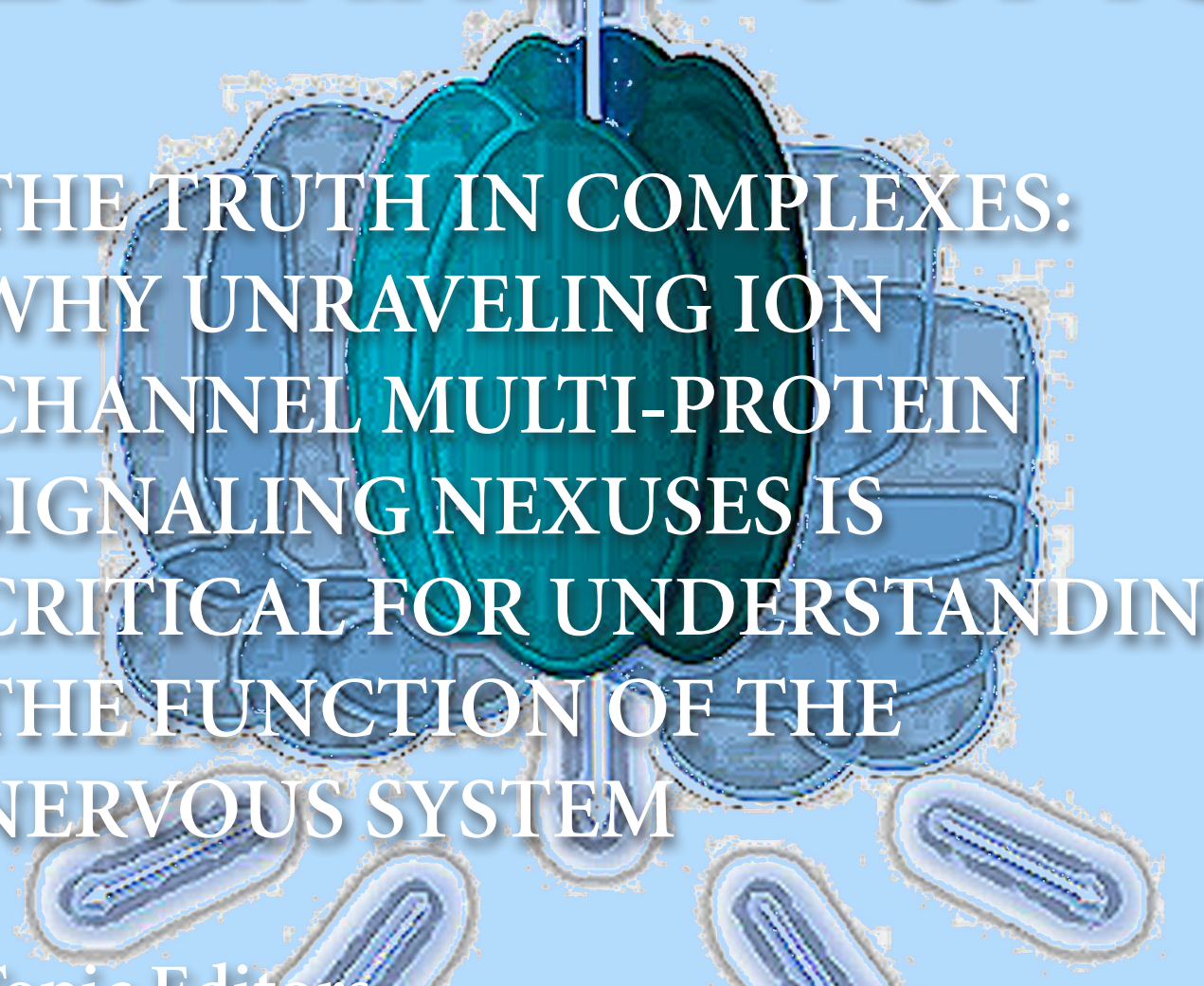


frontiers

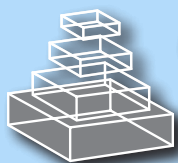
RESEARCH TOPICS



THE TRUTH IN COMPLEXES:
WHY UNRAVELING ION
CHANNEL MULTI-PROTEIN
SIGNALING NEXUSES IS
CRITICAL FOR UNDERSTANDING
THE FUNCTION OF THE
NERVOUS SYSTEM

Topic Editors

Leigh A. Swayne, Christophe Altier
and Gerald W. Zamponi



frontiers in
CELLULAR NEUROSCIENCE



frontiers

FRONTIERS COPYRIGHT STATEMENT

© Copyright 2007-2015
Frontiers Media SA.
All rights reserved.

All content included on this site, such as text, graphics, logos, button icons, images, video/audio clips, downloads, data compilations and software, is the property of or is licensed to Frontiers Media SA ("Frontiers") or its licensees and/or subcontractors. The copyright in the text of individual articles is the property of their respective authors, subject to a license granted to Frontiers.

The compilation of articles constituting this e-book, wherever published, as well as the compilation of all other content on this site, is the exclusive property of Frontiers. For the conditions for downloading and copying of e-books from Frontiers' website, please see the Terms for Website Use. If purchasing Frontiers e-books from other websites or sources, the conditions of the website concerned apply.

Images and graphics not forming part of user-contributed materials may not be downloaded or copied without permission.

Individual articles may be downloaded and reproduced in accordance with the principles of the CC-BY licence subject to any copyright or other notices. They may not be re-sold as an e-book.

As author or other contributor you grant a CC-BY licence to others to reproduce your articles, including any graphics and third-party materials supplied by you, in accordance with the Conditions for Website Use and subject to any copyright notices which you include in connection with your articles and materials.

All copyright, and all rights therein, are protected by national and international copyright laws.

The above represents a summary only. For the full conditions see the Conditions for Authors and the Conditions for Website Use.

ISSN 1664-8714

ISBN 978-2-88919-445-2

DOI 10.3389/978-2-88919-445-2

ABOUT FRONTIERS

Frontiers is more than just an open-access publisher of scholarly articles: it is a pioneering approach to the world of academia, radically improving the way scholarly research is managed. The grand vision of Frontiers is a world where all people have an equal opportunity to seek, share and generate knowledge. Frontiers provides immediate and permanent online open access to all its publications, but this alone is not enough to realize our grand goals.

FRONTIERS JOURNAL SERIES

The Frontiers Journal Series is a multi-tier and interdisciplinary set of open-access, online journals, promising a paradigm shift from the current review, selection and dissemination processes in academic publishing.

All Frontiers journals are driven by researchers for researchers; therefore, they constitute a service to the scholarly community. At the same time, the Frontiers Journal Series operates on a revolutionary invention, the tiered publishing system, initially addressing specific communities of scholars, and gradually climbing up to broader public understanding, thus serving the interests of the lay society, too.

DEDICATION TO QUALITY

Each Frontiers article is a landmark of the highest quality, thanks to genuinely collaborative interactions between authors and review editors, who include some of the world's best academicians. Research must be certified by peers before entering a stream of knowledge that may eventually reach the public - and shape society; therefore, Frontiers only applies the most rigorous and unbiased reviews.

Frontiers revolutionizes research publishing by freely delivering the most outstanding research, evaluated with no bias from both the academic and social point of view.

By applying the most advanced information technologies, Frontiers is catapulting scholarly publishing into a new generation.

WHAT ARE FRONTIERS RESEARCH TOPICS?

Frontiers Research Topics are very popular trademarks of the Frontiers Journals Series: they are collections of at least ten articles, all centered on a particular subject. With their unique mix of varied contributions from Original Research to Review Articles, Frontiers Research Topics unify the most influential researchers, the latest key findings and historical advances in a hot research area!

Find out more on how to host your own Frontiers Research Topic or contribute to one as an author by contacting the Frontiers Editorial Office: researchtopics@frontiersin.org

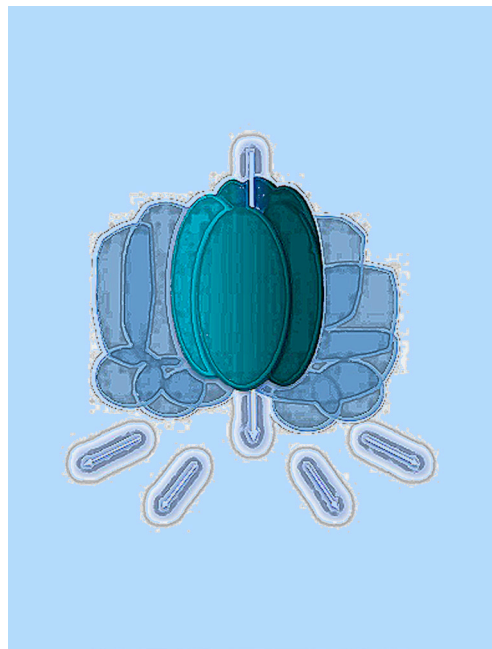
THE TRUTH IN COMPLEXES: WHY UNRAVELING ION CHANNEL MULTI-PROTEIN SIGNALING NEXUSES IS CRITICAL FOR UNDERSTANDING THE FUNCTION OF THE NERVOUS SYSTEM

Topic Editors:

Leigh A. Swayne, University of Victoria, Canada

Christophe Altier, University of Calgary, Canada

Gerald W. Zamponi, University of Calgary, Canada



Artistic rendering of an ion channel signaling nexus.

articles highlight how the complexity of ion channel signaling nexuses is critical to the proper functioning of the nervous system.

In the search for simple explanations of the natural world, its complicated textures are often filed down to a smoothened surface of our liking. The impetus for this Research Topic was borne out of a need to re-ignite interest in the complex – in this case in the context of ion channels in the nervous system. Ion channels are the large proteins that form regulated pores in the membranes of cells and, in the brain, are essential for the transfer, processing and storage of information. These pores full of twists and turns themselves are not just barren bridges into cells. More and more we are beginning to understand that ion channels are like bustling medieval bridges (packed with apartments and shops) rather than the more sleek modern variety – they are dynamic hubs connected with many structures facilitating associated activities. Our understanding of these networks continues to expand as our investigative tools advance. Together these

Table of Contents

- 05 *The Truth in Complexes: Perspectives on Ion Channel Signaling Nexuses in the Nervous System***
Leigh A. Swayne, Christophe Altier and Gerald W. Zamponi
- 08 *The NMDA Receptor Complex: A Multifunctional Machine at the Glutamatergic Synapse***
Xuelai Fan, Wu Yang Jin and Yu Tian Wang
- 17 *Ligand-Gated Ion Channel Interacting Proteins and their Role in Neuroprotection***
Shupeng Li, Albert H. C. Wong and Fang Liu
- 22 *Kir3 Channel Ontogeny – The Role of Gβγ Subunits in Channel Assembly and Trafficking***
Peter Zylbergold, Rory Sleno, Shahriar M. Khan, Ashley M. Jacobi, Mark A. Belhke and Terence E. Hébert
- 32 *Kir3 Channel Signaling Complexes: Focus on Opioid Receptor Signaling***
Karim Nagi and Graciela Pineyro
- 47 *Modulatory Mechanisms and Multiple Functions of Somatodendritic A-Type K⁺ Channel Auxiliary Subunits***
Henry H. Jerng and Paul J. Pfaffinger
- 67 *Signal Processing by T-Type Calcium Channel Interactions in the Cerebellum***
Jordan D.T. Engbers, Dustin Anderson, Gerald W. Zamponi and Ray W. Turner
- 82 *The Sodium Leak Channel, NALCN, in Health and Disease***
Maud Cochet-Bissuel, Philippe Lory and Arnaud Monteil
- 99 *The Emerging Pannexin 1 Signalome: A New Nexus Revealed?***
Leigh E. Wicki-Stordeur and Leigh A. Swayne
- 106 *CSPα – Chaperoning Presynaptic Proteins***
Julien Donnelier and Janice E. A. Braun
- 112 *The Essential Roles of Protein–Protein Interaction in Sigma-1 Receptor Functions***
Mohan Pabba
- 115 *STIM1-Mediated Bidirectional Regulation of Ca²⁺ Entry Through Voltage-Gated Calcium Channels (VGCC) and Calcium-Release Activated Channels (CRAC)***
Osama F. Harraz and Christophe Altier
- 121 *Differential Regulation of Collapsin Response Mediator Protein 2 (CRMP2) Phosphorylation by GSK3β and CDK5 Following Traumatic Brain Injury***
Sarah M. Wilson, Seul Ki Yeon, Xiao-Fang Yang, Ki Duk Park and Rajesh Khanna

135 *The Functionalized Amino Acid (S)-Lacosamide Subverts CRMP2-Mediated Tubulin Polymerization to Prevent Constitutive and Activity-Dependent Increase in Neurite Outgrowth*

Sarah M. Wilson, Aubin Moutal, Ohannes K. Melemedjian, Yuying Wang, Weina Ju, Liberty François-Moutal, May Khanna and Rajesh Khanna

150 *Novel Endogenous N-Acyl Amides Activate TRPV1-4 Receptors, BV-2 Microglia, and are Regulated in Brain in an Acute Model of Inflammation*

Siham Raboune, Jordyn M. Stuart, Emma Leishman, Sara M. Takacs, Brandon Rhodes, Arjun Basnet, Evan Jameyfield, Douglas McHugh, Theodore Widlanski and Heather B. Bradshaw



The truth in complexes: perspectives on ion channel signaling nexuses in the nervous system

Leigh A. Swayne^{1,2,3*}, Christophe Altier⁴ and Gerald W. Zamponi⁴

¹ Island Medical Program, Division of Medical Sciences, University of Victoria, Victoria, BC, Canada

² Department of Biology, University of Victoria, Victoria, BC, Canada

³ Department of Cellular and Physiological Sciences, University of British Columbia, Vancouver, BC, Canada

⁴ Department of Physiology and Pharmacology, University of Calgary, Calgary, AB, Canada

*Correspondence: lswayne@uvic.ca

Edited and reviewed by:

Egidio D'Angelo, University of Pavia, Italy

Keywords: interactome, ion channels, signaling networks, protein-protein interactions, protein-lipid interactions

ION CHANNELS AS SIGNALING NEXUSES

Ion channels are complex hetero-oligomeric structures characterized by large, dynamic interaction networks, or “interactomes.” In addition to directing channel localization, density and ion fluxes, these complexes facilitate downstream signaling events. Moreover, pathological modulation of these networks contributes to neurological dysfunction. Our contributors to this Research Topic, “*The truth in complexes: why unraveling ion channel multi-protein signaling nexuses is critical for understanding the function of the nervous system*” have considered interactomes from the perspective of the ion channel, from that of its intracellular protein modulators, and even from the point of view of lipid modulators. Together these diverse perspectives spin an intricate web of ion channel regulation in the nervous system.

MAJOR HUB: THE N-methyl-D-ASPARTATE RECEPTOR (NMDAR)

Described by Fan et al. (2014) as a “multifunctional machine,” the NMDAR interacts with a staggering number of proteins to shape synaptic plasticity, psychiatric disorders and ischemic neuronal damage. Notably, the authors outline arguably the most exciting example of interactome-based basic science leading to improved health outcomes: Tat-NR2B9c (also called NA-1). This cell-permeable peptide targets a specific NMDAR interaction, reducing ischemic brain damage in rodents, primates and humans (Sun et al., 2008; Cook et al., 2012; Hill et al., 2012). Li et al. (2014) similarly highlights interactions between several ligand-gated channels, including the NMDAR with other receptors and intracellular proteins, again focusing on these interactions as potential therapeutic targets for neuroprotection.

NOVEL NODES

Several other contributions shed light on the new insights into the function and composition of interactomes of various voltage-gated channels, regulated leak channels, and so called large pore channels.

VOLTAGE-GATED CHANNELS

Traditionally viewed as auxiliary subunits, K⁺ channel regulatory proteins are growing in complexity in terms of function

and type. Known to regulate activation and trafficking of muscarinic receptor-activated Kir3 channels, Zylbergold et al. (2014) provide evidence for an additional role of Gβγ subunits in Kir3 channel stability. Nagi and Pineyro (2014) focus specifically on opioid receptor signaling in the regulation of these channels. Jerng and Pfaffinger (2014) describe regulation of another K⁺ current, sub-threshold A-type (Kv4), by the so-called auxiliary subunits, dipeptidyl peptidase-like proteins (DPLPs) and Kv4 channel interacting proteins (KChIPs). While these were amongst the first identified interactors (e.g., for KChIP An et al., 2000), subsequent studies have significantly expanded the network. With respect to DPLPs and KChIPs, further study has also shed new light on their molecular diversity via alternative splicing as well as their roles in regulating several other channel types, such as voltage-gated Ca²⁺ channels and NMDARs. Connecting K⁺ channels with voltage-gated Ca²⁺ channels, Engbers et al. (2013) review how channel-channel interactions between intermediate conductance Ca²⁺-activated K⁺ channels (IKCa) and low voltage-activated Ca²⁺ channels (Cav3) functionally interact with other conductances to regulate signal processing in the cerebellum.

Na⁺ LEAK CHANNEL, NALCN

Elusive until recently, understanding of this regulated leak channel whose loss in mice is lethal (Lu et al., 2007), has greatly expanded by virtue of key insights into its interactome. Cochet-Bissuel et al. (2014) detail its ever-expanding list of interacting proteins, such as the M3 muscarinic receptor (Swayne et al., 2009). The authors highlight the involvement of the NALCN interactome in a number of disorders in the nervous system ranging from autism spectrum disorder (ASD) and schizophrenia to epilepsy and Alzheimer's disease.

PANNEXIN 1 (PANX1)

Permeable to ions and small metabolites like ATP, Panx1 channels gained early notoriety as “death pores” in ischemic stroke and seizure (Thompson et al., 2006, 2008; Weilingner et al., 2012). Highly expressed in neonatal brain (Ray et al., 2005; Vogt et al., 2005), Panx1 also positively regulates proliferation and differentiation, and negatively regulates neurite outgrowth in developing neurons (Wicki-Stordeur et al., 2012; Wicki-Stordeur

and Swayne, 2013). Wicki-Stordeur and Swayne (2014) reviewed the growing Panx1 interactome to shed clues on the signaling pathways in which Panx1 might be involved, highlighting roles in cytoskeletal remodeling and inflammation.

MULTI-TASKING INTRACELLULAR MODULATORS

A number of contributions underscore the capacity of “promiscuous” intracellular proteins to modulate a variety of ion channels and receptors through physical interaction. Reviewed by Donnelier and Braun (2014), cysteine string protein (CSP) is a resident pre-synaptic vesicle molecular chaperone targeting ion channels and vesicle-trafficking proteins. Not surprisingly, loss of, or mutation in CSP leads to synaptic dysfunction and neurodegeneration in a variety of systems (e.g., Zinsmaier et al., 1994; Fernandez-Chacon et al., 2004; Noskova et al., 2011). The sigma-1 receptor, reviewed by Pabba (2013), is an intracellular transmembrane protein that also acts in a chaperone-like way, modulating plasma membrane localized voltage- and ligand-gated channels with diverse neurophysiological and neuropathological implications. Harraz and Altier (2014) further link intracellular proteins to the regulation of plasma membrane channels, reviewing Stromal Interaction Molecule 1 (STIM1) in store-operated Ca^{2+} entry. They describe foundational work implicating STIM1 as the Ca^{2+} sensor in this process critical for maintaining neurotransmission. Further they outline key physical interactions between STIM1 with Ca^{2+} -release activated channels and voltage-gated Ca^{2+} channels that coordinate the activation and inhibition of these types of channels, respectively. Finally, two papers by Wilson et al. (2014a,b) focus on another intracellular multifunctional/multi-interactome protein, collapsin response mediator protein 2 (Crmp2). Best known as a microtubule stabilizer, Crmp2 is regulated in a context specific way by multiple kinases, and in turn, positively regulates both ligand- and voltage-gated Ca^{2+} channels.

NEW FRONTIERS: TOWARD MORE COMPREHENSIVE MACROMOLECULAR NETWORKS

Adding further complexity to ion channel networks is consideration of lipid membrane composition and lipid second messengers. In the sole lipidome-oriented contribution, Raboune et al. (2014) identify novel N-acyl amides regulating transient receptor potential vanilloid (TRPV) channels in the context of inflammatory pain. The future understanding of ion channel interactomes will undoubtedly include both proteome and lipidome components as technological advances in lipidomic research (Bou Khalil et al., 2010) become mainstream.

FINAL PERSPECTIVES: INTERACTOMES TO BEDSIDE

While daunting, elucidating these macromolecular intricacies has a translational silver lining: while difficult to identify and unravel, the myriad interaction loci revealed by studying these interactions present unique opportunities for discrete, and potentially safer therapeutic intervention. For example, selective blockade at key interaction loci with cell-permeable peptides now provides an infinite number of ways in which interactomes can be discretely modulated to improve health outcomes.

REFERENCES

- An, W. F., Bowlby, M. R., Betty, M., Cao, J., Ling, H. P., Mendoza, G., et al. (2000). Modulation of A-type potassium channels by a family of calcium sensors. *Nature* 403, 553–556. doi: 10.1038/35000592
- Bou Khalil, M., Hou, W., Zhou, H., Elisma, F., Swayne, L. A., Blanchard, A. P., et al. (2010). Lipidomics era: accomplishments and challenges. *Mass Spectrom. Rev.* 29, 877–929. doi: 10.1002/mas.20294
- Cochet-Bissuel, M., Lory, P., and Monteil, A. (2014). The sodium leak channel, NALCN, in health and disease. *Front. Cell. Neurosci.* 8:132. doi: 10.3389/fncel.2014.00132
- Cook, D. J., Teves, L., and Tymianski, M. (2012). Treatment of stroke with a PSD-95 inhibitor in the gyrencephalic primate brain. *Nature* 483, 213–217. doi: 10.1038/nature10841
- Donnelier, J., and Braun, J. E. (2014). CSPalpha-chaperoning presynaptic proteins. *Front. Cell. Neurosci.* 8:116. doi: 10.3389/fncel.2014.00116
- Engbers, J. D., Anderson, D., Zamponi, G. W., and Turner, R. W. (2013). Signal processing by T-type calcium channel interactions in the cerebellum. *Front. Cell. Neurosci.* 7:230. doi: 10.3389/fncel.2013.00230
- Fan, X., Jin, W. Y., and Wang, Y. T. (2014). The NMDA receptor complex: a multifunctional machine at the glutamatergic synapse. *Front. Cell. Neurosci.* 8:160. doi: 10.3389/fncel.2014.00160
- Fernandez-Chacon, R., Wolfel, M., Nishimune, H., Tabares, L., Schmitz, F., Castellano-Munoz, M., et al. (2004). The synaptic vesicle protein CSP alpha prevents presynaptic degeneration. *Neuron* 42, 237–251. doi: 10.1016/S0896-6273(04)00190-4
- Harraz, O. F., and Altier, C. (2014). STIM1-mediated bidirectional regulation of Ca^{2+} entry through voltage-gated calcium channels (VGCC) and calcium-release activated channels (CRAC). *Front. Cell. Neurosci.* 8:43. doi: 10.3389/fncel.2014.00043
- Hill, M. D., Martin, R. H., Mikulis, D., Wong, J. H., Silver, F. L., Terbrugge, K. G., et al. (2012). Safety and efficacy of NA-1 in patients with iatrogenic stroke after endovascular aneurysm repair (ENACT): a phase 2, randomised, double-blind, placebo-controlled trial. *Lancet Neurol.* 11, 942–950. doi: 10.1016/S1474-4422(12)70225-9
- Jerng, H. H., and Pfaffinger, P. J. (2014). Modulatory mechanisms and multiple functions of somatodendritic A-type K (+) channel auxiliary subunits. *Front. Cell. Neurosci.* 8:82. doi: 10.3389/fncel.2014.00082
- Li, S., Wong, A. H., and Liu, F. (2014). Ligand-gated ion channel interacting proteins and their role in neuroprotection. *Front. Cell. Neurosci.* 8:125. doi: 10.3389/fncel.2014.00125
- Lu, B., Su, Y., Das, S., Liu, J., Xia, J., and Ren, D. (2007). The neuronal channel NALCN contributes resting sodium permeability and is required for normal respiratory rhythm. *Cell* 129, 371–383. doi: 10.1016/j.cell.2007.02.041
- Nagi, K., and Pineyro, G. (2014). Kir3 channel signaling complexes: focus on opioid receptor signaling. *Front. Cell. Neurosci.* 8:186. doi: 10.3389/fncel.2014.00186
- Noskova, L., Stranecky, V., Hartmannova, H., Pristoupilova, A., Baresova, V., Ivanek, R., et al. (2011). Mutations in DNAJC5, encoding cysteine-string protein alpha, cause autosomal-dominant adult-onset neuronal ceroid lipofuscinosis. *Am. J. Hum. Genet.* 89, 241–252. doi: 10.1016/j.ajhg.2011.07.003
- Pabba, M. (2013). The essential roles of protein-protein interaction in sigma-1 receptor functions. *Front. Cell. Neurosci.* 7:50. doi: 10.3389/fncel.2013.00050
- Raboune, S., Stuart, J. M., Leishman, E., Takacs, S. M., Rhodes, B., Basnet, A., et al. (2014). Novel endogenous N-acyl amides activate TRPV1-4 receptors, BV-2 microglia, and are regulated in brain in an acute model of inflammation. *Front. Cell. Neurosci.* 8:195. doi: 10.3389/fncel.2014.00195
- Ray, A., Zoidl, G., Weickert, S., Wahle, P., and Dermietzel, R. (2005). Site-specific and developmental expression of pannexin1 in the mouse nervous system. *Eur. J. Neurosci.* 21, 3277–3290. doi: 10.1111/j.1460-9568.2005.04139.x
- Sun, H. S., Doucette, T. A., Liu, Y., Fang, Y., Teves, L., Aarts, M., et al. (2008). Effectiveness of PSD95 inhibitors in permanent and transient focal ischemia in the rat. *Stroke* 39, 2544–2553. doi: 10.1161/STROKEAHA.107.506048
- Swayne, L. A., Mezghrani, A., Varrault, A., Chemin, J., Bertrand, G., Dalle, S., et al. (2009). The NALCN ion channel is activated by M3 muscarinic receptors in a pancreatic beta-cell line. *EMBO Rep.* 10, 873–880. doi: 10.1038/embor.2009.125
- Thompson, R. J., Jackson, M. F., Olah, M. E., Rungta, R. L., Hines, D. J., Beazely, M. A., et al. (2008). Activation of pannexin-1 hemichannels augments aberrant bursting in the hippocampus. *Science* 322, 1555–1559. doi: 10.1126/science.1165209

- Thompson, R. J., Zhou, N., and Macvicar, B. A. (2006). Ischemia opens neuronal gap junction hemichannels. *Science* 312, 924–927. doi: 10.1126/science.1126241
- Vogt, A., Hormuzdi, S. G., and Monyer, H. (2005). Pannexin1 and Pannexin2 expression in the developing and mature rat brain. *Brain Res. Mol. Brain Res.* 141, 113–120. doi: 10.1016/j.molbrainres.2005.08.002
- Weilinger, N. L., Tang, P. L., and Thompson, R. J. (2012). Anoxia-induced NMDA receptor activation opens pannexin channels via Src family kinases. *J. Neurosci.* 32, 12579–12588. doi: 10.1523/JNEUROSCI.1267-12.2012
- Wicki-Stordeur, L. E., Dzugalo, A. D., Swansburg, R. M., Suits, J. M., and Swayne, L. A. (2012). Pannexin 1 regulates postnatal neural stem and progenitor cell proliferation. *Neural Dev.* 7, 11. doi: 10.1186/1749-8104-7-11
- Wicki-Stordeur, L. E., and Swayne, L. A. (2013). Panx1 regulates neural stem and progenitor cell behaviours associated with cytoskeletal dynamics and interacts with multiple cytoskeletal elements. *Cell Commun. Signal.* 11, 62. doi: 10.1186/1478-811X-11-62
- Wicki-Stordeur, L. E., and Swayne, L. A. (2014). The emerging Pannexin 1 signalome: a new nexus revealed? *Front. Cell. Neurosci.* 7:287. doi: 10.3389/fncel.2013.00287
- Wilson, S. M., Ki Yeon, S., Yang, X. F., Park, K. D., and Khanna, R. (2014a). Differential regulation of collapsin response mediator protein 2 (CRMP2) phosphorylation by GSK3 α and CDK5 following traumatic brain injury. *Front. Cell. Neurosci.* 8:135. doi: 10.3389/fncel.2014.00135
- Wilson, S. M., Moutal, A., Melemedjian, O. K., Wang, Y., Ju, W., Francois-Moutal, L., et al. (2014b). The functionalized amino acid (S)-Lacosamide subverts CRMP2-mediated tubulin polymerization to prevent constitutive and activity-dependent increase in neurite outgrowth. *Front. Cell. Neurosci.* 8:196. doi: 10.3389/fncel.2014.00196
- Zinsmaier, K. E., Eberle, K. K., Buchner, E., Walter, N., and Benzer, S. (1994). Paralysis and early death in cysteine string protein mutants of *Drosophila*. *Science* 263, 977–980.
- Zylbergold, P., Sleno, R., Khan, S. M., Jacobi, A. M., Belhke, M. A., and Hebert, T. E. (2014). Kir3 channel ontogeny - the role of Gbetagamma subunits in channel assembly and trafficking. *Front. Cell. Neurosci.* 8:108. doi: 10.3389/fncel.2014.00108

Conflict of Interest Statement: The authors declare that the research was conducted in the absence of any commercial or financial relationships that could be construed as a potential conflict of interest.

Received: 26 September 2014; accepted: 10 November 2014; published online: 26 November 2014.

Citation: Swayne LA, Altier C and Zamponi GW (2014) The truth in complexes: perspectives on ion channel signaling nexuses in the nervous system. *Front. Cell. Neurosci.* 8:406. doi: 10.3389/fncel.2014.00406

This article was submitted to the journal *Frontiers in Cellular Neuroscience*.

Copyright © 2014 Swayne, Altier and Zamponi. This is an open-access article distributed under the terms of the Creative Commons Attribution License (CC BY). The use, distribution or reproduction in other forums is permitted, provided the original author(s) or licensor are credited and that the original publication in this journal is cited, in accordance with accepted academic practice. No use, distribution or reproduction is permitted which does not comply with these terms.



The NMDA receptor complex: a multifunctional machine at the glutamatergic synapse

Xuelai Fan, Wu Yang Jin and Yu Tian Wang *

Brain Research Centre and Department of Medicine, Vancouver Coastal Health Research Institute, University of British Columbia, Vancouver, BC, Canada

Edited by:

Leigh Anne Swayne, University of Victoria, Canada

Reviewed by:

Carlo Sala, CNR Institute of Neuroscience, Italy

Jean-Claude Beique, University of Ottawa, Canada

*Correspondence:

Yu Tian Wang, Brain Research Centre and Department of Medicine, Vancouver Coastal Health Research Institute, University of British Columbia, 2211 Westbrook Mall, Vancouver, BC V6T2B5, Canada
e-mail: ytwang@brain.ubc.ca

The N-methyl-D-aspartate receptors (NMDARs) are part of a large multiprotein complex at the glutamatergic synapse. The assembly of NMDARs with synaptic proteins offers a means to regulate NMDAR channel properties and receptor trafficking, and couples NMDAR activation to distinct intracellular signaling pathways, thus contributing to the versatility of NMDAR functions. Receptor-protein interactions at the synapse provide a dynamic and powerful mechanism for regulating synaptic efficacy, but can also contribute to NMDAR overactivation-induced excitotoxicity and cellular damage under pathological conditions. An emerging concept is that by understanding the mechanisms and functions of disease-specific protein-protein interactions in the NMDAR complex, we may be able to develop novel therapies based on protein-NMDAR interactions for the treatment of brain diseases in which NMDAR dysfunction is at the root of their pathogenesis.

Keywords: NMDA receptors, protein-protein interaction, synaptic plasticity, dopamine receptors, excitotoxicity, ion channel complex, signaling pathways

N-methyl-D-aspartate receptors (NMDARs) are a major subtype of glutamate-gated ion channels at the excitatory synapses in the central nervous system (CNS), which mediate the flow of sodium (Na^+) and calcium (Ca^{2+}) ions into the cell and potassium ions (K^+) out of the cell. NMDARs are heterotetrameric plasma membrane channels composed of two obligatory GluN1 and two modulatory GluN2 (A-D) subunits (Cull-Candy et al., 2001; Collingridge et al., 2009), although sometimes the GluN2 subunits are replaced by GluN3(A-B) subunits (Ulbrich and Isacoff, 2008). NMDARs form a diheteromer when the two GluN2 subunits are identical, or a triheteromer when two different GluN2 subunits co-assemble with two identical GluN1 subunits (Ulbrich and Isacoff, 2008; Collingridge et al., 2010). At resting state, NMDARs are blocked by the presence of extracellular magnesium ions (Mg^{2+}) in the channel pore (Vargas-Caballero and Robinson, 2004). As such, the activation and opening of NMDARs is both voltage-dependent and ligand-gated, and requires the binding of two ligands, glutamate and either D-serine or glycine (Nong et al., 2003; Papouin et al., 2012), at a depolarized membrane potential to relieve Mg^{2+} block. The function of NMDARs in the CNS has been extensively studied in both genetic and pharmacological manipulations. NMDARs play a critical role in a wide range of cellular processes and brain functions, including synaptic plasticity, addiction and stroke (Schilström et al., 2006; Collingridge et al., 2010; Lai et al., 2011). The versatility of NMDAR functions may in part be attributed to its organization at the synapse. NMDARs are anchored to the plasma membrane as a multiprotein complex by binding to more than 70 adhesion proteins (Naisbitt et al., 1999; Husi et al., 2000; Grant and O'Dell, 2001). Upon activation, Ca^{2+} influxes through the opened channel pore and triggers various intracellular signaling cascades by activating calcium-sensitive

NMDAR-interacting proteins in the multiprotein complex (Lai et al., 2011; Martin and Wellman, 2011; Lisman et al., 2012). Increasing evidence suggest that it is these interacting proteins that confer the versatile functions of NMDARs. In this review, we will introduce several key NMDAR-interacting proteins in the NMDAR multiprotein complex and discuss their critical roles in mediating physiological and pathological functions in the brain.

INTERACTIONS BETWEEN NMDARs AND CALCIUM SENSING PROTEINS IN SYNAPTIC PLASTICITY

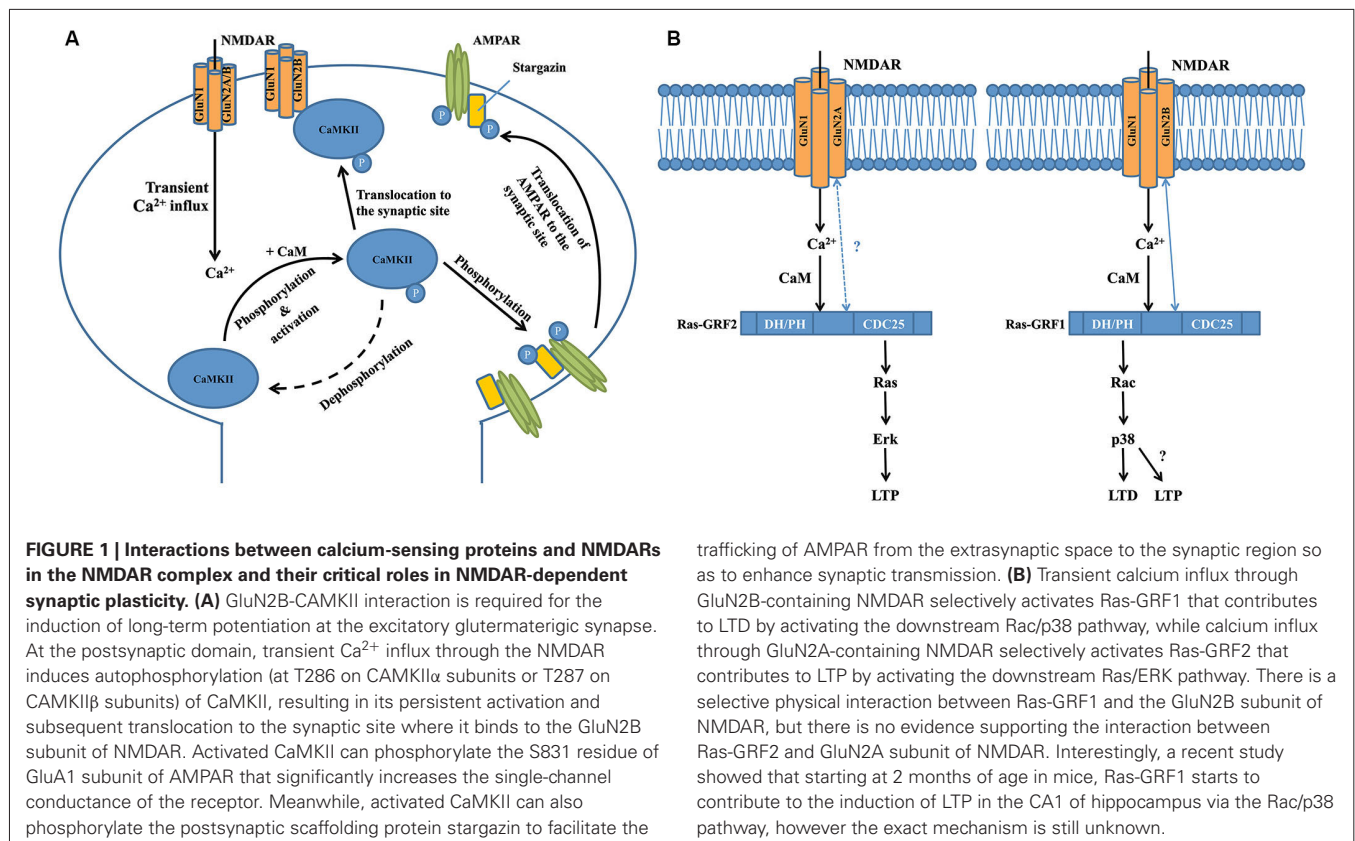
Two major forms of synaptic plasticity are long-term potentiation (LTP) and long-term depression (LTD), which are respectively characterized by long-lasting enhancement and reduction of synaptic transmission between two adjacent neurons after repetitive stimulation (Collingridge et al., 2010, 2004). Many proteins in the NMDAR complex contribute to these processes, with one of the most well-characterized proteins being Ca^{2+} /calmodulin-dependent protein kinase II (CaMKII; Hayashi et al., 2000; Pi et al., 2010; Lisman et al., 2012), a serine/threonine protein kinase that is highly enriched in the post-synaptic density region. CaMKII is a large holoenzyme consisting of 12 identical subunits (Lisman et al., 2012). Transient Ca^{2+} influx through the NMDAR channel pore induces autophosphorylation of CaMKII (at T286 on CaMKII α subunits or T287 on CaMKII β subunits), resulting in its persistent activation even after intracellular Ca^{2+} levels return to baseline (Rellos et al., 2010). As shown by a variety of real-time imaging studies and binding assays, activated CaMKII then rapidly and reversibly translocates to the spine and physically interacts with the 1260-1309aa domain in the carboxyl-terminal of the GluN2B NMDAR subunit (Figure 1A; Strack and Colbran,

1998; Bayer et al., 2001, 2006; Otmakhov et al., 2004; Zhang et al., 2008; Lisman et al., 2012). Although there is a basal level of association between CaMKII and NMDARs (Leonard et al., 1999), the translocation of these activated, phosphorylated CaMKII proteins greatly increases the total number of the kinase at the postsynaptic site. Introduction of a T286A mutation that prevents the autophosphorylation and activation of CaMKII α in mice significantly impairs NMDAR-dependent LTP in the hippocampal CA1 area and memory performance in a Morris water maze task (Giese et al., 1998), suggesting that CaMKII plays a vital role in NMDAR-dependent synaptic plasticity. This is further supported by several other lines of evidence. For example, overexpressing a GluN2B carboxyl-terminal fragment (839-1482aa) that disrupts the physiological interaction between NMDAR/CaMKII leads to severe deficits in hippocampal LTP and spatial learning in transgenic mice (Zhou et al., 2007). LTP in organotypic hippocampal slices is impaired either by acute replacement of the synaptic GluN2B with GluN2A subunit that shows less binding affinity with CaMKII, or by expression of a mutant synaptic GluN2B subunit that markedly reduces the binding affinity with CaMKII (Barria and Malinow, 2005). Taken together, these results suggest that association of activated CaMKII and NMDARs may be a necessary step for NMDAR-dependent synaptic plasticity.

How the NMDAR-CaMKII interaction contributes to the production of LTP is still not fully understood. Several recent studies report that normal levels of LTP in the CA1 neurons in adult hippocampal slices can be induced after GluN2B-containing NMDARs are fully blocked, suggesting that functional activation of GluN2B-containing NMDARs may not be essential (Köhr et al., 2003; Liu et al., 2004; Woo et al., 2005; Foster et al., 2010). In this regard, it is interesting to note that a recent study has found that GluN2B in the NMDAR complex may function as a key scaffolding protein at excitatory synapses, and thus plays a critical role in LTP by recruiting molecules important for LTP through interacting with them via its cytoplasmic tail (Foster et al., 2010). Thus, it is likely that GluN2B may have a structural, rather than a functional, role for LTP production, presumably through the GluN2B-CaMKII interaction to recruit CaMKII to the activated synapses, and CaMKII (as a calcium-dependent kinase) in turn playing an essential role in LTP induction; however, the mechanistic details have not yet been elucidated. Bath application of AC3-1, a selective peptide inhibitor for CaMKII, to acute hippocampal slices prevents LTP induction, but has little effect on NMDAR channel function (Chen et al., 2001). This suggests that although activated CaMKII is recruited to the synaptic site by interacting with the GluN2B carboxyl-terminal, it does not regulate NMDAR channel function during synaptic plasticity. Indeed, several other studies have reported that activated CaMKII phosphorylates the S831 residue of the GluA1 subunit of the α -amino-3-hydroxy-5-methyl-4-isoxazolepropionate glutamate receptor (AMPA), a major glutamate receptor that mediates fast synaptic transmission, and increases the single-channel conductance of GluA1-containing AMPARs (Figure 1A; Barria et al., 1997; Derkach et al., 1999; Kristensen et al., 2011). This effect can be mimicked by mutating the S831 residue of GluA1 to the phosphomimetic glutamate residue (Kristensen et al., 2011). Meanwhile, activated CaMKII can also phosphorylate stargazin (Tomita et al., 2005),

an important postsynaptic scaffolding protein that facilitates the trafficking of AMPARs from the extrasynaptic space to the synaptic region (Figure 1A; Schnell et al., 2002; Tsui and Malenka, 2006; Opazo et al., 2010; but see Kessels et al., 2009). Taken together, these processes markedly enhance synaptic transmission so as to promote the expression of LTP, in particular the initial phase of LTP. Given that LTP can exist for hours or even weeks, yet CaMKII is generally inactivated in a relatively short timeframe (~ 1 min) after transient synaptic stimulation (Lee et al., 2009), it is still unclear whether CaMKII plays any important roles in the maintenance of late-phase LTP. Furthermore, little is known about how activated CaMKII participates in LTD, the opposing form of synaptic plasticity to LTP, although several recent studies have suggested that autonomous CaMKII can lead to either LTP or LTD, depending on the phosphorylation state of the control point, T305/T306 (Pi et al., 2010; Coultrap et al., 2014). Answering these questions will further uncover details about the physiological functions of GluN2B-CaMKII interaction in the NMDAR multiprotein complex, and enhance our understanding of NMDAR-dependent synaptic plasticity.

Two other important calcium sensors in the NMDAR multiprotein complex are Ras-Guanine Nucleotide-Releasing Factor 1 (Ras-GRF1) and Ras-GRF2, a family of calcium-dependent guanine nucleotide exchange factors (GEF) that are predominantly expressed in adult CNS neurons (Feig, 2011). Structurally, Ras-GRF1 and Ras-GRF2 share many similarities, and contain several common functional domains, including the calmodulin-binding IQ domain, Ras GTPase-activating CDC25 domain and Rac GTPase-activating DH/PH domain (Feig, 2011). However, recent studies have shown that Ras-GRF1 and Ras-GRF2 interact with different NMDAR subunits and play strikingly different roles in NMDAR-dependent synaptic plasticity (Figure 1B; Feig, 2011). Knocking out Ras-GRF1 in mice shows minimal effects on both high frequency stimulation (HFS) and theta burst stimulation (TBS)-induced LTP in hippocampal slices, but leads to severe impairments in low frequency stimulation (LFS)-induced LTD (Li et al., 2006). In contrast, knocking out Ras-GRF2 significantly impairs both HFS and TBS-induced LTP in hippocampal slices, whereas LFS-induced LTD is not affected. More strikingly, as shown by immunoblotting studies in hippocampal brain slices, Ras-GRF2 mediates signaling from GluN2A-containing NMDARs to the Ras effector extracellular signal-related protein kinase 1/2 (Erk1/2) mitogen-activated protein (MAP) kinase, a promoter of LTP, whereas Ras-GRF1 mediates signaling from GluN2B-containing NMDARs to the Rac effector p38 MAP kinase, a promoter of LTD (Figure 1B; Li et al., 2006). Given that some evidence suggests that GluN2A-containing NMDARs promote LTP whereas GluN2B-containing NMDARs promote LTD (Liu et al., 2004; Massey et al., 2004), these distinct differences between Ras-GRF1 and Ras-GRF2 in synaptic plasticity may be partially explained by the selective interaction between Ras-GRF1 and the 886-1310aa domain in the carboxyl-terminal of GluN2B subunit (Krapivinsky et al., 2003). However, to date there is no clear evidence that supports the presence of a direct interaction between Ras-GRF2 and the GluN2A subunit, although it is suggested that Ras-GRF2 may localize in the vicinity of GluN2A-containing NMDARs at the postsynaptic site (Jin and Feig, 2010).



Furthermore, given that both Ras-GRF1 and Ras-GRF2 contain the activation domains for both Ras and Rac GTPases, it is also important to determine how and why these two proteins are coupled with different downstream signaling cascades during LTP and LTD. One explanation is that the selective association between the synaptic Ras GTPase-activating protein SynGAP and GluN2B-containing NMDARs in the synapse may help inhibit Ras-GRF1 from activating the Ras/Erk signaling cascade (Kim et al., 2005). Alternatively, scaffolding proteins that selectively associate with either GluN2A or GluN2B may specifically target Ras-GRF2 and Ras-GRF1 to the Ras and Rac signaling cascades, respectively (Buchsbaum et al., 2002; Feig, 2011). However, the detailed mechanism has yet to be determined.

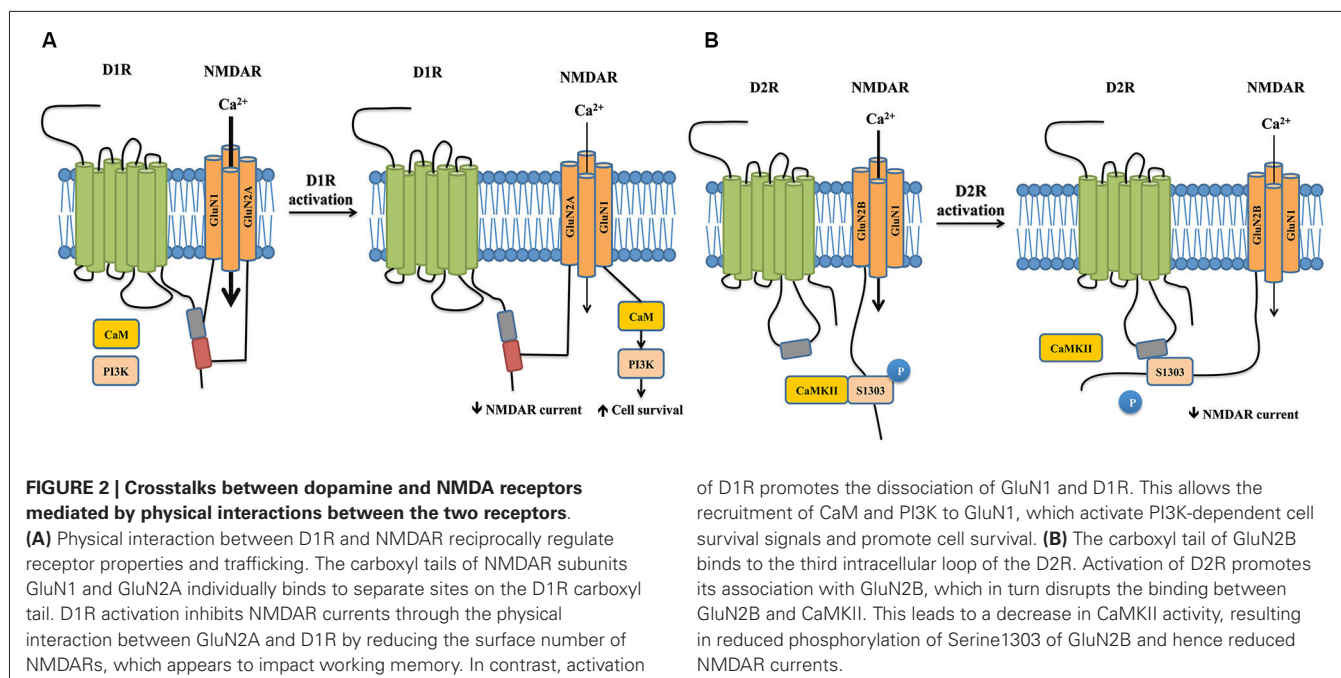
It is noteworthy that the contribution of Ras-GRFs to NMDAR-dependent synaptic plasticity is highly regulated by development in mice. Ras-GRF1 and Ras-GRF2 are only coupled to NMDARs in adult neurons beginning at 20 days of age in mice (Li et al., 2006), while the guanine nucleotide exchange factor Sos mediates NMDAR signaling in neurons derived from neonatal mice (Tian et al., 2004). As mentioned above (Figure 1B), previous studies report that beginning at 1 month of age, Ras-GRF1 preferentially mediates GluN2B-containing NMDAR-dependent LTD in the CA1 region of the hippocampus of mice via the Rac/p38 pathway (Li et al., 2006). Interestingly, beginning at 2 months of age in mice, the role of Ras-GRF1 dramatically shifts to support the induction of LTP, rather than LTD, in the CA1 region as a downstream effector of calcium-permeable, AMPA-type glutamate receptors (Jin et al., 2013). Surprisingly,

this induction of LTP is also mediated by the Rac/p38 pathway, which was previously thought to be mainly associated with LTD (Figure 1B; Jin et al., 2013). It is still unclear how these signaling pathways switch during development, but further investigation is likely to reveal additional details on the regulatory mechanisms of Ras-GRF in synaptic plasticity at the NMDAR complex.

INTERACTIONS BETWEEN NMDARs AND G-PROTEIN COUPLED RECEPTORS (GPCRs) IN PSYCHIATRIC DISORDERS

In addition to coupling to calcium sensing proteins, the NMDAR complex has extensive functional interactions with G-protein coupled receptors (GPCRs) through direct physical interaction. An example of this is the reciprocal modulation between NMDARs and dopamine receptors, a family of GPCRs that has been implicated in many psychiatric disorders, including schizophrenia (Seeman, 1987; Dolan et al., 1995).

Dopamine receptors comprise of five subtypes, D1R to D5R, which can be further classified pharmacologically into D1-like receptors consisting of D1R and D5R, and D2-like receptors consisting of D2R, D3R and D4R (Seeman, 1987; Tiberi et al., 1991; Dolan et al., 1995). Although earlier studies have shown presynaptic localization (Levey et al., 1993), it is now generally believed that D1-like receptors are strictly localized on cells that are postsynaptic to dopaminergic neurons (Hersch et al., 1995; Yung et al., 1995). In contrast, D2Rs and D3Rs are present both presynaptically and postsynaptically (Sokoloff et al., 2006). D1-like receptors increase intracellular cAMP concentrations through activation of the $G_{s/olf}$ class of G proteins and subsequent



activation of adenylyl cyclase (AC), whereas D2-like receptors couple to the $G_{i/o}$ class of G proteins to inhibit AC (Kebabian et al., 1972; Monsma et al., 1990). Numerous studies have demonstrated extensive crosstalk between DRs and NMDARs via direct physical association between the receptors (Figure 2, for a review, see Beaulieu and Gainetdinov, 2011).

D1Rs co-immunoprecipitates with both GluN1 and GluN2A subunits of the NMDAR in rat hippocampal tissue, suggesting a physical interaction between the two receptors (Lee et al., 2002). Further *in vitro* experiments confirm that the carboxyl tails of both the GluN1 subunit and GluN2A subunit (but not GluN2B) individually bind to the carboxyl tails of D1Rs (but not that of D5Rs). The 387-416aa domain of the D1R carboxyl-tail is sufficient for D1R-GluN1 binding, while the 417-446aa domain is required for the D1R-GluN2A interaction, suggesting that two distinct protein-protein interactions exist between the receptors. The binding between NMDARs and D1Rs occurs in the absence of D1R agonists, and D1R activation reduces the interaction between D1R-GluN1 but not that between D1R-GluN2A (Lee et al., 2002).

The functional consequences of these two interactions significantly differ. Following D1R stimulation with its agonist SKF81297, the D1R-GluN2A interaction functions to reduce the surface expression of NMDARs and hence the receptor-gated currents in both transfected cells and hippocampal neurons through a PKA/PKC independent pathway (Lee et al., 2002). It should be noted that SKF81297, in addition to activating D1Rs, has previously been shown to reduce NMDAR currents via a direct blockade of the NMDAR channel pore (Figure 2A, Cui et al., 2006). However, dissociation of D1R-GluN2A interaction using an interference peptide significantly reverses the attenuation of NMDAR currents, strongly arguing for a crucial role of the physical coupling between the two receptors, rather

than a direct channel blockade, in mediating D1R activation-induced NMDAR inhibition (Lee et al., 2002). As overactivation of NMDAR is crucial for excitotoxic neuronal death (Lai et al., 2011), this reduction of surface expression of NMDARs would be expected to decrease Ca^{2+} influx and hence be neuroprotective. However, peptide-mediated dissociation of D1R-GluN2A does not affect neuronal survival following a NMDA insult. Instead, the uncoupling of D1R-GluN1 following D1R activation confers neuroprotection through the recruitment of calmodulin and phosphatidylinositol 3-kinase to GluN1, which activates cell-survival signals (Figure 2A, Lee et al., 2002). These data suggest that D1R activation-induced inhibition of NMDAR-mediated currents and excitotoxicity are differentially mediated by distinct subunit-specific interactions in the NMDAR complex, further highlighting that specific protein-protein interactions dictate the functional outcomes of the NMDAR complex.

Further studies have demonstrated that D1R and NMDAR interactions may also reciprocally regulate receptor trafficking and surface expression in a NMDAR subunit-specific manner. D1Rs directly interact with the GluN1 subunit in cytoplasmic compartments, where they are retained, and the presence of the GluN2B subunit drives the translocation and insertion of the D1R-GluN1 receptor complex into the plasma membrane in medium spiny neurons and cotransfected cells (Fiorentini et al., 2003). This suggests that D1Rs and NMDARs are assembled as constitutive heteromeric complexes in cytoplasmic compartments prior delivery to functional sites, a process that does not depend on receptor activation (Fiorentini et al., 2003). Furthermore, constitutive association with GluN2B-containing NMDARs abolishes agonist-induced D1R internalization and stabilizes D1Rs at the post-synaptic density (Fiorentini et al., 2003). In contrast, although GluN2A-containing NMDARs can also recruit

D1Rs to the cell surface, this effect depends on NMDAR stimulation. In cotransfected cells, activation of GluN2A-containing NMDARs increases their physical association with D1Rs, which drives the insertion of D1Rs into the plasma membrane (Pei et al., 2004). These differences in agonist dependency may perhaps be attributed to functional differences between GluN2A or GluN2B-containing NMDARs (for a review, see Traynelis et al., 2010). In addition to regulating D1R surface expression, NMDAR activation can also reduce D1R lateral diffusion in medium spiny neurons via increased GluN1-D1R interaction, which stabilizes D1Rs at the synapse (Scott et al., 2006). It should be noted, however, that the observed increase in D1R surface levels may be transient or restricted to certain neuronal populations *in vivo*, as a 90% reduction in GluN1 expression in mice did not impair striatal D1R pharmacology and function (Ramsey et al., 2008).

Conversely, the binding between D1Rs and NMDARs also modulates NMDAR surface dynamics at glutamatergic synapses, which offers a more direct means to regulate synaptic plasticity. D1R activation, which reduces D1R-GluN1 interaction at the perisynapse, allows NMDARs to laterally diffuse into the post-synaptic density where they favor LTP, an effect that was recapitulated by dissociating D1R-GluN1 binding with an interference peptide (Ladepeche et al., 2013). Dissociation of D1R-GluN1 upon D1R activation promotes CaMKII-GluN1 interaction and increases CaMKII activity, which in turn upregulates NMDAR-mediated LTP in primary hippocampal neurons and promotes spatial working memory in the delayed match-to-place version of the water maze in intact animals (Nai et al., 2010). While this effect may be cautiously interpreted as a result of physical dissociation between D1R-GluN1, it should be noted that D1R activation may also affect synaptic plasticity through protein phosphatase-dependent pathways (Frey et al., 1993; Stramiello and Wagner, 2008) as well as network mechanisms (Xu and Yao, 2010). However, the relative contribution of each mechanism remains to be seen.

The long-form D2R, which is preferentially involved in post-synaptic signaling compared to short-form D2R (Lindgren et al., 2003) interacts with the carboxyl-tail of the GluN2B subunit of NMDARs in the post-synaptic density of striatal neurons. In contrast to D1Rs, this interaction is not mediated by the D2R carboxyl-tail, but by a TKRSSRAFR motif situated in the N-terminal of the third intracellular loop of D2Rs (Liu et al., 2006). The interaction between D2Rs and NMDARs is receptor- and subunit- specific: D3Rs, which are similar to D2Rs and also belong to the D2-class of dopamine receptors, do not associate with the GluN2B subunit, and D2Rs do not interact with the GluN1 subunit (Liu et al., 2006).

Activation of D2Rs with its agonist quinpirole inhibits NMDAR currents in acutely dissociated medium-sized striatal neurons, which can be blocked by disrupting D2R-GluN2B physical interaction (Liu et al., 2006). Acute treatment with cocaine, a psychostimulant known to exert its effects through both dopaminergic and glutamatergic signaling, enhances D2R-GluN2B coupling in the striatum. In turn, this increased association disrupts GluN2B-CaMKII binding, resulting in decreased CaMKII activity, reducing phosphorylation of GluN2B

at the Serine 1303 residue, and thereby resulting in reduced NMDAR currents (**Figure 2B**, Liu et al., 2006). Cocaine-enhanced D2R-GluN2B interaction seems to be specific to the striatum, as it was not observed in the hippocampus or frontal cortex. The D2R-GluN2B interaction may play a role in eliciting the locomotor effects of cocaine. In rats, systemic disruption of D2R-GluN2B interaction prior cocaine treatment markedly reverses the uncoupling between GluN2B-CaMKII induced by cocaine and rescues GluN2B S1303 phosphorylation in the striatum without affecting basal GluN2B-CaMKII interactions. Furthermore, blocking D2R-GluN2B interactions significantly, though not completely, reduces cocaine-stimulated locomotion in rats (Liu et al., 2006). This suggests the existence of other factors that contribute to the full-scale motor response to cocaine.

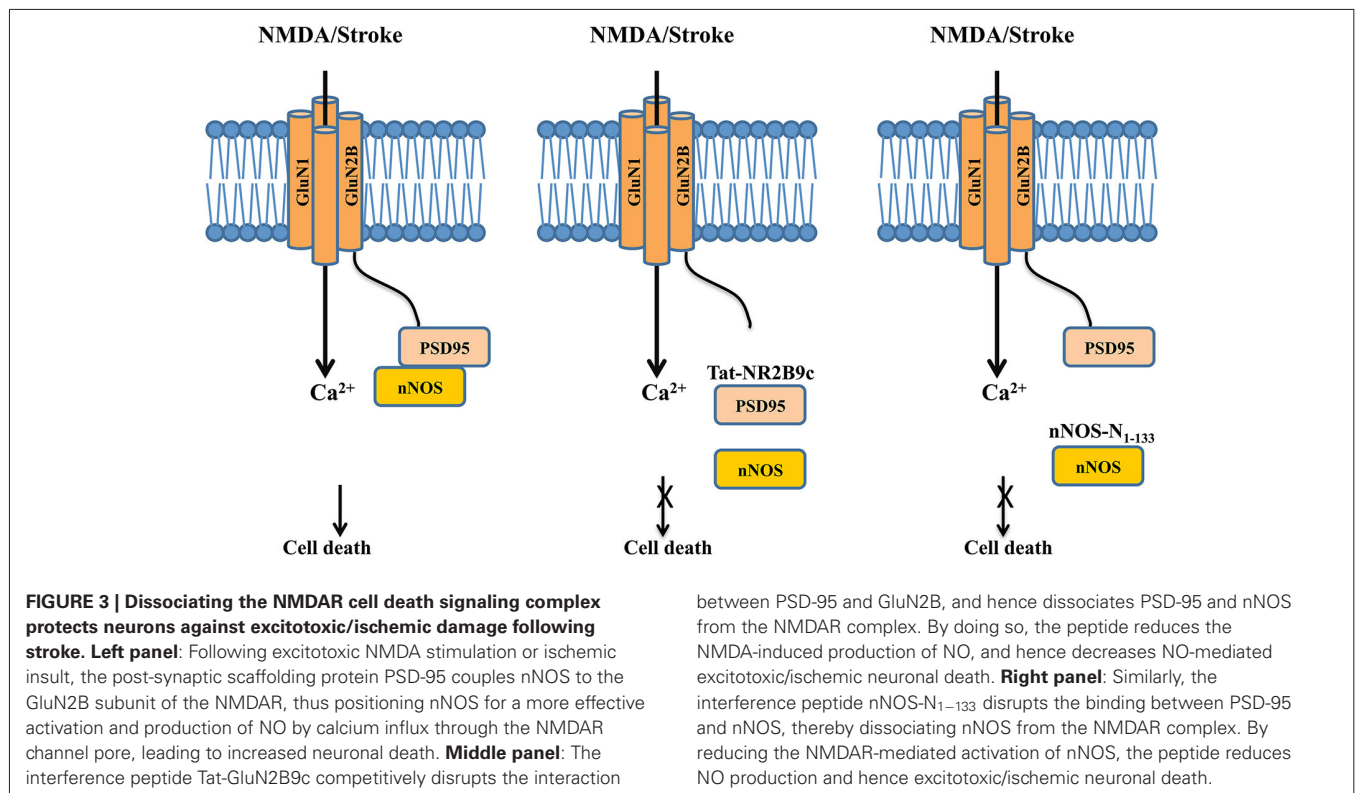
Going forward, it would be particularly interesting to see whether these findings extend to prefrontal dopaminergic neurotransmission. The prefrontal cortex, together with other corticolimbic areas including the cingulate gyrus and hippocampus, are implicated as part of the dysfunctional network that underlies schizophrenia (Fletcher, 1998). Furthermore, NMDAR hypofunction during development is gradually emerging as a convergence point for disease progression in schizophrenia (Snyder and Gao, 2013). Together, these findings, with the observation that the D1R-GluN1 physical interaction reciprocally regulates D1R and NMDAR surface expression and function, prompts the question of whether it is the initial failure in glutamatergic signaling that leads to reduced dopaminergic neurotransmission in schizophrenia through perturbed protein (receptor)-NMDAR interactions in the NMDAR complex.

In summary, NMDARs and dopamine receptors directly interact to reciprocally regulate receptor surface expression, channel properties and downstream intracellular signaling cascades. Together with functional interactions through shared downstream signaling molecules, the physical coupling between NMDARs and dopamine receptors adds another layer of regulation to both neurotransmitter systems to fine-tune neuronal function and behavior.

NMDAR COMPLEX AS A CRUX IN ISCHEMIC NEURONAL DAMAGES

Intensive investigations into the mechanisms and functions of protein-protein interactions in the NMDAR complex have not only further advanced our understanding of the roles of NMDARs in brain function and dysfunction, but also led to the development of novel protein-NMDAR interaction-based therapeutics for treating brain disorders in which NMDAR dysfunction is at the root of their pathogenesis. Well-characterized examples of such therapeutics are the newly developed and promising interventions that protect neurons against excitotoxic/ischemic damages following stroke by disrupting direct or indirect interactions between NMDARs and neuronal death signaling molecules, such as neuronal Nitric Oxide Synthase (nNOS; Aarts et al., 2002; Zhou et al., 2010), death associated protein kinase 1 (DAPK1; Tu et al., 2010; Fan et al., 2014) and PTEN (Zhang et al., 2013).

Overactivation of the NMDAR triggers rapid Ca^{2+} influx that could lead to excitotoxic neuronal death. This excitotoxicity is considered a common pathological step leading to neuronal



loss in many brain disorders, from acute brain injuries such as stroke to chronic neurodegenerative diseases such as Huntington's disease (Lai et al., 2014). Yet direct blockade of NMDARs has failed as a neuroprotective strategy in stroke, at least in part due to intolerable psychosomatic side effects as a result of blocking normal NMDAR function and/or relatively narrow windows for effective intervention (Ikonomidou and Turski, 2002; Lai et al., 2014). In an effort to overcome the shortcomings of NMDAR antagonists, scientists have focused on druggable protein-protein interactions in the NMDAR complex that specifically lead to neuronal death. These have led to not only the identification of several well-characterized cell death-promoting molecules that can form neuronal death signaling complexes downstream of NMDARs via either direct or indirect interactions with NMDAR subunits, but also the development of numerous promising interventions that protect neurons from brain insults by specifically disrupting these interactions (Lai et al., 2014).

One of the most exciting bench-to-bedside examples is the recent development of effective neuroprotectants based on disrupting the GluN2B-Post synaptic density-95 (PSD-95)-nNOS cell death complex (Christopherson, 1999; Sattler et al., 1999), which was first characterized over a decade ago. PSD-95 is a membrane-associated guanylate kinase (MAGUK) concentrated at glutamatergic synapses and is involved in synapse stabilization and plasticity (El-Husseini et al., 2000). nNOS catalyzes the production of nitric oxide (NO), a diffusible signaling molecule implicated in synaptic plasticity (Bredt et al., 1990) and glutamate neurotoxicity (Dawson et al., 1991). By binding to both nNOS and GluN2B through its different PDZ domains, PSD-95 functions as a scaffolding protein to bring nNOS to the NMDAR complex

(Kornau et al., 1995; Brenman et al., 1996). Following excitotoxic stimuli and/or ischemic insults, PSD-95 tethers nNOS to GluN2B, thus positioning nNOS to be more effectively activated by Ca^{2+} influx through the NMDAR channel pore and generation of the cytotoxic compound NO (Figure 3, left panel) (Dawson et al., 1991; Sattler et al., 1999).

In a proof-of-concept study, Aarts et al. (2002) disrupted this signaling complex with a 20-mer interference peptide Tat-NR2B9c, which comprises of the last nine amino acids of the carboxyl tail of GluN2B required for its interaction with PSD-95 and the 11-mer Tat protein transduction domain that renders the peptide plasma membrane permeable. The rationale behind the initial peptide design is to use it to disrupt GluN2B-PSD-95 interaction and hence to prevent PSD-95 from recruiting nNOS to the NMDAR complex, thereby reducing NO production and NO-mediated neuronal death (Figure 3, middle panel), although a later study suggests that the peptide may also somehow reduce the interaction between PSD-95 and nNOS (Cui et al., 2007). When bath applied to primary neuronal cultures and acute brain slices, Tat-NR2B9c does not affect NMDAR-mediated currents or Ca^{2+} fluxes, but can selectively disrupt the interaction between PSD-95 and NMDARs through competition with the binding of native GluN2B subunit (but not GluN2A) to PSD95, and thereby reduce the generation of NO and excitotoxicity (Aarts et al., 2002). When given systematically, a single dose of Tat-NR2B9c administered either before or after ischemic insults reduces ischemic brain damage with concurrent improvements in neurological scores in rats subjected to transient middle cerebral artery occlusion (MCAo), a well-characterized focal ischemia stroke model (Aarts et al., 2002).

Similar neuroprotective effects are seen by disrupting the interaction between PSD-95 and nNOS with an interference peptide derived from the PSD-95 binding domain of nNOS (nNOS-N₁₋₁₃₃; **Figure 3**, right panel; Zhou et al., 2010). Following viral infection of rats with a vector expressing this peptide, nNOS-N₁₋₁₃₃ effectively blocks the interaction between the two proteins and significantly reduces stroke-induced ischemic damage (Zhou et al., 2010).

These initial attempts at targeting GluN2B-PSD-95-nNOS signaling pathway for the treatment of stroke was quickly followed by a well-designed study in a focal ischemia model in gyrencephalic nonhuman primates (Cook et al., 2012a,b) and a successful phase 2, double-blind, placebo-controlled multicenter clinical trial of neuroprotection in procedurally-induced stroke (Hill et al., 2012). Treatment with Tat-NR2B9c (also named as NA-1 in these studies) results in reduced ischemic brain damage compared to the placebo treatment, as evidenced by diffusion weighted magnetic resonance imaging. These exciting bench-to-bedside results provide great promises for further understanding disease-specific protein-protein interactions in the NMDAR complex and thereby developing novel and effective therapeutics for brain diseases involving NMDAR-mediated neuronal degeneration.

CONCLUSIONS

Increasing evidence suggest that the NMDAR is not a solo player in the regulation of many brain functions and dysfunctions. By associating with various membrane receptors and extracellular or intracellular proteins in the complex, the NMDAR can contribute to various physiological processes such as learning and memory, and brain disorders such as stroke, schizophrenia and addiction. Many NMDAR-interacting proteins have recently been identified in the NMDAR complex; however, in the past only a few protein-protein interactions have been characterized in detail. Since NMDARs are widely expressed in all brain areas, it would be paramount to know whether and how the NMDAR plays vital roles in both brain function and dysfunction through these diverse protein-protein interactions in the receptor complex. Further investigation on this topic will not only deepen our understanding of the functions of the NMDAR multiprotein complex, but also greatly facilitate the development of innovative therapeutics in treating various NMDAR dysfunction-related brain disorders.

ACKNOWLEDGMENTS

We thank Dr. Loren Oschepok for his excellent editorial assistance. This work was in part supported by the Canadian Institutes of Health Research (CIHR). Yu Tian Wang is the holder of Heart and Stroke Foundation of British Columbia and Yukon Chair in Stroke Research.

REFERENCES

- Aarts, M., Liu, Y., Liu, L., Besshoh, S., Arundine, M., Gurd, J. W., et al. (2002). Treatment of ischemic brain damage by perturbing NMDA receptor-PSD-95 protein interactions. *Science* 298, 846–850. doi: 10.1126/science.1072873
- Barria, A., Derkach, V., and Soderling, T. (1997). Identification of the Ca²⁺/calmodulin-dependent protein kinase II regulatory phosphorylation site in the alpha-amino-3-hydroxyl-5-methyl-4-isoxazole-propionate-type glutamate receptor. *J. Biol. Chem.* 272, 32727–32730. doi: 10.1074/jbc.272.52.32727
- Bayer, K. U., De Koninck, P., Leonard, A. S., Hell, J. W., and Schulman, H. (2001). Interaction with the NMDA receptor locks CaMKII in an active conformation. *Nature* 411, 801–805. doi: 10.1038/35081080
- Bayer, K. U., LeBel, E., McDonald, G. L., O'Leary, H., Schulman, H., and De Koninck, P. (2006). Transition from reversible to persistent binding of CaMKII to postsynaptic sites and NR2B. *J. Neurosci.* 26, 1164–1174. doi: 10.1523/jneurosci.3116-05.2006
- Barria, A., and Malinow, R. (2005). NMDA receptor subunit composition controls synaptic plasticity by regulating binding to CaMKII. *Neuron* 48, 289–301. doi: 10.1016/j.neuron.2005.08.034
- Beaulieu, J. M., and Gainetdinov, R. R. (2011). The physiology, signaling and pharmacology of dopamine receptors. *Pharmacol. Rev.* 63, 182–217. doi: 10.1124/pr.110.002642
- Bredt, D. S., Hwang, P. M., and Snyder, S. H. (1990). Localization of nitric oxide synthase indicating a neural role for nitric oxide. *Nature* 347, 768–770. doi: 10.1038/347768a0
- Brenman, J. E., Chao, D. S., Gee, S. H., McGee, A. W., Craven, S. E., Santillano, D. R., et al. (1996). Interaction of nitric oxide synthase with the postsynaptic density protein PSD-95 and α 1-syntrophin mediated by PDZ domains. *Cell* 84, 757–767. doi: 10.1016/s0092-8674(00)81053-3
- Buchsbaum, R. J., Connolly, B. A., and Feig, L. A. (2002). Interaction of Rac exchange factors Tiam1 and Ras-GRF1 with a scaffold for the p38 mitogen-activated protein kinase cascade. *Mol. Cell. Biol.* 22, 4073–4085. doi: 10.1128/mcb.22.12.4073-4085.2002
- Chen, H. X., Otmakhov, N., Strack, S., Colbran, R. J., and Lisman, J. E. (2001). Is persistent activity of calcium/calmodulin-dependent kinase required for the maintenance of LTP? *J. Neurophysiol.* 85, 1368–1376.
- Christopherson, K. S. (1999). PSD-95 assembles a ternary complex with the N-Methyl-D-aspartic acid receptor and a bivalent neuronal nitric oxide synthase PDZ domain. *J. Biol. Chem.* 274, 27467–27473. doi: 10.1074/jbc.274.39.27467
- Collingridge, G. L., Isaac, J., and Wang, Y. T. (2004). Receptor trafficking and synaptic plasticity. *Nat. Rev. Neurosci.* 5, 952–962. doi: 10.1038/nrn1556
- Collingridge, G. L., Olsen, R. W., Peters, J., and Spedding, M. (2009). A nomenclature for ligand-gated ion channels. *Neuropharmacology* 56, 2–5. doi: 10.1016/j.neuropharm.2008.06.063
- Collingridge, G. L., Peineau, S., Howland, J. G., and Wang, Y. T. (2010). Long-term depression in the CNS. *Nat. Rev. Neurosci.* 11, 459–473. doi: 10.1038/nrn2867
- Cook, D. J., Teves, L., and Tymianski, M. (2012a). A translational paradigm for the preclinical evaluation of the stroke neuroprotectant tat-NR2B9c in gyrencephalic nonhuman primates. *Sci. Transl. Med.* 4:154ra133. doi: 10.1126/scitranslmed.3003824
- Cook, D. J., Teves, L., and Tymianski, M. (2012b). Treatment of stroke with a PSD-95 inhibitor in the gyrencephalic primate brain. *Nature* 483, 213–217. doi: 10.1038/nature10841
- Coultrap, S. J., Freund, R. K., O'Leary, H., Sanderson, J. L., Roche, K. W., Dell'Acqua, M. L., et al. (2014). Autonomous CaMKII mediates both LTP and LTD using a mechanism for differential substrate site selection. *Cell Rep.* 6, 431–437. doi: 10.1016/j.celrep.2014.01.005
- Cui, H., Hayashi, A., Sun, H. S., Belmares, M. P., Cobey, C., Phan, T., et al. (2007). PDZ protein interactions underlying NMDA receptor-mediated excitotoxicity and neuroprotection by PSD-95 inhibitors. *J. Neurosci.* 27, 9901–9915. doi: 10.1523/jneurosci.1464-07.2007
- Cui, C., Xu, M., and Atzori, M. (2006). Voltage-dependent block of N-Methyl-D-aspartate receptors by dopamine D1 receptor ligands. *Mol. Pharmacol.* 70, 1761–1770. doi: 10.1124/mol.106.028332
- Cull-Candy, S., Brickley, S., and Farrant, M. (2001). NMDA receptor subunits: diversity, development and disease. *Curr. Opin. Neurobiol.* 11, 327–335. doi: 10.1016/s0959-4388(00)00215-4
- Dawson, V. L., Dawson, T. M., London, E. D., Bredt, D. S., and Snyder, S. H. (1991). Nitric oxide mediates glutamate neurotoxicity in primary cortical cultures. *Proc. Natl. Acad. Sci. U S A* 88, 6368–6371. doi: 10.1073/pnas.88.14.6368
- Derkach, V., Barria, A., and Soderling, T. R. (1999). Ca²⁺/calmodulin-kinase II enhances channel conductance of alpha-amino-3-hydroxy-5-methyl-4-isoxazolepropionate type glutamate receptors. *Proc. Natl. Acad. Sci. U S A* 96, 3269–3274. doi: 10.1073/pnas.96.6.3269
- Dolan, R. J., Fletcher, P., Frith, C. D., Friston, K. J., Frackowiak, R. S. J., and Grasby, P. M. (1995). Dopaminergic modulation of impaired cognitive activation in the anterior cingulate cortex in schizophrenia. *Nature* 378, 180–182. doi: 10.1038/378180a0

- El-Husseini, A. E., Schnell, E., Chetkovich, D. M., Nicoll, R. A., and Brecht, D. S. (2000). PSD-95 involvement in maturation of excitatory synapses. *Science* 290, 1364–1368. doi: 10.1126/science.290.5495.1364
- Fan, X., Jin, W. Y., Lu, J., Wang, J., and Wang, Y. T. (2014). Rapid and reversible knockdown of endogenous proteins by peptide-directed lysosomal degradation. *Nat. Neurosci.* 17, 471–480. doi: 10.1038/nn.3637
- Feig, L. A. (2011). Regulation of neuronal function by Ras-GRF exchange factors. *Genes Cancer* 2, 306–319. doi: 10.1177/1947601911408077
- Fiorentini, C., Gardoni, F., Spano, P., Di Luca, M., and Missale, C. (2003). Regulation of dopamine D1 receptor trafficking and desensitization by oligomerization with glutamate N-Methyl-D-aspartate receptors. *J. Biol. Chem.* 278, 20196–20202. doi: 10.1074/jbc.m213140200
- Fletcher, P. (1998). The missing link: a failure of fronto-hippocampal integration in schizophrenia. *Nat. Neurosci.* 1, 266–267. doi: 10.1038/1078
- Foster, K. A., McLaughlin, N., Edbauer, D., Phillips, M., Bolton, A., Constantine-Paton, M., et al. (2010). Distinct roles of NR2A and NR2B cytoplasmic tails in long-term potentiation. *J. Neurosci.* 30, 2676–2685. doi: 10.1523/JNEUROSCI.4022-09.2010
- Frey, U., Huang, Y. Y., and Kandel, E. R. (1993). Effects of cAMP simulate a late stage of LTP in hippocampal CA1 neurons. *Science* 260, 1661–1664. doi: 10.1126/science.8389057
- Giese, K. P., Fedorov, N. B., Filipkowski, R. K., and Silva, A. J. (1998). Autophosphorylation at Thr286 of the alpha calcium-calmodulin kinase II in LTP and learning. *Science* 279, 870–873. doi: 10.1126/science.279.5352.870
- Grant, S. G., and O'Dell, T. J. (2001). Multiprotein complex signaling and the plasticity problem. *Curr. Opin. Neurobiol.* 11, 363–368. doi: 10.1016/s0959-4388(00)00220-8
- Hayashi, Y., Shi, S. H., Esteban, J. A., Piccini, A., Poncer, J. C., and Malinow, R. (2000). Driving AMPA receptors into synapses by LTP and CaMKII: requirement for GluR1 and PDZ domain interaction. *Science* 287, 2262–2267. doi: 10.1126/science.287.5461.2262
- Hersch, S. M., Ciliax, B. J., Gutekunst, C. A., Rees, H. D., Heilman, C. J., Yung, K. K., et al. (1995). Electron microscopic analysis of D1 and D2 dopamine receptor proteins in the dorsal striatum and their synaptic relationships with motor corticostriatal afferents. *J. Neurosci.* 15, 5222–5237.
- Hill, M. D., Martin, R. H., Mikulis, D., Wong, J. H., Silver, F. L., Terbrugge, K. G., et al. (2012). Safety and efficacy of NA-1 in patients with iatrogenic stroke after endovascular aneurysm repair (ENACT): a phase 2, randomised, double-blind, placebo-controlled trial. *Lancet Neurol.* 11, 942–950. doi: 10.1016/s1474-4422(12)70225-9
- Husi, H., Ward, M. A., Choudhary, J. S., Blackstock, W. P., and Grant, S. G. (2000). Proteomic analysis of NMDA receptor-adhesion protein signaling complexes. *Nat. Neurosci.* 3, 661–669. doi: 10.1038/76615
- Ikonomidou, C., and Turski, L. (2002). Why did NMDA receptor antagonists fail clinical trials for stroke and traumatic brain injury? *Lancet Neurol.* 1, 383–386. doi: 10.1016/s1474-4422(02)00164-3
- Jin, S. X., Arai, J., Tian, X., and Kumar-Singh, R. (2013). Acquisition of contextual discrimination involves the appearance of a RAS-GRF1/p38 mitogen-activated protein (MAP) kinase-mediated signaling pathway that promotes long term potentiation (LTP). *J. Biol. Chem.* 30, 21703–21713. doi: 10.1074/jbc.m113.471904
- Jin, S., and Feig, L. A. (2010). Long-term potentiation in the CA1 hippocampus induced by NR2A subunit-containing NMDA glutamate receptors is mediated by Ras-GRF2/Erk map kinase signalling. *PLoS One* 5:e11732. doi: 10.1371/journal.pone.0011732
- Kebabian, J. W., Petzold, G. L., and Greengard, P. (1972). Dopamine-sensitive adenylate cyclase in caudate nucleus of rat brain and its similarity to the "dopamine receptor". *Proc. Natl. Acad. Sci. U S A* 69, 2145–2149. doi: 10.1073/pnas.69.8.2145
- Kessels, H. W., Kopec, C. D., Klein, M. E., and Malinow, R. (2009). Roles of stargazin and phosphorylation in the control of AMPA receptor subcellular distribution. *Nat. Neurosci.* 12, 888–896. doi: 10.1038/nn.2340
- Kim, M. J., Dunah, A. W., Wang, Y. T., and Sheng, M. (2005). Differential roles of NR2A- and NR2B-containing NMDA receptors in Ras-ERK signaling and AMPA receptor trafficking. *Neuron* 46, 745–760. doi: 10.1016/j.neuron.2005.04.031
- Köhr, G., Jensen, V., Koester, H. J., Mihaljevic, A. L. A., Utvik, J. K., Kvello, A., et al. (2003). Intracellular domains of NMDA receptor subtypes are determinants for long-term potentiation induction. *J. Neurosci.* 23, 10791–10799.
- Kornau, H. C., Schenker, L. T., Kennedy, M. B., and Seeburg, P. H. (1995). Domain interaction between NMDA receptor subunits and the postsynaptic density protein PSD-95. *Science* 269, 1737–1740. doi: 10.1126/science.7569905
- Krapivinsky, G., Krapivinsky, L., Manasian, Y., Ivanov, A., Tyzio, R., Pellegrino, C., et al. (2003). The NMDA receptor is coupled to the ERK pathway by a direct interaction between NR2B and RasGRF1. *Neuron* 40, 775–784. doi: 10.1016/s0896-6273(03)00645-7
- Kristensen, A. S., Jenkins, M. A., Banke, T. G., Schousboe, A., Makino, Y., Johnson, R. C., et al. (2011). Mechanism of Ca²⁺/calmodulin-dependent kinase II regulation of AMPA receptor gating. *Nat. Neurosci.* 14, 727–735. doi: 10.1038/nn.2804
- Ladepeche, L., Dupuis, J. P., Bouchet, D., Doudnikoff, E., Yang, L., Campagne, Y., et al. (2013). Single-molecule imaging of the functional crosstalk between surface NMDA and dopamine D1 receptors. *Proc. Natl. Acad. Sci. U S A* 110, 18005–18010. doi: 10.1073/pnas.1310145110
- Lai, T. W., Shyu, W.-C., and Wang, Y. T. (2011). Stroke intervention pathways: NMDA receptors and beyond. *Trends Mol. Med.* 17, 266–275. doi: 10.1016/j.molmed.2010.12.008
- Lai, T. W., Zhang, S., and Wang, Y. T. (2014). Excitotoxicity and stroke: identifying novel targets for neuroprotection. *Prog. Neurobiol.* 115, 157–188. doi: 10.1016/j.pneurobio.2013.11.006
- Lee, F. J. S., Xue, S., Pei, L., Vukusic, B., Chéry, N., Wang, Y., et al. (2002). Dual regulation of NMDA receptor functions by direct protein-protein interactions with the dopamine D1 receptor. *Cell* 111, 219–230. doi: 10.1016/s0092-8674(02)00962-5
- Lee, S.-J. R., Escobedo-Lozoya, Y., Szatmari, E. M., and Yasuda, R. (2009). Activation of CaMKII in single dendritic spines during long-term potentiation. *Nature* 458, 299–304. doi: 10.1038/nature07842
- Leonard, A. S., Lim, I. A., and Hemsworth, D. E. (1999). Calcium/calmodulin-dependent protein kinase II is associated with the N-methyl-D-aspartate receptor. *Proc. Natl. Acad. Sci. U S A* 96, 3239–3244. doi: 10.1073/pnas.96.6.3239
- Levey, A. I., Hersch, S. M., Rye, D. B., Sunahara, R. K., Niznik, H. B., Kitt, C. A., et al. (1993). Localization of D1 and D2 dopamine receptors in brain with subtype-specific antibodies. *Proc. Natl. Acad. Sci. U S A* 90, 8861–8865. doi: 10.1073/pnas.90.19.8861
- Li, S., Tian, X., Hartley, D. M., and Feig, L. A. (2006). Distinct roles for Ras-guanine nucleotide-releasing factor 1 (Ras-GRF1) and Ras-GRF2 in the induction of long-term potentiation and long-term depression. *J. Neurosci.* 26, 1721–1729. doi: 10.1523/jneurosci.3990-05.2006
- Lindgren, N., Usiello, A., Gojny, M., Haycock, J., Erbs, E., Greengard, P., et al. (2003). Distinct roles of dopamine D2L and D2S receptor isoforms in the regulation of protein phosphorylation at presynaptic and postsynaptic sites. *Proc. Natl. Acad. Sci. U S A* 100, 4305–4309. doi: 10.1073/pnas.0730708100
- Lisman, J., Yasuda, R., and Raghavachari, S. (2012). Mechanisms of CaMKII action in long-term potentiation. *Nat. Rev. Neurosci.* 13, 169–182. doi: 10.1038/nrn3192
- Liu, L., Wong, T. P., Pozza, M. F., Lingenhoehl, K., Wang, Y., Sheng, M., et al. (2004). Role of NMDA receptor subtypes in governing the direction of hippocampal synaptic plasticity. *Science* 304, 1021–1024. doi: 10.1126/science.1096615
- Liu, X.-Y., Chu, X.-P., Mao, L.-M., Wang, M., Lan, H.-X., Li, M.-H., et al. (2006). Modulation of D2R-NR2B interactions in response to cocaine. *Neuron* 52, 897–909. doi: 10.1016/j.neuron.2006.10.011
- Martin, K. P., and Wellman, C. L. (2011). NMDA receptor blockade alters stress-induced dendritic remodeling in medial prefrontal cortex. *Cereb. Cortex* 21, 2366–2373. doi: 10.1093/cercor/bhr021
- Massey, P. V., Johnson, B. E., Moul, P. R., Auberson, Y. P., Brown, M. W., Molnar, E., et al. (2004). Differential roles of NR2A and NR2B-containing NMDA receptors in cortical long-term potentiation and long-term depression. *J. Neurosci.* 24, 7821–7828. doi: 10.1523/jneurosci.1697-04.2004
- Monsma, F. J., Mahan, L. C., McVittie, L. D., Gerfen, C. R., and Sibley, D. R. (1990). Molecular cloning and expression of a D1 dopamine receptor linked to adenyl cyclase activation. *Proc. Natl. Acad. Sci. U S A* 87, 6723–6727. doi: 10.1073/pnas.87.17.6723
- Nai, Q., Li, S., Wang, S. H., Liu, J., Lee, F. J. S., Frankland, P. W., et al. (2010). Uncoupling the D1-N-Methyl-D-aspartate (NMDA) receptor complex promotes NMDA-dependent long-term potentiation and working memory. *Biol. Psychiatry* 67, 246–254. doi: 10.1016/j.biopsych.2009.08.011

- Naisbitt, S., Kim, E., Tu, J. C., Xiao, B., Sala, C., Valtschanoff, J., et al. (1999). Shank, a novel family of postsynaptic density proteins that binds to the NMDA receptor/PSD-95/GKAP complex and cortactin. *Neuron* 23, 569–582. doi: 10.1016/s0896-6273(00)80809-0
- Nong, Y., Huang, Y.-Q., Ju, W., Kalia, L. V., Ahmadian, G., Wang, Y. T., et al. (2003). Glycine binding primes NMDA receptor internalization. *Nature* 422, 302–307. doi: 10.1038/nature01497
- Opazo, P., Labrecque, S., Tigaret, C. M., Frouin, A., Wiseman, P. W., De Koninck, P., et al. (2010). CaMKII triggers the diffusional trapping of surface AMPARs through phosphorylation of stargazin. *Neuron* 67, 239–252. doi: 10.1016/j.neuron.2010.06.007
- Otmakhov, N., Tao-Cheng, J.-H., Carpenter, S., Asrican, B., Dosemeci, A., Reese, T. S., et al. (2004). Persistent accumulation of calcium/calmodulin-dependent protein kinase II in dendritic spines after induction of NMDA receptor-dependent chemical long-term potentiation. *J. Neurosci.* 24, 9324–9331. doi: 10.1523/jneurosci.2350-04.2004
- Papouin, T., Ladépêche, L., Ruel, J., Sacchi, S., Labasque, M., Hanini, M., et al. (2012). Synaptic and extrasynaptic NMDA receptors are gated by different endogenous coagonists. *Cell* 150, 633–646. doi: 10.1016/j.cell.2012.06.029
- Pei, L., Lee, F. J., Moszczynska, A., Vukusic, B., and Liu, F. (2004). Regulation of dopamine D1 receptor function by physical interaction with the NMDA receptors. *J. Neurosci.* 24, 1149–1158. doi: 10.1523/jneurosci.3922-03.2004
- Pi, H. J., Otmakhov, N., and Lemelin, D. (2010). Autonomous CaMKII can promote either long-term potentiation or long-term depression, depending on the state of T305/T306 phosphorylation. *J. Neurosci.* 30, 8704–8709. doi: 10.1523/jneurosci.0133-10.2010
- Ramsey, A. J., Laakso, A., Cyr, M., Sotnikova, T. D., Salahpour, A., Medvedev, I. O., et al. (2008). Genetic NMDA receptor deficiency disrupts acute and chronic effects of cocaine but not amphetamine. *Neuropsychopharmacology* 33, 2701–2714. doi: 10.1038/sj.npp.1301663
- Rellos, P., Pike, A. C., Niesen, F. H., Salah, E., Lee, W. H., von Delft, F., et al. (2010). Structure of the CaMKII δ /calmodulin complex reveals the molecular mechanism of CaMKII kinase activation. *PLoS Biol.* 8:e1000426. doi: 10.1371/journal.pbio.1000426
- Sattler, R., Xiong, Z., Lu, W. Y., Hafner, M., MacDonald, J. F., and Tymianski, M. (1999). Specific coupling of NMDA receptor activation to nitric oxide neurotoxicity by PSD-95 protein. *Science* 284, 1845–1848. doi: 10.1126/science.284.5421.1845
- Schilström, B., Yaka, R., Argilli, E., Suvarna, N., Schumann, J., Chen, B. T., et al. (2006). Cocaine enhances NMDA receptor-mediated currents in ventral tegmental area cells via dopamine D5 receptor-dependent redistribution of NMDA receptors. *J. Neurosci.* 26, 8549–8558. doi: 10.1523/jneurosci.5179-05.2006
- Schnell, E., Sizemore, M., Karimzadegan, S., Chen, L., Brecht, D. S., and Nicoll, R. A. (2002). Direct interactions between PSD-95 and stargazin control synaptic AMPA receptor number. *Proc. Natl. Acad. Sci. U S A* 99, 13902–13907. doi: 10.1073/pnas.172511199
- Scott, L., Zelenin, S., Malmersjö, S., Kowalewski, J. M., Markus, E. Z., Nairn, A. C., et al. (2006). Allosteric changes of the NMDA receptor trap diffusible dopamine 1 receptors in spines. *Proc. Natl. Acad. Sci. U S A* 103, 762–767. doi: 10.1073/pnas.0505557103
- Seeman, P. (1987). Dopamine receptors and the dopamine hypothesis of schizophrenia. *Synapse* 1, 133–152. doi: 10.1002/syn.890010203
- Snyder, M. A., and Gao, W. J. (2013). NMDA hypofunction as a convergence point for progression and symptoms of schizophrenia. *Front. Cell. Neurosci.* 27:31. doi: 10.3389/fncel.2013.00031
- Sokoloff, P., Diaz, J., Le Foll, B., Guillin, O., Leriche, L., Bezaud, E., et al. (2006). The dopamine D3 receptor: a therapeutic target for the treatment of neuropsychiatric disorders. *CNS Neurol. Disord. Drug Targets* 5, 25–43. doi: 10.2174/187152706784111551
- Strack, S., and Colbran, R. J. (1998). Autophosphorylation-dependent targeting of calcium/calmodulin-dependent protein kinase II by the NR2B subunit of the N-methyl-D-aspartate receptor. *J. Biol. Chem.* 273, 20689–20692. doi: 10.1074/jbc.273.33.20689
- Stramiello, M., and Wagner, J. J. (2008). D1/5 receptor-mediated enhancement of LTP requires PKA, Src family kinases and NR2B-containing NMDARs. *Neuropharmacology* 55, 871–877. doi: 10.1016/j.neuropharm.2008.06.053
- Tian, X., Gotoh, T., Tsuji, K., Lo, E. H., Huang, S., and Feig, L. A. (2004). Developmentally regulated role for Ras-GRFs in coupling NMDA glutamate receptors to Ras, Erk and CREB. *EMBO J.* 23, 1567–1575. doi: 10.1038/sj.emboj.7600151
- Tiberi, M., Jarvie, K. R., Silvia, C., Falardeau, P., Gingrich, J. A., Godinot, N., et al. (1991). Cloning, molecular characterization and chromosomal assignment of a gene encoding a second D1 dopamine receptor subtype: differential expression pattern in rat brain compared with the D1A receptor. *Proc. Natl. Acad. Sci. U S A* 88, 7491–7495. doi: 10.1073/pnas.88.17.7491
- Tomita, S., Stein, V., Stocker, T. J., Nicoll, R. A., and Brecht, D. S. (2005). Bidirectional synaptic plasticity regulated by phosphorylation of stargazin-like TARPs. *Neuron* 45, 269–277. doi: 10.1016/j.neuron.2005.01.009
- Traynelis, S. F., Wollmuth, L. P., McBain, C. J., Menniti, F. S., Vance, K. M., Ogden, K. K., et al. (2010). Glutamate receptor ion channels: structure, regulation and function. *Pharmacol. Rev.* 62, 405–496. doi: 10.1124/pr.109.002451
- Tsui, J., and Malenka, R. C. (2006). Substrate localization creates specificity in calcium/calmodulin-dependent protein kinase II signaling at synapses. *J. Biol. Chem.* 281, 13794–13804. doi: 10.1074/jbc.m600966200
- Tu, W., Xu, X., Peng, L., Zhong, X., Zhang, W., Soundarapandian, M. M., et al. (2010). DAPK1 interaction with NMDA receptor NR2B subunits mediates brain damage in stroke. *Cell* 140, 222–234. doi: 10.1016/j.cell.2009.12.055
- Ulbrich, M. H., and Isacoff, E. Y. (2008). Rules of engagement for NMDA receptor subunits. *Proc. Natl. Acad. Sci. U S A* 105, 14163–14168. doi: 10.1073/pnas.0802075105
- Vargas-Caballero, M., and Robinson, H. P. C. (2004). Fast and slow voltage-dependent dynamics of magnesium block in the NMDA receptor: the asymmetric trapping block model. *J. Neurosci.* 24, 6171–6180. doi: 10.1523/jneurosci.1380-04.2004
- Woo, N. H., Teng, H. K., Siao, C.-J., Chiaruttini, C., Pang, P. T., Milner, T. A., et al. (2005). Activation of p75NTR by proBDNF facilitates hippocampal long-term depression. *Nat. Neurosci.* 8, 1069–1077. doi: 10.1038/nn1510
- Xu, T.-X., and Yao, W.-D. (2010). D1 and D2 dopamine receptors in separate circuits cooperate to drive associative long-term potentiation in the prefrontal cortex. *Proc. Natl. Acad. Sci. U S A* 107, 16366–16371. doi: 10.1073/pnas.1004108107
- Yung, K. K., Bolam, J. P., Smith, A. D., Hersch, S. M., Ciliax, B. J., and Levey, A. I. (1995). Immunocytochemical localization of D1 and D2 dopamine receptors in the basal ganglia of the rat: light and electron microscopy. *NSC* 65, 709–730. doi: 10.1016/0306-4522(94)00536-e
- Zhang, Y. P., Holbro, N., and Oertner, T. G. (2008). Optical induction of plasticity at single synapses reveals input-specific accumulation of α CaMKII. *Proc. Natl. Acad. Sci. U S A* 105, 12039–12044. doi: 10.1073/pnas.0802940105
- Zhang, S., Taghibiglou, C., Girling, K., Dong, Z., Lin, S. Z., Lee, W., et al. (2013). Critical role of increased PTEN nuclear translocation in excitotoxic and ischemic neuronal injuries. *J. Neurosci.* 33, 7997–8008. doi: 10.1523/jneurosci.5661-12.2013
- Zhou, L., Li, F., Xu, H.-B., Luo, C.-X., Wu, H.-Y., Zhu, M.-M., et al. (2010). Treatment of cerebral ischemia by disrupting ischemia-induced interaction of nNOS with PSD-95. *Nat. Med.* 16, 1439–1443. doi: 10.1038/nm.2245
- Zhou, Y., Takahashi, E., Li, W., Halt, A., Wiltgen, B., Ehninger, D., et al. (2007). Interactions between the NR2B receptor and CaMKII modulate synaptic plasticity and spatial learning. *J. Neurosci.* 27, 13843–13853. doi: 10.1523/jneurosci.4486-07.2007

Conflict of Interest Statement: The authors declare that the research was conducted in the absence of any commercial or financial relationships that could be construed as a potential conflict of interest.

Received: 13 April 2014; accepted: 26 May 2014; published online: 10 June 2014.

Citation: Fan X, Jin WY and Wang YT (2014) The NMDA receptor complex: a multifunctional machine at the glutamatergic synapse. *Front. Cell. Neurosci.* 8:160. doi: 10.3389/fncel.2014.00160

This article was submitted to the journal *Frontiers in Cellular Neuroscience*.

Copyright © 2014 Fan, Jin and Wang. This is an open-access article distributed under the terms of the Creative Commons Attribution License (CC BY). The use, distribution or reproduction in other forums is permitted, provided the original author(s) or licensor are credited and that the original publication in this journal is cited, in accordance with accepted academic practice. No use, distribution or reproduction is permitted which does not comply with these terms.



Ligand-gated ion channel interacting proteins and their role in neuroprotection

Shupeng Li, Albert H. C. Wong and Fang Liu*

Campbell Family Mental Health Research Institute, Centre for Addiction and Mental Health, University of Toronto, Toronto, ON, Canada

Edited by:

Gerald Zamponi, University of
Calgary, Canada

Reviewed by:

Laurent Fagni, University of
Montpellier, France
Stephen Ferguson, Western,
Canada

*Correspondence:

Fang Liu, Centre for Addiction and
Mental Health, 250 College Street,
Toronto, ON M5T 1R8, Canada
e-mail: fang.liu@camh.ca

Ion channel receptors are a vital component of nervous system signaling, allowing rapid and direct conversion of a chemical neurotransmitter message to an electrical current. In recent decades, it has become apparent that ionotropic receptors are regulated by protein-protein interactions with other ion channels, G-protein coupled receptors and intracellular proteins. These other proteins can also be modulated by these interactions with ion channel receptors. This bidirectional functional cross-talk is important for critical cellular functions such as excitotoxicity in pathological and disease states like stroke, and for the basic dynamics of activity-dependent synaptic plasticity. Protein interactions with ion channel receptors can therefore increase the computational capacity of neuronal signaling cascades and also represent a novel target for therapeutic intervention in neuropsychiatric disease. This review will highlight some examples of ion channel receptor interactions and their potential clinical utility for neuroprotection.

Keywords: ligand-gated ion channels, protein-protein interaction, receptor complex, glutamate receptors, dopamine receptors

Efficient neurotransmission requires the precise interplay of various neurotransmitter receptors at pre- and post-synaptic compartments. Ligand-gated ion channels play a central role in intercellular communication in the nervous system. Ion channels are the cellular machinery for ion flux across the membrane and therefore the basis of electrical excitation of neurons. Ligand-gated ion channels are oligomeric protein assemblies that convert a chemical signal into an ion flux through the post-synaptic membrane, and are involved in basic brain functions such as attention, learning, and memory (Ashcroft, 2006). This paper will review some interactions between ionotropic receptors and other proteins that affect signaling, metabolism, and trafficking. We will detail some of the interactions between G-protein coupled receptors and ion channels, ion channels with intracellular proteins, and ion channels with other ion channels. Specifically, we will discuss how these receptor-protein interactions may help to understand pathology of the nervous system, and offer the hope of new treatment targets for neuropsychiatric disease.

Most eukaryotic membrane channels are composed of several subunits. Pentameric ligand-gated ion channels have five subunits arranged in a pseudosymmetric rosette around the centrally located ion channel pore. Each subunit consists of an extracellular domain that contains the ligand-binding site and a transmembrane ion-pore domain (Kozuska and Paulsen, 2012). The agonist binding site is located at the boundary between subunits in the extracellular domain whereas the ion pore is formed by the transmembrane helices M2, which differentiate axial cationic and anionic channels (Dacosta and Baenziger, 2013).

The modular construction of ionotropic receptors increases the diversity of ligand binding and ion selectivity through the mixing and matching of various subunits (Rojas and Dingledine, 2013). Various other proteins are involved in controlling the type and position of particular subunits in a given channel, as

well as the function of the assembled channel. Thus, the function of many receptor proteins can only be fully understood in the context of their interactions with other proteins, the “interactome” (Li et al., 2013a). Through this extensive protein network, the binding of agonist to an ionotropic receptor can exert effects beyond simple current flow, including gene transcription, cytoskeletal rearrangement, and protein synthesis, degradation and transport.

The ligand-gated ion channel superfamily includes nicotinic acetylcholine receptors (nAChRs), adenosine triphosphate (ATP) receptors, γ -aminobutyric acid (GABA), glutamate, glycine, and 5-hydroxytryptamine (5-HT) receptors (Dent, 2010). The “Cys-loop” sub-family includes the ionotropic receptors for nicotine, GABA, glycine, and 5-HT. “Pore-loop” channels include inwardly-rectifying potassium channels and the glutamate receptors of the AMPA (α -amino-3-hydroxy-5-methyl-4-isoxazolepropionic acid) subtype and NMDA (N-methyl-D-aspartate) receptors (Connolly and Wafford, 2004). The structure and basic features of several important ion channel types is briefly reviewed below to provide some background, before discussing ion channel interactions with other proteins.

AMPA receptors are the major mediator of fast excitatory synaptic transmission in the mammalian central nervous system. Most of these ionotropic glutamate receptors are permeable to calcium and other cations, thus facilitating depolarization of the cell membrane. AMPA receptors contain four subunits, consisting of two dimers formed by combinations of four pore-forming subunits GluA 1–4. GluA 1/2, and GluA 2/3 are the predominant AMPA receptor types (Anggono and Huganir, 2012). Each subunit is an integral membrane protein with an extracellular amino terminal domain, three membrane-spanning domains (M1, M3, and M4), a hydrophobic hairpin domain (M2) that forms the channel pore, and three intracellular domains: Loop1, Loop2, and

the carboxyl tail. Although the carboxyl tail is crucial for receptor trafficking and function, other intracellular domains also play an important role in the regulation of AMPA receptor trafficking (Rojas and Dingledine, 2013). The pore lining domain also influences the AMPA receptor trafficking, early in the secretory pathway.

NMDA receptors are also ionotropic glutamate receptors permeable to calcium and sodium, and are critical for synaptic plasticity, learning, and memory. These receptors are involved in nicotine addiction and neurological disorders such as ischemic stroke (Dingledine et al., 1999; Albensi, 2007). NMDA channel opening is gated by several elements, including the binding of glutamate to the NR2 subunit, a co-ligand glycine which binds to a separate site on the NR1 subunit, and the removal of a magnesium ion block by depolarization. Thus NMDA channels require both agonist stimulation and depolarization of the post-synaptic membrane for current flow, effectively detecting coincident pre- and post-synaptic activation. Like AMPA receptors, NMDA receptors consist of four subunits, two of which are obligatory GluN1 and two which are modulatory GluN2. These subunits are present in various isoforms that in the NR1 subunit are generated by alternative splicing of the *GRIN1* gene. The GluN2 subunits are each encoded by different genes and the subunits are named: NR2A, B, C, and D (Durand et al., 1992; Sugihara et al., 1992; Hollmann et al., 1993; Michaelis, 1998). The exact subunit composition of native NMDARs remains unknown, but it has been suggested that native NMDARs in rat hippocampus largely contain NR1/2A subunits. The intracellular C-terminal (Allison et al., 1998) contains potential sites of protein phosphorylation by different kinases, and motifs for interacting with various protein partners.

For pentameric ligand-gated ion channels such as the GABA_A receptor, each subunit contains an extensive N-terminal extracellular domain and a short extracellular C-terminal sequence containing the ligand binding sites. Structurally, each receptor is composed of four closely-spaced transmembrane domains including the ion channel wall primarily in M2, and a variable length cytoplasmic loop between M3 and M4. With both the N-terminus and C-terminus of receptor subunits extending outside the cell membrane, the intracellular M3-M4 loop becomes the most important domain interacting with the intracellular environment. The M3-M4 intracellular loop (IL2) contains protein-protein interaction domains involved in regulating synaptic localization and intracellular trafficking (Maksay, 2009). Despite being highly variable in length and amino acid sequence, the IL2 loop usually contains numerous regulatory motifs and binding sites that differ in each subunit isoform. Moreover, this IL2 loop usually contains sites for phosphorylation, palmitoylation, ubiquitination and other modifications that modulate protein interactions and eventually determine the clustering, stability, and function of ligand-gated ion channels.

Within the central nervous system (CNS), nicotine acts on nicotinic receptors (nAChRs) to initiate various physiological and pathological processes at the cellular and circuit level. Similar to the NMDAR, nAChR is also a ligand-gated ion channel receptor with high Ca²⁺ permeability. The pentameric nAChR has a number of different subtypes, each with individual pharmacological

and physiological profiles and a distinct anatomical distribution in the brain (Gotti et al., 2009). There are 11 neuronal nAChR subunits identified in mammals, including eight α ($\alpha 2$ – $\alpha 9$) and three β ($\beta 2$ – $\beta 4$). Unlike NMDAR, nAChR can exist as both hetero-metric and homo-metric-assemblies of these subunits (Albuquerque et al., 2009). In rodents, the $\beta 2$ subunit is found throughout the CNS, mostly as part of the $\alpha 4\beta 2$ heteromeric receptor, which exhibits high affinity for nicotine. The second common AChR isoform is the $\alpha 7$ homopentamer, expressed mainly in the cortex, hippocampus, and limbic areas.

Numerous proteins are known to bind to the different subunits of pentameric ligand-gated ion channel receptors at specific subcellular localizations. These interacting proteins can both modulate ion channel function and influence the localization of the channel in the cell and in the membrane. There are several major categories of proteins that ligand-gated ion channels interact with: G-protein coupled receptors, intracellular proteins, and other ligand-gated ion channels (Kittler and Moss, 2003; Li et al., 2012; Rojas and Dingledine, 2013). We will discuss each of these types of interaction with examples drawn from our previous work.

LIGAND-GATED ION CHANNEL INTERACTIONS WITH G-PROTEIN COUPLED RECEPTORS

There are several ion channel interactions with G-protein coupled receptors reported by our group, all involving dopamine receptors: D5-GABA_A (Liu et al., 2000), D1-NMDA (Lee et al., 2002; Pei et al., 2004), and D2-AMPA (Zou et al., 2005).

First discovered in 2000, the interaction between γ -aminobutyric acid A receptors and the dopamine D5 receptor was one of the earliest examples of interactions between metabotropic and ionotropic receptors (Liu et al., 2000). The GABA_A receptor is the major inhibitory neurotransmitter receptor that conducts chloride ions, resulting in hyperpolarization of the cell membrane and thus inhibiting neuron depolarization. The second intracellular loop of the GABA_A $\gamma 2$ (short) receptor subunit binds directly to the carboxy-terminus of the D5 receptors. This interaction reduces D5 receptor-mediated cAMP accumulation without altering affinity of the D5 for endogenous and experimental ligands. Conversely, activation of D5 receptors reduces GABA_A currents and this is not dependent on PKC or PKA. Because these two receptors co-localize in hippocampal and cortical neurons, the bi-directional modulation is potentially important for a number of behaviors and brain disorders. A notable feature of this reciprocal modulation is that it is independent of the classical signaling pathways for each individual receptor.

The interaction between the D1 and NMDA receptor involves direct binding between the carboxy termini of the D1 receptor and the NR1-1a and NR2A subunits of the NMDA receptor (Lee et al., 2002). Because there are two interacting components in the NMDA receptor, the functional consequences are more complicated than with the D5-GABA_A interaction. Although the D1-NMDA interaction occurs in the absence of D1 receptor agonist stimulation, the D1 agonist SKF 81297 decreases the amount of D1-NMDA complex. However, the agonist affects only D1-NR1-1a binding, not the D1-NR2A interaction.

Similar to the D5-GABA_A interaction, D1 agonist stimulation reduces NMDA currents as well as reducing the slope of the current-voltage curve without altering the reversal potential. This decrease in NMDA conductance is accompanied by a reduction in NMDA cell surface expression. It is independent of PKA/PKC pathways and is mediated by the D1 interaction with the NR2A subunit. The D1-NR1-1a interaction mediates neuroprotective effects of D1 receptor activation, and these effects are not dependent on G-protein signaling but rather are dependent on a PI-3-kinase mechanism. The proposed model is that agonist activation of D1 receptors promotes dissociation of the D1-NR1-1a interaction, allowing the NR1-1a carboxy tail to bind CaM and PI-3 kinase, thereby initiating protective cellular cascades. Conversely, the D1 receptor is also regulated by NMDA receptor activation, which increases cell surface D1 receptor expression, and enhances cAMP accumulation in a SNARE-dependent fashion (Pei et al., 2004).

Dopamine D1 receptors also have a direct physical interaction with N-type calcium channels (Kisilevsky et al., 2008). In prefrontal cortex neurons dopamine D1 receptor activation reduced calcium influx through voltage-gated calcium channels, likely through both voltage-dependent G-protein-mediated pathways and through PKA-mediated pathways. The D1-Cav2.2 channel interaction also regulates cell surface expression and distribution of the channel, allowing effective dopaminergic regulation of backpropagating action potentials that are mediated by N-type calcium channels.

LIGAND-GATED ION CHANNEL INTERACTIONS WITH INTRACELLULAR PROTEINS

The second category of ion channel interactions to be considered is with intracellular proteins. For the GABA_A receptor, multiple interacting proteins have been characterized, that play a role in cytoskeletal coupling by gephyrin, radixin, and F-actin and in signaling modulation by RAFT1 and collybistin (Chen and Olsen, 2007). The functional characteristics of this modulation are related to their subcellular localization with receptors. For example, GABARAP, GODZ, and Plic1 interact with the intracellular parts of the GABA_A receptor, while GRIP1 and gephyrin are localized to sub-membrane and intracellular compartments.

Our group has recently reported an interaction between the N-terminus of the GluR2 sub-unit of the AMPA receptor and glyceraldehyde-3-phosphate dehydrogenase (GAPDH) (Wang et al., 2012; Zhai et al., 2013). GAPDH is a metabolic enzyme that participates in glycolysis and also plays a role in apoptosis (Tarze et al., 2007). AMPA receptor activation by agonist increases formation of the GluR2-GAPDH complex and promotes cellular internalization. Blocking this interaction with a peptide protects cells against glutamatergic excitotoxicity and ischemia-induced neuronal damage. This interaction is therefore of potential clinical interest for the treatment of ischemic stroke or other conditions with neuronal damage.

Another ion channel-protein interaction that has been of interest because of neuroprotective effects is between the PDZ domain of post-synaptic density 95 (PSD95) protein and carboxyl terminus of the NMDA NR2 subunit (Kornau et al., 1995; Niethammer

et al., 1996; Cui et al., 2007). This interaction couples NMDA receptor activation to nitric oxide neurotoxicity (Sattler et al., 1999), and disrupting this interaction can protect neurons from excitotoxicity and ischemic brain damage both *in vitro* and *in vivo* (Aarts et al., 2002). PSD-95 also interacts with and suppresses the tyrosine kinase Src and attenuates Src-mediated NMDA receptor upregulation (Kalia et al., 2006). Consistent with these findings, inhibitors of PSD-95 also show neuroprotective effects in animal models of stroke (Sun et al., 2008).

While several examples of direct interactions between ion channels and G-protein coupled receptors have been discussed above, these two types of receptors can also exert functional crosstalk through indirect interactions. For example, the presynaptic voltage-gated calcium channels that influence neurotransmitter release are regulated by G-protein activation and protein kinase C-dependent phosphorylation through binding to Gβγ (Zamponi et al., 1997). G-protein modulation of N-type calcium channels also involves syntaxin 1A, a member of the SNARE protein complex responsible for synaptic vesicle fusion during neurotransmitter release (Jarvis et al., 2000). An additional modulator is cysteine string protein or CSP, which also bind to N-type calcium channels in conjunction with G-proteins to exert a tonic inhibition of the channel (Maggia et al., 2000). In the case of G-protein activation in inwardly-rectifying potassium channels (GIRK), the Gβγ directly gates ion channel opening by binding to the intracellular pore of the channel (Nishida and MacKinnon, 2002).

LIGAND-GATED ION CHANNEL INTERACTIONS WITH OTHER ION CHANNELS

Ion channel receptors can also interact with other ion channels, such as the interaction between the α7 nicotinic acetylcholine receptors and NMDA receptors (α7nAChR-NMDA) (Li et al., 2012, 2013b). The carboxy tail of the NMDA receptor NR2 subunit binds directly with the second intracellular loop of the α7nACh receptor, and the interaction promotes ERK1/2 phosphorylation. This interaction is of clinical interest since nicotine increases formation of the complex, and disrupting the α7nAChR-NMDA interaction blocks cue-induced reinstatement of nicotine self-administration in the rat. This behavioral test is a model of relapse in nicotine addiction, suggesting that the α7nAChR-NMDA interaction could be a useful target for novel smoking cessation therapies.

TARGETING LIGAND-GATED ION CHANNEL INTERACTIONS FOR NEUROPROTECTION

Because of the involvement of ion channel receptors in neuronal death from excitatory glutamate stimulation, there has been considerable interest in these receptors as therapeutic targets for the treatment of brain disorders involving neuronal death, such as ischemic stroke. Ischemic stroke is a major medical problem that affects millions of people world-wide. Current acute post-stroke treatment is focused on lysing the clot obstructing arterial blood flow by using a tissue plasminogen-activator. Due to a very short time window for effectiveness and the potential for intracranial bleeding, few patients can benefit from this treatment (Grossman and Broderick, 2013). Therefore, there is a major need for new

and safer drugs that can reduce the extent of brain injury from ischemic stroke.

An alternative strategy for post-stroke treatment is to target neurotoxicity instead of focusing on the blood vessel blockade, or in addition to clot lysis. However, preventing excitotoxicity is difficult because glutamate receptors have a critical role in many brain functions. AMPA/kainate receptor antagonists such as NBQX or MPQX can reduce neurological deficits in animal models of autoimmune damage (Smith et al., 2000), but these drugs are too toxic for clinical use. Other strategies, such as blocking the glycine site of the NMDA receptor for treating ischemic stroke have been ineffective in improving outcomes (Lees et al., 2000; Sacco et al., 2001).

The interactions between ionic glutamate receptors and other proteins such as GluR2-GAPDH and NR2-PSD-95 can improve cell survival after ischemic insults, and thus represent another approach to neuroprotective treatments after stroke (Sattler et al., 1999; Zhai et al., 2013). This strategy is attractive because the basic signal transducing functions of the channels are not blocked as they would be by a conventional antagonist. Thus, a more subtle modulation of ion channel function can be achieved, with the hope of reducing excitotoxicity while sparing normal neurotransmission. Those *in vitro* and animal model experiments used small interfering peptides to disrupt the channel-protein interactions, but these peptides may not be ideal for human clinical use. Therefore, an important priority for future research is the development of suitable drugs targeting the ion channel-protein interactions involved in excitotoxicity.

In summary, ion channel function is modulated by interactions with other proteins. Various proteins influence the number and position of particular subunits in the assembled channel, the dynamics of receptor trafficking and targeting to designated subcellular areas, as well as the assembly, stability, and turnover of the receptor on the membrane and in intracellular signaling pathways. These interactions permit the function of ion channels to be fine-tuned according to both external stimuli and intracellular states. This network of molecular interactions allows for complex signal processing by neurons and also reveals new targets for pharmacological manipulation of neuron function that may be clinically useful. Knowledge of ion channel interactions has progressed rapidly and more such interactions are likely to emerge.

REFERENCES

- Aarts, M., Liu, Y., Liu, L., Besshoh, S., Arundine, M., Gurd, J. W., et al. (2002). Treatment of ischemic brain damage by perturbing NMDA receptor-PSD-95 protein interactions. *Science* 298, 846–850. doi: 10.1126/science.1072873
- Albensi, B. C. (2007). The NMDA receptor/ion channel complex: a drug target for modulating synaptic plasticity and excitotoxicity. *Curr. Pharm. Des.* 13, 3185–3194. doi: 10.2174/138161207782341321
- Albuquerque, E. X., Pereira, E. F., Alkondon, M., and Rogers, S. W. (2009). Mammalian nicotinic acetylcholine receptors: from structure to function. *Physiol. Rev.* 89, 73–120. doi: 10.1152/physrev.00015.2008
- Allison, D. W., Gelfand, V. I., Spector, I., and Craig, A. M. (1998). Role of actin in anchoring postsynaptic receptors in cultured hippocampal neurons: differential attachment of NMDA versus AMPA receptors. *J. Neurosci.* 18, 2423–2436.
- Anggono, V., and Huganir, R. L. (2012). Regulation of AMPA receptor trafficking and synaptic plasticity. *Curr. Opin. Neurobiol.* 22, 461–469. doi: 10.1016/j.conb.2011.12.006
- Ashcroft, F. M. (2006). From molecule to malady. *Nature* 440, 440–447. doi: 10.1038/nature04707
- Chen, Z. W., and Olsen, R. W. (2007). GABAA receptor associated proteins: a key factor regulating GABAA receptor function. *J. Neurochem.* 100, 279–294. doi: 10.1111/j.1471-4159.2006.04206.x
- Connolly, C. N., and Wafford, K. A. (2004). The Cys-loop superfamily of ligand-gated ion channels: the impact of receptor structure on function. *Biochem. Soc. Trans.* 32, 529–534. doi: 10.1042/BST0320529
- Cui, H., Hayashi, A., Sun, H. S., Belmares, M. P., Cobey, C., Phan, T., et al. (2007). PDZ protein interactions underlying NMDA receptor-mediated excitotoxicity and neuroprotection by PSD-95 inhibitors. *J. Neurosci.* 27, 9901–9915. doi: 10.1523/JNEUROSCI.1464-07.2007
- Dacosta, C. J., and Baenziger, J. E. (2013). Gating of pentameric ligand-gated ion channels: structural insights and ambiguities. *Structure* 21, 1271–1283. doi: 10.1016/j.str.2013.06.019
- Dent, J. A. (2010). The evolution of pentameric ligand-gated ion channels. *Adv. Exp. Med. Biol.* 683, 11–23. doi: 10.1007/978-1-4419-6445-8_2
- Dingledine, R., Borges, K., Bowie, D., and Traynelis, S. F. (1999). The glutamate receptor ion channels. *Pharmacol. Rev.* 51, 7–61.
- Durand, G. M., Gregor, P., Zheng, X., Bennett, M. V., Uhl, G. R., and Zukin, R. S. (1992). Cloning of an apparent splice variant of the rat N-methyl-D-aspartate receptor NMDAR1 with altered sensitivity to polyamines and activators of protein kinase C. *Proc. Natl. Acad. Sci. U.S.A.* 89, 9359–9363. doi: 10.1073/pnas.89.19.9359
- Gotti, C., Clementi, F., Fornari, A., Gaimarri, A., Guiducci, S., Manfredi, L., et al. (2009). Structural and functional diversity of native brain neuronal nicotinic receptors. *Biochem. Pharmacol.* 78, 703–711. doi: 10.1016/j.bcp.2009.05.024
- Grossman, A. W., and Broderick, J. P. (2013). Advances and challenges in treatment and prevention of ischemic stroke. *Ann. Neurol.* 74, 363–372. doi: 10.1002/ana.23993
- Hollmann, M., Boulter, J., Maron, C., Beasley, L., Sullivan, J., Pecht, G., et al. (1993). Zinc potentiates agonist-induced currents at certain splice variants of the NMDA receptor. *Neuron* 10, 943–954. doi: 10.1016/0896-6273(93)90209-A
- Jarvis, S. E., Magga, J. M., Beedle, A. M., Braun, J. E., and Zamponi, G. W. (2000). G protein modulation of N-type calcium channels is facilitated by physical interactions between syntaxin 1A and Gbetagamma. *J. Biol. Chem.* 275, 6388–6394. doi: 10.1074/jbc.275.9.6388
- Kalia, L. V., Pitcher, G. M., Pelkey, K. A., and Salter, M. W. (2006). PSD-95 is a negative regulator of the tyrosine kinase Src in the NMDA receptor complex. *EMBO J.* 25, 4971–4982. doi: 10.1038/sj.emboj.7601342
- Kisilevsky, A. E., Mulligan, S. J., Altier, C., Iftinca, M. C., Varela, D., Tai, C., et al. (2008). D1 receptors physically interact with N-type calcium channels to regulate channel distribution and dendritic calcium entry. *Neuron* 58, 557–570. doi: 10.1016/j.neuron.2008.03.002
- Kittler, J. T., and Moss, S. J. (2003). Modulation of GABAA receptor activity by phosphorylation and receptor trafficking: implications for the efficacy of synaptic inhibition. *Curr. Opin. Neurobiol.* 13, 341–347. doi: 10.1016/S0959-4388(03)00064-3
- Kornau, H. C., Schenker, L. T., Kennedy, M. B., and Seeburg, P. H. (1995). Domain interaction between NMDA receptor subunits and the postsynaptic density protein PSD-95. *Science* 269, 1737–1740. doi: 10.1126/science.7569905
- Kozuska, J. L., and Paulsen, I. M. (2012). The Cys-loop pentameric ligand-gated ion channel receptors: 50 years on. *Can. J. Physiol. Pharmacol.* 90, 771–782. doi: 10.1139/y2012-018
- Lee, F. J., Xue, S., Pei, L., Vukusic, B., Chery, N., Wang, Y., et al. (2002). Dual regulation of NMDA receptor functions by direct protein-protein interactions with the dopamine D1 receptor. *Cell* 111, 219–230. doi: 10.1016/S0092-8674(02)00962-5
- Lees, K. R., Asplund, K., Carolei, A., Davis, S. M., Diener, H. C., Kaste, M., et al. (2000). Glycine antagonist (gavestinel) in neuroprotection (GAIN International) in patients with acute stroke: a randomised controlled trial. GAIN International Investigators. *Lancet* 355, 1949–1954. doi: 10.1016/S0140-6736(00)02326-6
- Li, K. W., Chen, N., and Smit, A. B. (2013a). Interaction proteomics of the AMPA receptor: towards identification of receptor sub-complexes. *Amino Acids* 44, 1247–1251. doi: 10.1007/s00726-013-1461-9
- Li, S., Li, Z., Pei, L., Le, A. D., and Liu, F. (2012). The alpha7nACh-NMDA receptor complex is involved in cue-induced reinstatement of nicotine seeking. *J. Exp. Med.* 209, 2141–2147. doi: 10.1084/jem.20121270

- Li, S., Nai, Q., Lipina, T. V., Roder, J. C., and Liu, F. (2013b). $\alpha 7$ nAChR/NMDAR coupling affects NMDAR function and object recognition. *Mol. Brain* 6:58. doi: 10.1186/1756-6606-6-58
- Liu, F., Wan, Q., Pristupa, Z. B., Yu, X. M., Wang, Y. T., and Niznik, H. B. (2000). Direct protein-protein coupling enables cross-talk between dopamine D5 and gamma-aminobutyric acid A receptors. *Nature* 403, 274–280. doi: 10.1038/35001232
- Magga, J. M., Jarvis, S. E., Arnot, M. I., Zamponi, G. W., and Braun, J. E. (2000). Cysteine string protein regulates G protein modulation of N-type calcium channels. *Neuron* 28, 195–204. doi: 10.1016/S0896-6273(00)00096-9
- Maksay, G. (2009). Ligand-gated pentameric ion channels, from binding to gating. *Curr. Mol. Pharmacol.* 2, 253–262. doi: 10.2174/1874467210902030253
- Michaelis, E. K. (1998). Molecular biology of glutamate receptors in the central nervous system and their role in excitotoxicity, oxidative stress and aging. *Prog. Neurobiol.* 54, 369–415. doi: 10.1016/S0301-0082(97)00055-5
- Niethammer, M., Kim, E., and Sheng, M. (1996). Interaction between the C terminus of NMDA receptor subunits and multiple members of the PSD-95 family of membrane-associated guanylate kinases. *J. Neurosci.* 16, 2157–2163.
- Nishida, M., and MacKinnon, R. (2002). Structural basis of inward rectification: cytoplasmic pore of the G protein-gated inward rectifier GIRK1 at 1.8 Å resolution. *Cell* 111, 957–965. doi: 10.1016/S0092-8674(02)01227-8
- Pei, L., Lee, F. J., Moszczynska, A., Vukusic, B., and Liu, F. (2004). Regulation of dopamine D1 receptor function by physical interaction with the NMDA receptors. *J. Neurosci.* 24, 1149–1158. doi: 10.1523/JNEUROSCI.3922-03.2004
- Rojas, A., and Dingledine, R. (2013). Ionotropic glutamate receptors: regulation by G-protein-coupled receptors. *Mol. Pharmacol.* 83, 746–752. doi: 10.1124/mol.112.083352
- Sacco, R. L., DeRosa, J. T., Haley, E. C. Jr., Levin, B., Ordroneanu, P., Phillips, S. J., et al. (2001). Glycine antagonist in neuroprotection for patients with acute stroke: GAIN Americas: a randomized controlled trial. *JAMA* 285, 1719–1728. doi: 10.1001/jama.285.13.1719
- Sattler, R., Xiong, Z., Lu, W. Y., Hafner, M., MacDonald, J. F., and Tymianski, M. (1999). Specific coupling of NMDA receptor activation to nitric oxide neurotoxicity by PSD-95 protein. *Science* 284, 1845–1848. doi: 10.1126/science.284.5421.1845
- Smith, T., Groom, A., Zhu, B., and Turski, L. (2000). Autoimmune encephalomyelitis ameliorated by AMPA antagonists. *Nat. Med.* 6, 62–66. doi: 10.1038/71548
- Sugihara, H., Moriyoshi, K., Ishii, T., Masu, M., and Nakanishi, S. (1992). Structures and properties of seven isoforms of the NMDA receptor generated by alternative splicing. *Biochem. Biophys. Res. Commun.* 185, 826–832. doi: 10.1016/0006-291X(92)91701-Q
- Sun, H. S., Doucette, T. A., Liu, Y., Fang, Y., Teves, L., Aarts, M., et al. (2008). Effectiveness of PSD95 inhibitors in permanent and transient focal ischemia in the rat. *Stroke* 39, 2544–2553. doi: 10.1161/STROKEAHA.107.506048
- Tarze, A., Deniaud, A., Le Bras, M., Maillier, E., Molle, D., Larochette, N., et al. (2007). GAPDH, a novel regulator of the pro-apoptotic mitochondrial membrane permeabilization. *Oncogene* 26, 2606–2620. doi: 10.1038/sj.onc.1210074
- Wang, M., Li, S., Zhang, H., Pei, L., Zou, S., Lee, F. J., et al. (2012). Direct interaction between GluR2 and GAPDH regulates AMPAR-mediated excitotoxicity. *Mol. Brain* 5:13. doi: 10.1186/1756-6606-5-13
- Zamponi, G. W., Bourinet, E., Nelson, D., Nargeot, J., and Snutch, T. P. (1997). Crosstalk between G proteins and protein kinase C mediated by the calcium channel $\alpha 1$ subunit. *Nature* 385, 442–446. doi: 10.1038/385442a0
- Zhai, D., Li, S., Wang, M., Chin, K., and Liu, F. (2013). Disruption of the GluR2/GAPDH complex protects against ischemia-induced neuronal damage. *Neurobiol. Dis.* 54, 392–403. doi: 10.1016/j.nbd.2013.01.013
- Zou, S., Li, L., Pei, L., Vukusic, B., Van Tol, H. H., Lee, F. J., et al. (2005). Protein-protein coupling/uncoupling enables dopamine D2 receptor regulation of AMPA receptor-mediated excitotoxicity. *J. Neurosci.* 25, 4385–4395. doi: 10.1523/JNEUROSCI.5099-04.2005

Conflict of Interest Statement: The authors declare that the research was conducted in the absence of any commercial or financial relationships that could be construed as a potential conflict of interest.

Received: 14 March 2014; accepted: 21 April 2014; published online: 09 May 2014.

Citation: Li S, Wong AHC and Liu F (2014) Ligand-gated ion channel interacting proteins and their role in neuroprotection. *Front. Cell. Neurosci.* 8:125. doi: 10.3389/fncel.2014.00125

This article was submitted to the journal *Frontiers in Cellular Neuroscience*.

Copyright © 2014 Li, Wong and Liu. This is an open-access article distributed under the terms of the Creative Commons Attribution License (CC BY). The use, distribution or reproduction in other forums is permitted, provided the original author(s) or licensor are credited and that the original publication in this journal is cited, in accordance with accepted academic practice. No use, distribution or reproduction is permitted which does not comply with these terms.



Kir3 channel ontogeny – the role of G $\beta\gamma$ subunits in channel assembly and trafficking

Peter Zylbergold^{1†}, Rory Sleno^{1†}, Shahriar M. Khan¹, Ashley M. Jacobi², Mark A. Belhke² and Terence E. Hébert^{1*}

¹ Department of Pharmacology and Therapeutics, McGill University, Montréal, QC, Canada

² Integrated DNA Technologies, Inc., Coralville, IA, USA

Edited by:

Gerald Zamponi, University of Calgary, Canada

Reviewed by:

Leigh Anne Swayne, University of Victoria, Canada
Christophe Altier, University of Calgary, Canada

*Correspondence:

Terence E. Hébert, Department of Pharmacology and Therapeutics, McGill University, 3655 Promenade Sir-William-Osler, Room 1303, Montréal, QC H3G 1Y6, Canada
e-mail: terence.hebert@mcgill.ca

[†] Peter Zylbergold and Rory Sleno have contributed equally to this work.

The role of G $\beta\gamma$ subunits in Kir3 channel gating is well characterized. Here, we have studied the role of G $\beta\gamma$ dimers during their initial contact with Kir3 channels, prior to their insertion into the plasma membrane. We show that distinct G $\beta\gamma$ subunits play an important role in orchestrating and fine-tuning parts of the Kir3 channel life cycle. G $\beta_1\gamma_2$, apart from its role in channel opening that it shares with other G $\beta\gamma$ subunit combinations, may play a unique role in protecting maturing channels from degradation as they transit to the cell surface. Taken together, our data suggest that G $\beta_1\gamma_2$ prolongs the lifetime of the Kir3.1/Kir3.2 heterotetramer, although further studies would be required to shed more light on these early G $\beta\gamma$ effects on Kir3 maturation and trafficking.

Keywords: Kir3 channels, G proteins, G protein-coupled inwardly-rectifying potassium channels, G $\beta\gamma$ subunits, channel assembly

INTRODUCTION

Kir3 channels were first discovered in the context of the K_{ACh} channel (Kir3.1/Kir3.4), activated by the muscarinic acetylcholine receptor expressed in the heart. Logothetis et al. (1987) first noted that hyperpolarization of chick embryonic atrial cells via the iK_{ACh} depended on G $\beta\gamma$ but not G α subunits. It was later proposed that G $\beta\gamma$ acted on Kir3 through direct interactions with the channel (Huang et al., 1995; Inanobe et al., 1995; Krapivinsky et al., 1995b) and that different interacting domains underlie basal and agonist-induced activation. Specifically, it was shown that Leu339 on Kir3.4 and its counterpart Leu333 on Kir3.1 were critical for receptor-stimulated currents and that mutation of these residues to Glu completely abrogated channel activation (He et al., 1999). Surprisingly, these mutations did nothing to basal current, suggesting that distinct regions on the channel allowed G $\beta\gamma$ to facilitate basal activity. It was shown that both the N- (aa 34–86) and C-termini of Kir3.1 could bind G $\beta\gamma$ and that there was in fact two distinct binding domains on the C-terminus (aa 318–374 and aa 390–462), conferring greater G $\beta\gamma$ binding when Kir3.1 was part of the tetrameric channel (Huang et al., 1997). They also showed that the N- and C-termini of Kir3 channels interacted with each other and that when the C-terminus of Kir3.1 interacted with either the N-terminus of Kir3.1 or Kir3.4, substantial increases in G $\beta\gamma$ binding were observed (Huang et al., 1997). It was later found that mutation of single residues His57 and Leu262 on Kir3.1 (His64 and Leu268 on Kir3.4, respectively) were sufficient to reduce G $\beta\gamma$ activation of the channel complex (He et al., 2002). Glutathione-S-transferase-pull down experiments and competition assays demonstrated critical G $\beta\gamma$ binding domains on the Kir3.2 subunit. Using Kir3.1 and Kir3.2

as templates, Ivanina et al. (2003) confirmed that similar regions of the N-terminus of the two subunits bound G $\beta\gamma$, whereas significant differences were found at the level of the C-terminus. Consistent with Huang et al. (1997) Kir3.1 revealed two distinct G $\beta\gamma$ binding domains on its C-terminus, one proximal and one distal, while the Kir3.2 subunit possessed only one C-terminal binding site at its most distal end (Ivanina et al., 2003). Interestingly, mutation of these C-terminal sites on the Kir3.1 subunit, both proximal and distal, did little to the binding of G $\beta\gamma$ to the channel, but dramatically altered the current characteristics, suggesting these interacting domains were more involved in channel gating dynamics rather than G $\beta\gamma$ binding (Ivanina et al., 2003).

It was initially thought that Kir3 channels, like other effectors for G protein-coupled receptors (GPCRs), were trafficked independently of their cognate receptors, G proteins and auxiliary proteins to the plasma membrane. According to this model, functional interactions between signaling proteins would occur only upon receptor activation. However, this simple model does not account for the speed and specificity observed in signal transduction (Riven et al., 2006), and recent evidence suggests the existence of pre-assembled macromolecular signaling complexes containing Kir3 channels built before reaching the cell surface [(Nikolov and Ivanova-Nikolova, 2004; David et al., 2006; Rebois et al., 2006; Riven et al., 2006; Robitaille et al., 2009), reviewed in (Doupnik, 2008; Zylbergold et al., 2010)].

The notion of Kir3 signaling complexes arose initially from studies focusing on the interaction between D2- and D4-dopamine receptors, and Kir3 channels. We showed that the Kir3 channel could be co-immunoprecipitated in HEK 293 cells with either the

D2- or D4- dopamine receptor, and that this interaction required the presence of Gβγ as shown by sequestration of Gβγ by the carboxy-terminal domain of GPCR kinase 2 (GRK2, βARKct; Lavine et al., 2002). We also showed that Kir3 channels interacted with their cognate G proteins well before reaching the cell surface (Rebois et al., 2006). These interactions could be observed with Kir3.1, in the absence of expressed partner subunits, implying that this interaction occurred in the endoplasmic reticulum (ER; Robitaille et al., 2009). Using total internal reflection fluorescence (TIRF) microscopy combined with fluorescence resonance energy transfer (FRET), Riven et al. (2006) revealed that complexes of Kir3 and heterotrimeric G proteins exist at rest and that conformational changes in the channel facilitated opening of the channel gate. Furthermore, cell-surface interactions between Kir3, Gβγ, and the δ-opioid receptor (DOR), as detected by bioluminescence resonance energy transfer, have been described, supporting the notion that Kir3 complexes are stable in their journey from biosynthesis to functionality (Richard-Lalonde et al., 2013). Interactions between gamma-aminobutyric acid-B receptors and Kir3 channels have also been observed using an array of techniques (Fowler et al., 2007; Ciruela et al., 2010), with evidence suggesting that these interactions also occur soon after biosynthesis in the ER (David et al., 2006). Data suggesting that such complexes exist *in vivo* was first described by Nikolov and Ivanova-Nikolova (2004) whereby using rat atrial cardiomyocytes, they co-immunoprecipitated G proteins, GRKs, PKA, and protein phosphatases PP1/2, among others, with the KACH channel, indicating the presence of a highly coordinated complex for regulating cardiac excitability. Gβγ has been demonstrated to regulate many effectors [reviewed in (Khan et al., 2013)]. Early signaling complex formation has been observed for other effectors downstream of Gβγ signaling as well. Adenylyl cyclase has also been observed to stably associate with the β₂AR (Lavine et al., 2002), with this interaction likely occurring concurrently with biosynthesis of the enzyme (Dupré et al., 2007). The existence of such complexes during receptor and effector biosynthesis along with the fact that Gβγ interacts with multiple signaling partners in the ER suggests that these are organizational events related to the specificity of cellular signaling, and places Gβγ subunits in a good position for acting as a central organizer of signalosome regulation and stability (Dupré et al., 2009; Zylbergold et al., 2010).

The role of Gβγ subunits in channel gating is well established. This article will explore the role of Gβγ dimers during their initial contact with Kir3 channels. We suggest that distinct Gβγ subunits play an important role in orchestrating and fine-tuning parts of the Kir3 channel life cycle.

MATERIALS AND METHODS

REAGENTS

Blasticidin, hygromycin, Dulbecco's Modified Eagle's Medium (DMEM), fetal bovine serum (FBS), penicillin/streptomycin, and tetracycline were from Wisent (St-Bruno, QC, Canada). Lipofectamine 2000 was obtained from Invitrogen (Burlington, ON, Canada). Anti-FLAG M2 affinity agarose beads were from Sigma-Aldrich (St. Louis, MO, USA). Bradford reagent, acrylamide and polyvinylidene fluoride (PVDF) membranes were obtained from

Bio-Rad (Mississauga, ON, Canada). Enhanced chemiluminescence (ECL) Plus reagent was obtained from Perkin Elmer (Woodbridge, ON, Canada). The following primary antibodies were used: rabbit anti-Kir3.1 (Alomone Labs, Jerusalem, Israel), mouse anti-HA and mouse anti-myc (Covance, Princeton, NJ, USA), rabbit anti-FLAG (Sigma-Aldrich, St. Louis, MO, USA), mouse anti-glyceraldehyde 3-phosphate dehydrogenase (GAPDH) (Ambion, Burlington, ON, Canada), rabbit anti-Gβ₄ (Santa Cruz, Dallas, TX, USA), mouse anti-Na⁺/K⁺-ATPase (Sigma-Aldrich, St. Louis, MO, USA), and mouse anti-β-tubulin (Invitrogen, Burlington, ON, Canada). The rabbit anti-Gβ₁ antibody was a generous gift from Dr. Ron Taussig (UT Southwestern Medical Center). The following secondary antibodies were used: goat-anti-rabbit IgG (H+L) conjugated to Alexa488 (Invitrogen, Burlington, ON, Canada), goat-anti-mouse IgG (Fab specific) conjugated to peroxidase and goat-anti-rabbit IgG (whole molecule) conjugated to peroxidase (Sigma-Aldrich, St. Louis, MO, USA). PermaFluor aqueous mounting medium, bovine serum albumin and coverslips were obtained from ThermoScientific (Waltham, MA, USA). siRNAs targeted against Gβ₁, Gβ₄, Gγ₂, Gγ₄, Gγ₅, and Gγ₇ were purchased from Dharmacon (Ottawa, ON, Canada). Primetime qPCR 5' nuclease assays were provided by Integrated DNA Technologies (Coralville, IA, USA). Unless otherwise stated, chemicals were of reagent grade and were purchased from Sigma-Aldrich (St. Louis, MO, USA).

CLONING AND GENERATING THE INDUCIBLE CELL LINE

A previously developed inducible expression system was used to study pulses of Kir3.1 channels as they transit through biosynthetic pathways (Zylbergold et al., 2013). Briefly, extracellularly FLAG-tagged Kir3.1 was subcloned into the pcDNA5-FRT-TO inducible vector using BamHI and NotI restriction sites. The pcDNA5-FRT-TO-FLAG-Kir3.1 (2 μg) was co-transfected with the pOG44 recombinase gene (8 μg) into Flp-In™ T-Rex™ 293 parental cells in T75 flasks using Lipofectamine 2000 to generate inducible FLAG-Kir3.1 stables. 48 h post-transfection, cells were passaged and plated into new T75 flasks using fresh media (DMEM supplemented with 5% FBS and 1% penicillin/streptomycin – complete media) containing the selection antibiotics blasticidin (5 μg/mL) and hygromycin (200 μg/mL). Cells were grown to confluency and then used as required for subsequent experiments.

INDUCTION AND TRANSFECTION PROTOCOL

Inducible FLAG-Kir3.1 stable cells were plated in T75 flasks, allowed to grow for 48–72 h and subsequently transfected with 2 μg of Kir3.2-MYC, FLAG-Gβ₁, HA-Gγ₂, or various siRNAs (depending on the experiment) using Lipofectamine 2000 (1 μg:2 μL ratio of DNA:Lipofectamine 2000; 6.25 nM:1 μL siRNA:Lipofectamine 2000, as per manufacturer's protocol) in DMEM (0% FBS, 0% penicillin/streptomycin). Transfection media was then removed and replaced with complete media 5 h later. 24 h post-transfection, cells were induced with 1 μg/mL of tetracycline in DMEM for 30 min at 37°C, washed three times in DMEM and treated with 5 μg/mL of cycloheximide (CHX) in DMEM for 1 h at 37°C. Following CHX treatment, cells were washed twice in DMEM, and then incubated at 37°C in complete

media supplemented with blasticidin for varying periods of time as needed for subsequent experiments.

IMMUNOPRECIPITATION

Cells were plated in T75 flasks 48–72 h before transfection, co-transfected with 2 μ g of Kir3.2-MYC or FLAG-G β_1 , HA-G γ_2 , and then induced for Kir3.1-FLAG expression, 24–48 h post-transfection as described above. Transfected cells were washed twice with cold 1X phosphate buffered saline (PBS), harvested in 5 mL of cold 1X PBS, pelleted by centrifugation at 2000 rpm for 8 min at 4°C, and subsequently resuspended in a buffer containing 5 mM Tris pH 7.4, 2 mM EDTA, with protease inhibitor cocktail (10 μ g/mL trypsin inhibitor, 5 μ g/mL leupeptin, 50 μ g/mL benzamidine). Samples were then subjected to two 10 s bursts with a polytron homogenizer on ice. Debris and unlysed cells were spun down for 5 min at 1000 rpm (4°C), and the supernatant was then fractionated by a 20 min centrifugation step at 16000 rpm (4°C) to pellet down the membranes. Pelleted membranes were resuspended in solubilization buffer (75 mM Tris pH 8, 2 mM EDTA, 5 mM MgCl₂, 0.5% dodecylmaltoside, protease inhibitor cocktail) and incubated overnight with rotation at 4°C. The following day, membrane samples were spun for 5 min at 10,000 rpm (4°C) in order to remove unsolubilized membranes, resuspended in solubilization buffer and then quantified using the Bradford technique (Bio-Rad). In order to immunoprecipitate FLAG-tagged Kir3.1, 500 μ g of sample was added to 25 μ L of washed anti-FLAG M2 affinity agarose beads and incubated on a rotator overnight at 4°C. The following day, samples were washed three times [2 min at 1600 rpm (4°C)] in solubilization buffer supplemented with 300 mM potassium chloride. Bound proteins were eluted off of beads using 60 μ L of Tris-buffered saline (TBS) solution (50 mM Tris pH 7.4, 150 mM sodium chloride) containing competitive FLAG peptide (3 μ L/100 μ L TBS) for 20 min on a 4°C rotator. Eluted proteins were spun down for 2 min at 1600 rpm (4°C) and then the supernatant was collected and mixed with 4X sample buffer (62.5 mM Tris, 16.3% glycerol, 2% SDS, 5% β -mercaptoethanol, 0.025% bromophenol blue) in a 1:4 ratio. Samples were then subsequently analyzed by western blot.

WESTERN BLOTTING

For western blotting experiments, 60 μ L of samples obtained following immunoprecipitation (IP) and 50 μ g of samples from total lysate fractions were loaded on 8% polyacrylamide gels. Gels were electrophoresed for 90 min at 130 V and then transferred to PVDF membranes (Bio-Rad, Mississauga, ON, Canada) for 1 h at 100 V. Following transfer, PVDF membranes were blocked in 5% milk/TBS-containing 1% Tween (TBST) for 1 h at room temperature (RT). Membranes were probed with the primary antibodies as needed [anti-Kir3.1 (1/5000); anti-c-Myc (1/5000); anti-HA (1/5000); anti-G β_1 (1/5000); anti-G β_4 (1/400); anti-GAPDH (1/5000); anti- β -tubulin (1/5000); anti-Na⁺/K⁺-ATPase (1/5000)] in 5% milk/TBST overnight on a 4°C rotator. The following day, membranes were washed three times in TBST for 10 min, incubated in the appropriate secondary antibody [anti-rabbit or anti-mouse HRP (1/20000)] in 5% milk/TBST for 1 h at RT, and then subsequently washed again three times in TBST for

10 min. ECL Plus reagent was then added to the membranes and chemiluminescence was detected using a standard film developer.

IMMUNOFLUORESCENCE

Cells plated on coverslips in six well plates 48–72 h before transfection were transfected with 300 ng of Kir3.2-MYC or empty vector (pcDNA3), and then induced for Kir3.1-FLAG expression 24–48 h later. At the time of harvest, cells were washed once in 1X PBS pH 7.4 and then fixed in 2% paraformaldehyde (PFA) for 10 min at RT. Cells were then washed three times in 1X PBS pH 7.4 to remove remaining PFA and then blocked in blocking buffer (1X PBS supplemented with 2% BSA) for 1 h at RT. Immediately following blocking, 200 μ L blocking buffer with diluted rabbit anti-FLAG antibody (1/250) was applied to each coverslip and incubated overnight at 4°C. The following day, cells were washed three times in 1X PBS pH 7.4 and incubated with 200 μ L blocking buffer supplemented with anti-rabbit Alexa488 (1/500) for 1 h at RT in the dark. Cells were then washed three times in 1X PBS pH 7.4 and coverslips were mounted on glass slides using PermaFluor Aqueous Mounting Medium and then imaged using a Zeiss LSM510 confocal microscope.

REVERSE TRANSCRIPTION AND qPCR

For assessment of knockdown efficiency of G γ subunits, total RNA was isolated from siRNA transfected inducible FLAG-Kir3.1 stable cells with TRI reagent using a modified RNA isolation protocol from Ambion. 2 μ g of total RNA was reverse transcribed using a Moloney Murine Leukemia Virus Reverse Transcriptase (MMLV-RT, Promega) reaction assay as per the manufacturer's protocol. Reverse transcribed cDNA was subject to qPCR using Custom Primetime qPCR 5' Nuclease assays (IDT) as per the manufacturer's protocol in a Corbett Rotorgene 6000 qPCR instrument. Percentage knockdown efficiencies were calculated using C_t values obtained from the qPCR reaction that were subsequently analyzed using the 2^{− $\Delta\Delta$ C_t} method, using the levels of hypoxanthine-guanine phosphoribosyltransferase (HPRT) as the housekeeping gene.

RESULTS

In order to assess the role of G $\beta\gamma$ subunits in the maturation and stability of Kir3.1 channels, we combined our Kir3.1 inducible expression system with RNA interference to knockdown different G β and G γ subunits. Cells co-expressing Kir3.2 and control or different G β siRNAs were induced for 30 min with tetracycline and residual leak expression was silenced by a brief treatment with CHX. After washout, Kir3.1 maturation was followed at different time points. The advantage of our system is that it allows for a pulse of channel expression, at physiological protein levels, to mature and traffic to the plasma membrane without saturating the biosynthetic or quality control machinery (Zylbergold et al., 2013). After 6 h, it was observed that sufficient Kir3.1 is available for immunoprecipitation although the immature form is seen immediately after the 30 min pulse (**Figure 1A**; compare times 0 and 6 h in the FLAG IP and Total Lysate blots). The pulse of Kir3.1 expression also indicates that the channel reached maximum levels at 24 h post-induction and then levels subsequently begin to decline. Initial experiments demonstrated the selectivity

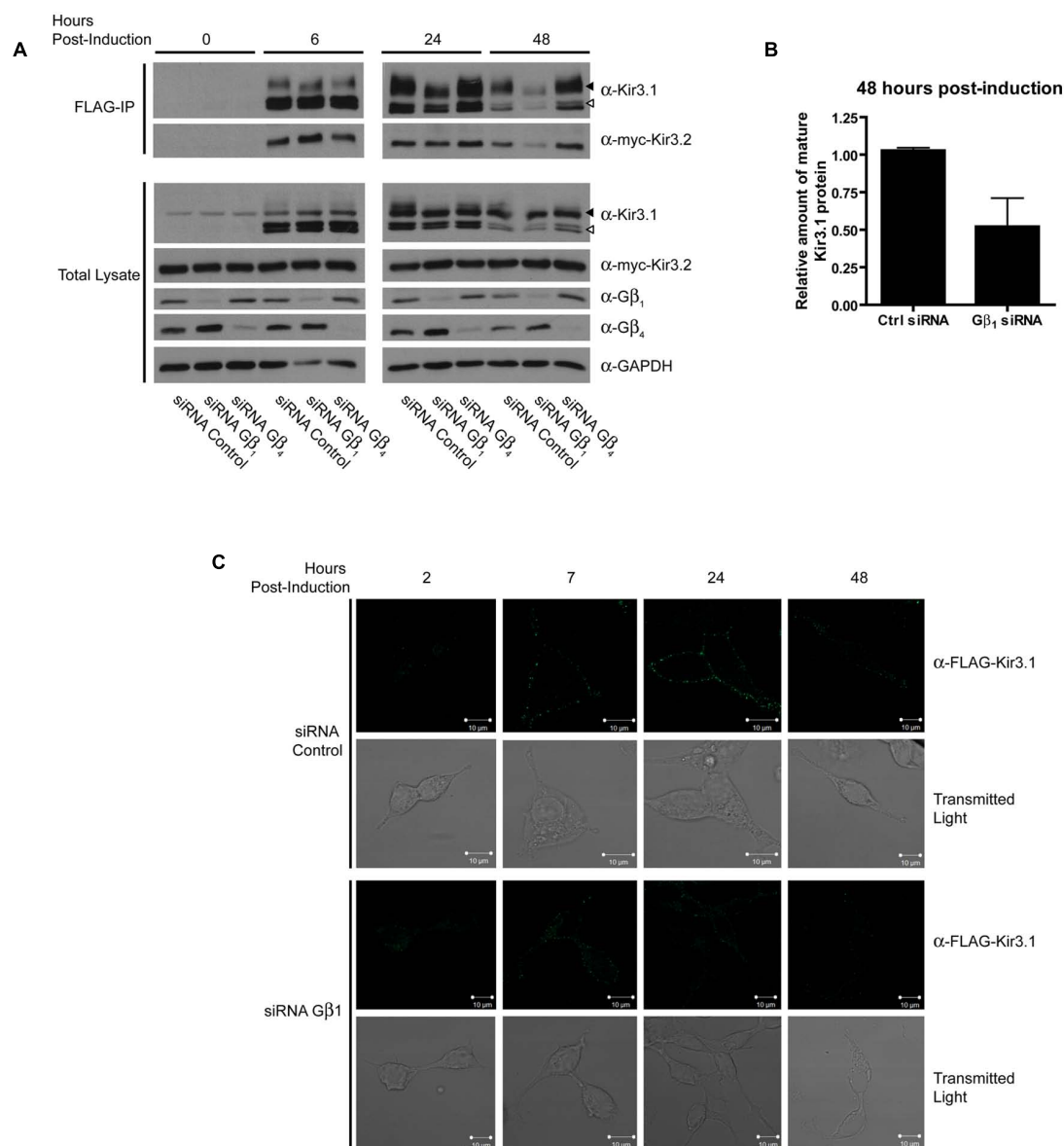


FIGURE 1 | G β ₁ but not G β ₄ knockdown reduces stability of Kir3.1.

(A) Flp-In-Trex-FLAG-Kir3.1 cells transfected with myc-Kir3.2 and G β ₁, G β ₄, or control siRNA were induced to express FLAG-Kir3.1 with 1 μ g/mL of tetracycline for 30 min and then chased for 0, 6, 24, or 48 h. Upper panel: cells were lysed and FLAG-Kir3.1 was immunoprecipitated using an α -FLAG antibody. Samples were then analyzed by western blot to detect levels of FLAG-Kir3.1 and myc-Kir3.2. Lower panel: total cell lysates showing expression of Kir3.1, Kir3.2, G β ₁, G β ₄, and GAPDH (loading control). Results are representative of three independent experiments. White arrow indicates immature channel proteins while black arrow indicates correctly processed Kir3.1. **(B)** Densitometric analysis of data

from experiments conducted above. The trend is clear and statistically significant at $p < 0.1$. **(C)** Flp-In Trex FLAG-Kir3.1 cells were plated on glass coverslips. The cells were transfected with siRNA targeted against G β ₁ and myc-Kir3.2. Cells were subsequently induced to express FLAG-Kir3.1 with 1 μ g/mL of tetracycline for 30 min followed by chase times of 2, 7, 24, or 48 h. Cells were fixed with 2% PFA and then labeled (top panels) with rabbit α -FLAG followed by an α -rabbit secondary antibody conjugated to Alexa488 or shown using transmitted light (lower panels). Slides were imaged using a Zeiss LSM510 confocal microscope. Results are representative of a single experiment with several independent fields of cells.

of the siRNAs for G β ₁ and G β ₄ and confirmed efficient silencing of their respective endogenous transcripts in HEK 293 cells as assessed by the depletion of their gene products at the protein level (**Figure 1A**; Total Lysate). Although both G β ₁ and G β ₄ are able to modulate channel function in response to GPCR stimulation (Lei et al., 2000), they are not identical with respect to their effects on

channel maturation. In the presence of Kir3.2, Kir3.1 adopts a mature glycosylation phenotype and is trafficked to the cell surface (**Figures 1A–C**). When we knocked down G β ₁, there was little effect on the initial interactions between Kir3.1 and Kir3.2 and early maturational events still occurred. However, the amount of mature and immature channel both decline by 24 h in the absence

of G β_1 , suggesting that the holo-channel is less stable and is likely targeted for early degradation. This observation is supported by the fact that much less channel appears on the cell surface when G β_1 was knocked down, as detected using confocal microscopy (Figure 1C). The punctate staining of surface Kir3.1 is consistent with more physiological levels of the channel and again represents one of the advantages of our expression system. The loss of G β_1 results in a more rapid life cycle for the channel. Knockdown of G β_1 had no effect on levels of Kir3.2 (Figure 1A, Total Lysate), possibly representing either a selective effect on Kir3.1 or a reflection of the fact that bulk expression of Kir3.2 may escape quality control. Future experiments with inducible Kir3.2 constructs may help resolve this issue. Unlike G β_1 , knockdown of G β_4 had no effect on the stability of the holo-channel, demonstrating a distinct role in channel function that may be restricted to activating the channel in response to receptor stimulation (Figure 1A). However, we did observe increased amounts of mature Kir3.1 when G β_4 was silenced. This may suggest that remaining G β_1 is now more able to interact with the channel in the absence of a competitor. Our data points to a clear demarcation between the functions of G β_1 and G β_4 with respect to Kir3.1 stability and trafficking. Consistent with our RNA interference data, we also noted that overexpression of G β_1 resulted in holo-channels that were more stable at 48 h post-induction (Figure 2). Loss of the G β_4 subunit also had no effect on levels of Kir3.2 in total cell lysates (Figure 1A, Total Lysate) suggesting that their effects are specific for Kir3.1 as well.

Curiously, we noted that knockdown of G β_4 slightly increased protein expression levels of G β_1 [also observed in a previous study (Krumins and Gilman, 2006)]. The reason for this is unclear at present but we have preliminary data that suggests it may be through transcriptional effects mediated by G β_1 (data not shown). This may also reflect the increased channel maturation in the absence of G β_4 , possibly independently of direct competition between the two G β subunits. Due to this potential confound of the effect of G β_4 knockdown on G β_1 expression, we next performed an experiment to see if a unique effect of G β_4 could be detected. We knocked down G β_4 in the presence of siRNA against G γ_2 . In the absence of G γ_2 , holo-channel stability was also reduced and was not rescued by knockdown of G β_4 (Figure 3A). This makes it likely that G β_1 and G γ_2 represent the G $\beta\gamma$ pair important for channel maturation. Further, we noted that in the absence of Kir3.2, the stability of the immature forms of Kir3.1 was not affected by knockdown of G $\beta_4\gamma_2$ (Figure 3B). This likely indicates that the functional effect of G $\beta\gamma$ on channel stability requires that Kir3.1 be associated with Kir3.2 and that the “stability clock” modulated by G $\beta\gamma$ begins ticking once the channel is set on a pathway of maturation. Additionally, we tested the effect of knockdown of other G γ subunits on holo-channel stability. Figure 3 indicates that knockdown of G γ_2 resulted in reduced stability for the Kir3.1/Kir3.2 holo-channel. However, knockdown of G γ_4 , G γ_5 , or G γ_7 had much more modest effects compared with control siRNA (Figure 4A). Knockdown efficiencies of individual G γ subunits was assessed using RT-qPCR, as endogenous protein expression levels of G γ isoforms in HEK 293 cells are difficult to visualize using current commercially available anti-G γ antibodies via western blotting (Figure 4B). Changes in expression of the G γ subunits assessed did not alter expression of Kir3.2

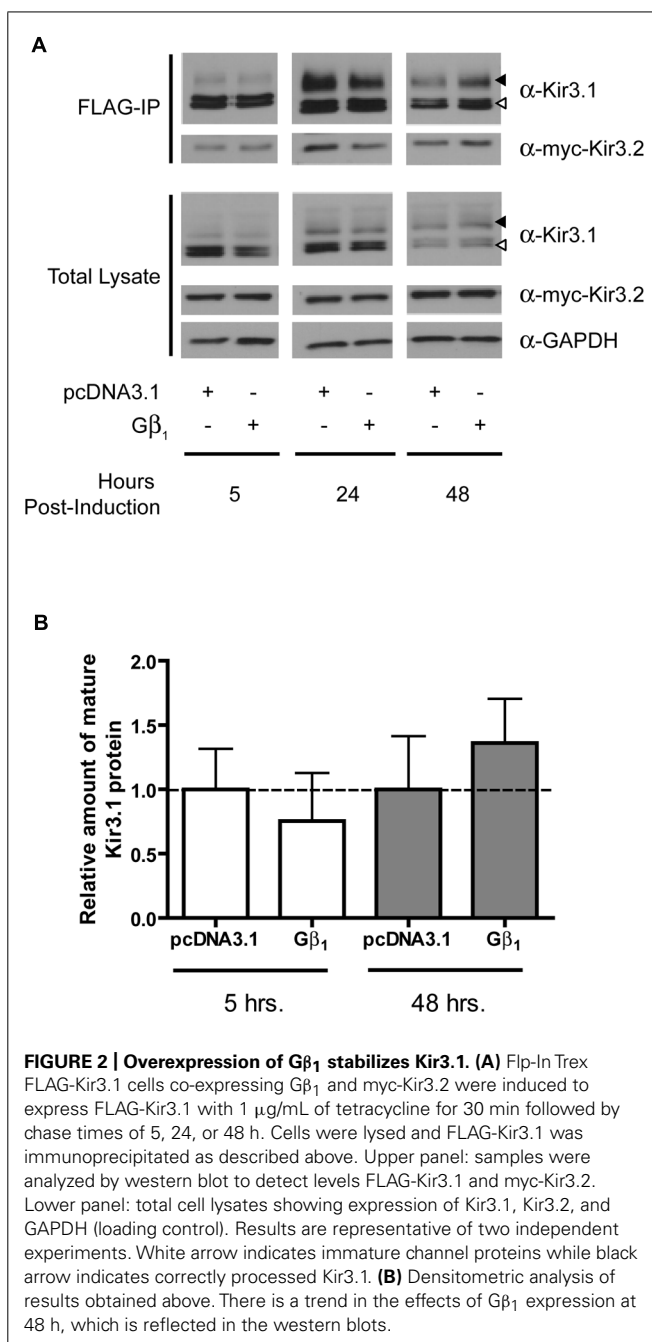


FIGURE 2 | Overexpression of G β_1 stabilizes Kir3.1. (A) Flp-In Trex FLAG-Kir3.1 cells co-expressing G β_1 and myc-Kir3.2 were induced to express FLAG-Kir3.1 with 1 μ g/mL of tetracycline for 30 min followed by chase times of 5, 24, or 48 h. Cells were lysed and FLAG-Kir3.1 was immunoprecipitated as described above. Upper panel: samples were analyzed by western blot to detect levels FLAG-Kir3.1 and myc-Kir3.2. Lower panel: total cell lysates showing expression of Kir3.1, Kir3.2, and GAPDH (loading control). Results are representative of two independent experiments. White arrow indicates immature channel proteins while black arrow indicates correctly processed Kir3.1. **(B)** Densitometric analysis of results obtained above. There is a trend in the effects of G β_1 expression at 48 h, which is reflected in the western blots.

(Figures 3 and 4). Finally, overexpression of G γ_2 resulted in holo-channels with increased stability (Figure 5). Taken together, our results suggest that G $\beta_1\gamma_2$ serve a unique role in channel trafficking that is distinct from their roles in channel activation, which can possibly be subserved by a number of G $\beta\gamma$ dimers with different isoform specificities.

DISCUSSION

Kir3 trafficking has been a topic of great interest to understand mechanisms mammalian cells use to regulate their excitability. Though much is known regarding Kir3 trafficking as it progresses along the initial stages of its synthesis and maturation, the role

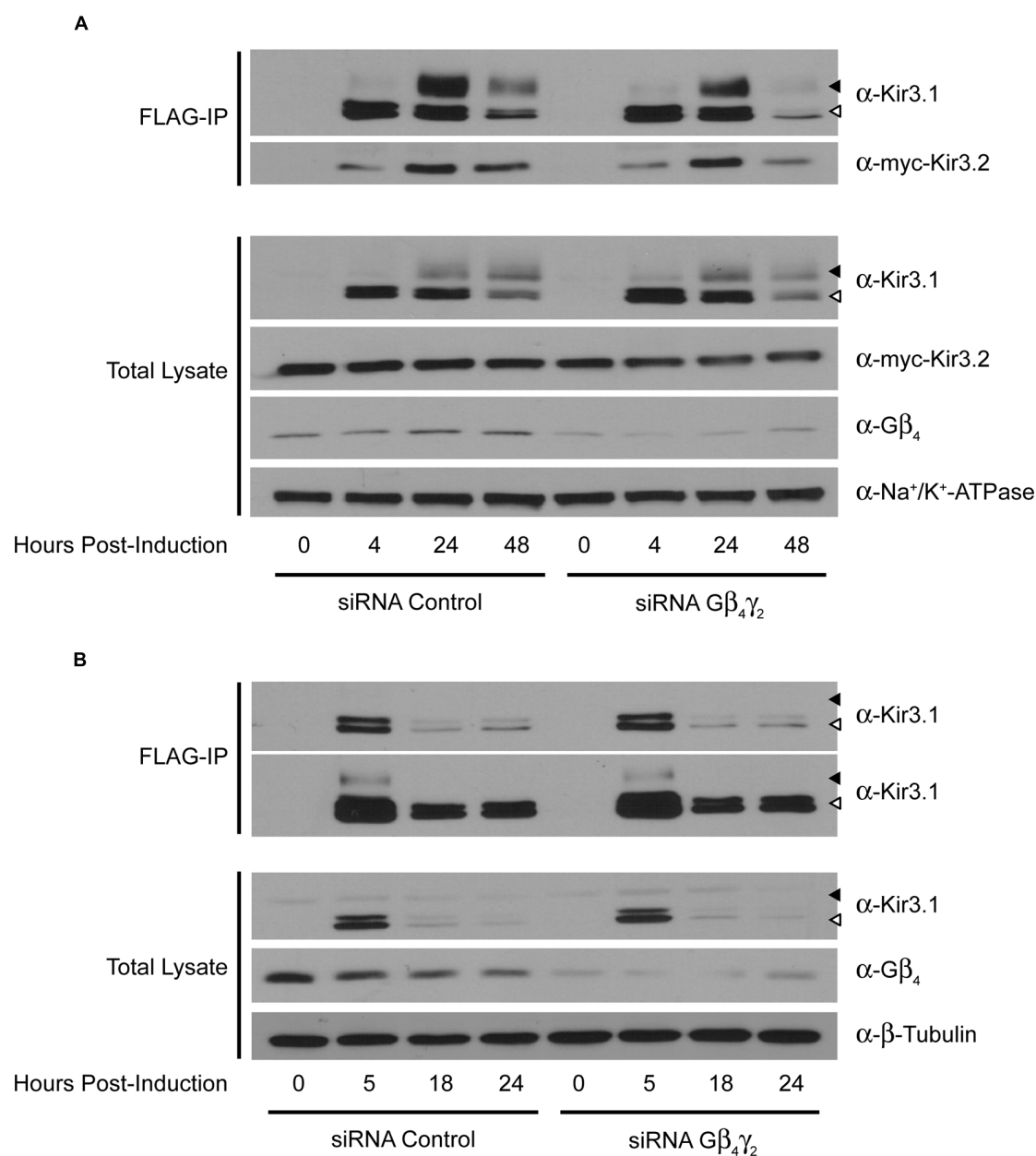
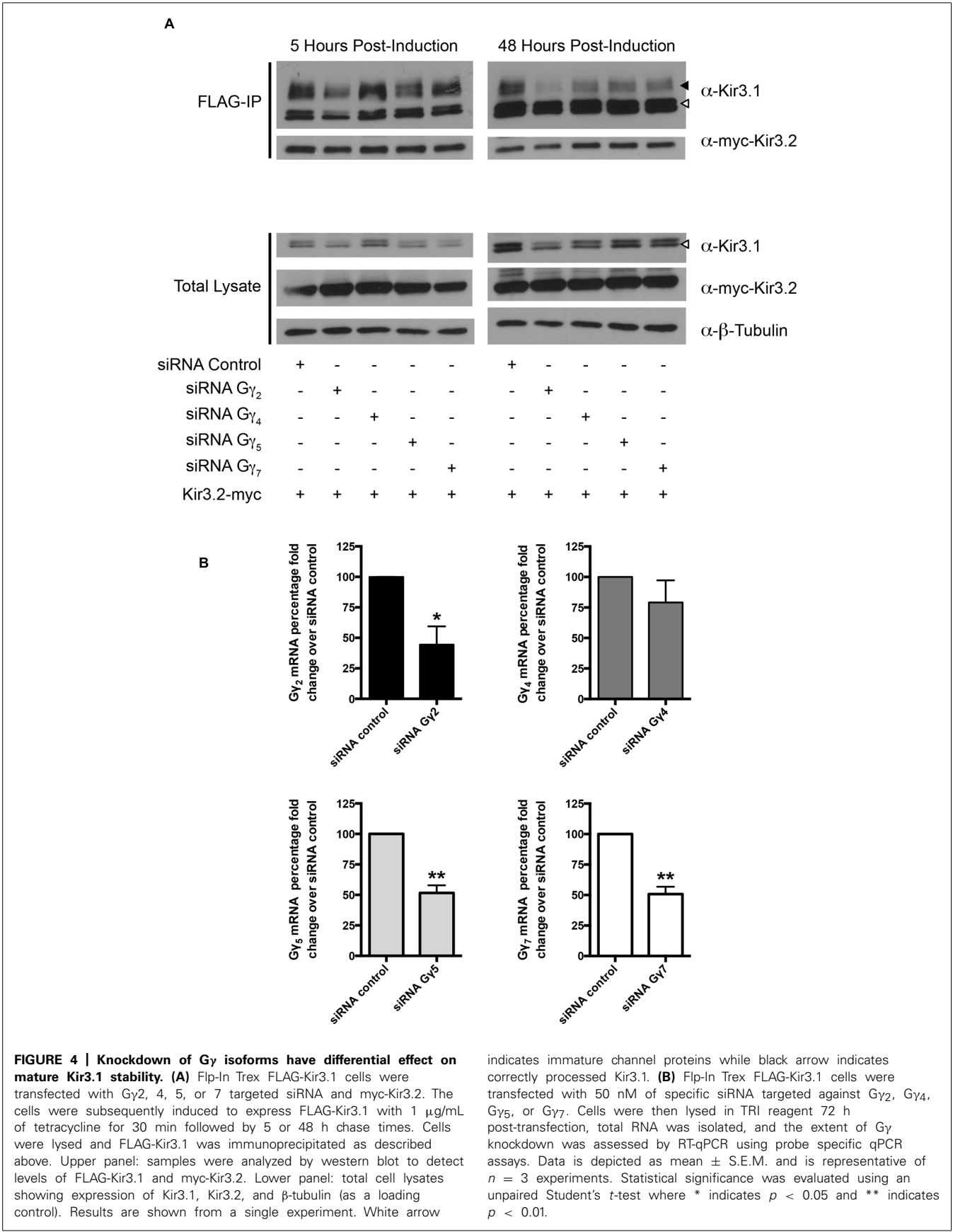


FIGURE 3 | Double knockdown of G β_4 and G γ_2 impairs Kir3.1 stability only in the presence of Kir3.2. (A) Flip-In T_{REX} FLAG-Kir3.1 cells transfected with myc-Kir3.2 and G β_4 /G γ_2 or control siRNA were induced to express FLAG-Kir3.1 with 1 μ g/mL of tetracycline for 30 min and chased for 0, 4, 24, or 48 h. Cells were lysed and FLAG-Kir3.1 was immunoprecipitated as described above. Upper panel: samples were analyzed by western blot to detect levels of FLAG-Kir3.1 and myc-Kir3.2. Lower panel: total cell lysates

showing expression of Kir3.1, Kir3.2, G β_4 , and Na⁺/K⁺ ATPase (loading control). **(B)** Experiment was the same as in panel **(A)** except Kir3.2 was not co-expressed and FLAG-Kir3.1 was chased for 0, 5, 18, or 24 h. Two different exposures are shown to highlight effects on both immature (top) and mature (bottom) forms of the channel, respectively. White arrow indicates immature channel proteins while black arrow indicates correctly processed Kir3.1. Results are from a single experiment.

that early interactions with signaling partners such as G β γ play in channel maturation remain unclear. When expressed alone, recombinant Kir3.1, which contains only one potential site for N-linked glycosylation, migrates as a doublet with a molecular mass of 54 and 56 kDa, with the upper band being the core-glycosylated, immature form of the protein (Krapivinsky et al., 1995a; Kennedy et al., 1999). Upon treatment with either endoglycosidase H, an

enzyme that selectively removes N-linked glycosyl moieties from proteins that have not been processed in the Golgi, or endoglycosidase F, an enzyme that non-selectively removes all N-linked sugar residues, the 56 kDa band is virtually abolished, confirming its residence in the ER (Kennedy et al., 1999). Co-expression of Kir3.4 with Kir3.1, results in a fully mature Kir3.1 subunit capable of being properly glycosylated (Kennedy et al., 1999). The role



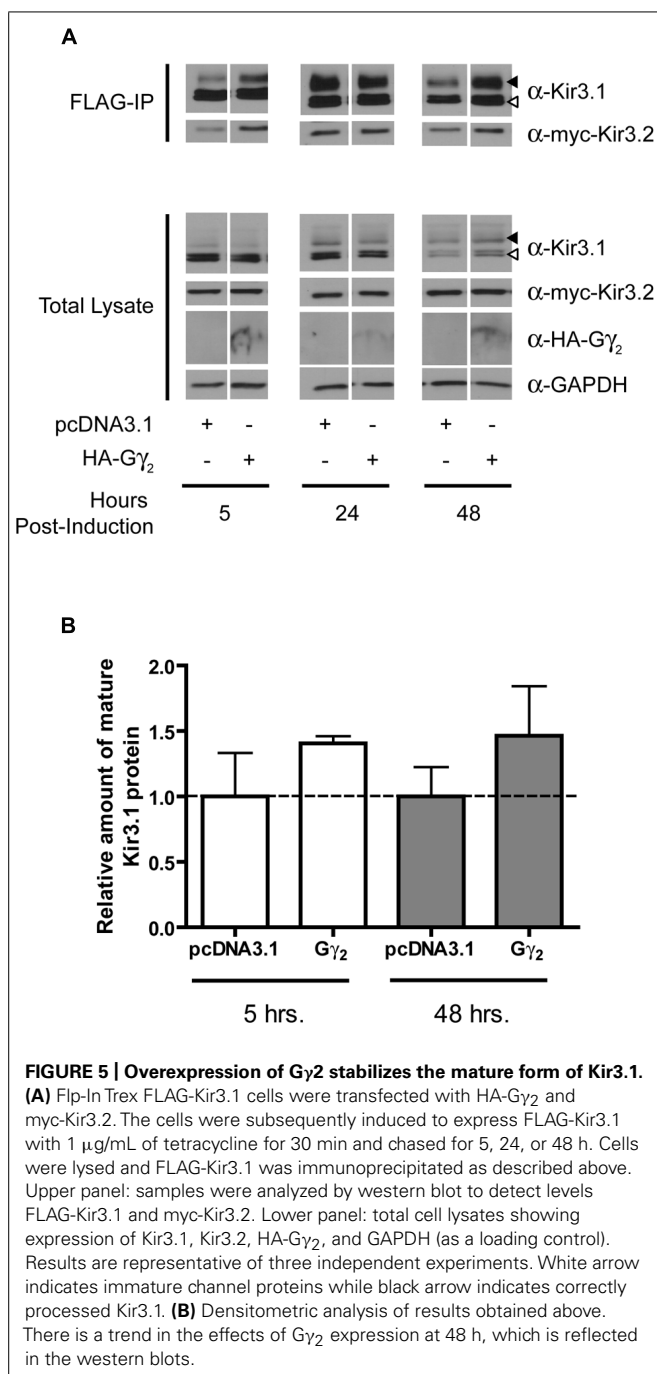


FIGURE 5 | Overexpression of G γ_2 stabilizes the mature form of Kir3.1. (A) Flp-In Trex FLAG-Kir3.1 cells were transfected with HA-G γ_2 and myc-Kir3.2. The cells were subsequently induced to express FLAG-Kir3.1 with 1 μ g/mL of tetracycline for 30 min and chased for 5, 24, or 48 h. Cells were lysed and FLAG-Kir3.1 was immunoprecipitated as described above. Upper panel: samples were analyzed by western blot to detect levels FLAG-Kir3.1 and myc-Kir3.2. Lower panel: total cell lysates showing expression of Kir3.1, Kir3.2, HA-G γ_2 , and GAPDH (as a loading control). Results are representative of three independent experiments. White arrow indicates immature channel proteins while black arrow indicates correctly processed Kir3.1. (B) Densitometric analysis of results obtained above. There is a trend in the effects of G γ_2 expression at 48 h, which is reflected in the western blots.

of Kir3.1 glycosylation may be one of quality control, as Kir3.1 subunits containing a mutation preventing glycosylation can still interact with partner subunits and traffic to the plasma membrane yielding typical current amplitudes (Pabon et al., 2000).

Here we show that a number of maturational steps for Kir3.1 are strictly dependent on the presence of Kir3.2. In the absence of Kir3.2, Kir3.1 subunits remain immature and the loss of G $\beta\gamma$ subunits does not affect this outcome. Though most studies have focused on the role of Kir3.4 in the trafficking of Kir3 channels, Kir3.2 subunits have been found to play a similar vital role in

forming functional Kir3.1-containing channels at the cell surface. Kir3.2 subunits are able to form both homotetramers as well as heterotetramers with either Kir3.1 or Kir3.3 which can then be targeted to the plasma membrane (Jelacic et al., 2000). Using deletion analysis, it was suggested that an ER export signal found at both the N- and C- terminus of Kir3.2 is vital for the cell surface delivery of Kir3.1/3.2 heterotetramers (Ma et al., 2002). Though no well-defined ER export motif has been characterized for Kir3.3, it has been shown to form tetrameric channels with both Kir3.1 and Kir3.2 subunits (Jelacic et al., 1999). Altogether, Kir3 trafficking from the ER appears to be a highly regulated process, with distinct combinations being available at the plasma membrane or targeted for degradation depending on the needs of the cell. Interestingly, when we inhibit the proteasome with MG-132, Kir3.1 can traffic to the cell surface (P.Z. unpublished observations), demonstrating a likely role for ER-associated degradation (ERAD) in the quality control of unpartnered Kir3.1 subunits.

Much attention has been paid to the specificity of G $\beta\gamma$ dimers in the activation of Kir3 channels. To date, G β_5 stands out as an outlier in the G β family in that G β_5 -G γ combinations significantly downregulate channel activation, leading to the suggestion that it acts as a competitive antagonist for Kir3 activation by other G $\beta\gamma$ subunit combinations (Lei et al., 2000, 2003). Interestingly, other G $\beta\gamma$ combinations show similar abilities to activate channels. Some G $\beta\gamma$ selectivity for Kir3.2 has been noted, in that G β subtypes 1–3 preferentially interact with this subunit (Robitaille et al., 2009). Most studies have found that any of the four G β subunits could be expressed with distantly related G γ subunits (i.e., G γ_2 vs. G γ_{11}) and all combinations could bind and activate Kir3 channels with similar efficacy (Lei et al., 2000).

G $\beta_1\gamma_2$, apart from its role in channel opening shared with other G $\beta\gamma$ dimers, seems to play a unique role in preserving maturing channels from degradation as they transit to the cell surface (summarized in Figure 6). Our data indicate that G $\beta_1\gamma_2$ prolongs the lifetime of the Kir3.1/Kir3.2 heterotetramer, although levels of Kir3.2 are not altered *per se*. This may suggest that Kir3.2 homotetramers might be differentially regulated by other factors although under conditions of bulk overexpression, it is difficult to prove this. Placing the other Kir3 isoforms under the control of inducible promoters using our label-free pulse-chase technique will help resolve these issues. It is clear that the roles G $\beta\gamma$ play in Kir3 activity and regulation are quite complex and likely exceed our current understanding. There are numerous potential G $\beta\gamma$ interacting domains on the tetrameric channel and it is evident that not all of these simply underlie channel activation and gating (i.e., G $\beta\gamma$ -associated channels need not be active until they reach the membrane). G $\beta\gamma$ subunits are involved in channel synthesis, trafficking, plasma membrane stability and degradation (Robitaille et al., 2009; Zylbergold et al., 2010), and it is likely that novel roles beyond mere channel activation will be uncovered in the years to come. Here, we have described some approaches that will allow these issues to be resolved with greater clarity.

ACKNOWLEDGMENTS

This study was supported by a Canadian Institutes of Health Research (CIHR) grant to Terence E. Hébert (CIHR; MOP-36379). Terence E. Hébert was a “Chercheur National” of the “Fonds de la

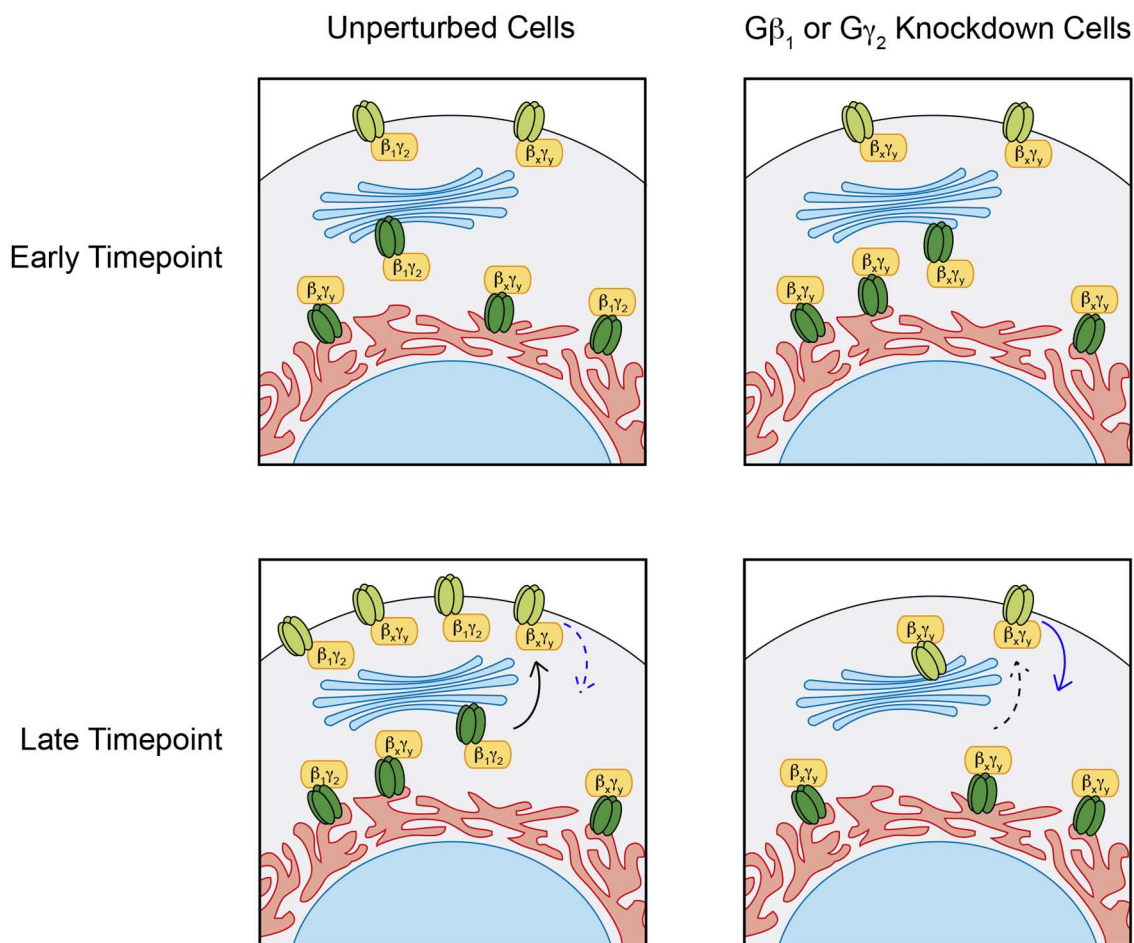


FIGURE 6 | Distinct G $\beta\gamma$ effects on Kir3 stability. Under normal conditions, pulse induction of Kir3.1 expression in the presence of Kir3.2 forms heterotetrameric channels of mature Kir3.1 and Kir3.2 (light green), which can traffic to the cell surface and remain expressed at the plasma membrane for up to 48 h. siRNA mediated knockdown of G β_1 or G γ_2 has negligible effects on immature Kir3.1 channels (dark green) but impairs Kir3.1 maturation and hastens the loss of channel at the cell surface suggesting a stabilizing role for the G $\beta_1\gamma_2$ dimer. These effects of G $\beta_1\gamma_2$

knockdown can be mediated through reduced anterograde trafficking (dashed black arrow) and/or enhanced channel internalization (solid blue arrow). Regardless of the G $\beta\gamma$ pair associated with Kir3 channels in the ER, these are trafficked out to the cell surface. However, those associated with G $\beta_1\gamma_2$ seem to persist longer than those associated with other G $\beta\gamma$ combinations. This suggests that additional functions exist for some G $\beta\gamma$ combinations, independent of their ability to open the channel in response to GPCR stimulation.

Recherche en Santé du Québec” (FRSQ) from 2008–2012. Peter Zylbergold, Rory Sleno, and Shahriar M. Khan were all supported by scholarships from the McGill CIHR Drug Development Training Program. Mark A. Belhke and Ashley M. Jacobi are employed by Integrated DNA Technologies, Inc. (IDT) which offers oligonucleotides for sale similar to some of the compounds described in the manuscript. IDT is however not a publicly traded company and these authors personally do not own any shares/equity in IDT.

REFERENCES

- Ciruela, F., Fernandez-Duenas, V., Sahlholm, K., Fernandez-Alacid, L., Nicolau, J. C., Watanabe, M., et al. (2010). Evidence for oligomerization between GABAB receptors and GIRK channels containing the GIRK1 and GIRK3 subunits. *Eur. J. Neurosci.* 32, 1265–1277. doi: 10.1111/j.1460-9568.2010.07356.x
- David, M., Richer, M., Mamarbachi, A. M., Villeneuve, L. R., Dupré, D. J., and Hébert, T. E. (2006). Interactions between GABA-B1 receptors and Kir 3 inwardly rectifying potassium channels. *Cell. Signal.* 18, 2172–2181. doi: 10.1016/j.cellsig.2006.05.014
- Doupnik, C. A. (2008). GPCR-Kir channel signaling complexes: defining rules of engagement. *J. Recept. Signal Transduct. Res.* 28, 83–91. doi: 10.1080/10799890801941970
- Dupré, D. J., Baragli, A., Rebois, R. V., Ethier, N., and Hébert, T. E. (2007). Signaling complexes associated with adenylyl cyclase II are assembled during their biosynthesis. *Cell. Signal.* 19, 481–489. doi: 10.1016/j.cellsig.2006.07.021
- Dupré, D. J., Robitaille, M., Rebois, R. V., and Hébert, T. E. (2009). The role of G $\beta\gamma$ subunits in the organization, assembly, and function of GPCR signaling complexes. *Annu. Rev. Pharmacol. Toxicol.* 49, 31–56. doi: 10.1146/annurev-pharmtox-061008-103038
- Fowler, C. E., Aryal, P., Suen, K. F., and Slesinger, P. A. (2007). Evidence for association of GABA(B) receptors with Kir3 channels and regulators of G protein signaling (RGS4) proteins. *J. Physiol.* 580, 51–65. doi: 10.1113/jphysiol.2006.123216
- He, C., Yan, X., Zhang, H., Mirshahi, T., Jin, T., Huang, A., et al. (2002). Identification of critical residues controlling G protein-gated inwardly rectifying K⁺ channel

- activity through interactions with the $\beta\gamma$ subunits of G proteins. *J. Biol. Chem.* 277, 6088–6096. doi: 10.1074/jbc.M104851200
- He, C., Zhang, H., Mirshahi, T., and Logothetis, D. E. (1999). Identification of a potassium channel site that interacts with G protein $\beta\gamma$ subunits to mediate agonist-induced signaling. *J. Biol. Chem.* 274, 12517–12524. doi: 10.1074/jbc.274.18.12517
- Huang, C. L., Jan, Y. N., and Jan, L. Y. (1997). Binding of the G protein $\beta\gamma$ subunit to multiple regions of G protein-gated inward-rectifying K⁺ channels. *FEBS Lett.* 405, 291–298. doi: 10.1016/S0014-5793(97)00197-X
- Huang, C. L., Slesinger, P. A., Casey, P. J., Jan, Y. N., and Jan, L. Y. (1995). Evidence that direct binding of G $\beta\gamma$ to the GIRK1 G protein-gated inwardly rectifying K⁺ channel is important for channel activation. *Neuron* 15, 1133–1143. doi: 10.1016/0896-6273(95)90101-9
- Inanobe, A., Morishige, K. I., Takahashi, N., Ito, H., Yamada, M., Takumi, T., et al. (1995). G $\beta\gamma$ directly binds to the carboxyl terminus of the G protein-gated muscarinic K⁺ channel, GIRK1. *Biochem. Biophys. Res. Commun.* 212, 1022–1028. doi: 10.1006/bbrc.1995.2072
- Ivanina, T., Rishal, I., Varon, D., Mullner, C., Frohnwieser-Steinecke, B., Schreibmayer, W., et al. (2003). Mapping the G $\beta\gamma$ -binding sites in GIRK1 and GIRK2 subunits of the G protein-activated K⁺ channel. *J. Biol. Chem.* 278, 29174–29183. doi: 10.1074/jbc.M304518200
- Jelacic, T. M., Kennedy, M. E., Wickman, K., and Clapham, D. E. (2000). Functional and biochemical evidence for G-protein-gated inwardly rectifying K⁺ (GIRK) channels composed of GIRK2 and GIRK3. *J. Biol. Chem.* 275, 36211–36216. doi: 10.1074/jbc.M007087200
- Jelacic, T. M., Sims, S. M., and Clapham, D. E. (1999). Functional expression and characterization of G-protein-gated inwardly rectifying K⁺ channels containing GIRK3. *J. Membr. Biol.* 169, 123–129. doi: 10.1007/s002329900524
- Kennedy, M. E., Nemec, J., Corey, S., Wickman, K., and Clapham, D. E. (1999). GIRK4 confers appropriate processing and cell surface localization to G-protein-gated potassium channels. *J. Biol. Chem.* 274, 2571–2582. doi: 10.1074/jbc.274.4.2571
- Khan, S. M., Sleno, R., Gora, S., Zylbergold, P., Laverdure, J. P., Labbe, J. C., et al. (2013). The expanding roles of G $\beta\gamma$ subunits in G protein-coupled receptor signaling and drug action. *Pharmacol. Rev.* 65, 545–577. doi: 10.1124/pr.111.005603
- Krapivinsky, G., Gordon, E. A., Wickman, K., Velimirovic, B., Krapivinsky, L., and Clapham, D. E. (1995a). The G-protein-gated atrial K⁺ channel IKACH is a heteromultimer of two inwardly rectifying K⁺-channel proteins. *Nature* 374, 135–141. doi: 10.1038/374135a0
- Krapivinsky, G., Krapivinsky, L., Wickman, K., and Clapham, D. E. (1995b). G $\beta\gamma$ binds directly to the G protein-gated K⁺ channel, IKACH. *J. Biol. Chem.* 270, 29059–29062. doi: 10.1074/jbc.270.49.29059
- Krumins, A. M., and Gilman, A. G. (2006). Targeted knockdown of G protein subunits selectively prevents receptor-mediated modulation of effectors and reveals complex changes in non-targeted signaling proteins. *J. Biol. Chem.* 281, 10250–10262. doi: 10.1074/jbc.M511551200
- Lavigne, N., Ethier, N., Oak, J. N., Pei, L., Liu, F., Trieu, P., et al. (2002). G protein-coupled receptors form stable complexes with inwardly rectifying potassium channels and adenylyl cyclase. *J. Biol. Chem.* 277, 46010–46019. doi: 10.1074/jbc.M205035200
- Lei, Q., Jones, M. B., Talley, E. M., Garrison, J. C., and Bayliss, D. A. (2003). Molecular mechanisms mediating inhibition of G protein-coupled inwardly-rectifying K⁺ channels. *Mol. Cells* 15, 1–9.
- Lei, Q., Jones, M. B., Talley, E. M., Schrier, A. D., McIntire, W. E., Garrison, J. C., et al. (2000). Activation and inhibition of G protein-coupled inwardly rectifying potassium (Kir3) channels by G protein $\beta\gamma$ subunits. *Proc. Natl. Acad. Sci. U.S.A.* 97, 9771–9776. doi: 10.1073/pnas.97.17.9771
- Logothetis, D. E., Kurachi, Y., Galper, J., Neer, E. J., and Clapham, D. E. (1987). The $\beta\gamma$ subunits of GTP-binding proteins activate the muscarinic K(+) channel in heart. *Nature* 325, 321–326. doi: 10.1038/325321a0
- Ma, D., Zerangue, N., Raab-Graham, K., Fried, S. R., Jan, Y. N., and Jan, L. Y. (2002). Diverse trafficking patterns due to multiple traffic motifs in G protein-activated inwardly rectifying potassium channels from brain and heart. *Neuron* 33, 715–729. doi: 10.1016/S0896-6273(02)00614-1
- Nikolov, E. N., and Ivanova-Nikolova, T. T. (2004). Coordination of membrane excitability through a GIRK1 signaling complex in the atria. *J. Biol. Chem.* 279, 23630–23636. doi: 10.1074/jbc.M312861200
- Pabon, A., Chan, K. W., Sui, J. L., Wu, X., Logothetis, D. E., and Thornhill, W. B. (2000). Glycosylation of GIRK1 at Asn119 and ROMK1 at Asn117 has different consequences in potassium channel function. *J. Biol. Chem.* 275, 30677–30682. doi: 10.1074/jbc.M005338200
- Rebois, R. V., Robitaille, M., Galès, C., Dupré, D. J., Baragli, A., Trieu, P., et al. (2006). Heterotrimeric G proteins form stable complexes with adenylyl cyclase and Kir3.1 channels in living cells. *J. Cell Sci.* 119, 2807–2818. doi: 10.1242/jcs.03021
- Richard-Lalonde, M., Nagi, K., Audet, N., Sleno, R., Amraei, M., Hogue, M., et al. (2013). Conformational dynamics of Kir3.1/Kir3.2 channel activation via δ -opioid receptors. *Mol. Pharmacol.* 83, 416–428. doi: 10.1124/mol.112.081950
- Riven, I., Iwanir, S., and Reuveny, E. (2006). GIRK channel activation involves a local rearrangement of a preformed G protein channel complex. *Neuron* 51, 561–573. doi: 10.1016/j.neuron.2006.08.017
- Robitaille, M., Ramakrishnan, N., Baragli, A., and Hébert, T. E. (2009). Intracellular trafficking and assembly of specific Kir3 channel/G protein complexes. *Cell. Signal.* 21, 488–501. doi: 10.1016/j.cellsig.2008.11.011
- Zylbergold, P., Ramakrishnan, N., and Hébert, T. (2010). The role of G proteins in assembly and function of Kir3 inwardly rectifying potassium channels. *Channels (Austin)* 4, 411–421. doi: 10.4161/chan.4.5.13327
- Zylbergold, P., Sleno, R., and Hébert, T. E. (2013). A novel, radiolabel-free pulse chase strategy to study Kir3 channel ontogeny. *J. Recept. Signal. Transduct. Res.* 33, 144–152. doi: 10.3109/10799893.2013.764898

Conflict of Interest Statement: The authors declare that the research was conducted in the absence of any commercial or financial relationships that could be construed as a potential conflict of interest.

Received: 11 February 2014; accepted: 25 March 2014; published online: 14 April 2014.
 Citation: Zylbergold P, Sleno R, Khan SM, Jacobi AM, Belhke MA and Hébert TE (2014) Kir3 channel ontogeny – the role of G $\beta\gamma$ subunits in channel assembly and trafficking. *Front. Cell. Neurosci.* 8:108. doi: 10.3389/fncel.2014.00108
 This article was submitted to the journal *Frontiers in Cellular Neuroscience*.
 Copyright © 2014 Zylbergold, Sleno, Khan, Jacobi, Belhke and Hébert. This is an open-access article distributed under the terms of the Creative Commons Attribution License (CC BY). The use, distribution or reproduction in other forums is permitted, provided the original author(s) or licensor are credited and that the original publication in this journal is cited, in accordance with accepted academic practice. No use, distribution or reproduction is permitted which does not comply with these terms.



Kir3 channel signaling complexes: focus on opioid receptor signaling

Karim Nagi^{1,2} and Graciela Pineyro^{1,2,3*}

¹ Département de Pharmacologie, Faculté de Médecine, Université de Montréal, Montréal, QC, Canada

² Centre de Recherche du CHU Sainte-Justine, Montréal, QC, Canada

³ Département de Psychiatrie, Faculté de Médecine, Université de Montréal, Montréal, QC, Canada

Edited by:

Leigh Anne Swayne, University of Victoria, Canada

Reviewed by:

Lin Tian, University of California, Davis, USA

Nathan Dascal, Tel Aviv University, Israel

*Correspondence:

Graciela Pineyro, Department of Psychiatry, Centre de Recherche du CHU Ste-Justine, University of Montreal, 3175, Côte Ste-Catherine, Bureau 2722, Montréal, QC H3T 1C5, Canada
e-mail: graciela.pineyro.filpo@umontreal.ca

Opioids are among the most effective drugs to treat severe pain. They produce their analgesic actions by specifically activating opioid receptors located along the pain perception pathway where they inhibit the flow of nociceptive information. This inhibition is partly accomplished by activation of hyperpolarizing G protein-coupled inwardly-rectifying potassium (GIRK or Kir3) channels. Kir3 channels control cellular excitability in the central nervous system and in the heart and, because of their ubiquitous distribution, they mediate the effects of a large range of hormones and neurotransmitters which, upon activation of corresponding G protein-coupled receptors (GPCRs) lead to channel opening. Here we analyze GPCR signaling via these effectors in reference to precoupling and collision models. Existing knowledge on signaling bias is discussed in relation to these models as a means of developing strategies to produce novel opioid analgesics with an improved side effects profile.

Keywords: GIRK, opioid, signaling, analgesia, bias, signaling complexes, functional selectivity, allosteric modulation

Opioids produce their actions via the activation of μ (MOR), δ (DOR), and κ (KOR) receptors (Pert and Snyder, 1973; Simon et al., 1973) all of which couple to heterotrimeric Gi/o proteins. As such they share adenylyl cyclase, Phospholipase C β [PLC β , N-type Ca²⁺ (Cav2.2)] channels and G-protein coupled inward rectifier K⁺ channels (GIRKs or Kir3 channels) as canonical G α and G $\beta\gamma$ effectors. The two channel effectors prominently mediate analgesic effects of opioids. For example, studies in rodents have shown that activation of MORs on small, unmyelinated nociceptors (Scherrer et al., 2009; Heinke et al., 2011; Bardoni et al., 2014) contribute to the analgesic effects of morphine (Wei et al., 1996; Andrade et al., 2010), and this is done via inhibition of N-type Ca²⁺ channels that control neurotransmitter release from these primary afferents (Glaum et al., 1994; Wrigley et al., 2010). Kir3 channel contribution to opioid analgesia has also been demonstrated in animal models (Ikeda et al., 2000; Mitrovic et al., 2003; Marker et al., 2005), and their relevance in the clinical response to opioid analgesics has been further confirmed by

gene linkage analyses (Nishizawa et al., 2009; Lotsch et al., 2010; Bruehl et al., 2013). In addition, the use of genetically modified mice lacking different channel subunits has further established activation of Kir3 channels as a pervasive analgesic mechanism which, in addition to opioids, also mediates pain modulation by $\alpha 2$ adrenergic, muscarinic, GABA $_B$ and cannabinoid receptor ligands (Blednov et al., 2003; Mitrovic et al., 2003). From this perspective the development of direct Kir3 channel activators may be considered a promising strategy for the development of novel analgesics. However, enthusiasm for this particular approach has remained limited given the possibility of widespread side-effects associated with administration of direct channel openers (Lujan et al., 2014). Indeed, these would result from the great variety of physiological responses mediated by Kir3 channels, including heart frequency control (Wickman et al., 1998; Bettahi et al., 2002), memory (Wickman et al., 2000), learning (Wickman et al., 2000; Cooper et al., 2012), as well as their participation in different pathological conditions including development of seizures (Signorini et al., 1997), generation of anxiety states (Blednov et al., 2001; Pravetoni and Wickman, 2008) and contribution to abnormal plasticity by drugs of abuse (Padgett et al., 2012; Hearing et al., 2013). Consequently, the prevailing strategy for engaging Kir3-mediated analgesia has remained the activation of pain-modulating GPCRs (McAllister et al., 1999; Lujan et al., 2014). Among them MORs, DORs and KORs all three mediate effective analgesia but display different side effects that distinctively limit their therapeutic use (Kieffer and Gaveriaux-Ruff, 2002; Bruchas and Chavkin, 2010; Gaveriaux-Ruff and Kieffer, 2011). Here we will summarize Kir3 channel contribution to desired and undesired responses of opioid analgesics and address

Abbreviations: GIRK, G protein activated inward rectifier K⁺; GPCRs, G protein-coupled receptors; DORs, Delta opioid receptors; MORs, Mu opioid receptors; KORs, Kappa opioid receptors; PLC, Phospholipase C; GABA, Gamma-aminobutyric acid; DRG, dorsal root ganglion; DAMGO, [D-Ala(2),N-Me-Phe(4),Gly(5)-ol]-enkephalin; KCNJ6, Inwardly-rectifying potassium channel, subfamily J, member 6; KCNJ3, Inwardly-rectifying potassium channel, subfamily J, member 3; 5-HT, 5-hydroxytryptamine; MAPK, Mitogen-activated protein kinases; $\bar{\text{barr}}$, $\bar{\text{barrestin}}$; cAMP, Cyclic adenosine monophosphate; VTA, Ventral tegmental area; PIP2, Phosphatidylinositol 4,5-bisphosphate; GDP, Guanosine diphosphate; GTP, Guanosine triphosphate; PSD95, Postsynaptic density protein 95; SAP97, Synapse-associated protein 97; FRET, Fluorescence resonance energy transfer; BRET, Bioluminescence resonance energy transfer; PC12, Neuron-like pheochromocytoma.

the question of whether biasing opioid signaling toward these effectors could help develop better opioid analgesics with a reduced side effects profile.

Kir3 CHANNEL SIGNALING AND OPIOID-DEPENDENT ANALGESIA

Kir3 channels are formed by tetrameric association of four different subunits (Kir3.1-3.4). Although all four of them are expressed in peripheral (Gao et al., 2007) and central nervous system (Wickman et al., 2000; Saenz Del Burgo et al., 2008; Fernandez-Alacid et al., 2011), neural channels are most frequently formed by association of Kir3.1, 3.2 and 3.3 subunits (Liao et al., 1996; Hibino et al., 2010; Luscher and Slesinger, 2010). The subunit combination that forms the channel will depend on the neuronal population involved (Inanobe et al., 1999; Cruz et al., 2004) and the cellular compartment (Koyrakh et al., 2005; Fernandez-Alacid et al., 2009) in which channels are found. Nonetheless, Kir3.1/3.2 heterotetramers are considered prototypical neuronal channels.

Kir3 channel contribution to opioid analgesia was initially suggested by the fact that mice carrying a missense mutation which renders Kir3.2 subunits insensitive to G protein activation (Patil et al., 1995; Navarro et al., 1996) displayed reduced analgesic responses to morphine (Ikeda et al., 2000, 2002). These observations were subsequently confirmed using null mice for different subunits (Mitrovic et al., 2003; Marker et al., 2005), which allowed to also implicate Kir3.1 (Marker et al., 2004) and Kir3.3 (Marker et al., 2002) in pain modulation. Knock-out of Kir3.2 and 3.3 was shown to interfere with morphine's ability to prolong avoidance behavior in the hot plate test. Since this response involves supraspinal integration, it can be concluded that both subunits contribute to mechanisms of opioid analgesia at this level (Marker et al., 2002; Mitrovic et al., 2003). Possible sites of supraspinal Kir3-mediated analgesia may include thalamus and limbic cortex, both of which express Kir3.1, 3.2 and 3.3 subunits (Saenz Del Burgo et al., 2008; Fernandez-Alacid et al., 2011) as well as opioid receptors (Le Merrer et al., 2009). The midbrain periaqueductal gray seems less likely since in this nucleus opioid actions are primarily presynaptic reducing neurotransmitter release via a mechanism that involves phospholipase A2, arachidonic acid and 12-lipoxygenase, which leads to modulation of voltage-dependent potassium channels (Vaughan and Christie, 1997; Vaughan et al., 1997).

Genetically engineered mice lacking Kir3.1 or Kir3.2 subunits also display reduced responses to intrathecal administration of morphine in the tail flick test (Marker et al., 2004, 2005) implicating both subunits in spinal mechanisms of opioid analgesia. This interpretation is supported by reports locating Kir3.1 and Kir3.2 subunits to lamina II interneurons that co-express μ opioid receptors (Marker et al., 2006). Functional studies also indicated that silencing of Kir3.1 or Kir3.2 subunits, or intrathecal infusion of Kir3 channel blocker tertiapin-Q interfered with the analgesic response by MOR and DOR agonists administered by the same route (Marker et al., 2005). In contrast, Kir3.3 ablation was without effect on the analgesic response elicited by intrathecal morphine (Marker et al., 2004), arguing against its significant contribution at this level. The latter observation is also in

keeping with immunohistological studies which reported absence of Kir3.3 labeling in the dorsal horn (Marker et al., 2004).

In addition to their participation in acute opioid analgesia, spinal Kir3 channels seem to mediate neuroadaptations that modulate responsiveness to opioids in conditions such as inflammatory or cancer-related pain. This possibility is particularly suggested by reports indicating that carrageenan-inflammation (Gonzalez-Rodriguez et al., 2010) and bone cancer (Gonzalez-Rodriguez et al., 2012) enhance the inhibitory effect of Kir3 channel blocker tertiapin-Q on analgesia induced by intrathecal administration of morphine.

Apart from brain and spinal cord, opioid receptors are also present in sensory neurons of the dorsal root ganglion (DRG) (Li et al., 1998; Gendron et al., 2006; Wu et al., 2008; Wang et al., 2010) and are transported to peripheral terminals where they mediate analgesic actions of peripherally injected opioids (Hassan et al., 1993; Obara et al., 2009; Vadivelu et al., 2011). Transcripts for Kir3.1/3.2 subunits have been detected in human DRGs and in rat nociceptors, but not in mice (Gao et al., 2007; Nockemann et al., 2013). This distribution parallels differences in species sensitivity to peripheral administration of opioids suggesting that when expressed, DRG Kir3 subunits actively participate in opioid analgesia. Indeed, intraplantar injection of MOR agonists does not produce analgesia in mice (Nockemann et al., 2013) but effectively mitigates pain in inflammatory or neuropathic rat models (Stein et al., 1989; Obara et al., 2009; Chung et al., 2013; Nockemann et al., 2013) as well as postoperative and arthritic pain in humans (Kalso et al., 2004; Vadivelu et al., 2011). Moreover, the active contribution of Kir3.2 channels to peripheral opioid analgesia has now been experimentally established using transgenic mice genetically engineered to express these subunits in sensory neurons. Unlike their wild-type counterparts, the latter display an analgesic response to plantar application of MOR agonist DAMGO (Nockemann et al., 2013).

It is important to bear in mind that most of the evidence analyzed thus far links Kir3 channel function to opioid analgesia in animal models. However, the latter have shown somewhat limited success in identifying and validating analgesic targets of clinical relevance (Mogil, 2009). Hence, from this perspective, any evidence linking Kir3 channels to therapeutic response in humans is of specific interest. At least three studies have now shown that variations in the gene coding for Kir3.2 subunits (*KCNJ6*) influence opioid dose requirements for both acute management of postoperative pain (Nishizawa et al., 2009; Bruehl et al., 2013) and for pain control in chronic patients (Lotsch et al., 2010). Similar assessment of Kir3.1 (*KCNJ3*) variations showed no effect (Bruehl et al., 2013).

OPIOID SIDE EFFECTS AND Kir3 CHANNEL SIGNALING

In spite of the established analgesic efficacy of MOR, DOR, and KOR agonists, activation of the different receptor subtypes results in a distinct set of side effects which limit therapeutic application of their agonists. Constipation, nausea, respiratory depression, tolerance, dependence, and abuse are among the most common undesired effects of clinically available MOR agonists (Ballantyne and Shin, 2008; Morgan and Christie, 2011). Many of these undesired actions, particularly respiratory depression (Cheng et al.,

1993; Gallantine and Meert, 2005), gastrointestinal side effects (Tavani et al., 1990; Gallantine and Meert, 2005; Feng et al., 2006) and physical dependence (Cowan et al., 1988; Codd et al., 2009) are less severe or absent with DOR agonists. Moreover, although DORs and MORs are both involved in reward response to physiological stimuli (Charbogne et al., 2014), DORs are not directly involved in assigning reward value to stimuli but instead facilitate predictive learning and influence the choice of action in face of contingencies that involve reward (Laurent et al., 2012). In keeping with this functional profile, DOR agonists do not facilitate intracranial self-stimulation (Do Carmo et al., 2009), are not discriminated as morphine substitutes (Gallantine and Meert, 2005) and do not display reinforcing properties in non-human primates (Banks et al., 2011). Nonetheless, despite these advantages, potential for tolerance (Pradhan et al., 2010; Audet et al., 2012) remains a limitation for long-term use of DOR agonists, as does their propensity to produce hippocampal hyperexcitability that may lead to seizures. The latter are produced both by DOR (De Sarro et al., 1992; Broom et al., 2002; Jutkiewicz et al., 2005) and MOR agonists (Drake et al., 2007). In the specific case of DOR agonists, hyperexcitability is brief and non-lethal. Moreover, seizures are rare at analgesic doses (Jutkiewicz et al., 2006), they do not appear with all ligands (Le Bourdonnec et al., 2008; Saitoh et al., 2011) and can be suppressed by controlling the rate of agonist administration (Jutkiewicz et al., 2005). Thus, overall, side effects of DOR agonists are considerably milder as compared to those of MORs, and their proven efficacy in chronic pain management make DORs especially attractive as targets for the development of novel analgesics (Gaveriaux-Ruff and Kieffer, 2011). This notion is further reinforced by the fact that DOR agonists display antidepressant properties (Chu Sin Chung and Kieffer, 2013) which could be of additional benefit in controlling negative affect, frequently associated with prolonged pain syndromes (Goldenberg, 2010). Unlike DOR agonists, KOR-mediated analgesia is typically associated with stress, depression, and dysphoria (Bruchas and Chavkin, 2010; Van't Veer and Carlezon, 2013) which, together with their tendency to induce tolerance (McLaughlin et al., 2004; Xu et al., 2004), would make these ligands less attractive for the treatment of chronic pain.

Kir3 channel function has been associated with some of the undesired effects of opioid analgesics. For example, reduced GABAergic activity in hippocampal dentate gyrus increases the excitability of glutamatergic granule cells and may reduce the threshold for seizures (Drake et al., 2007). MORs and DORs agonists silence hippocampal GABAergic interneurons by a mechanism that involves both Kir3 (Luscher et al., 1997) and voltage-dependent K^+ channels (Wimpey and Chavkin, 1991; Moore et al., 1994), explaining their documented tendency to produce seizures (Drake et al., 2007). MORs agonists also enhance excitability and firing activity of dopaminergic neurons of the ventral tegmental area (Gysling and Wang, 1983), and do so by hyperpolarization of local interneurons (Johnson and North, 1992; Bonci and Williams, 1997). Like in hippocampus, disinhibition is mediated through Kir3 channel activation (Luscher et al., 1997) and its consequence is the enhanced release of dopamine in corticolimbic areas which is thought to facilitate compulsive behaviors characteristic of addiction (Luscher and Ungless, 2006).

Finally, Kir3 channel activation by KORs modulates firing activity of dorsal raphe 5-HT neurons (Bruchas et al., 2007; Lemos et al., 2012). Dynorphin release during repeated stress exposure produces sustained activation of these receptors driving p38 α -MAPK activity and subsequent Kir3.1 subunit phosphorylation (Lemos et al., 2012). As a consequence 5-HT neuron firing activity becomes deregulated, possibly contributing to dysphoric effects of uncontrollable stress and to aversive actions of KOR agonists (Bruchas et al., 2007).

Additional undesired actions of opioids analgesics involve signaling effectors other than Kir3 channels. For example, constipation and respiratory depression have been associated with β arrestin (β arr)-mediated signaling by MOR agonists (Raehal et al., 2005; Dewire et al., 2013). The use of β arr-knockout mice has also suggested that DOR agonist tendency to induce seizures may involve this regulatory protein, and biased agonists that fail to recruit β arrs are being developed as a means of further improving the side effects profile of analgesics acting at this receptor subtype. Kir3-independent side effects also include compensatory changes in the cyclase pathway (cyclase superactivation). These are triggered by sustained inhibition of cAMP production (Christie, 2008) and have been shown to contribute to physical dependence (Han et al., 2006; Cao et al., 2010; Yang et al., 2014) and analgesic tolerance of opioid agonists (Javed et al., 2004; He and Whistler, 2007; Bobeck et al., 2014).

Data summarized thus far indicate that undesired actions of opioid ligands segregate according to receptor subtype, and within each subtype, desired and unwanted effects are not all necessarily mediated by the same effectors. Thus, undesired actions of DOR and KOR-activating analgesics are less than those of MOR ligands, and among the former, the presence of antidepressant properties and lack of dysphoric actions makes DOR specifically interesting as putative targets for the management of chronic pain syndromes (Gaveriaux-Ruff and Kieffer, 2011; Pradhan et al., 2011). Tolerance however, remains a drawback that limits further development of DOR-acting analgesics. This limitation could be, at least, partly addressed by taking advantage of biased signaling since effectors that mediate cellular tolerance and analgesia seem partly segregated. Indeed, as detailed above, while analgesic actions are generally mediated via modulation of channel effectors, adaptations of the cAMP cascade seem to account for at least some of the manifestations of tolerance (Javed et al., 2004; He and Whistler, 2007; Bobeck et al., 2014). Based on these observations, opioid ligands that specifically bias their pharmacological stimulus toward channel effectors could conceivably conserve analgesic properties while displaying reduced potential for tolerance, particularly the component that depends on cyclase adaptations. In the following sections, we will consider possible strategies to direct opioid signaling toward Kir3 channels. However, before doing so it is worth revising the events that lead to channel activation.

Kir3 CHANNEL ACTIVATION VIA GPCRS

It is now well established that Kir3 channels open via direct interaction with G $\beta\gamma$ dimers that are released from pertussis toxin sensitive heterotrimeric Gi/o proteins upon receptor activation (Logothetis et al., 1987; Wickman et al., 1994; Raveh

et al., 2009). G β γ activates the channel as long as the surface that contacts Kir3 subunits does not re-associate with G $\alpha_{i/o}$ -GDP, which results in signal termination (Schreibmayer et al., 1996). Biochemical, mutational and nuclear magnetic resonance studies have mapped several interaction sites for G β γ on all four channel subunits. These sites are summarized in **Table 1** and those in the C-terminal cytosolic domain have been largely confirmed

in recent crystallization of a complex formed by G β 1 γ 2 and the Kir3.2 homotetramer (Whorton and MacKinnon, 2013). Crystals of the complex revealed that the contact area between G β and the channel is approximately 700Å². The contact zone on channel subunits corresponds to the interface of two contiguous cytosolic domains encompassing β sheets/loops β K, β L, β M, and β N on one subunit and β D- β E elements from the adjacent one. The

Table 1 | G β γ interaction sites on different Kir3 subunits.

	Interaction sites	Methodology	References
Kir3.1	N-TERMINAL		
	N-terminal hydrophobic domain	Coaffinity precipitation	Huang et al., 1995
	Amino acids M1-N83	GST pull-down	Kunkel and Peralta, 1995
	Amino acids Q34-I86	Coprecipitation	Huang et al., 1997
	G β 1 γ 2 binds N-terminal domain	IP* and GST pull-down	Kawano et al., 2007
	Amino acids R45, F46, V47, N50, G51, N54	NMR*	Yokogawa et al., 2011
	C-TERMINAL		
	Amino acids V273-P462	Coaffinity precipitation	Huang et al., 1995
	Amino acids T290-Y356	GST pull-down	Huang et al., 1995
	Amino acids E318-P374 and D390-P462	Coprecipitation	Huang et al., 1997
	Amino acids M364-R383	G β γ binding assay	Krapivinsky et al., 1998
	Amino acids F181-G254 and to a lesser extent G254-P370	GST pull-down	Ivanina et al., 2003
	G β 1 γ 2 binds C-terminal domain	IP* and GST pull-down	Kawano et al., 2007
	Cytoplasmic pore with a binding site composed by amino acids A226, S235, R236, Q237, T238, E240, G241, E242, F243, L244, V253, G254, F255, S256, A259, D260, Q261, S278, T290, G307, M308, T317, E318, D319, E320, L333, E334, G336, F337, F338, K339, D341, Y342, S343, Q344, A347, T348, E350, and V358	NMR*	Yokogawa et al., 2011
Kir3.2	N-TERMINAL		
	N-terminal domain	Coprecipitation	Huang et al., 1997
	Amino acids I46-L96	GST pull-down	Ivanina et al., 2003
	G β 1 γ 2 binds amino acids T2-L96 with W91-L96 as crucial residues for G β 1 γ 2 binding	IP* and GST pull-down	Kawano et al., 2007
	C-TERMINAL		
	C-terminal domain	Coprecipitation	Huang et al., 1997
	Amino acids L310-E380	GST pull-down	Ivanina et al., 2003
	Amino acid L344 (β L- β M loop)	Coaffinity precipitation	Finley et al., 2004
Kir3.3	G β 1 γ 2 binds C-terminal domain	IP* and GST pull-down	Kawano et al., 2007
	N-TERMINAL		
	N-terminal domain	Coprecipitation	Huang et al., 1997
	C-TERMINAL		
	C-terminal domain	Coprecipitation	Huang et al., 1997
Kir3.4	N-TERMINAL		
	N-terminal domain	Coprecipitation	Huang et al., 1997
	Amino acids R41-V92 with H64 as a crucial residue in G β γ binding	GST pull-down	He et al., 2002
	G β 1 γ 2 binds N-terminal domain	IP* and GST pull-down	Kawano et al., 2007
	C-TERMINAL		
	C-terminal domain	Coprecipitation	Huang et al., 1997
	Amino acids S209-R225 and N226-K245 with C216 as crucial residue for G β γ binding	Co-IP*	Krapivinsky et al., 1998
	C-terminal domain with L339 as crucial residue for G β γ binding	GST pull-down	He et al., 1999
	Amino acids N253- Y348 with L268 as a crucial residue for G β γ binding	GST pull-down	He et al., 2002
	G β 1 γ 2 binds C-terminal domain	IP* and GST pull-down	Kawano et al., 2007

IP, Immunoprecipitation; NMR, Nuclear magnetic resonance spectroscopy.

channel's interaction surface on G β overlaps the G α binding site (Ford et al., 1998; Whorton and MacKinnon, 2013). The arrangement of Kir3.2 and G $\beta\gamma$ subunits within the crystal corresponds to a membrane-delimited signaling complex consisting of one channel tetramer, four G $\beta\gamma$ subunits, four phosphatidylinositol 4,5-bisphosphate (PIP₂) molecules and four Na⁺ ions bound to corresponding regulatory sites on the channel (Whorton and MacKinnon, 2011). This organization is compatible with G $\beta\gamma$ binding to the channel to induce an intermediate active state that is stabilized into the full open conformation by PIP₂ and Na⁺ ions (Whorton and MacKinnon, 2011, 2013). Interaction sites for G $\alpha_{i/o}$ have also been mapped to all four channel subunits, both in GDP- and GTP-bound states and these sites as summarized in Table 2.

Although structural determinants of channel activation are matter of considerable consensus, the dynamics that govern the process remain subject of active investigation. Originally, GPCRs, G proteins and channels were conceived as isolated membrane entities capable of conveying pharmacological stimuli from receptors to effectors through a series of collisions which included the G protein as intermediary (Orly and Schramm, 1976; Tolkovsky and Levitzki, 1978). However, the perception that this original formulation of the collision coupling model failed to account for the specificity and temporal resolution of Kir3 channel signaling has led to the proposal of alternative paradigms (Neubig, 1994). One

of such alternatives postulates that receptors and their signaling partners may be precoupled in the absence of agonist (Wreggett and De Lean, 1984; Tian et al., 1994) while another proposes that receptors, their G proteins and effectors are compartmentalized within microdomains (Neubig, 1994; Neer, 1995) where signaling partners are present in high enough concentrations to allow rapid interactions by collision (Gross and Lohse, 1991). In the case of neurons, postsynaptic densities are typically specialized domains where anchoring and scaffolding proteins control signaling partners present within dendritic spines (Romero et al., 2011; Fourie et al., 2014). Kir3.2c subunits directly interact with post synaptic density protein 95 (PSD95) and synapse-associated protein 97 (SAP97), two such proteins which not only regulate local concentration of channel subunits but their responsiveness to G proteins as well (Inanobe et al., 1999; Hibino et al., 2000; Nassirpour et al., 2010).

The idea that receptors and channels may associate to form a complex is supported by evidence obtained in native and heterologous systems. Thus, in co-immunoprecipitations from brain samples Kir3 subunits can be recovered with dopamine D₂ (Lavine et al., 2002) or GABA_B receptors (Ciruela et al., 2010). Functional evidence is also consistent with the notion that native receptors and channels may associate. For example, immobilization of MORs receptors expressed in cerebellar granule cells does not alter the rate of Kir3 channel activation, implying

Table 2 | G α interaction sites on different Kir3 subunits.

	Interaction sites	Methodology	References
Kir3.1	N-TERMINAL		
	G α -GDP binds N-terminal domain	Coaffinity precipitation	Huang et al., 1995
	G α_{i1} -GDP binds N-terminal domain	GST pull-down	Ivanina et al., 2004
	G α_q -GDP binds N-terminal domain	IP* and GST pull-down	Kawano et al., 2007
	G α_{i3} -GDP and G α_{i3} -GTP bind N-terminal domain	GST pull-down	Berlin et al., 2010
	C-TERMINAL		
	G α_{i3} -GDP binds amino acids F181-G254, G254-D319, and E320-P370	GST pull-down	Ivanina et al., 2004
	G α_{i1} -GDP binds amino acids G254-D319		
Kir3.2	G α_{i3} -GDP and G α_{i3} -GTP bind amino acids M184-E362	GST pull-down	Berlin et al., 2010
	G α_{i3} -GTP binds amino acids E242, V358, L365, L366, M367, S368, S369, L371, I372, and A373	NMR*	Mase et al., 2012
	N-TERMINAL		
	G α_{i3} -GDP binds amino acids I46-L96	GST pull-down	Ivanina et al., 2004
	G α_o -GDP and G α_q -GDP bind to N-terminal domain	Co-IP* and GST pull-down	Clancy et al., 2005
	G α_q -GDP binds amino acids T51-K90 with D81-K90 as crucial residues for G α_q -GDP binding	IP* and GST pull-down	Kawano et al., 2007
	C-TERMINAL		
	G α_{i3} -GDP binds amino acids L310-E380	GST pull-down	Ivanina et al., 2004
Kir3.4	G α_{i1} -GDP binds amino acids M191-G414	GST pull-down	Clancy et al., 2005
	G α_o -GDP binds amino acids E314-S330 with G318, C321, A323, I328, T329, and S330 as critical residues for G α_o -GDP binding		
	N-TERMINAL		
	G α_q -GDP binds N-terminal domain	IP* and GST pull-down	Kawano et al., 2007
	C-TERMINAL		
	G α_{i1} -GDP and G α_q -GDP bind C-terminal domain	GST pull-down	Rusinova et al., 2007

IP, Immunoprecipitation; NMR, Nuclear magnetic resonance spectroscopy.

that neither species freely diffuses within the membrane during signaling (Lober et al., 2006). More at a systems level, neuroadaptive changes induced by psychostimulants also suggests physical association between receptors and Kir3 channels. In particular, heterologous regulation of GABA_B receptors causes them to co-internalize with Kir3 subunits in the ventral tegmental area (VTA) (Padgett et al., 2012) and in pyramidal neurons of the prelimbic cortex (Hearing et al., 2013) following administration of cocaine or amphetamines. Similar conclusions were drawn from studying receptor trafficking in PC12 neurons where homologous desensitization of native muscarinic M2 receptors drives internalization and intracellular accumulation of Kir3 subunits (Clancy et al., 2007). However, a limitation with this group of observations is that native systems not always allow to rule out receptor activation by endogenous ligands, making it difficult to ascertain whether signaling complexes are spontaneously formed or if they result from receptor activation.

Spectroscopic studies in overexpression systems have proven valuable in assessing spontaneous interactions and in providing detailed kinetics of the steps involved in Kir3 activation. In heterologous systems, fluorescence resonance energy transfer (FRET) and bioluminescence resonance energy transfer (BRET)-based approaches have both revealed spontaneous energy transfer between channel subunits and G proteins (Riven et al., 2006; Robitaille et al., 2009; Berlin et al., 2010, 2011) and between the latter and receptors (Rebois et al., 2006; Audet et al., 2008). For opioid receptors in particular, DORs were shown to organize into multimeric arrays that also contain GαAβ1γ2 and Kir3.1/Kir3.2 subunits (Richard-Lalonde et al., 2013). However, some of these constitutive associations have not been consistently observed. For example, BRET studies show that α2A-adrenergic receptors precouple to Gαi1 (Gales et al., 2006) but FRET data indicate that precoupling occurs with Gαo (Nobles et al., 2005) but not Gαi1 (Hein et al., 2005). These discrepancies have been explained by different arguments: (a) differences in sensitivity between the two techniques would allow BRET to detect lower basal levels of interaction than FRET; (b) receptors do not display the same affinity for different Gα subunits, and (c) receptors with different levels of constitutive activity have different levels of G protein precoupling as reviewed in Lohse et al. (2012).

Kinetic approaches have also addressed the question of whether receptors and G protein precouple in the absence of ligand. For example, FRET assays have established that the time course of conformational changes undergone by the receptor's third intracellular loop upon its activation (50 ms–1 s) (Vilardaga et al., 2003) may be undistinguishable from the kinetics of receptor conformational rearrangements with respect to the G protein (Hein et al., 2005; Jensen et al., 2009). Although these findings argue in favor of precoupling, other observations can be taken as evidence of collision, particularly the fact that the speed of FRET changes that were observed at the interface of the receptor with the G protein varies with the concentration of agonist used to activate the receptor (Hein et al., 2005) and with the amount of G proteins expressed (Hein et al., 2005; Falkenburger et al., 2010). Indeed, both findings are consistent with the essence of the collision model, namely that activated receptors have free access to a common pool of G-proteins. Nonetheless these observations

can also be accommodated by a precoupling model if one conceives receptor signaling in terms of conformational ensembles (Kenakin and Onaran, 2002). According to the latter model, a FRET value can be considered representative of a macroscopic state which arises from an ensemble of different receptor states. Within this context, FRET changes corresponding to “receptor activation” represent a multiplicity of states undergoing some degree of conformational change which involves the displacement of the third intracellular loop, not all of which necessarily achieve the full conformational alteration that leads to G protein activation. As agonist concentrations increase and more receptors become permanently occupied by the ligand, the ensemble is progressively constrained so that all states achieve the conformational change that effectively modifies energy transfer between receptors and downstream signaling partners. The increased efficiency, with which higher concentrations of agonist allow the ensemble to attain conformational changes that fully modify the receptor G protein interface, may translate as an increase in the speed with which the two signaling partners reach maximal FRET. This enhanced efficiency to attain full activation may take place in a receptor ensemble that is precoupled to the G protein. Converse reasoning may be applied to explain how an increase in G protein concentrations may enhance the speed of FRET changes at its interface with the receptor in the context of a precoupling model. Indeed, when G proteins are a limiting factor, some receptors are precoupled and others not. As recently demonstrated in crystallographic studies, agonist-occupied receptors will not become fully activated unless coupled to a G protein (Rasmussen et al., 2011). In such case enhanced precoupling that takes place upon higher availability of the G protein will increase the probability of the receptor ensemble of achieving a full active state which evokes an effective conformational rearrangement vis a vis the G protein. As above, the ensemble's improved efficiency to achieve this activation state can be perceived as an increase in the speed with which energy is transferred between activated receptors and G proteins.

FRET technology has also been used in combination with total internal reflection to demonstrate that G protein subunits and Kir3 channels may organize into a membrane-delimited pre-formed complex (Riven et al., 2006). Constitutive association between Kir3 and Gβγ subunits has also been observed by means of BRET (Rebois et al., 2006; Robitaille et al., 2009; Richard-Lalonde et al., 2013). Moreover, the fact that kinetics of Kir3 channel currents are concordant with conformational changes undergone within the Gαβγ trimer upon activation (Bunemann et al., 2003), has been taken as an additional argument favoring pre-association between G proteins and channel effectors (Lohse et al., 2012).

An aspect upon which BRET and FRET data consistently agree, is the fact that G proteins remain associated with the receptor at least during initial stages of signaling (Gales et al., 2005, 2006; Hein et al., 2005, 2006) implying that at one point in time the receptor, the G protein and the effector are all part of the same complex. This reasoning is also in line with evidence summarized in the previous paragraph, which would place the transducer in direct contact with the effector even before activation. This kind of “triple multimeric array” has been described for DORs, GαAβ1γ2 and Kir3.1/Kir3.2 subunits using BRET

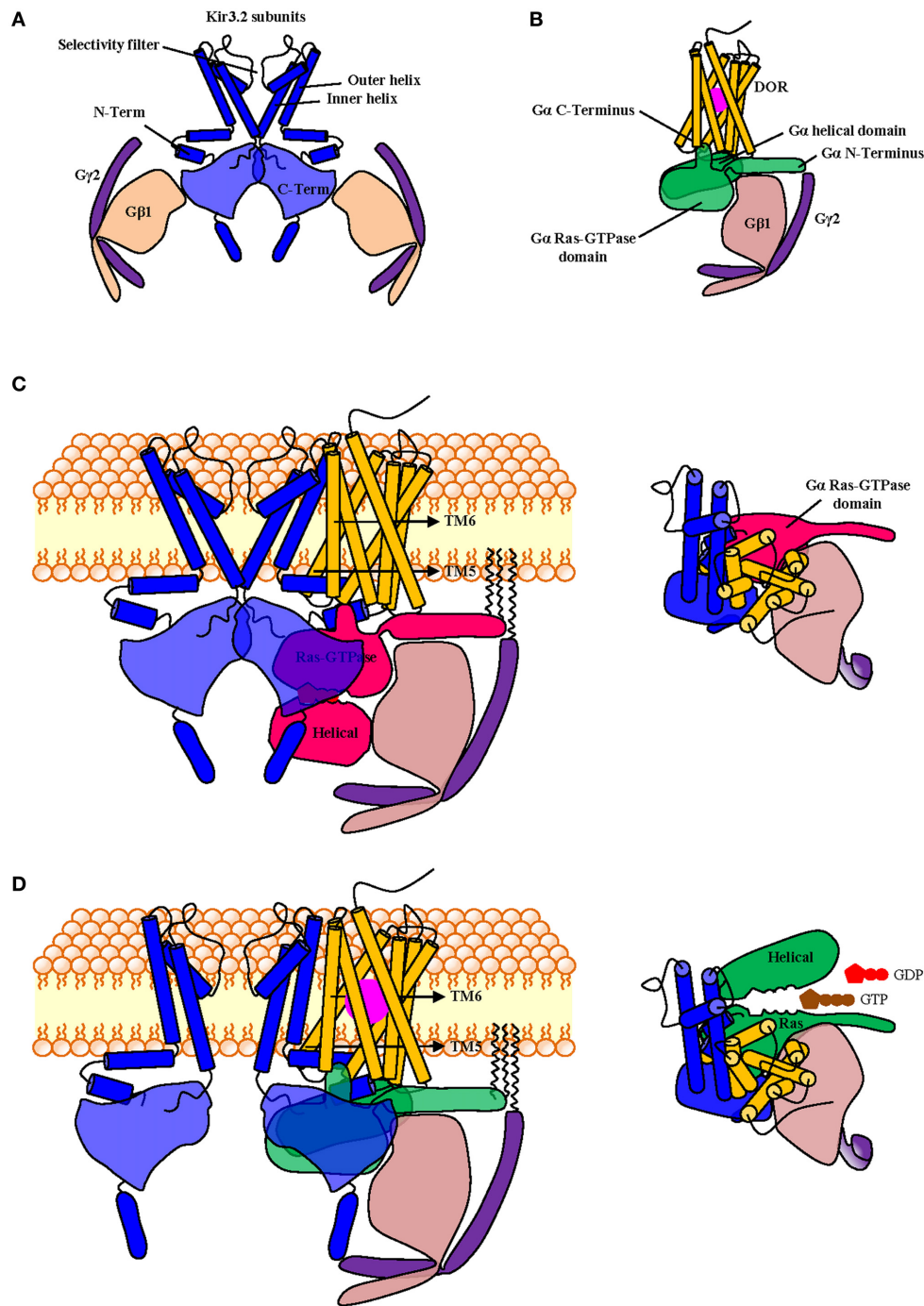


FIGURE 1 | Schematic representation of putative spatial organization of DORs, Kir3.2 and the $G\alpha\beta\gamma$ subunits within a signaling complex containing all signaling partners. The complex was constructed from diagrams based on the published crystal structures of the Kir3.2 tetramer in association with corresponding $G\beta_1\gamma_2$ subunits (PDB: 4KFM) (**A**) and that of the nucleotide-free $G\alpha\beta_1\gamma_2$ trimer in association with the active β_2 adrenergic receptor (PDB: 3sn6) where the latter was replaced by the topography corresponding to the DOR crystal (PDB: 4EJ4). Note that in the active receptor-G protein complex only the Ras-GTPase domain of $G\alpha$ is fully visible (**B**). To construct the multimeric array, the DOR- $G\alpha\beta\gamma$ complex shown in B was associated to the Kir3.2 channel shown in (A) by superimposing both $G\beta\gamma$ dimers and then removing the one corresponding to the channel. DOR and Kir3.2 subunits were both aligned with respect to the plain of the

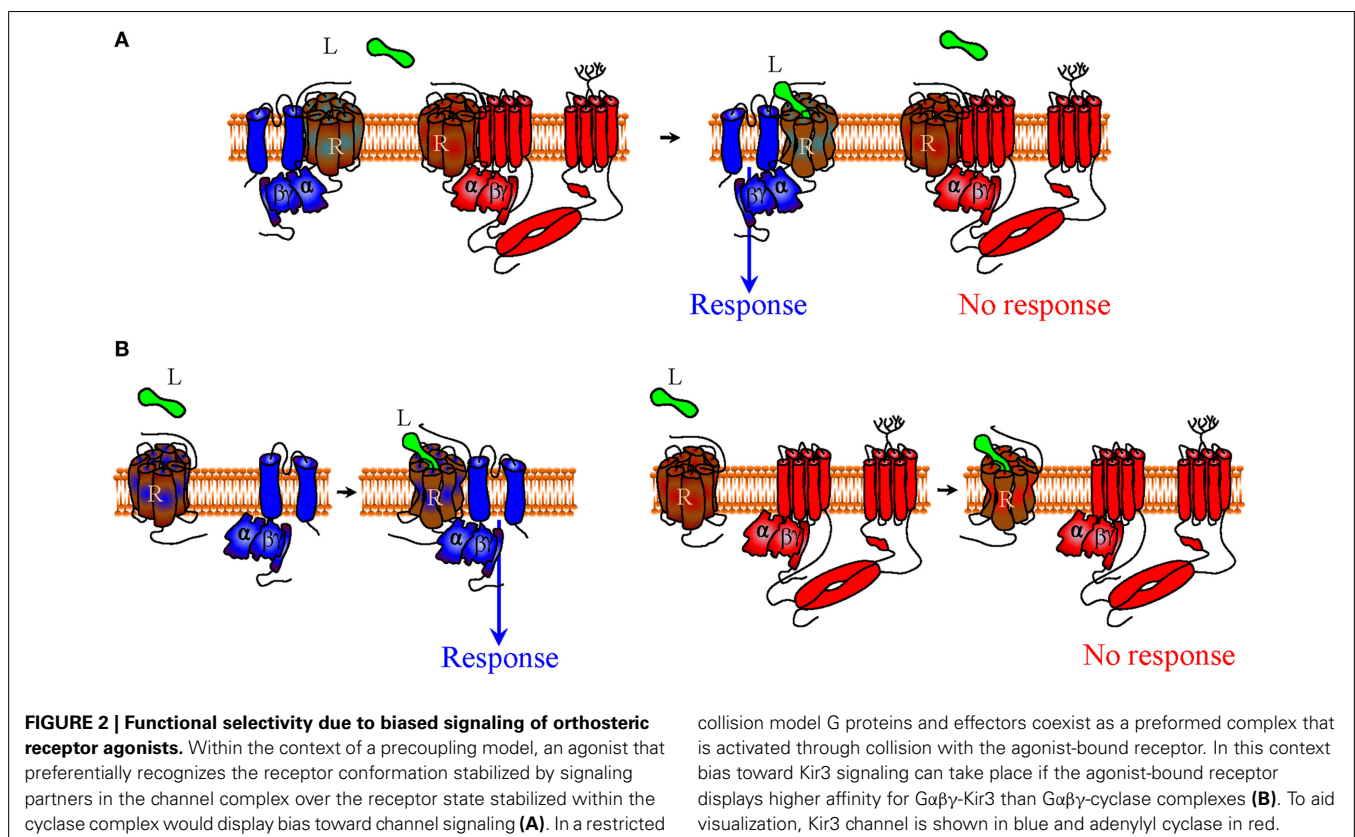
membrane. By completing this operation transmembrane domains 5 and 6 of the receptor came in close proximity of the outer helix of the channel subunit. The complex is shown in its inactive state where the helical and GTPase domains of $G\alpha$ are visible and in contact with $G\beta\gamma$. The inset shows topography of a single channel subunit with its corresponding $G\alpha\beta\gamma$ heterotrimer and DOR seen from above (**C**). In the active complex the agonist (violet) is bound to the receptor, the third intracellular loop is displaced toward the channel, the C-terminal end of $G\alpha$ insinuates between intracellular loops 2 and 3. For the proposed multimeric organization to be functional the complex must allow the displacement of the helical domain of $G\alpha$ upon nucleotide exchange; this is indeed the case since its helical domain moves laterally, from its initial position in the lower part of the inactive complex. Inset shows topography from above (**D**).

assays and co-immunoprecipitation in overexpression systems. Moreover, BRET changes that were observed among different interaction partners revealed that the conformational information that is codified by agonist binding to the receptor is relayed to the channel via the G protein (Richard-Lalonde et al., 2013). **Figure 1** shows a schematic representation of how DORs, Kir3.2 and $G\alpha\beta\gamma$ subunits could organize within a multimeric array with the receptor in its inactive (**Figure 1C**) or its active (**Figure 1D**) states. The proposed complex is based on published structures for the $G\beta\gamma$ -bound semi-open Kir3.2 channel (1A) (Whorton and MacKinnon, 2013) and an activated receptor-G protein complex (1B) (Rasmussen et al., 2011). In this putative array receptor and channel were allowed to maintain their positioning with respect to the plane of the membrane while receptor and G protein maintained their relative orientation with respect to one another, as described for the crystallized receptor-G protein complex (Rasmussen et al., 2011). Interestingly, if the diagram had been produced maintaining $G\beta\gamma$'s inclination with respect to the channel (Whorton and MacKinnon, 2013), the latter would have collided with the receptor. This suggests that, in order to organize into a complex, the different signaling partners most likely influence their mutual positions. If each of the four $G\beta\gamma$ subunits, that associate to Kir3.2 subunits in the crystal, interacts with one $G\alpha i/o$, and these in turn couple to a corresponding GPCR, it is conceivable that one receptor-G protein complex could occupy one of the grooves that correspond to the site of interaction between two adjacent Kir3 subunits (**Figures 1C,D**). A supramolecular organization which involves simultaneous association of all signaling

partners is compatible with the notion that ligand-specific conformational changes undergone by the receptor can translate into ligand-specific patterns of channel activation. Moreover, allosteric interactions within the array could allow a precoupling model to explain additional observations that are usually attributed to a collision model. For example, the fact that it is possible to attain maximal Kir3 channel currents at concentrations that produce submaximal conformational rearrangement of receptor-G protein interface (Hein et al., 2005) can be explained by positive cooperativity among channel subunits and with the activated $G\beta\gamma$ dimers, even if not all receptors have been occupied and undergone conformational changes associated with activation.

IS IT POSSIBLE TO BIAS PHARMACOLOGICAL STIMULI TOWARD Kir3 CHANNEL ACTIVATION?

Although DORs agonists effectively alleviate chronic pain and have milder side effects than ligands acting at other opioid receptors (Gallant and Meert, 2005; Feng et al., 2006; Codd et al., 2009), their potential for tolerance (Pradhan et al., 2010; Audet et al., 2012) limits their possible application as therapeutic agents. Given the contribution of cyclase pathway adaptations to the development of this side effect (Javed et al., 2004; He and Whistler, 2007; Bobeck et al., 2014), biasing pharmacological stimulus toward Kir3 channel activation and/or away from cyclase modulation was proposed as a rational means of reducing tolerance. Importantly, together with voltage-gated K^+ channels (Wimpey and Chavkin, 1991; Moore et al., 1994) and β arrs, Kir3



channels may also participate in hippocampal hyperexcitability (Luscher et al., 1997) induced by certain DOR ligands (Broom et al., 2002; Jutkiewicz et al., 2005). Depending on the degree of Kir3 involvement in this side effect, the incidence of seizures could increase for DOR ligands with Kir3 signaling bias. If this were the case, the alternative strategy based on obliteration of cyclase modulation would be of choice.

Biased agonism refers to the ability of orthosteric receptor ligands to selectively engage the activity of a distinct set of signaling partners over another (Urban et al., 2007), a type of selectivity that ensues from the stabilization of receptor conformations which activate a specific effector(s) while sparing the rest (Kenakin and Miller, 2010). Functional selectivity may also be indirect, driven by allosteric ligands (Leach et al., 2007; Kenakin, 2008). Sodium is an allosteric modulator of DORs and manipulation of its binding site provides an example of how allosteric influences may direct pharmacological stimuli toward different effectors (Fenalti et al., 2014). In particular, mutation of one of the residues (Asn131) in the first coordination shell of the Na⁺ ion produced an “efficacy switch” that changed DOR signaling from the canonical G*α*i/o pathway toward β arr recruitment. Furthermore, this effect was ligand sensitive since agonists lost G*α*i signaling while the antagonist naltrindole gained the ability to recruit β arr (Fenalti et al., 2014). Hence, by stabilizing receptor conformations that differentially favor one orthosteric response over another, *allosteric modulation of receptor conformations* offer

a great potential for directing pharmacological stimuli toward a desired response.

Let us first consider signaling bias within the context of the traditional shuttling-collision model. According to this paradigm the agonist interacts with a receptor which then travels within the membrane to interact and activate a G protein whose G*α* and G*βγ* subunits subsequently dissociate from the ligand-receptor complex to find and activate an effector (Orly and Schramm, 1976; Tolkovsky and Levitzki, 1978; Gilman, 1987; Bourne, 1997). Because in this model receptor and effector do not simultaneously interact with the G protein, the paradigm does not provide for a “memory” that would allow transferring conformational information codified by the agonist-bound receptor beyond the transducer stage. However, more recent spectroscopic studies of receptor-G protein-effector interaction point to greater restriction in mobility where G protein and effectors would be spontaneously coupled (Lohse et al., 2012). Moreover, independent of whether receptors form part of this constitutive complex or not, evidence analyzed in the previous section indicated that all three species may persistently associate during signaling. This association provides the basis for a “conformational memory” and the possibility of exploring novel bias strategies to specifically direct the pharmacological stimulus of a given receptor (in this case DORs) to a desired G protein coupled effector (Kir3 channels).

Being allosteric proteins (Kenakin and Miller, 2010), the conformation adopted by the receptor will not be solely determined

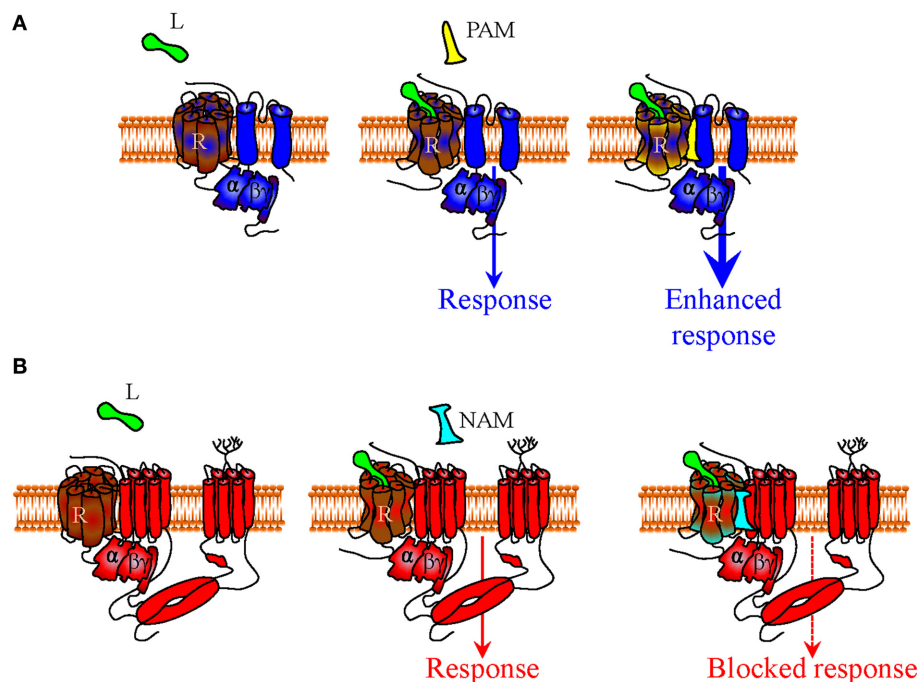


FIGURE 3 | Mechanisms of indirect bias involving allosteric modulators that specifically recognize a complex of desired composition. In a precoupling model or in a restricted collision model receptors, G proteins and effectors may all persistently associate during signaling. Within this context (only precoupling model represented in figure), small positive allosteric modulators (PAM) that specifically recognize the interface between DORs

and Kir3 channels (in blue) may specifically bias signaling of DOR orthosteric agonists toward this effector by stabilizing the complex and/or favoring channel opening (**A**). A negative allosteric modulator (NAM) that recognizes the DOR-adenylyl cyclase (in red) interface could distinctively block cAMP inhibition by the activated DOR, also allowing for bias in favor of channel effectors (**B**).

by orthosteric agonist binding, but also by its interaction with its cytosolic (G protein subunits) and membrane (Kir3 or cyclase) signaling partners, which therefore function as natural allosteric modulators. In cases where signaling complexes exist before activation, selectivity favoring Kir3 vs. cyclase signaling could be achieved by designing orthosteric ligands that display higher affinity for the conformation adopted by the receptor when contained within a Kir3 signaling complex than the one induced by its inclusion into cyclase multimers (**Figure 2A**). The idea that orthosteric agonists can indeed be tailored to specifically recognize receptors in association with distinct signaling partners is supported by studies indicating that the pharmacological properties of receptors contained in homodimers are different from those displayed by the same receptor when it is part of an heterodimer (Jordan and Devi, 1999; Waldhoer et al., 2005). Alternatively, if the complex is formed during signaling, bias toward Kir3 channel effectors would depend on the agonist's ability to stabilize a receptor conformation whose affinity for the G protein/Kir3 complex is higher than the one displayed for the G protein/cyclase complex (**Figure 2B**).

In addition, if at rest and/or during signaling receptors, G proteins and effectors associate through a distinct network of conformational influences, it is also conceivable that the pharmacological stimulus that is produced by an orthosteric ligand could be influenced by small *allosteric modulators* that specifically recognize the complex with the desired combination of DORs,

Gαβγ subunits and Kir3 channels. For example, small molecules that could bind the interface of DORs and Kir3 subunits to stabilize the complex and/or favor channel opening (*positive allosteric modulators*), would be of particular interest since they could selectively enhance Kir3 signaling by DORs and no other receptors that modulate this effector (**Figure 3A**). Alternatively, a *negative allosteric modulator* that recognizes the DOR/adenylyl cyclase interface could distinctively block cAMP inhibition by this receptor, resulting in another desired type of bias (**Figure 3B**). Finally, a variation of this strategy would be to design *complex-selective allosteric agonists* which are able to initiate signaling, independent of whether the orthosteric ligand is present or not (**Figure 4A**), or only when it is present for the case of restricted collision (**Figure 4B**). Such type of ligand could putatively recognize and stabilize the interface formed between the C-terminus of the activated Gαi/o subunit, the channel N-terminus and the third intracellular loop of the receptor. Admittedly, the structural information required for designing these compounds is not yet available but should become available once receptor/G proteins complexes are co-crystallized with their effectors.

In summary, we have analyzed evidence indicating that Kir3 channels are mediators of opioid analgesia. While they play a considerable role in undesired effects of MOR agonists, their contribution to those of DOR ligands is limited. Biasing DOR responses in favor of Kir3 channels and away from cyclase inhibition was suggested as a means of controlling analgesic tolerance

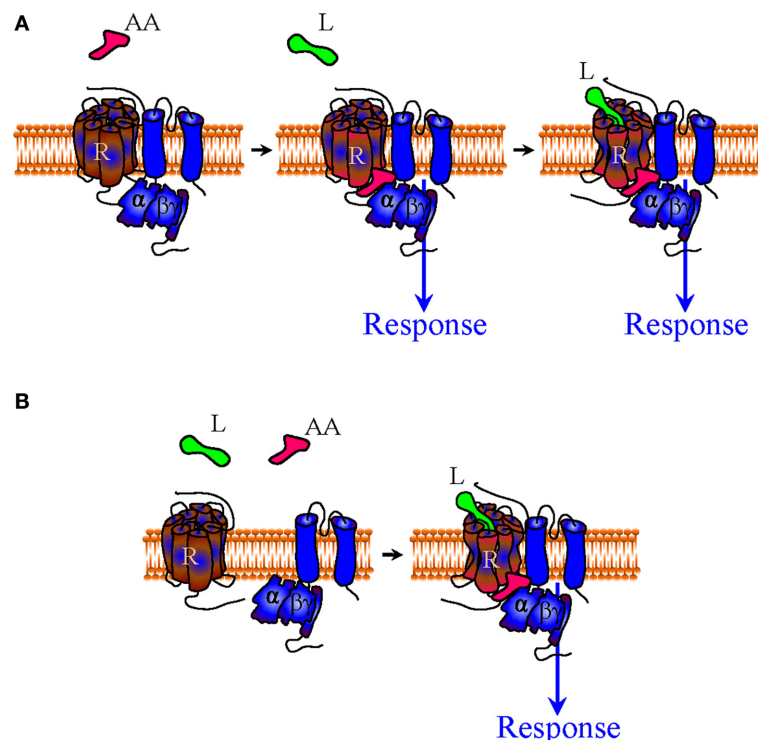


FIGURE 4 | Mechanisms of indirect bias involving allosteric agonists that specifically recognize a complex of desired composition. A complex-specific allosteric agonist (AA) may distinctively recognize an interface that is unique to the complex of interest. In the context of the

precoupling model AA may initiate signaling independent of whether the orthosteric agonist is present or not (**A**). In the restricted collision model the presence of the orthosteric agonist is necessary for the complex to be formed and provide the binding site for AA (**B**).

of DOR agonists, a side effect that limits their potential therapeutic application. Different modalities of GPCR association with G proteins and effectors were discussed, and putative bias strategies to ensure specific activation of a desired combination of receptors (DORs) and effectors (Kir3 channels) were provided.

ACKNOWLEDGMENTS

This work was supported by grants from the Natural Sciences and Engineering Research Council of Canada (NSERC) to Graciela Pineyro [311997]. Karim Nagi holds a studentship from Ste-Justine Hospital Research Center and the Faculty of Graduate and Postdoctoral Studies, University of Montreal.

REFERENCES

- Andrade, A., Denome, S., Jiang, Y. Q., Marangoudakis, S., and Lipscombe, D. (2010). Opioid inhibition of N-type Ca^{2+} channels and spinal analgesia couple to alternative splicing. *Nat. Neurosci.* 13, 1249–1256. doi: 10.1038/nn.2643
- Audet, N., Charfi, I., Mnie-Filali, O., Amraei, M., Chabot-Dore, A. J., Millicamps, M., et al. (2012). Differential association of receptor-Gbetagamma complexes with beta-arrestin2 determines recycling bias and potential for tolerance of delta opioid receptor agonists. *J. Neurosci.* 32, 4827–4840. doi: 10.1523/JNEUROSCI.3734-11.2012
- Audet, N., Gales, C., Archer-Lahlou, E., Vallieres, M., Schiller, P. W., Bouvier, M., et al. (2008). Bioluminescence resonance energy transfer assays reveal ligand-specific conformational changes within preformed signaling complexes containing delta-opioid receptors and heterotrimeric G proteins. *J. Biol. Chem.* 283, 15078–15088. doi: 10.1074/jbc.M707941200
- Ballantyne, J. C., and Shin, N. S. (2008). Efficacy of opioids for chronic pain: a review of the evidence. *Clin. J. Pain* 24, 469–478. doi: 10.1097/AJP.0b013e31816b2f26
- Banks, M. L., Roma, P. G., Folk, J. E., Rice, K. C., and Negus, S. S. (2011). Effects of the delta-opioid agonist SNC80 on the abuse liability of methadone in rhesus monkeys: a behavioral economic analysis. *Psychopharmacology (Berl)* 216, 431–439. doi: 10.1007/s00213-011-2235-2
- Bardoni, R., Tawfik, V. L., Wang, D., Francois, A., Solorzano, C., Shuster, S. A., et al. (2014). Delta opioid receptors presynaptically regulate cutaneous mechanosensory neuron input to the spinal cord dorsal horn. *Neuron* 81, 1312–1327. doi: 10.1016/j.neuron.2014.01.044
- Berlin, S., Keren-Raifman, T., Castel, R., Rubinstein, M., Dessauer, C. W., Ivanina, T., et al. (2010). G $\alpha(i)$ and G betagamma jointly regulate the conformations of a G betagamma effector, the neuronal G protein-activated K^+ channel (GIRK). *J. Biol. Chem.* 285, 6179–6185. doi: 10.1074/jbc.M109.085944
- Berlin, S., Tsemakhovich, V. A., Castel, R., Ivanina, T., Dessauer, C. W., Keren-Raifman, T., et al. (2011). Two distinct aspects of coupling between G $\alpha(i)$ protein and G protein-activated K^+ channel (GIRK) revealed by fluorescently labeled G $\alpha(i3)$ protein subunits. *J. Biol. Chem.* 286, 33223–33235. doi: 10.1074/jbc.M111.271056
- Bettahi, I., Marker, C. L., Roman, M. I., and Wickman, K. (2002). Contribution of the Kir3.1 subunit to the muscarinic-gated atrial potassium channel IKACH. *J. Biol. Chem.* 277, 48282–48288. doi: 10.1074/jbc.M209599200
- Blednov, Y. A., Stoffel, M., Alva, H., and Harris, R. A. (2003). A pervasive mechanism for analgesia: activation of GIRK2 channels. *Proc. Natl. Acad. Sci. U.S.A.* 100, 277–282. doi: 10.1073/pnas.012682399
- Blednov, Y. A., Stoffel, M., Chang, S. R., and Harris, R. A. (2001). GIRK2 deficient mice. Evidence for hyperactivity and reduced anxiety. *Physiol. Behav.* 74, 109–117. doi: 10.1016/S0031-9384(01)00555-8
- Bobeck, E. N., Chen, Q., Morgan, M. M., and Ingram, S. L. (2014). Contribution of adenylyl cyclase modulation of pre- and postsynaptic GABA neurotransmission to morphine antinociception and tolerance. *Neuropsychopharmacology*. doi: 10.1038/npp.2014.62. [Epub ahead of print].
- Bonci, A., and Williams, J. T. (1997). Increased probability of GABA release during withdrawal from morphine. *J. Neurosci.* 17, 796–803.
- Bourne, H. R. (1997). How receptors talk to trimeric G proteins. *Curr. Opin. Cell Biol.* 9, 134–142. doi: 10.1016/S0955-0674(97)80054-3
- Broom, D. C., Nitsche, J. F., Pintar, J. E., Rice, K. C., Woods, J. H., and Traynor, J. R. (2002). Comparison of receptor mechanisms and efficacy requirements for delta-agonist-induced convulsive activity and antinociception in mice. *J. Pharmacol. Exp. Ther.* 303, 723–729. doi: 10.1124/jpet.102.036525
- Bruchas, M. R., and Chavkin, C. (2010). Kinase cascades and ligand-directed signaling at the kappa opioid receptor. *Psychopharmacology (Berl)* 210, 137–147. doi: 10.1007/s00213-010-1806-y
- Bruchas, M. R., Land, B. B., Aita, M., Xu, M., Barot, S. K., Li, S., et al. (2007). Stress-induced p38 mitogen-activated protein kinase activation mediates kappa-opioid-dependent dysphoria. *J. Neurosci.* 27, 11614–11623. doi: 10.1523/JNEUROSCI.3769-07.2007
- Bruhll, S., Denton, J. S., Loneragan, D., Koran, M. E., Chont, M., Sobey, C., et al. (2013). Associations between KCNJ6 (GIRK2) gene polymorphisms and pain-related phenotypes. *Pain* 154, 2853–2859. doi: 10.1016/j.pain.2013.08.026
- Bunemann, M., Frank, M., and Lohse, M. J. (2003). Gi protein activation in intact cells involves subunit rearrangement rather than dissociation. *Proc. Natl. Acad. Sci. U.S.A.* 100, 16077–16082. doi: 10.1073/pnas.2536719100
- Cao, J. L., Vialou, V. F., Lobo, M. K., Robison, A. J., Neve, R. L., Cooper, D. C., et al. (2010). Essential role of the cAMP-cAMP response-element binding protein pathway in opiate-induced homeostatic adaptations of locus coeruleus neurons. *Proc. Natl. Acad. Sci. U.S.A.* 107, 17011–17016. doi: 10.1073/pnas.1010077107
- Charbogne, P., Kieffer, B. L., and Befort, K. (2014). 15 years of genetic approaches *in vivo* for addiction research: opioid receptor and peptide gene knockout in mouse models of drug abuse. *Neuropharmacology* 76(Pt B), 204–217. doi: 10.1016/j.neuropharm.2013.08.028
- Cheng, P. Y., Wu, D., Soong, Y., McCabe, S., Decena, J. A., and Szeto, H. H. (1993). Role of mu 1- and delta-opioid receptors in modulation of fetal EEG and respiratory activity. *Am. J. Physiol.* 265, R433–R438.
- Christie, M. J. (2008). Cellular neuroadaptations to chronic opioids: tolerance, withdrawal and addiction. *Br. J. Pharmacol.* 154, 384–396. doi: 10.1038/bjp.2008.100
- Chung, M. K., Cho, Y. S., Bae, Y. C., Lee, J., Zhang, X., and Ro, J. Y. (2013). Peripheral G protein-coupled inwardly rectifying potassium channels are involved in delta-opioid receptor-mediated anti-hyperalgesia in rat masseter muscle. *Eur. J. Pain* 18, 29–38. doi: 10.1002/j.1532-2149.2013.00343.x
- Chu Sin Chung, P., and Kieffer, B. L. (2013). Delta opioid receptors in brain function and diseases. *Pharmacol. Ther.* 140, 112–120. doi: 10.1016/j.pharmthera.2013.06.003
- Ciruela, F., Fernandez-Duenas, V., Sahlholm, K., Fernandez-Alacid, L., Nicolau, J. C., Watanabe, M., et al. (2010). Evidence for oligomerization between GABAB receptors and GIRK channels containing the GIRK1 and GIRK3 subunits. *Eur. J. Neurosci.* 32, 1265–1277. doi: 10.1111/j.1460-9568.2010.07356.x
- Clancy, S. M., Boyer, S. B., and Slesinger, P. A. (2007). Coregulation of natively expressed pertussis toxin-sensitive muscarinic receptors with G-protein-activated potassium channels. *J. Neurosci.* 27, 6388–6399. doi: 10.1523/JNEUROSCI.1190-07.2007
- Clancy, S. M., Fowler, C. E., Finley, M., Suen, K. F., Arrabit, C., Berton, F., et al. (2005). Pertussis-toxin-sensitive G $\alpha(i)$ subunits selectively bind to C-terminal domain of neuronal GIRK channels: evidence for a heterotrimeric G-protein-channel complex. *Mol. Cell. Neurosci.* 28, 375–389. doi: 10.1016/j.mcn.2004.10.009
- Codd, E. E., Carson, J. R., Colburn, R. W., Stone, D. J., Van Besien, C. R., Zhang, S. P., et al. (2009). JNJ-20788560 [9-(8-azabicyclo[3.2.1]oct-3-ylidene)-9H-xanthene-3-carboxylic acid diethylamide], a selective delta opioid receptor agonist, is a potent and efficacious antihyperalgesic agent that does not produce respiratory depression, pharmacologic tolerance, or physical dependence. *J. Pharmacol. Exp. Ther.* 329, 241–251. doi: 10.1124/jpet.108.146969
- Cooper, A., Grigoryan, G., Guy-David, L., Tsoory, M. M., Chen, A., and Reuveny, E. (2012). Trisomy of the G protein-coupled K^+ channel gene, *Kcnj6*, affects reward mechanisms, cognitive functions, and synaptic plasticity in mice. *Proc. Natl. Acad. Sci. U.S.A.* 109, 2642–2647. doi: 10.1073/pnas.1109099109
- Cowan, A., Zhu, X. Z., Mosberg, H. I., Omnaas, J. R., and Porreca, F. (1988). Direct dependence studies in rats with agents selective for different types of opioid receptor. *J. Pharmacol. Exp. Ther.* 246, 950–955.
- Cruz, H. G., Ivanova, T., Lunn, M. L., Stoffel, M., Slesinger, P. A., and Luscher, C. (2004). Bi-directional effects of GABA(B) receptor agonists on the mesolimbic dopamine system. *Nat. Neurosci.* 7, 153–159. doi: 10.1038/nn1181

- De Sarro, G. B., Marra, R., Spagnolo, C., and Nistico, G. (1992). Delta opioid receptors mediate seizures produced by intrahippocampal injection of ala-deltorphin in rats. *Funct. Neurol.* 7, 235–238.
- Dewire, S. M., Yamashita, D. S., Rominger, D. H., Liu, G., Cowan, C. L., Graczyk, T. M., et al. (2013). A G protein-biased ligand at the mu-opioid receptor is potently analgesic with reduced gastrointestinal and respiratory dysfunction compared with morphine. *J. Pharmacol. Exp. Ther.* 344, 708–717. doi: 10.1124/jpet.112.201616
- Do Carmo, G. P., Folk, J. E., Rice, K. C., Chartoff, E., Carlezon, W. A. Jr., and Negus, S. S. (2009). The selective non-peptidic delta opioid agonist SNC80 does not facilitate intracranial self-stimulation in rats. *Eur. J. Pharmacol.* 604, 58–65. doi: 10.1016/j.ejphar.2008.12.021
- Drake, C. T., Chavkin, C., and Milner, T. A. (2007). Opioid systems in the dentate gyrus. *Prog. Brain Res.* 163, 245–263. doi: 10.1016/S0079-6123(07)63015-5
- Falkenburger, B. H., Jensen, J. B., and Hille, B. (2010). Kinetics of M1 muscarinic receptor and G protein signaling to phospholipase C in living cells. *J. Gen. Physiol.* 135, 81–97. doi: 10.1085/jgp.200910344
- Fenalti, G., Giguere, P. M., Katritch, V., Huang, X. P., Thompson, A. A., Cherezov, V., et al. (2014). Molecular control of delta-opioid receptor signalling. *Nature* 506, 191–196. doi: 10.1038/nature12944
- Feng, P., Rahim, R. T., Cowan, A., Liu-Chen, L. Y., Peng, X., Gaughan, J., et al. (2006). Effects of mu, kappa or delta opioids administered by pellet or pump on oral Salmonella infection and gastrointestinal transit. *Eur. J. Pharmacol.* 534, 250–257. doi: 10.1016/j.ejphar.2006.01.048
- Fernandez-Alacid, L., Aguado, C., Ciruela, F., Martin, R., Colon, J., Cabanero, M. J., et al. (2009). Subcellular compartment-specific molecular diversity of pre- and post-synaptic GABA-activated GIRK channels in Purkinje cells. *J. Neurochem.* 110, 1363–1376. doi: 10.1111/j.1471-4159.2009.06229.x
- Fernandez-Alacid, L., Watanabe, M., Molnar, E., Wickman, K., and Lujan, R. (2011). Developmental regulation of G protein-gated inwardly-rectifying K⁺ (GIRK/Kir3) channel subunits in the brain. *Eur. J. Neurosci.* 34, 1724–1736. doi: 10.1111/j.1460-9568.2011.07886.x
- Finley, M., Arrabit, C., Fowler, C., Suen, K. F., and Slesinger, P. A. (2004). betaL-betaM loop in the C-terminal domain of G protein-activated inwardly rectifying K(+) channels is important for G(betagamma) subunit activation. *J. Physiol.* 555, 643–657. doi: 10.1113/jphysiol.2003.056101
- Ford, C. E., Skiba, N. P., Bae, H., Daaka, Y., Reuveny, E., Shekter, L. R., et al. (1998). Molecular basis for interactions of G protein betagamma subunits with effectors. *Science* 280, 1271–1274. doi: 10.1126/science.280.5367.1271
- Fourie, C., Li, D., and Montgomery, J. M. (2014). The anchoring protein SAP97 influences the trafficking and localisation of multiple membrane channels. *Biochim. Biophys. Acta* 1838, 589–594. doi: 10.1016/j.bbame.2013.03.015
- Gales, C., Rebois, R. V., Hogue, M., Trieu, P., Breit, A., Hebert, T. E., et al. (2005). Real-time monitoring of receptor and G-protein interactions in living cells. *Nat. Methods* 2, 177–184. doi: 10.1038/nmeth743
- Gales, C., Van Durm, J. J., Schaak, S., Pontier, S., Percherancier, Y., Audet, M., et al. (2006). Probing the activation-promoted structural rearrangements in preassembled receptor-G protein complexes. *Nat. Struct. Mol. Biol.* 13, 778–786. doi: 10.1038/nsmb1134
- Gallantini, E. L., and Meert, T. F. (2005). A comparison of the antinociceptive and adverse effects of the mu-opioid agonist morphine and the delta-opioid agonist SNC80. *Basic Clin. Pharmacol. Toxicol.* 97, 39–51. doi: 10.1111/j.1742-7843.2005.pto_97107.x
- Gao, X. F., Zhang, H. L., You, Z. D., Lu, C. L., and He, C. (2007). G protein-coupled inwardly rectifying potassium channels in dorsal root ganglion neurons. *Acta Pharmacol. Sin.* 28, 185–190. doi: 10.1111/j.1745-7254.2007.00478.x
- Gaveriaux-Ruff, C., and Kieffer, B. L. (2011). Delta opioid receptor analgesia: recent contributions from pharmacology and molecular approaches. *Behav. Pharmacol.* 22, 405–414. doi: 10.1097/FBP.0b013e32834a1f2c
- Gendron, L., Lucido, A. L., Mennicken, F., O'Donnell, D., Vincent, J. P., Stroh, T., et al. (2006). Morphine and pain-related stimuli enhance cell surface availability of somatic delta-opioid receptors in rat dorsal root ganglia. *J. Neurosci.* 26, 953–962. doi: 10.1523/JNEUROSCI.3598-05.2006
- Gilman, A. G. (1987). G proteins: transducers of receptor-generated signals. *Annu. Rev. Biochem.* 56, 615–649. doi: 10.1146/annurev.bi.56.070187.003151
- Glaum, S. R., Miller, R. J., and Hammond, D. L. (1994). Inhibitory actions of delta 1-, delta 2-, and mu-opioid receptor agonists on excitatory transmission in lamina II neurons of adult rat spinal cord. *J. Neurosci.* 14, 4965–4971.
- Goldenberg, D. L. (2010). Pain/Depression dyad: a key to a better understanding and treatment of functional somatic syndromes. *Am. J. Med.* 123, 675–682. doi: 10.1016/j.amjmed.2010.01.014
- Gonzalez-Rodriguez, S., Hidalgo, A., Baamonde, A., and Menendez, L. (2010). Involvement of Gi/o proteins and GIRK channels in the potentiation of morphine-induced spinal analgesia in acutely inflamed mice. *Naunyn-Schmiedeberg's Arch. Pharmacol.* 381, 59–71. doi: 10.1007/s00210-009-0471-3
- Gonzalez-Rodriguez, S., Llamas, S., Hidalgo, A., Baamonde, A., and Menendez, L. (2012). Potentiation of acute morphine-induced analgesia measured by a thermal test in bone cancer-bearing mice. *Fundam. Clin. Pharmacol.* 26, 363–372. doi: 10.1111/j.1472-8206.2010.00921.x
- Gross, W., and Lohse, M. J. (1991). Mechanism of activation of A2 adenosine receptors. II. A restricted collision-coupling model of receptor-effector interaction. *Mol. Pharmacol.* 39, 524–530.
- Gysling, K., and Wang, R. Y. (1983). Morphine-induced activation of A10 dopamine neurons in the rat. *Brain Res.* 277, 119–127. doi: 10.1016/0006-8993(83)90913-7
- Han, M. H., Bolanos, C. A., Green, T. A., Olson, V. G., Neve, R. L., Liu, R. J., et al. (2006). Role of cAMP response element-binding protein in the rat locus ceruleus: regulation of neuronal activity and opiate withdrawal behaviors. *J. Neurosci.* 26, 4624–4629. doi: 10.1523/JNEUROSCI.4701-05.2006
- Hassan, A. H., Ableitner, A., Stein, C., and Herz, A. (1993). Inflammation of the rat paw enhances axonal transport of opioid receptors in the sciatic nerve and increases their density in the inflamed tissue. *Neuroscience* 55, 185–195. doi: 10.1016/0306-4522(93)90465-R
- He, C., Yan, X., Zhang, H., Mirshahi, T., Jin, T., Huang, A., et al. (2002). Identification of critical residues controlling G protein-gated inwardly rectifying K(+) channel activity through interactions with the beta gamma subunits of G proteins. *J. Biol. Chem.* 277, 6088–6096. doi: 10.1074/jbc.M104851200
- He, C., Zhang, H., Mirshahi, T., and Logothetis, D. E. (1999). Identification of a potassium channel site that interacts with G protein betagamma subunits to mediate agonist-induced signaling. *J. Biol. Chem.* 274, 12517–12524.
- He, L., and Whistler, J. L. (2007). The biochemical analysis of methadone modulation on morphine-induced tolerance and dependence in the rat brain. *Pharmacology* 79, 193–202. doi: 10.1159/000100893
- Hearing, M., Kotecki, L., Marron Fernandez De Velasco, E., Fajardo-Serrano, A., Chung, H. J., Lujan, R., et al. (2013). Repeated cocaine weakens GABA(B)-GIRK signaling in layer 5/6 pyramidal neurons in the prefrontal cortex. *Neuron* 80, 159–170. doi: 10.1016/j.neuron.2013.07.019
- Hein, P., Frank, M., Hoffmann, C., Lohse, M. J., and Bunemann, M. (2005). Dynamics of receptor/G protein coupling in living cells. *EMBO J.* 24, 4106–4114. doi: 10.1038/sj.emboj.7600870
- Hein, P., Rochais, F., Hoffmann, C., Dorsch, S., Nikolaev, V. O., Engelhardt, S., et al. (2006). Gs activation is time-limiting in initiating receptor-mediated signaling. *J. Biol. Chem.* 281, 33345–33351. doi: 10.1074/jbc.M606713200
- Heinke, B., Gingl, E., and Sandkuhler, J. (2011). Multiple targets of mu-opioid receptor-mediated presynaptic inhibition at primary afferent Aδ- and C-fibers. *J. Neurosci.* 31, 1313–1322. doi: 10.1523/JNEUROSCI.4060-10.2011
- Hibino, H., Inanobe, A., Furutani, K., Murakami, S., Findlay, I., and Kurachi, Y. (2010). Inwardly rectifying potassium channels: their structure, function, and physiological roles. *Physiol. Rev.* 90, 291–366. doi: 10.1152/physrev.00021.2009
- Hibino, H., Inanobe, A., Tanemoto, M., Fujita, A., Doi, K., Kubo, T., et al. (2000). Anchoring proteins confer G protein sensitivity to an inward-rectifier K(+) channel through the GK domain. *EMBO J.* 19, 78–83. doi: 10.1093/emboj/19.1.78
- Huang, C. L., Jan, Y. N., and Jan, L. Y. (1997). Binding of the G protein betagamma subunit to multiple regions of G protein-gated inward-rectifying K⁺ channels. *FEBS Lett.* 405, 291–298. doi: 10.1016/S0014-5793(97)00197-X
- Huang, C. L., Slesinger, P. A., Casey, P. J., Jan, Y. N., and Jan, L. Y. (1995). Evidence that direct binding of G beta gamma to the GIRK1 G protein-gated inwardly rectifying K⁺ channel is important for channel activation. *Neuron* 15, 1133–1143.
- Ikeda, K., Kobayashi, T., Kumanishi, T., Niki, H., and Yano, R. (2000). Involvement of G-protein-activated inwardly rectifying K (GIRK) channels in opioid-induced analgesia. *Neurosci. Res.* 38, 113–116. doi: 10.1016/S0168-0102(00)00144-9
- Ikeda, K., Kobayashi, T., Kumanishi, T., Yano, R., Sora, I., and Niki, H. (2002). Molecular mechanisms of analgesia induced by opioids and ethanol: is the

- GIRK channel one of the keys? *Neurosci. Res.* 44, 121–131. doi: 10.1016/S0168-0102(02)00094-9
- Inanobe, A., Yoshimoto, Y., Horio, Y., Morishige, K. I., Hibino, H., Matsumoto, S., et al. (1999). Characterization of G-protein-gated K⁺ channels composed of Kir3.2 subunits in dopaminergic neurons of the substantia nigra. *J. Neurosci.* 19, 1006–1017.
- Ivanina, T., Rishal, I., Varon, D., Mullner, C., Frohnwieser-Steinbeck, B., Schreibmayer, W., et al. (2003). Mapping the Gbetagamma-binding sites in GIRK1 and GIRK2 subunits of the G protein-activated K⁺ channel. *J. Biol. Chem.* 278, 29174–29183. doi: 10.1074/jbc.M304518200
- Ivanina, T., Varon, D., Peleg, S., Rishal, I., Porozov, Y., Dessauer, C. W., et al. (2004). Galphai1 and Galphai3 differentially interact with, and regulate, the G protein-activated K⁺ channel. *J. Biol. Chem.* 279, 17260–17268. doi: 10.1074/jbc.M313425200
- Javed, R. R., Dewey, W. L., Smith, P. A., and Smith, F. L. (2004). PKC and PKA inhibitors reverse tolerance to morphine-induced hypothermia and supraspinal analgesia in mice. *Eur. J. Pharmacol.* 492, 149–157. doi: 10.1016/j.ejphar.2004.03.061
- Jensen, J. B., Lyssand, J. S., Hague, C., and Hille, B. (2009). Fluorescence changes reveal kinetic steps of muscarinic receptor-mediated modulation of phosphoinositides and Kv7.2/7.3 K⁺ channels. *J. Gen. Physiol.* 133, 347–359. doi: 10.1085/jgp.200810075
- Johnson, S. W., and North, R. A. (1992). Opioids excite dopamine neurons by hyperpolarization of local interneurons. *J. Neurosci.* 12, 483–488.
- Jordan, B. A., and Devi, L. A. (1999). G-protein-coupled receptor heterodimerization modulates receptor function. *Nature* 399, 697–700.
- Jutkiewicz, E. M., Baladi, M. G., Folk, J. E., Rice, K. C., and Woods, J. H. (2006). The convulsive and electroencephalographic changes produced by nonpeptidic delta-opioid agonists in rats: comparison with pentylenetetrazol. *J. Pharmacol. Exp. Ther.* 317, 1337–1348. doi: 10.1124/jpet.105.095810
- Jutkiewicz, E. M., Rice, K. C., Traynor, J. R., and Woods, J. H. (2005). Separation of the convulsions and antidepressant-like effects produced by the delta-opioid agonist SNC80 in rats. *Psychopharmacology (Berl)* 182, 588–596. doi: 10.1007/s00213-005-0138-9
- Kalso, E., Edwards, J. E., Moore, R. A., and McQuay, H. J. (2004). Opioids in chronic non-cancer pain: systematic review of efficacy and safety. *Pain* 112, 372–380. doi: 10.1016/j.pain.2004.09.019
- Kawano, T., Zhao, P., Floreani, C. V., Nakajima, Y., Kozasa, T., and Nakajima, S. (2007). Interaction of Galphaq and Kir3, G protein-coupled inwardly rectifying potassium channels. *Mol. Pharmacol.* 71, 1179–1184. doi: 10.1124/mol.106.032508
- Kenakin, T. (2008). Functional selectivity in GPCR modulator screening. *Comb. Chem. High Throughput Screen.* 11, 337–343. doi: 10.2174/138620708784534824
- Kenakin, T., and Miller, L. J. (2010). Seven transmembrane receptors as shapeshifting proteins: the impact of allosteric modulation and functional selectivity on new drug discovery. *Pharmacol. Rev.* 62, 265–304. doi: 10.1124/pr.108.000992
- Kenakin, T., and Onaran, O. (2002). The ligand paradox between affinity and efficacy: can you be there and not make a difference? *Trends Pharmacol. Sci.* 23, 275–280. doi: 10.1016/S0165-6147(02)02036-9
- Kieffer, B. L., and Gaveriaux-Ruff, C. (2002). Exploring the opioid system by gene knockout. *Prog. Neurobiol.* 66, 285–306. doi: 10.1016/S0301-0082(02)00008-4
- Koyrakh, L., Lujan, R., Colon, J., Karschin, C., Kurachi, Y., Karschin, A., et al. (2005). Molecular and cellular diversity of neuronal G-protein-gated potassium channels. *J. Neurosci.* 25, 11468–11478. doi: 10.1523/JNEUROSCI.3484-05.2005
- Krapivinsky, G., Kennedy, M. E., Nemec, J., Medina, I., Krapivinsky, L., and Clapham, D. E. (1998). Gbeta binding to GIRK4 subunit is critical for G protein-gated K⁺ channel activation. *J. Biol. Chem.* 273, 16946–16952. doi: 10.1074/jbc.273.27.16946
- Kunkel, M. T., and Peralta, E. G. (1995). Identification of domains conferring G protein regulation on inward rectifier potassium channels. *Cell* 83, 443–449. doi: 10.1016/0092-8674(95)90122-1
- Laurent, V., Leung, B., Maidment, N., and Balleine, B. W. (2012). mu- and delta-opioid-related processes in the accumbens core and shell differentially mediate the influence of reward-guided and stimulus-guided decisions on choice. *J. Neurosci.* 32, 1875–1883. doi: 10.1523/JNEUROSCI.4688-11.2012
- Lavigne, N., Ethier, N., Oak, J. N., Pei, L., Liu, F., Trieu, P., et al. (2002). G protein-coupled receptors form stable complexes with inwardly rectifying potassium channels and adenylyl cyclase. *J. Biol. Chem.* 277, 46010–46019. doi: 10.1074/jbc.M205035200
- Leach, K., Sexton, P. M., and Christopoulos, A. (2007). Allosteric GPCR modulators: taking advantage of permissive receptor pharmacology. *Trends Pharmacol. Sci.* 28, 382–389. doi: 10.1016/j.tips.2007.06.004
- Le Bourdonnec, B., Windh, R. T., Ajello, C. W., Leister, L. K., Gu, M., Chu, G. H., et al. (2008). Potent, orally bioavailable delta opioid receptor agonists for the treatment of pain: discovery of N,N-diethyl-4-(5-hydroxyspiro[chromene-2,4'-piperidine]-4-yl)benzamide (ADL5859). *J. Med. Chem.* 51, 5893–5896. doi: 10.1021/jm8008986
- Le Merrier, J., Becker, J. A., Befort, K., and Kieffer, B. L. (2009). Reward processing by the opioid system in the brain. *Physiol. Rev.* 89, 1379–1412. doi: 10.1152/physrev.00005.2009
- Lemos, J. C., Roth, C. A., Messinger, D. I., Gill, H. K., Phillips, P. E., and Chavkin, C. (2012). Repeated stress dysregulates kappa-opioid receptor signaling in the dorsal raphe through a p38alpha MAPK-dependent mechanism. *J. Neurosci.* 32, 12325–12336. doi: 10.1523/JNEUROSCI.2053-12.2012
- Li, J. L., Ding, Y. Q., Li, Y. Q., Li, J. S., Nomura, S., Kaneko, T., et al. (1998). Immunocytochemical localization of mu-opioid receptor in primary afferent neurons containing substance P or calcitonin gene-related peptide. A light and electron microscope study in the rat. *Brain Res.* 794, 347–352. doi: 10.1016/S0006-8993(98)00332-1
- Liao, Y. J., Jan, Y. N., and Jan, L. Y. (1996). Heteromultimerization of G-protein-gated inwardly rectifying K⁺ channel proteins GIRK1 and GIRK2 and their altered expression in weaver brain. *J. Neurosci.* 16, 7137–7150.
- Lober, R. M., Pereira, M. A., and Lambert, N. A. (2006). Rapid activation of inwardly rectifying potassium channels by immobile G-protein-coupled receptors. *J. Neurosci.* 26, 12602–12608. doi: 10.1523/JNEUROSCI.4020-06.2006
- Logothetis, D. E., Kurachi, Y., Galper, J., Neer, E. J., and Clapham, D. E. (1987). The beta gamma subunits of GTP-binding proteins activate the muscarinic K⁺ channel in heart. *Nature* 325, 321–326. doi: 10.1038/325321a0
- Lohse, M. J., Nuber, S., and Hoffmann, C. (2012). Fluorescence/bioluminescence resonance energy transfer techniques to study G-protein-coupled receptor activation and signaling. *Pharmacol. Rev.* 64, 299–336. doi: 10.1124/pr.110.004309
- Lotsch, J., Pruss, H., Veh, R. W., and Doehring, A. (2010). A KCNJ6 (Kir3.2, GIRK2) gene polymorphism modulates opioid effects on analgesia and addiction but not on pupil size. *Pharmacogenet. Genomics* 20, 291–297. doi: 10.1097/FPC.0b013e3283386bda
- Lujan, R., Marron Fernandez De Velasco, E., Aguado, C., and Wickman, K. (2014). New insights into the therapeutic potential of Girk channels. *Trends Neurosci.* 37, 20–29. doi: 10.1016/j.tins.2013.10.006
- Luscher, C., Jan, L. Y., Stoffel, M., Malenka, R. C., and Nicoll, R. A. (1997). G protein-coupled inwardly rectifying K⁺ channels (GIRKs) mediate postsynaptic but not presynaptic transmitter actions in hippocampal neurons. *Neuron* 19, 687–695. doi: 10.1016/S0896-6273(00)80381-5
- Luscher, C., and Slesinger, P. A. (2010). Emerging roles for G protein-gated inwardly rectifying potassium (GIRK) channels in health and disease. *Nat. Rev. Neurosci.* 11, 301–315. doi: 10.1038/nrn2834
- Luscher, C., and Ungless, M. A. (2006). The mechanistic classification of addictive drugs. *PLoS Med.* 3:e437. doi: 10.1371/journal.pmed.0030437
- Marker, C. L., Cintora, S. C., Roman, M. I., Stoffel, M., and Wickman, K. (2002). Hyperalgesia and blunted morphine analgesia in G protein-gated potassium channel subunit knockout mice. *Neuroreport* 13, 2509–2513. doi: 10.1097/00001756-200212200-00026
- Marker, C. L., Lujan, R., Colon, J., and Wickman, K. (2006). Distinct populations of spinal cord lamina II interneurons expressing G-protein-gated potassium channels. *J. Neurosci.* 26, 12251–12259. doi: 10.1523/JNEUROSCI.3693-06.2006
- Marker, C. L., Lujan, R., Loh, H. H., and Wickman, K. (2005). Spinal G-protein-gated potassium channels contribute in a dose-dependent manner to the analgesic effect of mu- and delta- but not kappa-opioids. *J. Neurosci.* 25, 3551–3559. doi: 10.1523/JNEUROSCI.4899-04.2005
- Marker, C. L., Stoffel, M., and Wickman, K. (2004). Spinal G-protein-gated K⁺ channels formed by GIRK1 and GIRK2 subunits modulate thermal nociception and contribute to morphine analgesia. *J. Neurosci.* 24, 2806–2812. doi: 10.1523/JNEUROSCI.5251-03.2004
- Mase, Y., Yokogawa, M., Osawa, M., and Shimada, I. (2012). Structural basis for modulation of gating property of G protein-gated inwardly rectifying potassium

- ion channel (GIRK) by i/o-family G protein alpha subunit (Galphai/o). *J. Biol. Chem.* 287, 19537–19549. doi: 10.1074/jbc.M112.353888
- McAllister, S. D., Griffin, G., Satin, L. S., and Abood, M. E. (1999). Cannabinoid receptors can activate and inhibit G protein-coupled inwardly rectifying potassium channels in a xenopus oocyte expression system. *J. Pharmacol. Exp. Ther.* 291, 618–626.
- McLaughlin, J. P., Myers, L. C., Zarek, P. E., Caron, M. G., Lefkowitz, R. J., Czyzyk, T. A., et al. (2004). Prolonged kappa opioid receptor phosphorylation mediated by G-protein receptor kinase underlies sustained analgesic tolerance. *J. Biol. Chem.* 279, 1810–1818. doi: 10.1074/jbc.M305796200
- Mitrovic, I., Margeta-Mitrovic, M., Bader, S., Stoffel, M., Jan, L. Y., and Basbaum, A. I. (2003). Contribution of GIRK2-mediated postsynaptic signaling to opiate and alpha 2-adrenergic analgesia and analgesic sex differences. *Proc. Natl. Acad. Sci. U.S.A.* 100, 271–276. doi: 10.1073/pnas.0136822100
- Mogil, J. S. (2009). Are we getting anywhere in human pain genetics? *Pain* 146, 231–232. doi: 10.1016/j.pain.2009.07.023
- Moore, S. D., Madamba, S. G., Schweitzer, P., and Siggins, G. R. (1994). Voltage-dependent effects of opioid peptides on hippocampal CA3 pyramidal neurons *in vitro*. *J. Neurosci.* 14, 809–820.
- Morgan, M. M., and Christie, M. J. (2011). Analysis of opioid efficacy, tolerance, addiction and dependence from cell culture to human. *Br. J. Pharmacol.* 164, 1322–1334. doi: 10.1111/j.1476-5381.2011.01335.x
- Nassirpour, R., Bahima, L., Lalive, A. L., Luscher, C., Lujan, R., and Slesinger, P. A. (2010). Morphine- and CaMKII-dependent enhancement of GIRK channel signaling in hippocampal neurons. *J. Neurosci.* 30, 13419–13430. doi: 10.1523/JNEUROSCI.2966-10.2010
- Navarro, B., Kennedy, M. E., Velimirovic, B., Bhat, D., Peterson, A. S., and Clapham, D. E. (1996). Nonselective and G betagamma-insensitive weaver K⁺ channels. *Science* 272, 1950–1953. doi: 10.1126/science.272.5270.1950
- Neer, E. J. (1995). Heterotrimeric G proteins: organizers of transmembrane signals. *Cell* 80, 249–257. doi: 10.1016/0092-8674(95)90407-7
- Neubig, R. R. (1994). Membrane organization in G-protein mechanisms. *FASEB J.* 8, 939–946.
- Nishizawa, D., Nagashima, M., Katoh, R., Satoh, Y., Tagami, M., Kasai, S., et al. (2009). Association between KCNJ6 (GIRK2) gene polymorphisms and post-operative analgesic requirements after major abdominal surgery. *PLoS ONE* 4:e7060. doi: 10.1371/journal.pone.0007060
- Nobles, M., Benians, A., and Tinker, A. (2005). Heterotrimeric G proteins precouple with G protein-coupled receptors in living cells. *Proc. Natl. Acad. Sci. U.S.A.* 102, 18706–18711. doi: 10.1073/pnas.0504778102
- Nockemann, D., Rouault, M., Labuz, D., Hublitz, P., McKnelly, K., Reis, F. C., et al. (2013). The K(+) channel GIRK2 is both necessary and sufficient for peripheral opioid-mediated analgesia. *EMBO Mol. Med.* 5, 1263–1277. doi: 10.1002/emmm.201201980
- Obara, I., Parkitna, J. R., Korostynski, M., Makuch, W., Kaminska, D., Przewlocka, B., et al. (2009). Local peripheral opioid effects and expression of opioid genes in the spinal cord and dorsal root ganglia in neuropathic and inflammatory pain. *Pain* 141, 283–291. doi: 10.1016/j.pain.2008.12.006
- Orly, J., and Schramm, M. (1976). Coupling of catecholamine receptor from one cell with adenylate cyclase from another cell by cell fusion. *Proc. Natl. Acad. Sci. U.S.A.* 73, 4410–4414. doi: 10.1073/pnas.73.12.4410
- Padgett, C. L., Lalive, A. L., Tan, K. R., Terunuma, M., Munoz, M. B., Pangalos, M. N., et al. (2012). Methamphetamine-evoked depression of GABA(B) receptor signaling in GABA neurons of the VTA. *Neuron* 73, 978–989. doi: 10.1016/j.neuron.2011.12.031
- Patil, N., Cox, D. R., Bhat, D., Faham, M., Myers, R. M., and Peterson, A. S. (1995). A potassium channel mutation in weaver mice implicates membrane excitability in granule cell differentiation. *Nat. Genet.* 11, 126–129. doi: 10.1038/ng1095-126
- Pert, C. B., and Snyder, S. H. (1973). Opiate receptor: demonstration in nervous tissue. *Science* 179, 1011–1014. doi: 10.1126/science.179.4077.1011
- Pradhan, A. A., Befort, K., Nozaki, C., Gaveriaux-Ruff, C., and Kieffer, B. L. (2011). The delta opioid receptor: an evolving target for the treatment of brain disorders. *Trends Pharmacol. Sci.* 32, 581–590. doi: 10.1016/j.tips.2011.06.008
- Pradhan, A. A., Walwyn, W., Nozaki, C., Filliol, D., Erbs, E., Matifas, A., et al. (2010). Ligand-directed trafficking of the delta-opioid receptor *in vivo*: two paths toward analgesic tolerance. *J. Neurosci.* 30, 16459–16468. doi: 10.1523/JNEUROSCI.3748-10.2010
- Pravetoni, M., and Wickman, K. (2008). Behavioral characterization of mice lacking GIRK/Kir3 channel subunits. *Genes Brain Behav.* 7, 523–531. doi: 10.1111/j.1601-183X.2008.00388.x
- Rahal, K. M., Walker, J. K., and Bohn, L. M. (2005). Morphine side effects in beta-arrestin 2 knockout mice. *J. Pharmacol. Exp. Ther.* 314, 1195–1201. doi: 10.1124/jpet.105.087254
- Rasmussen, S. G., Devree, B. T., Zou, Y., Kruse, A. C., Chung, K. Y., Kobilka, T. S., et al. (2011). Crystal structure of the beta2 adrenergic receptor-Gs protein complex. *Nature* 477, 549–555. doi: 10.1038/nature10361
- Raveh, A., Riven, I., and Reuveny, E. (2009). Elucidation of the gating of the GIRK channel using a spectroscopic approach. *J. Physiol.* 587, 5331–5335. doi: 10.1113/jphysiol.2009.180158
- Rebois, R. V., Robitaille, M., Gales, C., Dupre, D. J., Baragli, A., Trieu, P., et al. (2006). Heterotrimeric G proteins form stable complexes with adenylyl cyclase and Kir3.1 channels in living cells. *J. Cell Sci.* 119, 2807–2818. doi: 10.1242/jcs.03021
- Richard-Lalonde, M., Nagi, K., Audet, N., Sleno, R., Amraei, M., Hogue, M., et al. (2013). Conformational dynamics of Kir3.1/Kir3.2 channel activation via delta-opioid receptors. *Mol. Pharmacol.* 83, 416–428. doi: 10.1124/mol.112.081950
- Riven, I., Iwanir, S., and Reuveny, E. (2006). GIRK channel activation involves a local rearrangement of a preformed G protein channel complex. *Neuron* 51, 561–573. doi: 10.1016/j.neuron.2006.08.017
- Robitaille, M., Ramakrishnan, N., Baragli, A., and Hebert, T. E. (2009). Intracellular trafficking and assembly of specific Kir3 channel/G protein complexes. *Cell. Signal.* 21, 488–501. doi: 10.1016/j.cellsig.2008.11.011
- Romero, G., Von Zastrow, M., and Friedman, P. A. (2011). Role of PDZ proteins in regulating trafficking, signaling, and function of GPCRs: means, motif, and opportunity. *Adv. Pharmacol.* 62, 279–314. doi: 10.1016/B978-0-12-385952-5.00003-8
- Rusinova, R., Mirshahi, T., and Logothetis, D. E. (2007). Specificity of Gbetagamma signaling to Kir3 channels depends on the helical domain of pertussis toxin-sensitive Galpha subunits. *J. Biol. Chem.* 282, 34019–34030. doi: 10.1074/jbc.M704928200
- Saenz Del Burgo, L., Cortes, R., Mengod, G., Zarate, J., Echevarria, E., and Salles, J. (2008). Distribution and neurochemical characterization of neurons expressing GIRK channels in the rat brain. *J. Comp. Neurol.* 510, 581–606. doi: 10.1002/cne.21810
- Saitoh, A., Sugiyama, A., Nemoto, T., Fujii, H., Wada, K., Oka, J., et al. (2011). The novel delta opioid receptor agonist KNT-127 produces antidepressant-like and antinociceptive effects in mice without producing convulsions. *Behav. Brain Res.* 223, 271–279. doi: 10.1016/j.bbr.2011.04.041
- Scherrer, G., Imachi, N., Cao, Y. Q., Contet, C., Mennicken, F., O'Donnell, D., et al. (2009). Dissociation of the opioid receptor mechanisms that control mechanical and heat pain. *Cell* 137, 1148–1159. doi: 10.1016/j.cell.2009.04.019
- Schreibmayer, W., Dessauer, C. W., Vorobiov, D., Gilman, A. G., Lester, H. A., Davidson, N., et al. (1996). Inhibition of an inwardly rectifying K⁺ channel by G-protein alpha-subunits. *Nature* 380, 624–627. doi: 10.1038/380624a0
- Signorini, S., Liao, Y. J., Duncan, S. A., Jan, L. Y., and Stoffel, M. (1997). Normal cerebellar development but susceptibility to seizures in mice lacking G protein-coupled, inwardly rectifying K⁺ channel GIRK2. *Proc. Natl. Acad. Sci. U.S.A.* 94, 923–927. doi: 10.1073/pnas.94.3.923
- Simon, E. J., Hiller, J. M., and Edelman, I. (1973). Stereospecific binding of the potent narcotic analgesic (3H) Etorphine to rat-brain homogenate. *Proc. Natl. Acad. Sci. U.S.A.* 70, 1947–1949. doi: 10.1073/pnas.70.7.1947
- Stein, C., Millan, M. J., Shippenberg, T. S., Peter, K., and Herz, A. (1989). Peripheral opioid receptors mediating antinociception in inflammation. Evidence for involvement of mu, delta and kappa receptors. *J. Pharmacol. Exp. Ther.* 248, 1269–1275.
- Tavani, A., Petrillo, P., La Regina, A., and Sbacchi, M. (1990). Role of peripheral mu, delta and kappa opioid receptors in opioid-induced inhibition of gastrointestinal transit in rats. *J. Pharmacol. Exp. Ther.* 254, 91–97.
- Tian, W. N., Duzic, E., Lanier, S. M., and Deth, R. C. (1994). Determinants of alpha 2-adrenergic receptor activation of G proteins: evidence for a precoupled receptor/G protein state. *Mol. Pharmacol.* 45, 524–531.
- Tolkovsky, A. M., and Levitzki, A. (1978). Mode of coupling between the beta-adrenergic receptor and adenylate cyclase in turkey erythrocytes. *Biochemistry* 17, 3795. doi: 10.1021/bi00611a020

- Urban, J. D., Clarke, W. P., Von Zastrow, M., Nichols, D. E., Kobilka, B., Weinstein, H., et al. (2007). Functional selectivity and classical concepts of quantitative pharmacology. *J. Pharmacol. Exp. Ther.* 320, 1–13. doi: 10.1124/jpet.106.104463
- Vadivelu, N., Mitra, S., and Hines, R. L. (2011). Peripheral opioid receptor agonists for analgesia: a comprehensive review. *J. Opioid Manag.* 7, 55–68. doi: 10.5055/jom.2011.0049
- Van't Veer, A., and Carlezon, W. A. Jr. (2013). Role of kappa-opioid receptors in stress and anxiety-related behavior. *Psychopharmacology (Berl.)* 229, 435–452. doi: 10.1007/s00213-013-3195-5
- Vaughan, C. W., and Christie, M. J. (1997). Presynaptic inhibitory action of opioids on synaptic transmission in the rat periaqueductal grey *in vitro*. *J. Physiol.* 498(Pt 2), 463–472.
- Vaughan, C. W., Ingram, S. L., Connor, M. A., and Christie, M. J. (1997). How opioids inhibit GABA-mediated neurotransmission. *Nature* 390, 611–614. doi: 10.1038/37610
- Vilardaga, J. P., Bunemann, M., Krasel, C., Castro, M., and Lohse, M. J. (2003). Measurement of the millisecond activation switch of G protein-coupled receptors in living cells. *Nat. Biotechnol.* 21, 807–812. doi: 10.1038/nbt838
- Waldhoer, M., Fong, J., Jones, R. M., Lunzer, M. M., Sharma, S. K., Kostenis, E., et al. (2005). A heterodimer-selective agonist shows *in vivo* relevance of G protein-coupled receptor dimers. *Proc. Natl. Acad. Sci. U.S.A.* 102, 9050–9055. doi: 10.1073/pnas.050112102
- Wang, H. B., Zhao, B., Zhong, Y. Q., Li, K. C., Li, Z. Y., Wang, Q., et al. (2010). Coexpression of delta- and mu-opioid receptors in nociceptive sensory neurons. *Proc. Natl. Acad. Sci. U.S.A.* 107, 13117–13122. doi: 10.1073/pnas.1008382107
- Wei, Z. Y., Karim, F., and Roerig, S. C. (1996). Spinal morphine/clonidine antinociceptive synergism: involvement of G proteins and N-type voltage-dependent calcium channels. *J. Pharmacol. Exp. Ther.* 278, 1392–1407.
- Whorton, M. R., and MacKinnon, R. (2011). Crystal structure of the mammalian GIRK2 K⁺ channel and gating regulation by G proteins, PIP₂, and sodium. *Cell* 147, 199–208. doi: 10.1016/j.cell.2011.07.046
- Whorton, M. R., and MacKinnon, R. (2013). X-ray structure of the mammalian GIRK2-beta gamma G-protein complex. *Nature* 498, 190–197. doi: 10.1038/nature12241
- Wickman, K., Karschin, C., Karschin, A., Picciotto, M. R., and Clapham, D. E. (2000). Brain localization and behavioral impact of the G-protein-gated K⁺ channel subunit GIRK4. *J. Neurosci.* 20, 5608–5615.
- Wickman, K., Nemec, J., Gendler, S. J., and Clapham, D. E. (1998). Abnormal heart rate regulation in GIRK4 knockout mice. *Neuron* 20, 103–114. doi: 10.1016/S0896-6273(00)80438-9
- Wickman, K. D., Iniguez-Lluhl, J. A., Davenport, P. A., Taussig, R., Krapivinsky, G. B., Linder, M. E., et al. (1994). Recombinant G-protein beta gamma-subunits activate the muscarinic-gated atrial potassium channel. *Nature* 368, 255–257. doi: 10.1038/368255a0
- Wimpey, T. L., and Chavkin, C. (1991). Opioids activate both an inward rectifier and a novel voltage-gated potassium conductance in the hippocampal formation. *Neuron* 6, 281–289. doi: 10.1016/0896-6273(91)90363-5
- Wreggett, K. A., and De Lean, A. (1984). The ternary complex model. Its properties and application to ligand interactions with the D2-dopamine receptor of the anterior pituitary gland. *Mol. Pharmacol.* 26, 214–227.
- Wrigley, P. J., Jeong, H. J., and Vaughan, C. W. (2010). Dissociation of mu- and delta-opioid inhibition of glutamatergic synaptic transmission in superficial dorsal horn. *Mol. Pain* 6:71. doi: 10.1186/1744-8069-6-71
- Wu, Z. Z., Chen, S. R., and Pan, H. L. (2008). Distinct inhibition of voltage-activated Ca²⁺ channels by delta-opioid agonists in dorsal root ganglion neurons devoid of functional T-type Ca²⁺ currents. *Neuroscience* 153, 1256–1267. doi: 10.1016/j.neuroscience.2008.03.031
- Xu, M., Petraschka, M., McLaughlin, J. P., Westenbroek, R. E., Caron, M. G., Lefkowitz, R. J., et al. (2004). Neuropathic pain activates the endogenous kappa opioid system in mouse spinal cord and induces opioid receptor tolerance. *J. Neurosci.* 24, 4576–4584. doi: 10.1523/JNEUROSCI.5552-03.2004
- Yang, H. Y., Wu, Z. Y., Wood, M., Whiteman, M., and Bian, J. S. (2014). Hydrogen sulfide attenuates opioid dependence by suppression of adenylate cyclase/cAMP pathway. *Antioxid. Redox Signal.* 20, 31–41. doi: 10.1089/ars.2012.5119
- Yokogawa, M., Osawa, M., Takeuchi, K., Mase, Y., and Shimada, I. (2011). NMR analyses of the Gbetagamma binding and conformational rearrangements of the cytoplasmic pore of G protein-activated inwardly rectifying potassium channel 1 (GIRK1). *J. Biol. Chem.* 286, 2215–2223. doi: 10.1074/jbc.M110.160754

Conflict of Interest Statement: The authors declare that the research was conducted in the absence of any commercial or financial relationships that could be construed as a potential conflict of interest.

Received: 16 March 2014; accepted: 18 June 2014; published online: 08 July 2014.

Citation: Nagi K and Pineyro G (2014) Kir3 channel signaling complexes: focus on opioid receptor signaling. *Front. Cell. Neurosci.* 8:186. doi: 10.3389/fncel.2014.00186

This article was submitted to the journal *Frontiers in Cellular Neuroscience*.

Copyright © 2014 Nagi and Pineyro. This is an open-access article distributed under the terms of the Creative Commons Attribution License (CC BY). The use, distribution or reproduction in other forums is permitted, provided the original author(s) or licensor are credited and that the original publication in this journal is cited, in accordance with accepted academic practice. No use, distribution or reproduction is permitted which does not comply with these terms.



Modulatory mechanisms and multiple functions of somatodendritic A-type K⁺ channel auxiliary subunits

Henry H. Jerng* and Paul J. Pfaffinger

Department of Neuroscience, Baylor College of Medicine, Houston, TX, USA

Edited by:

Leigh Anne Swayne, University of Victoria, Canada

Reviewed by:

Stefan H. Heinemann, Friedrich-Schiller-Universität, Germany
Douglas A. Bayliss, University of Virginia, USA

*Correspondence:

Henry H. Jerng, Department of Neuroscience, Baylor College of Medicine, One Baylor Plaza, S630, Houston, TX 77030, USA
e-mail: hjerng@cns.bcm.edu

Auxiliary subunits are non-conducting, modulatory components of the multi-protein ion channel complexes that underlie normal neuronal signaling. They interact with the pore-forming α -subunits to modulate surface distribution, ion conductance, and channel gating properties. For the somatodendritic subthreshold A-type potassium (I_{SA}) channel based on Kv4 α -subunits, two types of auxiliary subunits have been extensively studied: Kv channel-interacting proteins (KChIPs) and dipeptidyl peptidase-like proteins (DPLPs). KChIPs are cytoplasmic calcium-binding proteins that interact with intracellular portions of the Kv4 subunits, whereas DPLPs are type II transmembrane proteins that associate with the Kv4 channel core. Both KChIPs and DPLPs genes contain multiple start sites that are used by various neuronal populations to drive the differential expression of functionally distinct N-terminal variants. In turn, these N-terminal variants generate tremendous functional diversity across the nervous system. Here, we focus our review on (1) the molecular mechanism underlying the unique properties of different N-terminal variants, (2) the shaping of native I_{SA} properties by the concerted actions of KChIPs and DPLP variants, and (3) the surprising ways that KChIPs and DPLPs coordinate the activity of multiple channels to fine-tune neuronal excitability. Unlocking the unique contributions of different auxiliary subunit N-terminal variants may provide an important opportunity to develop novel targeted therapeutics to treat numerous neurological disorders.

Keywords: somatodendritic A-type current, potassium channel, auxiliary subunit, Kv channel-interacting protein, dipeptidyl peptidase-like protein, N-terminal variant, modulatory mechanism, excitability

INTRODUCTION TO I_{SA}

The membranes of neurons contain multiple sets of voltage-sensitive K⁺ (Kv) channels that open and close in response to changes in membrane potential, giving rise to outward K⁺ currents with differing voltage dependence, kinetic properties, and pharmacological sensitivities. One distinct K⁺ current, the subthreshold A-type transient current (I_{SA}), has garnered a great deal of interest since its initial discovery in the neuronal somata by Hagiwara et al. (1961). Later characterized in detail by Connor and Stevens (1971b) and Neher (1971), I_{SA} activates rapidly in the subthreshold range of membrane potentials but rapidly inactivates. At resting membrane potentials more positive than around -50 mV, no I_{SA} current can be elicited unless the membrane is first conditioned to more hyperpolarized potentials to allow recovery from inactivation (Connor and Stevens, 1971a,b; Neher, 1971). Pharmacologically, I_{SA} is identifiable by its elevated sensitivity to block by 4-aminopyridine and considerably reduced sensitivity to tetraethylammonium compared to most other Kv channel currents (Thompson, 1977). Currents with properties matching I_{SA} are found in nearly all excitable cells, both neuronal and non-neuronal (Rudy, 1988).

Studies on I_{SA} functional properties and subcellular localization in neurons have suggested important roles for I_{SA} in neurophysiology. In repetitively firing cells, an inactivation-and-recovery cycle for I_{SA} during the interspike interval regulates spiking timing and firing frequency (Connor and Stevens, 1971a).

Because of its rapid activation, I_{SA} is also capable of suppressing synaptic excitatory potentials and delaying spike firing in response to a superthreshold stimulus (Schoppa and Westbrook, 1999; Shibata et al., 2000; Nadin and Pfaffinger, 2010). In the late 1990's, it was discovered that I_{SA} has an important role in regulating signaling thought to be critical for Hebbian plasticity. In hippocampal pyramidal neurons, in addition to firing an all-or-nothing orthodromic spike down the axon, a graded spike is backpropagated up the dendritic tree. Due to its high density in the dendrites and its rapid activation, I_{SA} suppresses action potential backpropagation (Hoffman et al., 1997). However, in regions of the dendritic tree that experienced recent depolarizing synaptic activity sufficient to inactivate I_{SA} , the backpropagating action potential remains large and induces a large influx of Ca²⁺ that is critical for long-term potentiation (LTP; Johnston et al., 2003). The ability of I_{SA} to compartmentalize excitability and information storage in the dendrites may have been a critical factor in the evolution of the nervous system.

THE I_{SA} CHANNEL IS A MULTI-PROTEIN SUPERMOLECULAR COMPLEX

In the 1980s, genetic analysis of the fruit fly *Drosophila melanogaster* provided an opportunity to probe the molecular basis of I_{SA} . The identification of the *Shaker* gene mutants led to the discovery of the first voltage-gated K⁺ channel, Shaker, and the identification of other subfamilies of Kv channels in the fly

(Shab, Shaw, and Shal) as well as their mammalian homologs (Kv1, Kv2, Kv3, and Kv4; Papazian et al., 1987; Pongs et al., 1988; Butler et al., 1989; Chandy and Gutman, 1993). Of these initial four subfamilies of cloned Kv channels, Kv4 was identified as the best candidate for underlying I_{SA} since Kv4 channels show localization in the soma and dendrites (Sheng et al., 1992) and exhibit biophysical and pharmacological properties that most resemble native I_{SA} in heterologous expression systems (Jerng et al., 2004a). Subsequent breakthrough studies examining the native I_{SA} using genetic knockouts, dominant negative suppression, and RNA interference (RNAi) techniques confirm that indeed Kv4 channels underlie I_{SA} (Johns et al., 1997; Malin and Nerbonne, 2000; Chen et al., 2006b; Lauver et al., 2006).

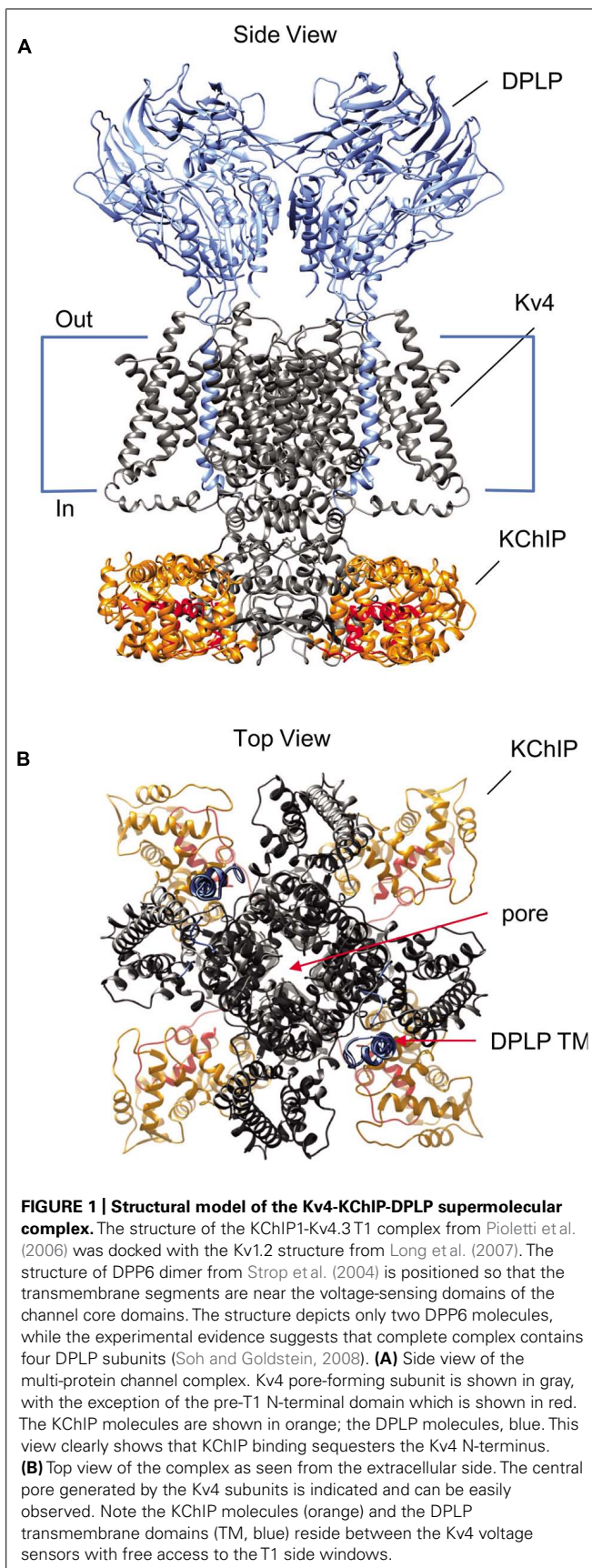
Although Kv4 subunits underlie I_{SA}, the functional properties of Kv4 channels in heterologous cells differ from those of native I_{SA}, especially the kinetics of activation, inactivation and recovery from inactivation (Serodio et al., 1994). As accumulating research began to show that ion channels and receptors function as large macromolecular complexes, An et al. (2000) discovered the first Kv4 auxiliary subunit by using yeast two-hybrid screens with a Kv4 N-terminal domain as bait. Named Kv channel-interacting proteins, KChIPs are cytoplasmic Ca²⁺-binding proteins that significantly increased surface expression of Kv4 current and remodeled current biophysical properties. However, reconstitution studies in heterologous cells showed that co-expression of KChIP with Kv4 channels alone is insufficient to generate the native I_{SA}. Especially critical is the failure of KChIPs to recapitulate the characteristic features of I_{SA}: rapid kinetics of activation, inactivation, and recovery from inactivation.

In the search for additional Kv4 interacting proteins, the discovery of KChIP was quickly followed by another Kv4 modulatory protein, the dipeptidyl peptidase-like proteins (DPLPs). DPLPs are single-pass type II transmembrane proteins belonging to the S9B family of serine proteases, and they consist of DPP6 (aka DPPX) and DPP10 (aka DPPY; Wada et al., 1992; Qi et al., 2003; Takimoto et al., 2006). Although DPLPs are closely related to the DPP4 family of serine proteases, they lack both the active site serine and the molecular architecture necessary for catalytic activity (Kin et al., 2001; Strop et al., 2004). Instead of proteolytic activity, DPP6 and DPP10 interact with Kv4 proteins and modulate Kv4 channel trafficking, surface expression, and gating function (Nadal et al., 2003; Jerng et al., 2004b; Ren et al., 2005; Zagha et al., 2005). Importantly, DPLPs profoundly and fundamentally accelerate Kv4 channel activation and inactivation gating, as well as shifting the voltage dependence of activation and inactivation in the hyperpolarizing direction, accelerating inactivation, altering channel conductance, and changing toxin sensitivity (Kaulin et al., 2009; Maffie et al., 2013). Although DPLPs form homo- or heterodimers in solutions (Strop et al., 2004), the relationship between structures in solution and those fully integrated into the channel remains unknown. Nevertheless, Soh and Goldstein (2008) studied the functional properties of channels from Kv4 and DPP6 subunits linked in tandem as well as the molar ratios of DPP6 and Kv4.2 subunits purified from assembled channels and concluded that channel complexes are composed of four subunits of Kv4.2 and DPP6. Studies of heteromultimeric channel complexes with DPP6a and DPP6K also suggest that

there are four DPP6 subunits per channel (Jerng and Pfaffinger, 2012).

Multiple lines of evidence suggest that the KChIP and DPLP auxiliary subunits work in concert to modulate Kv4 channel function, and that the Kv4, KChIP, and DPLP subunits together form the macromolecular complex responsible for producing I_{SA} (**Figure 1**). Kv4, KChIP, and DPLP transcripts and proteins have overlapping expression patterns throughout the CNS (Rhodes et al., 2004; Zagha et al., 2005; Clark et al., 2008). Kv4, KChIP, and DPLP proteins can be co-immunoprecipitated from brain samples (Nadal et al., 2003; Jerng et al., 2005; Marionneau et al., 2009). Co-assembly of Kv4, KChIP, and DPLP subunits can generate K⁺ currents in heterologous studies with functional properties similar to those found in native I_{SA} (Nadal et al., 2003; Jerng et al., 2005). In cultured cerebellar granule (CG) cells and hippocampal neurons, genetic knockout and RNAi of DPP6 simultaneously reduces the protein level of all ternary channel complex subunits (Nadin and Pfaffinger, 2010; Sun et al., 2011). Meanwhile, genetic knockout of Kv4 expression leads to down-regulation of KChIP protein levels (Menegola and Trimmer, 2006; Norris et al., 2010).

In addition to KChIP and DPLP proteins, various published reports suggest that additional ancillary, cytoskeletal, and molecular chaperone proteins may interact with the I_{SA} channel complex, including Kvβ subunit, Navβ1 subunit, MinK-related protein 1 (MiRP1), kinesin isoform Kif17, Kv channel-associated protein (KChAP), post-synaptic density protein 95 (PSD-95), and filamin (Petrecca et al., 2000; Yang et al., 2001; Zhang et al., 2001; Deschenes and Tomaselli, 2002; Wong et al., 2002; Marionneau et al., 2012a; **Table 1**). All of these proteins have been reported to co-immunoprecipitate with Kv4 subunits from native tissues or transfected culture cells, suggesting that these candidates either directly interact with Kv4 proteins or associate indirectly as part of the large multi-protein complex. However, questions remain as to whether these proteins play a fundamental role in the function of I_{SA}. Compared to KChIPs and DPLPs, their overall abundance in the I_{SA} complex in the brain appears to be low or undetectable (Marionneau et al., 2012b). In addition, the chaperone and cytoskeletal proteins tested so far (KChAP, PSD-95, Kif17, filamin) exert minimal effects on functional properties and increase peak current amplitude significantly less than KChIPs and DPLPs (**Table 1**). Furthermore, studies on the ancillary proteins Kvβ1, Navβ1, and MiRP1, well-known partners of Kv1, Nav, and KCNQ channels, respectively, have yielded conflicting results for their modulatory effects on Kv4 channels. Their facilitative effect on Kv4 peak current is highly variable, between 0.2- to 3-fold increase and significantly less than KChIPs and DPLPs. Moreover, unlike KChIPs and DPLPs, their molecular interaction with Kv4 channels remains controversial. For example, based on crystal structures, Kvβ1 interacts with the T1 domains of Kv1 channels (Gulbis et al., 2000); however, the motif used by Kv1 channels is not conserved in Kv4 channels, and it is currently unclear whether Kvβ interacts with Kv4 channels at the N- or C-terminal domain (Nakahira et al., 1996; Yang et al., 2001; Wang et al., 2003). Finally, it is possible that the regulatory effects observed under high expression conditions in heterologous cells are not normally seen in the nervous system. For these reasons,



discussions of these other ancillary proteins are not included in this review.

N-TERMINAL VARIANTS OF AUXILIARY SUBUNITS AND THEIR DIFFERENTIAL EXPRESSION PATTERNS

Following their discovery, it was quickly realized that KChIP and DPLP proteins exist as N-terminal variants, products of different start sites and/or alternative splicing (Jerng et al., 2004a; Pruunsild and Timmusk, 2005; Pongs and Schwarz, 2010). All genes encoding KChIP and DPLP contain a core set of exons that are included in every transcript, but they also contain alternative promoters and optional exons that can be alternatively spliced into the final transcript (**Figure 2**). As a result, the different transcripts encode a set of proteins with variable N-termini attached to a common C-terminal core. As shown by Northern hybridization, RT-PCR, and *in situ* hybridization, the expression of N-terminal variant transcripts is not uniform throughout the brain; instead, each variant exhibits a specific expression pattern with variable levels of transcripts in different neuronal populations. Importantly, when combined with variant-specific functional effects (discussed later), the overlapping of distinct KChIP and DPLP variants is an important contributor to functional or regulatory differences in I_{SA} of different neurons.

KChIPs

As members of the neuronal calcium sensor (NCS) gene family, KChIPs have existed as a distinct gene family predating the divergence of cnidarians such as *Nematostella* (An et al., 2000). In common with other members of the NCS-1 gene family, KChIP proteins have N- and C-terminal lobules each containing two EF-hands surrounding a deep hydrophobic pocket. Under normal circumstances, it appears that only EF-3 and EF-4 of the C-terminal lobule binds Ca²⁺; in the N-terminal lobule, EF-1 is unbound and EF-2 binds Mg²⁺. In mammals, four separate genes (KCINP1, KCINP2, KCINP3, KCINP4) encode the four families of KChIP proteins: KChIP1, KChIP2, KChIP3, and KChIP4 (**Figure 2A**). As for gene structure, all KChIP1–4 genes contain a homologs set of 7 C-terminal exons encoding the four EF-hands of the core domain, which are preceded by multiple transcription start sites and alternative exons (**Figure 2A**). The resulting transcripts create sets of 17 different proteins with variable N-terminal domains that comprise the most diverse class of Kv channel auxiliary subunits.

Further analysis of KChIP transcript expression in various tissues yields distinctive tissue specificity and expression patterns, as summarized in **Figure 3A** with references provided in the figure legend. Among the four KChIP families, only KChIP4 is expressed exclusively in the brain, while the others can be found in other tissues such as heart, lung, and testis. Although the mRNA transcripts of nearly all the KChIP N-terminal variants are detected in the brain, the expression levels vary significantly between neuronal populations, with some expressing strongly only in very specific neuronal populations. In addition, some KChIP variants exhibit preferential expression along the anterior–posterior axis. For example, whereas KChIP3a and KChIP3x transcripts have mostly strong expression throughout the brain regions, other

Table 1 | Validation of auxiliary subunits and accessory proteins.

Proteins	Kv4.2-IP PAF	Kv4 CoIP	Δ Ipeak	Δ Functional properties
Auxiliary subunits				
KChIP1	–	Brain	↑ 7.5-fold	Slowed inactivation; rightward shift in SSI; accelerated recovery; accelerated closing (An et al., 2000; Holmqvist et al., 2002; Morohashi et al., 2002)
KChIP2	1.7	Brain	↑ 5.5-fold	
KChIP3	1.4	Brain	↑ 5.8-fold	
KChIP4	5.6	Brain	↑ 2- to 3-fold	
DPP6	5.3	Brain	↑ 4- to 18-fold	Accelerated activation and inactivation; leftward shifts in SSI and G-V relationship; accelerated recovery; accelerated channel closing (Nadal et al., 2003, 2006; Jerng et al., 2004b; Zagha et al., 2005)
DPP10	2.0	Brain	↑ 5.9-fold	
Accessory proteins				
Kvβ1	0.7	Brain	↑ 0.2- to 3-fold	Moderate acceleration of inactivation; moderate to no effect on SSI; no effect on recovery; Kv1 preference (Nakahira et al., 1996; Yang et al., 2001; Wang et al., 2003; Aimond et al., 2005)
Navβ1	0.8	Brain Heart	↑ 0.3- to 2-fold	Inconsistent effects reported (Chabala et al., 1993; Deschenes and Tomaselli, 2002; Deschenes et al., 2008; Hu et al., 2012; Marionneau et al., 2012a)
MiRP1	–	<i>In vitro</i>	Variable	Inconsistent effects reported (Zhang et al., 2001; Deschenes and Tomaselli, 2002; Radicke et al., 2006)
KChAP	–	Heart	↑ 0.8-fold	None (Kuryshv et al., 2000, 2001)
NCS-1	–	Heart	↑ 0.5-fold	Inconsistent effects reported (Nakamura et al., 2001; Guo et al., 2002; Ren et al., 2003)
PSD-95	–	<i>In vitro</i>	↑ 2-fold	None (Wong et al., 2002; Wong and Schlichter, 2004)
Filamin	–	Brain	↑ 2.5-fold	None (Petrecca et al., 2000)
Kinesin isoform Kif17	–	Brain	ND	ND (Chu et al., 2006)

PAF, protein abundance factor; PAF (Kv4.2) = 2.1 (Marionneau et al., 2011); (–), not detected; ND, not determined; SSI, steady-state inactivation; G-V, conductance-voltage.

Other proteins (*Gabra-6*, *Gpr158*, *Prkcb1*) have not undergone validation.

variants show general preferences for expression in the fore-brain (KChIP2a) or hindbrain (KChIP2g, KChIP4bL, KChIP4a, KChIP4d, KChIP4e).

Although the KChIP core is cytoplasmic by nature, the variable N-termini of KChIPs play a major role in controlling the protein's subcellular localization by encoding motifs that induce the protein to associate with membranes (**Figure 4**). Mammalian KChIPs can be divided into four classes based on the presence or absence of specific N-terminal membrane association motifs: cytoplasmic, N-myristoylated, S-palmitoylated, and transmembrane. N-myristoylation occurs in KChIP1a and KChIP1b when a shared glycine residue at position two is modified with a myristoylate group (O'Callaghan et al., 2003; **Figure 4B**). N-terminal myristoylation is a common feature of other NCS-1 family proteins and is often seen in invertebrate KChIPs; however, only these two KChIP1 variants are known to be myristoylated in mammals. In other NCS-1 family proteins, like recoverin, the membrane association can be regulated by a Ca²⁺-myristoyl switch, whereby Ca²⁺ binding to EF-hands 2 and 3 leads to sequestration of the fatty acid chain by the protein's hydrophobic pocket (Tanaka et al., 1995). However, KChIP1a and KChIP1b appear to remain membrane-anchored regardless of the Ca²⁺ concentration, and N-myristoylation causes the KChIP1 proteins to localize to the post-ER trafficking vesicles,

possibly the secretory vesicles of the Golgi body (O'Callaghan et al., 2003). It is hypothesized that N-myristoylation of these KChIPs help regulate the trafficking of Kv4 channels to the plasma membrane.

A second form of fatty acid modification of KChIPs, S-palmitoylation, appears to have evolved more recently but prior to the divergence of vertebrate KChIPs into different families (**Figure 4C**). S-palmitoylation motifs are found in both Exon 1 and Exon 2 of different KChIP genes, based on analysis by a palmitoylation site prediction algorithm (CSS-Palm 4.0) and mutational analysis (Takimoto et al., 2002; Ren et al., 2008). S-palmitoylation is a major post-translational modification (8 out of 17 variants) of the KChIP N-terminal variants, and for S-palmitoylated variants, the fatty acid attachment is required for the facilitation of Kv4 expression at the cell surface by KChIPs (Takimoto et al., 2002). Interestingly, the S-palmitoylation of these KChIPs may have important implications in the trafficking of Kv4 channel complexes to post-synaptic lipid rafts in the brain. Kv4.2 from rat brain preparations is found in the lipid rafts, a detergent-insoluble glycolipid-enriched membrane fraction (Wong and Schlichter, 2004), but the recruitment of Kv4.2 to lipid rafts cannot be explained by an interaction between Kv4.2 and the major post-synaptic density protein (PSD-95). Since S-palmitoylated proteins are known to accumulate in the lipid rafts, perhaps

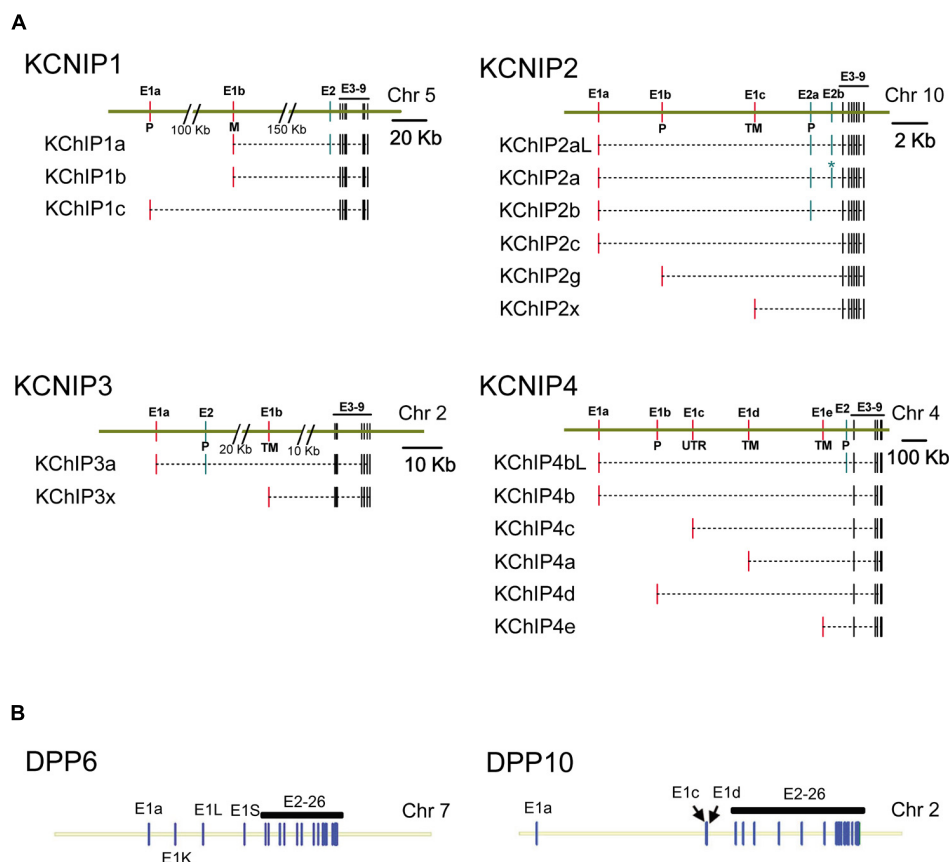


FIGURE 2 | Genomic structure of KChIP and DPLP genes. Gene structures for Kv4.2 auxiliary subunit proteins show a common core with variable N-terminal exons. **(A)** KChIP genes show a common set of 3' exons 3–9 with 1 to 2 alternative 5' exons used to construct the final mRNA transcript. **(B)** DPLP genes show a common set of 3' exons 2–26 with alternative 5' first exons. Maps were constructed using exon locations in human chromosomes as given in Consensus CDS data base (<http://www.ncbi.nlm.nih.gov/CCDS>) or determined from published mRNA sequences using Splign (<http://www.ncbi.nlm.nih.gov/sutils/splign>). Additional splice variants of these genes have been

proposed that are not shown. **(A)** KChIP1: KChIP1a-CCDS34286, KChIP1b-CCDS4374, KChIP1c-CCDS34285. KChIP2: KChIP2aL-CCDS7521, KChIP2a-CCDS7522, KChIP2b-CCDS41562, KChIP2c-CCDS7524, KChIP2g-CCDS7525, KChIP2x- Jerng and Pfaffinger (2008). KChIP3: KChIP3a-CCDS2013, KChIP3x-CCDS33245. KChIP4: KChIP4bL-CCDS43216, KChIP4b-CCDS43215, KChIP4c-CCDS47035, KChIP4a-CCDS3428, KChIP4d-CCDS43217, KChIP4e- Jerng and Pfaffinger (2008). **(B)** DPP6: splicing based on Jerng et al. (2009). DPP10: DPP10a-CCDS46400, DPP10c-CCDS54388, DPP10d-CCDS33278. P, S-palmitoylation; M, N-myristoylation; TM, transmembrane.

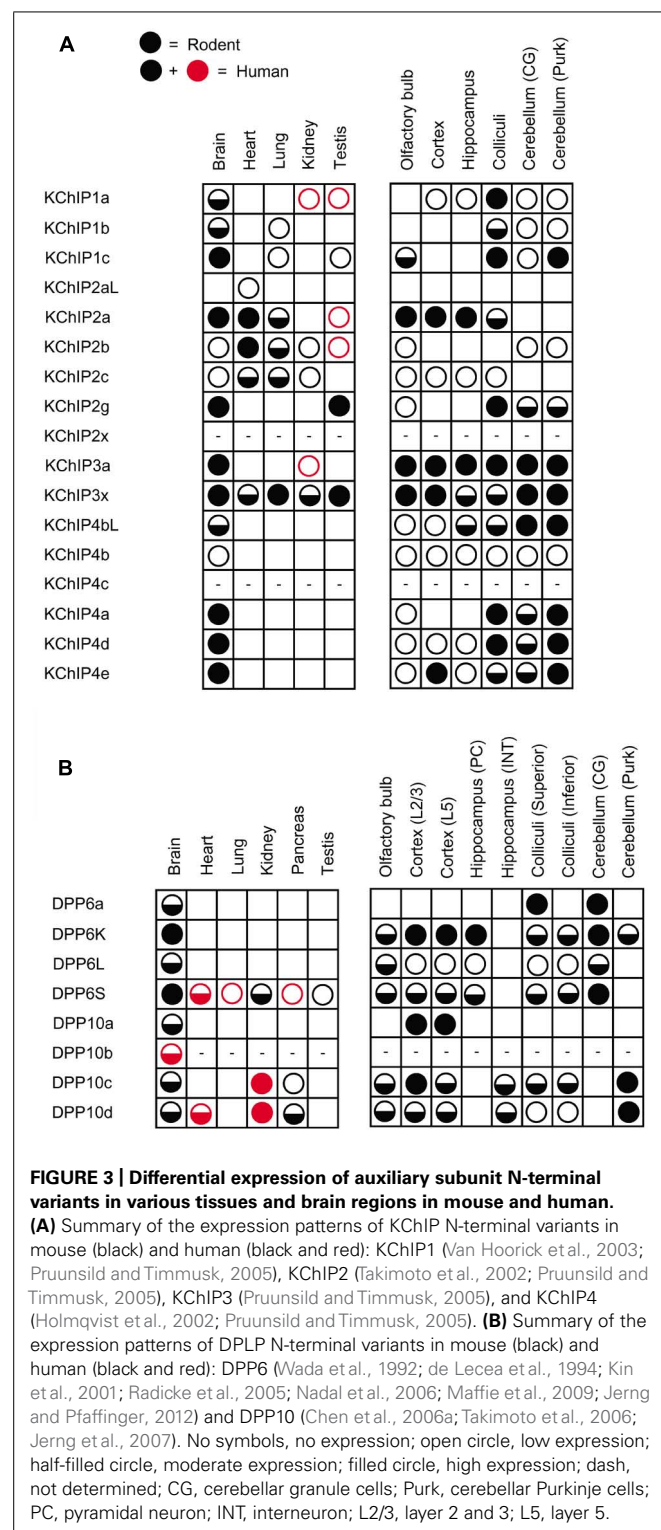
S-palmitoylation of KChIPs play an important role in transporting Kv4 channels to lipid rafts. Furthermore, S-palmitoylation is a reversible process, suggesting that trafficking of Kv4 channels may be regulated by the cell. Indeed, studies by Pruunsild and Timmusk (2012) using over-expression of tagged KChIP variants in neurons indicate that, while N-myristoylated and transmembrane KChIPs consistently show respectively cytoplasmic punctuate and perinuclear localization, many of the supposed S-palmitoylated KChIPs were diffusely distributed throughout the neuron (Pruunsild and Timmusk, 2012).

In addition to N-myristoylation and S-palmitoylation, some KChIP N-terminal variants (KChIP2x, KChIP3x, KChIP4a, KChIP4e) contain a transmembrane domain capable of modulating both surface expression and gating (Figure 4D). Based on sequence similarity, it is likely that the transmembrane-encoding N-terminal exons of KChIP2x, KChIP3x, and KChIP4a have been retained from the ancestral KChIP gene, and they all show similar

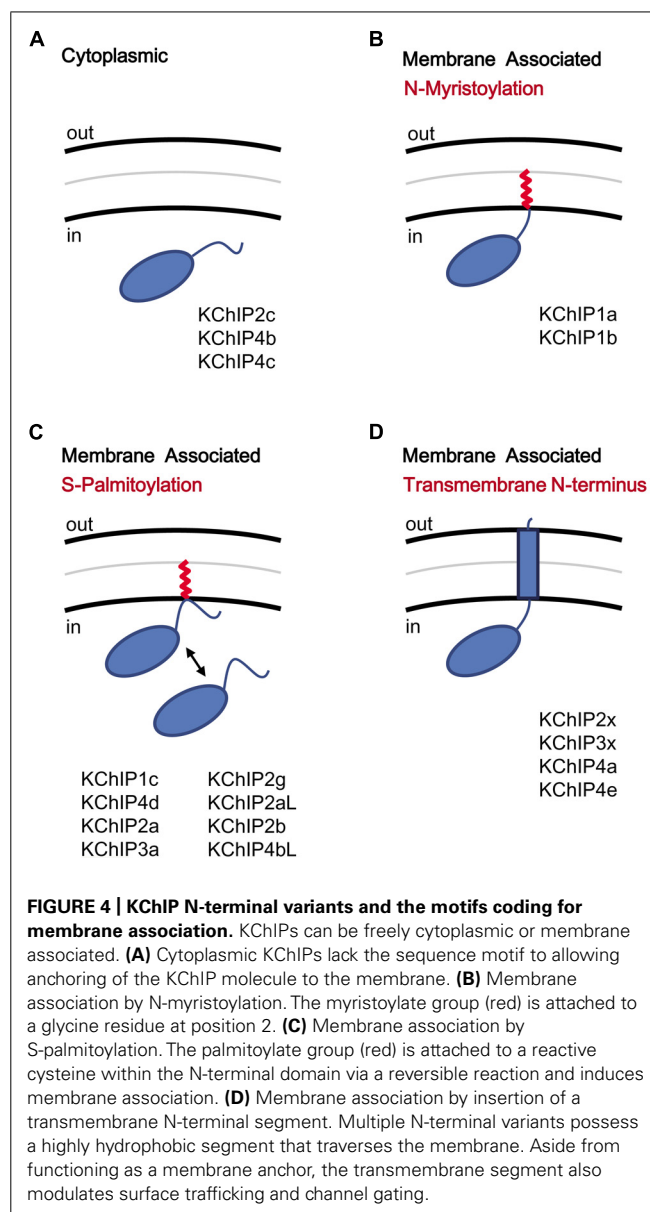
functional effects, including ER retention, suppression of Kv4 functional expression, and modulation of channel gating properties (Jerng and Pfaffinger, 2008). KChIP4e, which is also predicted to have a transmembrane domain, likewise has a perinuclear sub-cellular localization, even though a fusion protein between the KChIP4e variable N-terminus with eGFP was not found to associate with the membrane fraction (Pruunsild and Timmusk, 2012). In summary, while N-myristoylation and S-palmitoylation can specifically promote trafficking of KChIPs to the post-ER or the Golgi bodies, the transmembrane segment found in KChIP2x, KChIP3x, and KChIP4a affect both channel gating as well as trafficking.

DPLPs

The two DPLP genes, DPP6 and DPP10, are homologous genes with significant sequence identity and are likely products of gene duplication early during the evolution of vertebrates (Figure 2B).



The overall genomic structures of DPP6 and DPP10 are strikingly similar, with alternative first Exons encoding the variable cytoplasmic N-termini and a common core set of 25 exons encoding the transmembrane domain and globular extracellular domain (Takimoto et al., 2006; Jerng et al., 2009). Exon 1a shares significant



functional and sequence homology between DPP6 and DPP10 and thus likely predates the ancestral split into separate genes (Jerng et al., 2009). Thus far, five DPP6 (DPP6a, DPP6K, DPP6L, DPP6D, DPP6S) and four DPP10 (DPP10a, DPP10b, DPP10c, DPP10d) N-terminal variants have been isolated in mammals for a combined total of nine variants, and all but DPP6D has been functionally characterized (Nadal et al., 2006; Takimoto et al., 2006).

The expression profiles of DPP6 and DPP10 N-terminal variants have revealed some interesting findings (Figure 3B). First, the precise DPLP N-terminal variants expressed vary even between mammalian species. For example, DPP10c is found in human but not in rodents (Takimoto et al., 2006). Second, in both humans and mice, DPP6S, DPP10c, and DPP10d are widely expressed in non-brain tissues (Wada et al., 1992; Radicke et al., 2005; Takimoto et al., 2006). Interestingly, the first exons that encode DPP6S and DPP10d N-termini are the alternative exons closest to Exon

2, suggesting that perhaps they share a promoter with decreased specificity for brain expression. Third, the expression patterns of DPP6a and DPP10a paralogs are the most specific; DPP10a is expressed specifically in the cortex, whereas DPP6a is expressed in superior colliculus, CG cells, red nucleus, and other specific brain structures (Jerng et al., 2007; Maffie et al., 2009; Jerng and Pfaffinger, 2012). Fourth, DPP6 prefers to be expressed in neurons that also express Kv4.2, such as hippocampal pyramidal neurons and CG cells (Nadal et al., 2006; Clark et al., 2008). DPP10 prefers to be expressed in neurons that also express Kv4.3, such as hippocampal interneurons and cerebellar Purkinje neurons (Zagha et al., 2005).

HOW Kv4 FUNCTIONAL PROPERTIES ARE MODULATED BY AUXILIARY SUBUNITS CORE REGIONS

In the past two decades, tremendous progress has been made in our understanding of the molecular basis underlying the functional properties of Kv channels. Kv4 channels, like other voltage-gated K⁺ channels, are rotationally symmetrical homo- or heterotetrameric arrangements of Kv4.1, Kv4.2, and Kv4.3 pore-forming α -subunits (Long et al., 2007; **Figure 1**). The Kv4 pore-forming subunits consist of cytoplasmic N- and C-terminal domains and a central transmembrane core region consisting of six transmembrane segments (S1–S6), a pore loop region (P), and the associated inter-segment linkers. The transmembrane core region can be divided into the voltage-sensing region (S1–S4) and the pore-lining region (S5–P–S6; Kubo et al., 1993). The pore-lining region of Kv channel α -subunits contains the minimal elements required for K⁺ selectivity, conductance, and certain forms of inactivation. In the cytoplasmic N-terminus, the T1 domain controls the organized subfamily specific tetramerization of Kv4 subunits and plays an important role in KChIP protein assembly (Shen and Pfaffinger, 1995). In the mature channel, the T1 domain hangs down from the central axis of the channel core in a manner that has been likened to a gondola. The structural organization of the cytoplasmic C-terminal portion of the channel is less well understood, but this region contains important phosphorylation sites as well as a PDZ-binding motif (Jerng et al., 2004a).

Structure-function studies in heterologous expression systems have contributed significantly to our understanding of how KChIP and DPLP auxiliary subunits modulate the Kv4 channel. Generally, these studies have shown that auxiliary subunits have certain effects that are attributed to the core domain and thus common to all variants of a particular subunit class, as well as additional modulatory effects that are only produced by certain N-terminal variants. We will first consider the effects that are produced in common.

MODULATION OF EXPRESSION AND GATING BY THE KCHIP CORE DOMAIN

When Kv4 channels are expressed alone in heterologous systems, the N-terminal portion of the peptide forms an intracellular pore blocker that produces open-state inactivation (OSI) similar to the rapid “ball-and-chain” N-type inactivation of Shaker channels (Gebauer et al., 2004). In addition to producing N-type inactivation, the N-terminal domain also performs a separate

function, one of suppressing the surface expression of Kv4 channels by inducing ER retention (Shibata et al., 2003). Both of these N-terminal functions are suppressed by KChIP molecules. KChIP proteins use their hydrophobic pockets to bind the hydrophobic Kv4 N-terminal domain, with critical interactions involving highly conserved Trp8 and Phe11 residues in the Kv4 channel N-terminus (**Figure 1**; Scannevin et al., 2004; Zhou et al., 2004; Pioletti et al., 2006; Wang et al., 2007). When all four Kv4 N-termini are bound to KChIPs, the channel complex is released from ER retention and placed at high levels on the cell surface (Kunjilwar et al., 2013). As expected, these channels also have slowed inactivation due to the sequestration of the Kv4 N-terminus.

In addition, KChIP binding accelerates recovery from inactivation by modulating a second inactivation phenomenon present in Kv4 channels often described as closed-state inactivation (CSI). As opposed to OSI, CSI occurs while the channel is undergoing activation or deactivation transitions, and it has been proposed to involve a decoupling of voltage sensor movement from channel opening (Jerng et al., 1999; Bähring et al., 2001; Bähring and Covarrubias, 2011). Channels that undergo N-type inactivation often transition over to CSI, and thus recovery from this state is a key determinant of inactivation recovery kinetics. While the exact mechanism of KChIP-mediated acceleration of recovery is not entirely clear, a key factor appears to involve KChIP interactions at a second binding site on the side of the Kv4 subunit T1 domain (Site 2; Scannevin et al., 2004; Pioletti et al., 2006; Wang et al., 2007). KChIP protein binding at Site 2 bridges two T1 domains, stabilizing the T1 domain assembly interface and helps to drive Kv4 channel assembly. The T1 domain has been shown to affect recovery from CSI, and it is most likely that the KChIP-mediated stabilization of the T1 domain structure restricts its potential conformations and leads to an acceleration of recovery kinetics.

MODULATION OF EXPRESSION AND GATING BY THE DPLP CORE DOMAIN

Using their single-pass transmembrane domains, DPLPs interact with Kv4 channels via the channel core transmembrane region rather than the cytoplasmic N-terminus used by KChIPs (**Figure 1**; Dougherty et al., 2009). As for the sites of interaction on Kv4 subunits, some preliminary evidence suggests that the DPLP transmembrane domain is interacting with portions of the S1 and S2 segments, although the exact binding site is not yet clear (Ren et al., 2003). Since DPLPs can affect both single-channel conductance and toxin binding, two properties that depend on the pore structure, it is likely that DPLP transmembrane binding has an impact on the packing of the transmembrane pore domain. These packing effects may restrict the intermediate gating states available to the channel, thereby accelerating the channel gating kinetics.

The interaction between DPLP and Kv4 subunits also promote surface expression of Kv4 channels in heterologous expression studies, similar to the effects of KChIP co-expression; however, the mechanism appears to be different and does not involve sequestration of the Kv4 channel N-terminus (Kunjilwar et al., 2013). Instead, it appears that DPLP-mediated enhancement of

Kv4 expression depends on the glycosylation state of the channel. By binding to the Kv4 channel, DPLPs provide a large extracellular domain with multiple glycosylation sites and, in effect, alter the glycosylation state of the channel. The trafficking effects of DPLPs, at least in part, depends on proper glycosylation of the DPLP extracellular domain, since treatment with tunicamycin or mutations that disrupt glycosylation results in a loss of the enhanced expression associated with DPLPs (Cotella et al., 2010; Kunjilwar et al., 2013).

FUNCTIONAL IMPACT OF THE N-TERMINAL “TOOL KIT” AND THEIR MECHANISM OF ACTION

Kv channel-interacting protein and DPLP N-terminal variants have distinct expression patterns and unique functional effects that are likely important for shaping channel functional properties, post-translational regulation, and subcellular localization. Some of the unique properties of KChIP and DPLP variants have been identified in heterologous expression systems, but other functional effects may require native expression environments to be observed. Since most of the variable N-terminal exons found in KChIP and DPLP genes are highly conserved throughout vertebrate evolution, it is very likely that every variant encodes some important specialized functions. In this section, we will discuss some of the known functional effects of specific N-terminal variants.

KChIP2x, KChIP3x, KChIP4a, AND KChIP4e: THE tmKChIPs

The variable N-terminal domains of KChIP2x, KChIP3x, and KChIP4a feature a stretch of hydrophobic amino acids that folds into a transmembrane segment, facilitates membrane partition, and promotes ER retention (Figure 5A; Jerng and Pfaffinger, 2008; Pruunsild and Timmusk, 2012). In intact cells, biotinylation studies of N-terminal cysteine mutants show that the KChIP4a N-terminus is extracellular and the transmembrane segment begins with leucine at residue 3. In their *in vitro* studies of KChIP4a, Schwenk et al. (2008) and Liang et al. (2009) show that a 21-residue-long segment beginning with Leu-3 or Glu-4 forms a 6-turn α -helix in solution NMR and in X-ray crystallography, and under *in vitro* conditions, this helix can fold back onto the core domain and bind the same hydrophobic pocket that sequesters Kv4 N-terminal domain (Schwenk et al., 2008; Liang et al., 2009). However, this autoinhibitory state of KChIP4a appears short-lived, since the Kv4.3 N-terminus can out-compete the KChIP4a N-terminus for the hydrophobic pocket and free the KChIP4a N-terminus (Liang et al., 2009), thereby allowing it to become ultimately anchored in the membrane. The final N-terminal variant with a putative transmembrane N-terminus, KChIP4e, is considerably different from the paralogs of KChIP2x, KChIP3x, and KChIP4a. Based on analysis by The Eukaryotic Linear Motif website (<http://elm.eu.org>), the putative transmembrane domain of KChIP4e begins at residue 10 and ends at 32, giving a longer extracellular N-terminal stretch. Because the transmembrane nature of their N-termini, in this review these variants are collectively referred to as transmembrane KChIPs, or tmKChIPs.

Although KChIP2x, KChIP3x, and KChIP4a are in many ways functionally similar, specific functional differences between these tmKChIPs and KChIP4e suggest that the regulatory effects

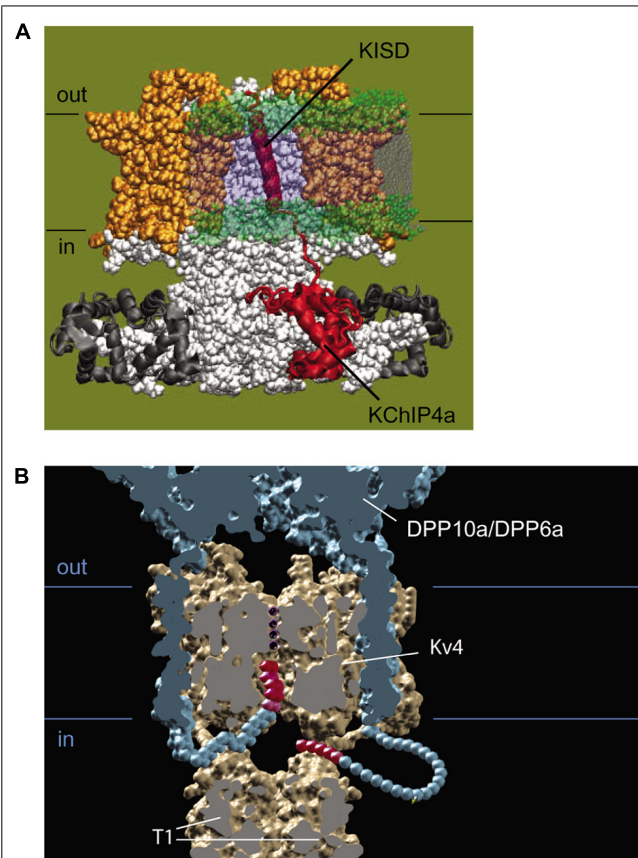


FIGURE 5 | Molecular mechanism of functional regulation by KChIP4a, DPP6a, and DPP10a. (A) Working molecular model of the transmembrane Kv-channel inactivation suppressor domain (KISD) inserting through the membrane and making contacts with the Kv4 channel core, as adapted from Jerng and Pfaffinger (2008). As reported by Tang et al. (2013), separate domains within the KISD determine ER retention and regulation of channel gating. KChIP4a is shown in red, voltage sensors in yellow, and the remaining Kv4 channels in white. **(B)** Side view of a model illustrating the basis for fast inactivation mediated by DPP6a and DPP10a. Two of the four subunits have been removed to reveal the inner channel structure, including the permeation pathway with K^+ , DPLP extracellular and transmembrane domain (blue), and the DPLP N-termini with inactivation particles (red).

involve more than just the insertion of transmembrane domains into the lipid bilayer. For example, even though KChIP4e has a putative transmembrane N-terminus and shows perinuclear localization, KChIP4e increases surface expression of Kv4.2 channels, does not slow inactivation kinetics, and accelerates recovery from inactivation (Jerng and Pfaffinger, 2008; Pruunsild and Timmusk, 2012). Also, while KChIP2x and Kv3x slow inactivation similar to KChIP4a, they accelerated recovery like typical KChIPs (Jerng and Pfaffinger, 2008). It therefore seems likely that certain differences in the N-terminal sequence may confer different properties to the channel complex, perhaps by altering how the transmembrane region of the protein interacts with the transmembrane portion of the channel or other membrane regulatory proteins. The difference in surface expression between KChIP4e and the other tmKChIPs may be due to differences in specific ER retention motifs between these variants (Shibata

et al., 2003; Jerng and Pfaffinger, 2008; Liang et al., 2010; Prunsild and Timmusk, 2012; Tang et al., 2013). Indeed, Tang et al. (2013) have identified the ER retention motif which consists of six hydrophobic and aliphatic residues (LIVIVL) within KChIP4a N-terminus (Tang et al., 2013). These residues are also highly conserved within KChIP2x and KChIP3x but not in KChIP4e.

Differences in functional effects may also reflect specific regulatory sequences. Residues 19–21 of KChIP4a (VKL motif) have been identified as those responsible for promoting CSI of Kv4.3 channels, with Leu-21 being the critical residue (Tang et al., 2013). CSI is the predominant form of inactivation for Kv4 channels bound to KChIPs (Kaulin et al., 2008). The similarity in the sequence between KChIP4a (VKL) and KChIP2x (VKV), and KChIP3x (IAV) may explain why all these variants slow the inactivation time courses whereas the more distinct sequences in KChIP4e (LLH) at the homologous position does not. Lys-20 is conserved between KChIP4a and KChIP2x and may explain why the inactivation time courses are more similar between Kv4.2+KChIP4a and Kv4.2+KChIP2x than Kv4.2+KChIP3x (Jerng and Pfaffinger, 2008). Also, Val-21 for both KChIP2x and KChIP3x may explain why their steady-state inactivation (SSI) properties are vastly different from that of KChIP4a. In summary, available evidence suggests that discrete portions of the tmKChIP transmembrane domain induces ER retention and interacts with Kv4 pore-forming subunits to produce dramatic changes in the functional properties. At present, despite the widespread expression of tmKChIPs throughout the brain and the potential impact they have on I_{SA} channel expression and gating in neurons, nothing is known about the binding partner for the tmKChIP transmembrane domain on the Kv4 subunits, and further research is required to elucidate the precise interactions needed for tmKChIP-mediated modulation.

DPP10a AND DPP6a: DPLPs MEDIATING N-TYPE INACTIVATION

Although the transmembrane domain of DPLP imparts most of the functional effects associated with DPLP co-expression, such as accelerated gating kinetics and hyperpolarizing shifts in the voltage-dependence of activation and inactivation, early experiments studying DPP10a found significantly faster inactivation kinetics than DPP6S (Jerng et al., 2004b). This fast inactivation associated with DPP10a is transferrable to DPP6S by transplanting the DPP10a N-terminus, and among the DPP10 N-terminal variants, only DPP10a produced this effect (Jerng et al., 2004b, 2007). The DPP6a variant also confers a similar fast inactivation, suggesting that a conserved determinant within the N-terminus is responsible (Jerng et al., 2009; Maffie et al., 2009). This N-terminus-mediated fast inactivation occurs when Kv4 is bound by KChIP or in the absence of the endogenous Kv4 N-type inactivation, suggesting a direct action of the N-terminus (Figure 6; Jerng et al., 2009). This direction action by the N-terminus is a dominant feature in heteromeric DPLP channels, suggesting that fast inactivation can be generated with even less than 4 DPP10a or DPP6a on a single channel (Jerng et al., 2007; Jerng and Pfaffinger, 2012). Finally, deletion of the N-terminal 5 residues is sufficient to prevent the

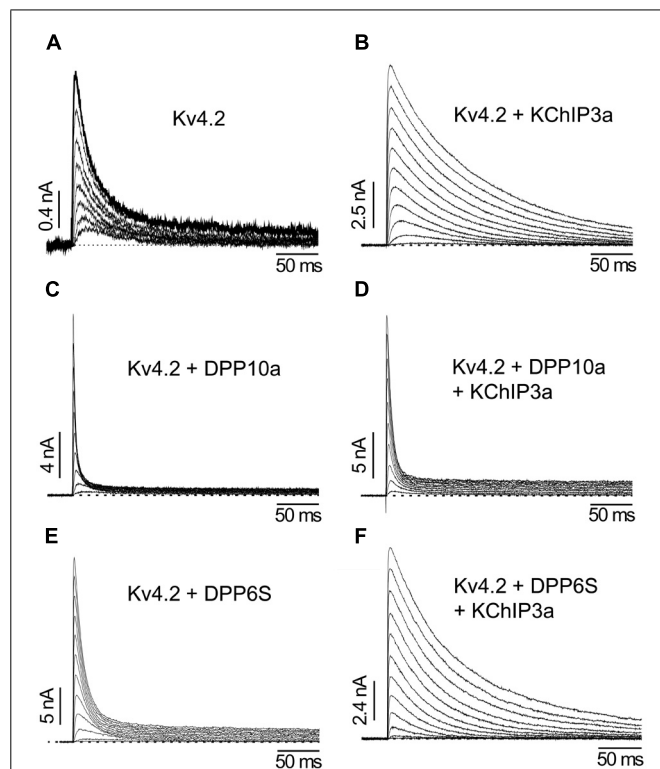


FIGURE 6 | The differential functional effects of DPLP N-terminal variants (Adapted from Jerng et al., 2005). (A) Kv4.2 outward currents elicited by membrane depolarization in CHO cells. (B) After co-expression with KChIP3a, Kv4.2 channels significantly increase in surface expression and exhibit slower inactivation. (C) Similar to KChIP3a, co-expression of Kv4.2 with DPP10a results in a dramatic increase in peak current; however, the inactivation kinetics is markedly accelerated. (D) Channel complexes co-expressing KChIP3a and DPP10a results in currents that are more like that of Kv4.2+DPP10a channels, indicating the dominance of DPP10a-mediated fast inactivation. (E) DPP6-S accelerates inactivation of Kv4.2 channels. (F) Co-expression of DPP6-S with Kv4.2+KChIP3a channels does not produce dramatic acceleration of inactivation observed with DPP10a.

DPP10a- or DPP6a-mediated fast inactivation, and perfusion of the N-terminal peptide can also produce block (Jerng et al., 2009).

How do DPP10a and DPP6a mediate fast inactivation? Fast inactivation of K⁺ channels is commonly produced by a “ball-and-chain” or N-type mechanism, whereby the distal N-terminus occludes the inner pore and produce inactivation (Hoshi et al., 1990). Furthermore, in Shaker K⁺ channels, it has been shown that an internal blocker called tetraethylammonium (TEA) can compete with the blocking particle and the degree of block is proportional to the slowing of inactivation (Demo and Yellen, 1991). Moreover, the blocking particle is trapped by the channel closing during repolarization, and the relief from block is equivalent to channel recovery as observed in the tail current. Diagnostic tests prove that DPP10a and DPP6a confer fast inactivation by this Shaker N-type inactivation mechanism (Jerng et al., 2009); therefore, fast inactivation mediated by DPP6a or DPP10a is produced when the N-terminal inactivation particle blocks the

open pore (**Figure 5B**). In addition, heterologous expression studies show that, similar to Shaker N-type inactivation found in Kv1.4, DPP6a- and DPP10a-conferred N-type inactivation is regulated by oxidation and reduction through a highly conserved N-terminal cysteine at position 13 (Ruppersberg et al., 1991; Jerng et al., 2012). These results suggest that (1) neurons expressing these DPLP variants are likely to have I_{SA} with fast inactivation, and (2) this fast inactivation is sensitive to the cell's redox state.

DPP6K

DPP6K modifies the functional properties of Kv4 channels in a very distinct way. Co-expressed with Kv4.2 channels, DPP6K produces the typical modulatory effects of increasing the current amplitude, decreasing the time to peak current, accelerating inactivation kinetics, and introducing leftward shifts in SSI and conductance-voltage relationship (Nadal et al., 2006). However, when compared to DPP6S and DPP6L, the recovery kinetics in the presence of DPP6K is significantly slower and the voltage dependence of SSI is markedly more hyperpolarized. In the Kv4-KChIP3a-DPP6K ternary complex, the unique DPP6K effects are even more pronounced (Jerng and Pfaffinger, 2012). Unlike other DPP6 variants, DPP6K dampens the ability of KChIP3a to promote an acceleration of recovery from inactivation and shift SSI to more positive potentials. Named after a high content of lysines in the N-terminus, DPP6K has four lysine residues (Lys-2, Lys-4, Lys-8, and Lys-11) within the 17-residue-long variable N-terminus (Nadal et al., 2006). However, alanine substitutions of these lysines have no effect on their modulation of Kv4 channel complexes, and the significance of these lysine residues remains certain (Jerng and Pfaffinger, 2011). Instead, deletion and point mutation analysis shows that the DPP6K functional effects come from a stretch of residues between Met-12 and Met-17, with Met-12 and Val-16 being the critical residues. Therefore, it is hypothesized that Met-12 and Val-16 directly interacts with some cytoplasmic domain of Kv4 subunits to oppose the effects of KChIPs and thereby slow recovery and regulate SSI. Furthermore, heterologous expression studies using different KChIP variants indicate that the functional effects associated with DPP6K are highly dependent on the variants of KChIP subunits present, suggesting that the precise combination of KChIP and DPLP N-terminal variants expressed by neurons play a critical role in determining the functional properties of I_{SA} and therefore AP firing properties.

THE Kv4-KChIP-DPLP TERNARY COMPLEX AND DIVERSITY OF NEURONAL I_{SA}

THE TERNARY COMPLEX AND SURFACE TRAFFICKING

Most KChIPs and all DPLPs subunits increase surface trafficking and functional expression of Kv4 channels. The apparent redundancy of this functional effect among the two classes of auxiliary subunits has been addressed in detail by knockout or RNAi studies in native neurons where one class of subunit is deleted. KChIP3-specific knockout has no effect on Kv4.2 protein level (Alexander et al., 2009), and in hippocampal neurons, KChIP2 deletion (*Kcnp2*^{-/-}) diminished I_{SA} only moderately (Wang et al., 2013). In cortical pyramidal neurons from mice, the results show that RNAi suppression of individual KChIPs

(KChIP2, KChIP3, and KChIP4) can be compensated by the reciprocal increases in the expression of other KChIPs (Norris et al., 2010). In dealing with compensation, simultaneous suppression of KChIP2–4 by miRNA reportedly eliminated a significant fraction of the current (~50%) without altering the voltage dependence of activation and the kinetics of inactivation. On the other hand, targeted deletion of Kv4.2 in neurons produces dramatic reduction in the level of KChIP proteins that precisely tracks the loss of Kv4.2 protein normally found a given region (Menegola and Trimmer, 2006; Nadin and Pfaffinger, 2010; Norris et al., 2010). These findings suggest that perhaps the binding of Kv4 subunits by KChIP proteins inhibits or suppresses degradation by the ubiquitin-proteasome pathway (Jang et al., 2011).

Compared to KChIPs, DPLPs clearly play a central role in the surface expression of I_{SA} channels. In contrast to the moderate reduction associated with the inhibition of KChIP expression, suppression of DPP6 by RNAi dramatically decreases the protein levels (90%) of Kv4.2, Kv4.3, and KChIP3 in CG cells and hippocampal neurons (Nadin and Pfaffinger, 2010). Genetic knockout of DPP6 produces a marked reduction of Kv4.2 and KChIP2/KChIP4 proteins in hippocampus, particularly in the distal dendrites (Sun et al., 2011). On the contrary, targeted deletion of Kv4.2 and/or Kv4.3 in neurons has little to no effect on the DPP6 proteins levels (Nadin and Pfaffinger, 2010; Foeger et al., 2012). Together, these results suggest a model of ternary channel complex trafficking where KChIP stability is dependent upon Kv4 protein, Kv4 protein stability is dependent upon DPLP binding, and DPLPs can exist in a neuron independently of the I_{SA} channel complex.

What mechanism underlies this dependence of surface expression on DPLP? In other words, why would Kv4.2 channels, despite KChIP's innate ability to promote surface expression by sequestering Kv4's N-terminal ER retention motif, continue to be prevented from reaching the cell surface? The answer may lie with the ability of KChIP2x, KChIP3x, and KChIP4a to mediate ER retention and potentially targeted for degradation (Jerng and Pfaffinger, 2008), and more experiments will be required to investigate the neuronal machinery involved in the quality control of I_{SA} channels arriving on the cell surface.

A final important question is how are these three proteins regulated to determine the level of I_{SA} produced in a given neuron. Based on a variety of analyses, it seems that all surface I_{SA} channels in neurons minimally contain all three subunit types. In CG cells, rescue of DPP6 knockdown by over-expression of RNAi-insensitive DPP6 constructs returns I_{SA} back to normal levels, suggesting that DPP6 expression level is normally high enough to drive all available I_{SA} channels to the cell surface (Nadin and Pfaffinger, 2010). On the other hand, when Kv4.2 has been over-expressed in neuron, the amplitude of I_{SA} undergoes dramatic increases, suggesting that sufficient KChIP and DPP6 subunits are normally expressed in neurons to accommodate the additional Kv4.2 subunits being produced (Johns et al., 1997; Lauer et al., 2006). It therefore seems likely that in most neurons, the overall level of I_{SA} may be normally limited by the level of Kv4 subunit expression.

THE TERNARY COMPLEX AND FUNCTIONAL PROPERTIES

In native cells, the association of KChIP and DPLP subunits with Kv4 also has important consequence for channel functional properties. Studies using heterologous expression systems suggest that, for most channel properties, the combined modulation of Kv4 channels by KChIP and DPLP are usually the summed effects of the individual subunits. For example, KChIPs shift the SSI curve rightward, whereas DPLPs shift it leftward. Thus, a channel containing both KChIP and DPLP will have a SSI curve intermediate between either subunit alone. On the other hand, since both KChIP and DPLPs accelerate recovery from inactivation, the ternary complex exhibits recovery from inactivation faster than with either subunit alone (Jerng et al., 2005).

Examining the specific KChIP and DPLP variants being expressed in different neuronal populations explains how the interaction of KChIP and DPLP modulatory effects shape distinctive I_{SA} in these different neurons. For example, DPP10a and DPP6a distinctly produce fast N-type inactivation by blocking the internal pore with their N-terminal domains (**Figure 5B**). In the ternary complex, the fast inactivation associated with these unique subunits dominates and characteristically produces inactivation that accelerates with increasing depolarization and is unaltered by the presence of KChIPs (Jerng et al., 2005, 2009; Maffie et al., 2009). In contrast, in the presence of other DPLP subunits, the binding of KChIP to the Kv4 N-terminus eliminates endogenous N-type inactivation of Kv4 channels and reveals the underlying CSI, which slows with increasing depolarization.

Cortical pyramidal neurons

Cortical pyramidal neurons express I_{SA} with rapid inactivation kinetics ($\tau = \sim 10$ ms) relatively independent of voltage at positive membrane potentials (Zhou and Hablitz, 1996; Korngreen and Sakmann, 2000). A combination of Kv4.2, Kv4.3, KChIP2–4, DPP6S, and DPP10a transcripts is expressed in these neurons (**Figures 3A,B**), and a recent report indicates that miRNA-mediated simultaneous knockout of KChIP2–4 in Kv1.4^{-/-} cortical pyramidal neurons produced a significant reduction in I_{SA} peak current with no observed changes in the inactivation kinetics (Norris et al., 2010). Since the KChIP component does not significantly influence inactivation properties and the phenotypically dominant DPP10a variant is expressed at high levels, co-expression of Kv4.2, KChIP3a, and DPP10a in heterologous cells was sufficient to generate an A-type current with inactivation kinetics and voltage dependence very similar to that of the cortical I_{SA} (Jerng et al., 2007). Co-expression of Kv4.2 and KChIP3a with the other DPLP present, DPP6S, did not produce cortical I_{SA}-like fast inactivation. These results suggest that DPP10a-mediated N-type inactivation is critically important to the inactivation kinetics of cortical I_{SA}.

Superior colliculus neurons

I_{SA} among superior colliculus neurons exhibits varying inactivation rates and voltage-dependent properties (Saito and Isa, 2000). The time constant of inactivation ranges between 12 and 65 ms, but the voltage dependence of inactivation kinetics at positive potential remains monotonic and suggests DPP10a- or DPP6a-mediated N-type inactivation. In situ hybridization studies indicate that

DPP6a is highly expressed in superior colliculus, but in addition DPP6S and DPP6K are also expressed at moderate levels (Nadal et al., 2006; Maffie et al., 2009; Jerng and Pfaffinger, 2012). These results suggest that varying ratios between DPP6a and other DPP6 variants in individual neurons may produce the observed variable functional properties, and the differences are physiologically significant since different I_{SA} properties are associated with different firing properties among the superior colliculus neurons (Saito and Isa, 2000).

Cerebellar granule cells

During prolonged depolarization, the I_{SA} from CG cells features a prominent biphasic inactivation, where the fast inactivation is voltage-independent and the slow inactivation becomes slower with increasing potential (Zegarra-Moran and Moran, 1994). As a result, in contrast with I_{SA} from cortical and superior colliculus neurons, I_{SA} from CG cells inactivates overall more slowly at higher membrane potential (Amarillo et al., 2008). *In situ* hybridization and RT-PCR studies of the I_{SA} subunits present show that CG cells express a mixture of Kv4.2, Kv4.3, DPP6, and KChIP3, with some contribution from various KChIP4 variants (**Figure 3**). The levels of Kv4.2 and Kv4.3 transcripts are not uniform among CG cell layer, since they exhibit opposite anterior–posterior gradients (Amarillo et al., 2008). Among the DPP6 variants, DPP6K and DPP6a comprise the vast majority of DPP6 expressed in CG cells, with DPP6K being the predominant variant (Jerng and Pfaffinger, 2012). DPP6K appears to be important to the Kv4.2 channel complexes since it shares the same anterior–posterior gradient of expression in the CG cell layer (Nadal et al., 2006). Co-expression of Kv4.2 and KChIP with DPP6K and DPP6a at the experimentally derived ratio (2:1) in *Xenopus* oocytes reconstitutes a transient current that highly resembles the native I_{SA} in CG cells (**Figure 7A, left panel**; Jerng and Pfaffinger, 2012). Like the native I_{SA}, the reconstituted current inactivated with two components of inactivation characterized by different voltage dependent properties (**Figure 7A, right panel**). In another co-expression study, Maffie et al. (2009) also generated the best match between the inactivation kinetics of reconstituted and native currents using DPP6S and DPP6a at a 2-to-1 ratio. The contribution of DPP6a-conferred N-type inactivation to native I_{SA} inactivation was further addressed by RNAi experiments conducted on CG cells. Suppression of DPP6 expression by RNAi in mouse CG cells markedly slowed I_{SA} inactivation kinetics and altered its voltage dependence (**Figure 7B**; Nadin and Pfaffinger, 2010), suggesting that DPP6a-conferred N-type inactivation contribute significantly to the inactivation of I_{SA}. Furthermore, fast N-type inactivation is restored when rat DPP6a rescue protein is over-expressed in mouse CG cells treated with DPP6 RNAi. Therefore, significant dilution of DPP6a by DPP6K and other DPP6 variants very likely results in the bi-phasic inactivation of I_{SA} in CG cells, rather than other factors such as a loss of N-type inactivation associated with DPP6a.

Hippocampal neurons

Hippocampal I_{SA} displays inactivation kinetics that slows with increasing depolarization (Hoffman et al., 1997), and this voltage dependence of inactivation appears consistent with the finding

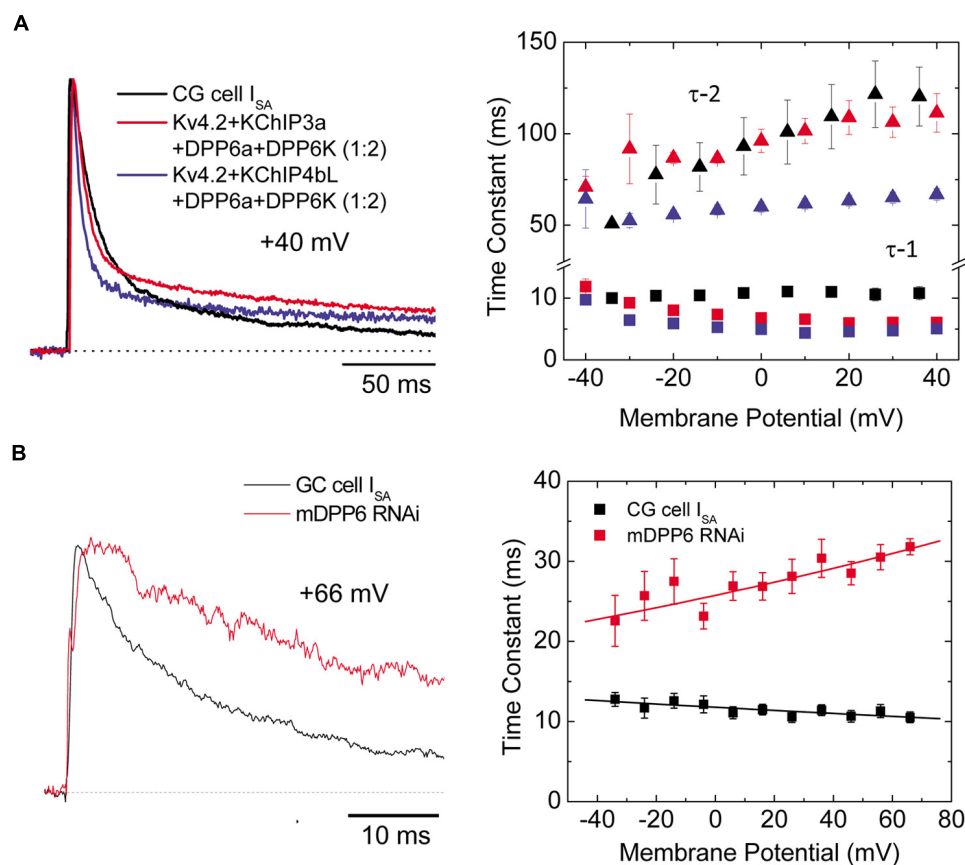


FIGURE 7 | Ternary channel complex consisting of Kv4.2, KChIP3a, DPP6a, and DPP6K express A-type current similar to I_{SA} from CG cells (Adapted from Nadin and Pfaffinger, 2010; Jerng and Pfaffinger, 2012). (A) Comparison between native I_{SA} from CG cells and reconstituted currents expressed by Kv4.2, KChIP, and DPP6 subunits. Based on real-time RT-PCR results, the ratio between DPP6a and DPP6K was determined to be 1-to-2 (Jerng and Pfaffinger, 2012). Native and reconstituted current traces elicited by +40 mV depolarizations are quite similar (left panel). The incorporation of KChIP3a versus KChIP4bL produces negligible effect on

overall current waveforms. The overall inactivation is best described by the sum of two exponential components, and the two corresponding time constants (τ-1, τ-2) have different dependence on membrane potential (right panel). (B) In the absence of DPP6, I_{SA} inactivation significantly slows (left panel). The loss of DPP6 altered the inactivation-voltage profile (right panel). Control I_{SA} shows inactivation with time constant relatively insensitive to depolarization. After DPP6 knockdown by RNAi, inactivation time constant slows with increasing depolarization. Note that panels A and B have separate legends.

that neither DPP10a nor DPP6a is highly expressed in these neurons (Jerng et al., 2007; Jerng and Pfaffinger, 2012). Overall, knockout experiments show that KChIP and DPP6 play an important role in suppressing excitability in hippocampal neurons. In hippocampal pyramidal neurons, the deletion of KChIP2 gene (*Kcni2*^{-/-}) moderately reduced peak I_{SA} and shifted the V_{1/2} of SSI to more hyperpolarized potentials (Wang et al., 2013). As a result, hippocampal neurons with the KChIP2 gene knocked out show increased excitability; in fact, the average spontaneous firing rate increased 10-fold. In hippocampal interneurons, suppression of KChIP1 by siRNA moderately reduced peak I_{SA} and slowdown recovery from inactivation (Bourdeau et al., 2011). As a result, firing frequency during suprathreshold depolarizations was increased. Meanwhile, hippocampal CA1 neurons with DPP6 knockout show a reduction of I_{SA} in distal dendrites (Sun et al., 2011). In contrast with the KChIP2 knockout, the decreased I_{SA} is associated with depolarizing shift in the

voltage-dependence of activation, and these effects result in more backpropagation of action potentials, increased excitability of dendrites, enhanced electrical activities, and increased induction of synaptic LTP.

KChIPs AND DPLPs: BEYOND THE I_{SA} CHANNEL

Kv channel-interacting proteins and DPLPs, as constitutive components of the I_{SA} channel complex, contribute to neuronal excitability by tuning the properties of I_{SA}. However, recent studies suggest that these proteins are more than just auxiliary subunits of I_{SA} channels; KChIPs and DPLPs directly modulate other ion channels or receptors, or act as intermediaries between I_{SA} channels and other membrane proteins.

KChIPs AND Cav CHANNEL (T-TYPE, L-TYPE)

Voltage-gated Ca²⁺ (Cav) channels are activated by membrane depolarization, and their opening allows Ca²⁺ to enter the cell

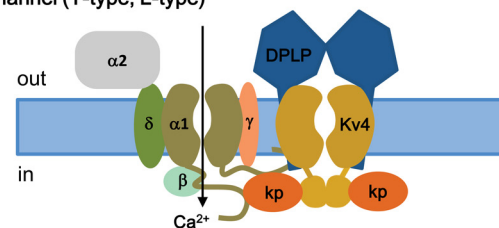
and initiate intracellular Ca^{2+} signaling events. In the brain, the T-type Ca^{2+} channel and Kv4 channels are widely expressed with high expression in the somatodendritic regions of neurons (McKay et al., 2006), and they both operate at the subthreshold range of membrane potential. Anderson et al. (2010) showed that in cerebellar stellate cells the Ca^{2+} influx mediated by T-type Cav channels modulates I_{SA}, by producing a depolarizing shift in the SSI of I_{SA} by approximately 10 mV and modulating I_{SA} window current and spike firing (Anderson et al., 2010). This effect of Ca^{2+} on SSI is specific and has no effect on the voltage dependence of activation, the kinetics of inactivation and recovery, or the I_{SA} current density. The Ca^{2+} sensitivity of the Kv4 complex is specifically produced by KChIP3 and not by KChIP1 or KChIP2, indicating a critical role for KChIP3 in the modulation of I_{SA} in CG cells. In addition, there must be a close proximity between Cav channels and I_{SA} channels, since Cav3.2 and Cav3.3 co-immunoprecipitate with Kv4.2 and KChIP3 proteins from rat brain homogenates, including those from cerebellum, hippocampus, and neocortex (**Figure 8A**; Anderson et al., 2010). This co-immunoprecipitation depends on the C-terminal regions of Cav3.2 and Cav3.3, suggesting that the Cav3 C-terminus interacts with the I_{SA} complex. However, it remains unclear whether the Cav3 C-terminus binds Kv4 or KChIP3 subunits. Physiologically, in the cerebellum the Cav-Kv4 channel complex acts as a Ca^{2+} sensor that responds to a decrease in extracellular Ca^{2+} by dynamically adjusting stellate cell excitability to maintain inhibitory charge transfer to Purkinje cells (Anderson et al., 2013). The pre-synaptic N-type Cav2.2 channels which are activated by high voltage have no effect on Kv4.2 availability (Anderson et al., 2010), suggesting that only post-synaptic Cav channels have evolved to function alongside KChIP and I_{SA} channel complex.

In cardiac myocytes, it was found that *Kcnp2*^{-/-} mice have reduced L-type Ca^{2+} current (I_{Ca,L}) by 28% compared to wild-type myocyte (Thomsen et al., 2009b). L-type Cav channels are also found in the dendrites and dendritic spines of cortical neurons, and recently a Ca^{2+} -independent regulation of I_{Ca,L} by KChIP2 was found in neurons (Thomsen et al., 2009a). Biochemical analysis shows that there is a direct interaction between KChIP2 and the Cav1.2 alpha-1C subunit N-terminus, and the binding of KChIP2 to the N-terminal inhibitory (NTI) module of alpha-1C augments the I_{Ca,L} current density without increasing protein expression or trafficking to the plasma membrane. More studies will be required to decipher the different Ca^{2+} dependence observed between T- and L-type Cav channels, although these studies suggest important ways that different KChIPs may function separately from their direct effects on Kv4 channels.

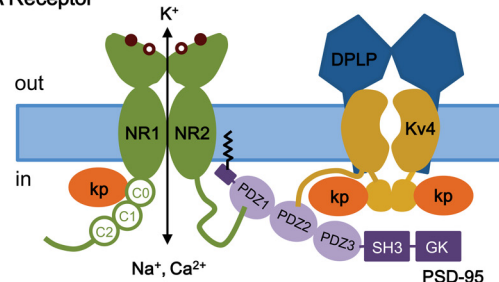
KChIPs AND NMDA RECEPTOR

The N-methyl-D-aspartate receptors (NMDA receptors, NMDARs) make up a major class of ionotropic glutamate receptors that, like I_{SA} channels, are involved in controlling synaptic plasticity and memory function (Maren and Baudry, 1995; Asztely and Gustafsson, 1996). The NMDA receptor is a non-specific cation channel located in the postsynaptic membrane that allows Ca^{2+} and Na^{+} to pass into the cell while K^{+} flows out, with

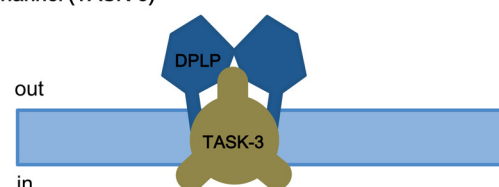
A Cav Channel (T-type, L-type)



B NMDA Receptor



C K2P Channel (TASK-3)



D Prion Protein (PrPC)

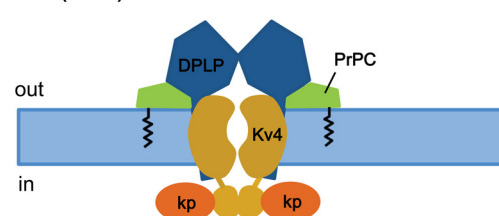


FIGURE 8 | KChIP and DPLP are also involved in binding and regulating other channels and receptors. (A) T- and L-type Cav channels.

Depolarization-activated Cav channels, like I_{SA} channels, are multi-protein complexes. The cytoplasmic N- and C-termini of Cav channels have been shown to interact with the I_{SA} channel complex, via Kv4 or KChIP subunits. **(B)** NMDA receptor. The NMDA receptors are opened by 2 simultaneous events: activation by extracellular ligand binding and depolarization-mediated relief of block by Mg^{2+} (coincidence detector). Both NMDA receptor and I_{SA} channels are localized post-synaptically, and KChIPs have been shown to regulate NMDA receptor activities. **(C)** TASK-3 two-pore K^{+} channels. DPP6 co-assembles with TASK-3 channels in the dendritic membrane to regulate membrane excitability. **(D)** Prion proteins (PrPC) bind to DPP6, thereby regulating I_{SA} expression and gating. Kp, KChIP; NR1, glycine-binding subunit; NR2, glutamate-binding subunit; SH3, SRC homology 3 domain; GK, guanylate kinase.

an equilibrium potential near 0 mV (Dingledine et al., 1999). At rest, the NMDA receptor is blocked by Mg^{2+} , which can be cleared by depolarization. Since both glutamate binding and postsynaptic depolarization are required for channel opening, the NMDA receptor functions as a “coincidence detector.” The

NMDR receptor is a heterotetramer between two NR1 (glycine-binding) and two NR2 (glutamate-binding) subunits (Traynelis et al., 2010; **Figure 8B**). The extracellular ligand-binding domain is attached to the transmembrane core domain that determines conductance, Ca²⁺-permeability, and voltage-dependent Mg²⁺ block. The cytoplasmic domain contains residues that can be modified by protein kinases and phosphatases as well as residues that interact with structural proteins. The C-terminus of NMDA receptor binds to the postsynaptic density-95 (PSD-95) at a PDZ domain, which anchors itself through S-palmitoylation of an N-terminal domain (**Figure 8B**; Craven et al., 1999; Sturgill et al., 2009).

Like several receptors and Kv1 channels, Kv4.2 subunits bind to PSD-95 via an amino acid sequence motif (VSAL) in its C-terminal tail, allowing channel clustering and promoting localization into lipid rafts (**Figure 8B**; Wong et al., 2002; Wong and Schlichter, 2004). Although the exact detail remains unclear, in addition to its role as a Kv4 auxiliary subunit, KChIP3a can directly bind in a Ca²⁺-dependent manner to a region of the NMDAR juxta-transmembrane C-terminus (C0 cassette, amino acids 834–863) of the NR1 subunit, thereby inhibiting NMDAR-mediated current and excitotoxicity (Zhang et al., 2010). As for the region of KChIP3a that binds NMDAR, the first 50 residues as well as the core domain are important for interaction. It appears that, in addition to S-palmitoylation to allow membrane association and localization to lipid rafts, the N-terminal cytoplasmic domain of KChIP3a is involved in association with NMDA receptors. At this time, it is unknown whether KChIP3a, when interacting with NR1 subunits, is associated or unassociated with Kv4. In either case, the KChIP subunit apparently again acts as a Ca²⁺ sensor that, with NMDRs, functions as a negative regulator to protect neurons from cytotoxic injury.

DPP6 AND K2P CHANNEL (TASK-3)

Two-pore K⁺ channels (K2P) channels generate a K⁺ leak conductance (I_{K(SO)}) and set the resting membrane potential in many neuronal populations. Opening of K2P channels promote hyperpolarization, and inhibition of K2P channels lead to depolarization. TASK-3 channels are members of the K2P channel family that is sensitive to acid and inhalation anesthetics at clinically relevant concentrations and widely expressed in the rodent brain (Talley et al., 2001; Vega-Saenz de Miera et al., 2001; Aller et al., 2005; Aller and Wisden, 2008). At a subcellular level, TASK-3 channels are expressed in the somatodendritic regions of the neuron, much like Kv4 channels (Marinc et al., 2012).

RNAi-mediated suppression of DPP6 expression in CG cells from Kv4.2 knockout mouse reveals that DPP6 is affecting the resting membrane potential by influencing a channel other than Kv4 (Nadin and Pfaffinger, 2013), most likely the K2P channel TASK-3. TASK-3 is the most highly expressed K2P subunit in CG cells, and consistent with TASK-3, the DPP6-modulated resting membrane conductance is sensitive to acidic pH and Zn. In addition, reconstitution and immunoprecipitation studies in CHO-K1 cells show that DPP6 co-immunoprecipitates with TASK-3 and its co-expression increases the TASK-3 current, suggesting that DPP6 interacts with TASK-3 channels (**Figure 8C**).

DPP6 AND CELLULAR PRION PROTEIN

Cellular prion proteins (PrPC), products of the *PRNP* gene, are cell surface proteins that are widely expressed in various tissues but with the highest levels in neurons in the central nervous system (Bendheim et al., 1992). Under pathological conditions, the alpha-helix-rich PrPC can give rise to the abnormal beta-sheet-rich PrPSc, and the accumulation of PrPSc in the brain produces neurodegenerative disorders known as prion diseases. The transmission and development of prion disease is proposed to occur by a process of homotypic conversion from normal to abnormal prion protein, whereby the endogenous PrPC interacts with an incoming PrPSc or *de novo* PrPSc generated by some unknown post-translational process (Telling et al., 1995; Kaneko et al., 1997).

Currently, the normal biological function of PrPC remains mostly unknown. PrPC knockout studies in mice initially suggest that PrPC is not required for embryonic development or normal neuronal excitability and synaptic transmission in hippocampal CA1 region (Bueler et al., 1992; Lledo et al., 1996). However, subsequent studies suggest that PrPC knockout is linked to abnormalities in motor, cognitive, and emotional functions, along with increased susceptibility to seizures and alterations in excitability and synaptic plasticity (Roesler et al., 1999; Walz et al., 2002; Criado et al., 2005; Prestori et al., 2008). The strongest evidence for PrPC function comes from *in vitro* studies, which suggest that PrPC may be involved in neuriteogenesis, cell adhesion, and binding of neurotrophic factors. Neurons from PrPC knockout mice in culture shows reduced Ca²⁺-dependent K⁺ current (Colling et al., 1996; Herms et al., 2001; Mallucci et al., 2002) and reduced cytoplasmic Ca²⁺ levels (Herms et al., 2000). The reduction in Ca²⁺ levels is proposed to be due to PrPC modulation of L-type Cav channels in CG cells (Korte et al., 2003), which can subsequently affect the Ca-dependent K current.

To further understand the normal physiological role of PrPC, studies were conducted to identify PrPC-interacting proteins by analyzing high-density protein microarrays and by protein cross-linking followed by purification and mass spectrometry (tbTPC; Schmitt-Ulms et al., 2004; Satoh et al., 2009). The tbTPC technique identifies DPP6 as part of the molecular microenvironment of PrPC (Schmitt-Ulms et al., 2004), and just recently Mercer et al. (2013) demonstrated that PrPC co-immunoprecipitates with DPP6 and modulates Kv4.2 channels in a DPP6-dependent manner (**Figure 8D**; Mercer et al., 2013). PrPC modulates the I_{SA} channel complex by increasing peak current amplitude, rightward shifting the voltage dependence of SSI, slowing inactivation kinetics, and accelerating recovery from inactivation. These functional effects overall decrease membrane excitability and susceptibility to seizures and explains why the PrPC knockout alters excitability, synaptic plasticity, and susceptibility to seizures. In addition, since DPP6 also associates with the K2P channel TASK-3, PrPC may also interact with the K2P-DPP6 channel complex.

THE ROLE OF I_{SA} AND ITS AUXILIARY SUBUNITS IN REGULATING EXCITABILITY

The roles that I_{SA} and its regulation play in controlling neuronal excitability is complex and involves the dynamic interplay

between I_{SA} and multiple other channel types. The regulation of excitability is the net effect of the strengths of synaptic inputs, the integrative properties of the somatodendritic compartment, and the threshold firing properties of the axon initial segment. I_{SA} directly or indirectly affects all of these steps. Being a K⁺ current, I_{SA} primarily plays a regulatory function, controlling how readily depolarizing currents gain control of the membrane potential and how effectively action potential firing is back-propagated to the synapse to regulate synapse strength. The unique regulatory properties of I_{SA} compared to other K⁺ currents involve the voltage range over which the channel gates, the kinetics of the channel's gating, its subcellular localization in the neuron, as well as the sensitivity of I_{SA} to specific post-translational regulatory phenomena. A few of the ways in which rapid activation of I_{SA} at subthreshold potentials directly regulates excitability includes: (1) suppression of AMPA responses (Schoppa and Westbrook, 1999), (2) suppression of back propagating action potentials (Hoffman et al., 1997), and (3) delayed firing in response to current injections (Nadin and Pfaffinger, 2010). Because I_{SA} inactivates rapidly, these regulatory responses are all time limited and rapidly lost unless reset by a subsequent hyperpolarization. This timing dependence for I_{SA} regulation is an additional coincidence detection mechanism that operates in parallel with the well described coincidence detection role for Mg²⁺ block of NMDA receptors (Schrader et al., 2002). For example, in hippocampal pyramidal neurons, incoming AMPA response depolarize dendrites enough to drive I_{SA} inactivation (Watanabe et al., 2002). If the drive is enough to initiate the firing of an action potential, the backpropagation of this spike will be suppressed by I_{SA} in regions of the dendritic tree that were not

previously depolarized (Hoffman et al., 1997). However, in the region of the active synapses, the inactivation of I_{SA} will allow a large spike to propagate resulting in a large Ca²⁺ flux through NMDA receptors (Johnston et al., 2003). The sensitivity of this response is modified during LTP protocols by phosphorylation of I_{SA} and thus is a tunable mechanism capable of refining the assignment of Hebbian synaptic strengthening to the synapses in dendritic regions that drove action potential firing (Frick et al., 2004).

Because I_{SA} gating properties are strongly regulated by auxiliary subunit proteins, excitability and coincidence detection in different neuronal types are likely to be extensively tuned by the I_{SA} auxiliary subunit protein variants that are being expressed. The interaction of KChIPs and DPLPs with other channels and receptors will also modulate the overall excitability properties of the neuron. As an illustration of the important role of non-Kv4 proteins in excitability, knockout of Kv4.2 effectively eliminates I_{SA} from hippocampal neuronal dendrites, but compensatory changes in glutamatergic transmission and inhibitory connections occur and likely compensate for much of the impact of this knockout (Andrasfalvy et al., 2008; Jung et al., 2008; Kim and Hoffman, 2012; Kaufmann et al., 2013). It is likely that many of the compensatory effects noted in ion channel knockout studies are due to the integrative effects of auxiliary subunit protein (Lin et al., 2013; Wang et al., 2013). In addition, I_{SA} is reported to be regulated by auxiliary subunits proteins for other channels, further implicating auxiliary protein in the integrative regulation of excitability. For now, however, the specific manner in which these integrative interactions work together to control neuronal functional phenotypes is not well understood. A key question for

Table 2 | Genetic association between I_{SA} subunits and disease/disorders.

Subunit	Phenotype	Subject	Conclusion and analysis method	Reference
Kv4.2	Temporal lobe epilepsy	Human-Japanese	Yes: electrophysiology	Singh et al. (2006)
KChIP	Ventricular tachycardia	Mouse	Yes: KChIP2 knockout	Kuo et al. (2001)
	Pain	Mouse	Yes: KChIP3 knockout	Cheng et al. (2002)
DPP6	Amyotrophic lateral sclerosis	Human-multi-ethnic	Inconsistent: GWAS analysis SNP analysis CNV association	Cronin et al. (2008), van Es et al. (2008), Chio et al. (2009), Li et al. (2009), Blauw et al. (2010), Fogh et al. (2011)
	Progressive multiple sclerosis	Human-Italian	Yes: SNP analysis	Brambilla et al. (2012)
	Tardive dyskinesia schizophrenia	Human-Japanese	Yes: GWAS analysis	Tanaka et al. (2013)
	Autism spectrum disorder	Human-multi-ethnic	Yes: ID mutations CNV association	Marshall et al. (2008), Noor et al. (2010)
	Microcephaly	Human-Chinese	Yes: CNV association	Liao et al. (2013)
DPP10	Asthma	Human-multi-ethnic	Yes: SNP association GWAS analysis Positional cloning	Allen et al. (2003), Zhou et al. (2009), Wu et al. (2010), Torgerson et al. (2012)
	Autism spectrum disorder	Human-mixed	Yes: CNV analysis	Girirajan et al. (2013)
	Bipolar disorder schizophrenia	Human-Norwegian	Yes: GWAS analysis	Djurovic et al. (2010)

GWAS, genome-wide association studies; CNV, copy-number variants; SNP, single-nucleotide polymorphism.

future studies is the extent to which compensatory remodeling is being driven at the systems level or is the direct result of signals being generated by loss of ion channel complexes and the protein-protein interactions that these channel complexes normally participate in.

SUMMARY AND CONCLUSION

With the physiological role of I_{SA} firmly established and the central role of Kv4 subunits in I_{SA} generation clearly recognized, in recently years the attention has been focused on the modulatory roles of Kv4 auxiliary subunits and their contribution to the tuning of I_{SA} biophysical properties, the creation of functional diversity in neurons, the regulated trafficking and subcellular localization of I_{SA} channels, and the expanding interaction between I_{SA} and other signal transduction pathways within neurons. What we have learned from the detailed molecular understanding of I_{SA} channels is that, at a minimal level, I_{SA} is the product of Kv4 channels and a complex network of interactions, between Kv4 and a “tool kit” of auxiliary subunits that also senses and feeds back modulatory signals to alter the I_{SA}. This modulatory signal may include the environment redox state that specifically regulates fast inactivation, or the local Ca²⁺ concentration that alters I_{SA} function through KChIP. Furthermore, we have also learned that auxiliary subunits play a critical role in the proper assembly and trafficking of I_{SA} channels to the cell surface and the recruitment of these channels to lipid rafts and then post-synaptic densities.

Lastly, as part of a greater network, KChIP and DPLPs have been proposed to have functions independent of their helper roles on I_{SA}, and substantially more study is required to further explore define their roles in neuronal physiology. Just recently, Lin et al. (2013) show that DPP6 interacts with a filopodia-associated myosin and fibronectin in the extracellular matrix, and DPP6 is important to cell adhesion and motility that ultimately impact synaptic development and function. Because of their potential multi-faceted roles, it is perhaps not surprising that KChIPs and DPLPs are increasingly linked to various diseases and disorders, including autism spectrum disorder and schizophrenia (Table 2). Only with better understanding of functional roles of these auxiliary subunits can we begin to further unravel the mystery behind these disorders and develop targeted treatments.

REFERENCES

- Aimond, F., Kwak, S. P., Rhodes, K. J., and Nerbonne, J. M. (2005). Accessory Kvbeta1 subunits differentially modulate the functional expression of voltage-gated K⁺ channels in mouse ventricular myocytes. *Circ. Res.* 96, 451–458. doi: 10.1161/01.RES.0000156890.25876.63
- Alexander, J. C., McDermott, C. M., Tunur, T., Rands, V., Stelly, C., Karhson, D., et al. (2009). The role of calsenilin/DREAM/KChIP3 in contextual fear conditioning. *Learn. Mem.* 16, 167–177. doi: 10.1101/lm.1261709
- Allen, M., Heinzmann, A., Noguchi, E., Abecasis, G., Broxholme, J., Ponting, C. P., et al. (2003). Positional cloning of a novel gene influencing asthma from chromosome 2q14. *Nat. Genet.* 35, 258–263. doi: 10.1038/ng1256
- Aller, M. I., Veale, E. L., Linden, A. M., Sandu, C., Schwaninger, M., Evans, L. J., et al. (2005). Modifying the subunit composition of TASK channels alters the modulation of a leak conductance in cerebellar granule neurons. *J. Neurosci.* 25, 11455–11467. doi: 10.1523/JNEUROSCI.3153-05.2005
- Aller, M. I., and Wisden, W. (2008). Changes in expression of some two-pore domain potassium channel genes (KCNK) in selected brain regions of developing mice. *Neuroscience* 151, 1154–1172. doi: 10.1016/j.neuroscience.2007.12.011
- Amarillo, Y., De Santiago-Castillo, J. A., Dougherty, K., Maffie, J., Kwon, E., Covarrubias, M., et al. (2008). Ternary Kv4.2 channels recapitulate voltage-dependent inactivation kinetics of A-type K⁺ channels in cerebellar granule neurons. *J. Physiol.* 586, 2093–2106. doi: 10.1113/jphysiol.2007.150540
- An, W. F., Bowlby, M. R., Betty, M., Cao, J., Ling, H. P., Mendoza, G., et al. (2000). Modulation of A-type potassium channels by a family of calcium sensors. *Nature* 403, 553–556. doi: 10.1038/35000592
- Anderson, D., Engbers, J. D., Heath, N. C., Bartoletti, T. M., Mehaffey, W. H., Zamponi, G. W., et al. (2013). The Cav3-Kv4 complex acts as a calcium sensor to maintain inhibitory charge transfer during extracellular calcium fluctuations. *J. Neurosci.* 33, 7811–7824. doi: 10.1523/JNEUROSCI.5384-12.2013
- Anderson, D., Mehaffey, W. H., Iftinca, M., Rehak, R., Engbers, J. D., Hameed, S., et al. (2010). Regulation of neuronal activity by Cav3-Kv4 channel signaling complexes. *Nat. Neurosci.* 13, 333–337. doi: 10.1038/nn.2493
- Andrasfalvy, B. K., Makara, J. K., Johnston, D., and Magee, J. C. (2008). Altered synaptic and non-synaptic properties of CA1 pyramidal neurons in Kv4.2 knockout mice. *J. Physiol.* 586, 3881–3892. doi: 10.1113/jphysiol.2008.154336
- Asztely, F., and Gustafsson, B. (1996). Ionotropic glutamate receptors. Their possible role in the expression of hippocampal synaptic plasticity. *Mol. Neurobiol.* 12, 1–11. doi: 10.1007/BF02740744
- Bähring, R., Boland, L. M., Varghese, A., Gebauer, M., and Pongs, O. (2001). Kinetic analysis of open- and closed-state inactivation transitions in human Kv4.2 A-type potassium channels. *J. Physiol.* 535, 65–81. doi: 10.1111/j.1469-7793.2001.00065.x
- Bähring, R., and Covarrubias, M. (2011). Mechanisms of closed-state inactivation in voltage-gated ion channels. *J. Physiol.* 589, 461–479. doi: 10.1113/jphysiol.2010.191965
- Bendheim, P. E., Brown, H. R., Rudelli, R. D., Scala, L. J., Goller, N. L., Wen, G. Y., et al. (1992). Nearly ubiquitous tissue distribution of the scrapie agent precursor protein. *Neurology* 42, 149–156. doi: 10.1212/WNL.42.1.149
- Blauw, H. M., Al-Chalabi, A., Andersen, P. M., van Vught, P. W., Diekstra, F. P., van Es, M. A., et al. (2010). A large genome scan for rare CNVs in amyotrophic lateral sclerosis. *Hum. Mol. Genet.* 19, 4091–4099. doi: 10.1093/hmg/ddq323
- Bourdeau, M. L., Laplante, I., Laurent, C. E., and Lacaille, J. C. (2011). KChIP1 modulation of Kv4.3-mediated A-type K(+) currents and repetitive firing in hippocampal interneurons. *Neuroscience* 176, 173–187. doi: 10.1016/j.neuroscience.2010.11.051
- Brambilla, P., Esposito, F., Lindstrom, E., Sorosina, M., Giacalone, G., Clarelli, F., et al. (2012). Association between DPP6 polymorphism and the risk of progressive multiple sclerosis in Northern and Southern Europeans. *Neurosci. Lett.* 530, 155–160. doi: 10.1016/j.neulet.2012.10.008
- Bueler, H., Fischer, M., Lang, Y., Bluethmann, H., Lipp, H. P., DeArmond, S. J., et al. (1992). Normal development and behaviour of mice lacking the neuronal cell-surface PrP protein. *Nature* 356, 577–582. doi: 10.1038/356577a0
- Butler, A., Wei, A. G., Baker, K., and Salkoff, L. (1989). A family of putative potassium channel genes in *Drosophila*. *Science* 243, 943–947. doi: 10.1126/science.2493160
- Chabala, L. D., Bakry, N., and Covarrubias, M. (1993). Low molecular weight poly(A)⁺ mRNA species encode factors that modulate gating of a non-Shaker A-type K⁺ channel. *J. Gen. Physiol.* 102, 713–728. doi: 10.1085/jgp.102.4.713
- Chandy, K. G., and Gutman, G. A. (1993). Nomenclature for mammalian potassium channel genes. *Trends Pharmacol. Sci.* 14, 434. doi: 10.1016/0165-6147(93)90181-I
- Chen, T., Ajami, K., McCaughan, G. W., Gai, W. P., Gorrell, M. D., and Abbott, C. A. (2006a). Molecular characterization of a novel dipeptidyl peptidase like 2-short form (DPL2-s) that is highly expressed in the brain and lacks dipeptidyl peptidase activity. *Biochim. Biophys. Acta* 1764, 33–43. doi: 10.1016/j.bbapap.2005.09.013
- Chen, X., Yuan, L. L., Zhao, C., Birnbaum, S. G., Frick, A., Jung, W. E., et al. (2006b). Deletion of Kv4.2 gene eliminates dendritic A-type K⁺ current and enhances induction of long-term potentiation in hippocampal CA1 pyramidal neurons. *J. Neurosci.* 26, 12143–12151. doi: 10.1523/JNEUROSCI.2667-06.2006
- Cheng, H. Y., Pitcher, G. M., Laviolette, S. R., Whishaw, I. Q., Tong, K. I., Kockeritz, L. K., et al. (2002). DREAM is a critical transcriptional repressor for pain modulation. *Cell* 108, 31–43. doi: 10.1016/S0092-8674(01)00629-8
- Chio, A., Schymick, J. C., Restagno, G., Scholz, S. W., Lombardo, F., Lai, S. L., et al. (2009). A two-stage genome-wide association study of sporadic amyotrophic lateral sclerosis. *Hum. Mol. Genet.* 18, 1524–1532. doi: 10.1093/hmg/ddp059
- Chu, P. J., Rivera, J. F., and Arnold, D. B. (2006). A role for Kif17 in transport of Kv4.2. *J. Biol. Chem.* 281, 365–373. doi: 10.1074/jbc.M508897200

- Clark, B. D., Kwon, E., Maffie, J., Jeong, H. Y., Nadal, M., Strop, P., et al. (2008). DPP6 localization in brain supports function as a Kv4 channel associated protein. *Front. Mol. Neurosci.* 1:8. doi: 10.3389/neuro.02.008.2008
- Colling, S. B., Collinge, J., and Jefferys, J. G. (1996). Hippocampal slices from prion protein null mice: disrupted Ca(2+)-activated K+ currents. *Neurosci. Lett.* 209, 49–52. doi: 10.1016/0304-3940(96)12596-9
- Connor, J. A., and Stevens, C. F. (1971a). Prediction of repetitive firing behaviour from voltage clamp data on an isolated neurone soma. *J. Physiol.* 213, 31–53.
- Connor, J. A., and Stevens, C. F. (1971b). Voltage clamp studies of a transient outward membrane current in gastropod neural somata. *J. Physiol.* 213, 21–30.
- Cotella, D., Radicke, S., Bortoluzzi, A., Ravens, U., Wettwer, E., Santoro, C., et al. (2010). Impaired glycosylation blocks DPP10 cell surface expression and alters the electrophysiology of Ito channel complex. *Pflugers Arch.* 460, 87–97. doi: 10.1007/s00424-010-0824-2
- Craven, S. E., El-Husseini, A. E., and Brecht, D. S. (1999). Synaptic targeting of the postsynaptic density protein PSD-95 mediated by lipid and protein motifs. *Neuron* 22, 497–509. doi: 10.1016/S0896-6273(00)80705-9
- Criado, J. R., Sanchez-Alavez, M., Conti, B., Giacchino, J. L., Wills, D. N., Henriksen, S. J., et al. (2005). Mice devoid of prion protein have cognitive deficits that are rescued by reconstitution of PrP in neurons. *Neurobiol. Dis.* 19, 255–265. doi: 10.1016/j.nbd.2005.01.001
- Cronin, S., Berger, S., Ding, J., Schymick, J. C., Washecka, N., Hernandez, D. G., et al. (2008). A genome-wide association study of sporadic ALS in a homogeneous Irish population. *Hum. Mol. Genet.* 17, 768–774. doi: 10.1093/hmg/ddm361
- de Lecea, L., Soriano, E., Criado, J. R., Steffensen, S. C., Henriksen, S. J., and Sutcliffe, J. G. (1994). Transcripts encoding a neural membrane CD26 peptidase-like protein are stimulated by synaptic activity. *Brain Res. Mol. Brain Res.* 25, 286–296. doi: 10.1016/0169-328X(94)90164-3
- Demo, S. D., and Yellen, G. (1991). The inactivation gate of the Shaker K+ channel behaves like an open-channel blocker. *Neuron* 7, 743–753. doi: 10.1016/0896-6273(91)90277-7
- Deschenes, I., Armoundas, A. A., Jones, S. P., and Tomaselli, G. F. (2008). Post-transcriptional gene silencing of KChIP2 and Na(v)beta1 in neonatal rat cardiac myocytes reveals a functional association between Na and I(to) currents. *J. Mol. Cell. Cardiol.* 45, 336–346. doi: 10.1016/j.yjmcc.2008.05.001
- Deschenes, I., and Tomaselli, G. F. (2002). Modulation of Kv4.3 current by accessory subunits. *FEBS Lett.* 528, 183–188. doi: 10.1016/S0014-5793(02)03296-9
- Dingledine, R., Borges, K., Bowie, D., and Traynelis, S. F. (1999). The glutamate receptor ion channels. *Pharmacol. Rev.* 51, 7–61.
- Djurovic, S., Gustafsson, O., Mattingsdal, M., Athanasou, L., Bjella, T., Tesli, M., et al. (2010). A genome-wide association study of bipolar disorder in Norwegian individuals, followed by replication in Icelandic sample. *J. Affect. Disord.* 126, 312–316. doi: 10.1016/j.jad.2010.04.007
- Dougherty, K., Tu, L., Deutsch, C., and Covarrubias, M. (2009). The dipeptidyl-aminopeptidase-like protein 6 is an integral voltage sensor-interacting beta-subunit of neuronal K(V)4.2 channels. *Channels (Austin)* 3, 122–128. doi: 10.4161/chan.3.2.8333
- Foeger, N. C., Norris, A. J., Wren, L. M., and Nerbonne, J. M. (2012). Augmentation of Kv4.2-encoded currents by accessory dipeptidyl peptidase 6 and 10 subunits reflects selective cell surface Kv4.2 protein stabilization. *J. Biol. Chem.* 287, 9640–9650. doi: 10.1074/jbc.M111.324574
- Fogh, I., D'Alfonso, S., Gellera, C., Ratti, A., Cereda, C., Penco, S., et al. (2011). No association of DPP6 with amyotrophic lateral sclerosis in an Italian population. *Neurobiol. Aging* 32, 966–967. doi: 10.1016/j.neurobiolaging.2009.05.014
- Frick, A., Magee, J., and Johnston, D. (2004). LTP is accompanied by an enhanced local excitability of pyramidal neuron dendrites. *Nat. Neurosci.* 7, 126–135. doi: 10.1038/nn1178
- Gebauer, M., Isbrandt, D., Sauter, K., Callsen, B., Nolting, A., Pongs, O., et al. (2004). N-type inactivation features of Kv4.2 channel gating. *Biophys. J.* 86, 210–223. doi: 10.1016/S0006-3495(04)74097-7
- Girirajan, S., Dennis, M. Y., Baker, C., Ratti, A., Malig, M., Coe, B. P., Campbell, C. D., et al. (2013). Refinement and discovery of new hotspots of copy-number variation associated with autism spectrum disorder. *Am. J. Hum. Genet.* 92, 221–237. doi: 10.1016/j.ajhg.2012.12.016
- Gulbis, J. M., Zhou, M., Mann, S., and MacKinnon, R. (2000). Structure of the cytoplasmic beta subunit-T1 assembly of voltage-dependent K+ channels. *Science* 289, 123–127. doi: 10.1126/science.289.5476.123
- Guo, W., Malin, S. A., Johns, D. C., Jeromin, A., and Nerbonne, J. M. (2002). Modulation of Kv4-encoded K(+) currents in the mammalian myocardium by neuronal calcium sensor-1. *J. Biol. Chem.* 277, 26436–26443. doi: 10.1074/jbc.M201431200
- Hagiwara, S., Kusano, K., and Saito, N. (1961). Membrane changes of Onchidium nerve cell in potassium-rich media. *J. Physiol.* 155, 470–489.
- Hermes, J. W., Korte, S., Gall, S., Schneider, I., Dunker, S., and Kretzschmar, H. A. (2000). Altered intracellular calcium homeostasis in cerebellar granule cells of prion protein-deficient mice. *J. Neurochem.* 75, 1487–1492. doi: 10.1046/j.1471-4159.2000.0751487.x
- Hermes, J. W., Tings, T., Dunker, S., and Kretzschmar, H. A. (2001). Prion protein affects Ca2+-activated K+ currents in cerebellar purkinje cells. *Neurobiol. Dis.* 8, 324–330. doi: 10.1006/nbdi.2000.0369
- Hoffman, D. A., Magee, J. C., Colbert, C. M., and Johnston, D. (1997). K+ channel regulation of signal propagation in dendrites of hippocampal pyramidal neurons. *Nature* 387, 869–875. doi: 10.1038/42571
- Holmqvist, M. H., Cao, J., Hernandez-Pineda, R., Jacobson, M. D., Carroll, K. I., Sung, M. A., et al. (2002). Elimination of fast inactivation in Kv4 A-type potassium channels by an auxiliary subunit domain. *Proc. Natl. Acad. Sci. U.S.A.* 99, 1035–1040. doi: 10.1073/pnas.022509299
- Hoshi, T., Zagotta, W. N., and Aldrich, R. W. (1990). Biophysical and molecular mechanisms of Shaker potassium channel inactivation. *Science* 250, 533–538. doi: 10.1126/science.2122519
- Hu, D., Barajas-Martinez, H., Medeiros-Domingo, A., Crotti, L., Veltmann, C., Schimpf, R., et al. (2012). A novel rare variant in SCN1Bb linked to Brugada syndrome and SIDS by combined modulation of Na(v)1.5 and K(v)4.3 channel currents. *Heart Rhythm* 9, 760–769. doi: 10.1016/j.hrthm.2011.12.006
- Jang, C., Choi, J. K., Kim, E., Park, E. S., Wasco, W., Buxbaum, J. D., et al. (2011). Calsenilin is degraded by the ubiquitin-proteasome pathway. *Biochem. Biophys. Res. Commun.* 405, 180–185. doi: 10.1016/j.bbrc.2010.12.137
- Jerng, H. H., Dougherty, K., Covarrubias, M., and Pfaffinger, P. J. (2009). A novel N-terminal motif of dipeptidyl peptidase-like proteins produces rapid inactivation of Kv4.2 channels by a pore-blocking mechanism. *Channels (Austin)* 3, 448–461. doi: 10.4161/chan.3.6.10216
- Jerng, H. H., Kunjilwar, K., and Pfaffinger, P. J. (2005). Multiprotein assembly of Kv4.2, KChIP3 and DPP10 produces ternary channel complexes with ISA-like properties. *J. Physiol.* 568, 767–788. doi: 10.1113/jphysiol.2005.087858
- Jerng, H. H., Lauver, A. D., and Pfaffinger, P. J. (2007). DPP10 splice variants are localized in distinct neuronal populations and act to differentially regulate the inactivation properties of Kv4-based ion channels. *Mol. Cell. Neurosci.* 35, 604–624. doi: 10.1016/j.mcn.2007.03.008
- Jerng, H. H., and Pfaffinger, P. J. (2008). Multiple Kv channel-interacting proteins contain an N-terminal transmembrane domain that regulates Kv4 channel trafficking and gating. *J. Biol. Chem.* 283, 36046–36059. doi: 10.1074/jbc.M806852200
- Jerng, H. H., and Pfaffinger, P. J. (2011). The cytoplasmic N-terminal domain of DPP6K disrupts KChIP modulation of Kv4 channels. *Biophys. J.* 100, 98a. doi: 10.1016/j.bpj.2010.12.742
- Jerng, H. H., and Pfaffinger, P. J. (2012). Incorporation of DPP6a and DPP6K variants in ternary Kv4 channel complex reconstitutes properties of A-type K current in rat cerebellar granule cells. *PLoS ONE* 7:e38205. doi: 10.1371/journal.pone.0038205
- Jerng, H. H., Kunjilwar, P. J., and Covarrubias, M. (2004a). Molecular physiology and modulation of somatodendritic A-type potassium channels. *Mol. Cell. Neurosci.* 27, 343–369. doi: 10.1016/j.mcn.2004.06.011
- Jerng, H. H., Qian, Y., and Pfaffinger, P. J. (2004b). Modulation of Kv4.2 channel expression and gating by dipeptidyl peptidase 10 (DPP10). *Biophys. J.* 87, 2380–2396. doi: 10.1529/biophysj.104.042358
- Jerng, H. H., Schaefer, M. K., and Pfaffinger, P. J. (2012). DPP6a confers redox sensitivity to Kv4 channel inactivation. *Biophys. J.* 102, 133a. doi: 10.1016/j.bpj.2011.11.736
- Jerng, H. H., Shahidullah, M., and Covarrubias, M. (1999). Inactivation gating of Kv4 potassium channels: molecular interactions involving the inner vestibule of the pore. *J. Gen. Physiol.* 113, 641–660. doi: 10.1085/jgp.113.5.641
- Johns, D. C., Nuss, H. B., and Marban, E. (1997). Suppression of neuronal and cardiac transient outward currents by viral gene transfer of dominant-negative Kv4.2 constructs. *J. Biol. Chem.* 272, 31598–31603. doi: 10.1074/jbc.272.50.31598

- Johnston, D., Christie, B. R., Frick, A., Gray, R., Hoffman, D. A., Schexnayder, L. K., et al. (2003). Active dendrites, potassium channels and synaptic plasticity. *Philos. Trans. R. Soc. Lond. B Biol. Sci.* 358, 667–674. doi: 10.1098/rstb.2002.1248
- Jung, S. C., Kim, J., and Hoffman, D. A. (2008). Rapid, bidirectional remodeling of synaptic NMDA receptor subunit composition by A-type K⁺ channel activity in hippocampal CA1 pyramidal neurons. *Neuron* 60, 657–671. doi: 10.1016/j.neuron.2008.08.029
- Kaneko, K., Zulianello, L., Scott, M., Cooper, C. M., Wallace, A. C., James, T. L., et al. (1997). Evidence for protein X binding to a discontinuous epitope on the cellular prion protein during scrapie prion propagation. *Proc. Natl. Acad. Sci. U.S.A.* 94, 10069–10074. doi: 10.1073/pnas.94.19.10069
- Kaufmann, W. A., Matsui, K., Jeromin, A., Nerbonne, J. M., and Ferraguti, F. (2013). Kv4.2 potassium channels segregate to extrasynaptic domains, and influence intrasynaptic NMDA receptor NR2B subunit expression. *Brain Struct. Funct.* 218, 1115–1132. doi: 10.1007/s00429-012-0450-1
- Kaulin, Y. A., De Santiago-Castillo, J. A., Nadal, M., Rudy, B., and Covarrubias, M. (2009). The dipeptidyl-peptidase-like-protein DPP6 determines the unitary conductance of neuronal Kv4.2 channels. *J. Neurosci.* 29, 3242–3251. doi: 10.1523/JNEUROSCI.4767-08.2009
- Kaulin, Y. A., De Santiago-Castillo, J. A., Rocha, C. A., and Covarrubias, M. (2008). Mechanism of the modulation of Kv4.2KChIP-1 channels by external K⁺. *Biophys. J.* 94, 1241–1251. doi: 10.1529/biophysj.107.117796
- Kim, E., and Hoffman, D. A. (2012). Dynamic regulation of synaptic maturation state by voltage-gated A-type K⁺ channels in CA1 hippocampal pyramidal neurons. *J. Neurosci.* 32, 14427–14432. doi: 10.1523/JNEUROSCI.2373-12.2012
- Kin, Y., Misumi, Y., and Ikehara, Y. (2001). Biosynthesis and characterization of the brain-specific membrane protein DPPX, a dipeptidyl peptidase IV-related protein. *J. Biochem.* 129, 289–295. doi: 10.1093/oxfordjournals.jbchem.a002856
- Korngreen, A., and Sakmann, B. (2000). Voltage-gated K⁺ channels in layer 5 neocortical pyramidal neurones from young rats: subtypes and gradients. *J. Physiol.* 525(Pt 3), 621–639. doi: 10.1111/j.1469-7793.2000.00621.x
- Korte, S., Vassallo, N., Kramer, M. L., Kretzschmar, H. A., and Herms, J. (2003). Modulation of L-type voltage-gated calcium channels by recombinant prion protein. *J. Neurochem.* 87, 1037–1042. doi: 10.1046/j.1471-4159.2003.02080.x
- Kubo, Y., Baldwin, T. J., Jan, Y. N., and Jan, L. Y. (1993). Primary structure and functional expression of a mouse inward rectifier potassium channel. *Nature* 362, 127–133. doi: 10.1038/362127a0
- Kunjilwar, K., Qian, Y., and Pfaffinger, P. J. (2013). Functional stoichiometry underlying KChIP regulation of Kv4.2 functional expression. *J. Neurochem.* 126, 462–472. doi: 10.1111/jnc.12309
- Kuo, H. C., Cheng, C. F., Clark, R. B., Lin, J. J., Lin, J. L., Hoshijima, M., et al. (2001). A defect in the Kv channel-interacting protein 2 (KChIP2) gene leads to a complete loss of I(to) and confers susceptibility to ventricular tachycardia. *Cell* 107, 801–813. doi: 10.1016/S0092-8674(01)00588-8
- Kuryshv, Y. A., Gudzt, T. I., Brown, A. M., and Wible, B. A. (2000). KChAP as a chaperone for specific K(+) channels. *Am. J. Physiol. Cell Physiol.* 278, C931–C941.
- Kuryshv, Y. A., Wible, B. A., Gudzt, T. I., Ramirez, A. N., and Brown, A. M. (2001). KChAP/Kvbeta1.2 interactions and their effects on cardiac Kv channel expression. *Am. J. Physiol. Cell Physiol.* 281, C290–C299.
- Laufer, A., Yuan, L. L., Jeromin, A., Nadin, B. M., Rodriguez, J. J., Davies, H. A., et al. (2006). Manipulating Kv4.2 identifies a specific component of hippocampal pyramidal neuron A-current that depends upon Kv4.2 expression. *J. Neurochem.* 99, 1207–1223. doi: 10.1111/j.1471-4159.2006.04185.x
- Li, X. G., Zhang, J. H., Xie, M. Q., Liu, M. S., Li, B. H., Zhao, Y. H., et al. (2009). Association between DPP6 polymorphism and the risk of sporadic amyotrophic lateral sclerosis in Chinese patients. *Chin. Med. J. (Engl.)* 122, 2989–2992.
- Liang, P., Chen, H., Cui, Y., Lei, L., and Wang, K. (2010). Functional rescue of Kv4.3 channel tetramerization mutants by KChIP4a. *Biophys. J.* 98, 2867–2876. doi: 10.1016/j.bpj.2010.03.044
- Liang, P., Wang, H., Chen, H., Cui, Y., Gu, L., Chai, J., et al. (2009). Structural insights into KChIP4a modulation of Kv4.3 inactivation. *J. Biol. Chem.* 284, 4960–4967. doi: 10.1074/jbc.M807704200
- Liao, C., Fu, F., Li, R., Yang, W. Q., Liao, H. Y., Yan, J. R., et al. (2013). Loss-of-function variation in the DPP6 gene is associated with autosomal dominant microcephaly and mental retardation. *Eur. J. Med. Genet.* 56, 484–489. doi: 10.1016/j.ejmg.2013.06.008
- Lin, L., Sun, W., Throesch, B., Kung, F., Decoster, J. T., Berner, C. J., et al. (2013). DPP6 regulation of dendritic morphogenesis impacts hippocampal synaptic development. *Nat. Commun.* 4, 2270. doi: 10.1038/ncomms3270
- Lledo, P. M., Tremblay, P., DeArmond, S. J., Prusiner, S. B., and Nicoll, R. A. (1996). Mice deficient for prion protein exhibit normal neuronal excitability and synaptic transmission in the hippocampus. *Proc. Natl. Acad. Sci. U.S.A.* 93, 2403–2407. doi: 10.1073/pnas.93.6.2403
- Long, S. B., Tao, X., Campbell, E. B., and MacKinnon, R. (2007). Atomic structure of a voltage-dependent K⁺ channel in a lipid membrane-like environment. *Nature* 450, 376–382. doi: 10.1038/nature06265
- Maffie, J., Blenkinsop, T., and Rudy, B. (2009). A novel DPP6 isoform (DPP6-E) can account for differences between neuronal and reconstituted A-type K(+) channels. *Neurosci. Lett.* 449, 189–194. doi: 10.1016/j.neulet.2008.10.098
- Maffie, J. K., Dvoretzskova, E., Bougis, P. E., Martin-Eauclaire, M. F., and Rudy, B. (2013). Dipeptidyl-peptidase-like-proteins confer high sensitivity to the scorpion toxin AmmTX3 to Kv4-mediated A-type K⁺ channels. *J. Physiol.* 591, 2419–2427. doi: 10.1113/jphysiol.2012.248831
- Malin, S. A., and Nerbonne, J. M. (2000). Elimination of the fast transient in superior cervical ganglion neurons with expression of KV4.2W362F: molecular dissection of IA. *J. Neurosci.* 20, 5191–5199.
- Mallucci, G. R., Ratte, S., Asante, E. A., Linehan, J., Gowland, I., Jefferys, J. G., et al. (2002). Post-natal knockout of prion protein alters hippocampal CA1 properties, but does not result in neurodegeneration. *EMBO J.* 21, 202–210. doi: 10.1093/emboj/21.3.202
- Maren, S., and Baudry, M. (1995). Properties and mechanisms of long-term synaptic plasticity in the mammalian brain: relationships to learning and memory. *Neurobiol. Learn. Mem.* 63, 1–18. doi: 10.1006/nlme.1995.1001
- Marinc, C., Pruss, H., Derst, C., and Veh, R. W. (2012). Immunocytochemical localization of TASK-3 channels in rat motor neurons. *Cell. Mol. Neurobiol.* 32, 309–318. doi: 10.1007/s10571-011-9762-6
- Marionneau, C., Carrasquillo, Y., Norris, A. J., Townsend, R. R., Isom, L. L., Link, A. J., et al. (2012a). The sodium channel accessory subunit Navbeta1 regulates neuronal excitability through modulation of repolarizing voltage-gated K(+) channels. *J. Neurosci.* 32, 5716–5727. doi: 10.1523/JNEUROSCI.6450-11.2012
- Marionneau, C., Lichti, C. F., Lindenbaum, P., Charpentier, F., Nerbonne, J. M., Townsend, R. R., et al. (2012b). Mass spectrometry-based identification of native cardiac Nav1.5 channel alpha subunit phosphorylation sites. *J. Proteome Res.* 11, 5994–6007. doi: 10.1021/pr300702c
- Marionneau, C., LeDuc, R. D., Rohrs, H. W., Link, A. J., Townsend, R. R., and Nerbonne, J. M. (2009). Proteomic analyses of native brain K(V)4.2 channel complexes. *Channels (Austin)* 3, 284–294. doi: 10.4161/chan.3.4.9553
- Marionneau, C., Townsend, R. R., and Nerbonne, J. M. (2011). Proteomic analysis highlights the molecular complexities of native Kv4 channel macromolecular complexes. *Semin. Cell Dev. Biol.* 22, 145–152. doi: 10.1016/j.semcdb.2010.10.004
- Marshall, C. R., Noor, A., Vincent, J. B., Lionel, A. C., Feuk, L., Skaug, J., et al. (2008). Structural variation of chromosomes in autism spectrum disorder. *Am. J. Hum. Genet.* 82, 477–488. doi: 10.1016/j.ajhg.2007.12.009
- McKay, B. E., McRory, J. E., Molineux, M. L., Hamid, J., Snutch, T. P., Zamponi, G. W., et al. (2006). Ca(V)3 T-type calcium channel isoforms differentially distribute to somatic and dendritic compartments in rat central neurons. *Eur. J. Neurosci.* 24, 2581–2594. doi: 10.1111/j.1460-9568.2006.05136.x
- Menegola, M., and Trimmer, J. S. (2006). Unanticipated region- and cell-specific downregulation of individual KChIP auxiliary subunit isoforms in Kv4.2 knockout mouse brain. *J. Neurosci.* 26, 12137–12142. doi: 10.1523/JNEUROSCI.2783-06.2006
- Mercer, R. C., Ma, L., Watts, J. C., Strome, R., Wohlgemuth, S., Yang, J., et al. (2013). The prion protein modulates A-type K⁺ currents mediated by Kv4.2 complexes through dipeptidyl aminopeptidase-like protein 6. *J. Biol. Chem.* 288, 37241–37255. doi: 10.1074/jbc.M113.488650
- Morohashi, Y., Hatano, N., Ohya, S., Takikawa, R., Watabiki, T., Takasugi, N., et al. (2002). Molecular cloning and characterization of CALP/KChIP4, a novel EF-hand protein interacting with presenilin 2 and voltage-gated potassium channel subunit Kv4. *J. Biol. Chem.* 277, 14965–14975. doi: 10.1074/jbc.M200897200
- Nadal, M. S., Amarillo, Y., Vega-Saenz de Miera, E., and Rudy, B. (2006). Differential characterization of three alternative spliced isoforms of DPPX. *Brain Res.* 1094, 1–12. doi: 10.1016/j.brainres.2006.03.106
- Nadal, M. S., Ozaita, A., Amarillo, Y., Vega-Saenz de Miera, E., Ma, Y., Mo, W., et al. (2003). The CD26-related dipeptidyl aminopeptidase-like protein DPPX is

- a critical component of neuronal A-type K⁺ channels. *Neuron* 37, 449–461. doi: 10.1016/S0896-6273(02)01185-6
- Nadin, B. M., and Pfaffinger, P. J. (2010). Dipeptidyl peptidase-like protein 6 is required for normal electrophysiological properties of cerebellar granule cells. *J. Neurosci.* 30, 8551–8565. doi: 10.1523/JNEUROSCI.5489-09.2010
- Nadin, B. M., and Pfaffinger, P. J. (2013). A new TASK for dipeptidyl peptidase-like protein 6. *PLoS ONE* 8:e60831. doi: 10.1371/journal.pone.0060831
- Nakahira, K., Shi, G., Rhodes, K. J., and Trimmer, J. S. (1996). Selective interaction of voltage-gated K⁺ channel beta-subunits with alpha-subunits. *J. Biol. Chem.* 271, 7084–7089. doi: 10.1074/jbc.271.12.7084
- Nakamura, T. Y., Pountney, D. J., Ozaita, A., Nandi, S., Ueda, S., Rudy, B., et al. (2001). A role for frequenin, a Ca²⁺-binding protein, as a regulator of Kv4 K⁺-currents. *Proc. Natl. Acad. Sci. U.S.A.* 98, 12808–12813. doi: 10.1073/pnas.221168498
- Neher, E. (1971). Two fast transient current components during voltage clamp on snail neurons. *J. Gen. Physiol.* 58, 36–53. doi: 10.1085/jgp.58.1.36
- Noor, A., Whibley, A., Marshall, C. R., Gianakopoulos, P. J., Piton, A., Carson, A. R., et al. (2010). Disruption at the PTC1D1 locus on Xp22.11 in autism spectrum disorder and intellectual disability. *Sci. Transl. Med.* 2, 49ra68. doi: 10.1126/scitranslmed.3001267
- Norris, A. J., Foeger, N. C., and Nerbonne, J. M. (2010). Interdependent roles for accessory KChIP2, KChIP3, and KChIP4 subunits in the generation of Kv4-encoded IA channels in cortical pyramidal neurons. *J. Neurosci.* 30, 13644–13655. doi: 10.1523/JNEUROSCI.2487-10.2010
- O'Callaghan, D. W., Hasdemir, B., Leighton, M., and Burgoyne, R. D. (2003). Residues within the myristoylation motif determine intracellular targeting of the neuronal Ca²⁺ sensor protein KChIP1 to post-ER transport vesicles and traffic of Kv4 K⁺ channels. *J. Cell Sci.* 116, 4833–4845. doi: 10.1242/jcs.00803
- Papazian, D. M., Schwarz, T. L., Tempel, B. L., Jan, Y. N., and Jan, L. Y. (1987). Cloning of genomic and complementary DNA from Shaker, a putative potassium channel gene from *Drosophila*. *Science* 237, 749–753. doi: 10.1126/science.2441470
- Petrecce, K., Miller, D. M., and Shrier, A. (2000). Localization and enhanced current density of the Kv4.2 potassium channel by interaction with the actin-binding protein filamin. *J. Neurosci.* 20, 8736–8744.
- Pioletti, M., Findeisen, F., Hura, G. L., and Minor, D. L. Jr. (2006). Three-dimensional structure of the KChIP1-Kv4.3 T1 complex reveals a cross-shaped octamer. *Nat. Struct. Mol. Biol.* 13, 987–995. doi: 10.1038/nsmb1164
- Pongs, O., Kecskemethy, N., Müller, R., Krah-Jentgens, I., Baumann, A., Kiltz, H. H., et al. (1988). Shaker encodes a family of putative potassium channel proteins in the nervous system of *Drosophila*. *EMBO J.* 7, 1087–1096.
- Pongs, O., and Schwarz, J. R. (2010). Ancillary subunits associated with voltage-dependent K⁺ channels. *Physiol. Rev.* 90, 755–796. doi: 10.1152/physrev.00020.2009
- Prestori, F., Rossi, P., Bearzatto, B., Laine, J., Necchi, D., Diwakar, S., et al. (2008). Altered neuron excitability and synaptic plasticity in the cerebellar granular layer of juvenile prion protein knock-out mice with impaired motor control. *J. Neurosci.* 28, 7091–7103. doi: 10.1523/JNEUROSCI.0409-08.2008
- Pruunsild, P., and Timmusk, T. (2005). Structure, alternative splicing, and expression of the human and mouse KCNIP gene family. *Genomics* 86, 581–593. doi: 10.1016/j.ygeno.2005.07.001
- Pruunsild, P., and Timmusk, T. (2012). Subcellular localization and transcription regulatory potency of KCNIP/Calsenilin/DREAM/KChIP proteins in cultured primary cortical neurons do not provide support for their role in CRE-dependent gene expression. *J. Neurochem.* 123, 29–43. doi: 10.1111/j.1471-4159.2012.07796.x
- Qi, S. Y., Riviere, P. J., Trojnar, J., Junien, J. L., and Akinsanya, K. O. (2003). Cloning and characterization of dipeptidyl peptidase 10, a new member of an emerging subgroup of serine proteases. *Biochem. J.* 373, 179–189. doi: 10.1042/BJ20021914
- Radicke, S., Cotella, D., Graf, E. M., Banse, U., Jost, N., Varro, A., et al. (2006). Functional modulation of the transient outward current I_{to} by KCNE beta-subunits and regional distribution in human non-failing and failing hearts. *Cardiovasc. Res.* 71, 695–703. doi: 10.1016/j.cardiores.2006.06.017
- Radicke, S., Cotella, D., Graf, E. M., Ravens, U., and Wettwer, E. (2005). Expression and function of dipeptidyl-aminopeptidase-like protein 6 as a putative beta-subunit of human cardiac transient outward current encoded by Kv4.3. *J. Physiol.* 565, 751–756. doi: 10.1113/jphysiol.2005.087312
- Ren, J., Wen, L., Gao, X., Jin, C., Xue, Y., and Yao, X. (2008). CSS-Palm 2.0: an updated software for palmitoylation sites prediction. *Protein Eng. Des. Sel.* 21, 639–644. doi: 10.1093/protein/gzn039
- Ren, X., Hayashi, Y., Yoshimura, N., and Takimoto, K. (2005). Transmembrane interaction mediates complex formation between peptidase homologues and Kv4 channels. *Mol. Cell. Neurosci.* 29, 320–332. doi: 10.1016/j.mcn.2005.02.003
- Ren, X., Shand, S. H., and Takimoto, K. (2003). Effective association of Kv channel-interacting proteins with Kv4 channel is mediated with their unique core peptide. *J. Biol. Chem.* 278, 43564–43570. doi: 10.1074/jbc.M302337200
- Rhodes, K. J., Carroll, K. I., Sung, M. A., Doliveira, L. C., Monaghan, M. M., Burke, S. L., et al. (2004). KChIPs and Kv4 alpha subunits as integral components of A-type potassium channels in mammalian brain. *J. Neurosci.* 24, 7903–7915. doi: 10.1523/JNEUROSCI.0776-04.2004
- Roesler, R., Walz, R., Quevedo, J., de-Paris, F., Zanata, S. M., Graner, E., et al. (1999). Normal inhibitory avoidance learning and anxiety, but increased locomotor activity in mice devoid of PrP(C). *Brain Res. Mol. Brain Res.* 71, 349–353. doi: 10.1016/S0169-328X(99)00193-X
- Rudy, B. (1988). Diversity and ubiquity of K channels. *Neuroscience* 25, 729–749. doi: 10.1016/0306-4522(88)90033-4
- Ruppersberg, J. P., Stocker, M., Pongs, O., Heinemann, S. H., Frank, R., and Koenen, M. (1991). Regulation of fast inactivation of cloned mammalian IK(A) channels by cysteine oxidation. *Nature* 352, 711–714. doi: 10.1038/352711a0
- Saito, Y., and Isa, T. (2000). Voltage-gated transient outward currents in neurons with different firing patterns in rat superior colliculus. *J. Physiol.* 528(Pt 1), 91–105. doi: 10.1111/j.1469-7793.2000.00091.x
- Satoh, J., Obayashi, S., Misawa, T., Sumiyoshi, K., Oosumi, K., and Tabunoki, H. (2009). Protein microarray analysis identifies human cellular prion protein interactors. *Neuropathol. Appl. Neurobiol.* 35, 16–35. doi: 10.1111/j.1365-2990.2008.00947.x
- Scannevin, R. H., Wang, K., Jow, F., Megules, J., Kopsco, D. C., Edris, W., et al. (2004). Two N-terminal domains of Kv4 K(+) channels regulate binding to and modulation by KChIP1. *Neuron* 41, 587–598. doi: 10.1016/S0896-6273(04)00049-2
- Schmitt-Ulms, G., Hansen, K., Liu, J., Cowdrey, C., Yang, J., DeArmond, S. J., et al. (2004). Time-controlled transcatheter perfusion cross-linking for the study of protein interactions in complex tissues. *Nat. Biotechnol.* 22, 724–731. doi: 10.1038/nbt969
- Schoppa, N. E., and Westbrook, G. L. (1999). Regulation of synaptic timing in the olfactory bulb by an A-type potassium current. *Nat. Neurosci.* 2, 1106–1113. doi: 10.1038/16033
- Schrader, L. A., Anderson, A. E., Mayne, A., Pfaffinger, P. J., and Sweatt, J. D. (2002). PKA modulation of Kv4.2-encoded A-type potassium channels requires formation of a supramolecular complex. *J. Neurosci.* 22, 10123–10133.
- Schwenk, J., Zolles, G., Kandas, N. G., Neubauer, I., Kalbacher, H., Covarrubias, M., et al. (2008). NMR analysis of KChIP4a reveals structural basis for control of surface expression of Kv4 channel complexes. *J. Biol. Chem.* 283, 18937–18946. doi: 10.1074/jbc.M800976200
- Serodio, P., Kentros, C., and Rudy, B. (1994). Identification of molecular components of A-type channels activating at subthreshold potentials. *J. Neurophysiol.* 72, 1516–1529.
- Shen, N. V., and Pfaffinger, P. J. (1995). Molecular recognition and assembly sequences involved in the subfamily-specific assembly of voltage-gated K⁺ channel subunit proteins. *Neuron* 14, 625–633. doi: 10.1016/0896-6273(95)90319-4
- Sheng, M., Tsaur, M. L., Jan, Y. N., and Jan, L. Y. (1992). Subcellular segregation of two A-type K⁺ channel proteins in rat central neurons. *Neuron* 9, 271–284. doi: 10.1016/0896-6273(92)90166-B
- Shibata, R., Misonou, H., Campomanes, C. R., Anderson, A. E., Schrader, L. A., Doliveira, L. C., et al. (2003). A fundamental role for KChIPs in determining the molecular properties and trafficking of Kv4.2 potassium channels. *J. Biol. Chem.* 278, 36445–36454. doi: 10.1074/jbc.M306142200
- Shibata, R., Nakahira, K., Shibasaki, K., Wakazono, Y., Imoto, K., and Ikenaka, K. (2000). A-type K⁺ current mediated by the Kv4 channel regulates the generation of action potential in developing cerebellar granule cells. *J. Neurosci.* 20, 4145–4155.
- Singh, B., Ogiwara, I., Kaneda, M., Tokonami, N., Mazaki, E., Baba, K., et al. (2006). A Kv4.2 truncation mutation in a patient with temporal lobe epilepsy. *Neurobiol. Dis.* 24, 245–253. doi: 10.1016/j.nbd.2006.07.001

- Soh, H., and Goldstein, S. A. (2008). I_{SA} channel complexes include four subunits each of DPP6 and Kv4.2. *J. Biol. Chem.* 283, 15072–15077. doi: 10.1074/jbc.M706964200
- Strop, P., Bankovich, A. J., Hansen, K. C., Garcia, K. C., and Brunger, A. T. (2004). Structure of a human A-type potassium channel interacting protein DPPX, a member of the dipeptidyl aminopeptidase family. *J. Mol. Biol.* 343, 1055–1065. doi: 10.1016/j.jmb.2004.09.003
- Sturgill, J. F., Steiner, P., Czervionke, B. L., and Sabatini, B. L. (2009). Distinct domains within PSD-95 mediate synaptic incorporation, stabilization, and activity-dependent trafficking. *J. Neurosci.* 29, 12845–12854. doi: 10.1523/JNEUROSCI.1841-09.2009
- Sun, W., Maffie, J. K., Lin, L., Petralia, R. S., Rudy, B., and Hoffman, D. A. (2011). DPP6 establishes the A-type K(+) current gradient critical for the regulation of dendritic excitability in CA1 hippocampal neurons. *Neuron* 71, 1102–1115. doi: 10.1016/j.neuron.2011.08.008
- Takimoto, K., Hayashi, Y., Ren, X., and Yoshimura, N. (2006). Species and tissue differences in the expression of DPPY splicing variants. *Biochem. Biophys. Res. Commun.* 348, 1094–1100. doi: 10.1016/j.bbrc.2006.07.157
- Takimoto, K., Yang, E. K., and Conforti, L. (2002). Palmitoylation of KChIP splicing variants is required for efficient cell surface expression of Kv4.3 channels. *J. Biol. Chem.* 277, 26904–26911. doi: 10.1074/jbc.M203651200
- Talley, E. M., Solorzano, G., Lei, Q., Kim, D., and Bayliss, D. A. (2001). Cns distribution of members of the two-pore-domain (KCNK) potassium channel family. *J. Neurosci.* 21, 7491–7505.
- Tanaka, S., Syu, A., Ishiguro, H., Inada, T., Horiuchi, Y., Ishikawa, M., et al. (2013). DPP6 as a candidate gene for neuroleptic-induced tardive dyskinesia. *Pharmacogenomics J.* 13, 27–34. doi: 10.1038/tpj.2011.36
- Tanaka, T., Ames, J. B., Harvey, T. S., Stryer, L., and Ikura, M. (1995). Sequestration of the membrane-targeting myristoyl group of recoverin in the calcium-free state. *Nature* 376, 444–447. doi: 10.1038/376444a0
- Tang, Y. Q., Liang, P., Zhou, J., Lu, Y., Lei, L., Bian, X., et al. (2013). Auxiliary KChIP4a suppresses A-type K⁺ current through endoplasmic reticulum (ER) retention and promoting closed-state inactivation of Kv4 channels. *J. Biol. Chem.* 288, 14727–14741. doi: 10.1074/jbc.M113.466052
- Telling, G. C., Scott, M., Mastrianni, J., Gabizon, R., Torchia, M., Cohen, F. E., et al. (1995). Prion propagation in mice expressing human and chimeric PrP transgenes implicates the interaction of cellular PrP with another protein. *Cell* 83, 79–90. doi: 10.1016/0092-8674(95)90236-8
- Thompson, S. H. (1977). Three pharmacologically distinct potassium channels in molluscan neurones. *J. Physiol.* 265, 465–488.
- Thomsen, M. B., Foster, E., Nguyen, K. H., and Sosunov, E. A. (2009a). Transcriptional and electrophysiological consequences of KChIP2-mediated regulation of CaV1.2. *Channels (Austin)* 3, 308–310. doi: 10.4161/chan.3.5.9560
- Thomsen, M. B., Wang, C., Ozgen, N., Wang, H. G., Rosen, M. R., and Pitt, G. S. (2009b). Accessory subunit KChIP2 modulates the cardiac L-type calcium current. *Circ. Res.* 104, 1382–1389. doi: 10.1161/CIRCRESAHA.109.196972
- Torgerson, D. G., Capurso, D., Mathias, R. A., Graves, P. E., Hernandez, R. D., Beaty, T. H., et al. (2012). Resequencing candidate genes implicates rare variants in asthma susceptibility. *Am. J. Hum. Genet.* 90, 273–281. doi: 10.1016/j.ajhg.2012.01.008
- Traynelis, S. F., Wollmuth, L. P., McBain, C. J., Menniti, F. S., Vance, K. M., Ogden, K. K., et al. (2010). Glutamate receptor ion channels: structure, regulation, and function. *Pharmacol. Rev.* 62, 405–496. doi: 10.1124/pr.109.002451
- van Es, M. A., van Vught, P. W., Blauw, H. M., Franke, L., Saris, C. G., Van den Bosch, L., et al. (2008). Genetic variation in DPP6 is associated with susceptibility to amyotrophic lateral sclerosis. *Nat. Genet.* 40, 29–31. doi: 10.1038/ng.2007.52
- Van Hoerick, D., Raes, A., Keyers, W., Mayeur, E., and Snyders, D. J. (2003). Differential modulation of Kv4 kinetics by KChIP1 splice variants. *Mol. Cell. Neurosci.* 24, 357–366. doi: 10.1016/S1044-7431(03)00174-X
- Vega-Saenz de Miera, E., Lau, D. H., Zhadina, M., Pountney, D., Coetzee, W. A., and Rudy, B. (2001). KT3.2 and KT3.3, two novel human two-pore K(+) channels closely related to TASK-1. *J. Neurophysiol.* 86, 130–142.
- Wada, K., Yokotani, N., Hunter, C., Doi, K., Wenthold, R. J., and Shimasaki, S. (1992). Differential expression of two distinct forms of mRNA encoding members of a dipeptidyl aminopeptidase family. *Proc. Natl. Acad. Sci. U.S.A.* 89, 197–201. doi: 10.1073/pnas.89.1.197
- Walz, R., Castro, R. M., Velasco, T. R., Carlotti, C. G. Jr., Sakamoto, A. C., et al. (2002). Cellular prion protein: implications in seizures and epilepsy. *Cell. Mol. Neurobiol.* 22, 249–257. doi: 10.1023/A:1020711700048
- Wang, H., Yan, Y., Liu, Q., Huang, Y., Shen, Y., Chen, L., et al. (2007). Structural basis for modulation of Kv4 K⁺ channels by auxiliary KChIP subunits. *Nat. Neurosci.* 10, 32–39. doi: 10.1038/nn1822
- Wang, H. G., He, X. P., Li, Q., Madison, R. D., Moore, S. D., McNamara, J. O., et al. (2013). The auxiliary subunit KChIP2 is an essential regulator of homeostatic excitability. *J. Biol. Chem.* 288, 13258–13268. doi: 10.1074/jbc.M112.434548
- Wang, L., Takimoto, K., and Levitan, E. S. (2003). Differential association of the auxiliary subunit Kvbeta2 with Kv1.4 and Kv4.3 K⁺ channels. *FEBS Lett.* 547, 162–164. doi: 10.1016/S0014-5793(03)00705-1
- Watanabe, S., Hoffman, D. A., Migliore, M., and Johnston, D. (2002). Dendritic K⁺ channels contribute to spike-timing dependent long-term potentiation in hippocampal pyramidal neurons. *Proc. Natl. Acad. Sci. U.S.A.* 99, 8366–8371. doi: 10.1073/pnas.122210599
- Wong, W., Newell, E. W., Jugloff, D. G., Jones, O. T., and Schlichter, L. C. (2002). Cell surface targeting and clustering interactions between heterologously expressed PSD-95 and the Shal voltage-gated potassium channel, Kv4.2. *J. Biol. Chem.* 277, 20423–20430. doi: 10.1074/jbc.M109412200
- Wong, W., and Schlichter, L. C. (2004). Differential recruitment of Kv1.4 and Kv4.2 to lipid rafts by PSD-95. *J. Biol. Chem.* 279, 444–452. doi: 10.1074/jbc.M304675200
- Wu, H., Romieu, I., Shi, M., Hancock, D. B., Li, H., Sienra-Monge, J. J., et al. (2010). Evaluation of candidate genes in a genome-wide association study of childhood asthma in Mexicans. *J. Allergy Clin. Immunol.* 125, 321.e13–327.e13. doi: 10.1016/j.jaci.2009.09.007
- Yang, E. K., Alvira, M. R., Levitan, E. S., and Takimoto, K. (2001). Kvbeta subunits increase expression of Kv4.3 channels by interacting with their C termini. *J. Biol. Chem.* 276, 4839–4844. doi: 10.1074/jbc.M004768200
- Zagha, E., Ozaita, A., Chang, S. Y., Nadal, M. S., Lin, U., Saganich, M. J., et al. (2005). DPP10 modulates Kv4-mediated A-type potassium channels. *J. Biol. Chem.* 280, 18853–18861. doi: 10.1074/jbc.M410613200
- Zegarra-Moran, O., and Moran, O. (1994). Properties of the transient potassium currents in cerebellar granule cells. *Exp. Brain Res.* 98, 298–304. doi: 10.1007/BF00228417
- Zhang, M., Jiang, M., and Tseng, G. N. (2001). minK-related peptide 1 associates with Kv4.2 and modulates its gating function: potential role as beta subunit of cardiac transient outward channel? *Circ. Res.* 88, 1012–1019. doi: 10.1161/hh1001.090839
- Zhang, Y., Su, P., Liang, P., Liu, T., Liu, X., Liu, X. Y., et al. (2010). The DREAM protein negatively regulates the NMDA receptor through interaction with the NR1 subunit. *J. Neurosci.* 30, 7575–7586. doi: 10.1523/JNEUROSCI.1312-10.2010
- Zhou, F. M., and Hablitz, J. J. (1996). Layer I neurons of the rat neocortex. II. Voltage-dependent outward currents. *J. Neurophysiol.* 76, 668–682.
- Zhou, H., Hong, X., Jiang, S., Dong, H., and Xu, X. (2009). Analyses of associations between three positionally cloned asthma candidate genes and asthma or asthma-related phenotypes in a Chinese population. *BMC Med. Genet.* 10:123. doi: 10.1186/1471-2350-10-123
- Zhou, W., Qian, Y., Kunjilwar, K., Pfaffinger, P. J., and Choe, S. (2004). Structural insights into the functional interaction of KChIP1 with Shal-type K(+) channels. *Neuron* 41, 573–586. doi: 10.1016/S0896-6273(04)00045-5

Conflict of Interest Statement: The authors declare that the research was conducted in the absence of any commercial or financial relationships that could be construed as a potential conflict of interest.

Received: 15 January 2014; accepted: 3 March 2014; published online: 27 March 2014.

Citation: Jerng HH and Pfaffinger PJ (2014) Modulatory mechanisms and multiple functions of somatodendritic A-type K⁺ channel auxiliary subunits. *Front. Cell. Neurosci.* 8:82. doi: 10.3389/fncel.2014.00082

This article was submitted to the journal *Frontiers in Cellular Neuroscience*.

Copyright © 2014 Jerng and Pfaffinger. This is an open-access article distributed under the terms of the Creative Commons Attribution License (CC BY). The use, distribution or reproduction in other forums is permitted, provided the original author(s) or licensor are credited and that the original publication in this journal is cited, in accordance with accepted academic practice. No use, distribution or reproduction is permitted which does not comply with these terms.



Signal processing by T-type calcium channel interactions in the cerebellum

Jordan D. T. Engbers¹, Dustin Anderson¹, Gerald W. Zamponi² and Ray W. Turner^{1,2 *}

¹ Department of Cell Biology and Anatomy, Hotchkiss Brain Institute, University of Calgary, Calgary, Canada

² Department of Physiology and Pharmacology, Hotchkiss Brain Institute, University of Calgary, Calgary, Canada

Edited by:

Leigh Anne Swayne, University of Victoria, Canada

Reviewed by:

Terrance P. Snutch, The University of British Columbia, Canada

Philippe Isope, Centre National Pour la Recherche Scientifique, France

*Correspondence:

Ray W. Turner, Department of Cell Biology and Anatomy, Hotchkiss Brain Institute, University of Calgary, HRIC 1AA14, 3330 Hospital Dr. N.W., Calgary, AB T2N 4N1, Canada
e-mail: rwtturner@ucalgary.ca

T-type calcium channels of the Cav3 family are unique among voltage-gated calcium channels due to their low activation voltage, rapid inactivation, and small single channel conductance. These special properties allow Cav3 calcium channels to regulate neuronal processing in the subthreshold voltage range. Here, we review two different subthreshold ion channel interactions involving Cav3 channels and explore the ability of these interactions to expand the functional roles of Cav3 channels. In cerebellar Purkinje cells, Cav3 and intermediate conductance calcium-activated potassium (IKCa) channels form a novel complex which creates a low voltage-activated, transient outward current capable of suppressing temporal summation of excitatory postsynaptic potentials (EPSPs). In large diameter neurons of the deep cerebellar nuclei, Cav3-mediated calcium current (I_T) and hyperpolarization-activated cation current (I_H) are activated during trains of inhibitory postsynaptic potentials. These currents have distinct, and yet synergistic, roles in the subthreshold domain with I_T generating a rebound burst and I_H controlling first spike latency and rebound spike precision. However, by shortening the membrane time constant the membrane returns towards resting value at a faster rate, allowing I_H to increase the efficacy of I_T and increase the range of burst frequencies that can be generated. The net effect of Cav3 channels thus depends on the channels with which they are paired. When expressed in a complex with a K_{Ca} channel, Cav3 channels reduce excitability when processing excitatory inputs. If functionally coupled with an HCN channel, the depolarizing effect of Cav3 channels is accentuated, allowing for efficient inversion of inhibitory inputs to generate a rebound burst output. Therefore, signal processing relies not only on the activity of individual subtypes of channels but also on complex interactions between ion channels whether based on a physical complex or by indirect effects on membrane properties.

Keywords: Cav3, HCN, T-type, IKCa, KCa3.1, channel complex

INTRODUCTION

Voltage- or calcium-gated ion channels can alter the output of a postsynaptic cell by modulating temporal or spatial summation of synaptic responses and thus the ability to attain spike threshold. Since the majority of a synaptic potential is subthreshold to spike generation, ion channels must be activated within a low voltage range or even during membrane hyperpolarizations. A limited subset of ion channels have the requisite properties to function in this manner, with low voltage-activated Cav3 T-type calcium channels directly activated during subthreshold postsynaptic potentials, and HCN channels activated within the negative voltage range traversed by inhibitory postsynaptic potentials (IPSPs; Magee and Johnston, 1995; Magee et al., 1995; Luthi and McCormick, 1998b; Swensen and Bean, 2003; Kole et al., 2006; Hildebrand et al., 2009; Engbers et al., 2011; Gastrein et al., 2011; Engbers et al., 2012). However, the ability for these channels to regulate synaptic responses can differ depending on direct or indirect interactions with other ion channels.

Interactions between calcium and potassium channels can be detected simply at a functional level, in which calcium influx is shown to drive potassium channel activation, or as an actual

association at the molecular level based on either a direct interaction between alpha subunits or indirectly through an accessory protein. Cav3 channels have been shown to at least functionally couple to small conductance (SK, KCa2.x) calcium-dependent potassium channels (Wolfart et al., 2001; Wolfart and Roeper, 2002; Yanovsky et al., 2005; Cueni et al., 2008) or big conductance (BK, KCa1.1) potassium channels (Smith et al., 2002). More recently Cav3 channels have been found to associate at the molecular level with a host of potassium channels, including BK channels (Engbers et al., 2013; Rehak et al., 2013), intermediate conductance calcium-dependent potassium channels (IKCa, KCa3.1; Engbers et al., 2012), and the voltage-gated Kv4 family (Anderson et al., 2010a,b). Interactions between these channels allow Cav3-mediated calcium influx to modulate spike repolarization (Gittis and du Lac, 2007; Rehak et al., 2013), firing rate gain (Smith et al., 2002; Anderson et al., 2010a, 2013), and temporal summation of EPSPs (Engbers et al., 2012), all over a wider range of membrane voltage than would be possible with high voltage-activated (HVA) calcium channels. The roles for Cav3 calcium influx in modulating subthreshold responses can also reflect a synergistic interplay with other channels through their respective effects on membrane

potential, such as the well-recognized case of Cav3 calcium and HCN channels that drive subthreshold oscillations in thalamic neurons (McCormick and Pape, 1990; McCormick and Bal, 1997; Kim et al., 2001; Cheong and Shin, 2013). HCN channels that give rise to I_H are also recognized to modulate temporal summation of both excitatory (Magee, 1999; Angelo et al., 2007; Tsay et al., 2007) and inhibitory (McCormick and Pape, 1990; Atherton et al., 2010) synaptic responses.

Several reviews of the functional roles of Cav3 calcium channels and HCN channels have been published (Luthi and McCormick, 1998a; Perez-Reyes, 2003; Robinson and Siegelbaum, 2003; Yunker and McEnery, 2003; Biel et al., 2009; Cueni et al., 2009; Wahl-Schott and Biel, 2009; Cain and Snutch, 2010, 2013; Cheong and Shin, 2013; Weiss and Zamponi, 2013). In the current review, we contrast and compare the effects of a new direct molecular interaction between Cav3 and IKCa channels to that of a synergistic interaction between Cav3 and HCN channels on synaptic processing in cerebellar Purkinje cells and deep cerebellar nuclear (DCN) cells, the postsynaptic target of Purkinje cells. These two examples serve to emphasize how ion channel interactions involving Cav3 channels can result in a wide range of functional effects.

CEREBELLAR SYNAPTIC INPUTS

The cerebellum is a highly organized cortical structure that receives information from the periphery as well as input from descending cortical projections relayed through pontine nuclei in the form of excitatory synaptic inputs. The majority of input arrives as mossy fibers to granule cells that in turn project parallel fibers (PF) to the molecular layer, providing upwards of 150,000 inputs to individual Purkinje cells. Not all of these inputs are active, as long-term depression results in the silencing of up to 85% of the PF-PC synapses (Ekerot and Jorntell, 2001; Isope and Barbour, 2002). However, even accounting for silenced synapses, the Purkinje cell can still receive input from over 20,000 granule cells. Granule cell projections are highly organized in the context of sensory input but even a low rate of spontaneous activity (~ 1 –4 Hz) can lead to an enormous level of background PF activity that Purkinje cells must discriminate from sensory-relevant bursts of input in a small subset of PFs (Chadderton et al., 2004; Rancz et al., 2007; Ekerot and Jorntell, 2008; D'Angelo and De Zeeuw, 2009). Purkinje cells that are excited by granule cells project inhibitory GABAergic output to cells in the DCN, a set of three bilateral nuclei at the base of cerebellum. The neural coding strategies used by DCN cells are still being determined, but extensive work *in vitro* has established that they have the capacity to respond to inhibition with a rebound increase in firing rate (Jahnsen, 1986a; Aizenman and Linden, 1999; Molineux et al., 2006, 2008; Tadayonnejad et al., 2009, 2010; Hoebeek et al., 2010; Sangrey and Jaeger, 2010; Engbers et al., 2011). The extent to which this occurs in response to physiological stimuli has recently been debated (Alvina et al., 2008; Person and Raman, 2012), although some consensus begins to emerge from both *in vivo* and *in vitro* work that DCN cells can exhibit a rebound increase in firing frequency given a significantly large inhibitory input that could arise in relation to the frequency, number, and in particular, synchronous input from Purkinje cells (Aizenman and Linden, 1999; Zhang et al., 2004; Wetmore et al., 2008; Tadayonnejad et al., 2009, 2010; Hoebeek et al., 2010; Bengtsson et al.,

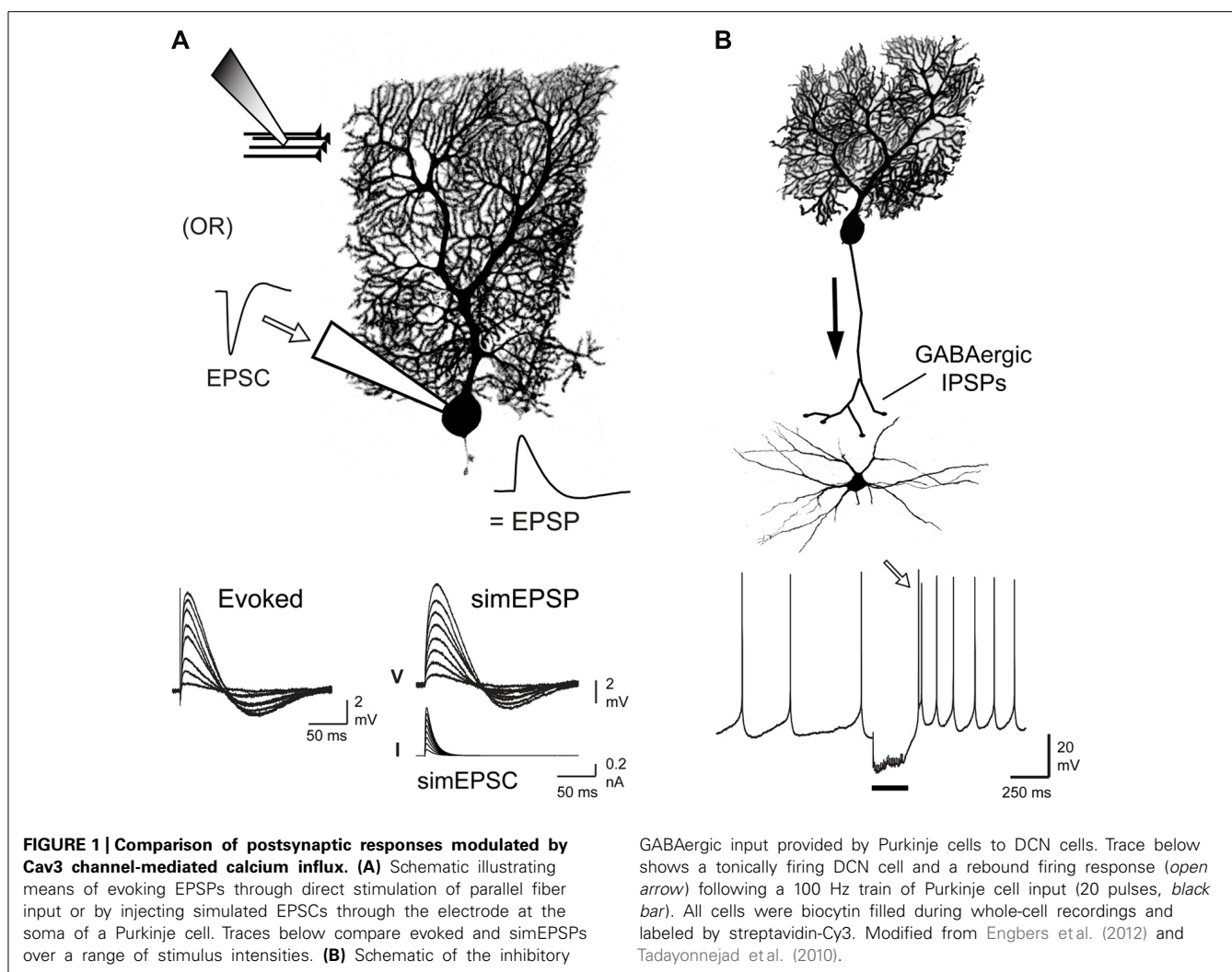
2011). Nevertheless, the ionic mechanisms that could facilitate a rebound response are still under investigation. The effects of PF input to Purkinje cells or Purkinje cell input onto DCN cells can be studied in an *in vitro* slice preparation either by directly stimulating synaptic inputs or by simulating synaptic potentials by injecting postsynaptic current waveforms at the soma (**Figure 1**). The current review compares the means by which Cav3 channels can interact with other ion channels to produce markedly different results between the PF-Purkinje cell synapse and the Purkinje-DCN cell synapse.

THE ROLE OF CAV3 CHANNELS IN SUPPRESSING TEMPORAL SUMMATION

Parallel fibers EPSPs are followed by an afterhyperpolarization (AHP) lasting up to ~ 200 ms, a striking feature given that these AHPs can be seen to follow even small amplitude EPSPs. Part of this AHP is due to deactivation of I_H during the depolarizing phase of the EPSP, resulting in a hyperpolarizing voltage overshoot (Angelo et al., 2007). However, we recently showed that the remaining portion of the AHP is due to activation of IKCa channels via Cav3 channel-mediated calcium influx at hyperpolarized potentials (Engbers et al., 2012). This finding improves on our understanding of Cav3 ion channel interactions in three ways: (1) Cav3 channels can activate at much lower voltages than previously thought, (2) small amplitude Cav3-mediated current is sufficient to activate KCa channels, and (3) the functional role of Cav3 inward current can be inverted by association with a K^+ channel.

Cav3 channels are known to be low voltage-activated, with the voltage for initial activation usually identified by the presence of measureable current on conductance plots derived from whole-cell voltage clamp recordings. However, it is important to recognize that activation of channels in the membrane may occur at voltage levels below those necessary to appear under whole-cell recording conditions. In this regard, voltage clamp analyses have established that Cav3 calcium channels exhibit overlap in the activation and inactivation profiles. This overlap establishes a window current that, while small near resting membrane potential ($\sim 2\%$ of total available current), is constitutively active and sufficient to raise intracellular calcium concentration and affect neuronal firing (**Figures 2A,B**; Huguenard, 1996; Swensen and Bean, 2003; Perez-Reyes, 2006; Talavera and Nilius, 2006; Dreyfus et al., 2010; Engbers et al., 2012). Careful inspection of the degree of overlap of these curves recorded even under whole cell conditions reveals a Cav3 window current that extends from well below -65 mV all the way to ~ -20 mV (**Figure 2B**). These values agree with previous work reporting that a significant proportion of calcium current activated during a sodium spike in Purkinje cells is mediated Cav3 channels (Chemin et al., 2002; Swensen and Bean, 2003). Therefore, LVA Cav3 channels can be a significant source of calcium at subthreshold and suprathreshold voltages, and provide a constitutive inward current even during rest.

Activation curves derived by voltage steps in whole-cell voltage clamp might suggest that no significant activation of Cav3 current will occur at potentials negative to -70 mV. However, in a study of HVA calcium channel-mediated transmitter release, the use of slow voltage ramps revealed Cav2.1 (P/Q-type) channel



activation ~ 20 mV more negative than the activation threshold suggested by macroscopic activation curves (Awatramani et al., 2005). Experimental results had also suggested that Cav3 channels were capable of being activated at potentials as low as -75 mV (Engbers et al., 2012). Indeed, slow ramp commands (-100 to -40 mV) applied to Purkinje cells in whole-cell configuration established initial activation of a Ni^{2+} -sensitive inward current at voltages as low as -90 mV (Figures 2C,D). These and other measures confirm that Cav3 channel window current can extend over a far wider range than previously anticipated, potentially providing a calcium current that can be activated by even small amplitude PF EPSPs. While this does not suggest that potentials of -90 mV will ever be reached under physiological conditions, it does indicate that Cav3 channels can act as a significant source of calcium influx over the entire subthreshold range and their availability as a functional current should not be discounted based solely on membrane potential in relation to the voltage for inactivation. In fact, Cav3 channels are known to contribute to Purkinje cell activity during tonic firing at a depolarized state (Swensen and Bean, 2003; Engbers et al., 2012). Furthermore, Cav3 activation properties are known to vary between cell types and even be regulated by

their association with other structures, such as mGluR1 receptors (Hildebrand et al., 2009).

In addition to the Ni^{2+} -sensitive inward current, ramp commands in Purkinje cells revealed a Ni^{2+} -sensitive outward current that activated from ~ -80 mV with a later onset than the initial Cav3 calcium current (Figure 2C), presumably the same current responsible for the PF-associated AHP. This finding indicated at least a functional coupling between Cav3 channels and KCa channel(s) of some identity. BK and SK2 channels are both expressed in Purkinje cells and are known to be activated by calcium influx. A functional coupling and molecular association between HVA calcium and BK channels is well-established and characterized (Raman and Bean, 1999; Swensen and Bean, 2003; Grunnet and Kaufmann, 2004; Womack et al., 2004; Berkefeld et al., 2006; Alvin and Khodakhah, 2008; Berkefeld and Fakler, 2008; Fakler and Adelman, 2008). A functional coupling between BK and Cav3 channels has also been demonstrated in some cells (Smith et al., 2002; Engbers et al., 2013; Rehak et al., 2013). A higher sensitivity of SK channels to intracellular calcium compared to BK channels allows the SK channel family to couple with a wide range of Ca^{2+} sources, including Cav1, Cav2.3, and Cav3 calcium

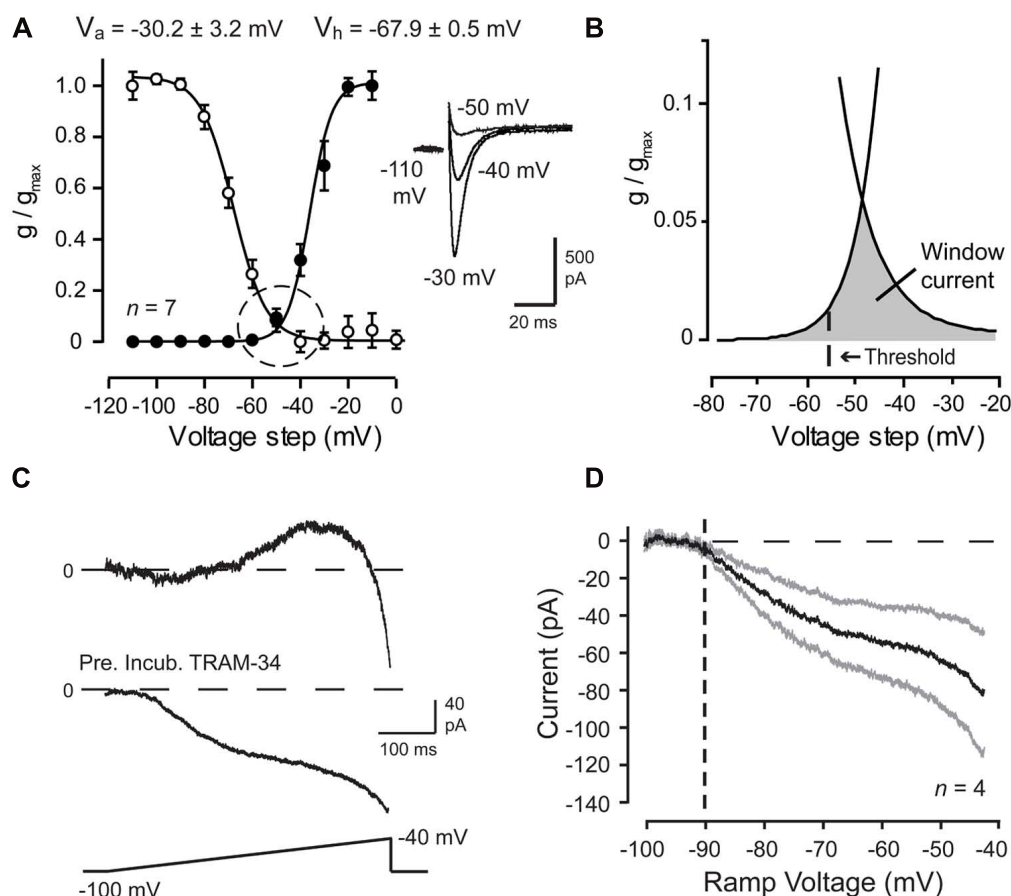


FIGURE 2 | Cav3 T-type calcium current is evoked over a wide membrane voltage range in Purkinje cells. (A,B) Mean conductance and inactivation plots calculated for whole-cell Cav3 current recorded from P10–12 Purkinje cells. *Inset* shows Cav3 current evoked over relatively negative step commands. **(B)** Expanded image of the fits for activation and inactivation curves from plots in **(A)** (*dashed circle*) showing a wide voltage range for Cav3 window current (*gray*) in relation to spike threshold (*dashed line*). **(C,D)** Whole-cell recordings from mature (P18–30) Purkinje cells evoked by a ramp from -100 mV to -40 mV (500 ms) and

Ni^{2+} -sensitive currents extracted by applying $300 \mu M Ni^{2+}$. Shown are records of sequential inward-outward currents activated in one cell (*top trace*) and in another cell purely inward current when recorded in the presence of the potassium channel blocker TRAM-34 (100 nM) (*bottom trace*). **(D)** Current-voltage plot of the average Ni^{2+} -sensitive Cav3 current evoked by a ramp command in the presence of TRAM-34. Inward current exhibits initial activation from a voltage of ~ -90 mV (*dashed line*). Standard errors are shown by gray traces. Modified from Engbers et al. (2012).

channels, NMDA receptors, and Ca^{2+} -permeable nicotinic acetylcholine receptors (Marrion and Tavalin, 1998; Oliver et al., 2000; Wolfart and Roeper, 2002; Ngo-Anh et al., 2005; Yanovsky et al., 2005; Bloodgood and Sabatini, 2007; Cueni et al., 2008; Fakler and Adelman, 2008; Faber, 2010).

Given the wide range of calcium sources capable of activating BK and SK channels, it was fully expected that one of these KCa channel subtypes would account for the PF-evoked AHP. However, a pharmacological assay established that the PF EPSP-AHP simulated by postsynaptic injection of a PF EPSC waveform (simEPSP) was fully *insensitive* to blockers of SK or BK channels as well as a range of HVA calcium channel blockers (Engbers et al., 2012). Instead the PF EPSP rate of decay and AHP were reduced by low Ni^{2+} and mibefradil, two established blockers of Cav3 current in Purkinje cells (McDonough and Bean, 1998; Isope and Murphy, 2005; **Figure 3A**). The rate of decay of the simEPSP and AHP were also blocked by charybdotoxin (ChTx) or TRAM-34, two

blockers of IKCa channels (**Figure 3A**). This was surprising given that IKCa channels were only believed to be expressed in central regions in activated microglia and endothelial cells (Kaushal et al., 2007; Pedarzani and Stocker, 2008). However, applying TRAM-34 during ramp commands effectively blocked all Ni^{2+} -sensitive outward current (**Figures 2C,D**). Moreover, a series of protein biochemical tests established that IKCa channels are expressed in Purkinje cells and exhibit an association with Cav3 channels at the molecular level (see Engbers et al., 2012). These results then established the existence of a Cav3-IKCa channel complex, adding to the number of complexes recognized between calcium and potassium channels.

It is interesting to contemplate the pairing of Cav3 and IKCa channels. Cav3 channels have a small single channel conductance, low maximal open probability and exhibit rapid inactivation, resulting in small changes in intracellular calcium during sub-threshold voltage changes. Therefore, any KCa channel depending

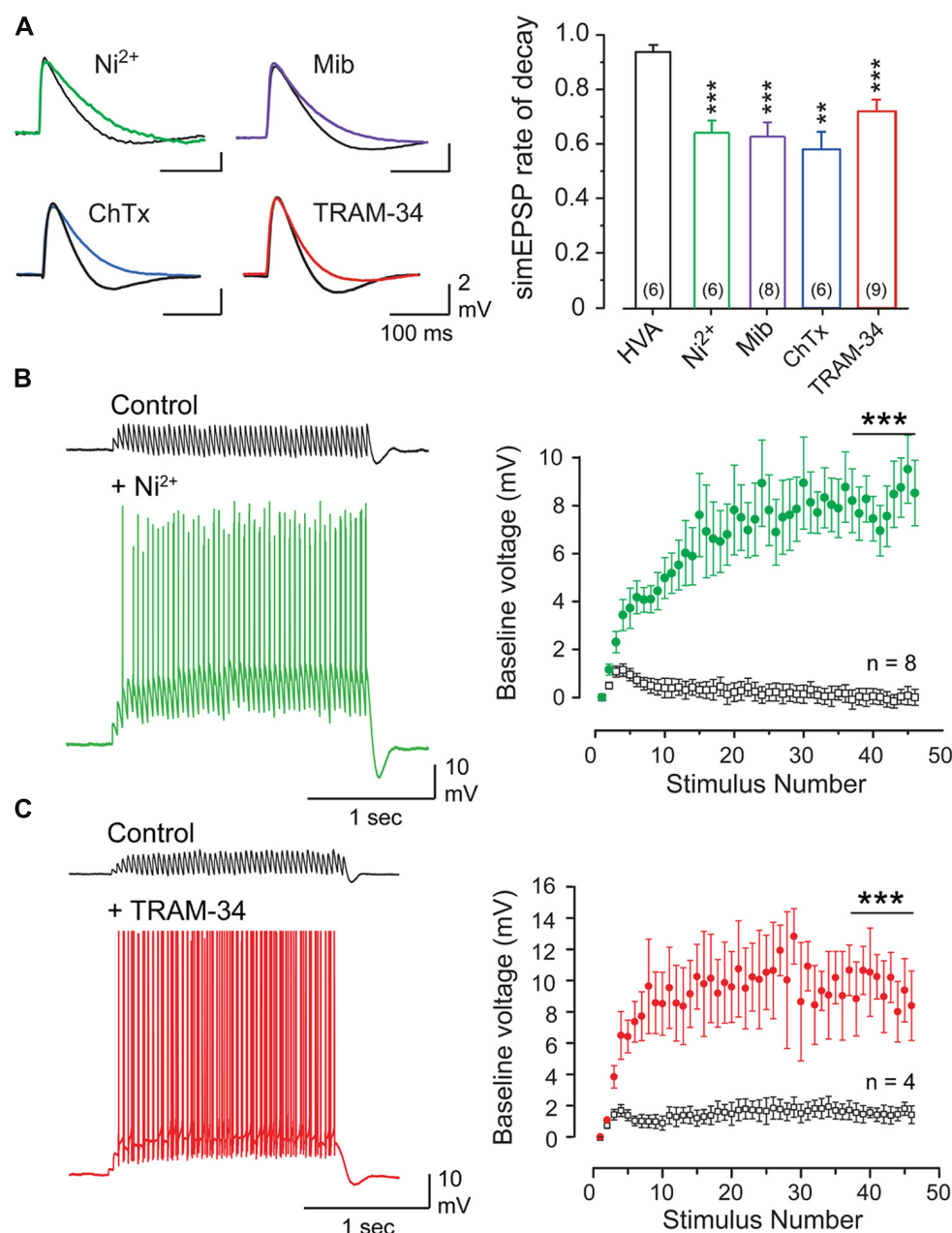


FIGURE 3 | The parallel fiber EPSP activates a Cav3- and KCa3. 1-mediated AHP that suppresses temporal summation. **(A)** Superimposed records of simEPSPs in Purkinje cells before and after 100 μM Ni^{2+} , 1 μM mibefradil (Mib), 100 nM ChTx, or 100 nM TRAM-34. Bar graphs show mean values of the reduction of simEPSP rate of decay. HVA refers to a cocktail of ω -conotoxin GVIA (1 μM), nifedipine (1 μM), and SNX-482 (200 nM). **(B,C)**

Recordings and plots of the mean baseline voltage during 25 Hz trains of parallel fiber-evoked EPSPs before and after applying Ni^{2+} [**(B)**, 100 μM] or TRAM-34 [**(C)**, 100 nM]. Recordings in **(B,C)** were conducted in 50 μM picrotoxin. Statistical significance tested for last 10 pulses of stimulus trains in **(B,C)** is denoted by bars. Sample values in **(A)** are shown in brackets within bar plots. ** $p < 0.01$, *** $p < 0.001$. Modified from Engbers et al. (2012).

on Cav3-mediated calcium influx would have to be exquisitely sensitive to calcium concentration. Interestingly, IKCa is the most sensitive of the KCa channels and exhibits a slow rate of deactivation once activated (Ishii et al., 1997; Joiner et al., 1997). Furthermore, the larger conductance of IKCa channels (20–90 pS) compared to SK channels (10–20 pS) allows small changes in open probability to have a greater effect on membrane voltage. The

molecular association between Cav3 and IKCa channels is thus an ideal pairing of signal and transducer, with the KCa channel being tuned to sense the range of intracellular calcium concentration changes associated with Cav3 influx at the level of a nanodomain.

Given the factors that allow Cav3 calcium influx to activate IKCa channels, this ion channel complex should exhibit activation in the subthreshold region. Repetitive PF stimulation revealed an

initial temporal summation of EPSPs over the first few stimuli, but then a marked suppression of summation for the remainder of the stimulus train (**Figures 3B,C**). This result was obtained in the presence or absence of picrotoxin to block GABAergic inhibition (not shown), revealing that suppression of temporal summation did not involve feedforward inhibition activated by PF inputs (Hausser and Clark, 1997; Mittmann et al., 2005). Rather, perfusion of either Ni^{2+} (100 μM) to block Cav3 calcium influx or TRAM-34 (100 nM) to block IKCa channels restored temporal summation to reveal a substantial increase in EPSP peak amplitude and repetitive spike output from Purkinje cells throughout the stimulus train (**Figures 3B,C**). Therefore, when coupled to IKCa channels, the Cav3 channel does not provide a net depolarizing effect, but has its influence effectively inverted by the IKCa channel, resulting in a net hyperpolarizing effect. The close association between these channels further allow a rapid response to subthreshold depolarizations and a pronounced effect on temporal summation of excitatory inputs.

These studies were important in demonstrating that Cav3 calcium current has the capacity to activate at very negative membrane voltages, providing an inward current that could potentially accentuate temporal summation and other membrane depolarizations. However, by forming a complex with IKCa channels, Cav3 calcium influx instead provides a net inhibitory influence over temporal summation. These and other experiments help support the hypothesis that the purpose of a Cav3-IKCa mediated inhibition is to suppress the background level of PF input expected to be transmitted to Purkinje cells (Engbers et al., 2012). In this way Purkinje cells will be able to respond to the high frequency bursts of PF input that convey sensory-relevant information.

SYNERGISTIC INTERPLAY BETWEEN CAV3 AND HCN CHANNELS BOOSTS A REBOUND RESPONSE

A different interaction between Cav3 and HCN channels becomes apparent in the integration of inhibitory synaptic input to DCN cells. Recordings *in vitro* have primarily focused on large diameter cells that exhibit a characteristic rebound increase in firing rate following a period of membrane hyperpolarization or train of IPSPs evoked by stimulation of Purkinje cell input (Molineux et al., 2008; Tadayonnejad et al., 2009, 2010; Pedroarena, 2010; Sangrey and Jaeger, 2010; Engbers et al., 2011). Transient calcium current through Cav3 channels (I_T) and the inward tail current associated with hyperpolarization-activated HCN channels (I_H) have been proposed to contribute to rebound responses from some of the earliest recordings (Jahnsen, 1986b; McCormick and Pape, 1990; Muri and Knopfel, 1994; Huguenard, 1996). We also found a correlation between the expression of the Cav3.1 calcium channel isoform in DCN cells and the generation of a high frequency Transient Burst phenotype, and for Cav3.3 channels to a form of Weak Burst response (Molineux et al., 2006). For the purpose of this review we will restrict examples to Transient Burst DCN cells.

I_T recorded under steady-state whole-cell voltage clamp conditions is shown in **Figure 4**, where a step from a negative holding potential to -50 mV (a value just below spike threshold) reveals a large amplitude calcium current. The correspondence of this current to Cav3 channels is supported by an insensitivity to the general

HVA calcium channel blocker Cd^{2+} (50 μM) but full block by 300 μM Ni^{2+} (**Figures 4A,B**). I_H recorded under whole cell conditions and isolated as Cs^+ -sensitive current is evident as a slowly activating and non-inactivating inward current that activates at physiological temperatures negative to -50 mV (**Figures 4C,D**). Of most apparent relevance to a rebound response is a prolonged inward I_H tail current (~ 500 ms) that follows the end of a negative command pulse (Engbers et al., 2011). This is important in that a prolonged I_H deactivation will be expected to generate a depolarization with potential influence on the rebound response (Aizenman and Linden, 1999; Engbers et al., 2011; Steuber et al., 2011). Indeed, perfusion of either a low concentration of Ni^{2+} (300 μM) or Cs^+ (2 mM) under current clamp conditions reduced the frequency of the rebound response (**Figure 4E**), results consistent with a depolarizing influence for both I_T and I_H . In fact, the ability for calcium channel blockers to reduce the rebound response has been reported using voltage clamp step commands (Molineux et al., 2006, 2008), calcium imaging experiments (Muri and Knopfel, 1994; Zhang et al., 2004; Zheng and Raman, 2009; Schneider et al., 2013), and recently more selective I_T blockers (Alvina et al., 2009; Boehme et al., 2011). Blocking I_H with external Cs^+ uncovered an additional influence of I_H in controlling the first spike latency (FSL) to the burst response, an effect that was graded with the stimulus (**Figure 4F**; Sangrey and Jaeger, 2010; Tadayonnejad et al., 2010). Thus, the greater the number of stimuli (and the longer the hyperpolarization) the shorter the FSL when expressed as a ratio to the control interspike interval (ISI). Similar results on FSL/ISI were not obtained by perfusing Cav3 channel blockers (not shown; Engbers et al., 2011).

The most direct interpretation of these results is that both Cav3 and HCN channels contribute a membrane depolarization that directly increases rebound spike frequency and reduces the FSL. To more carefully compare the roles for I_T and I_H in either aspect of a rebound, we used available data on these currents (**Figures 2 and 4**) to construct a two compartment reduced model based on Hodgkin–Huxley formalism (for details, see Engbers et al., 2011). Importantly, this model proved capable of reproducing the stimulus-dependent decrease in FSL/ISI and increase in spike frequency of the rebound response (**Figure 5A**). We note that the frequency response here was measured over only the first 100 ms of the rebound, and does not account for the longer duration depolarizations that reflect contributions by HVA calcium channels or I_{NaP} (Zheng and Raman, 2009; Sangrey and Jaeger, 2010; Steuber et al., 2011). Comparing the output of the model upon removing I_T or I_H was highly instructive in first showing that if only I_H was present the model preserved the inverse relationship between FSL/ISI and hyperpolarization strength (greater depth and longer duration) but also exhibited a significant decrease in rebound frequency (**Figure 5B**). If only I_T was present, the FSL/ISI relationship was reversed, with longer hyperpolarizations resulting in a longer FSL/ISI ratio (**Figure 5C**). However, the rebound response was only present when the model contained I_T (**Figures 5A,C**). Removing both I_T and I_H caused the FSL/ISI relationship to become directly proportional to the depth and duration of hyperpolarization, as would be expected without active currents in the subthreshold range, and abolished the rebound response (**Figure 5D**).

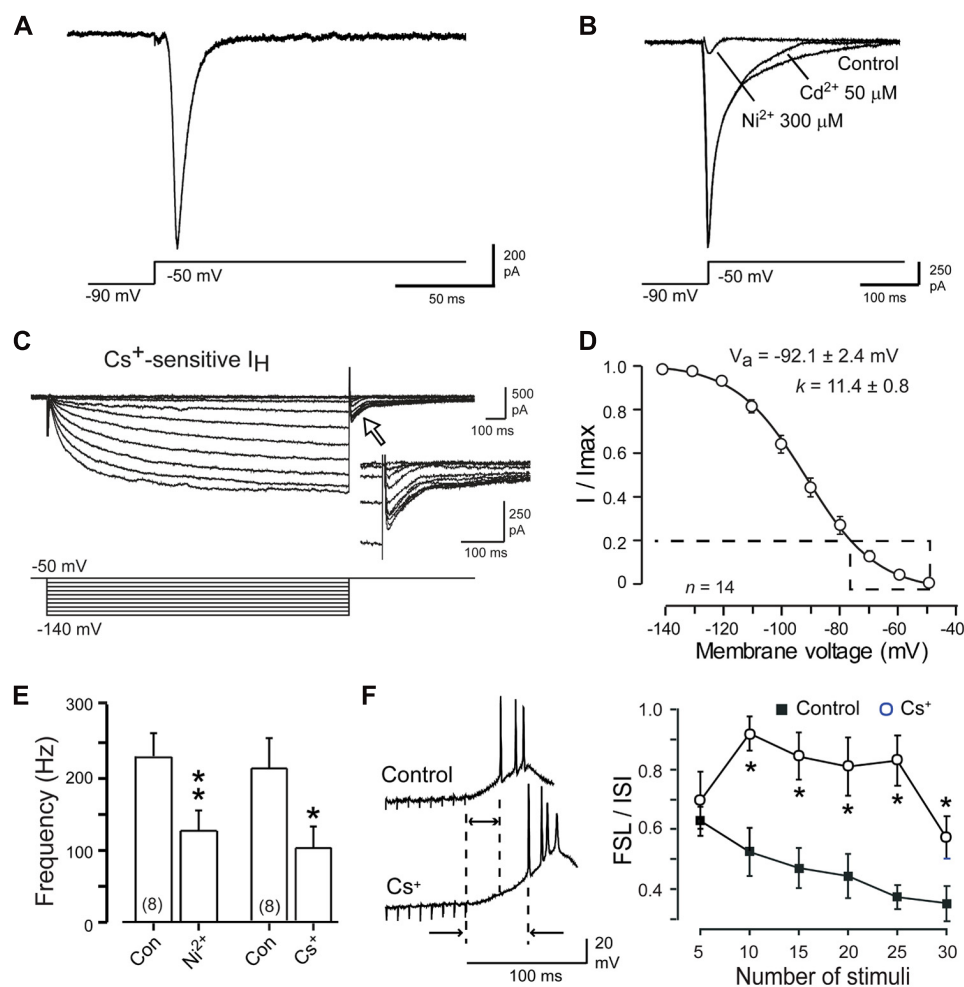


FIGURE 4 | DCN cells express both I_T and I_H . (A) I_T recorded from a Transient Burst DCN cell under whole-cell conditions at physiological temperature for a single step to -50 mV. (B) I_T recorded in a separate cell reveals no effects of applying Cd^{2+} but nearly full block by Ni^{2+} . (C) I_H recorded from a DCN cell at physiological temperature and identified as Cs^+ -sensitive current. An inward tail current is evident following the end of step commands (inset, open arrow). (D) Mean conductance plot for Cs^+ -sensitive I_H . Dashed line and box denotes the physiological range of

membrane voltage traversed by IPSPs. (E) Recordings and mean bar plots of rebound responses in DCN cells evoked by a hyperpolarizing current pulse reveal a decrease in burst frequency after blocking either Cav3 (Ni^{2+}) or HCN (Cs^+) channels. (F) Blocking I_H with Cs^+ reveals an increase in FSL during the rebound response evoked by a train of Purkinje cell IPSPs that increases in a graded fashion with the number of stimuli. * $p < 0.05$, ** $p < 0.01$. Modified from Molineux et al. (2008) and Engbers et al. (2011).

These results emphasize that I_H is the primary determinant of the FSL of a rebound response, while I_T by itself failed to reproduce the normal FSL response. In addition, the large reduction in rebound frequency when I_H was removed revealed that I_H has a key role in controlling the frequency of a rebound response. The most straightforward explanation for this would be that I_H increases rebound frequency by way of a direct depolarization of the membrane following hyperpolarization. However, further examination revealed that the contribution by I_H to rebound frequency could instead be accounted for by a synergistic effect of I_H on I_T , revealing an *indirect* interaction between HCN and Cav3 channels.

Recognition of an I_T – I_H interaction was gained when considering a well-established role for HCN channels in regulating resting membrane conductance. In hippocampal cells, I_H has been shown

to account for a large percentage of the resting conductance and acts to normalize dendritic EPSPs (Magee, 1999). In Purkinje cells, basal activation of I_H at resting membrane potentials shortens the width of PF EPSPs (Angelo et al., 2007) and reduces the bistable range (Williams et al., 2002; Fernandez et al., 2007). To determine if I_H exerted its role through a direct depolarization or by modifying the membrane conductance, we compared charging curves of the three models for I_T alone, I_T – I_H , and when I_T was expressed alone and membrane capacitance adjusted in the somatic compartment (I_T –C; **Figure 6A**). This test showed that the model of I_T alone had a slower rate of charging compared to I_T – I_H or I_T –C, but that a model of I_T could be adjusted to the same time constant when model capacitance was increased as a substitute for I_H (**Figure 6A**). When compared in current clamp, it was apparent that spikes discharged at a shorter latency for either the I_T – I_H

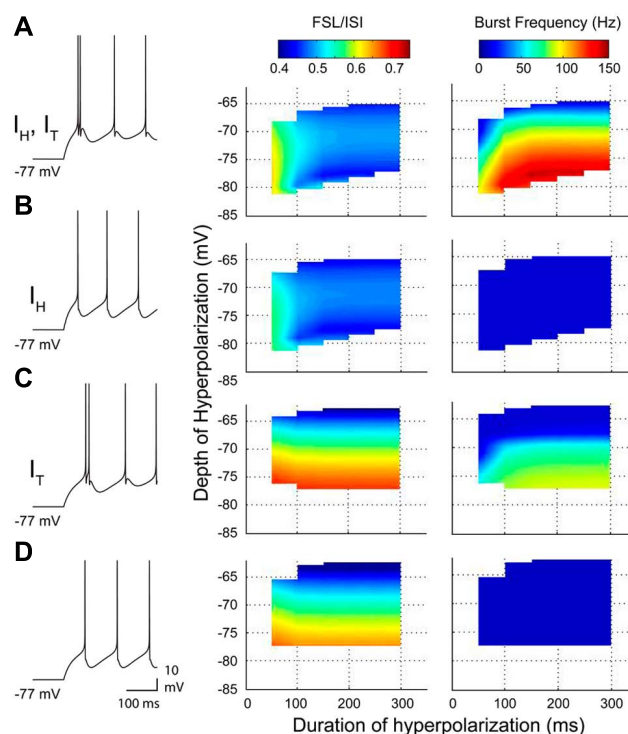


FIGURE 5 | A reduced model of the roles for I_T and I_H in rebound response frequency and FSL. (A–D), Output from a two compartment model containing combinations of I_T and/or I_H , with representative spike output following a 300 ms hyperpolarizing step to -77 mV from a resting potential of ~ -60 mV (10 Hz baseline firing) (left). Changes in frequency and FSL/ISI are plotted in three dimensions in relation to the frequency and ISI present at a resting membrane potential of

~ -60 mV. Note a decrease in FSL/ISI and increase in frequency with longer durations or larger amplitude hyperpolarizations when both I_T and I_H are present (A). Removing I_T dramatically abolishes all rebound responses (B), while removing I_H reverses the FSL/ISI relationship and reduces rebound frequency (C). Removing both I_T and I_H blocks the shifts in both FSL/ISI and spike frequency found when both are present (D).

model or I_T -C than for I_T alone (Figure 6B). These results were borne out when comparing three dimensional plots of the rebound burst frequency for different levels and durations of hyperpolarization, where the profile of burst frequency for the I_T -C strongly resembled that of I_T - I_H (Figure 6C). In contrast, adjusting the capacitance in a model with just I_T could not replicate the FSL/ISI relationship generated by a model of I_T - I_H (Figure 6D), indicating that the voltage dependence and kinetics of I_H determine the FSL/ISI relationship. Finally, a comparison of the degree of I_T inactivation for different depths of hyperpolarization revealed that without I_H the membrane potential returned to rest at the end of the stimulus slowly enough to induce greater I_T inactivation, and thus less ability to contribute to a rebound response (Figure 6E). Thus, a normally slow rate of return of membrane potential at the end of a stimulus is rescued by virtue of the effects of I_H on the membrane time constant, an effect that can be mimicked by lowering cell capacitance.

A second important parameter of FSL is the degree of precision of the first spike, as measured by the standard deviation of the latency of jitter in a population of spike discharges. To test the contribution of I_H and I_T to this parameter, we injected the models with stochastic excitatory and inhibitory synaptic conductances and injected current to hyperpolarize the model to -75 mV for 300 ms (Figures 7A,B). The standard deviation of the latency of

discharge of the first spike for each of the different models was used as a measure of spike precision. In a model of I_T - I_H the latency to first spike displayed a high degree of precision or minimal standard deviation (Figures 7A,B). By comparison, the model with I_T alone presented a much greater degree of variation in FSL, the majority of which were at longer latencies than for the model of I_T - I_H (Figures 7A,B). Here, a model of I_T alone with an adjustment of membrane capacitance could not restore spike precision despite a decrease in latency (Figures 7A,B). This suggests that the direct depolarizing effect of I_H following hyperpolarization affects the precision of the first spike. These data were important in showing that I_H modifies the actions of I_T both by decreasing latency and increasing precision of first spike discharge, but through different mechanisms.

CONCLUDING REMARKS

The processing of synaptic input requires the activation of ion channels in a low voltage range in order to modify subthreshold potentials. Cav3 calcium channels are low voltage-activated and are unique among calcium channels in exhibiting fast activation and voltage-dependent inactivation, leading to only a transient current when activated. These characteristics suggest that T-type current would have rapid but only short lasting effects on membrane excitability given the extent to which membrane

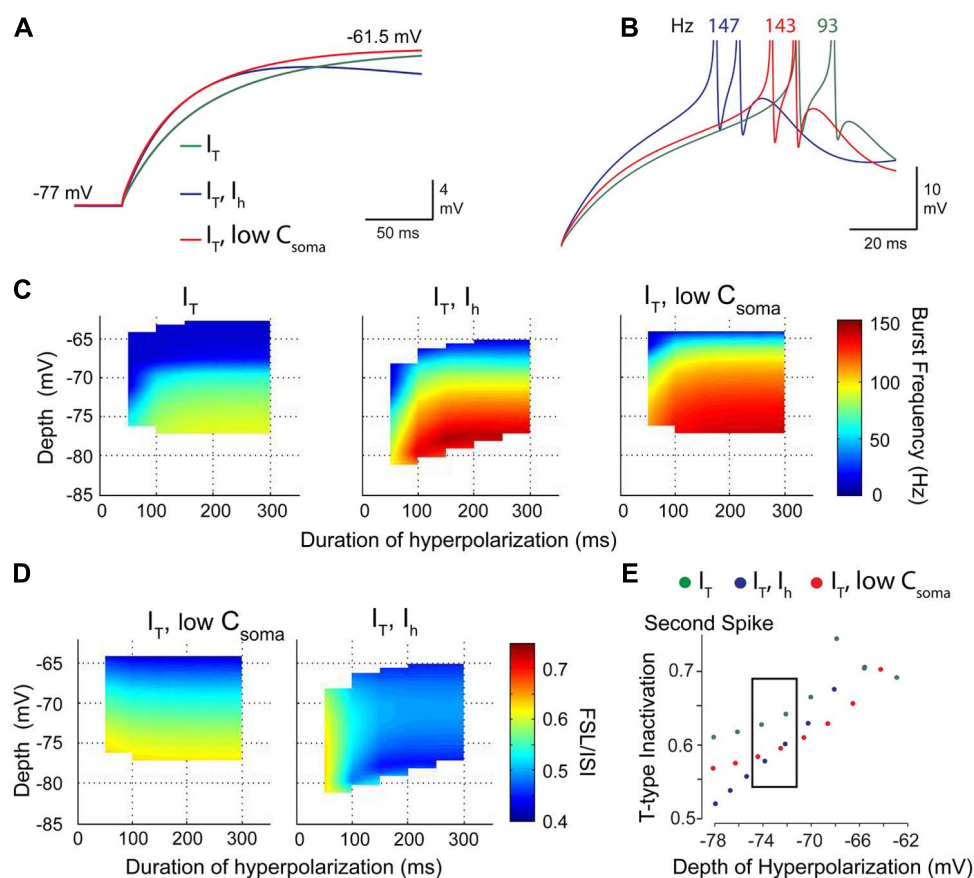


FIGURE 6 | I_H acts to increase the role of I_T in determining rebound burst frequency by modifying the membrane time constant. (A)

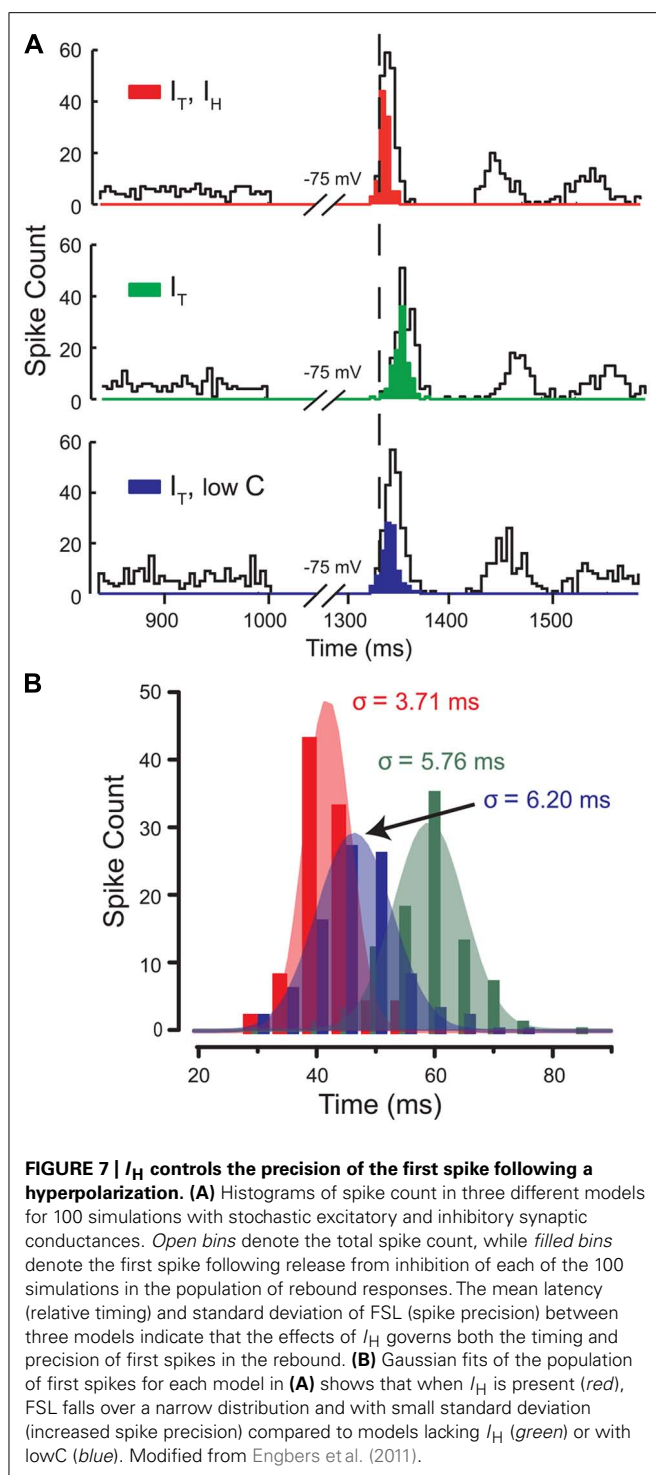
Expanded image of membrane charging profiles during repolarization from -77 mV. Superimposed traces are for models containing I_T and I_H (I_T-I_H), I_T alone, and a model with only I_T in which membrane capacitance was lowered (red trace) to match the time constant for a model containing I_H (purple trace). (B) In the absence of I_H , a decrease in capacitance increases burst frequency and decreases FSL (red trace) when compared to a model with I_T alone (green trace). (C) Three dimensional colour plots comparing the response of models containing I_T ,

I_T-I_H , and I_T with a low somatic membrane capacitance to simulate the effect of I_H . Note that the $I_T\text{-LowC}$ model reaches the same peak frequency of 150 Hz as the I_T-I_H model, indicating that a reduction in time constant increases burst frequency. (D) A comparison of models of $I_T\text{-LowC}$ to I_T-I_H indicate that the voltage-dependence and kinetics of I_H determine the normal voltage-FSL relationship. (E) A comparison of the amount of I_T inactivation during the rebound between the three models shows that incorporating low C or I_H reduces the extent of I_T inactivation compared to a model of I_T alone. Modified from Engbers et al. (2011).

depolarizations will inactivate the channels. In addition, unlike HVA calcium channels, Cav3 channels were long believed not to associate with any particular potassium or ligand-gated channel. However, in recent years this outlook has changed with identification of functional and even molecular associations between Cav3 calcium and other channels. Some of the first reports revealed that Cav3 channels can at least functionally couple to activation of BK and SK potassium channels (Smith et al., 2002; Cueni et al., 2008). More recently Cav3 channels were shown to associate at the molecular level with BK and IKCa channels and even Kv4 A-type potassium channels (Anderson et al., 2010a,b; Engbers et al., 2012, 2013; Rehak et al., 2013). These associations prove capable of greatly expanding the role for Cav3 calcium channels in processing input signals and modifying cell output.

A critical determinant of Cav3 channel activity is the extent of window current defined by the overlap of activation and

inactivation curves. We now recognize that the extent of this overlap can be far greater than expected and to extend well above spike threshold, allowing evoked spikes to incorporate a significant component of T-type calcium current (Chemin et al., 2002; Swensen and Bean, 2003). More recently it was shown that activation of Cav3 calcium current can be detected electrophysiologically from potentials as low as -90 mV in cerebellar Purkinje cells (Engbers et al., 2012) and -70 mV in MVN neurons (Rehak et al., 2013). This is important in indicating that inward T-type current can be activated well within the range of subthreshold depolarizations or hyperpolarizations. While activation of inward current should provide a depolarizing drive, the influx of calcium can secondarily alter the net effect of calcium influx in ways we are only beginning to appreciate. In addition, other channels not known to physically associate with Cav3 channels but which affect voltage transitions can secondarily affect the functional role of Cav3 channels. The current review focused on two recently identified



interactions between Cav3 and IKCa channels and Cav3 and HCN channels as a means of highlighting two very different forms of interactions involving Cav3 channels.

Cav3-IKCa MODULATION OF TEMPORAL SUMMATION

In cerebellar Purkinje cells a direct association between Cav3 and IKCa channels enables the activation of outward potassium

current well into the subthreshold voltage range. Thus, even small amplitude PF EPSPs are capable of activating Cav3 channels and subsequently IKCa outward current to control the rate of decay of the EPSP and a subsequent AHP. The effect this has on temporal summation is dramatic in that only the first few stimuli of a train of EPSPs prove capable of summing, with marked suppression of any further summation even during a long stimulus train. This interaction is important in acting as a high pass filter to reduce the inherent level of excitability of Purkinje cells that would result from the constant barrage of even spontaneous PF EPSPs. Instead, only high frequency bursts of PF input representative of sensory input can exceed the barrier put in place by the Cav3-IKCa association to produce spike output (Engbers et al., 2012). The effects of the Cav3-IKCa complex can be compared to hippocampal and cortical pyramidal cells, where Cav3 channels activated during EPSPs act to amplify EPSP amplitude (Markram and Sakmann, 1994; Magee and Johnston, 1995; Gillessen and Alzheimer, 1997; Urban et al., 1998). In the case of the Cav3-IKCa complex, however, trains of EPSPs are suppressed and excitability is reduced. Similar results have been seen for BK channel activation in MVN neurons, where activation of BK channels by Cav3 calcium influx reduces the gain of spike output, thus reducing cell excitability (du Lac and Lisberger, 1995; Smith et al., 2002; Rehak et al., 2013). Therefore, Cav3 channels can play either an excitatory or a net *inhibitory* role in signal processing depending on the ion channels with which they interact.

HCN CHANNELS INDIRECTLY MODIFY Cav3 FUNCTIONAL INFLUENCE

Both I_H and I_T act within the subthreshold range and often play complementary roles. Early recordings in thalamocortical relay neurons demonstrated that an interplay of I_H and I_T generates oscillatory burst output (McCormick and Pape, 1990). In DCN neurons, I_H and I_T interact to play distinct yet complementary roles. The direct depolarizing effects of I_H performs two functions. The first is to drive a graded reduction in FSL as hyperpolarizations are increased, creating an inverse relationship between the strength of the hyperpolarization and the time to burst output (Sangrey and Jaeger, 2010; Engbers et al., 2011). Increased activation of I_H during hyperpolarization also increases the precision of the rebound burst, improving temporal fidelity. However, activation of I_H also improves the efficacy of I_T . By reducing the membrane time constant, I_H decreases the inactivation of I_T during repolarization, resulting in more Ca^{2+} influx and higher burst frequency. I_H thus acts synergistically with I_T to increase rebound frequency by at least 60% of the total response. As short-term facilitation and depression are known to be highly frequency-dependent (Dittman et al., 2000), the ability for I_H to increase the range of frequencies generated during rebound responses (compare Figures 5A,C) could have important physiological consequences at downstream postsynaptic targets of DCN cells (Babalyan and Fanardzhyan, 1991).

LEVEL OF INTERACTION BETWEEN Cav3 AND IKCa/HCN CHANNELS

It is clear that very different outcomes can arise from the expression of Cav3 calcium channels when their conductance or actions on

the membrane potential are combined with IKCa or HCN channels. It would thus seem advantageous to employ mechanisms that could coexpress, colocalize, or otherwise ensure the pairing of these channels to mediate their effects in a given cell if not on a regional and subcellular basis. It is interesting to compare our current state of knowledge on the nature of interactions between Cav3 and either IKCa or HCN channels in terms of distribution and mechanisms of co-localization.

All protein biochemistry conducted thus far on the Cav3-IKCa complex has focused on the Cav3.2 channel isoform (Engbers et al., 2012), one of three known members of this family (Cav3.1, Cav3.2, Cav3.3; Perez-Reyes et al., 1998). Western blot analysis indicated coimmunoprecipitation between Cav3.2 and IKCa proteins from cerebellar lysates. This association also appears to be specific to the low voltage Cav3.2 isoform in finding no coimmunoprecipitation between IKCa protein and Cav2.1 (P/Q-type) channels from cerebellar lysates (Engbers et al., 2012), one of the principle HVA calcium channels expressed in Purkinje cells. The physiological interaction between Cav3 calcium influx and IKCa activation in Purkinje cells is also inferred to reflect activity of the Cav3.2 isoform given the ability to block the PF-evoked AHP with 100 μM Ni^{2+} , a dose that preferentially blocks Cav3.2 (Zamponi et al., 1996; Lee et al., 1999). Dual immunolabel experiments also revealed a remarkable correspondence in colocalization of both Cav3.2 and IKCa protein to the cell body region and specific patches of proximal dendritic membrane of Purkinje cells. A close proximity of these channels was further indicated by the ability of internal BAPTA, but not EGTA, to block a TRAM-34-sensitive outward current evoked in outside-out recordings from Purkinje cells. This test is argued to support an interaction between channels that function within a calcium nanodomain (<50 nm distance; Berkefeld and Fakler, 2008; Fakler and Adelman, 2008). Together these data indicate that Cav3 and IKCa channels can be associated as a physical complex, although the specific sites for interaction between the subunits have not been reported thus far. We also do not know if there are mechanisms in place to establish this association at the level of the Golgi complex or if the channels are translocated to the membrane (or endocytosed) in any coordinated fashion. This is particularly the case for IKCa channels that can be highly regulated in terms of stimulus-induced transcription, translation, and translocation to and from the plasma membrane (Ghanshani et al., 2000; Toyama et al., 2008; Wulff and Castle, 2010; Bouhy et al., 2011; Schwab et al., 2012). The current evidence only identifies a coimmunoprecipitation between Cav3.2 and IKCa from brain lysates, and a functional interaction at the plasma membrane level with minimal physical separation. Further work will thus be required to establish where and how the Cav3.2-IKCa interaction is formed and the extent to which it might influence functions of the complex.

The ability to identify a Cav3.2-IKCa interaction also does not guarantee that all cells expressing Cav3.2 and IKCa proteins will form these ion channel complexes. Precedence for this can be found in previous work showing that activation of BK channels by calcium influx through N-type channels can be detected in close association in a given cell (as recognized by paired activation of N-type and BK channels; Marrion and Tavalin, 1998; Berkefeld et al., 2006; Loane et al., 2007; Berkefeld and Fakler, 2008). L-type

calcium channels can complex with SK potassium channels and still be recorded in adjacent membrane in isolation (Marrion and Tavalin, 1998). These factors must therefore be considered when one attempts to predict where a Cav3-IKCa complex might be active in cerebellum or other brain regions. The reported expression pattern of Cav3 channels differs according to available reports on mRNA expression through *in situ* hybridization or protein distribution by immunocytochemistry. Indeed, the most thorough *in situ* hybridization work predicted that Purkinje cells express Cav3.1 mRNA (Craig et al., 1999). In contrast, immunolocalization suggests that all three isoforms are expressed in Purkinje cells, but differentially across the soma-dendritic axis (Craig et al., 1999; McKay et al., 2006; Molineux et al., 2006; Hildebrand et al., 2009). The Cav3.2 isoform was primarily localized to the somatic region and restricted segments of the primary trunk of apical dendrites, and a lower detectable level on some secondary branches. As indicated above, this distribution proves to be extremely well matched to that of IKCa immunolabel in these cells (Engbers et al., 2012). However, attempting to generalize or predict what other cells might use this complex physiologically is difficult at this time given that the single report of IKCa channels in Purkinje cells represents the first demonstration of this channel type in any central neuron. Comparisons between the pattern of Cav3.2 and IKCa protein in other cells thus awaits a study on the localization of IKCa channels in other brain regions, at which time tentative predictions could be made as to how generalized this interaction might be in controlling cell output.

Much less is known of any potential relationship between Cav3.2 and HCN channels in DCN cells. *In situ* hybridization suggested that the primary mRNA expressed in DCN cells is for Cav3.1. As indicated, a detailed comparison of Cav3 channel immunolabel and rebound burst phenotypes in DCN cells found evidence for a correlation between the expression of Cav3.1 immunolabel and Transient Burst neurons, and Cav3.3 to a Weak Burst phenotype. While Cav3.2 immunolabel could be detected in some group of neurons in the DCN, none of the Transient or Weak Burst cells examined in that study tested positive for this Cav3 isoform. DCN cells have been shown to express immunolabel (Notomi and Shigemoto, 2004) and mRNA (Monteggia et al., 2000; Santoro et al., 2000) for at least HCN1, HCN2, and HCN4 isoforms. However, no comparisons have been made between the pattern of Cav3 and HCN channel labeling to detect any potential colocalization.

Interestingly, at least a functional coupling has been detected between calcium influx and HCN channels in some systems. Thus, calcium influx has been found to augment I_H in both sino-atrial node cells (Hirano and Hagiwara, 1989) and thalamocortical cells (Luthi and McCormick, 1998b, 1999a,b) by right shifting the voltage-dependence for I_H activation. In thalamocortical cells the increase in I_H promotes a slow depolarization of seconds duration that depends on preceding calcium influx from rebound calcium spikes, a response attributed primarily to T-type calcium channels. The increase in I_H then decreases input resistance and the magnitude of calcium spikes, slowing if not blocking the generation of oscillatory activity (Luthi and McCormick, 1998b). An I_H -dependent process has also been shown to generate a slow depolarization that depends on prior membrane hyperpolarizations in a subset (23%) of cortical neurons, although the

calcium dependence of this process was not definitively established (Winograd et al., 2008). Also, this effect was not found in all cortical cell types including those that otherwise expressed I_H , indicating that calcium-dependent regulation of I_H is not a property of all cells (Winograd et al., 2008).

The calcium dependent increase of I_H in thalamocortical cells could be blocked by external application of 2–5 mM Ni^{2+} or internal perfusion of BAPTA or EGTA (Budde et al., 1997; Luthi and McCormick, 1998b). While the effects of Ni^{2+} were interpreted as reflecting a block of T-type calcium influx, this concentration is not selective enough to provide strong support for a discrete action on Cav3 channels (Zamponi et al., 1996). The best evidence of a role for T-type channels is the dependence of I_H augmentation in thalamocortical cells on the generation of rebound calcium spikes (Luthi and McCormick, 1998b). Calcium-dependent regulation of I_H in these cells was also concluded to be indirect through a calcium-dependent increase of PKA that modifies these cyclic nucleotide-dependent channels (Luthi and McCormick, 1999b). Therefore, at this time, there is evidence that calcium influx can modify I_H in a subset of neurons, but a direct interaction, like that shown for Cav3 and IKCa channels, has not been demonstrated, with no further work carried out in DCN cells.

It is interesting to note that in cortical layer III pyramidal cells, HCN1 channels colocalize with Cav3.2 channels in the presynaptic terminals of glutamatergic inputs, where they act to increase Cav3 inactivation by depolarizing the terminal (Huang et al., 2011). Similar effects of I_H increasing I_T inactivation have been reported for dendrites of hippocampal CA1 pyramidal neurons (Tsai et al., 2007). However, these effects are different from the results summarized here for DCN cells in which the effect of I_H on membrane time constant instead decreases Cav3 inactivation (Figure 6). Thus, at this time we have no reason to suspect that the interplay between Cav3- or HCN-mediated components of the rebound response in DCN cells reflects anything more than coexpressing these channels in isolation in the membrane, with concomitant effects on the membrane time constant and degree of Cav3 channel inactivation.

In summary, work in this area is converging to a growing realization that Cav3 calcium channels do not operate in isolation as long believed, but in fact can interact with other ion channels or receptors indirectly or as functional channel complexes to determine the final influence on membrane excitability. All of this work emphasizes the need for a detailed knowledge of the biophysical properties of ion channels, but also underscores the fact that their functional role depends on what other ion channels they interact with in the membrane simply through coexpression or by direct interaction in a growing number of ion channel complexes.

ACKNOWLEDGMENTS

We gratefully acknowledge previous and current laboratory members who assisted in some aspects of data collection in the work summarized here, including M. Molineux, R. Rehak, R. Tadayonnejad, and M. Kruskic. This work was supported by grants from the Canadian Institutes of Health Research (CIHR) by Ray W. Turner and Gerald W. Zamponi and studentships through Alberta Innovates – Health Solutions (Jordan D. T. Engbers, Dustin Anderson), T. Chen Fong awards (Jordan D. T. Engbers, Dustin Anderson),

the Killam Foundation (Jordan D. T. Engbers, Dustin Anderson), an AIMs award (Dustin Anderson) and a CIHR-CGS PhD studentship (Jordan D. T. Engbers). Ray W. Turner and Gerald W. Zamponi are AI-HS Scientists and Gerald W. Zamponi holds a Canada Research Chair.

AUTHOR CONTRIBUTIONS

Ray W. Turner and Gerald W. Zamponi received grant support for the study; Jordan D. T. Engbers, Dustin Anderson, and Ray W. Turner designed the experiments; Jordan D. T. Engbers and Dustin Anderson conducted the experiments and analyzed the data; Ray W. Turner and Jordan D. T. Engbers wrote the manuscript.

REFERENCES

- Aizenman, C. D., and Linden, D. J. (1999). Regulation of the rebound depolarization and spontaneous firing patterns of deep nuclear neurons in slices of rat cerebellum. *J. Neurophysiol.* 82, 1697–1709.
- Alvina, K., Ellis-Davies, G., and Khodakhah, K. (2009). T-type calcium channels mediate rebound firing in intact deep cerebellar neurons. *Neuroscience* 158, 635–641. doi: 10.1016/j.neuroscience.2008.09.052
- Alvina, K., and Khodakhah, K. (2008). Selective regulation of spontaneous activity of neurons of the deep cerebellar nuclei by N-type calcium channels in juvenile rats. *J. Physiol.* 586, 2523–2538. doi: 10.1113/jphysiol.2007.148197
- Alvina, K., Walter, J. T., Kohn, A., Ellis-Davies, G., and Khodakhah, K. (2008). Questioning the role of rebound firing in the cerebellum. *Nat. Neurosci.* 11, 1256–1258. doi: 10.1038/nn.2195
- Anderson, D., Engbers, J. D., Heath, N. C., Bartoletti, T. M., Mehaffey, W. H., Zamponi, G. W., et al. (2013). The Cav3-Kv4 complex acts as a calcium sensor to maintain inhibitory charge transfer during extracellular calcium fluctuations. *J. Neurosci.* 33, 7811–7824. doi: 10.1523/JNEUROSCI.5384-12.2013
- Anderson, D., Mehaffey, W. H., Ifitca, M., Rehak, R., Engbers, J. D., Hameed, S., et al. (2010a). Regulation of neuronal activity by Cav3-Kv4 channel signaling complexes. *Nat. Neurosci.* 13, 333–337. doi: 10.1038/nn.2493
- Anderson, D., Rehak, R., Hameed, S., Mehaffey, W. H., Zamponi, G. W., and Turner, R. W. (2010b). Regulation of the K(V)4.2 complex by Ca(V)3.1 calcium channels. *Channels (Austin)* 4, 163–167. doi: 10.4161/chan.4.3.11955
- Angelo, K., London, M., Christensen, S. R., and Hausser, M. (2007). Local and global effects of I(h) distribution in dendrites of mammalian neurons. *J. Neurosci.* 27, 8643–8653. doi: 10.1523/JNEUROSCI.5284-06.2007
- Atherton, J. F., Kitano, K., Baufreton, J., Fan, K., Wokosin, D., Tkatch, T., et al. (2010). Selective participation of somatodendritic HCN channels in inhibitory but not excitatory synaptic integration in neurons of the subthalamic nucleus. *J. Neurosci.* 30, 16025–16040. doi: 10.1523/JNEUROSCI.3898-10.2010
- Awatramani, G. B., Price, G. D., and Trussell, L. O. (2005). Modulation of transmitter release by presynaptic resting potential and background calcium levels. *Neuron* 48, 109–121. doi: 10.1016/j.neuron.2005.08.038
- Babalyan, A. L., and Fanardzhyan, V. V. (1991). Electrophysiological properties of red nucleus neurons in the rat brain slices. *Neurophysiology* 23, 454–461. doi: 10.1007/BF01052452
- Bengtsson, F., Ekerot, C. F., and Jorntell, H. (2011). In vivo analysis of inhibitory synaptic inputs and rebounds in deep cerebellar nuclear neurons. *PLoS ONE* 6:e18822. doi: 10.1371/journal.pone.0018822
- Berkefeld, H., and Fakler, B. (2008). Repolarizing responses of BKCa-Cav complexes are distinctly shaped by their Cav subunits. *J. Neurosci.* 28, 8238–8245. doi: 10.1523/JNEUROSCI.2274-08.2008
- Berkefeld, H., Sailer, C. A., Bildl, W., Rohde, V., Thumfart, J. O., Eble, S., et al. (2006). BKCa-Cav channel complexes mediate rapid and localized Ca^{2+} -activated K^{+} signaling. *Science* 314, 615–620. doi: 10.1126/science.1132915
- Biel, M., Wahl-Schott, C., Michalak, S., and Zong, X. (2009). Hyperpolarization-activated cation channels: from genes to function. *Physiol. Rev.* 89, 847–885. doi: 10.1152/physrev.00029.2008
- Bloodgood, B. L., and Sabatini, B. L. (2007). Nonlinear regulation of unitary synaptic signals by Cav(2.3) voltage-sensitive calcium channels located in dendritic spines. *Neuron* 53, 249–260. doi: 10.1016/j.neuron.2006.12.017
- Boehme, R., Uebele, V. N., Renger, J. J., and Pedroarena, C. (2011). Rebound excitation triggered by synaptic inhibition in cerebellar nuclear neurons is suppressed

- by selective T-type calcium channel block. *J. Neurophysiol.* 106, 2653–2661. doi: 10.1152/jn.00612.2011
- Bouhy, D., Ghasemlou, N., Lively, S., Redensek, A., Rathore, K. I., Schlichter, L. C., et al. (2011). Inhibition of the Ca(2+)-dependent K(+) channel, KCNN4/KCa3.1, improves tissue protection and locomotor recovery after spinal cord injury. *J. Neurosci.* 31, 16298–16308. doi: 10.1523/JNEUROSCI.0047-11.2011
- Budde, T., Biella, G., Munsch, T., and Pape, H. C. (1997). Lack of regulation by intracellular Ca²⁺ of the hyperpolarization-activated cation current in rat thalamic neurones. *J. Physiol.* 503 (Pt 1), 79–85. doi: 10.1111/j.1469-7793.1997.079bi.x
- Cain, S. M., and Snutch, T. P. (2010). Contributions of T-type calcium channel isoforms to neuronal firing. *Channels (Austin)* 4, 475–482. doi: 10.4161/chan.4.6.14106
- Cain, S. M., and Snutch, T. P. (2013). T-type calcium channels in burst-firing, network synchrony, and epilepsy. *Biochim. Biophys. Acta* 1828, 1572–1578. doi: 10.1016/j.bbame.2012.07.028
- Chadderton, P., Margrie, T. W., and Hausser, M. (2004). Integration of quanta in cerebellar granule cells during sensory processing. *Nature* 428, 856–860. doi: 10.1038/nature02442
- Chemin, J., Monteil, A., Perez-Reyes, E., Bourinet, E., Nargeot, J., and Lory, P. (2002). Specific contribution of human T-type calcium channel isoforms (alpha(1G), alpha(1H) and alpha(1I)) to neuronal excitability. *J. Physiol.* 540, 3–14. doi: 10.1113/jphysiol.2001.013269
- Cheong, E., and Shin, H. S. (2013). T-type Ca(2+)(+) channels in absence epilepsy. *Biochim. Biophys. Acta* 1828, 1560–1571. doi: 10.1016/j.bbame.2013.02.002
- Craig, P. J., Beattie, R. E., Folly, E. A., Banerjee, M. D., Reeves, M. B., Priestley, J. V., et al. (1999). Distribution of the voltage-dependent calcium channel alpha1G subunit mRNA and protein throughout the mature rat brain. *Eur. J. Neurosci.* 11, 2949–2964. doi: 10.1046/j.1460-9568.1999.00711.x
- Cueni, L., Canepari, M., Adelman, J. P., and Luthi, A. (2009). Ca(2+) signaling by T-type Ca(2+) channels in neurons. *Pflugers Arch.* 457, 1161–1172. doi: 10.1007/s00424-008-0582-6
- Cueni, L., Canepari, M., Lujan, R., Emmenegger, Y., Watanabe, M., Bond, C. T., et al. (2008). T-type Ca²⁺ channels, SK2 channels and SERCAs gate sleep-related oscillations in thalamic dendrites. *Nat. Neurosci.* 11, 683–692. doi: 10.1038/nn.2124
- D'Angelo, E., and De Zeeuw, C. I. (2009). Timing and plasticity in the cerebellum: focus on the granular layer. *Trends Neurosci.* 32, 30–40. doi: 10.1016/j.tins.2008.09.007
- Dittman, J. S., Kreitzer, A. C., and Regehr, W. G. (2000). Interplay between facilitation, depression, and residual calcium at three presynaptic terminals. *J. Neurosci.* 20, 1374–1385.
- Dreyfus, F. M., Tschertner, A., Errington, A. C., Renger, J. J., Shin, H. S., Uebele, V. N., et al. (2010). Selective T-type calcium channel block in thalamic neurons reveals channel redundancy and physiological impact of I(T) window. *J. Neurosci.* 30, 99–109. doi: 10.1523/JNEUROSCI.4305-09.2010
- du Lac, S., and Lisberger, S. G. (1995). Cellular processing of temporal information in medial vestibular nucleus neurons. *J. Neurosci.* 15, 8000–8010.
- Ekerot, C. F., and Jorntell, H. (2001). Parallel fibre receptive fields of Purkinje cells and interneurons are climbing fibre-specific. *Eur. J. Neurosci.* 13, 1303–1310. doi: 10.1046/j.0953-816x.2001.01499.x
- Ekerot, C. F., and Jorntell, H. (2008). Synaptic integration in cerebellar granule cells. *Cerebellum* 7, 539–541. doi: 10.1007/s12311-008-0064-6
- Engbers, J. D., Anderson, D., Asmara, H., Rehak, R., Mehaffey, W. H., Hameed, S., et al. (2012). Intermediate conductance calcium-activated potassium channels modulate summation of parallel fiber input in cerebellar Purkinje cells. *Proc. Natl. Acad. Sci. U.S.A.* 109, 2601–2606. doi: 10.1073/pnas.1115024109
- Engbers, J. D., Anderson, D., Tadayonnejad, R., Mehaffey, W. H., Molineux, M. L., and Turner, R. W. (2011). Distinct roles for I(T) and I(H) in controlling the frequency and timing of rebound spike responses. *J. Physiol.* 589, 5391–5413. doi: 10.1113/jphysiol.2011.215632
- Engbers, J. D., Zamponi, G. W., and Turner, R. W. (2013). Modeling interactions between voltage-gated Ca²⁺ channels and KCa1.1 channels. *Channels (Austin)* 7, 24–25.
- Faber, E. S. (2010). Functional interplay between NMDA receptors, SK channels and voltage-gated Ca²⁺ channels regulates synaptic excitability in the medial prefrontal cortex. *J. Physiol.* 588, 1281–1292. doi: 10.1113/jphysiol.2009.185645
- Fakler, B., and Adelman, J. P. (2008). Control of K(Ca) channels by calcium nano/microdomains. *Neuron* 59, 873–881. doi: 10.1016/j.neuron.2008.09.001
- Fernandez, F. R., Engbers, J. D., and Turner, R. W. (2007). Firing dynamics of cerebellar purkinje cells. *J. Neurophysiol.* 98, 278–294. doi: 10.1152/jn.00306.2007
- Gastrein, P., Campanac, E., Gassel, C., Cudmore, R., Bialowas, A., Carlier, E., et al. (2011). The role of hyperpolarization-activated cationic current (Ih) in spike-time precision and intrinsic resonance in cortical neurons in vitro. *J. Physiol.* 589, 3753–3773. doi: 10.1113/jphysiol.2011.209148
- Ghanshani, S., Wulff, H., Miller, M. J., Rohm, H., Neben, A., Gutman, G. A., et al. (2000). Upregulation of the IKCa1 potassium channel during T-cell activation. Molecular mechanism and functional consequences. *J. Biol. Chem.* 275, 37137–37149. doi: 10.1074/jbc.M003941200
- Gillesen, T., and Alzheimer, C. (1997). Amplification of EPSPs by low Ni(2+)- and amiloride-sensitive Ca²⁺ channels in apical dendrites of rat CA1 pyramidal neurons. *J. Neurophysiol.* 77, 1639–1643.
- Gittis, A. H., and du Lac, S. (2007). Firing properties of GABAergic versus non-GABAergic vestibular nucleus neurons conferred by a differential balance of potassium currents. *J. Neurophysiol.* 97, 3986–3996. doi: 10.1152/jn.00141.2007
- Grunnet, M., and Kaufmann, W. A. (2004). Coassembly of big conductance Ca²⁺-activated K⁺ channels and L-type voltage-gated Ca²⁺ channels in rat brain. *J. Biol. Chem.* 279, 36445–36453. doi: 10.1074/jbc.M402254200
- Hausser, M., and Clark, B. A. (1997). Tonic synaptic inhibition modulates neuronal output pattern and spatiotemporal synaptic integration. *Neuron* 19, 665–678. doi: 10.1016/S0896-6273(00)80379-7
- Hildebrand, M. E., Isope, P., Miyazaki, T., Nakaya, T., Garcia, E., Feltz, A., et al. (2009). Functional coupling between mGluR1 and Cav3.1 T-type calcium channels contributes to parallel fiber-induced fast calcium signaling within Purkinje cell dendritic spines. *J. Neurosci.* 29, 9668–9682. doi: 10.1523/JNEUROSCI.0362-09.2009
- Hirano, T., and Hagiwara, S. (1989). Kinetics and distribution of voltage-gated Ca, Na and K channels on the somata of rat cerebellar Purkinje cells. *Pflugers Arch.* 413, 463–469. doi: 10.1007/BF00594174
- Hoebeek, F. E., Witter, L., Ruigrok, T. J., and De Zeeuw, C. I. (2010). Differential olivo-cerebellar cortical control of rebound activity in the cerebellar nuclei. *Proc. Natl. Acad. Sci. U.S.A.* 107, 8410–8415. doi: 10.1073/pnas.0907118107
- Huang, Z., Lujan, R., Kadurin, I., Uebele, V. N., Renger, J. J., Dolphin, A. C., et al. (2011). Presynaptic HCN1 channels regulate Cav3.2 activity and neurotransmission at select cortical synapses. *Nat. Neurosci.* 14, 478–486. doi: 10.1038/nn.2757
- Huguenard, J. R. (1996). Low-threshold calcium currents in central nervous system neurons. *Annu. Rev. Physiol.* 58, 329–348. doi: 10.1146/annurev.ph.58.030196.001553
- Ishii, T. M., Silvia, C., Hirschberg, B., Bond, C. T., Adelman, J. P., and Maylie, J. (1997). A human intermediate conductance calcium-activated potassium channel. *Proc. Natl. Acad. Sci. U.S.A.* 94, 11651–11656. doi: 10.1073/pnas.94.21.11651
- Isope, P., and Barbour, B. (2002). Properties of unitary granule cell – Purkinje cell synapses in adult rat cerebellar slices. *J. Neurosci.* 22, 9668–9678.
- Isope, P., and Murphy, T. H. (2005). Low threshold calcium currents in rat cerebellar Purkinje cell dendritic spines are mediated by T-type calcium channels. *J. Physiol.* 562, 257–269. doi: 10.1113/jphysiol.2004.074211
- Jahnsen, H. (1986a). Electrophysiological characteristics of neurones in the guinea-pig deep cerebellar nuclei in vitro. *J. Physiol.* 372, 129–147.
- Jahnsen, H. (1986b). Extracellular activation and membrane conductances of neurones in the guinea-pig deep cerebellar nuclei in vitro. *J. Physiol.* 372, 149–168.
- Joiner, W. J., Wang, L. Y., Tang, M. D., and Kaczmarek, L. K. (1997). hSK4, a member of a novel subfamily of calcium-activated potassium channels. *Proc. Natl. Acad. Sci. U.S.A.* 94, 11013–11018. doi: 10.1073/pnas.94.20.11013
- Kaushal, V., Koeberle, P. D., Wang, Y., and Schlichter, L. C. (2007). The Ca²⁺-activated K⁺ channel KCNN4/KCa3.1 contributes to microglia activation and nitric oxide-dependent neurodegeneration. *J. Neurosci.* 27, 234–244. doi: 10.1523/JNEUROSCI.3593-06.2007
- Kim, D., Song, I., Keum, S., Lee, T., Jeong, M. J., Kim, S. S., et al. (2001). Lack of the burst firing of thalamocortical relay neurons and resistance to absence seizures in mice lacking alpha(1G) T-type Ca(2+) channels. *Neuron* 31, 35–45. doi: 10.1016/S0896-6273(01)00343-9

- Kole, M. H., Hallermann, S., and Stuart, G. J. (2006). Single Ih channels in pyramidal neuron dendrites: properties, distribution, and impact on action potential output. *J. Neurosci.* 26, 1677–1687. doi: 10.1523/JNEUROSCI.3664-05.2006
- Lee, J. H., Gomora, J. C., Cribbs, L. L., and Perez-Reyes, E. (1999). Nickel block of three cloned T-type calcium channels: low concentrations selectively block $\alpha 1H$. *Biophys. J.* 77, 3034–3042. doi: 10.1016/S0006-3495(99)77134-1
- Loane, D. J., Lima, P. A., and Marrion, N. V. (2007). Co-assembly of N-type Ca^{2+} and BK channels underlies functional coupling in rat brain. *J. Cell Sci.* 120, 985–995. doi: 10.1242/jcs.03399
- Luthi, A., and McCormick, D. A. (1998a). H-current: properties of a neuronal and network pacemaker. *Neuron* 21, 9–12. doi: 10.1016/S0896-6273(00)80509-7
- Luthi, A., and McCormick, D. A. (1998b). Periodicity of thalamic synchronized oscillations: the role of Ca^{2+} -mediated upregulation of Ih. *Neuron* 20, 553–563. doi: 10.1016/S0896-6273(00)80994-0
- Luthi, A., and McCormick, D. A. (1999a). Ca^{2+} -mediated up-regulation of Ih in the thalamus. How cell-intrinsic ionic currents may shape network activity. *Ann. N. Y. Acad. Sci.* 868, 765–769. doi: 10.1111/j.1749-6632.1999.tb11354.x
- Luthi, A., and McCormick, D. A. (1999b). Modulation of a pacemaker current through Ca^{2+} -induced stimulation of cAMP production. *Nat. Neurosci.* 2, 634–641. doi: 10.1038/10189
- Magee, J. C. (1999). Dendritic Ih normalizes temporal summation in hippocampal CA1 neurons. *Nat. Neurosci.* 2, 848. doi: 10.1038/12229
- Magee, J. C., Christofi, G., Miyakawa, H., Christie, B., Lasser-Ross, N., and Johnston, D. (1995). Subthreshold synaptic activation of voltage-gated Ca^{2+} channels mediates a localized Ca^{2+} influx into the dendrites of hippocampal pyramidal neurons. *J. Neurophysiol.* 74, 1335–1342.
- Magee, J. C., and Johnston, D. (1995). Synaptic activation of voltage-gated channels in the dendrites of hippocampal pyramidal neurons. *Science* 268, 301–304. doi: 10.1126/science.7716525
- Markram, H., and Sakmann, B. (1994). Calcium transients in dendrites of neocortical neurons evoked by single subthreshold excitatory postsynaptic potentials via low-voltage-activated calcium channels. *Proc. Natl. Acad. Sci. U.S.A.* 91, 5207–5211. doi: 10.1073/pnas.91.11.5207
- Marrion, N. V., and Tavalin, S. J. (1998). Selective activation of Ca^{2+} -activated K^{+} channels by co-localized Ca^{2+} channels in hippocampal neurons. *Nature* 395, 900–905. doi: 10.1038/27674
- McCormick, D. A., and Bal, T. (1997). Sleep and arousal: thalamocortical mechanisms. *Annu. Rev. Neurosci.* 20, 185–215. doi: 10.1146/annurev.neuro.20.1.185
- McCormick, D. A., and Pape, H. C. (1990). Properties of a hyperpolarization-activated cation current and its role in rhythmic oscillation in thalamic relay neurones. *J. Physiol.* 431, 291–318.
- McDonough, S. I., and Bean, B. P. (1998). Mibefradil inhibition of T-type calcium channels in cerebellar purkinje neurons. *Mol. Pharmacol.* 54, 1080–1087.
- McKay, B. E., McRory, J. E., Molineux, M. L., Hamid, J., Snutch, T. P., Zamponi, G. W., et al. (2006). Cav3 T-type calcium channel isoforms differentially distribute to somatic and dendritic compartments in rat central neurons. *Eur. J. Neurosci.* 24, 2581–2594. doi: 10.1111/j.1460-9568.2006.05136.x
- Mittmann, W., Koch, U., and Hausser, M. (2005). Feed-forward inhibition shapes the spike output of cerebellar Purkinje cells. *J. Physiol.* 563, 369–378. doi: 10.1113/jphysiol.2004.075028
- Molineux, M. L., McRory, J. E., McKay, B. E., Hamid, J., Mehaffey, W. H., Rehak, R., et al. (2006). Specific T-type calcium channel isoforms are associated with distinct burst phenotypes in deep cerebellar nuclear neurons. *Proc. Natl. Acad. Sci. U.S.A.* 103, 5555–5560. doi: 10.1073/pnas.0601261103
- Molineux, M. L., Mehaffey, W. H., Tadayonnejad, R., Anderson, D., Tennent, A. F., and Turner, R. W. (2008). Ionic factors governing rebound burst phenotype in rat deep cerebellar neurons. *J. Neurophysiol.* 100, 2684–2701. doi: 10.1152/jn.90427.2008
- Monteggia, L. M., Eisch, A. J., Tang, M. D., Kaczmarek, L. K., and Nestler, E. J. (2000). Cloning and localization of the hyperpolarization-activated cyclic nucleotide-gated channel family in rat brain. *Brain Res. Mol. Brain Res.* 81, 129–139. doi: 10.1016/S0169-328X(00)00155-8
- Muri, R., and Knopfel, T. (1994). Activity induced elevations of intracellular calcium concentration in neurons of the deep cerebellar nuclei. *J. Neurophysiol.* 71, 420–428.
- Ngo-Anh, T. J., Bloodgood, B. L., Lin, M., Sabatini, B. L., Maylie, J., and Adelman, J. P. (2005). SK channels and NMDA receptors form a Ca^{2+} -mediated feedback loop in dendritic spines. *Nat. Neurosci.* 8, 642–649. doi: 10.1038/nn1449
- Notomi, T., and Shigemoto, R. (2004). Immunohistochemical localization of Ih channel subunits, HCN1–4, in the rat brain. *J. Comp. Neurol.* 471, 241–276. doi: 10.1002/cne.11039
- Oliver, D., Klocker, N., Schuck, J., Baukowitz, T., Ruppersberg, J. P., and Fakler, B. (2000). Gating of Ca^{2+} -activated K^{+} channels controls fast inhibitory synaptic transmission at auditory outer hair cells. *Neuron* 26, 595–601. doi: 10.1016/S0896-6273(00)81197-6
- Pedarzani, P., and Stocker, M. (2008). Molecular and cellular basis of small – and intermediate-conductance, calcium-activated potassium channel function in the brain. *Cell. Mol. Life Sci.* 65, 3196–3217. doi: 10.1007/s00018-008-8216-x
- Pedroarena, C. M. (2010). Mechanisms supporting transfer of inhibitory signals into the spike output of spontaneously firing cerebellar nuclear neurons in vitro. *Cerebellum* 9, 67–76. doi: 10.1007/s12311-009-0153-1
- Perez-Reyes, E. (2003). Molecular physiology of low-voltage-activated t-type calcium channels. *Physiol. Rev.* 83, 117–161.
- Perez-Reyes, E. (2006). Molecular characterization of T-type calcium channels. *Cell Calcium* 40, 89–96. doi: 10.1016/j.ceca.2006.04.012
- Perez-Reyes, E., Cribbs, L. L., Daud, A., Lacerda, A. E., Barclay, J., Williamson, M. P., et al. (1998). Molecular characterization of a neuronal low-voltage-activated T-type calcium channel. *Nature* 391, 896–900. doi: 10.1038/36110
- Person, A. L., and Raman, I. M. (2012). Purkinje neuron synchrony elicits its time-locked spiking in the cerebellar nuclei. *Nature* 481, 502–505. doi: 10.1038/nature10732
- Raman, I. M., and Bean, B. P. (1999). Ionic currents underlying spontaneous action potentials in isolated cerebellar Purkinje neurons. *J. Neurosci.* 19, 1663–1674.
- Rancz, E. A., Ishikawa, T., Duguid, I., Chadderton, P., Mahon, S., and Hausser, M. (2007). High-fidelity transmission of sensory information by single cerebellar mossy fibre boutons. *Nature* 450, 1245–1248. doi: 10.1038/nature05995
- Rehak, R., Bartoletti, T. M., Engbers, J. D. T., Berecki, G., Turner, R. W., and Zamponi, G. W. (2013). Low voltage activation of $KCa_{1.1}$ current by Cav3-KCa $_{1.1}$ complexes. *PLoS ONE* 8:e61844. doi: 10.1371/journal.pone.0061844
- Robinson, R. B., and Siegelbaum, S. A. (2003). Hyperpolarization-activated cation currents: from molecules to physiological function. *Annu. Rev. Physiol.* 65, 453–480. doi: 10.1146/annurev.physiol.65.092101.142734
- Sangrey, T., and Jaeger, D. (2010). Analysis of distinct short and prolonged components in rebound spiking of deep cerebellar nucleus neurons. *Eur. J. Neurosci.* 32, 1646–1657. doi: 10.1111/j.1460-9568.2010.07408.x
- Santoro, B., Chen, S., Luthi, A., Pavlidis, P., Shumyatsky, G. P., Tibbs, G. R., et al. (2000). Molecular and functional heterogeneity of hyperpolarization-activated pacemaker channels in the mouse CNS. *J. Neurosci.* 20, 5264–5275.
- Schneider, E. R., Civillico, E. F., and Wang, S. S. (2013). Calcium-based dendritic excitability and its regulation in the deep cerebellar nuclei. *J. Neurophysiol.* 109, 2282–2292. doi: 10.1152/jn.00925.2012
- Schwab, A., Nechiporuk-Zloy, V., Gassner, B., Schulz, C., Kessler, W., Mally, S., et al. (2012). Dynamic redistribution of calcium sensitive potassium channels (hKCa $_{3.1}$) in migrating cells. *J. Cell. Physiol.* 227, 686–696. doi: 10.1002/jcp.22776
- Smith, M. R., Nelson, A. B., and Du Lac, S. (2002). Regulation of firing response gain by calcium-dependent mechanisms in vestibular nucleus neurons. *J. Neurophysiol.* 87, 2031–2042.
- Steuber, V., Schultheiss, N. W., Silver, R. A., De Schutter, E., and Jaeger, D. (2011). Determinants of synaptic integration and heterogeneity in rebound firing explored with data-driven models of deep cerebellar nucleus cells. *J. Comput. Neurosci.* 30, 633–658. doi: 10.1007/s10827-010-0282-z
- Swensen, A. M., and Bean, B. P. (2003). Ionic mechanisms of burst firing in dissociated Purkinje neurons. *J. Neurosci.* 23, 9650–9663.
- Tadayonnejad, R., Anderson, D., Molineux, M. L., Mehaffey, W. H., Jayasuriya, K., and Turner, R. W. (2010). Rebound discharge in deep cerebellar nuclear neurons in vitro. *Cerebellum* 9, 352–374. doi: 10.1007/s12311-010-0168-7
- Tadayonnejad, R., Mehaffey, W. H., Anderson, D., and Turner, R. W. (2009). Reliability of triggering postinhibitory rebound bursts in deep cerebellar neurons. *Channels (Austin)* 3, 149–155. doi: 10.4161/chan.3.3.8872
- Talavera, K., and Nilius, B. (2006). Biophysics and structure-function relationship of T-type Ca^{2+} channels. *Cell Calcium* 40, 97–114. doi: 10.1016/j.ceca.2006.04.013
- Toyama, K., Wulff, H., Chandy, K. G., Azam, P., Raman, G., Saito, T., et al. (2008). The intermediate-conductance calcium-activated potassium channel $KCa_{3.1}$ contributes to atherogenesis in mice and humans. *J. Clin. Invest.* 118, 3025–3037. doi: 10.1172/JCI30836

- Tsay, D., Dudman, J. T., and Siegelbaum, S. A. (2007). HCN1 channels constrain synaptically evoked Ca^{2+} spikes in distal dendrites of CA1 pyramidal neurons. *Neuron* 56, 1076–1089. doi: 10.1016/j.neuron.2007.11.015
- Urban, N. N., Henze, D. A., and Barrionuevo, G. (1998). Amplification of perforant-path EPSPs in CA3 pyramidal cells by LVA calcium and sodium channels. *J. Neurophysiol.* 80, 1558–1561.
- Wahl-Schott, C., and Biel, M. (2009). HCN channels: structure, cellular regulation and physiological function. *Cell. Mol. Life Sci.* 66, 470–494. doi: 10.1007/s00018-008-8525-0
- Weiss, N., and Zamponi, G. W. (2013). Control of low-threshold exocytosis by T-type calcium channels. *Biochim. Biophys. Acta* 1828, 1579–1586. doi: 10.1016/j.bbamem.2012.07.031
- Wetmore, D. Z., Mukamel, E. A., and Schnitzer, M. J. (2008). Lock-and-key mechanisms of cerebellar memory recall based on rebound currents. *J. Neurophysiol.* 100, 2328–2347. doi: 10.1152/jn.00344.2007
- Williams, S. R., Christensen, S. R., Stuart, G. J., and Häusser, M. (2002). Membrane potential bistability is controlled by the hyperpolarization-activated current $I(\text{H})$ in rat cerebellar Purkinje neurons in vitro. *J. Physiol.* 539, 469–483. doi: 10.1113/jphysiol.2001.013136
- Winograd, M., Destexhe, A., and Sanchez-Vives, M. V. (2008). Hyperpolarization-activated graded persistent activity in the prefrontal cortex. *Proc. Natl. Acad. Sci. U.S.A.* 105, 7298–7303. doi: 10.1073/pnas.0800360105
- Wolfart, J., Neuhoﬀ, H., Franz, O., and Roeper, J. (2001). Differential expression of the small-conductance, calcium-activated potassium channel SK3 is critical for pacemaker control in dopaminergic midbrain neurons. *J. Neurosci.* 21, 3443–3456.
- Wolfart, J., and Roeper, J. (2002). Selective coupling of T-type calcium channels to SK potassium channels prevents intrinsic bursting in dopaminergic midbrain neurons. *J. Neurosci.* 22, 3404–3413.
- Womack, M. D., Chevez, C., and Khodakhah, K. (2004). Calcium-activated potassium channels are selectively coupled to P/Q-type calcium channels in cerebellar Purkinje neurons. *J. Neurosci.* 24, 8818–8822. doi: 10.1523/JNEUROSCI.2915-04.2004
- Wulff, H., and Castle, N. A. (2010). Therapeutic potential of $\text{KCa}_{3.1}$ blockers: recent advances and promising trends. *Exp. Rev. Clin. Pharmacol.* 3, 385–396. doi: 10.1586/ecp.10.11
- Yanovsky, Y., Zhang, W., and Misgeld, U. (2005). Two pathways for the activation of small-conductance potassium channels in neurons of substantia nigra pars reticulata. *Neuroscience* 136, 1027–1036. doi: 10.1016/j.neuroscience.2005.08.026
- Yunker, A. M., and McEnery, M. W. (2003). Low-voltage-activated (“T-Type”) calcium channels in review. *J. Bioenerg. Biomembr.* 35, 533–575. doi: 10.1023/B:JOB.0000008024.77488.48
- Zamponi, G. W., Bourinet, E., and Snutch, T. P. (1996). Nickel block of a family of neuronal calcium channels: subtype- and subunit-dependent action at multiple sites. *J. Membr. Biol.* 151, 77–90. doi: 10.1007/s002329900059
- Zhang, W., Shin, J. H., and Linden, D. J. (2004). Persistent changes in the intrinsic excitability of rat deep cerebellar nuclear neurons induced by EPSPs or IPSP bursts. *J. Physiol. (Lond.)* 561.3, 703–719. doi: 10.1113/jphysiol.2004.071696
- Zheng, N., and Raman, I. M. (2009). Ca currents activated by spontaneous firing and synaptic disinhibition in neurons of the cerebellar nuclei. *J. Neurosci.* 29, 9826–9838. doi: 10.1523/JNEUROSCI.2069-09.2009

Conflict of Interest Statement: The authors declare that the research was conducted in the absence of any commercial or financial relationships that could be construed as a potential conflict of interest.

Received: 10 September 2013; accepted: 06 November 2013; published online: 27 November 2013.

Citation: Engbers JD, Anderson D, Zamponi GW and Turner RW (2013) Signal processing by T-type calcium channel interactions in the cerebellum. *Front. Cell. Neurosci.* 7:230. doi: 10.3389/fncel.2013.00230

This article was submitted to the journal *Frontiers in Cellular Neuroscience*.

Copyright © 2013 Engbers, Anderson, Zamponi and Turner. This is an open-access article distributed under the terms of the Creative Commons Attribution License (CC BY). The use, distribution or reproduction in other forums is permitted, provided the original author(s) or licensor are credited and that the original publication in this journal is cited, in accordance with accepted academic practice. No use, distribution or reproduction is permitted which does not comply with these terms.



The sodium leak channel, NALCN, in health and disease

Maud Cochet-Bissuel^{1,2,3}, Philippe Lory^{1,2,3} and Arnaud Monteil^{1,2,3*}

¹ Institut de Génomique Fonctionnelle, CNRS UMR 5203, Universités Montpellier 1&2, Montpellier, France

² INSERM, U 661, Montpellier, France

³ LabEx 'Ion Channel Science and Therapeutics', Montpellier, France

Edited by:

Christophe Altier, University of
Calgary, Canada

Reviewed by:

Zhong-Ping Feng, University of
Toronto, Canada

Laurens Bosman, Erasmus MC,
Netherlands

David Specia, University of
California, Davis, USA

*Correspondence:

Arnaud Monteil, Institut de
Génomique Fonctionnelle,
Université Montpellier 1 & 2, CNRS
UMR 5203, 141 rue de la Cardonille,
Montpellier F-34094, France
e-mail: arnaud.monteil@igf.cnrs.fr

Ion channels are crucial components of cellular excitability and are involved in many neurological diseases. This review focuses on the sodium leak, G protein-coupled receptors (GPCRs)-activated NALCN channel that is predominantly expressed in neurons where it regulates the resting membrane potential and neuronal excitability. NALCN is part of a complex that includes not only GPCRs, but also UNC-79, UNC-80, NLF-1 and src family of Tyrosine kinases (SFKs). There is growing evidence that the NALCN channelosome critically regulates its ion conduction. Both in mammals and invertebrates, animal models revealed an involvement in many processes such as locomotor behaviors, sensitivity to volatile anesthetics, and respiratory rhythms. There is also evidence that alteration in this NALCN channelosome can cause a wide variety of diseases. Indeed, mutations in the *NALCN* gene were identified in *Infantile Neuroaxonal Dystrophy (INAD)* patients, as well as in patients with an *Autosomal Recessive Syndrome with severe hypotonia, speech impairment, and cognitive delay*. Deletions in *NALCN* gene were also reported in diseases such as 13q syndrome. In addition, genes encoding NALCN, NLF-1, UNC-79, and UNC-80 proteins may be susceptibility loci for several diseases including bipolar disorder, schizophrenia, Alzheimer's disease, autism, epilepsy, alcoholism, cardiac diseases and cancer. Although the physiological role of the NALCN channelosome is poorly understood, its involvement in human diseases should foster interest for drug development in the near future. Toward this goal, we review here the current knowledge on the NALCN channelosome in physiology and diseases.

Keywords: NALCN, UNC-79, UNC-80, ion channel, excitability

INTRODUCTION

Ion channels are integral membrane proteins that allow specific ions to pass through lipid membranes following a concentration gradient (Hille, 2001). More than 400 genes are known that encode ion channel subunits. In addition, alternative splicing and heteromeric assembly of different subunits increase tremendously the variety of ion channels. They are involved in many signaling and control processes in the cell as well as in pathologies referred to as "channelopathies" (reviewed in Ashcroft, 2006; Camerino et al., 2008). In addition, pharmaceutical companies view ion channels as therapeutic targets of choice (Kaczorowski et al., 2008; Clare, 2010). In the present review, we focus on the *Na⁺-leak channel* (NALCN), a major player in determining the influence of extracellular *Na⁺* on a neuron's basal excitability and its modulation by hormones and neurotransmitters.

STRUCTURE OF NALCN

NALCN (also named Rb21, VGCNL-1, NA in *Drosophila melanogaster* and NCA-1/2 in *Caenorhabditis elegans*) was first cloned from rat brain and described by Perez-Reyes and colleagues who named it Rb21 (Lee et al., 1999). With the exception of the nematode *Caenorhabditis*, the cnidarian *Nematostella* and the sponge *Amphimedon* that have two related channels, there is only one gene encoding NALCN in other organisms (Liebeskind et al., 2012; Senatore et al., 2013). In mammals, NALCN is a 1738

amino-acids protein that forms the channel pore of the complex and has a predicted topology similar to voltage-gated sodium and calcium channels (Snutch and Monteil, 2007) (Figure 1A). Unlike other members of the four-domain ion channel family, the S4 transmembrane segments have fewer positive residues, especially in domains 2 and 4, possibly explaining NALCN's voltage insensitivity. The predicted pore region is also unique in that its ionic selectivity motif differs from that of calcium channels (EEEE or EEDD) and sodium channels (DEKA). NALCN's ion selectivity motif (EEKE) is implicated in its specific permeation properties. With the exception of *C. elegans* and *D. melanogaster*, alternative splicing events in the pore-forming region of invertebrate NALCN result in a calcium channel-like EEEE motif or a sodium channel-like EEKE (or EKEE) motif that remain to be explored at the functional level (Senatore et al., 2013). These findings suggest that NALCN could behave as a sodium or calcium channel depending on the expressed isoform (Senatore et al., 2013).

In humans, the gene encoding NALCN is located on chromosome 13q33.1 and comprises at least 44 exons (43 coding exons). Several splice variants were identified during our cloning step and by database scanning (*unpublished results* Figure 1B). Alternative splicing events were found in the intracellular loop linking domains 2 and 3 and in the carboxy-terminus region. Interestingly, there is a long non-coding RNA

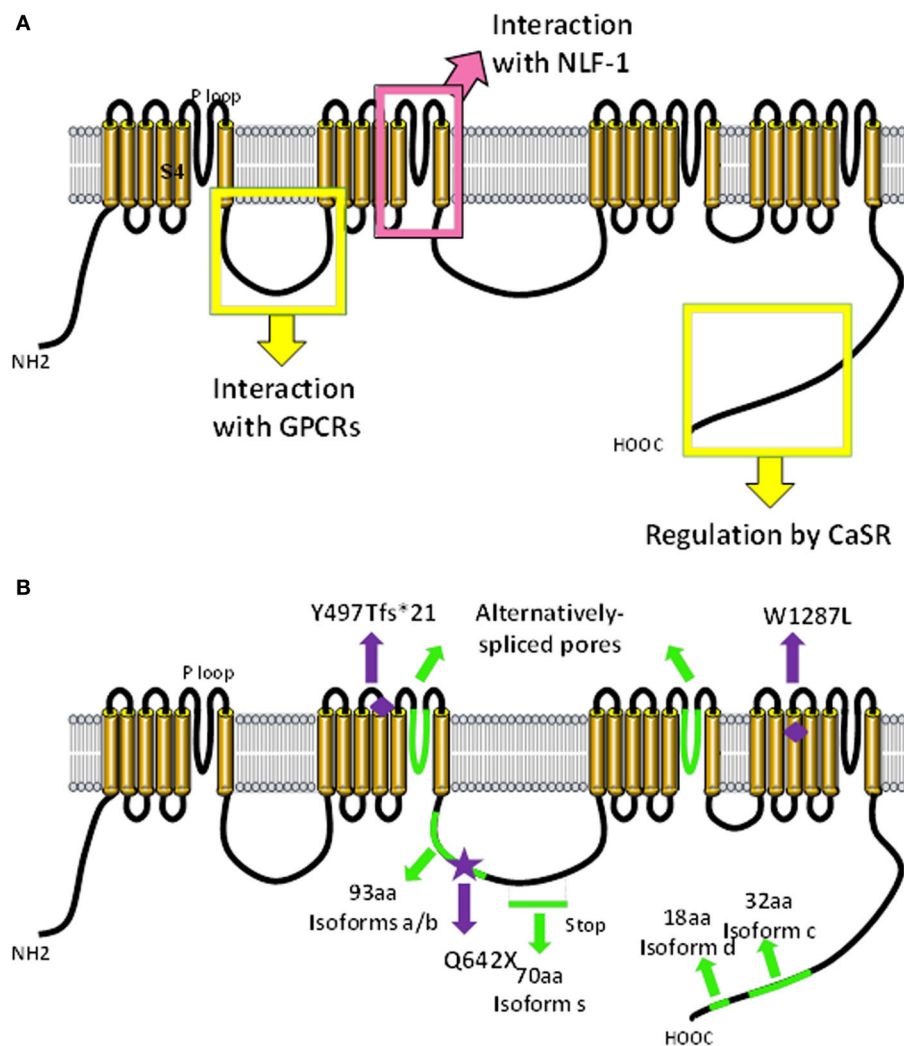


FIGURE 1 | Predicted molecular make-up of NALCN. The predicted structure of NALCN is similar to $\alpha_1\alpha_1$ subunits of voltage-gated Na^+ and Ca^{2+} channels (Lee et al., 1999). **(A)** It has four homologous repeats (domains I–IV) each composed of six transmembrane segments (S1–S6). Four pore-forming loops (P-loops) spanning from S5 to S6 make up the ion selectivity filter. The intracellular loop linking domains I and II of NALCN interacts with M3R and molecular determinants involved in the regulation by CaSR are located in the carboxy-terminus (Swayne et al.,

2009; Lu et al., 2010). The S5/P loop/S6 segment of transmembrane domain II is required for the interaction with NLF-1 (Xie et al., 2013). **(B)** Alternative events (shown in green) are detected in the intracellular loop linking domains II and III, in the P-loops of domains II and III, as well as in the carboxy-terminus (Senatore et al., 2013; data not shown). Mutations found in patients with INAD and an autosomal recessive syndrome with severe hypotonia, speech impairment, and cognitive delay are shown (Al-Sayed et al., 2013; Koroglu et al., 2013).

(lncRNA) gene named *NALCN-AS1* partially overlapping with *NALCN* on the reverse strand (Gene ID: 100885778; <http://www.ncbi.nlm.nih.gov/>). lncRNAs are thought to function in various cellular contexts, including post-transcriptional regulation, post-translational regulation of protein activity, organization of protein complexes, cell–cell signaling, as well as recombination (reviewed in Geisler and Coller, 2013; Sabin et al., 2013). Importantly, lncRNAs would be associated with a wide range of neurodevelopmental, neurodegenerative and psychiatric diseases, as well as brain cancer (reviewed in Barry, 2014). The specific function of *NALCN-AS1* remains to be elucidated.

NALCN FUNCTION

GATING PROPERTIES

The first functional characterization of NALCN was described by Ren and colleagues, who identified NALCN as the channel responsible for a tetrodotoxin (TTX)-resistant sodium leak current in mouse hippocampal neurons (Lu et al., 2007). In *Nalcn* knockout mice, they found that hippocampal neurons were hyperpolarized by ~ 10 mV compared to wild-type mice (Lu et al., 2007). They concluded that NALCN would contribute to the resting membrane potential in these neurons by eliciting a depolarizing current to counterbalance the hyperpolarizing current induced by two-pore potassium channels (reviewed in Ren, 2011;

Lu and Feng, 2012). A similar NALCN-like channel activity was described in neurons from *L. stagnalis* and *C. elegans* (Lu and Feng, 2011; Xie et al., 2013). Contrasting with these data, NALCN does not conduct a background current but rather drives an acetylcholine-activated sodium current in the MIN-6 cell line, a pancreatic β -cell model (Swayne et al., 2009). This acetylcholine-activated NALCN current requires the M3 muscarinic receptor (M3R) and occurs through a G protein-independent, Src family of tyrosine kinases (SFK)-dependent pathway. Similarly, NALCN current was found to be activated by substance P (SP) and neurotensin through a SFK-dependent pathway in mouse hippocampal and ventral tegmental area neurons (Lu et al., 2009). It is not clear why NALCN behaves as a leak channel (e.g., looks like spontaneously active) in neuronal cells and not in MIN-6 cells and whether NALCN may be considered as a GPCR-activated channel with a cell type-dependent basal activity or as a constitutively open channel regulated by GPCRs. Although these studies provide the first demonstration for the functional properties and regulation of NALCN channels, much remains to be determined about the functionality of NALCN and the mechanism(s) responsible for its activation. Indeed, it has also been hypothesized that NALCN may not be an ion channel *per se* but rather an ion sensor (Senatore and Spafford, 2013). Discordance in the field indicates that more work is clearly required to reveal the real “channel” identity of NALCN. In the context of this review, we will consider NALCN as a pore-forming subunit.

THE NALCN CHANNELOSOME

Like many ion channels, NALCN is associated with several proteins to form a larger channel complex (**Figure 2, Table 1**). These interacting proteins are involved in the folding, stabilization, cellular localization, and activation of NALCN.

UNC-80

UNC-80 (also named KIAA1843, c2orf21) is located on human chromosome 2q34 and has at least 45 exons. UNC-80 is a large protein of about 3300 amino acids without any predicted transmembrane segments or particular functional domains. UNC-80 contributes to the neuronal localization and/or stabilization of NALCN channel in *C. elegans* and *D. melanogaster* (Jospin et al., 2007; Yeh et al., 2008; Lear et al., 2013). In addition, UNC-80 acts as a scaffold protein for the SFKs and UNC-79. In fact, NALCN can interact with UNC-80 in the absence of UNC-79 and UNC-79 can interact with UNC-80 in the absence of NALCN. The interaction of NALCN and UNC-80 is required for the NALCN activation/inhibition by GPCRs in neurons (Wang and Ren, 2009; Lu et al., 2010). Similar to *NALCN*, databases indicate the existence of several *UNC-80* splice variants.

UNC-79

UNC-79 (also named KIAA1409) is located on human chromosome 14q32.12 and has at least 48 exons. UNC-79 is also a large protein (~2800 amino acids) without any predicted

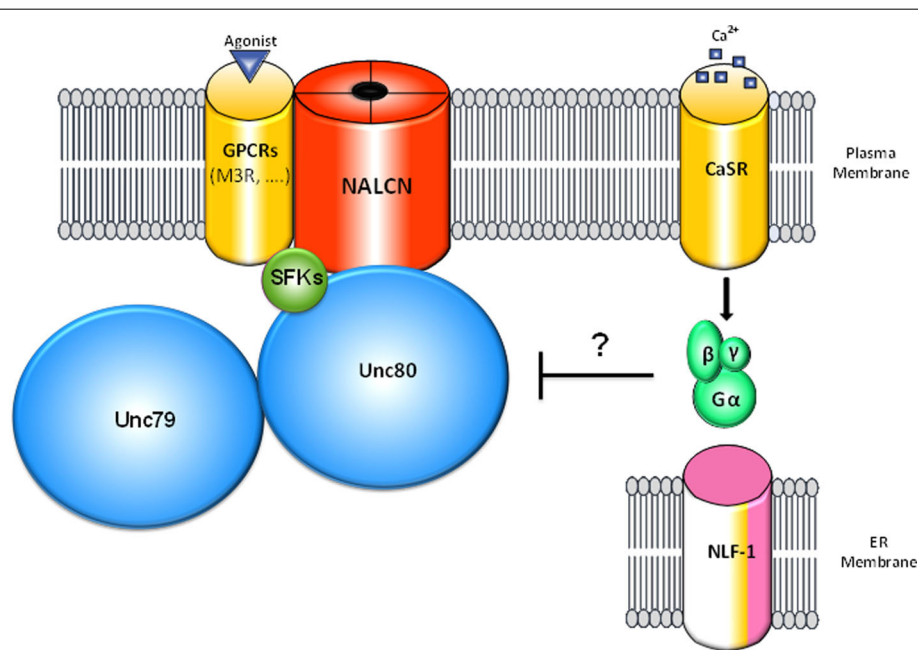


FIGURE 2 | Schematic representation of the NALCN channelosome.

The NALCN ion channel interacts with the M3 muscarinic receptor (M3R) that activates the channel through a G protein-independent and Src Family of Tyrosine Kinases (SFK)-dependent pathway upon activation by acetylcholine (Swayne et al., 2009). UNC-80 interacts with NALCN and SFKs and acts as a scaffolding protein (Wang and Ren, 2009; Lu et al., 2010). In addition, UNC-80 is involved in the expression levels of NALCN and UNC-79 as well as their neuronal localization (Jospin et al., 2007;

Yeh et al., 2008). UNC-79 interacts with UNC-80 but not NALCN and is involved in the expression levels and the neuronal localization of NALCN and UNC-80 (Yeh et al., 2008). CaSR was found to regulate NALCN channel activity by an uncharacterized mechanism involving G-proteins activation and UNC-80 (Lu et al., 2010). For clarity, NLF-1, an endoplasmic reticulum-resident protein that interacts with NALCN and is possibly involved in its folding is shown apart. It is not known whether the interactions mentioned above are direct or not.

Table 1 | Genes involved in the NALCN channelosome and their known roles.

Gene	Cytogenetic location	Coordinates (GRCh37 genome assembly)	Gene product function	References
<i>NALCN</i>	13q33.1	101,706,129–102,068,812	Ion channel	Lu et al., 2007, 2009; Swayne et al., 2009
<i>UNC-80</i>	2q34	210,636,716–210,864,023	Scaffold protein for the SFKs and UNC-79 Neuronal localization	Wang and Ren, 2009; Lu et al., 2010 Jospin et al., 2007; Yeh et al., 2008
<i>UNC-79</i>	14q32.12	93,799,565–94,174,222	Expression level of NALCN and UNC-80 Neuronal localization	Humphrey et al., 2007; Yeh et al., 2008; Lu et al., 2010 Yeh et al., 2008
<i>NLF-1</i>	13q33.3	107,822,318–108,519,083	Expression level of NALCN	Xie et al., 2013
<i>CHRM3</i>	1q43	239,549,876–240,078,750	NALCN activator	Swayne et al., 2009
<i>SRC</i>	20q12-q13	35,973,088–36,033,835	Tyrosine kinase	Lu et al., 2009; Swayne et al., 2009

transmembrane segments or particular functional domains. UNC-79 was found to be involved in regulating the neuronal localization of the NALCN channel complex both in *C. elegans* and *D. melanogaster* (Humphrey et al., 2007; Yeh et al., 2008; Lear et al., 2013). UNC-79 has been found to regulate the expression level of UNC-80 and, as a pair, UNC-79 and UNC-80 regulate the expression level of NALCN. This likely occurs through a post-transcriptional mechanism as no difference in the corresponding mRNA levels was found (Humphrey et al., 2007; Yeh et al., 2008). This regulation may not be conserved in mammals. As a matter of fact, *Unc-79* mutant mice lack detectable levels of the UNC-80 protein but NALCN is still present (Lu et al., 2010; Specca et al., 2010). Another difference between invertebrates and mammals concerns the redundant functions of these proteins. Indeed, in *D. melanogaster*, transgenic expression of NALCN, UNC-79, or UNC-80 does not relieve the requirement for the other subunits while, in mouse primary neurons, UNC-80 can bypass the requirement for UNC-79 (Lu et al., 2010; Lear et al., 2013).

NLF-1

NLF-1 (*NCA Localization Factor 1*, also named FAM155A) is an endoplasmic reticulum (ER) resident protein of around 438–468 amino-acids, depending on the species, that interacts with NALCN and promotes its neuronal localization in *C. elegans* (Xie et al., 2013). The gene encoding NLF-1 is located on human chromosome 13q33.3 and contains 3 exons. An intronic and non-coding transcript gene, *FAM155A-IT1*, is described on the same strand (Gene ID: 100874375; <http://www.ncbi.nlm.nih.gov/>) with no known function. In *C. elegans*, the loss of function of *nlf-1* results in a reduced leak current and a hyperpolarized resting membrane potential in premotor interneurons. NLF-1 function is conserved across species as the mouse homolog functionally substitutes to the *C. elegans* one. In addition, knockdown of the *D. melanogaster* ortholog gene, *CG33988* results in similar phenotypes as for *na* (see below; Ghezzi et al., 2014). Also, knockdown of *Nlf-1* in primary mouse cortical cultures effectively reduced the background Na^+ current. It has been postulated that NLF-1 could function as a chaperone to facilitate the folding and assembly of NALCN channels. This interaction involves the

second transmembrane domain of NALCN and requires its S5/P loop/S6 segment. The topology of NLF-1 is predicted to have one single transmembrane domain within 40 residues of the carboxy-terminus and lack known amino-terminal signal sequences. There are putative ER retention motifs (RXR) at the amino-terminus region. *nlf-1* is expressed in sensory neurons, interneurons, and excitatory motor neurons in *C. elegans*. Endogenous UNC-79 level is also significantly decreased in *nlf-1* mutants but the NLF-1 level is unaffected by the absence of UNC-79 and UNC-80. In humans, there is another gene homologous to *NLF-1*, *FAM155B* that is localized to Xq13.1 and encodes for a putative protein of 473 amino-acids. It is not known if this putative protein belongs to the NALCN channel complex. Both NLF-1 and FAM155B have a cysteine-rich domain (CRD) involved in signal transduction in other proteins (Pei and Grishin, 2012). In addition, these two proteins are related to Mid1, a fungal stretch-activated calcium channel component that forms a complex with the transmembrane calcium channel Cch1 (Maruoka et al., 2002).

G protein-coupled receptors (GPCRs)

In addition to its baseline activity, NALCN activity is enhanced/modulated by several GPCRs. Acetylcholine-induced NALCN current requires the interaction of NALCN and M3R proteins through the 1–2 loop of NALCN and the i3 and carboxy-terminus of M3R (Swayne et al., 2009). Other GPCRs, the Neurokinin 1 receptor (NK1R) and a neurotensin receptor that remains to be identified, activate NALCN upon the binding of their ligands SP and neurotensin in primary mouse pyramidal hippocampal neurons and dopaminergic neurons from the ventral tegmental area (Lu et al., 2009). However, whether NK1R interacts with NALCN remains to be shown. This raises the possibility that several GPCRs may activate NALCN and the challenge to determine the repertoire of NALCN-activating GPCRs persists. A full analysis of the literature gives some clues on this point. For example, it has been reported that 5-HT modulates a non-selective leak current involved in the resting membrane potential in the pre-Bötzinger complex and motor neurons likely through activation of the 5-HT_{2A} receptor (Ptak et al., 2009). Also, a cation conductance activated by glutamatergic

metabotropic receptors through a G protein-independent pathway was described in CA3 hippocampal pyramidal neurons (Guerineau et al., 1995). In addition to its activation by several GPCRs, NALCN was found to be inhibited by another GPCR, the calcium-sensing receptor (CaSR) (Lu et al., 2010). This regulation is G-protein-dependent and SFK-independent, requires UNC-80 and involves molecular determinants in the carboxy-terminal portion of NALCN. It is not known if CaSR belongs to the NALCN channel complex.

EXPRESSION PATTERN

NALCN is mainly expressed in the central nervous system (CNS) but also in heart, adrenal gland, thyroid gland, lymph node, and islets of Langerhans (both in α - and β -cells) (Lee et al., 1999; Kutlu et al., 2009; Swayne et al., 2009; Koroglu et al., 2013; Rorsman and Braun, 2013; see <http://t1dbase.org>). In the CNS, NALCN is expressed mainly in neurons, to a lesser extent in oligodendrocytes, and at a very low level in astrocytes (Cahoy et al., 2008). The temporal expression of NALCN is strongly correlated with the expression of genes involved in synapse development and with synaptic density in several areas of the human brain (Kang et al., 2011; see <http://hbatlas.org/>). The spatial expression of NALCN is also correlated with genes expressed in specific neural cell types such as *CALB1* (Cortical GABA interneurons), *CTGF* and *UNC-5C* (Subplate cortical glutamatergic neurons). In invertebrates, NALCN-orthologs are concentrated at the synapse in *D. melanogaster*, and along the axon in *C. elegans* and *L. stagnalis* (Nash et al., 2002; Humphrey et al., 2007; Yeh et al., 2008; Senatore et al., 2013). The cellular sub-localization of NALCN in mammals is not known.

PHYSIOLOGICAL ROLES OF NALCN: LESSONS FROM ANIMAL MODELS

Mutations in genes coding for NALCN channel proteins, both in mammals and invertebrates, yield a wide range of phenotypes. Functional knock-out or hypomorphic mutations in these genes produce viable offspring (but fewer compared to wild-type) in *C. elegans* and *D. melanogaster*, whereas it is post-embryonic lethal in homozygous null mice (Krishnan and Nash, 1990; Nakayama et al., 2006; Lu et al., 2007; Specca et al., 2010). While no obvious developmental defects, including neuronal development, were found in *Nalcn* and *Unc-79* mutant mice, these mice die as a result of disrupted respiratory rhythm (Lu et al., 2007, see below). The depletion of *nca1/2*, *unc-79* or *unc-80* in *C. elegans* does not result in any gross abnormality in neuronal cell body position, neuronal processes, or fasciculation suggesting that these mutations do not interfere with the nervous system development (Pierce-Shimomura et al., 2008). We present below the phenotypes observed for the animal mutants in NALCN channel complex (Table 2).

LOCOMOTOR ACTIVITY

Wild-type *C. elegans* travels on a culture plate through the continuous and rhythmic propagation of sinusoidal body bends. A simultaneous loss of both *nca-1* and *nca-2*, or the individual loss of *unc-79*, *unc-80* or *nlf-1* results in fainting, a unique motor deficit characterized by periodic halting during movement

(Sedensky and Meneely, 1987; Morgan et al., 1988; Rajaram et al., 1999; Humphrey et al., 2007; Jospin et al., 2007; Xie et al., 2013). A dysfunction of premotor interneurons was found to be the primary cause of the failure in the initiation and maintenance of rhythmic locomotion exhibited by fainters (Xie et al., 2013). A “hesitant” walking phenotype (e.g., the walk is interrupted by pauses) is also observed when *na* or *unc-79* are invalidated in *D. melanogaster* (Krishnan and Nash, 1990; Mir et al., 1997; Guan et al., 2000; Nash et al., 2002; Humphrey et al., 2007). Conversely, gain-of-function mutations in *nca-1* lead to exaggerated body bending, termed coiling, in *C. elegans* (Yeh et al., 2008).

When transitioned between solid and liquid environments, *C. elegans* switch between two patterns of rhythmic locomotion, crawling and swimming that are distinct in both kinematics and pattern of muscle activity (Pierce-Shimomura et al., 2008). A genetic screen was performed in order to find mutants capable of normal crawling but incapable of normal swimming. *unc-79*, *unc-80* and *nca-1;nca-2* mutants were found to be paralyzed upon immersion in liquid. The paralytic defect in swimming does not seem to be explained by general defects in neuronal excitability, synaptic function, or development because the fainting phenotype was not observed in mutants defective in voltage-gated calcium channels or major synaptic proteins.

SENSITIVITY TO GENERAL VOLATILE ANESTHETICS (GAs) AND ETHANOL

Several studies reported an altered sensitivity to GAs both in invertebrates and mice mutants with some discrepancies. In *C. elegans*, *nca-1;nca-2*, *unc-79*, and *unc-80* mutants are hypersensitive to the immobilizing effect of halothane (~2–3 fold increase compared to controls) and other anesthetic agents (Sedensky and Meneely, 1987; Morgan et al., 1988, 1990; Humphrey et al., 2007). In fact, *unc-79* mutants are hypersensitive to thiomethoxyflurane, methoxyflurane, chloroform, and halothane. They are also more resistant to flurothyl and enflurane, insensitive to fluroxene and isoflurane, and mildly more sensitive to diethylether (Morgan and Cascorbi, 1985; Morgan et al., 1988, 1990; Humphrey et al., 2007). By contrast, hypomorphic *na^{har38}* and *na^{har85}* drosophila mutants were first described as resistant to halothane, methoxyflurane, chloroform and trichloroethylene but not to diethylether, isoflurane, and enflurane (Krishnan and Nash, 1990; Nash et al., 1991; Campbell and Nash, 1994; Mir et al., 1997). However, it was then reported that *unc-79* and *na* mutants are hypersensitive to halothane but not enflurane (Guan et al., 2000; Humphrey et al., 2007). The fact that *na* mutants were first described as resistant instead of hypersensitive may be explained by the method used to score anesthetic sensitivity but in some cases also by the fact that different alleles were tested. In another study, *na^{har38}* mutation was found to be hypersensitive to isoflurane and to increase the potency with which isoflurane alters local field potentials recorded directly from fly brains (Van Swinderen, 2006). It was also shown that halothane presynaptically depresses synaptic transmission in wild-type drosophila larvae but not in *na^{har38}* and *na^{har85}* mutants (Nishikawa and Kidokoro, 1999). In mammals, heterozygous *Lightweight* mice, that carry a hypomorphic mutation in *Unc-79*, exhibit no alteration in Minimum Alveolar Concentration (MAC) in response to

Table 2 | Physiological roles of NALCN: lessons from animal models.

Phenotype	Gene	Species	Reference
Locomotor activity	<i>nca1/2, unc-79, unc-80, nlf-1</i> <i>na,</i> <i>unc-79</i>	<i>C. elegans</i> <i>D. melanogaster</i>	Sedensky and Meneely, 1987; Morgan et al., 1988; Krishnan and Nash, 1990 Mir et al., 1997; Rajaram et al., 1999; Guan et al., 2000; Nash et al., 2002; Humphrey et al., 2007; Pierce-Shimomura et al., 2008; Yeh et al., 2008; Xie et al., 2013
Sensitivity to volatile anesthetics	<i>nca1/2, unc-79, unc-80</i> <i>na,</i> <i>unc-79</i> <i>unc-79</i>	<i>C. elegans</i> <i>D. melanogaster</i> <i>M. Musculus</i>	Morgan and Cascorbi, 1985; Sedensky and Meneely, 1987; Morgan et al., 1988, 1990 Krishnan and Nash, 1990; Nash et al., 1991; Campbell and Nash, 1994; Mir et al., 1997; Guan et al., 2000; Van Swinderen, 2006; Humphrey et al., 2007 Specia et al., 2010
Sensitivity to ethanol	<i>nca1/2, unc-79, unc-80</i> <i>Unc-79</i>	<i>C. elegans</i> <i>M. musculus</i>	Morgan and Sedensky, 1995; Specia et al., 2010 Specia et al., 2010
Respiratory rhythm	<i>Nalcn</i> <i>nalcn</i>	<i>M. Musculus</i> <i>L. stagnalis</i>	Lu et al., 2007 Lu and Feng, 2011
Photic control of locomotion, circadian rhythms	<i>na, nlf-1, unc-79, unc-80</i>	<i>D. melanogaster</i>	Campbell and Nash, 2001; Nash et al., 2002; Lear et al., 2005, 2013; Ghezzi et al., 2014
Abdominal morphology	<i>na,</i> <i>unc-79</i>	<i>D. melanogaster</i>	Krishnan and Nash, 1990; Mir et al., 1997; Nash et al., 2002; Humphrey et al., 2007
Social clustering	<i>na, nlf-1</i>	<i>D. melanogaster</i>	Burg et al., 2013; Ghezzi et al., 2014
Metabolism	<i>Unc-79</i>	<i>M. musculus</i>	Specia et al., 2010
Ethanol consumption	<i>Unc-79</i>	<i>M. musculus</i>	Specia et al., 2010
Systemic osmoregulation	<i>Nalcn</i>	<i>M. musculus</i>	Sinke et al., 2011
Pacemaker activity	<i>Nalcn</i>	<i>M. musculus</i>	Kim et al., 2012
Hyperactivity	<i>Unc-79</i>	<i>M. musculus</i>	Specia et al., 2010
Reproduction	<i>na</i>	<i>D. melanogaster</i>	Krishnan and Nash, 1990

halothane, cyclopropane, or sevoflurane. However, a significant resistance to isoflurane-induced anesthesia was described (Specia et al., 2010).

It remains to be determined if the NALCN channel complex is a direct target for GAs, is important for the function of cells that contain such targets, or influences anesthesia more indirectly. GAs produce a widespread neurodepression in the CNS by enhancing inhibitory neurotransmission and reducing excitatory neurotransmission. However, the action mechanisms of GAs are not completely understood. Several ion channels and GPCRs are affected by these compounds (reviewed in Chau, 2010; Minami and Uezono, 2013). Of interest, it is known for a long time that GAs such as halothane, hyperpolarize neurons by acting on the potassium currents likely by activating two-pore potassium channels (Patel et al., 1999; Gruss et al., 2004; Liu et al., 2004). Considering that neurons from *Nalcn* knockout animals exhibit a ~10 mV hyperpolarization of their resting membrane potential, it is tempting to hypothesize that, in the case of an observed hypersensitivity, the absence of NALCN could remove a kind of brake for some GAs to act on their targets such as two-pore potassium channels. In this scheme, it would explain why, contrasting with *C. elegans* and *D. melanogaster unc-79* and

unc-80 mutants, heterozygous *lightweight* mice do not display any hypersensitivity to halothane. In fact, NALCN current and protein were found to be still present in *Unc-79* deficient mice whereas this is not the case in *C. elegans* and *D. melanogaster* (Yeh et al., 2008; Lu et al., 2010; Specia et al., 2010; Lear et al., 2013). An observed resistance to other GAs implies that the NALCN channel complex is a direct target while an absence of phenotype to other GAs would indicate that other targets beside NALCN are involved.

In addition to GAs, alteration in ethanol sensitivity was described in animal mutants for the NALCN channelosome. Morgan and Sedensky, in 1995, found mutations in several genes in *C. elegans* which seem to control the sensitivity to ethanol, including *unc-79* (Morgan and Sedensky, 1995). As a matter of fact, *unc-79* mutants showed a decrease by about 25% in ethanol sensitivity. By contrast, it was recently reported that *unc-79, unc-80*, and *nca-1;nca-2* mutants show hypersensitivity to ethanol (Specia et al., 2010). This hypersensitivity seems to be conserved in mammals as heterozygous *Lightweight* mice exhibit a highly significant increase in the sensitivity to the acute sedative effects of ethanol (Specia et al., 2010). Heterozygous *Lightweight* mice also present an increased ethanol preference and consumption,

compared to wild-type mice, particularly at higher alcohol concentrations (Specia et al., 2010). As with GAs, the nature of the interaction between ethanol and NALCN physiology remains to be studied.

RESPIRATORY RHYTHM

In 2007, it was shown that the *Nalcn* gene is crucial for survival in mammals (Lu et al., 2007). Homozygous *Nalcn* knockout mice pups appear normal up to 12 h after birth and then die within 12 h due to severely disrupted respiratory rhythms (Lu et al., 2007). While wild-type mice had no abnormalities, knockout animals' respiration was highly sporadic. Breathing was characterized by ~5 s of apnea, followed by a burst of deep breathing for ~5 s, and this occurred at a rate of ~5 apnea events/minute. Interestingly, this pattern is reminiscent of the periodic breathing of Cheyne-Stokes respiration found in humans with CNS damage (reviewed in Strohl, 2003). Electrophysiological recording from the fourth cervical nerve root that innervates the diaphragm revealed that rhythmic electrical activity present in wild-type mice was largely absent. Thus, the defects observed in the respiratory rhythm in knockout mice are likely to reflect defects in electrical signaling in the nervous system (Lu et al., 2007).

More recently, Lu and Feng, 2011, investigated the properties of a NALCN ortholog in the snail *L. stagnalis* and its role in the activity of a respiratory pacemaker neuron (Lu and Feng, 2011). An *in vivo* investigation of its role on regulating respiratory behavior was performed by using RNA interference approaches. Animals in which *nalcn* was knocked down showed a reduced total breathing time compared to the naïve control. The resting membrane potential of the right pedal dorsal 1 (RPeD1) neuron that initiates the respiratory rhythm was found to be hyperpolarized by ~15 mV and its rhythmic firing was abolished. Thus, NALCN also plays a role in maintaining the respiratory activity in adult animal. It remains to be demonstrated if NALCN plays the same role in mammals by studying its functional properties in the preBötzinger complex and the retrotrapezoidnucleus/parafacial respiratory group that are involved in the respiratory rhythmogenesis (reviewed in Feldman et al., 2013).

PHOTIC CONTROL OF LOCOMOTION, CIRCADIAN RHYTHMS

Several studies performed with *D. melanogaster* mutants revealed the NALCN channelosome as an important player of circadian rhythms. Indeed, null *na* mutants display disrupted circadian rhythm. Typically, wild-type *D. melanogaster* are diurnal, with a greater proportion of their activity occurring during the daytime but null *na* mutants exhibit most of their activity at night (Nash et al., 2002). Furthermore, light enhances the climbing deficit that is induced by GAs in these flies (Campbell and Nash, 2001). Interestingly, the amount of NA protein does not fluctuate over time or light cycles indicating that expression of NA is not under circadian regulation. The phenotype seems to be the result of a broad aberrant motor response to photic input. Central to this, *na* is expressed in circadian pacemaker neurons and regulates the output of these neurons (Lear et al., 2005). An accumulation of Pigment-Dispersing factor (PDF), a neuropeptide essential for robust circadian behavior, is observed in these neurons from *na* mutants. This suggests that *na* may be required for PDF release.

It is not surprising to observe a disturbance of circadian rhythms in *na* null mutants as electrical activity is an important regulator of clock function both in invertebrates and mammals (Nitabach et al., 2002; Belle et al., 2009). Null mutations of *unc-79* and *unc-80* in *D. melanogaster* also display severe defects in circadian locomotor rhythmicity that are indistinguishable from *na* mutant phenotypes, and support the role of this channelosome in circadian rhythms (Lear et al., 2013). Knockdown of *nlf-1* in *D. melanogaster* was also found to phenocopy *na* knockdown for the circadian locomotion phenotype (Ghezzi et al., 2014).

SOCIAL CLUSTERING

Involvement of the NALCN channelosome in social clustering, the natural tendency of animals of the same species to congregate in close proximity within a group, was recently described. Indeed, in a study aiming to investigate resource-independent local enhancement (RILE) in *D. melanogaster*, Burg et al., 2013, reported that *na^{har38}* mutants display a deficient social phenotype compared to wild-type flies (Burg et al., 2013). This deficiency is rescued by the expression of *na* under the control of its native promoter. In addition, a complete rescue of the phenotype is also observed when *na* is expressed in cholinergic neurons and a partial rescue is obtained when *na* is expressed in glutamatergic neurons. *na* is strongly expressed in the mushroom body, a structure known to play a role in olfactory and visual learning and memory and the specific blockade of *na* expression in this structure affects RILE behavior. Knockdown of *nlf-1* in *D. melanogaster* was also found to significantly suppress the social clustering phenotype as for *na* (Ghezzi et al., 2014).

ABDOMINAL MORPHOLOGY (NARROW ABDOMEN)

The *na* mutant flies are noticeably smaller than controls and their abdomens are more slender and elongated but no obvious deformity has been identified (Krishnan and Nash, 1990; Mir et al., 1997; Nash et al., 2002). *D. melanogaster* bearing mutations in *unc-79* also exhibit a cylindric shaped abdomen (Humphrey et al., 2007). It is not known if this alteration represents a developmental defect or reflects altered physiology. However, *Nalcn* knockout mice neonates do not display gross abnormalities in embryonic development, righting responses, spontaneous limb movement, and toe/tail pinch responses (Lu et al., 2007).

METABOLISM (BODY COMPOSITION AND FOOD CONSUMPTION)

Heterozygous *Lightweight* mice are smaller (shorter in length and lower in body weight) and have a leaner body composition (increased lean tissue and decreased body fat) than wild-type mice (Specia et al., 2010). Interestingly, heterozygous *Lightweight* mice display an increased food intake in comparison with wild-type mice of the same weight.

SYSTEMIC OSMOREGULATION (SERUM SODIUM CONCENTRATION)

A genetic analysis performed in mice demonstrated that *Nalcn* is involved in systemic osmoregulation by controlling the serum sodium concentration (Sinke et al., 2011). Furthermore, this study reported that heterozygous *Nalcn* knockout mice exhibit a significant hypernatremia.

PACEMAKER ACTIVITY (INTERSTITIAL CELLS OF CAJAL)

With others channels, such as transient receptor potential canonical (TRPC) channels, NALCN is partly responsible for the SP-induced depolarization and regulation of the intestinal pacemaker activity in the interstitial cells of Cajal (Kim et al., 2012). This activity generates the phasic contractions of the gastrointestinal muscles. Of note, in this study, the authors found that NALCN is not required for the basal pacemaking activity in ICCs.

POSSIBLE IMPLICATIONS OF NALCN IN HUMAN DISEASES

The NALCN channelosome was shown to be vital in mammals (Nakayama et al., 2006; Lu et al., 2007). Considering its role in regulating neuronal resting membrane potential, it is expected that polymorphisms, copy number variations (CNVs) and mutations in the corresponding genes may significantly impact neuronal physiology and lead to diseases. In this section, we review our current knowledge on data involving the NALCN channel complex in human diseases. We have also included a review of genetic data that loosely link the NALCN channel complex genes to diseases, which may provide insights into candidate genes involved in neuronal diseases (Table 3).

INFANTILE NEUROAXONAL DYSTROPHY (INAD)

Infantile neuroaxonal dystrophy (INAD) is a rare neurodegenerative disease characterized by progressive motor, mental and visual deterioration that begins in infancy. Onset is usually between the age of 6 months and 3 years and death typically ensues before the age of 10 years (reviewed in Gregory et al., 1993). Early clinical manifestations include bilateral pyramidal tract signs, truncal hypotonia, cognitive decline and optic atrophy. Most cases present with distal axonal swelling and spheroid bodies in tissue biopsies (Cowen and Olmstead, 1963; Morgan et al., 2006). Originally, this recessive disorder was linked solely to mutations in the *PLA2G6* gene, which encodes the calcium-independent phospholipase A2 β (iPLA2 β) enzyme, also designated iPLA2-VIA (Khateeb et al., 2006; Morgan et al., 2006). Recently, a study reported a mutation in the *NALCN* gene in two affected siblings with additional atypical features including facial dysmorphism, pectus carinatum, scoliosis, pes varus, zygodactyly and bilateral cryptorchidism. The patients also exhibit cerebellar atrophy and seizures and are still alive at 18 years-old (Koroglu et al., 2013; also see Seven et al., 2002). The identified mutation was a C to T conversion in *NALCN* coding exon 16 (c.1924C > T), creating a premature translational termination signal at codon 642 (Q642X) and truncated NALCN channel (Figure 1B). Interestingly, our unpublished data indicate that this exon is alternatively spliced resulting in the loss of one isoform but not NALCN in its entirety and may explain why the mutation is not lethal. It remains to be established whether this mutation results in a mRNA decay or expression of a truncated two-domain isoform. The fact that *PL2G6* and *NALCN* genes mutations result in a similar disease raises the possibility that iPLA2 β could be a regulator of NALCN.

AUTOSOMAL RECESSIVE SYNDROME WITH SEVERE HYPOTONIA, SPEECH IMPAIRMENT, AND COGNITIVE DELAY

Mutations in the *NALCN* gene were recently reported in six patients with an autosomal-recessive syndrome characterized by

Table 3 | Possible implications of the NALCN channel complex in diseases.

Disease	Gene	Reference
Infantile neuroaxonal dystrophy (INAD)	<i>NALCN</i>	Koroglu et al., 2013
Autosomal-recessive syndrome with severe hypotonia, speech impairment, and cognitive delay	<i>NALCN</i>	Al-Sayed et al., 2013
Cervical dystonia	<i>NALCN</i>	Mok et al., 2013
Cancer		
Pancreas	<i>NALCN</i>	Biankin et al., 2012
Non-small cell lung	<i>NALCN, UNC-80</i>	Lee et al., 2013
Tumor-derived endothelial cells	<i>NLF-1</i>	McGuire et al., 2012
Glioblastoma	<i>NALCN, NLF-1</i>	Fontanillo et al., 2012
Psychiatric disorders		
Bipolar disorder	<i>NALCN, UNC-79</i>	Baum et al., 2008; Askland et al., 2009; Wang et al., 2010
Schizophrenia	<i>NALCN</i>	Wang et al., 2010
Depression	<i>NLF-1</i>	Terracciano et al., 2010
Attention-deficit/hyperactivity disorder with conduct disorder	<i>NLF-1</i>	Anney et al., 2008
Epilepsy	<i>UNC-80</i>	Ratnapriya et al., 2010; EPICURE Consortium et al., 2012
Autism	<i>UNC-80</i>	Iossifov et al., 2012
13q syndrome	<i>NALCN, NLF-1</i>	Brown et al., 1995; Kirchhoff et al., 2009; Huang et al., 2012; Lalani et al., 2013
Alzheimer's disease	<i>UNC-80</i> <i>UNC-79</i>	Scott et al., 2003 Lee et al., 2008; Grupe et al., 2007
Alcoholism	<i>NALCN</i> <i>UNC-79</i> <i>UNC-80</i>	Wetherill et al., 2014 Lind et al., 2010 Nurnberger et al., 2001; Schuckit et al., 2001
Restless legs syndrome	<i>NALCN</i>	Balaban et al., 2012
Primary biliary cirrhosis	<i>NLF-1</i>	Hirschfield et al., 2009
Hypertension	<i>NLF-1</i>	Adeyemo et al., 2009
Polyglutamine disorders	<i>NLF-1</i>	Whan et al., 2010

severe hypotonia, speech impairment, and cognitive delay from two large consanguineous families (Al-Sayed et al., 2013). Three male patients (ranging from 4 to 7 years-old) from one family are homozygous for a single nucleotide deletion c.1489delT located in the coding region for the S4 helix from domain II (Figure 1B). This mutation results in a frame shift creating a stop codon 21 amino-acids downstream, which likely results in the production of a truncated protein or mRNA decay. Unless the involved exon is alternatively spliced, it is not clear why this deletion is not lethal as reported for *Nalcn* knockout mice (Lu et al., 2007). These patients have an absence of speech development, severe

hypotonia, chronic constipation, global developmental delay, and facial dysmorphism which is reminiscent of infantile hypotonia with psychomotor retardation and characteristic facies (IHPRF, OMIM #615419). Three female patients (ranging from 9 to 17 years-old) from a second family are homozygous for a missense mutation c.3860G > T (W1287L) in exon 34 that encodes for the S4 helix from domain IV (**Figure 1B**). These patients have a milder but similar phenotype as the first family with additional features such as seizure disorder and hyperactivity.

CERVICAL DYSTONIA

Dystonia is a “syndrome of sustained muscle contractions, frequently causing twisting and repetitive movements or abnormal postures” (reviewed in Fahn et al., 1998). Estimates of the prevalence of dystonia range from ~1:10,000 to more than 1:200 (Nutt et al., 1988; Nakashima et al., 1995; Epidemiological Study of Dystonia in Europe Collaborative, G., 2000; Muller et al., 2002). Clinical presentation of dystonia is heterogeneous, from focal involvement such as cervical dystonia to generalized torsional dystonia. Cervical dystonia is the most common form of dystonia (Butler et al., 2004; Jankovic et al., 2007; Groen et al., 2013). The majority of cervical dystonia is transmitted in a non-Mendelian pattern, which suggests cervical dystonia is likely a complex disease rather than monogenic form. A recent genome-wide association study (GWAS) in 212 patients with this form of dystonia revealed a possible association with *NALCN* (Mok et al., 2013). However, this study did not find any single nucleotide polymorphisms (SNPs) with genome-wide significance (defined as $P < 5 \times 10^{-8}$) but a few clusters of possible association (defined as $P < 5 \times 10^{-6}$). Six SNPs within or in the vicinity of the *NALCN* gene with *P*-values ranging from 2.54×10^{-6} to 9.76×10^{-7} were found. Additional GWAS with larger cohorts of patients are required since the small sample size for this initial study was underpowered to detect loci with small disease effects.

PSYCHIATRIC DISORDERS

Schizophrenia and Bipolar disorder

Schizophrenia (SCZ) is a chronic, severe disabling brain disorder characterized by abnormalities in the perception of reality. It most commonly manifests as auditory hallucinations, delusions, disorganized speech and thinking with significant social or occupational dysfunction (reviewed in Silveira et al., 2012). Bipolar disorder (BD), also known as manic-depressive illness, is a serious medical illness that causes shifts in a person's mood, energy, and ability to function (reviewed in Smith et al., 2012). Different from the normal ups and downs that everyone goes through, the symptoms of BD are severe. SCZ and BD affect around 1% of the population each. Both diseases have strong inherited components and growing evidence indicates that BD and SCZ may be closely related.

Interestingly, the *NALCN* gene lies within a region on chromosome 13q that has shown linkage to both BD and SCZ (reviewed in Detera-Wadleigh and McMahon, 2006). More specifically, the correlation between *NALCN* mRNA expression and the SCZ-associated gene *GABRB2* in human brain (Kang et al., 2011), along with the association between the *Drosophila* homolog, *na*

with circadian rhythms (disruptions of which are a hallmark of BD) suggest that *NALCN* may play a role in these two disorders (reviewed in Lenox et al., 2002). Importantly, while some genetic studies point out *NALCN* as a susceptibility locus in SCZ and BD, other studies have not concurred with these findings. A GWAS performed by genotyping more than 550,000 SNPs in two independent cohorts of European origin (for a total of 1233 patients and 1439 controls) revealed a significant association between *NALCN* and BD (SNP rs9513877; Baum et al., 2008). This finding was confirmed by Askland et al. (2009). A genome-wide meta-analysis also identified a significant association of *NALCN* (SNP rs2044117) with both SCZ and BD in cohorts of 1172 (SCZ) and 653 (BD) European-American patients (Wang et al., 2010). However, no significant association between BD and *NALCN* was found in a Finnish cohort of 723 individuals from 180 families with type I BD (Ollila et al., 2009). Furthermore, there was no association of *NALCN* with SCZ in a cohort of 583 patients (Souza et al., 2011), nor in a group of 240 individuals with treatment-resistant SCZ (Teo et al., 2012). The discrepancies in candidate gene studies may partly result from the clinical and genetic heterogeneity of BD and SCZ and their complex inheritance model, but also from methodological issues such as the definition of clinical phenotype. More work is needed to confirm that *NALCN* is a susceptibility locus in BD and SCZ.

Several findings suggest that *UNC-79* and *UNC-80* are also associated with these disorders, further implicating the *NALCN* channelosome with SCZ and BD. The *UNC-79* encoding gene lies within a region on chromosome 14q that has shown linkage to BD. Askland et al., 2009, also suggested an association between SNP rs17125698 located at around 4Mb from the *UNC-79* gene and BD (Askland et al., 2009). Another study also reported an association of SNP rs11622475 located in 14q32 in BD (Wellcome Trust Case Control, C, 2007). However, this SNP is located at around 100Mb from *UNC-79*. A proteomic study suggested that *UNC-80* could belong to the same protein complex as dysbindin, a SCZ susceptibility gene product (Mead et al., 2010).

Major depressive and Attention-deficit/hyperactivity disorders

NLF-1 has been loosely associated with both major depressive disorder and attention-deficit/hyperactivity disorder. Major depressive disorder (MDD) is a syndrome characterized by a number of behavioral, cognitive and emotional features. It is most commonly associated with a sad or depressed mood, a reduced capacity to feel pleasure, hopelessness, loss of energy, altered sleep patterns, weight fluctuations, difficulty in concentrating and suicidal ideation (reviewed in Uher et al., 2013). A GWAS of depression traits found a possible association between MDD and SNPs in the vicinity of *NLF-1* (SNPs rs9634463, rs7329003, rs713548, rs9301191, and rs1924397), but statistical significance was not reached for any gene (Terracciano et al., 2010). Attention-deficit/hyperactivity disorder (ADHD) is characterized by inattention, excessive motor activity, impulsivity and distractibility and affects 8–12% of school-age children worldwide (reviewed in Sharma and Couture, 2014). Individuals with ADHD show high co-morbidity with a wide range of psychiatric disorders. In a study aiming to identify susceptibility loci for ADHD with conduct disorder, Anney et al., 2008, did not find any

significant association with any SNP but two of the strongest associations were found with SNPs rs10492664 and rs8002852 that are located in the vicinity of *NLF-1* (Anney et al., 2008). Interestingly, phenotypes observed for *Nk1R* knockout mice strongly parallel abnormalities expressed by patients with ADHD and heterozygous *Lightweight* mice are modestly but significantly hyperactive (Specia et al., 2010; Yan et al., 2010).

EPILEPSY

Epilepsy, a very common neurological disorder, is defined by the occurrence of unprovoked seizures caused by the synchronous discharge of large number of neurons (reviewed in Sander, 2003; Khan and Al Baradie, 2012). Abnormal expression or function of ion channels may be involved in the pathophysiology of both acquired and inherited epilepsy (reviewed in Mantegazza et al., 2010; Lerche et al., 2013). Considering the importance of the NALCN channel complex in setting the resting membrane potential of neurons, the NALCN channelosome gene mutations are clear candidates for epilepsy. As mentioned in this review, patients with INAD or an autosomal-recessive syndrome with severe hypotonia, speech impairment, and cognitive delay have seizures (Al-Sayed et al., 2013; Koroglu et al., 2013). Seizures were also reported for patients with chromosome 13q deletions in regions that contain the *NALCN* gene (Kirchhoff et al., 2009; Lalani et al., 2013). Recently, a whole genome linkage analysis in three-generations of a south Indian family who had multiple members affected with juvenile myoclonic epilepsy (JME) found a critical genetic interval of 24 Mb between markers D2S116 and D2S2390 (Ratnapriya et al., 2010). The *UNC-80* gene lies in this region. In addition, a region-wide linkage analysis carried out in 118 European families with an aggregation of JME indicated a significant linkage with marker rsD2S143 located on chromosome 2q34 at around 4Mb of the *UNC-80* gene (EPICURE Consortium et al., 2012).

AUTISM

Autism Spectrum Disorders (ASDs) are neurodevelopmental disorders characterized by impairments in social interaction and communication, and the presence of restrictive and repetitive behaviors (reviewed in Jones et al., 2014). Exome sequencing of 343 families, each with a single child on the autism spectrum and at least one unaffected sibling, revealed *de novo* small indels and point substitutions in the affected sibling (Iossifov et al., 2012). One of the discovered mutations resulted in a truncating R518X mutation in one copy of *UNC-80*, suggesting that *UNC-80* is a susceptibility locus in autistic spectrum.

13q SYNDROME

The 13q syndrome is caused by structural and functional monosomy of the 13q chromosomal region and was first described in 1963 and consequently delineated as a specific syndrome in 1969 (Lele et al., 1963; Allderdice et al., 1969). Large numbers of patients with deletions of the long arm of chromosome 13, which includes *NALCN* and *NLF-1*, have been described in the literature. The phenotypes of these patients varied widely. Some showed severe malformations involving the brain, heart, kidneys, lungs, other organ systems, and digits while others were only

mildly affected with minor dysmorphic features, developmental delay, and growth failure. The characteristic features of 13q deletions include growth retardation with microcephaly, facial dysmorphism, congenital heart, brain, and kidney defects (Brown et al., 1995). Several studies addressed karyotype-phenotype correlations depending on the extent of the deletions (Brown et al., 1995; Luo et al., 2000; McCormack et al., 2002; Alanay et al., 2005; Garcia et al., 2006; Ballarati et al., 2007; Walczak-Sztulpa et al., 2008; Kirchhoff et al., 2009; Quelin et al., 2009). It was reported that the severely malformed phenotype results from the deletion of a critical region lying between markers D13S136 and D13S147 (Brown et al., 1995). This region of around 2.3 Mb contains several genes including *NALCN*. Recently, a molecular-karyotyping study reported that a female with congenital heart defects, facial anomalies, developmental delay, and intellectual disability had a deletion of 12.75 Mb extending from 13q33.1 to 13q34 (Huang et al., 2012). The deleted region harbors 55 genes, including *NALCN* and *NLF-1*. Another study further refined a critical region for all CNS anomalies and neural tube defects taken together, to a region of 1.6 Mb (Kirchhoff et al., 2009). Only seven known genes are located within this region, including *NALCN*. A recent study aiming to identify rare DNA copy number variants in cardiovascular malformations with extracardiac abnormalities revealed the deletion of 641 kb in the *NALCN* gene region in 3 patients (Lalani et al., 2013). The extracardiac phenotypes of these patients include agenesis of corpus callosum, growth retardation, facial dysmorphism, and seizures.

ALZHEIMER'S DISEASE

Alzheimer's disease (AD) is the most common form of dementia and the most frequent degenerative brain disorder encountered in old age. The risk of developing AD substantially increases after 65 years of age (reviewed in Nussbaum and Ellis, 2003). With the exception of rare cases of early onset familial Alzheimer's disease caused by mutations in the amyloid precursor protein or presenilins genes, the etiology of the vast majority of cases remains misunderstood. There is evidence for substantial genetic influence (reviewed in St. George-Hyslop and Petit, 2005; Tanzi and Bertram, 2005). A linkage analysis to detect novel AD loci from 437 families (1252 individuals) revealed a statistically significant linkage with marker D2S2944 located in 2q34 in 31 American families with a minimum age at onset between 50 and 60 years (Scott et al., 2003). This marker is located at less than 4Mb from the *UNC-80* gene. Another study reported the existence of a susceptibility locus in 14q32.12 near marker D14S617 in a Caribbean Hispanic cohort of 1161 individuals from 209 families (Lee et al., 2008). The *UNC-79* gene lies in a region at less than 3Mb from this marker. The existence of a susceptibility locus for AD in the vicinity of the *UNC-79* gene (SNP rs11622883) was also reported by Grupe et al., 2007, from a cohort of 1808 American-European patients (Grupe et al., 2007).

ALCOHOLISM

Alcohol dependence is one of the most common and costly public health problems. Several studies suggest a role of genetic factors and few genes have been shown to be associated with alcohol dependence (reviewed in Morozova et al., 2014). A recent

GWAS performed in 118 European-American families (2322 individuals) demonstrated a significant linkage of SNP rs17484734, located in the *NALCN* gene, and high-risk of alcohol dependence (Wetherill et al., 2014). Interestingly, mice that heterologously carry a hypomorphic mutation in the *Unc-79* gene voluntarily consume more ethanol than wild-type littermates (Specia et al., 2010). A GWAS on comorbid alcohol/nicotine dependence in 599 cases and 488 controls found SNP rs12882384 as one of the three top findings, which is located within the *UNC-79* gene (Lind et al., 2010). Genome-wide significance was found for joint alcohol/nicotine comorbidity but not for nicotine or alcohol dependence alone suggesting the existence of genes that mediate the combined effect of these two addictive substances. In addition, two previous studies suggest the existence of a susceptibility locus located on chromosome 2, near the *UNC-80* gene, linked to alcohol tolerance (markers D2S425, D2S434, D2S424, D2S1323, D2S1333) and the comorbidity of alcoholism and depression (marker DS1371) respectively (Nurnberger et al., 2001; Schuckit et al., 2001).

RESTLESS LEGS SYNDROME

Restless legs syndrome (RLS) is a sensorimotor disorder characterized by abnormal sensations in the limbs that are both dependent on activity and time of day, such that symptoms are promoted by rest and relieved by activity and peak in the evening or at night (reviewed in Winkelmann et al., 2013). RLS is a genetically heterogeneous complex trait with high prevalence but large phenotype variability. Current theories of RLS pathophysiology emphasize brain iron deficiency with abnormal dopaminergic consequences, together with a strong underlying genetic background (reviewed in Dauvilliers and Winkelmann, 2013). A recent study analyzing 11 individuals from the same family indicated the existence of a locus on chromosome 13q, between SNPs rs2182885 and rs7333498 (around 5.3 Mb in size; Balaban et al., 2012). The *NALCN* gene lies in this region.

PRIMARY BILIARY CIRRHOSIS

Primary biliary cirrhosis is a chronic granulomatous cholangitis, characteristically associated with antimitochondrial antibodies. Analysis of both aggregation data from families and concordance data from twins revealed a genetic predisposition for the disease (reviewed in Hirschfield and Gershwin, 2013). A GWAS with a cohort of 2072 North-American individuals (536 patients and 1536 controls) was carried out by genotyping more than 300,000 SNPs (Hirschfield et al., 2009). Although this study reported the strongest association of the disease with HLA-related genes, a significant association was found with SNP rs2211312 in the *NLF-1* gene.

HYPERTENSION AND BLOOD PRESSURE

Hypertension is a common human disease affecting over one billion people world-wide and a major contributor to cerebrovascular accidents, myocardial infarction, congestive cardiac failure and chronic renal failure (reviewed in Zhao et al., 2013). A GWAS performed by genotyping more than 800,000 SNPs in a sample of 1017 African-American individuals led to the identification

of several potential loci involved in the regulation of blood pressure (Adeyemo et al., 2009). A significant association was found between systolic blood pressure and SNP rs9301196 located within the *NLF-1* gene.

POLYGLUTAMINE DISORDERS

Polyglutamine (polyQ)-expansions in different proteins cause at least eleven neurodegenerative diseases including Huntington disease and spinocerebellar ataxias (reviewed in Todd and Lim, 2013). These human diseases are caused by extreme expansion of the repeats, which adversely impact protein structure, often causing intracellular protein aggregation and altered protein function. Bovine NLF-1 exhibits a polymorphic polyQ tract in its sequence (Whan et al., 2010). This polyQ tract is also found in other species including human beings suggesting that aggregation of NLF-1 could be involved in neurodegenerative diseases.

CANCER

Biankin et al. examined pancreatic cancer genomes using exome sequencing and copy number analysis from a cohort of 142 patients of early (stages I and II) sporadic pancreatic ductal adenocarcinoma (Biankin et al., 2012). Analysis of genes with non-silent mutations occurring in 2 or more individual cancers identified 16 genes including *NALCN* (mutated in 4 patients). Pathway analysis allowed not only the identification of genes involved in mechanisms already known to be involved in cancer but also genes known to be involved in axon guidance. This latter finding was strengthened by the inclusion of data from another study (Jones et al., 2008). It is tempting to speculate that *NALCN* could also be involved in axon guidance.

An association of *NALCN* with non-small cell lung cancer was also suggested by a study where 217,817 SNPs were genotyped in 348 advanced patients who received chemotherapy (Lee et al., 2013). These genetic association studies revealed that SNP rs9557635, located in the genomic regions of the *NALCN* gene, was associated with this disease. Interestingly, this study also reported a strongly significant association with SNP rs2371030 located 25 kb downstream to the *CPS1* gene on chromosome 2q34, which contains the *UNC-80* gene. Further linking the channelosome to cancer, a recent study reported an *NLF-1* copy number increase in populations of tumor-derived endothelial cells that are resistant to anti-angiogenic cancer therapies (McGuire et al., 2012). Finally, in a search for key altered genomic regions in human glioblastomas, Fontanillo et al., 2012, found a high correlation between the malignant state and copy number alterations in the *NALCN* and *NLF-1* regions with a decrease in expression level (Fontanillo et al., 2012).

CONCLUDING REMARKS AND FUTURE DIRECTIONS IS NALCN REALLY A CHANNEL PER SE?

From a fundamental point of view, it remains unclear whether *NALCN* is truly an ion channel. The early findings by Ren and colleagues supported that *NALCN* was an ion channel, based on mutations in the putative selectivity filter (EEKE) that alter the permeation properties and the gadolinium block (EEKA) or inhibit the observed currents in HEK-293 cells (EEEE) (Lu et al., 2007). Further supporting this, in *D. melanogaster*, the expression

of a *na^{EEEE}* mutant in *na* neurons using the UAS-GAL4 system did not restore the studied phenotype as *na^{wt}* does (Lear et al., 2005). However, functional expression of NALCN channel in heterologous expression systems is difficult to obtain and these data do not demonstrate unambiguously that NALCN is a pore forming subunit. A clear proof of its channel activity would come from electrophysiological data exploring NALCN channel activity when rebuilt in lipid bilayers.

WHAT ARE THE GATING PROPERTIES OF NALCN?

The mechanism(s) that gate NALCN have yet to be established. On one hand, NALCN channel is described as conducting a sodium leak current in neurons both in mammals and invertebrates (Lu et al., 2007; Lu and Feng, 2011; Xie et al., 2013). On the other hand, NALCN channel also conducts a sodium current activated by acetylcholine through the M3R in a pancreatic β -cell line without any evidence for a leak current (Swayne et al., 2009). One may hypothesize that the NALCN-mediated leak current observed in neurons may result from a constitutive activity of some GPCRs (Swayne et al., 2009). In this case, it would require UNC-80 and SFKs. However, this hypothesis may not be valid for two main reasons. First, considering that HEK-293 cells do not express *UNC-79* and *UNC-80* (Swayne et al., 2009), the expression of NALCN alone is sufficient to observe a sodium leak current in these cells (Lu et al., 2007). Second, it was shown that a sodium leak current mediated by NALCN is still present in hippocampal neurons from *Unc-79* knockout mice where *UNC-80* is not detected (Lu et al., 2010). Thus, the gating properties of NALCN remain mysterious and should be investigated further. In keeping with this idea, the search for additional proteins that belong to the NALCN channelosome could give clues regarding modulation of the NALCN gating mechanism.

WHAT IS THE REPERTOIRE OF GPCRS CAPABLE OF MODULATING NALCN CHANNEL?

Recent studies have established that NALCN can be activated/potentiated or inhibited by different GPCRs (Lu et al., 2009; Swayne et al., 2009; Lu et al., 2010). Therefore, one may expect additional GPCRs to be involved in these processes. Identification of this repertoire is an important challenge and understanding why some GPCRs modulate NALCN, and some others do not, would help to understand further how NALCN is activated/regulated in neurons and how neurotransmitters and hormones affect neuronal electrophysiological properties.

WHAT ARE THE FUNCTIONAL CONSEQUENCES OF ALTERNATIVE SPLICING ON NALCN CHANNELOSOME GENES?

Alternative splicing events were demonstrated in many ion channels and can significantly impact their biophysical properties, cellular localization, and functional regulations (reviewed in Noel et al., 2011; Jan and Jan, 2012; Lipscombe et al., 2013). Alternative splicing was identified in NALCN channelosome genes (Senatore et al., 2013; Monteil unpublished data). The physiological consequences of these alternative splicing events remain to be elucidated.

ARE UNC-79, UNC-80, AND NLF-1 SPECIFIC NALCN-ANCILLARY SUBUNITS?

In *C. elegans*, *nlf-1*, *unc-79*, *unc-80*, and *nca-1;nca-2* mutants exhibit exactly similar phenotypes and both *Unc-79* and *Nalcn* knockout mice die soon after birth. However, the post-natal lethality observed in these mouse models could mask phenotypes more specific to one subunit compared to the others. As a matter of fact, we cannot exclude that *UNC-79*, *UNC-80*, and *NLF-1* may have NALCN-independent physiological roles. Conditional knockout mice for each component of the NALCN channelosome would be very helpful to clarify this point.

ARE THERE MORE PROTEINS IN THE NALCN CHANNELOSOME?

The NALCN channelosome is probably not restricted to NALCN, *UNC-79*, *UNC-80*, *NLF-1*, SFKs, and GPCRs. As an example, there is another gene highly related to *NLF-1*, *FAM155B* in mammals (accession number NG_021282.1). Whether the *FAM155B* gene product belongs to the NALCN channel complex should be investigated. Also, the mechanisms involved in the regulation of the NALCN channel by CaSR are not known and could imply a co-inclusion in the same protein complex. Some studies indicate genetic interactions between *nca-1;nca-2* and other genes in *C. elegans*. As a matter of fact, null mutants of stomatins (*unc-1* and *unc-24*) and innexins (*unc-7* and *unc-9*) were found to restore the altered sensitivity to GAs and ethanol (Sedensky and Meneely, 1987; Morgan et al., 1990; Morgan and Sedensky, 1995; Sedensky et al., 2001; Humphrey et al., 2007). It was also found that *nca-1;nca-2* mutants exhibit a reduced evoked post-synaptic current at the neuromuscular junction and this phenotype is rescued by *unc-7* mutants (Bouhours et al., 2011). However, in this latter study, co-immunofluorescent staining experiments do not show obvious neuronal co-localization of *UNC-7* and *NCA-1/NCA-2*. Thus, the reported genetic interaction between *unc-7* and *nca-1;nca-2* probably reflects a functional, rather than a physical interaction. A genetic interaction was also described between *unc-26* null mutants and *unc-80* and *nca-1;nca-2* (Jospin et al., 2007). *unc-26* encodes for Synaptojanin, a lipid phosphatase required to degrade phosphatidylinositol 4,5 bisphosphate (PIP2) at cell membranes during synaptic vesicle recycling (Cremona et al., 1999). It was found that *unc-80* and *nca-1;nca-2* mutants ameliorate the recycling defects of synaptic vesicles as well as the synaptic transmission in *unc-26* null mutants and it was suggested that *nca-1;nca-2* function could be regulated by PIP2 (Jospin et al., 2007). Whether Synaptojanin belongs to the NALCN channelosome remains to be investigated. Interestingly, *NALCN* and *PLA2G6* mutations results in similar phenotypes in humans suggesting that iPLA2 β could be a regulator of NALCN. Complementary techniques such as two-hybrid and immunoprecipitation studies followed by mass spectrometry approaches will certainly lead to the discovery of new components of the NALCN channelosome.

HOW IS NALCN FUNCTIONS MODULATED?

In addition to their regulation by binding partners, ion channels are known to be post-translationally modulated. For example, ion channel complexes can be phosphorylated by a variety of kinases which regulate their physiological roles (reviewed in

Smart, 1997; Dai et al., 2009; Cerda et al., 2011; Scheuer, 2011; Vacher and Trimmer, 2011). An *in silico* analysis of primary amino-acid sequences of NALCN, UNC-79, UNC-80, and NLF-1 reveals the existence of several predicted phosphorylation sites that are conserved in mammals and for some of these sites, are also conserved in *C. elegans*, *D. Melanogaster*, and *L. Stagnalis* (not shown). The physiological relevance of the NALCN channelosome phosphorylation, as well as the identification of the kinases involved, remains to be explored.

IN WHICH NEURONAL SUBTYPE(S) IS NALCN EXPRESSED?

NALCN, and probably UNC-79, UNC-80, and NLF-1, is widely expressed throughout the CNS in mammals (Lee et al., 1999; Swayne et al., 2009; Kang et al., 2011). To better assess the physiological role of NALCN, it is crucial to identify whether expression is restricted to some specific neuronal populations. In addition, NALCN is localized along the axons in *C. elegans* and in synaptic regions in *D. melanogaster* (Nash et al., 2002; Humphrey et al., 2007; Yeh et al., 2008), but the neuronal localization of NALCN channel proteins in mammals is unknown. The development of specific antibodies for immunohistochemistry experiments will be crucial for this purpose.

LACK OF PHARMACOLOGY OF NALCN BUT RELEVANCE OF NALCN AS A DRUG TARGET

To date, no specific pharmacology for NALCN has been reported and this clearly represents a significant hurdle in the study of NALCN properties and activity. The discovery of specific NALCN agonists/antagonists is critically needed. Such molecules would be tools to investigate NALCN's physiological roles and may also hold interest to develop innovative therapeutic strategies. Whether the NALCN channelosome represents a drug target of interest remains unclear at the present time. Considering that NALCN channel is expressed in pancreatic islets, both in α - and β -cells, and is possibly involved in the regulation of insulin secretion (Kutlu et al., 2009 and <http://t1dbase.org>; Swayne et al., 2010), targeting NALCN might be relevant to treat type 2 diabetes. It is tempting to speculate that agonists of NALCN would have beneficial effects in pancreatic β -cells on insulin secretion (reviewed in Gilon and Rorsman, 2009). NALCN blockers might be relevant to treat pain considering that SP plays a pivotal role in the transmission of noxious stimuli in the spinal cord (reviewed in Seybold, 2009) and that NALCN is highly expressed in the dorsal spinal cord compared to the ventral spinal cord (Sun et al., 2002). Based on the potential implication of NALCN channel in human physiology and diseases, its pharmacological targeting might also be relevant to treat epilepsy, bowel motility disorders, osmoregulation disorders and psychiatric disorders.

SUMMARY

The NALCN channelosome is vital in mammals: homozygous mutant mice exhibit neonatal lethal phenotype and NALCN plays a crucial role in neuronal excitability. NALCN is involved in the regulation of resting membrane potential and is modulated by hormones and neurotransmitters. In the present article, we provide an extensive review of the literature describing the molecular and functional properties of the NALCN channelosome, the

various phenotypes observed in NALCN animal models, as well as the recent implications of NALCN in human diseases. We also discuss how NALCN could represent a therapeutic target to treat a wide variety of human diseases, especially neurological and psychiatric diseases. Unfortunately, the lack of specific pharmacology is clearly a brake to all the NALCN investigations. In the coming years, the expected development of selective agonists/antagonists, as well as new animal models, should foster our understanding of the functional properties and physiological roles of the NALCN channelosome.

ACKNOWLEDGMENTS

The authors are grateful to Stephanie Knapp who participated to the early writing steps of this review article. We thank Sarah England, Erin Reinl, and Natalia Prevarskaia for critical readings and comments on the manuscript and Drs. Céline Lemmers, Isabelle Bidaud, Samer Khoury-Hanna, Hamid Gholamipour-Badie, and Adriano Senatore for their contribution to the work performed in the laboratory. Our laboratory is supported by a grant from "Agence Nationale de la Recherche" 11 BSV1 004 01 and is part of the Laboratory of Excellence "Ion Channel Science and Therapeutics" (<http://www.labex-icst.fr/en>; ANR-11-LABX-0015-01_ICST).

REFERENCES

- Adeyemo, A., Gerry, N., Chen, G., Herbert, A., Doumatey, A., Huang, H., et al. (2009). A genome-wide association study of hypertension and blood pressure in African Americans. *PLoS Genet.* 5:e1000564. doi: 10.1371/journal.pgen.1000564
- Alanay, Y., Aktas, D., Utine, E., Talim, B., Onderoglu, L., Caglar, M., et al. (2005). Is Dandy-Walker malformation associated with "distal 13q deletion syndrome?" Findings in a fetus supporting previous observations. *Am. J. Med. Genet. A* 136, 265–268. doi: 10.1002/ajmg.a.30808
- Allderdice, P. W., Davis, J. G., Miller, O. J., Klinger, H. P., Warburton, D., Miller, D. A., et al. (1969). The 13q-deletion syndrome. *Am. J. Hum. Genet.* 21, 499–512.
- Al-Sayed, M. D., Al-Zaidan, H., Albakheet, A., Hakami, H., Kenana, R., Al-Yafee, Y., et al. (2013). Mutations in NALCN cause an autosomal-recessive syndrome with severe hypotonia, speech impairment, and cognitive delay. *Am. J. Hum. Genet.* 93, 721–726. doi: 10.1016/j.ajhg.2013.08.001
- Anney, R. J., Lasky-Su, J., O'Dushlaine, C., Kenny, E., Neale, B. M., Mulligan, A., et al. (2008). Conduct disorder and ADHD: evaluation of conduct problems as a categorical and quantitative trait in the international multicentre ADHD genetics study. *Am. J. Med. Genet. B Neuropsychiatr. Genet.* 147B, 1369–1378. doi: 10.1002/ajmg.b.30871
- Ashcroft, F. M. (2006). From molecule to malady. *Nature* 440, 440–447. doi: 10.1038/nature04707
- Askland, K., Read, C., and Moore, J. (2009). Pathways-based analyses of whole-genome association study data in bipolar disorder reveal genes mediating ion channel activity and synaptic neurotransmission. *Hum. Genet.* 125, 63–79. doi: 10.1007/s00439-008-0600-y
- Balaban, H., Bayrakli, F., Kartal, U., Pinarbasi, E., Topaktas, S., and Kars, H. Z. (2012). A novel locus for restless legs syndrome on chromosome 13q. *Eur. Neurol.* 68, 111–116. doi: 10.1159/000338779
- Ballarati, L., Rossi, E., Bonati, M. T., Gimelli, S., Maraschio, P., Finelli, P., et al. (2007). 13q Deletion and central nervous system anomalies: further insights from karyotype-phenotype analyses of 14 patients. *J. Med. Genet.* 44, e60. doi: 10.1136/jmg.2006.043059
- Barry, G. (2014). Integrating the roles of long and small non-coding RNA in brain function and disease. *Mol. Psychiatry* 19, 410–416. doi: 10.1038/mp.2013.196
- Baum, A. E., Akula, N., Cabanero, M., Cardona, I., Corona, W., Klemens, B., et al. (2008). A genome-wide association study implicates diacylglycerol kinase ϵ (DGKH) and several other genes in the etiology of bipolar disorder. *Mol. Psychiatry* 13, 197–207. doi: 10.1038/sj.mp.4002012

- Belle, M. D., Diekmann, C. O., Forger, D. B., and Piggins, H. D. (2009). Daily electrical silencing in the mammalian circadian clock. *Science* 326, 281–284. doi: 10.1126/science.1169657
- Biankin, A. V., Waddell, N., Kassahn, K. S., Gingras, M. C., Muthuswamy, L. B., Johns, A. L., et al. (2012). Pancreatic cancer genomes reveal aberrations in axon guidance pathway genes. *Nature* 491, 399–405. doi: 10.1038/nature11547
- Bouhours, M., Po, M. D., Gao, S., Hung, W., Li, H., Georgiou, J., et al. (2011). A co-operative regulation of neuronal excitability by UNC-7 innexin and NCA/NALCN leak channel. *Mol. Brain* 4:16. doi: 10.1186/1756-6606-4-16
- Brown, S., Russo, J., Chitayat, D., and Warburton, D. (1995). The 13q- syndrome: the molecular definition of a critical deletion region in band 13q32. *Am. J. Hum. Genet.* 57, 859–866.
- Burg, E. D., Langan, S. T., and Nash, H. A. (2013). *Drosophila* social clustering is disrupted by anesthetics and in narrow abdomen ion channel mutants. *Genes Brain Behav.* 12, 338–347. doi: 10.1111/gbb.12025
- Butler, A. G., Duffey, P. O., Hawthorne, M. R., and Barnes, M. P. (2004). An epidemiologic survey of dystonia within the entire population of northeast England over the past nine years. *Adv. Neurol.* 94, 95–99.
- Cahoy, J. D., Emery, B., Kaushal, A., Foo, L. C., Zamanian, J. L., Christopherson, K. S., et al. (2008). A transcriptome database for astrocytes, neurons, and oligodendrocytes: a new resource for understanding brain development and function. *J. Neurosci.* 28, 264–278. doi: 10.1523/JNEUROSCI.4178-07.2008
- Camerino, D. C., Desaphy, J. F., Tricarico, D., Pierno, S., and Liantonio, A. (2008). Therapeutic approaches to ion channel diseases. *Adv. Genet.* 64, 81–145. doi: 10.1016/S0065-2660(08)00804-3
- Campbell, D. B., and Nash, H. A. (1994). Use of *Drosophila* mutants to distinguish among volatile general anesthetics. *Proc. Natl. Acad. Sci. U.S.A.* 91, 2135–2139. doi: 10.1073/pnas.91.6.2135
- Campbell, J. L., and Nash, H. A. (2001). Volatile general anesthetics reveal a neurobiological role for the white and brown genes of *Drosophila melanogaster*. *J. Neurobiol.* 49, 339–349. doi: 10.1002/neu.10009
- Cerda, O., Baek, J. H., and Trimmer, J. S. (2011). Mining recent brain proteomic databases for ion channel phosphosite nuggets. *J. Gen. Physiol.* 137, 3–16. doi: 10.1085/jgp.201010555
- Chau, P. L. (2010). New insights into the molecular mechanisms of general anesthetics. *Br. J. Pharmacol.* 161, 288–307. doi: 10.1111/j.1476-5381.2010.00891.x
- Clare, J. J. (2010). Targeting ion channels for drug discovery. *Discov. Med.* 9, 253–260.
- Cowen, D., and Olmstead, E. V. (1963). Infantile neuroaxonal dystrophy. *J. Neuropathol. Exp. Neurol.* 22, 175–236. doi: 10.1097/00005072-196304000-00001
- Cremona, O., Di Paolo, G., Wenk, M. R., Luthi, A., Kim, W. T., Takei, K., et al. (1999). Essential role of phosphoinositide metabolism in synaptic vesicle recycling. *Cell* 99, 179–188. doi: 10.1016/S0092-8674(00)81649-9
- Dai, S., Hall, D. D., and Hell, J. W. (2009). Supramolecular assemblies and localized regulation of voltage-gated ion channels. *Physiol. Rev.* 89, 411–452. doi: 10.1152/physrev.00029.2007
- Dauvilliers, Y., and Winkelmann, J. (2013). Restless legs syndrome: update on pathogenesis. *Curr. Opin. Pulm. Med.* 19, 594–600. doi: 10.1097/MCP.0b013e328365ab07
- Detera-Wadleigh, S. D., and McMahon, F. J. (2006). G72/G30 in schizophrenia and bipolar disorder: review and meta-analysis. *Biol. Psychiatry* 60, 106–114. doi: 10.1016/j.biopsych.2006.01.019
- EPICURE Consortium, Leu, C., De Kovel, C. G., Zara, F., Striano, P., Pezzella, M., et al. (2012). Genome-wide linkage meta-analysis identifies susceptibility loci at 2q34 and 13q31.3 for genetic generalized epilepsies. *Epilepsia* 53, 308–318. doi: 10.1111/j.1528-1167.2011.03379.x
- Epidemiological Study of Dystonia in Europe Collaborative, G. (2000). A prevalence study of primary dystonia in eight European countries. *J. Neurol.* 247, 787–792. doi: 10.1007/s004150070094
- Fahn, S., Bressman, S. B., and Marsden, C. D. (1998). Classification of dystonia. *Adv. Neurol.* 78, 1–10.
- Feldman, J. L., Del Negro, C. A., and Gray, P. A. (2013). Understanding the rhythm of breathing: so near, yet so far. *Annu. Rev. Physiol.* 75, 423–452. doi: 10.1146/annurev-physiol-040510-130049
- Fontanillo, C., Aibar, S., Sanchez-Santos, J. M., and De Las Rivas, J. (2012). Combined analysis of genome-wide expression and copy number profiles to identify key altered genomic regions in cancer. *BMC Genomics* 13(Suppl. 5):S5. doi: 10.1186/1471-2164-13-S5-S5
- Garcia, N. M., Allgood, J., Santos, L. J., Lonergan, D., Batanian, J. R., Henkemeyer, M., et al. (2006). Deletion mapping of critical region for hypospadias, penoscrotal transposition and imperforate anus on human chromosome 13. *J. Pediatr. Urol.* 2, 233–242. doi: 10.1016/j.jpuro.2006.03.006
- Geisler, S., and Coller, J. (2013). RNA in unexpected places: long non-coding RNA functions in diverse cellular contexts. *Nat. Rev. Mol. Cell Biol.* 14, 699–712. doi: 10.1038/nrm3679
- Ghezzi A., Liebeskind, B. J., Thompson A., Atkinson, N. S., and Zakonm H. H. (2014). Ancient association between cation leak channels and Mid1 proteins is conserved in fungi and animals. *Front. Mol. Neurosci.* 7:15. doi: 10.3389/fnmol.2014.00015
- Gilon, P., and Rorsman, P. (2009). NALCN: a regulated leak channel. *EMBO Rep.* 10, 963–964. doi: 10.1038/embor.2009.185
- Gregory, A., Kurian, M. A., Maher, E. R., Hogarth, P., and Hayflick, S. J. (1993). “PLA2G6-associated neurodegeneration,” in *GeneReviews*, eds R. A. Pagon, M. P. Adam, T. D. Bird, C. R. Dolan, C. T. Fong, and K. Stephens (Seattle, WA). Available online at: <http://www.ncbi.nlm.nih.gov/books/NBK1675/>
- Groen, J. L., Simon-Sanchez, J., Ritz, K., Bochdanovits, Z., Fang, Y., Van Hilten, J. J., et al. (2013). Cervical dystonia and genetic common variation in the dopamine pathway. *Parkinsonism Relat. Disord.* 19, 346–349. doi: 10.1016/j.parkreldis.2012.08.016
- Grupe, A., Abraham, R., Li, Y., Rowland, C., Hollingworth, P., Morgan, A., et al. (2007). Evidence for novel susceptibility genes for late-onset Alzheimer's disease from a genome-wide association study of putative functional variants. *Hum. Mol. Genet.* 16, 865–873. doi: 10.1093/hmg/ddm031
- Gruss, M., Bushell, T. J., Bright, D. P., Lieb, W. R., Mathie, A., and Franks, N. P. (2004). Two-pore-domain K⁺ channels are a novel target for the anesthetic gases xenon, nitrous oxide, and cyclopropane. *Mol. Pharmacol.* 65, 443–452. doi: 10.1124/mol.65.2.443
- Guan, Z., Scott, R. L., and Nash, H. A. (2000). A new assay for the genetic study of general anesthesia in *Drosophila melanogaster*: use in analysis of mutations in the X-chromosomal 12E region. *J. Neurogenet.* 14, 25–42. doi: 10.3109/01677060009083475
- Guerineau, N. C., Bossu, J. L., Gahwiler, B. H., and Gerber, U. (1995). Activation of a nonselective cationic conductance by metabotropic glutamatergic and muscarinic agonists in CA3 pyramidal neurons of the rat hippocampus. *J. Neurosci.* 15, 4395–4407.
- Hille, B. (2001). *Ion Channels of Excitable Membranes*. Sunderland, MA: Sinauer Associates, Inc.
- Hirschfield, G. M., and Gershwin, M. E. (2013). The immunobiology and pathophysiology of primary biliary cirrhosis. *Annu. Rev. Pathol.* 8, 303–330. doi: 10.1146/annurev-pathol-020712-164014
- Hirschfield, G. M., Liu, X., Xu, C., Lu, Y., Xie, G., Lu, Y., et al. (2009). Primary biliary cirrhosis associated with HLA, IL12A, and IL12RB2 variants. *N. Engl. J. Med.* 360, 2544–2555. doi: 10.1056/NEJMoa0810440
- Huang, C., Yang, Y. F., Yin, N., Chen, J. L., Wang, J., Zhang, H., et al. (2012). Congenital heart defect and mental retardation in a patient with a 13q33.1-34 deletion. *Gene* 498, 308–310. doi: 10.1016/j.gene.2012.01.083
- Humphrey, J. A., Hamming, K. S., Thacker, C. M., Scott, R. L., Sedensky, M. M., Snutch, T. P., et al. (2007). A putative cation channel and its novel regulator: cross-species conservation of effects on general anesthesia. *Curr. Biol.* 17, 624–629. doi: 10.1016/j.cub.2007.02.037
- Iossifov, I., Ronemus, M., Levy, D., Wang, Z., Hakker, I., Rosenbaum, J., et al. (2012). De novo gene disruptions in children on the autistic spectrum. *Neuron* 74, 285–299. doi: 10.1016/j.neuron.2012.04.009
- Jan, L. Y., and Jan, Y. N. (2012). Voltage-gated potassium channels and the diversity of electrical signalling. *J. Physiol.* 590, 2591–2599. doi: 10.1113/jphysiol.2011.224212
- Jankovic, J., Tsui, J., and Bergeron, C. (2007). Prevalence of cervical dystonia and spasmodic torticollis in the United States general population. *Parkinsonism Relat. Disord.* 13, 411–416. doi: 10.1016/j.parkreldis.2007.02.005
- Jones, E. J., Gliga, T., Bedford, R., Charman, T., and Johnson, M. H. (2014). Developmental pathways to autism: a review of prospective studies of infants at risk. *Neurosci. Biobehav. Rev.* 39C, 1–33. doi: 10.1016/j.neubiorev.2013.12.001
- Jones, S., Zhang, X., Parsons, D. W., Lin, J. C., Leary, R. J., Angenendt, P., et al. (2008). Core signaling pathways in human pancreatic cancers revealed by global genomic analyses. *Science* 321, 1801–1806. doi: 10.1126/science.1164368
- Jospin, M., Watanabe, S., Joshi, D., Young, S., Hamming, K., Thacker, C., et al. (2007). UNC-80 and the NCA ion channels contribute to endocytosis defects

- in synaptotagmin mutants. *Curr. Biol.* 17, 1595–1600. doi: 10.1016/j.cub.2007.08.036
- Kaczorowski, G. J., McManus, O. B., Priest, B. T., and Garcia, M. L. (2008). Ion channels as drug targets: the next GPCRs. *J. Gen. Physiol.* 131, 399–405. doi: 10.1085/jgp.200709946
- Kang, H. J., Kawasawa, Y. I., Cheng, F., Zhu, Y., Xu, X., Li, M., et al. (2011). Spatio-temporal transcriptome of the human brain. *Nature* 478, 483–489. doi: 10.1038/nature10523
- Khan, S., and Al Baradie, R. (2012). Epileptic encephalopathies: an overview. *Epilepsy Res. Treat.* 2012:403592. doi: 10.1155/2012/403592
- Khateeb, S., Flusser, H., Ofir, R., Shelef, I., Narkis, G., Vardi, G., et al. (2006). PLA2G6 mutation underlies infantile neuroaxonal dystrophy. *Am. J. Hum. Genet.* 79, 942–948. doi: 10.1086/508572
- Kim, B. J., Chang, I. Y., Choi, S., Jun, J. Y., Jeon, J. H., Xu, W. X., et al. (2012). Involvement of Na⁺-leak channel in substance P-induced depolarization of pacemaking activity in interstitial cells of Cajal. *Cell. Physiol. Biochem.* 29, 501–510. doi: 10.1159/000338504
- Kirchhoff, M., Bisgaard, A. M., Stoeve, R., Dimitrov, B., Gillesen-Kaesbach, G., Fryns, J. P., et al. (2009). Phenotypic and 244k array-CGH characterization of chromosome 13q deletions: an update of the phenotypic map of 13q21.1-qter. *Am. J. Med. Genet. A* 149A, 894–905. doi: 10.1002/ajmg.a.32814
- Koroglu, C., Seven, M., and Tolun, A. (2013). Recessive truncating NALCN mutation in infantile neuroaxonal dystrophy with facial dysmorphism. *J. Med. Genet.* 50, 515–520. doi: 10.1136/jmedgenet-2013-101634
- Krishnan, K. S., and Nash, H. A. (1990). A genetic study of the anesthetic response: mutants of *Drosophila melanogaster* altered in sensitivity to halothane. *Proc. Natl. Acad. Sci. U.S.A.* 87, 8632–8636. doi: 10.1073/pnas.87.21.8632
- Kutlu, B., Burdick, D., Baxter, D., Rasschaert, J., Flamez, D., Eizirik, D. L., et al. (2009). Detailed transcriptome atlas of the pancreatic beta cell. *BMC Med. Genomics* 2:3. doi: 10.1186/1755-8794-2-3
- Lalani, S. R., Shaw, C., Wang, X., Patel, A., Patterson, L. W., Kolodziejaska, K., et al. (2013). Rare DNA copy number variants in cardiovascular malformations with extracardiac abnormalities. *Eur. J. Hum. Genet.* 21, 173–181. doi: 10.1038/ejhg.2012.155
- Lear, B. C., Darrah, E. J., Aldrich, B. T., Gebre, S., Scott, R. L., Nash, H. A., et al. (2013). UNC79 and UNC80, putative auxiliary subunits of the NARROW ABDOMEN ion channel, are indispensable for robust circadian locomotor rhythms in *Drosophila*. *PLoS ONE* 8:e78147. doi: 10.1371/journal.pone.0078147
- Lear, B. C., Lin, J. M., Keath, J. R., McGill, J. J., Raman, I. M., and Allada, R. (2005). The ion channel narrow abdomen is critical for neural output of the *Drosophila* circadian pacemaker. *Neuron* 48, 965–976. doi: 10.1016/j.neuron.2005.10.030
- Lee, J. H., Barral, S., Cheng, R., Chacon, I., Santana, V., Williamson, J., et al. (2008). Age-at-onset linkage analysis in Caribbean Hispanics with familial late-onset Alzheimer's disease. *Neurogenetics* 9, 51–60. doi: 10.1007/s10048-007-0103-3
- Lee, J. H., Cribbs, L. L., and Perez-Reyes, E. (1999). Cloning of a novel four repeat protein related to voltage-gated sodium and calcium channels. *FEBS Lett.* 445, 231–236. doi: 10.1016/S0014-5793(99)00082-4
- Lee, Y., Yoon, K. A., Joo, J., Lee, D., Bae, K., Han, J. Y., et al. (2013). Prognostic implications of genetic variants in advanced non-small cell lung cancer: a genome-wide association study. *Carcinogenesis* 34, 307–313. doi: 10.1093/carcin/bgs356
- Lele, K. P., Penrose, L. S., and Stallard, H. B. (1963). Chromosome Deletion in a Case of Retinoblastoma. *Ann. Hum. Genet.* 27, 171–174. doi: 10.1111/j.1469-1809.1963.tb00209.x
- Lenox, R. H., Gould, T. D., and Manji, H. K. (2002). Endophenotypes in bipolar disorder. *Am. J. Med. Genet.* 114, 391–406. doi: 10.1002/ajmg.10360
- Lerche, H., Shah, M., Beck, H., Noebels, J., Johnston, D., and Vincent, A. (2013). Ion channels in genetic and acquired forms of epilepsy. *J. Physiol.* 591, 753–764. doi: 10.1113/jphysiol.2012.240606
- Liesbeskind, B. J., Hillis, D. M., and Zakon, H. H. (2012). Phylogeny unites animal sodium leak channels with fungal calcium channels in an ancient, voltage-insensitive clade. *Mol. Biol. Evol.* 29, 3613–3616. doi: 10.1093/molbev/mss182
- Lind, P. A., Macgregor, S., Vink, J. M., Pergadia, M. L., Hansell, N. K., De Moor, M. H., et al. (2010). A genome-wide association study of nicotine and alcohol dependence in Australian and Dutch populations. *Twin Res. Hum. Genet.* 13, 10–29. doi: 10.1375/twin.13.1.10
- Lipscombe, D., Andrade, A., and Allen, S. E. (2013). Alternative splicing: functional diversity among voltage-gated calcium channels and behavioral consequences. *Biochim. Biophys. Acta* 1828, 1522–1529. doi: 10.1016/j.bbame.2012.09.018
- Liu, C., Au, J. D., Zou, H. L., Cotten, J. E., and Yost, C. S. (2004). Potent activation of the human tandem pore domain K channel TRESK with clinical concentrations of volatile anesthetics. *Anesth. Analg.* 99, 1715–1722. doi: 10.1213/01.ANE.0000136849.07384.44
- Lu, B., Su, Y., Das, S., Liu, J., Xia, J., and Ren, D. (2007). The neuronal channel NALCN contributes resting sodium permeability and is required for normal respiratory rhythm. *Cell* 129, 371–383. doi: 10.1016/j.cell.2007.02.041
- Lu, B., Su, Y., Das, S., Wang, H., Wang, Y., Liu, J., et al. (2009). Peptide neurotransmitters activate a cation channel complex of NALCN and UNC-80. *Nature* 457, 741–744. doi: 10.1038/nature07579
- Lu, B., Zhang, Q., Wang, H., Wang, Y., Nakayama, M., and Ren, D. (2010). Extracellular calcium controls background current and neuronal excitability via an UNC79-UNC80-NALCN cation channel complex. *Neuron* 68, 488–499. doi: 10.1016/j.neuron.2010.09.014
- Lu, T. Z., and Feng, Z. P. (2011). A sodium leak current regulates pacemaker activity of adult central pattern generator neurons in *Limnaea stagnalis*. *PLoS ONE* 6:e18745. doi: 10.1371/journal.pone.0018745
- Lu, T. Z., and Feng, Z. P. (2012). NALCN: a regulator of pacemaker activity. *Mol. Neurobiol.* 45, 415–423. doi: 10.1007/s12035-012-8260-2
- Luo, J., Balkin, N., Stewart, J. F., Sarwark, J. F., Charrow, J., and Nye, J. S. (2000). Neural tube defects and the 13q deletion syndrome: evidence for a critical region in 13q33–34. *Am. J. Med. Genet.* 91, 227–230. doi: 10.1002/(SICI)1096-8628(20000320)91:3<227::AID-AJMG14>3.0.CO;2-I
- Mantegazza, M., Rusconi, R., Scalmani, P., Avanzini, G., and Franceschetti, S. (2010). Epileptogenic ion channel mutations: from bedside to bench and, hopefully, back again. *Epilepsy Res.* 92, 1–29. doi: 10.1016/j.eplepsyres.2010.08.003
- Maruoka, T., Nagasoe, Y., Inoue, S., Mori, Y., Goto, J., Ikeda, M., et al. (2002). Essential hydrophilic carboxyl-terminal regions including cysteine residues of the yeast stretch-activated calcium-permeable channel Mid1. *J. Biol. Chem.* 277, 11645–11652. doi: 10.1074/jbc.M111603200
- McCormack, W. M. Jr., Shen, J. J., Curry, S. M., Berend, S. A., Kashork, C., Pinar, H., et al. (2002). Partial deletions of the long arm of chromosome 13 associated with holoprosencephaly and the Dandy-Walker malformation. *Am. J. Med. Genet.* 112, 384–389. doi: 10.1002/ajmg.10659
- McGuire, T. F., Sajithlal, G. B., Lu, J., Nicholls, R. D., and Prochownik, E. V. (2012). *In vivo* evolution of tumor-derived endothelial cells. *PLoS ONE* 7:e37138. doi: 10.1371/journal.pone.0037138
- Mead, C. L., Kuzyk, M. A., Moradian, A., Wilson, G. M., Holt, R. A., and Morin, G. B. (2010). Cytosolic protein interactions of the schizophrenia susceptibility gene dysbindin. *J. Neurochem.* 113, 1491–1503. doi: 10.1111/j.1471-4159.2010.06690.x
- Minami, K., and Uezono, Y. (2013). The recent progress in research on effects of anesthetics and analgesics on G protein-coupled receptors. *J. Anesth.* 27, 284–292. doi: 10.1007/s00540-012-1507-2
- Mir, B., Iyer, S., Ramaswami, M., and Krishnan, K. S. (1997). A genetic and mosaic analysis of a locus involved in the anesthesia response of *Drosophila melanogaster*. *Genetics* 147, 701–712.
- Mok, K. Y., Schneider, S. A., Trabzuni, D., Stamelou, M., Edwards, M., Kasperavičiute, D., et al. (2013). Genomewide association study in cervical dystonia demonstrates possible association with sodium leak channel. *Mov. Disord.* 29, 245–251. doi: 10.1002/mds.25732
- Morgan, N. V., Westaway, S. K., Morton, J. E., Gregory, A., Gissen, P., Sonek, S., et al. (2006). PLA2G6, encoding a phospholipase A2, is mutated in neurodegenerative disorders with high brain iron. *Nat. Genet.* 38, 752–754. doi: 10.1038/ng1826
- Morgan, P. G., and Cascorbi, H. F. (1985). Effect of anesthetics and a convulsant on normal and mutant *Caenorhabditis elegans*. *Anesthesiology* 62, 738–744. doi: 10.1097/0000542-198506000-00007
- Morgan, P. G., Sedensky, M., and Meneely, P. M. (1990). Multiple sites of action of volatile anesthetics in *Caenorhabditis elegans*. *Proc. Natl. Acad. Sci. U.S.A.* 87, 2965–2969. doi: 10.1073/pnas.87.8.2965
- Morgan, P. G., and Sedensky, M. M. (1995). Mutations affecting sensitivity to ethanol in the nematode, *Caenorhabditis elegans*. *Alcohol. Clin. Exp. Res.* 19, 1423–1429. doi: 10.1111/j.1530-0277.1995.tb01002.x
- Morgan, P. G., Sedensky, M. M., Meneely, P. M., and Cascorbi, H. F. (1988). The effect of two genes on anesthetic response in the nematode *Caenorhabditis elegans*. *Anesthesiology* 69, 246–251. doi: 10.1097/0000542-198808000-00015
- Morozova, T. V., Mackay, T. F., and Anholt, R. R. (2014). Genetics and genomics of alcohol sensitivity. *Mol. Genet. Genomics*. doi: 10.1007/s00438-013-0808-y. [Epub ahead of print].

- Muller, J., Kiechl, S., Wenning, G. K., Seppi, K., Willeit, J., Gasperi, A., et al. (2002). The prevalence of primary dystonia in the general community. *Neurology* 59, 941–943. doi: 10.1212/01.WNL.0000026474.12594.0D
- Nakashima, K., Kusumi, M., Inoue, Y., and Takahashi, K. (1995). Prevalence of focal dystonias in the western area of Tottori Prefecture in Japan. *Mov. Disord.* 10, 440–443. doi: 10.1002/mds.870100406
- Nakayama, M., Iida, M., Koseki, H., and Ohara, O. (2006). A gene-targeting approach for functional characterization of KIAA genes encoding extremely large proteins. *FASEB J.* 20, 1718–1720. doi: 10.1096/fj.06-5952fj
- Nash, H. A., Campbell, D. B., and Krishnan, K. S. (1991). New mutants of *Drosophila* that are resistant to the anesthetic effects of halothane. *Ann. N.Y. Acad. Sci.* 625, 540–544. doi: 10.1111/j.1749-6632.1991.tb33885.x
- Nash, H. A., Scott, R. L., Lear, B. C., and Allada, R. (2002). An unusual cation channel mediates photic control of locomotion in *Drosophila*. *Curr. Biol.* 12, 2152–2158. doi: 10.1016/S0960-9822(02)01358-1
- Nishikawa, K., and Kidokoro, Y. (1999). Halothane presynaptically depresses synaptic transmission in wild-type *Drosophila* larvae but not in halothane-resistant (har) mutants. *Anesthesiology* 90, 1691–1697. doi: 10.1097/0000542-199906000-00026
- Nitabach, M. N., Blau, J., and Holmes, T. C. (2002). Electrical silencing of *Drosophila* pacemaker neurons stops the free-running circadian clock. *Cell* 109, 485–495. doi: 10.1016/S0092-8674(02)00737-7
- Noel, J., Sandoz, G., and Lesage, F. (2011). Molecular regulations governing TREK and TRAAK channel functions. *Channels (Austin)* 5, 402–409. doi: 10.4161/chan.5.5.16469
- Nurnberger, J. I. Jr., Foroud, T., Flury, L., Su, J., Meyer, E. T., Hu, K., et al. (2001). Evidence for a locus on chromosome 1 that influences vulnerability to alcoholism and affective disorder. *Am. J. Psychiatry* 158, 718–724. doi: 10.1176/appi.ajp.158.5.718
- Nussbaum, R. L., and Ellis, C. E. (2003). Alzheimer's disease and Parkinson's disease. *N. Engl. J. Med.* 348, 1356–1364. doi: 10.1056/NEJM2003ra020003
- Nutt, J. G., Muenster, M. D., Aronson, A., Kurland, L. T., and Melton, L. J., 3rd. (1988). Epidemiology of focal and generalized dystonia in Rochester, Minnesota. *Mov. Disord.* 3, 188–194. doi: 10.1002/mds.870030302
- Ollila, H. M., Soronen, P., Silander, K., Palo, O. M., Kiesepa, T., Kaunisto, M. A., et al. (2009). Findings from bipolar disorder genome-wide association studies replicate in a Finnish bipolar family-cohort. *Mol. Psychiatry* 14, 351–353. doi: 10.1038/mp.2008.122
- Patel, A. J., Honore, E., Lesage, F., Fink, M., Romey, G., and Lazdunski, M. (1999). Inhalational anesthetics activate two-pore-domain background K⁺ channels. *Nat. Neurosci.* 2, 422–426. doi: 10.1038/8084
- Pei, J., and Grishin, N. V. (2012). Cysteine-rich domains related to Frizzled receptors and Hedgehog-interacting proteins. *Protein Sci.* 21, 1172–1184. doi: 10.1002/pro.2105
- Pierce-Shimomura, J. T., Chen, B. L., Mun, J. J., Ho, R., Sarkis, R., and McIntire, S. L. (2008). Genetic analysis of crawling and swimming locomotory patterns in *C. elegans*. *Proc. Natl. Acad. Sci. U.S.A.* 105, 20982–20987. doi: 10.1073/pnas.0810359105
- Ptak, K., Yamanishi, T., Aungst, J., Milescu, L. S., Zhang, R., Richerson, G. B., et al. (2009). Raphe neurons stimulate respiratory circuit activity by multiple mechanisms via endogenously released serotonin and substance P. *J. Neurosci.* 29, 3720–3737. doi: 10.1523/JNEUROSCI.5271-08.2009
- Quelin, C., Bendavid, C., Dubourg, C., De La Rochebrochard, C., Lucas, J., Henry, C., et al. (2009). Twelve new patients with 13q deletion syndrome: genotype-phenotype analyses in progress. *Eur. J. Med. Genet.* 52, 41–46. doi: 10.1016/j.ejmg.2008.10.002
- Rajaram, S., Spangler, T. L., Sedensky, M. M., and Morgan, P. G. (1999). A stomatin and a degenerin interact to control anesthetic sensitivity in *Caenorhabditis elegans*. *Genetics* 153, 1673–1682.
- Ratnapriya, R., Vijai, J., Kadandale, J. S., Iyer, R. S., Radhakrishnan, K., and Anand, A. (2010). A locus for juvenile myoclonic epilepsy maps to 2q33-q36. *Hum. Genet.* 128, 123–130. doi: 10.1007/s00439-010-0831-6
- Ren, D. (2011). Sodium leak channels in neuronal excitability and rhythmic behaviors. *Neuron* 72, 899–911. doi: 10.1016/j.neuron.2011.12.007
- Rorsman, P., and Braun, M. (2013). Regulation of insulin secretion in human pancreatic islets. *Annu. Rev. Physiol.* 75, 155–179. doi: 10.1146/annurev-physiol-030212-183754
- Sabin, L. R., Delas, M. J., and Hannon, G. J. (2013). Dogma derailed: the many influences of RNA on the genome. *Mol. Cell* 49, 783–794. doi: 10.1016/j.molcel.2013.02.010
- Sander, J. W. (2003). The epidemiology of epilepsy revisited. *Curr. Opin. Neurol.* 16, 165–170. doi: 10.1097/01.wco.0000063766.15877.8e
- Scheuer, T. (2011). Regulation of sodium channel activity by phosphorylation. *Semin. Cell Dev. Biol.* 22, 160–165. doi: 10.1016/j.semcdb.2010.10.002
- Schuckit, M. A., Edenberg, H. J., Kalmijn, J., Flury, L., Smith, T. L., Reich, T., et al. (2001). A genome-wide search for genes that relate to a low level of response to alcohol. *Alcohol. Clin. Exp. Res.* 25, 323–329. doi: 10.1111/j.1530-0277.2001.tb02217
- Scott, W. K., Hauser, E. R., Schmechel, D. E., Welsh-Bohmer, K. A., Small, G. W., Roses, A. D., et al. (2003). Ordered-subsets linkage analysis detects novel Alzheimer disease loci on chromosomes 2q34 and 15q22. *Am. J. Hum. Genet.* 73, 1041–1051. doi: 10.1086/379083
- Sedensky, M. M., and Meneely, P. M. (1987). Genetic analysis of halothane sensitivity in *Caenorhabditis elegans*. *Science* 236, 952–954. doi: 10.1126/science.3576211
- Sedensky, M. M., Siefker, J. M., and Morgan, P. G. (2001). Model organisms: new insights into ion channel and transporter function. Stomatin homologues interact in *Caenorhabditis elegans*. *Am. J. Physiol. Cell Physiol.* 280, C1340–C1348.
- Senatore, A., Monteil, A., Van Minnen, J., Smit, A. B., and Spafford, J. D. (2013). NALCN ion channels have alternative selectivity filters resembling calcium channels or sodium channels. *PLoS ONE* 8:e55088. doi: 10.1371/journal.pone.0055088
- Senatore, A., and Spafford, J. D. (2013). A uniquely adaptable pore is consistent with NALCN being an ion sensor. *Channels (Austin)* 7, 60–68. doi: 10.4161/chan.23981
- Seven, M., Ozkiliç, A., and Yuksel, A. (2002). Dysmorphic face in two siblings with infantile neuroaxonal dystrophy. *Genet. Couns.* 13, 465–473.
- Seybold, V. S. (2009). The role of peptides in central sensitization. *Handb. Exp. Pharmacol.* 451–491. doi: 10.1007/978-3-540-79090-7_13
- Sharma, A., and Couture, J. (2014). A review of the pathophysiology, etiology, and treatment of attention-deficit hyperactivity disorder (ADHD). *Ann. Pharmacother.* 48, 209–225. doi: 10.1177/1060028013510699
- Silveira, C., Marques-Teixeira, J., and De Bastos-Leite, A. J. (2012). More than one century of schizophrenia: an evolving perspective. *J. Nerv. Ment. Dis.* 200, 1054–1057. doi: 10.1097/NMD.0b013e318275d249
- Sinke, A. P., Caputo, C., Tsai, S. W., Yuan, R., Ren, D., Deen, P. M., et al. (2011). Genetic analysis of mouse strains with variable serum sodium concentrations identifies the Nalcn sodium channel as a novel player in osmoregulation. *Physiol. Genomics* 43, 265–270. doi: 10.1152/physiolgenomics.00188.2010
- Smart, T. G. (1997). Regulation of excitatory and inhibitory neurotransmitter-gated ion channels by protein phosphorylation. *Curr. Opin. Neurobiol.* 7, 358–367. doi: 10.1016/S0959-4388(97)80063-3
- Smith, D. J., Whitham, E. A., and Ghaemi, S. N. (2012). Bipolar disorder. *Handb. Clin. Neurol.* 106, 251–263. doi: 10.1016/B978-0-444-52002-9.00015-2
- Snutch, T. P., and Monteil, A. (2007). The sodium “leak” has finally been plugged. *Neuron* 54, 505–507. doi: 10.1016/j.neuron.2007.05.005
- Souza, R. P., Rosa, D. V., Romano-Silva, M. A., Zhen, M., Meltzer, H. Y., Lieberman, J. A., et al. (2011). Lack of association of NALCN genetic variants with schizophrenia. *Psychiatry Res.* 185, 450–452. doi: 10.1016/j.psychres.2010.07.009
- Specia, D. J., Chihara, D., Ashique, A. M., Bowers, M. S., Pierce-Shimomura, J. T., Lee, J., et al. (2010). Conserved role of unc-79 in ethanol responses in lightweight mutant mice. *PLoS Genet.* 6:e1057. doi: 10.1371/journal.pgen.1001057
- St. George-Hyslop, P. H., and Petit, A. (2005). Molecular biology and genetics of Alzheimer's disease. *C. R. Biol.* 328, 119–130. doi: 10.1016/j.crv.2004.10.013
- Strohl, K. P. (2003). Periodic breathing and genetics. *Respir. Physiol. Neurobiol.* 135, 179–185. doi: 10.1016/S1569-9048(03)00036-3
- Sun, H., Xu, J., Della Penna, K. B., Benz, R. J., Kinose, F., Holder, D. J., et al. (2002). Dorsal horn-enriched genes identified by DNA microarray, *in situ* hybridization and immunohistochemistry. *BMC Neurosci.* 3:11. doi: 10.1186/1471-2202-3-11
- Swayne, L. A., Mezghrani, A., Lory, P., Nargeot, J., and Monteil, A. (2010). The NALCN ion channel is a new actor in pancreatic beta-cell physiology. *Islets* 2, 54–56. doi: 10.4161/isl.2.1.10522

- Swayne, L. A., Mezghrani, A., Varrault, A., Chemin, J., Bertrand, G., Dalle, S., et al. (2009). The NALCN ion channel is activated by M3 muscarinic receptors in a pancreatic beta-cell line. *EMBO Rep.* 10, 873–880. doi: 10.1038/embor.2009.125
- Tanzi, R. E., and Bertram, L. (2005). Twenty years of the Alzheimer's disease amyloid hypothesis: a genetic perspective. *Cell* 120, 545–555. doi: 10.1016/j.cell.2005.02.008
- Teo, C., Zai, C., Borlido, C., Tomasetti, C., Strauss, J., Shinkai, T., et al. (2012). Analysis of treatment-resistant schizophrenia and 384 markers from candidate genes. *Pharmacogenet. Genomics* 22, 807–811. doi: 10.1097/FPC.0b013e3283586c04
- Terracciano, A., Tanaka, T., Sutun, A. R., Sanna, S., Deiana, B., Lai, S., et al. (2010). Genome-wide association scan of trait depression. *Biol. Psychiatry* 68, 811–817. doi: 10.1016/j.biopsych.2010.06.030
- Todd, T. W., and Lim, J. (2013). Aggregation formation in the polyglutamine diseases: protection at a cost? *Mol. Cells* 36, 185–194. doi: 10.1007/s10059-013-0167-x
- Uher, R., Payne, J. L., Pavlova, B., and Perlis, R. H. (2013). Major depressive disorder in Dsm-5: implications for clinical practice and research of changes from Dsm-IV. *Depress. Anxiety*. doi: 10.1002/da.22217. [Epub ahead of print].
- Vacher, H., and Trimmer, J. S. (2011). Diverse roles for auxiliary subunits in phosphorylation-dependent regulation of mammalian brain voltage-gated potassium channels. *Pflugers Arch.* 462, 631–643. doi: 10.1007/s00424-011-1004-8
- Van Swinderen, B. (2006). A succession of anesthetic endpoints in the *Drosophila* brain. *J. Neurobiol.* 66, 1195–1211. doi: 10.1002/neu.20300
- Walczak-Sztulpa, J., Wisniewska, M., Latos-Bielenska, A., Linne, M., Kelbova, C., Belitz, B., et al. (2008). Chromosome deletions in 13q33-34: report of four patients and review of the literature. *Am. J. Med. Genet. A* 146, 337–342. doi: 10.1002/ajmg.a.32127
- Wang, H., and Ren, D. (2009). UNC80 functions as a scaffold for Src kinases in NALCN channel function. *Channels (Austin)*. 3, 161–163. doi: 10.4161/chan.3.3.8853
- Wang, K. S., Liu, X. F., and Aragam, N. (2010). A genome-wide meta-analysis identifies novel loci associated with schizophrenia and bipolar disorder. *Schizophr. Res.* 124, 192–199. doi: 10.1016/j.schres.2010.09.002
- Wellcome Trust Case Control, C. (2007). Genome-wide association study of 14,000 cases of seven common diseases and 3,000 shared controls. *Nature* 447, 661–678. doi: 10.1038/nature05911
- Wetherill, L., Kapoor, M., Agrawal, A., Bucholz, K., Koller, D., Bertelsen, S. E., et al. (2014). Family-based association analysis of alcohol dependence criteria and severity. *Alcohol. Clin. Exp. Res.* 38, 354–366. doi: 10.1111/acer.12251
- Whan, V., Hobbs, M., McWilliam, S., Lynn, D. J., Lutzow, Y. S., Khatkar, M., et al. (2010). Bovine proteins containing poly-glutamine repeats are often polymorphic and enriched for components of transcriptional regulatory complexes. *BMC Genomics* 11:654. doi: 10.1186/1471-2164-11-654
- Winkelman, J. W., Gagnon, A., and Clair, A. G. (2013). Sensory symptoms in restless legs syndrome: the enigma of pain. *Sleep Med.* 14, 934–942. doi: 10.1016/j.sleep.2013.05.017
- Xie, L., Gao, S., Alcaire, S. M., Aoyagi, K., Wang, Y., Griffin, J. K., et al. (2013). NLF-1 delivers a sodium leak channel to regulate neuronal excitability and modulate rhythmic locomotion. *Neuron* 77, 1069–1082. doi: 10.1016/j.neuron.2013.01.018
- Yan, T. C., McQuillin, A., Thapar, A., Asherson, P., Hunt, S. P., Stanford, S. C., et al. (2010). NK1 (TACR1) receptor gene 'knockout' mouse phenotype predicts genetic association with ADHD. *J. Psychopharmacol.* 24, 27–38. doi: 10.1177/0269881108100255
- Yeh, E., Ng, S., Zhang, M., Bouhours, M., Wang, Y., Wang, M., et al. (2008). A putative cation channel, NCA-1, and a novel protein, UNC-80, transmit neuronal activity in *C. elegans*. *PLoS Biol.* 6:e55. doi: 10.1371/journal.pbio.0060055
- Zhao, Q., Kelly, T. N., Li, C., and He, J. (2013). Progress and future aspects in genetics of human hypertension. *Curr. Hypertens. Rep.* 15, 676–686. doi: 10.1007/s11906-013-0388-6

Conflict of Interest Statement: The authors declare that the research was conducted in the absence of any commercial or financial relationships that could be construed as a potential conflict of interest.

Received: 05 March 2014; accepted: 28 April 2014; published online: 20 May 2014.

Citation: Cochet-Bissuel M, Lory P and Monteil A (2014) The sodium leak channel, NALCN, in health and disease. *Front. Cell. Neurosci.* 8:132. doi: 10.3389/fncel.2014.00132

This article was submitted to the journal *Frontiers in Cellular Neuroscience*.

Copyright © 2014 Cochet-Bissuel, Lory and Monteil. This is an open-access article distributed under the terms of the Creative Commons Attribution License (CC BY). The use, distribution or reproduction in other forums is permitted, provided the original author(s) or licensor are credited and that the original publication in this journal is cited, in accordance with accepted academic practice. No use, distribution or reproduction is permitted which does not comply with these terms.



The emerging Pannexin 1 signalome: a new nexus revealed?

Leigh E. Wicki-Stordeur¹ and Leigh A. Swayne^{1,2,3,4} *

¹ Division of Medical Sciences, University of Victoria, Victoria, BC, Canada

² Department of Biology, University of Victoria, Victoria, BC, Canada

³ Department of Biochemistry and Microbiology, University of Victoria, Victoria, BC, Canada

⁴ Department of Cellular and Physiological Sciences and Island Medical Program, University of British Columbia, Vancouver, BC, Canada

Edited by:

Christophe Altier, University of
Calgary, Canada

Reviewed by:

Michael F. Jackson, University of
Manitoba, Canada

Tuan Trang, University of Calgary,
Canada

*Correspondence:

Leigh A. Swayne, Division of Medical
Sciences, University of Victoria, 3800
Finnerty Road, Victoria, BC V8P 5C2,
Canada
e-mail: lswayne@uvic.ca

Pannexins (Panxs) are a family of single-membrane, large-pore ion, and metabolite permeable channels. Of the three Panx proteins, Panx1 has been most extensively studied, and has recently emerged as an exciting, clinically relevant target in many physiological and pathophysiological settings. This channel is widely expressed across various cell and tissue types; however its links to precise signaling pathways are largely unknown. Here we review the current literature surrounding presently identified Panx1–protein interactions, a critical first step to unraveling the Panx1 signalome. First we elucidate the reported associations of Panx1 with other ion channels, receptors, and channel signaling complexes. Further, we highlight recently identified Panx1–cytoskeleton interactions. Finally, we discuss the implications of these protein–protein interactions for Panx1 function in various cell and tissue types, and identify key outstanding questions arising from this work.

Keywords: Pannexin 1, Panx1, pannexins, interactome, P2X7, inflammasome, cytoskeleton

WHAT IS THE VALUE OF UNRAVELING THE PANX1 SIGNALOME?

Panx1 forms large pore channels permeable to ions and small molecules, and is a clinically relevant protein in inflammatory conditions (Kanneganti et al., 2007; Silverman et al., 2009; Gulbransen et al., 2012; Diezmos et al., 2013), stroke (Thompson et al., 2006; Bargiotas et al., 2011; Bargiotas et al., 2012; Dvorianchikova et al., 2012), and cancer (Lai et al., 2007; Cowan et al., 2012; Penuela et al., 2012). Panx1 is ubiquitously found in many cell and tissue types throughout the body, while Panx2 and Panx3 exhibit slightly more restricted organ and tissue expression patterns. Because of its widespread distribution, future attempts to develop Panx1-based therapeutic strategies will optimally incorporate tissue/cell type specificity to minimize side effects. Knowledge of the signaling pathways in which Panx1 participates, more precisely, its unique cell- and tissue-specific protein interaction partners, will be important for the development of such targeted therapeutic strategies. Thus, not only will unraveling the web of the Panx1 signalome be key for understanding the depth and breadth of its tissue and cell-specific functions, it will also be critically important for Panx1-based drug development.

PANX1 PERSPECTIVES, THEN AND NOW

Panx1 was cloned in 1998, and the pannexin family was first described as putative gap junction proteins in 2000 (Panchin et al., 2000) based on their homology to innexins, the invertebrate gap-junction forming proteins. Of the three Panx family members, Panx1 has been the primary focus of research. A large body of work has developed the current consensus that Panx1 forms single membrane channels (recently reviewed MacVicar and Thompson, 2009; Sosinsky et al., 2011). Individual four-pass transmembrane domain Panx1 subunits come together as

hexamers. Panx1 channels appear to be relatively non-selective, permitting the passage of small ions and molecules up to one kilodalton in size. Panx1 is perhaps most well-known for its role in facilitating ATP release from a variety of cell types under both physiological and pathophysiological contexts, by several mechanisms of activation (recently reviewed Sandilos and Bayliss, 2012).

There are still significant gaps in the knowledge of the molecular mechanisms regulating Panx1 function and its downstream effects. Since its discovery, only a handful of studies have captured small snapshots of the Panx1 interactome. Here we unite these somewhat disparate pieces in order to develop a clearer picture of the cellular signaling network of Panx1. We also highlight data from our recent study that included the first unbiased proteomics analysis of Panx1 interacting proteins (Wicki-Stordeur and Swayne, 2013). In this minireview, we have grouped these interacting proteins into two major categories: (1) ion channels, receptors, and their signaling complexes and (2) cytoskeletal proteins (summarized in **Table 1; Figure 1**).

ION CHANNELS, RECEPTORS, AND THEIR SIGNALING COMPLEXES

PANX1–PANXIN INTERACTIONS

An early starting point was other members of the Pannexin protein family (Bruzzone et al., 2005). The initial impetus for investigation into Panx–Panx interactions likely arose from a rich literature detailing the intermixing of connexins (reviewed in Koval, 2006), the vertebrate gap junction protein family. Connexins share structural similarity to pannexins, but no sequence similarity. The first identified Panx1 binding protein was its family member, Panx2 (Bruzzone et al., 2005).

Table 1 | Summary of Panx1 protein interaction partners, supporting evidence, functional significance, and relevant references.

Interactor	Evidence	Function	Reference
Ion channels and receptors (and signaling complexes)			
Pannexin 2 (Panx2)	MYC IPs (OE) Functional coupling (OE) Panx1 and Panx2 IPs (OE) Purified channels (OE)	Modification of Panx1 channel function Panx2 trafficking and localization	Bruzzzone et al. (2003, 2005), Penuela et al. (2009), Ambrosi et al. (2010)
Pannexin 3 (Panx3)	Co-loc (OE and Endg) Panx1 and Panx3 IPs (OE)	Unknown	Penuela et al. (2009)
Purinergic receptor, P2X, ligand-gated ion channel 7 (P2X7 receptor)	MYC IP (OE) Functional coupling (OE) EGFP IP (OE) Panx1 and P2X7 IPs P2X7 IP Panx1 IP MYC and FLAG IPs (OE)	Panx1 forms the large pore of the P2X7 receptor complex known as the “death pore” Inflammasome activation	Pelegri and Surprenant (2006), Locovei et al. (2007), Iglesias et al. (2008), Silverman et al. (2009), Poornima et al. (2012), Xu et al. (2012), Kanjanamekanant et al. (2013), Wang et al. (2013)
Inflammasome (associated with P2X7)		Inflammasome activation	
NOD-like receptor family, pyrin-domain containing 1 (NLRP1)	Panx1 IP	(NLRP and/or cell-type dependent)	Silverman et al. (2009)
NOD-like receptor family, pyrin-domain containing 2 (NLRP2)	NLRP2 IP		Minkiewicz et al. (2013)
NOD-like receptor family, pyrin-domain containing 2 (NLRP3)	FLAG and HA IPs		Wang et al. (2013)
Apoptosis-associated speck-like protein containing CARD (ASC)	Panx1 and ASC IP ASC IP		Silverman et al. (2009), Minkiewicz et al. (2013)
X-linked inhibitor of apoptosis (XIAP)	Panx1 IP		Silverman et al. (2009)
Caspase 1 (Casp1)	Panx1 IP		Silverman et al. (2009)
Caspase 11 (Casp11)	Panx1 IP		Silverman et al. (2009)
Purinergic receptor, P2X, ligand-gated ion channel 4 (P2X4 receptor)	P2X4 IP	ATP-induced ROS production	Hung et al. (2013)
Voltage-gated potassium channel subunit beta-3 (Kcnab3)	B2H and co-loc HA and MYC IPs	Modulating Panx1 redox sensitivity and Panx1 inactivation	Bunse et al. (2005, 2009)
α -1D adrenergic receptor (Adra1d)	Panx1 and Adra1d IPs	Panx1 activation coupled to adrenoceptor function Possible role in blood pressure regulation	Billaud et al. (2011)
Cytoskeletal Proteins			
Actin	Panx1 (OE) IP and BA Panx1 IP and co-loc (OE)	Panx1 trafficking and stabilization	Bhalla-Gehi et al. (2010), Wicki-Stordeur and Swayne (2013)
Actin-related protein 3 (Arp3)	GFP IP and LC-MS/MS, Panx1 IP and co-loc (OE)	Unknown	Wicki-Stordeur and Swayne (2013)

B2H, bacterial two-hybrid; BA, binding assay; Co-loc, Co-localization; Endg, endogenous; IP, immunoprecipitation; OE, overexpressed; LC-MS/MS, high performance liquid chromatography coupled to tandem mass spectrometry analysis.

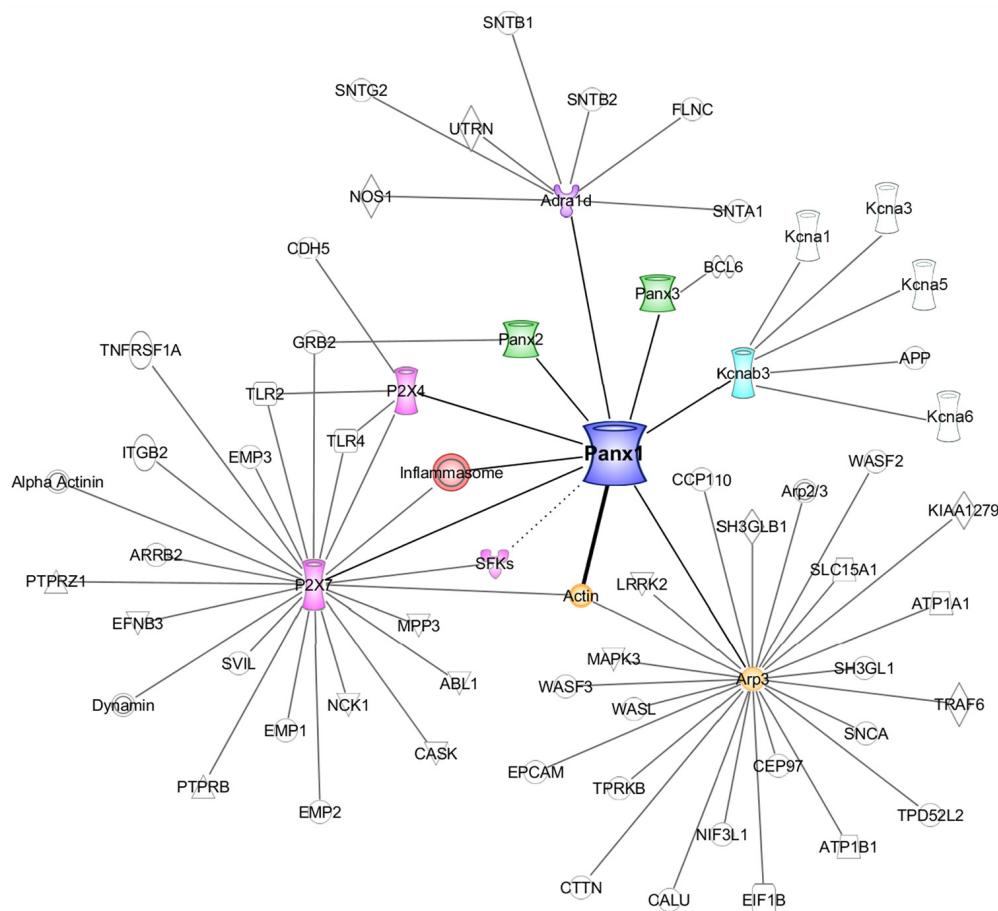


FIGURE 1 | The Panx1 interactome. A diagram generated using Ingenuity Pathways Analysis (IPA; Ingenuity Systems (Qiagen), Redwood City, CA, USA) representing a curated list of the Panx1 interacting proteins, and the subsequent IPA-derived interaction networks of these interactors (excluding

actin). The thick line between Panx1 and actin represents a direct interaction. The dotted line between Panx1 and SFKs indicates a likely link between the two proteins, however, no physical interaction data is yet available.

Panx2 is a much larger protein than Panx1, owing to its exceptionally longer C-terminus. It is particularly enriched in the brain (Baranova et al., 2004). The discovery of this interaction by Bruzzone et al. (2005) arose subsequent to an earlier observation by the same group, that depolarization-evoked currents in *Xenopus* oocytes injected with RNA for both Panx1 and Panx2 were significantly smaller and had modified gating kinetics in comparison with currents from *Xenopus* oocytes injected with Panx1 RNA alone (Bruzzone et al., 2003). The RNA encoding Panx2 itself did not lead to a depolarization-activated current. The authors proposed that Panx1/Panx2 heteromerization was the underlying cause for the difference in depolarization-evoked currents. Their later discovery of the interaction between epitope-tagged Panx1 and Panx2 supported this hypothesis (Bruzzone et al., 2005).

Key questions arose from these initial findings. For these findings to be physiologically relevant, Panx1 and Panx2 must be found in the same cells, and need to come into close proximity. Whether Panx1 and Panx2 are found in the same subcellular compartments is still an open question. To date, several studies have shown that ectopically and endogenously expressed Panx1 are found primarily

at the cell surface, with some reports of intracellular expression. In contrast, ectopically (Lai et al., 2009; Penuela et al., 2009) and endogenously (Swayne et al., 2010; Wicki-Stordeur et al., 2013) expressed Panx2 are largely found primarily in intracellular compartments. Whether Panx2 forms functional channels at the cell membrane is contentious (but see Penuela et al., 2009). Further, if Panx2 forms functional channels, are they activated in the same way as Panx1 channels? Does the interaction occur early in the secretory pathway, and could it impact on the trafficking of Panx1?

Penuela et al. (2009) later demonstrated that co-expression with Panx1 in HEK293T cells dramatically increased the cell surface expression of Panx2, measured by cell surface biotinylation and confocal microscopy. In HEK 293T cells ectopically co-expressing Panx1 and Panx2, the authors confirmed reciprocal co-precipitation of the two proteins. Interestingly, immunoprecipitation of Panx2 co-precipitates the immature glycosylation species of Panx1 specific to the early secretory pathway (gly0 and gly1). This suggests the proteins are able to interact early in the secretory pathway, not long after translation. Somewhat paradoxically, the ability of Panx1 to increase the cell surface expression of Panx2

suggests that Panx1/Panx2 reaches the plasma membrane. In a similar set of experiments, this group also demonstrated overlapping distributions of Panx1 and Panx3 using confocal microscopy, and an interaction by immunoprecipitation. The extent of Panx1 and Panx3 co-precipitation was modulated by the glycosylation state of Panx1, but the physiological implications of these findings have not yet been fully elucidated.

Interestingly, Ambrosi et al. (2010) found that purified Panx1/Panx2 heteromeric channels from insect cells were unstable over time (present at 1 h, but not 24 h post-purification). Additional experiments led the authors to suggest these findings could have resulted from size differences between Panx1 and Panx2, as well as experimentally identified differences in oligomeric symmetry (their study suggested that Panx1 forms hexamers while Panx2 forms octamers).

How Panx1 and Panx2 might functionally interact in cells remains to be determined. In the context of the nervous system, the distribution of Panx2 appears to change from intracellular to cell surface during the course of hippocampal neurogenesis (Swayne et al., 2010), but whether Panx1 and Panx2 have overlapping distributions in mature neurons is currently unknown. Recent work investigating the role of Panxs in stroke recovery has demonstrated that knockout of both Panx1 and Panx2 improves histological and behavioral outcomes (Bargiotas et al., 2011; Kindo et al., 2011). Thus elucidation of the functional and physical relationships between members of the pannexin family will provide us with both fundamental and clinically relevant information. Although much progress has been made, there are still many unanswered questions relating to the crosstalk between Panx glycosylation and trafficking and the role of the Panx family interactions in this respect.

P2X7 RECEPTORS

It is perhaps not surprising that the physiological and pathophysiological roles of pannexins and P2 purinergic receptors are connected given the former is perhaps best known as an ATP release channel, and the latter act as receptors for ATP and its metabolite, ADP. Pelegrin and Surprenant (2006) first reported a physical and functional interaction between overexpressed Panx1 and P2X7 receptors in 2006. The authors also demonstrated that P2X7 receptor activation in macrophage led to the opening of a large pore permeable to dye and IL-1 β release. Based on their data, the authors concluded that Panx1 channels formed the large pore previously ascribed to P2X7 receptors alone. Subsequent work by Locovei et al. (2007) in the *Xenopus* oocyte heterologous expression model further supported this work. They showed that P2X7 receptors formed a non-selective ion channel, but co-expression with Panx1 was necessary to form a larger channel referred to as the “death pore.” Poornima et al. (2012) also reported an interaction between Panx1 and P2X7 receptors overexpressed in N2a cells. Recently, Kanjanamekanant et al. (2013) demonstrated an interaction between endogenous Panx1 and P2X7 receptor in human periodontal ligament cells using reciprocal immunoprecipitations, and found this interaction was strengthened following mechanical stress. Interestingly, Xu et al. (2012) observed a functional interaction only between Panx1 and the P2X7a receptor splice variant using dye uptake studies in overexpressing HEK293 cells. It now

appears that such a Panx1-P2X7 receptor complex may also involve P2X4 receptor components in some cell types, as Hung et al. (2013) recently co-precipitated these three proteins from immortalized gingival epithelial cells.

Extending on the earlier findings by Pelegrin and colleagues, in the J774 monocyte macrophage cell line derived from a BALB/C mouse tumor, Iglesias et al. (2008) showed that Panx1 activation was tightly coupled to P2X7 receptor activation via a Panx1/P2X7 receptor complex involving a Src family tyrosine kinase (SFK). This group demonstrated interaction between the endogenously expressed proteins and were able to block the functional interaction with a membrane permanent TAT-P2X7 peptide targeting the SH3 domain of the P2X7 receptor. Interestingly, Weilingner et al. (2012) have further linked SFKs more directly to Panx1 function using a Panx1 C-terminal competitive peptide strategy; however a physical interaction between the two proteins has not yet been illustrated. Alberto et al. (2013) observed conflicting findings with respect to the Panx1-P2X7 receptor coupling; in primary mouse and rat peritoneal macrophage cultures, RNAi targeting Panx1, as well as probenecid and carbenoxolone treatment to block Panx1, had no effect on ATP-induced P2X7 currents. It should be noted that these two studies used substantially different recording solutions. More importantly, there are likely substantial differences arising from the use of two different macrophage models. Macrophages are found in all tissues. As a result of their extreme inherent plasticity, these distinct tissue-subsets have a high level of diversity in terms of gene expression and functional capabilities (Wynn et al., 2013). Even within peritoneal macrophages, it has been recently revealed that there are two physical, functionally and developmentally distinct subsets (Ghosh et al., 2010). Thus, the Panx1/P2X7 receptor relationship in macrophages is likely state- and subset-dependent. Moreover microglia, the macrophage-like resident immune cells of the brain, also possess a P2X7-Panx1 functional unit. Rigato et al. (2012) recently observed that microglial proliferation is dependent on P2X7 receptor and not Panx1, however, initial microglial activation and/or recruitment may still possess a Panx1 component.

The inflammasome, P2X7 receptors, and Panx1 in cytokine activation and immune cell recruitment

Interestingly, Panx1 has recently been linked to the inflammasome, a large cytoplasmic complex involved in cytokine activation and immune cell recruitment (Martinon et al., 2002, 2009). P2X7 receptors and Panx1 have been reported to be associated with inflammasomes in a variety of cell types (Silverman et al., 2009). As critical components of the inflammasome, Nod-like receptor proteins (NLRPs) link the detection of “danger signals” [or danger associated molecular pattern molecules (DAMP)], arising under scenarios such as metabolic stress, to proteolytic activation of the pro-inflammatory cytokines IL-1 β and IL-18. Other key complex proteins include the adaptor protein ASC (Apoptosis-associated speck-like protein containing a CARD), and the inflammatory caspases-1 and -11. While P2X7 receptors are established inflammasome components, a recent report (Silverman et al., 2009) in cortical neurons revealed the potential involvement of Panx1. Silverman and colleagues immunoprecipitated Panx1 from

cultured primary cortical neurons. Major components of the neuronal inflammasome including the P2X7 receptor, NLRP1, ASC, caspase-1, caspase-11, and X-linked inhibitor of apoptosis protein (XIAP) co-precipitated with Panx1. Reciprocally, ASC co-precipitated Panx1 as well as NLRP1, caspase-1, caspase-11, and XIAP. The authors further showed that elevating extracellular potassium above the normal resting range opened Panx1 channels leading to caspase-1 activation, and that this was sensitive to the Panx1 blocker probenecid. They determined that potassium-dependent activation of Panx1 was independent of changes in the membrane potential, which suggested that stimulation of inflammasome signaling was mediated by an allosteric effect of potassium binding to Panx1.

Minkiewicz et al. (2013) recently described a novel inflammasome in human astrocytes. They detected NLRP2 protein in human astrocytes and investigated the putative involvement of Panx1 in an NLRP2-based astrocytic inflammasome. Immunoprecipitation of NLRP2 from human primary astrocyte cultures co-precipitated Panx1, ASC, caspase-1, and P2X7 receptor. Reciprocally Panx1, P2X7 receptor, NLRP2, and caspase-1 co-precipitated with ASC. A more recent study (Wang et al., 2013) showed that while overexpressed Panx1 and NLRP3, or Panx1 and P2X7 receptors co-precipitated, overexpressed ASC and Panx1 did not interact in HEK293T cells. Interestingly, there were no deficiencies in NLRP3-inflammasome activation in macrophage of Panx1 knock-out mice (Qu et al., 2011; Wang et al., 2013; but see, Hung et al., 2013).

Gulbrandsen and colleagues confirmed *in vivo* Panx1 involvement in the NLRP3 inflammasome. They found that blocking Panx1 channels in enteric neurons ameliorates some of the effects of experimental colitis, including neuronal death (Gulbrandsen et al., 2012). Further, enteric neuronal death was dependent on P2X7 receptor, ASC, and caspase function, but not that of NLRP3, implying that a separate Panx1-inflammasome complex may be involved. Therefore, whether Panx1 is universally involved in inflammasome complexes may be characterized by cell type specific NLRP expression and utilization. Furthermore, the precise functional role of the physical association between Panx1 and inflammasome components remains to be determined.

POTASSIUM CHANNEL AUXILIARY SUBUNIT K ν β 3

One of the initial Panx1 interactome studies was performed by Bunse et al. (2005). They employed an *E. coli* two-hybrid system to search for potential Panx1 interactors. This study identified the potassium channel accessory subunit, K ν β 3 (Kcnab3) as a putative interactor with the Panx1 C-terminus. K ν β 3 interacts with the shaker related voltage-gated potassium channels K ν 1.1, 1.3, 1.5, and 1.6 to modify voltage-dependent activation, and inactivation kinetics (Leicher et al., 1998; Bähring et al., 2004; Tipparaju et al., 2012). A follow-up study confirmed the Panx1-K ν β 3 interaction in a double-overexpression system by co-precipitation for the tagged proteins. An additional functional investigation indicated that ectopically expressed Panx1 currents became somewhat desensitized to redox- and pharmacological-based inhibition upon co-expression of K ν β 3 in oocytes (Bunse et al., 2009). The authors postulated that K ν β 3 is important for regulating Panx1 channel function by modulating its sensitivity

to redox potentials. Bunse et al. (2011) further confirmed redox modulation of Panx1 activity, however, the molecular mechanisms underlying this sensitivity remain unknown. This will likely prove to be important in pathological contexts such as stroke and hypoxia, where redox signaling plays an important role (reviewed in Valko et al., 2007).

α 1D-ADRENORECEPTOR

Because of the established role of Panx1 in the release of ATP, a signaling molecule important for vasoconstriction, Billaud et al. (2011) performed Panx1 immunoprecipitations from thoracodorsal resistance arteries to examine its role in vascular smooth muscle cell communication. They identified an interaction between endogenous Panx1 and the α 1D-adrenoreceptor. Further, they noted that ATP release via Panx1 was necessary to facilitate phenylephrine-evoked α 1D-adrenoreceptor-mediated vessel constriction. Moreover, results from a HEK293 expression system indicated a Panx1-dependent component to ATP release evoked by α 1D-adrenoreceptor activation (Sumi et al., 2010). Taken together, these studies indicate a mechanism for Panx1 activation downstream of adrenoreceptor stimulation, and imply a role for this channel in systemic blood pressure regulation.

CYTOSKELETAL PROTEINS

Perhaps unsurprisingly, due to its known mechanosensitive nature, Panx1 has recently been found to associate with cytoskeletal proteins. Bhalla-Gehi et al. (2010) initially noted a role of the actin-based microfilament cytoskeleton in the cell-surface trafficking and stabilization of Panx1. Further study revealed an interaction between ectopically expressed Panx1 and actin. Interestingly, *in vitro* binding assays with purified proteins revealed the Panx1 C-terminus as the region responsible for the direct interaction.

More recently, our group confirmed this Panx1-actin association with endogenous Panx1 immunoprecipitations from a neuroblastoma cell line (Wicki-Stordeur and Swayne, 2013). Moreover, immunofluorescence and confocal microscopy illustrated co-localization of Panx1-EGFP with actin.

Our study also uncovered several novel Panx1 interactors. We performed immunoprecipitations from Panx1-EGFP expressing cells, coupled to mass spectrometry-based identification. From these, a putative association of Panx1 with actin-related protein 3 (Arp3) was revealed. This interaction was confirmed through endogenous Panx1 co-precipitations, and co-localization by immunofluorescence. Arp3 is a component of the large Arp2/3 actin-regulating complex involved in nucleation and branching of microfilaments (reviewed in Firat-Karalar and Welch, 2011). Because of its key role in controlling the dynamic actin cytoskeleton, the Arp2/3 complex is key in several cellular processes dependent on actin remodeling, such as filopodia (Korobova and Svitkina, 2008; Spillane et al., 2011) and lamellipodia (Ingberman et al., 2013) formation, cell migration (Sawa et al., 2003; Schaefer et al., 2008), and neurite outgrowth (Schaefer et al., 2008; Firat-Karalar et al., 2011).

Using gene ontology (GO) analysis we determined that 10% of the mass spectrometry-identified putative Panx1 interactors in neuroblastoma cells fell under a cytoskeleton classification. While most of these have yet to be validated, the large proportion of

cytoskeletal interactors implies a significant role for the cytoskeleton in regulation of Panx1 trafficking and function. Potentially further connecting Panx1 with the cytoskeleton and other ion channels, a novel interaction between stomatin and Panx1 has also recently been identified that inhibits Panx1 currents (Zhan et al., 2012). Much work will clearly be needed to begin to untangle the complexities of emerging Panx1 nexus.

CONCLUDING REMARKS

The Panx1 interactome is beginning to emerge, however, many key questions remain unanswered. For instance, which of the Panx1 interactions are direct, and which occur indirectly through other bridging proteins? At present, the Panx1-actin relationship stands alone as the only proven direct interaction. The functional significance of many of these interactions is also currently unknown. Moreover, questions arise regarding the tissue and cell-type specificity of these interactions. For example, the Panx1-inflammasome connection not only seems to depend on which NLRP is forming the complex, but also on the cell type in question. Finally, little is understood regarding alterations to the Panx1 interactome under pathophysiological conditions, such as stroke. In order to fill such knowledge gaps in our understanding of the role of Panx1 in both physiological and pathophysiological settings, the Panx1 interactome must be more fully elucidated and understood. In this way we will uncover key molecular players involved in Panx1 regulation and function, and thus be able to consider Panx1 as a viable therapeutic target within clinical settings.

AUTHOR CONTRIBUTIONS

Leigh E. Wicki-Stordeur and Leigh A. Swayne wrote and revised the manuscript. Leigh E. Wicki-Stordeur created the Table and Figure. Both authors approve of the manuscript and its contents.

ACKNOWLEDGMENTS

Research in the Swayne lab is supported by NSERC Discovery, Heart and Stroke Foundation Partnership for Stroke Recovery, Canadian Foundation for Innovation and British Columbia Knowledge Development Fund grants awarded to Leigh A. Swayne. Leigh E. Wicki-Stordeur is supported by a Vanier Canada Graduate Scholarship (NSERC) and an A. James and Laurette Agnew Memorial Award. LEWS was previously supported by an NSERC CGSM, a Howard E. Petch research scholarship, an Edythe Hembroff-Schleicher graduate scholarship, and the Victoria Foundation Willard and Elva Dawson Fund.

REFERENCES

- Alberto, A. V., Faria, R. X., Couto, C. G., Ferreira, L. G., Souza, C. A., Teixeira, P. C., et al. (2013). Is pannexin the pore associated with the P2X7 receptor? *Naunyn Schmiedeberg's Arch. Pharmacol.* 386, 775–787. doi: 10.1007/s00210-013-0868-x
- Ambrosi, C., Gassmann, O., Pranskevich, J. N., Boassa, D., Smock, A., Wang, J., et al. (2010). Pannexin1 and Pannexin2 channels show quaternary similarities to connexons and different oligomerization numbers from each other. *J. Biol. Chem.* 285, 24420–24431. doi: 10.1074/jbc.M110.115444
- Bähring, R., Vardanyan, V., and Pongs, O. (2004). Differential modulation of Kv1 channel-mediated currents by co-expression of Kvbeta3 subunit in a mammalian cell-line. *Mol. Membr. Biol.* 21, 19–25. doi: 10.1080/09687680310001597749
- Baranova, A., Ivanov, D., Petrash, N., Pestova, A., Skoblov, M., Kelmanson, I., et al. (2004). The mammalian pannexin family is homologous to the invertebrate innexin gap junction proteins. *Genomics* 83, 706–716. doi: 10.1016/j.ygeno.2003.09.025
- Bargiotas, P., Krenz, A., Hormuzdi, S. G., Ridder, D. A., Herb, A., Barakat, W., et al. (2011). Pannexins in ischemia-induced neurodegeneration. *Proc. Natl. Acad. Sci. U.S.A.* 108, 20772–20777. doi: 10.1073/pnas.1018262108
- Bargiotas, P., Krenz, A., Monyer, H., and Schwanninger, M. (2012). Functional outcome of pannexin-deficient mice after cerebral ischemia. *Channels* 6, 453–456. doi: 10.4161/chan.22315
- Bhalla-Gehi, R., Penuela, S., Churko, J. M., Shao, Q., and Laird, D. W. (2010). Pannexin1 and pannexin3 delivery, cell surface dynamics, and cytoskeletal interactions. *J. Biol. Chem.* 285, 9147–9160. doi: 10.1074/jbc.M109.082008
- Billaud, M., Lohman, A. W., Straub, A. C., Looft-Wilson, R., Johnstone, S. R., Araj, C. A., et al. (2011). Pannexin1 regulates alpha1-adrenergic receptor-mediated vasoconstriction. *Circ. Res.* 109, 80–85. doi: 10.1161/CIRCRESAHA.110.237594
- Bruzzone, R., Barbe, M. T., Jakob, N. J., and Monyer, H. (2005). Pharmacological properties of homomeric and heteromeric pannexin hemichannels expressed in *Xenopus* oocytes. *J. Neurochem.* 92, 1033–1043. doi: 10.1111/j.1471-4159.2004.02947.x
- Bruzzone, R., Hormuzdi, S. G., Barbe, M. T., Herb, A., and Monyer, H. (2003). Pannexins, a family of gap junction proteins expressed in brain. *Proc. Natl. Acad. Sci. U.S.A.* 100, 13644–13649.
- Bunse, S., Haghika, A., Zoidl, G., and Dermietzel, R. (2005). Identification of a potential regulator of the gap junction protein pannexin1. *Cell Commun. Adhes.* 12, 231–236. doi: 10.1080/15419060500511834
- Bunse, S., Locovei, S., Schmidt, M., Qiu, F., Zoidl, G., Dahl, G., et al. (2009). The potassium channel subunit Kvbeta3 interacts with pannexin 1 and attenuates its sensitivity to changes in redox potentials. *FEBS J.* 276, 6258–6270. doi: 10.1111/j.1742-4658.2009.07334.x
- Bunse, S., Schmidt, M., Hoffmann, S., Engelhardt, K., Zoidl, G., and Dermietzel, R. (2011). Single cysteines in the extracellular and transmembrane regions modulate pannexin 1 channel function. *J. Membr. Biol.* 244, 21–33. doi: 10.1007/s00232-011-9393-3
- Cowan, K. N., Langlois, S., Penuela, S., Cowan, B. J., and Laird, D. W. (2012). Pannexin1 and Pannexin3 exhibit distinct localization patterns in human skin appendages and are regulated during keratinocyte differentiation and carcinogenesis. *Cell Commun. Adhes.* 19, 45–53. doi: 10.3109/15419061.2012.712575
- Diezmos, E. F., Sandow, S. L., Markus, I., Shevy Perera, D., Lubowski, D. Z., King, D. W., et al. (2013). Expression and localization of pannexin-1 hemichannels in human colon in health and disease. *Neurogastroenterol. Motil.* 25, e395–e405. doi: 10.1111/nmo.12130
- Dvorianchikova, G., Ivanov, D., Barakat, D., Grinberg, A., Wen, R., Slepak, V. Z., et al. (2012). Genetic ablation of Pannexin1 protects retinal neurons from ischemic injury. *PLoS ONE* 7:e31991. doi: 10.1371/journal.pone.0031991
- Firat-Karalar, E. N., Hsiue, P. P., and Welch, M. D. (2011). The actin nucleation factor JMY is a negative regulator of neuritogenesis. *Mol. Biol. Cell* 22, 4563–4574. doi: 10.1091/mbc.E11-06-0585
- Firat-Karalar, E. N., and Welch, M. D. (2011). New mechanisms and functions of actin nucleation. *Curr. Opin. Cell Biol.* 23, 4–13. doi: 10.1016/j.ceb.2010.10.007
- Ghosn, E. E., Cassado, A. A., Govoni, G. R., Fukuhara, T., Yang, Y., Monack, D. M., et al. (2010). Two physically, functionally, and developmentally distinct peritoneal macrophage subsets. *Proc. Natl. Acad. Sci. U.S.A.* 107, 2568–2573. doi: 10.1073/pnas.0915000107
- Gulbransen, B. D., Bashashati, M., Hirota, S. A., Gui, X., Roberts, J. A., MacDonald, J. A., et al. (2012). Activation of neuronal P2X7 receptor-pannexin-1 mediates death of enteric neurons during colitis. *Nat. Med.* 18, 600–604. doi: 10.1038/nm.2679
- Hung, S. C., Choi, C. H., Said-Sadier, N., Johnson, L., Atanasova, K. R., Sellami, H., et al. (2013). P2X4 assembles with P2X7 and pannexin-1 in gingival epithelial cells and modulates ATP-induced reactive oxygen species production and inflammasome activation. *PLoS ONE* 8:e70210. doi: 10.1371/journal.pone.0070210
- Iglesias, R., Locovei, S., Roque, A., Alberto, A. P., Dahl, G., Spray, D. C., et al. (2008). P2X7 receptor-Pannexin1 complex: pharmacology and signaling. *Am. J. Physiol. Cell Physiol.* 295, C752–C760. doi: 10.1152/ajpcell.00228.2008
- Ingerman, E., Hsiao, J. Y., and Mullins, R. D. (2013). Arp2/3 complex ATP hydrolysis promotes lamellipodial actin network disassembly but is dispensable for assembly. *J. Cell Biol.* 200, 619–633. doi: 10.1083/jcb.201211069
- Kanjanamekanant, K., Luckprom, P., and Pavasant, P. (2013). P2X7 receptor-Pannexin1 interaction mediates stress-induced interleukin-1 beta expression in human periodontal ligament cells. *J. Periodontol. Res.* doi: 10.1111/jre.12139 [Epub ahead of print].

- Kanneganti, T. D., Lamkanfi, M., Kim, Y. G., Chen, G., Park, J. H., Franchi, L., et al. (2007). Pannexin-1-mediated recognition of bacterial molecules activates the cryopyrin inflammasome independent of Toll-like receptor signaling. *Immunity* 26, 433–443. doi: 10.1016/j.immuni.2007.03.008
- Kindo, M., Gerelli, S., Billaud, P., and Mazzucotelli, J. P. (2011). Flash pulmonary edema in an orthotopic heart transplant recipient. *Interact. Cardiovasc. Thorac. Surg.* 12, 323–325. doi: 10.1510/icvts.2010.254755
- Korobova, F., and Svitkina, T. (2008). Arp2/3 complex is important for filopodia formation, growth cone motility, and neuritogenesis in neuronal cells. *Mol. Biol. Cell* 19, 1561–1574. doi: 10.1091/mbc.E07-09-0964
- Koval, M. (2006). Pathways and control of connexin oligomerization. *Trends Cell Biol.* 16, 159–166. doi: 10.1016/j.tcb.2006.01.006
- Lai, C. P., Bechberger, J. F., and Naus, C. C. (2009). Pannexin2 as a novel growth regulator in C6 glioma cells. *Oncogene* 28, 4402–4408. doi: 10.1038/ncr.2009.283
- Lai, C. P., Bechberger, J. F., Thompson, R. J., MacVicar, B. A., Bruzzone, R., and Naus, C. C. (2007). Tumor-suppressive effects of pannexin 1 in C6 glioma cells. *Cancer Res.* 67, 1545–1554. doi: 10.1158/0008-5472.CAN-06-1396
- Leicher, T., Bähring, R., Isbrandt, D., and Pongs, O. (1998). Coexpression of the KCNA3B gene product with Kv1.5 leads to a novel A-type potassium channel. *J. Biol. Chem.* 273, 35095–35101. doi: 10.1074/jbc.273.52.35095
- Locovei, S., Scemes, E., Qiu, F., Spray, D. C., and Dahl, G. (2007). Pannexin1 is part of the pore forming unit of the P2X(7) receptor death complex. *FEBS Lett.* 581, 483–488. doi: 10.1016/j.febslet.2006.12.056
- MacVicar, B. A., and Thompson, R. J. (2009). Non-junction functions of pannexin-1 channels. *Trends Neurosci.* 33, 93–102. doi: 10.1016/j.tins.2009.11.007
- Martinon, F., Burns, K., and Tschopp, J. (2002). The inflammasome: a molecular platform triggering activation of inflammatory caspases and processing of proIL-beta. *Mol. Cell* 10, 417–426. doi: 10.1016/S1097-2765(02)00599-3
- Martinon, F., Mayor, A., and Tschopp, J. (2009). The inflammasomes: guardians of the body. *Annu. Rev. Immunol.* 27, 229–265. doi: 10.1146/annurev.immunol.021908.132715
- Minkiewicz, J., De Rivero Vaccari, J. P., and Keane, R. W. (2013). Human astrocytes express a novel NLRP2 inflammasome. *Glia* 61, 1113–1121. doi: 10.1002/glia.22499
- Panchin, Y., Kelmanson, I., Matz, M., Lukyanov, K., Usman, N., and Lukyanov, S. (2000). A ubiquitous family of putative gap junction molecules. *Curr. Biol.* 10, R473–R474. doi: 10.1016/S0960-9822(00)00576-5
- Pelegrin, P., and Surprenant, A. (2006). Pannexin-1 mediates large pore formation and interleukin-1beta release by the ATP-gated P2X7 receptor. *EMBO J.* 25, 5071–5082. doi: 10.1038/sj.emboj.7601378
- Penuela, S., Bhalla, R., Nag, K., and Laird, D. W. (2009). Glycosylation regulates pannexin intermixing and cellular localization. *Mol. Biol. Cell* 20, 4313–4323. doi: 10.1091/mbc.E09-01-0067
- Penuela, S., Gyenis, L., Ablack, A., Churko, J. M., Berger, A. C., Litchfield, D. W., et al. (2012). Loss of pannexin 1 attenuates melanoma progression by reversion to a melanocytic phenotype. *J. Biol. Chem.* 287, 29184–29193. doi: 10.1074/jbc.M112.377176
- Poornima, V., Madhupriya, M., Kootar, S., Sujatha, G., Kumar, A., and Bera, A. K. (2012). P2X7 receptor-pannexin 1 hemichannel association: effect of extracellular calcium on membrane permeabilization. *J. Mol. Neurosci.* 46, 585–594. doi: 10.1007/s12031-011-9646-8
- Qu, Y., Misaghi, S., Newton, K., Gilmour, L. L., Louie, S., Cupp, J. E., et al. (2011). Pannexin-1 is required for ATP release during apoptosis but not for inflammasome activation. *J. Immunol.* 186, 6553–6561. doi: 10.4049/jimmunol.1100478
- Rigato, C., Swinnen, N., Buckinx, R., Couillin, I., Mangin, J. M., Rigo, J. M., et al. (2012). Microglia proliferation is controlled by P2X7 receptors in a Pannexin-1-independent manner during early embryonic spinal cord invasion. *J. Neurosci.* 32, 11559–11573. doi: 10.1523/JNEUROSCI.1042-12.2012
- Sandilos, J. K., and Bayliss, D. A. (2012). Physiological mechanisms for the modulation of pannexin 1 channel activity. *J. Physiol.* 590, 6257–6266. doi: 10.1111/jphysiol.2012.240911
- Sawa, M., Suetsugu, S., Sugimoto, A., Miki, H., Yamamoto, M., and Takenawa, T. (2003). Essential role of the C. elegans Arp2/3 complex in cell migration during ventral enclosure. *J. Cell Sci.* 116, 1505–1518. doi: 10.1242/jcs.00362
- Schaefer, A. W., Schoonderwoert, V. T., Ji, L., Medeiros, N., Danuser, G., and Forscher, P. (2008). Coordination of actin filament and microtubule dynamics during neurite outgrowth. *Dev. Cell* 15, 146–162. doi: 10.1016/j.devcel.2008.05.003
- Silverman, W. R., De Rivero Vaccari, J. P., Locovei, S., Qiu, F., Carlsson, S. K., Scemes, E., et al. (2009). The pannexin 1 channel activates the inflammasome in neurons and astrocytes. *J. Biol. Chem.* 284, 18143–18151. doi: 10.1074/jbc.M109.004804
- Sosinsky, G. E., Boassa, D., Dermietzel, R., Duffy, H. S., Laird, D. W., MacVicar, B., et al. (2011). Pannexin channels are not gap junction hemichannels. *Channels* 5, 193–197. doi: 10.4161/chan.5.3.15765
- Spillane, M., Ketschek, A., Jones, S. L., Korobova, F., Marsick, B., Lanier, L., et al. (2011). The actin nucleating Arp2/3 complex contributes to the formation of axonal filopodia and branches through the regulation of actin patch precursors to filopodia. *Dev. Neurobiol.* 71, 747–758. doi: 10.1002/dneu.20907
- Sumi, Y., Woehrle, T., Chen, Y., Yao, Y., Li, A., and Junger, W. G. (2010). Adrenergic receptor activation involves ATP release and feedback through purinergic receptors. *Am. J. Physiol. Cell Physiol.* 299, C1118–C1126. doi: 10.1152/ajpcell.00122.2010
- Swayne, L. A., Sorbara, C. D., and Bennett, S. A. (2010). Pannexin 2 is expressed by postnatal hippocampal neural progenitors and modulates neuronal commitment. *J. Biol. Chem.* 285, 24977–24986. doi: 10.1074/jbc.M110.130054
- Thompson, R. J., Zhou, N., and MacVicar, B. A. (2006). Ischemia opens neuronal gap junction hemichannels. *Science* 312, 924–927. doi: 10.1126/science.1126241
- Tippiraju, S. M., Li, X. P., Kilfoil, P. J., Xue, B., Uversky, V. N., Bhatnagar, A., et al. (2012). Interactions between the C-terminus of Kv1.5 and Kvbeta regulate pyridine nucleotide-dependent changes in channel gating. *Pflugers Arch.* 463, 799–818. doi: 10.1007/s00424-012-1093-z
- Valko, M., Leibfritz, D., Moncol, J., Cronin, M. T., Mazur, M., and Telser, J. (2007). Free radicals and antioxidants in normal physiological functions and human disease. *Int. J. Biochem. Cell Biol.* 39, 44–84. doi: 10.1016/j.biocel.2006.07.001
- Wang, H., Xing, Y., Mao, L., Luo, Y., Kang, L., and Meng, G. (2013). Pannexin-1 influences peritoneal cavity cell population but is not involved in NLRP3 inflammasome activation. *Protein Cell* 4, 259–265. doi: 10.1007/s13238-013-2114-1
- Weiling, N. L., Tang, P. L., and Thompson, R. J. (2012). Anoxia-induced NMDA receptor activation opens pannexin channels via Src family kinases. *J. Neurosci.* 32, 12579–12588. doi: 10.1523/JNEUROSCI.1267-12.2012
- Wicki-Stordeur, L. E., Boyce, A. K., and Swayne, L. A. (2013). Analysis of a pannexin 2-pannexin 1 chimeric protein supports divergent roles for pannexin C-termini in cellular localization. *Cell Commun. Adhes.* 20, 73–79. doi: 10.3109/15419061.2013.791681
- Wicki-Stordeur, L. E., and Swayne, L. A. (2013). Panx1 regulates neural stem and progenitor cell behaviours associated with cytoskeletal dynamics and interacts with multiple cytoskeletal elements. *Cell Commun. Signal.* 11, 62. doi: 10.1186/1478-811X-11-62
- Wynn, T. A., Chawla, A., and Pollard, J. W. (2013). Macrophage biology in development, homeostasis and disease. *Nature* 496, 445–455. doi: 10.1038/nature12034
- Xu, X. J., Boumechache, M., Robinson, L. E., Marschall, V., Gorecki, D. C., Masin, M., et al. (2012). Splice variants of the P2X7 receptor reveal differential agonist dependence and functional coupling with pannexin-1. *J. Cell Sci.* 125, 3776–3789. doi: 10.1242/jcs.099374
- Zhan, H., Moore, C. S., Chen, B., Zhou, X., Ma, X.-M., Ijichi, K., et al. (2012). Stomatin inhibits pannexin-1-mediated whole-cell currents by interacting with its carboxyl terminal. *PLoS ONE* 7:e39489. doi: 10.1371/journal.pone.0039489

Conflict of Interest Statement: The authors declare that the research was conducted in the absence of any commercial or financial relationships that could be construed as a potential conflict of interest.

Received: 04 December 2013; paper pending published: 16 December 2013; accepted: 23 December 2013; published online: 08 January 2014.

Citation: Wicki-Stordeur LE and Swayne LA (2014) The emerging Pannexin 1 signalome: a new nexus revealed? *Front. Cell. Neurosci.* 7:287. doi: 10.3389/fncel.2013.00287

This article was submitted to the journal *Frontiers in Cellular Neuroscience*.

Copyright © 2014 Wicki-Stordeur and Swayne. This is an open-access article distributed under the terms of the Creative Commons Attribution License (CC BY). The use, distribution or reproduction in other forums is permitted, provided the original author(s) or licensor are credited and that the original publication in this journal is cited, in accordance with accepted academic practice. No use, distribution or reproduction is permitted which does not comply with these terms.



CSP α —chaperoning presynaptic proteins

Julien Donnelier and Janice E. A. Braun*

Department of Physiology and Pharmacology, The Hotchkiss Brain Institute, Faculty of Medicine, University of Calgary, Calgary, AB, Canada

Edited by:

Leigh Anne Swayne, University of Victoria, Canada

Reviewed by:

Robert Burgoyne, University of Liverpool, UK

Luke Chamberlain, University of Strathclyde, UK

*Correspondence:

Janice E. A. Braun, Department of Physiology and Pharmacology, The Hotchkiss Brain Institute, Faculty of Medicine, The University of Calgary, 3330 Hospital Dr. N.W., Calgary, AB T2N 4N1, Canada
e-mail: braunj@ucalgary.ca

Synaptic transmission relies on precisely regulated and exceedingly fast protein-protein interactions that involve voltage-gated channels, the exocytosis/endocytosis machinery as well as signaling pathways. Although we have gained an ever more detailed picture of synaptic architecture much remains to be learned about how synapses are maintained. Synaptic chaperones are “folding catalysts” that preserve proteostasis by regulating protein conformation (and therefore protein function) and prevent unwanted protein-protein interactions. Failure to maintain synapses is an early hallmark of several degenerative diseases. Cysteine string protein (CSP α) is a presynaptic vesicle protein and molecular chaperone that has a central role in preventing synaptic loss and neurodegeneration. Over the past few years, a number of different “client proteins” have been implicated as CSP α substrates including voltage-dependent ion channels, signaling proteins and proteins critical to the synaptic vesicle cycle. Here we review the ion channels and synaptic protein complexes under the influence of CSP α and discuss gaps in our current knowledge.

Keywords: CSP, cysteine string protein, DnaJC5, J protein, chaperones, neurodegeneration, neural differentiation

ONE J PROTEIN: THE TOTAL PROTECTION PLAN

Cysteine String Protein (CSP α) is a presynaptic vesicle protein with neuroprotective activity. In humans, mutations in the DNAJC5 gene encoding CSP α that produce heterozygous CSP α point mutations or point deletions cause autosomal-dominant, adult onset neuronal ceroid lipofuscinosis (ANCL), a neurodegenerative disorder characterized by accumulation of lysosomal cellular debris (Benitez et al., 2011; Nosková et al., 2011; Velinov et al., 2012). Disease onset is between 20–30 years of age and the course and outcome of ANCL involves, increased anxiety, speech difficulties, ataxia, involuntary movements, seizures, cognitive deterioration, dementia with a shortened life expectancy. In mice, CSP α KO causes activity-dependent synapse loss, progressive defects in neurotransmission and neurodegeneration verifying CSP α 's anti-neurodegenerative function (Fernández-Chacón et al., 2004; García-Junco-Clemente et al., 2010). CSP α heterozygote mice, which have reduced levels of CSP α , are phenotypically normal suggesting that wild type mice normally have “extra” CSP α protection (Fernández-Chacón et al., 2004). In *Drosophila melanogaster*, CSP α KOs that survive to adulthood demonstrate temperature-sensitive paralysis, uncoordinated movement, shaking and early death (Zinsmaier et al., 1994). It is clear that the function of CSP α is to protect the synapse, what is not known is the mechanism(s) underlying the prevention of synapse loss by CSP α . Understandably, much effort has focused on delineating the cellular pathway of CSP α -mediated protection.

THE CSP α TRIMERIC COMPLEX

CSP α contains a “J-domain” which is a ~70-amino acid region of homology shared by bacterial DnaJ and all other J proteins

as well as a palmitoylated cysteine-rich “string” region used for membrane attachment to the outer leaflet of synaptic vesicles (Braun and Scheller, 1995). Rather than being “constitutively active” CSP α becomes active upon assembly with SGT (small glutamine-rich tetratricopeptide repeat-containing protein) and Hsc70 (70-kDa heat-shock cognate protein) (Braun et al., 1996; Tobaben et al., 2001). Hsc70 is a central hub of the cellular chaperone network (Craig et al., 2006; Kakkar et al., 2012), and it follows that collapse of Hsc70 would be expected to cause collapse of the J protein network. Each member of the J protein family—there are 49 J proteins in *Homo sapiens*—has a J domain that activates Hsc70's ATPase activity for conformational work on diverse “client proteins” (Kakkar et al., 2012). Outside of the J domain, J proteins have little, if any, structural similarity. These non-homologous regions are, almost certainly, determinants of J protein specificity but do not provide much clarity into the functionality of specific J proteins. Since other J proteins do not compensate, CSP α is generally viewed as facilitating highly specific folding events. *In vitro*, mutation of the invariant tripeptide of histidine, proline and aspartic acid (HPD motif) located between helices II and III of CSP α 's four α helical J domain creates a loss-of-function mutant that does not activate Hsc70 (Chamberlain and Burgoyne, 1997). CSP α is also found in non-neuronal secretory cells including exocrine (Braun and Scheller, 1995; Zhao et al., 1997; Weng et al., 2009), endocrine (Brown et al., 1998; Zhang et al., 2002) and neuroendocrine (Kohan et al., 1995; Chamberlain et al., 1996) secretory granules and mammary cell small vesicles (Gleave et al., 2001). That said, the reduced life-span in CSP α KO mice is due to neurodegeneration.

THE INTERVAL PRECEDING FULMINANT NEURODEGENERATION

CSP α KO mice appear normal at birth, but around postnatal day 20, they develop progressive motor deficits and CNS degeneration, followed by early lethality between days 40–80 (Fernández-Chacón et al., 2004). In this context it is noteworthy that CSP α is not required for neurotransmitter release but only necessary to maintain synaptic function and architecture. *Which client proteins are critical for triggering the cascade of events leading to degeneration?* The field is now turning to better appreciate the age interval of CSP α KO mice when the demise of the synapse is likely to begin. While this early window remains to be fully dissected, we know that around 20 proteins have altered expression patterns by P28 and that these proteins represent potential primary “misfolding events” (Zhang et al., 2012). Activity-dependent degeneration in mice and temperature-sensitive paralysis in *Drosophila* are distinguishing features of CSP α null models. In mice, synapses that fire frequently, such as those associated with photoreceptors and GABAergic neurons, are lost first (Schmitz et al., 2006; García-Junco-Clemente et al., 2010). Early impairments in motor terminals are characterized by a failure to sustain prolonged release and impaired synaptic vesicle recycling (Rozas et al., 2012). In *Drosophila*, the $\sim 50\%$ reduction of nerve-evoked neurotransmitter release at 18–22°C and a drastic temperature-sensitive reduction in evoked release above 29°C is well established (Umbach et al., 1994; Zinsmaier et al., 1994; Nie et al., 1999; Dawson-Scully et al., 2000, 2007; Arnold et al., 2004; Bronk et al., 2005). Activity- and temperature-dependent degeneration in CSP α KO reflect the idea that nerve terminals are particularly vulnerable to misfolding and that CSP α is indispensable to refolding and repair. It is likely that CSP α is designed to facilitate folding of multiple “client proteins” whose unfolding leads to a second set of separate downstream degenerative events. However, many questions remain regarding CSP α ’s “protein client lineup”.

“RESCUE” OF CSP α KO MICE

Endogenous J proteins do not serve as “back ups” for the deletion of CSP α , however, overexpression of α -synuclein abrogates motor impairments and lethality in CSP α KO mice while KO of endogenous α -synuclein speeds up neurodegeneration (Chandra et al., 2005). Of note, mice deficient in α -synuclein do not have an obvious phenotype (Chandra et al., 2005). α -synuclein is a soluble presynaptic protein of unknown function that associates with synaptic vesicles and is the major component of Lewy bodies, a landmark of Parkinson’s disease and other neurodegenerative disorders (Maroteaux et al., 1988; Burré et al., 2010). CSP α / α -synuclein do not interact and Hsc70 ATPase is not activated by α -synuclein, hence, while CSP α and α -synuclein may target common “client proteins” they are nonetheless mechanistically distinct (Chandra et al., 2005). Somewhat paradoxically, treatment of CSP α KO mice with proteasome inhibitors ameliorates neurodegeneration and extends the life-span of CSP α KO mice (Sharma et al., 2012b). Thus, the neurodegeneration observed in CSP α KO mice is not due to a reduction in the proteasome capacity and the consequential elevation of ubiquitinated

synaptic proteins. While the physiological implications of these findings have not yet been elucidated, rescue of degeneration in CSP α KO mice serves as proof-of-principle for intervention in nerve terminal failure and synapse loss and may pave the way for development of therapeutic agents that prevent neurodegeneration.

EXOCYTOSIS AND ENDOCYTOSIS MACHINERY

SNARE (soluble N-ethylmaleimide-sensitive factor attachment receptors) proteins are fundamental to presynaptic vesicle-release events and for that reason have been closely scrutinized as possible CSP α “clients”. The t-SNARE, SNAP25 (synaptosomal associated protein of 25 kDa) expression is decreased in CSP α KO mice (Chandra et al., 2005; Zhang et al., 2012). However, it is the effective assembly/disassembly of SNAP25 into the SNARE complex during repeated rounds of exocytosis/endocytosis that correlates with the maintenance of synaptic function rather than cellular levels of SNAP25 (Sharma et al., 2011b, 2012a). While neurodegeneration is rescued by overexpression of wild-type, but not inactive mutants of SNAP-25, the decline in SNAP25 expression *per se* is unlikely to be a primary cause of neurodegeneration, as SNAP25 heterozygous mice with $\sim 50\%$ reduction in SNAP25 levels are phenotypically normal (Washbourne et al., 2002; Sharma et al., 2011b). Furthermore, the dramatic rescue of neurodegeneration in CSP α KO mice by α -synuclein, rescues the association of SNAP25 with other SNAREs but does not ameliorate the decrease in SNAP-25 expression (Sharma et al., 2011b, 2012a). More recently, it was shown that treatment of CSP α KO mice with proteasome inhibitors reverses impairment of SNARE-complex assembly and alleviates neurodegeneration (Sharma et al., 2012b). CSP α has also been shown to interact with the t-SNARE, syntaxin (Nie et al., 1999; Evans et al., 2001) and the Ca²⁺ binding protein, synaptotagmin (Evans and Morgan, 2002), emphasizing its role in chaperoning the exocytosis machinery. Taken together, degeneration in CSP α KO mice is halted by interventions that correct SNARE complex function including interventions that influence SNARE complex assembly without elevating SNAP25 levels. A separate line of investigation has revealed that CSP α KO mice also have an endocytosis defect resulting in the failure to recycle and maintain the size of the synaptic vesicle pool during prolonged stimulation (Rozas et al., 2012). In fact, early on (P28) in the course of degeneration the GTPase, dynamin 1, which is essential for endocytosis, is reduced by $\sim 40\%$ in CSP α KO mice (Zhang et al., 2012). CSP α directly interacts with dynamin 1 to promote polymerization, a process required in membrane fission (Zhang et al., 2012), however the mechanistic details linking endocytosis and CSP α dysfunction remain to be established. Insights into exocytosis/endocytosis defects will undoubtedly prove to be important in understanding the pathological uncoupling between presynaptic exocytosis and endocytosis.

PRESYNAPTIC ION CHANNELS: CHANNEL PROTEOSTASIS AND MULTI-PROTEIN COMPLEXES

Do changes in presynaptic ion channels or ion channel complexes trigger the activity-dependent and temperature-dependent

neurodegeneration in CSP α -KO mice? We have shown that large conductance Ca²⁺- and voltage-activated K⁺ (BK) channels are ~2.5 fold higher in the brain of CSP α null mice compared with age-matched wild types (Kyle et al., 2013). This increase in expression is observed at an early age (i.e., P23–P27), when levels of neuronal K_v1.1, K_v1.2 and Ca_v2.2 do not change. Physiologically, BK channels are activated by membrane depolarization and/or elevations in intracellular Ca²⁺ and drive the membrane potential towards the K⁺ equilibrium potential. Under normal conditions, BK channels regulate repolarization of the action potential, thereby regulating excitability of neurons, as well as presynaptic neurotransmitter release. Further, ectopic expression of dysfunctional CSP α mutants (i.e., CSP α _{HPD-AAA}, CSP α _{L116 Δ} , CSP α _{L115R}) also elicits elevation of BK channel expression and macroscopic current density (Kyle et al., 2013; Ahrendt et al., 2014) suggesting that the observed increase, at least initially, reflects an elevation of functional, rather than misfolded or aggregated BK channel protein. CSP α _{HPD-AAA} is a loss-of-function mutant in which the essential J domain required for activation of Hsc70ATPase is disrupted but the cysteine string anchor is functional. The increase found in the presence of this loss-of-function mutant is consistent with the increase in BK channel expression observed in CSP α null mice. On the other hand, while CSP α _{L116 Δ} and CSP α _{L115R} increase BK channel density at the membrane, the increase is not as large as that observed with CSP α _{HPD-AAA} (Kyle et al., 2013), suggesting that CSP α _{L116 Δ} and CSP α _{L115R} are partial loss-of-function mutants. In humans, deletion of residue 116 or replacement of Lys115 by Arg in the cysteine string region results in ANCL (Benitez et al., 2011; Nosková et al., 2011; Velinov et al., 2012), however the mechanism(s) underlying disease pathology is not known. It is becoming increasingly clear that changes in the cysteine string region can promote oligomerization. Wild type CSP α self-associates (Braun and Scheller, 1995) and this dimerization is eliminated in the absence of the cysteine string region (Xu et al., 2010). When expressed in bacteria, which lack eukaryotic palmitoyltransferase enzymes, CSP α forms oligomers and the cysteine string region is important for the self-association (Swayne et al., 2003). Two mutations in the cysteine string region of CSP α , L116 Δ and L115R, do not effectively anchor to synaptic vesicles and form oligomers indicating the cysteine string region is closely tied to oligomerization properties (Greaves et al., 2012). Clearly, identification of the neuronal location of CSP α _{L116 Δ} /CSP α _{L115R} oligomers is central to understanding ANCL disease progression. Thus, disruption of the anchor to the synaptic vesicle while maintaining the functional J domain in the CSP α _{L116 Δ} and CSP α _{L115R} mutants and subsequent CSP α oligomerization and cellular mislocalization likely leads to indiscriminate chaperone activity. We speculate that CSP α _{L116 Δ} and CSP α _{L115R} cause both a partial loss-of-function (i.e., reduced chaperone activity at the synaptic vesicle) as well as gain-of-function (i.e., increased chaperone activity at a different cellular location). Consistent with this notion, CSP α heterozygote mice do not show neurodegeneration while ANCL patients show adult-onset neurodegeneration most likely due to mislocalized/oligomerized mutant CSP α chaperone activity outside the presynapse. *Do changes in BK channel activity link to neurological disorders or neurodegeneration?* Several studies

have reported that alterations in the expression and function of BK channels give rise to neural dysfunction. For example, genetic deletion of BK channel subunits in mice (Sausbier et al., 2004; Brenner et al., 2005) and a gain-of-function channel mutation in humans (Du et al., 2005; Díez-Sampedro et al., 2006) are associated with ataxia and epilepsy, while functional alterations are associated with retardation, schizophrenia and autism (Laumonnier et al., 2006; Zhang et al., 2006; Higgins et al., 2008; Deng et al., 2013). Clearly, when BK channel activity is disrupted, neural excitability and neurotransmitter release are disrupted, but neurodegeneration *per se* does not typically ensue raising a number of interesting questions. *Does the fulminant, activity-dependent neurodegeneration seen in CSP α KO mice result from a coupling of aberrant BK channel expression with synaptic vesicle release/recycling defects? What underlies the rapid rate of degeneration in CSP α KO mice. Further, are complexes of BK channels with other synaptic proteins regulated by CSP α ?* BK channels are subject to a wide array of regulatory processes, including interactions with SNARE proteins (Ling et al., 2003); however the precise details of these channel complexes in CSP α KO mice remain to be investigated. We speculate that CSP α directly modulates BK channel density, nonetheless this is not a foregone conclusion. Future experiments will undoubtedly establish whether CSP α acts indirectly via one of the known regulators of BK channel activity or by directly targeting the channels.

Do functional and/or structural changes in voltage-dependent Ca²⁺ channels occur early in the pathological sequence of events underlying neurodegeneration in CSP α KO mice? Whether CSP α directly regulates Ca²⁺ currents remains contentious. Ca²⁺ entry into presynaptic nerve terminals is fundamental to neurotransmission and consequently subject to multiple levels of control. A large body of work has clarified that neurotransmission defects at the neuromuscular junction involve a decrease in quantal content, a reduction in the calcium sensitivity of evoked exocytosis and anomalous bursts of spontaneous neurotransmitter release (Umbach et al., 1994; Zinsmaier et al., 1994; Dawson-Scully et al., 2000, 2007; Ruiz et al., 2008). Further, recruitment of Ca²⁺ channels (Chen et al., 2002) as well as physical interactions of CSP α with N-type and P/Q type voltage-dependent Ca²⁺ channels have been demonstrated (Leveque et al., 1998; Miller et al., 2003a,b; Swayne et al., 2005, 2006). Whether it is the synaptic vesicle-anchored monomeric CSP α or the mislocalized CSP α oligomers that regulate Ca²⁺ currents requires further investigation. We have found that CSP α influences the regulation of N-type Ca²⁺ channels by heterotrimeric GTP binding proteins (Maggia et al., 2000; Miller et al., 2003b; Natochin et al., 2005). There are still many unanswered questions regarding the role of CSP α in regulating synaptic channels and synaptic channel complexes. The CSP α KO mouse model offers an excellent opportunity to study channel proteostasis and channel complexes that may contribute to activity-dependent neurodegeneration. How CSP α might function in different secretory cells (e.g., pancreatic exocrine and endocrine cells), given the differences in their complement of ion channels, also remains to be determined. Further efforts will be needed to untangle the neuroprotective pathway(s) involving CSP α at the synapse and to establish precisely the complement

of synaptic channels involved in the cascade of neurodegenerative events triggered by the absence of CSP α .

In summary, ion channels are physiologically regulated within tight limits and present evidence implicates the presynaptic molecular chaperone CSP α in the fine-tuning of functional channel levels and regulation of synaptic channel complexes. In the future, it will be interesting to determine whether CSP α is also important for the quality control of mis-folded/aberrant channels. The time course of the expression changes in SNAP25, dynamin 1 and synaptic channels in CSP α KO mice remains a key question.

JEOPARDIZING THE SYNAPSE: LINKS TO ALZHEIMER'S AND PARKINSON'S DISEASE

Clearly, the dysfunction of CSP α is linked to undesired consequences. Neurodegenerative diseases such as Alzheimer's disease and Parkinson's disease show a characteristic loss of neurons and synapses (Muchowski and Wacker, 2005). The identification of CSP α as a central chaperone for the maintenance of synapses raises the questions: *are cellular CSP α -neuroprotective pathways compromised in neurodegenerative disorders other than ANCL? Do functionally impaired proteins that build up in neurodegenerative disorders interfere with CSP α chaperone activity?* It is noteworthy that lysosomal lipofuscin inclusions, like those seen in ANCL, are present in very early onset (age 30) and rapidly progressing Alzheimer's disease caused by presenilin 1 mutations (Dolzanskaya et al., 2014). Moreover, CSP α is reduced in the frontal cortex of humans with Alzheimer's disease (Zhang et al., 2012) and SNARE complex assembly is impaired in human brain tissue from patients with Alzheimer's Disease and Parkinson's Disease (Sharma et al., 2012b). Interference with CSP α , SNARE complex assembly, dynamin 1 assembly and ion channel complexes by impaired/toxic proteins typically found in neurodegenerative disorders may, at least in part, contribute to neurodegeneration and these possibilities will undoubtedly be the focus of future investigations.

FUTURE PERSPECTIVES

When CSP α is compromised, protein surveillance and proteostasis mechanisms in the neuron fail and the integrity of pre-synaptic terminals is compromised. The field is now poised to tackle in detail the pathogenic sequence of events responsible for activity-dependent neurodegeneration in the absence of CSP α chaperone activity. The emerging detailed molecular blueprint will undoubtedly serve investigators well in the development of therapeutics that protect against synaptic loss in neurodegenerative disorders.

REFERENCES

- Ahrendt, E., Kyle, B., Braun, A. P., and Braun, J. E. (2014). Cysteine string protein limits expression of the large conductance, calcium-activated K(+) (BK) channel. *PLoS One* 9:e86586. doi: 10.1371/journal.pone.0086586
- Arnold, C., Reisch, N., Leibold, C., Becker, S., Prufert, K., Sautter, K., et al. (2004). Structure-function analysis of the cysteine string protein in *Drosophila*: cysteine string, linker and C terminus. *J. Exp. Biol.* 207, 1323–1334. doi: 10.1242/jeb.00898
- Benitez, B. A., Alvarado, D., Cai, Y., Mayo, K., Chakraverty, S., Norton, J., et al. (2011). Exome-sequencing confirms DNAJC5 mutations as cause of adult neuronal ceroid-lipofuscinosis. *PLoS One* 6:e26741. doi: 10.1371/journal.pone.0026741
- Braun, J. E., and Scheller, R. H. (1995). Cysteine string protein, a DnaJ family member, is present on diverse secretory vesicles. *Neuropharmacology* 34, 1361–1369. doi: 10.1016/0028-3908(95)00114-1
- Braun, J. E., Wilbanks, S. M., and Scheller, R. H. (1996). The cysteine string secretory vesicle protein activates Hsc70 ATPase. *J. Biol. Chem.* 271, 25989–25993. doi: 10.1074/jbc.271.42.25989
- Brenner, R., Chen, Q. H., Vilaythong, A., Toney, G. M., Noebels, J. L., and Aldrich, R. W. (2005). BK channel beta4 subunit reduces dentate gyrus excitability and protects against temporal lobe seizures. *Nat. Neurosci.* 8, 1752–1759. doi: 10.1038/nn1573
- Bronk, P., Nie, Z., Klose, M. K., Dawson-Scully, K., Zhang, J., Robertson, R. M., et al. (2005). The multiple functions of cysteine-string protein analyzed at *Drosophila* nerve terminals. *J. Neurosci.* 25, 2204–2214. doi: 10.1523/jneurosci.3610-04.2005
- Brown, H., Larsson, O., Branstrom, R., Yang, S., Leibiger, B., Leibiger, I., et al. (1998). Cysteine string protein (CSP) is an insulin secretory granule-associated protein regulating beta-cell exocytosis. *EMBO J.* 17, 5048–5058. doi: 10.1093/emboj/17.17.5048
- Burré, J., Sharma, M., Tsetsenis, T., Buchman, V., Etherton, M. R., and Sudhof, T. C. (2010). Alpha-synuclein promotes SNARE-complex assembly in vivo and in vitro. *Science* 329, 1663–1667. doi: 10.1126/science.1195227
- Chamberlain, L. H., and Burgoyne, R. D. (1997). The molecular chaperone function of the secretory vesicle cysteine string proteins. *J. Biol. Chem.* 272, 31420–31426. doi: 10.1074/jbc.272.50.31420
- Chamberlain, L. H., Henry, J., and Burgoyne, R. D. (1996). Cysteine string proteins are associated with chromaffin granules. *J. Biol. Chem.* 271, 19514–19517. doi: 10.1074/jbc.271.32.19514
- Chandra, S., Gallardo, G., Fernandez-Chacon, R., Schluter, O. M., and Sudhof, T. C. (2005). Alpha-synuclein cooperates with CSP alpha in preventing neurodegeneration. *Cell* 123, 383–396. doi: 10.1016/j.cell.2005.09.028
- Chen, S., Zheng, X., Schulze, K. L., Morris, T., Bellen, H., and Stanley, E. F. (2002). Enhancement of presynaptic calcium current by cysteine string protein. *J. Physiol.* 538, 383–389. doi: 10.1113/jphysiol.2001.013397
- Craig, E. A., Huang, P., Aron, R., and Andrew, A. (2006). The diverse roles of J-proteins, the obligate Hsp70 co-chaperone. *Rev. Physiol. Biochem. Pharmacol.* 156, 1–21. doi: 10.1007/s10254-005-0001-0
- Dawson-Scully, K., Bronk, P., Atwood, H. L., and Zinsmaier, K. E. (2000). Cysteine-string protein increases the calcium sensitivity of neurotransmitter exocytosis in *Drosophila*. *J. Neurosci.* 20, 6039–6047.
- Dawson-Scully, K., Lin, Y., Imad, M., Zhang, J., Marin, L., Horne, J. A., et al. (2007). Morphological and functional effects of altered cysteine string protein at the *Drosophila* larval neuromuscular junction. *Synapse* 61, 1–16. doi: 10.1002/syn.20335
- Deng, P. Y., Rotman, Z., Blundon, J. A., Cho, Y., Cui, J., Cavalli, V., et al. (2013). FMRP regulates neurotransmitter release and synaptic information transmission by modulating action potential duration via BK channels. *Neuron* 77, 696–711. doi: 10.1016/j.neuron.2012.12.018
- Díez-Sampedro, A., Silverman, W. R., Bautista, J. F., and Richerson, G. B. (2006). Mechanism of increased open probability by a mutation of the BK channel. *J. Neurophysiol.* 96, 1507–1516. doi: 10.1152/jn.00461.2006
- Dolzanskaya, N., Gonzalez, M. A., Sperziani, F., Steff, S., Messing, J., Wen, G. Y., et al. (2014). A novel p.Leu(381)Phe mutation in presenilin 1 is associated with very early onset and unusually fast progressing dementia as well as lysosomal inclusions typically seen in Kufs disease. *J. Alzheimers Dis.* 39, 23–27. doi: 10.3233/JAD-131340
- Du, W., Bautista, J. F., Yang, H., Díez-Sampedro, A., You, S. A., Wang, L., et al. (2005). Calcium-sensitive potassium channelopathy in human epilepsy and paroxysmal movement disorder. *Nat. Genet.* 37, 733–738. doi: 10.1038/ng1585
- Evans, G. J., and Morgan, A. (2002). Phosphorylation-dependent interaction of the synaptic vesicle proteins cysteine string protein and synaptotagmin I. *Biochem. J.* 364, 343–347. doi: 10.1042/bj20020123
- Evans, G. J., Wilkinson, M. C., Graham, M. E., Turner, K. M., Chamberlain, L. H., Burgoyne, R. D., et al. (2001). Phosphorylation of cysteine string protein by protein kinase A. Implications for the modulation of exocytosis. *J. Biol. Chem.* 276, 47877–47885. doi: 10.1074/jbc.M108186200
- Fernández-Chacón, R., Wolfel, M., Nishimune, H., Tabares, L., Schmitz, F., Castellano-Munoz, M., et al. (2004). The synaptic vesicle protein CSP alpha prevents presynaptic degeneration. *Neuron* 42, 237–251. doi: 10.1016/s0896-6273(04)00190-4

- García-Junco-Clemente, P., Cantero, G., Gomez-Sanchez, L., Linares-Clemente, P., Martinez-Lopez, J. A., Lujan, R., et al. (2010). Cysteine string protein- α prevents activity-dependent degeneration in GABAergic synapses. *J. Neurosci.* 30, 7377–7391. doi: 10.1523/jneurosci.0924-10.2010
- Gleave, T. L., Beechey, R. B., and Burgoyne, R. D. (2001). Cysteine string protein expression in mammary epithelial cells. *Pflugers Arch.* 441, 639–649. doi: 10.1007/s004240000478
- Greaves, J., Lemonidis, K., Gorleku, O. A., Cruchaga, C., Grefen, C., and Chamberlain, L. H. (2012). Palmitoylation-induced aggregation of cysteine-string protein mutants that cause neuronal ceroid lipofuscinosis. *J. Biol. Chem.* 287, 37330–37339. doi: 10.1074/jbc.M112.389098
- Higgins, J. J., Hao, J., Kosofsky, B. E., and Rajadhyaksha, A. M. (2008). Dysregulation of large-conductance Ca^{2+} -activated K^{+} channel expression in nonsyndromal mental retardation due to a cereblon p.R419X mutation. *Neurogenetics* 9, 219–223. doi: 10.1007/s10048-008-0128-2
- Kakkar, V., Prins, L. C., and Kampinga, H. H. (2012). DNAJ proteins and protein aggregation diseases. *Curr. Top. Med. Chem.* 12, 2479–2490. doi: 10.2174/1568026611212220004
- Kohan, S. A., Pescatori, M., Brecha, N. C., Mastrogiacomio, A., Umbach, J. A., and Gundersen, C. B. (1995). Cysteine string protein immunoreactivity in the nervous system and adrenal gland of rat. *J. Neurosci.* 15, 6230–6238.
- Kyle, B. D., Ahrendt, E., Braun, A. P., and Braun, J. E. (2013). The large conductance, calcium-activated K^{+} (BK) channel is regulated by cysteine string protein. *Sci. Rep.* 3:2447. doi: 10.1038/srep02447
- Laumonnier, F., Roger, S., Guerin, P., Molinari, E., M'rad, R., Cahard, D., et al. (2006). Association of a functional deficit of the BKCa channel, a synaptic regulator of neuronal excitability, with autism and mental retardation. *Am. J. Psychiatry* 163, 1622–1629. doi: 10.1176/appi.ajp.163.9.1622
- Leveque, C., Pupier, S., Marquize, B., Geslin, L., Kataoka, M., Takahashi, M., et al. (1998). Interaction of cysteine string proteins with the $\alpha 1A$ subunit of the P/Q-type calcium channel. *J. Biol. Chem.* 273, 13488–13492. doi: 10.1074/jbc.273.22.13488
- Ling, S., Sheng, J.-Z., Braun, J. E. A., and Braun, A. P. (2003). Syntaxin 1A co-associates with native rat brain and cloned large conductance, calcium-activated K^{+} channels in situ. *J. Physiol.* 533, 65–81. doi: 10.1113/jphysiol.2003.051631
- Magga, J. M., Jarvis, S. E., Arnot, M. I., Zamponi, G. W., and Braun, J. E. (2000). Cysteine string protein regulates G-protein modulation of N-type calcium channels. *Neuron* 28, 195–204. doi: 10.1016/S0896-6273(00)00096-9
- Maroteaux, L., Campanelli, J. T., and Scheller, R. H. (1988). Synuclein: a neuron-specific protein localized to the nucleus and presynaptic nerve terminal. *J. Neurosci.* 8, 2804–2815.
- Miller, L. C., Swayne, L. A., Chen, L., Feng, Z. P., Wacker, J. L., Muchowski, P. J., et al. (2003a). Cysteine string protein (CSP) inhibition of N-type calcium channels is blocked by mutant huntingtin. *J. Biol. Chem.* 278, 53072–53081. doi: 10.1074/jbc.M306230200
- Miller, L. C., Swayne, L. A., Kay, J. G., Feng, Z. P., Jarvis, S. E., Zamponi, G. W., et al. (2003b). Molecular determinants of cysteine string protein modulation of N-type calcium channels. *J. Cell Sci.* 116, 2967–2974. doi: 10.1242/jcs.00595
- Muchowski, P. J., and Wacker, J. L. (2005). Modulation of neurodegeneration by molecular chaperones. *Nat. Rev. Neurosci.* 6, 11–22. doi: 10.1038/nrn1587
- Natochin, M., Campbell, T. N., Barren, B., Miller, L. C., Hameed, S., Artemyev, N. O., et al. (2005). Characterization of the G $\alpha(s)$ regulator cysteine string protein. *J. Biol. Chem.* 280, 30236–30241. doi: 10.1074/jbc.M500722200
- Nie, Z., Ranjan, R., Wenniger, J. J., Hong, S. N., Bronk, P., and Zinsmaier, K. E. (1999). Overexpression of cysteine-string proteins in *Drosophila* reveals interactions with syntaxin. *J. Neurosci.* 19, 10270–10279.
- Nosková, L., Stranecky, V., Hartmannova, H., Pristoupilova, A., Baresova, V., Ivanek, R., et al. (2011). Mutations in DNAJC5, encoding cysteine-string protein α , cause autosomal-dominant adult-onset neuronal ceroid lipofuscinosis. *Am. J. Hum. Genet.* 89, 241–252. doi: 10.1016/j.ajhg.2011.09.003
- Rozas, J. L., Gomez-Sanchez, L., Mircheski, J., Linares-Clemente, P., Nieto-Gonzalez, J. L., Vazquez, M. E., et al. (2012). Motorneurons require cysteine string protein- α to maintain the readily releasable vesicular pool and synaptic vesicle recycling. *Neuron* 74, 151–165. doi: 10.1016/j.neuron.2012.02.019
- Ruiz, R., Casanas, J. J., Sudhof, T. C., and Tabares, L. (2008). Cysteine string protein- α is essential for the high calcium sensitivity of exocytosis in a vertebrate synapse. *Eur. J. Neurosci.* 27, 3118–3131. doi: 10.1111/j.1460-9568.2008.06301.x
- Sausbier, M., Hu, H., Arntz, C., Feil, S., Kamm, S., Adelsberger, H., et al. (2004). Cerebellar ataxia and Purkinje cell dysfunction caused by Ca^{2+} -activated K^{+} channel deficiency. *Proc. Natl. Acad. Sci. U S A* 101, 9474–9478. doi: 10.1073/pnas.0401702101
- Schmitz, F., Tabares, L., Khimich, D., Strenke, N., de la Villa-Polo, P., Castellano-Munoz, M., et al. (2006). CSP α -deficiency causes massive and rapid photoreceptor degeneration. *Proc. Natl. Acad. Sci. U S A* 103, 2926–2931. doi: 10.1073/pnas.0510060103
- Sharma, M., Burre, J., and Sudhof, T. C. (2011b). CSP α promotes SNARE-complex assembly by chaperoning SNAP-25 during synaptic activity. *Nat. Cell Biol.* 13, 30–39. doi: 10.1038/ncb0211-182a
- Sharma, M., Burre, J., Bronk, P., Zhang, Y., Xu, W., and Sudhof, T. C. (2012a). CSP α knockout causes neurodegeneration by impairing SNAP-25 function. *EMBO J.* doi: 10.1038/emboj.2011.467
- Sharma, M., Burre, J., and Sudhof, T. C. (2012b). Proteasome inhibition alleviates SNARE-dependent neurodegeneration. *Sci. Transl. Med.* 4, 147ra113. doi: 10.1126/scitranslmed.3004028
- Swayne, L. A., Beck, K. E., and Braun, J. E. (2006). The cysteine string protein multimeric complex. *Biochem. Biophys. Res. Commun.* 348, 83–91. doi: 10.1016/j.bbrc.2006.07.033
- Swayne, L. A., Blattler, C., Kay, J. G., and Braun, J. E. A. (2003). Oligomerization characteristics of cysteine string protein. *Biochem. Biophys. Res. Commun.* 300, 921–926. doi: 10.1016/S0006-291X(02)02964-9
- Swayne, L. A., Chen, L., Hameed, S., Barr, W., Charlesworth, E., Colicos, M. A., et al. (2005). Crosstalk between huntingtin and syntaxin 1A regulates N-type calcium channels. *Mol. Cell. Neurosci.* 30, 339–351. doi: 10.1016/j.mcn.2005.07.016
- Tobaben, S., Thakur, P., Fernandez-Chacon, R., Sudhof, T. C., Rettig, J., and Stahl, B. (2001). A trimeric protein complex functions as a synaptic chaperone machine. *Neuron* 31, 987–999. doi: 10.1016/S0896-6273(01)00427-5
- Umbach, J. A., Zinsmaier, K. E., Eberle, K. K., Buchner, E., Benzer, S., and Gundersen, C. B. (1994). Presynaptic dysfunction in *Drosophila* csp mutants. *Neuron* 13, 899–907. doi: 10.1016/0896-6273(94)90255-0
- Velinov, M., Dolzhanskaya, N., Gonzalez, M., Powell, E., Konidari, I., Hulme, W., et al. (2012). Mutations in the gene DNAJC5 cause autosomal dominant kufs disease in a proportion of cases: study of the parry family and 8 other families. *PLoS One* 7:e29729. doi: 10.1371/journal.pone.0029729
- Washbourne, P., Thompson, P. M., Carta, M., Costa, E. T., Mathews, J. R., Lopez-Bendito, G., et al. (2002). Genetic ablation of the t-SNARE SNAP-25 distinguishes mechanisms of neuroexocytosis. *Nat. Neurosci.* 5, 19–26. doi: 10.1038/nn783
- Weng, N., Baumler, M. D., Thomas, D. D., Falkowski, M. A., Swayne, L. A., Braun, J. E., et al. (2009). Functional role of J domain of cysteine string protein in Ca^{2+} -dependent secretion from acinar cells. *Am. J. Physiol. Gastrointest. Liver Physiol.* 296, G1030–G1039. doi: 10.1152/ajpgi.90592.2008
- Xu, F., Proft, J., Gibbs, S., Winkfein, B., Johnson, J. N., Syed, N., et al. (2010). Quercetin targets cysteine string protein (CSP α) and impairs synaptic transmission. *PLoS One* 5:e11045. doi: 10.1371/journal.pone.0011045
- Zhang, Y. Q., Henderson, M. X., Colangelo, C. M., Ginsberg, S. D., Bruce, C., Wu, T., et al. (2012). Identification of CSP α clients reveals a role in dynamin 1 regulation. *Neuron* 74, 136–150. doi: 10.1016/j.neuron.2012.01.029
- Zhang, W., Khan, A., Ostenson, C. G., Berggren, P. O., Efendic, S., and Meister, B. (2002). Down-regulated expression of exocytotic proteins in pancreatic islets of diabetic GK rats. *Biochem. Biophys. Res. Commun.* 291, 1038–1044. doi: 10.1006/bbrc.2002.6555
- Zhang, L., Li, X., Zhou, R., and Xing, G. (2006). Possible role of potassium channel, big K in etiology of schizophrenia. *Med. Hypotheses* 67, 41–43. doi: 10.1016/j.mehy.2005.09.055
- Zhao, C. M., Jacobsson, G., Chen, D., Hakanson, R., and Meister, B. (1997). Exocytotic proteins in enterochromaffin-like (ECL) cells of the rat stomach. *Cell Tissue Res.* 290, 539–551. doi: 10.1007/s004410050960

Zinsmaier, K. E., Eberle, K. K., Buchner, E., Walter, N., and Benzer, S. (1994). Paralysis and early death in cysteine string protein mutants of *Drosophila*. *Science* 263, 977–980. doi: 10.1126/science.8310297

Conflict of Interest Statement: The authors declare that the research was conducted in the absence of any commercial or financial relationships that could be construed as a potential conflict of interest.

Received: 14 March 2014; accepted: 09 April 2014; published online: 29 April 2014.

Citation: Donnelier J and Braun JEA (2014) CSP α —chaperoning presynaptic proteins. *Front. Cell. Neurosci.* 8:116. doi: 10.3389/fncel.2014.00116

This article was submitted to the journal *Frontiers in Cellular Neuroscience*.

Copyright © 2014 Donnelier and Braun. This is an open-access article distributed under the terms of the Creative Commons Attribution License (CC BY). The use, distribution or reproduction in other forums is permitted, provided the original author(s) or licensor are credited and that the original publication in this journal is cited, in accordance with accepted academic practice. No use, distribution or reproduction is permitted which does not comply with these terms.



The essential roles of protein–protein interaction in sigma-1 receptor functions

Mohan Pabba*

Neurosciences Unit, Department of Cellular and Molecular Medicine, Faculty of Medicine, University of Ottawa, Ottawa, ON, Canada

*Correspondence: mpabb044@uottawa.ca; mpabba@ohri.ca

Edited by:

Christophe Altier, University of Calgary, Canada

Reviewed by:

Christophe Altier, University of Calgary, Canada

σ -1R is the well-known subtype of σ -Rs that were originally proposed in 1976 (Martin et al., 1976). σ -1R is a 223 amino acid integral membrane protein consisting of a short N-terminus, a large C-terminus tail, and two transmembrane domains: one at the N-terminus and the other in the middle of the protein (Su et al., 2010). σ -1Rs are distributed throughout the brain. At the subcellular level, σ -1Rs are mainly localized at the endoplasmic reticulum (ER)/mitochondrial associated membranes (MAM) and at very low levels in post-synaptic thickenings of the neuron (Alonso et al., 2000; Su et al., 2010). σ -1Rs at ER/MAM membranes exist in clustered globular structures that are enriched with cholesterol and neutral lipids (Hayashi and Su, 2003, 2005). Several categories of drugs bind to σ -1Rs, for example: cocaine, dihydroepiandrosterone, dimethyl tryptamine (DMT), psychotomimetic compounds, and haloperidol (antagonist). The steroids and DMT were proposed to act as endogenous ligands for the σ -1R. Studies from various laboratories performed on heterologous, *in vivo* and *ex vivo* systems by employing multidisciplinary techniques demonstrated that the σ -1R interacts with numerous cellular components (Su et al., 2010), e.g., different classes of ion channels, kinases, G-protein coupled receptors (GPCRs), etc. The σ -1R associates with voltage-gated ion channels, e.g., Na^+ , K^+ , and Ca^{2+} . Interaction of the σ -1R with voltage-gated K^+ and Ca^{2+} channels results in either inhibition or enhancement in the activities of these ion channels, whereas σ -1R interaction with voltage-gated Na^+ channels results in inhibition of the channel activity (Kourrich et al., 2012). On the other hand, σ -1R enhances the activity of *N*-methyl-D-aspartate receptors (NMDARs) (a ligand-gated ion channel)

and dopamine D_1 receptors (a GPCR) (Monnet et al., 1990; Navarro et al., 2010). The σ -1R modulation of D_1 R is through protein–protein interactions (Navarro et al., 2010). However, it is yet to be determined whether σ -1R modulates the NMDAR function through protein–protein interactions. Nevertheless, a recent study demonstrated that σ -1R inhibits the activity of small conductance Ca^{2+} -activated K^+ -channels (SK channels), and consequently potentiates the NMDAR function (Martina et al., 2007). It is still unknown if there is any physical association between SK channels and σ -1Rs.

How does the σ -1R, being an intracellular protein, modulate the functions of numerous cellular components that are present at the plasma membrane? The prevailing hypothesis is that under resting conditions, at ER/MAM, σ -1Rs are associated with chaperone called BiP. Upon activation of σ -1Rs by their agonists (at concentrations \sim equal to or less than 10 times their K_i value), σ -1R dissociates from BiP and modulates the function of inositol triphosphate (IP_3) receptors. The σ -1R modulation of IP_3 receptor function consequently affects Ca^{2+} influx and signaling into the mitochondria (Hayashi and Su, 2007). However, if σ -1R agonists are present at high concentrations ($\sim >10$ times their K_i value) or during the ER stress, σ -1R dissociates from BiP and translocates to the plasma membrane or plasmalemma and modulates the activities of various cellular components via protein–protein interactions (Su et al., 2010). While this model is promising, several outstanding questions remain to be addressed with respect to σ -1Rs and their association with cellular components, especially different classes of ion

channels (**Figure 1**). For instance, first, it needs to be clarified whether the σ -1R modulates multiple cellular components at the plasma membrane or at the plasmalemma of neurons (Su et al., 2010). Second, it is unclear at the moment if the σ -1R associates with ion channels (e.g., voltage-gated Na^+ or K^+ channels) at the ER/MAM, and after association, whether or not the entire complex (σ -1R-ion channel) is translocated to the plasma membrane. Third, investigations from different laboratories demonstrated that the treatment of animals with several σ -1R ligands alter the behavior of animals in various behavioral paradigms such as cocaine-induced behavioral response, NMDAR-antagonism induced amnesia, etc. Hence, it remains to be investigated if there is any link between σ -1Rs association with voltage-gated and/or ligand-gated ion channels, and the alteration in animal behavior, at least in the above-mentioned conditions. Forth, how the σ -1R modulates the functions of voltage-gated and ligand-gated ion channels heterogeneously and to a varying degree remains elusive. Although there can be multiple factors involved, the following reasons could play an important role in differential regulation of voltage-gated and ligand-gated ion channels by σ -1Rs. (a) Recently, it is shown that the σ -1R could exist in dimers (Chu et al., 2013); therefore, do the dimers of σ -1R associate with ion channels? (b) What is the stoichiometry of the σ -1R interaction with ion channels? (c) Several lines of evidence demonstrate that there exist subtypes within the σ -1Rs (Bergeron and Debonnel, 1997; Shioda et al., 2012); thus, do these subtypes display differences in association with ion channels? (d) What is the conformational crystal structure of the σ -1R

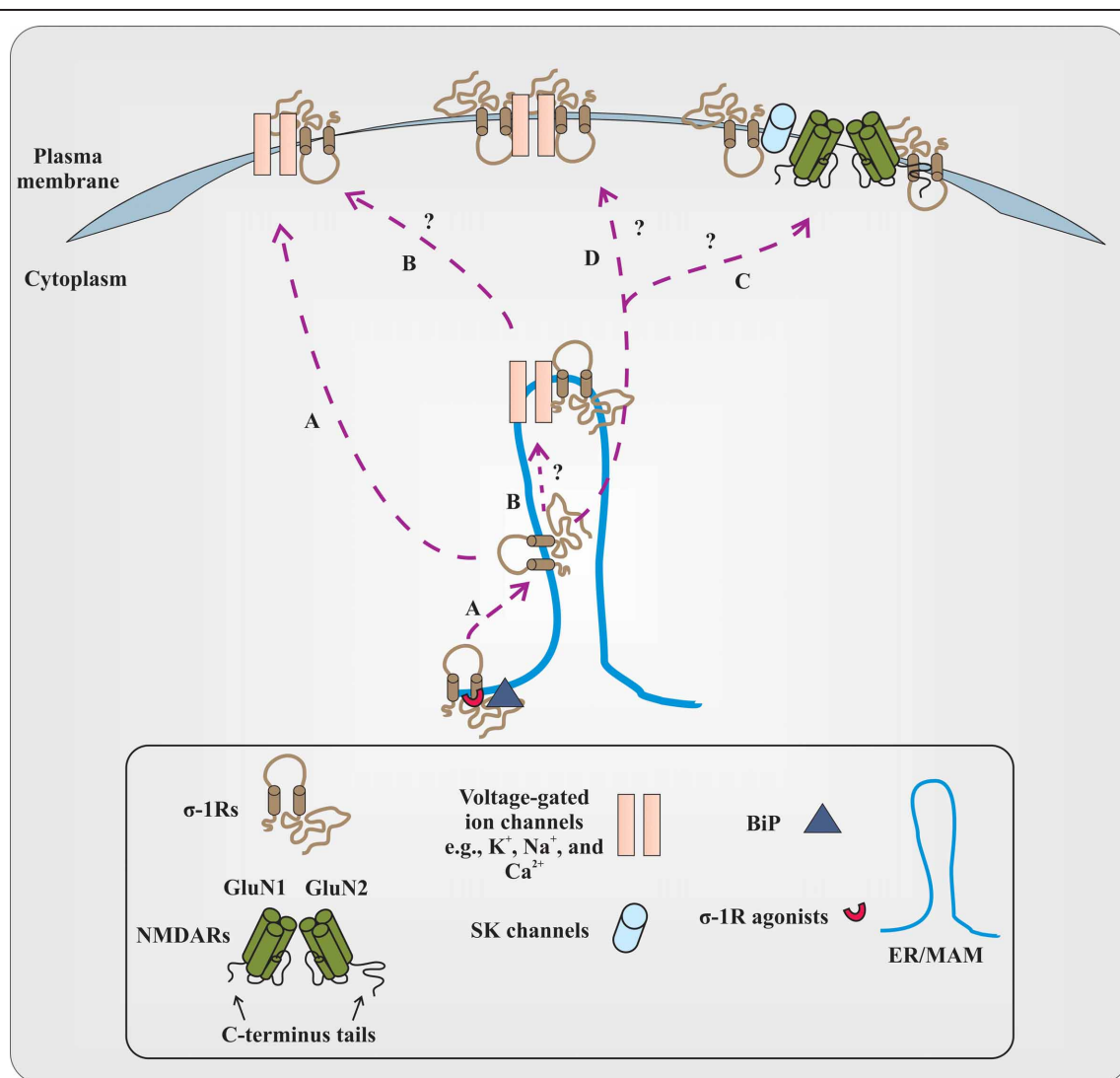


FIGURE 1 | Proposed and elusive mechanism(s) of σ -1R modulation of the function of voltage-gated and ligand-gated ion channels. (A) The prevailing hypothesis is that activation of σ -1Rs with high concentrations of their agonists (red colored semi-circle) causes σ -1Rs two transmembrane domains (black colored line boundaries and respective tails in a light brown color), at the ER/MAM, to dissociate from the chaperone called BiP (dark gray colored triangle). The dissociated σ -1Rs translocate to the plasma membrane or plasmalemma and in a subtype dependent manner, either inhibit or enhance the function of ion channels by forming protein-protein interactions. **(B)** It remains to be identified if the dissociated σ -1Rs associate with ion channels at the ER/MAM, and after association, whether or not the entire complex is translocated

toward the plasma membrane. The study from Kourrich et al. (2013) supports this possibility, at least with voltage-gated K^+ -channel Kv1.2. **(C)** It is unclear if dissociated and translocated σ -1Rs associate with SK channels or NMDARs. The functional NMDARs are tetrameric assemblies of two obligatory GluN1 subunits with either two GluN2 subunits (different combinations of GluN2 subunits) or GluN3 subunits. For representation, the dimer form of NMDARs (GluN1 and GluN2 subunits) and their C-terminus tails are presented in the figure. The N-terminus domain of NMDAR subunits and GluN3 subunits are not shown. **(D)** The other possibilities that remain unexplored are whether the dimers of the σ -1R interact with ion channels, and the stoichiometry of interaction between the σ -1R and ion channels.

in association with either voltage-gated or ligand-gated ion channels? (e) Which amino acid residues or motif(s) in the σ -1R determine the σ -1R association with various classes of ion channels? (f) Which polar and non-polar amino acid residues of the σ -1R influence the biophysical properties of σ -1R-associated ion channels?

The crystallographic data could provide enough evidence regarding the residues and domains of the σ -1R involved in physical association with ion channels. Additionally, it could also provide information regarding the differences in associations between σ -1Rs and various ion channels, if there are any. Finally, are

there any spatial requirements for the σ -1R to associate with ion channels, given σ -1R-modulated ion channels (e.g., voltage-gated Na^+ and K^+ channels) have some overlapping distribution in the neuron (Trimmer and Rhodes, 2004)?

However, a recent study by employing a multidisciplinary approach elegantly

demonstrated that the σ -1R's interaction with voltage-gated K^+ channel Kv1.2 plays an important role in the cocaine-induced locomotor sensitization (Kourrich et al., 2013). Using pharmacological blockers and knockdown of σ -1Rs, Kourrich et al. (2013) first identified that σ -1Rs are involved in cocaine-induced long-lasting neuronal and behavioral adaptation. Then, by employing electrophysiological recordings as well as biochemical studies on *ex vivo* tissue and heterologous cells, they confirmed that the σ -1R's interaction with voltage-gated K^+ channel Kv1.2 contributes/participates in the behavioral response (locomotor sensitization) to cocaine. Studies from Kourrich et al. (2013) have provided valuable information in terms of the σ -1R's association with ion channels, at least with voltage-gated K^+ -channels such as: (a) the σ -1R could possibly associate with these ion channels at the ER/MAM, and then the entire complex is trafficked toward the plasma membrane; (b) the potential link between σ -1R association with these ion channels and alteration in the behavior of animals; and importantly, (c) the structural orientation of the σ -1R at the plasma membrane during the association with these ion channels, for example, both N-terminus and C-terminus tails of the σ -1R are extracellular. Additionally, this study also provided first direct and unequivocal evidence for the presence of σ -1Rs at the plasma membrane. Nonetheless, even though Kourrich et al. (2013) demonstrated that both N-terminus and C-terminus tails of the σ -1R are extracellular, the orientation of the σ -1R *in vivo* needs to be confirmed. Also, future studies are necessary to test if the σ -1R's interaction with other ion channels alters the behavior of animals similar to what is shown by Kourrich et al. (2013). For example, is there any interaction between σ -1Rs and NMDARs that could ameliorate the behavioral phenotype observed in mouse models of amnesia induced by the blockade of NMDARs (Maurice et al., 1994)?

It is essential to identify and understand the molecular details of the σ -1R association with cellular components (Su et al., 2010) such as different classes

of ion channels, kinases, GPCRs, etc. Gaining substantial knowledge on the details about σ -1Rs and their structural determinants responsible for association with ion channels as well as other cellular components could help decipher the σ -1R's role in pathological conditions such as addiction, amnesia, frontotemporal degeneration in motor neuron disease (FTLD-MND), etc. (Hayashi et al., 2011). Furthermore, insights on molecular features of the σ -1R interactions with various classes of ion channels provide the opportunity to understand the critical role of σ -1Rs in neuronal plasticity (Su et al., 2010; Kourrich et al., 2012). Defining the intricacies underlying the relationship between σ -1Rs and their interacting partners during physiological and pathological conditions will form a venue for the development of novel therapeutic strategies.

ACKNOWLEDGMENTS

I am thankful to Wissam B. Nassrallah for helpful feedback on the manuscript.

REFERENCES

- Alonso, G., Phan, V., Guillemain, I., Saunier, M., Legrand, A., Anol, M., et al. (2000). Immunocytochemical localization of the sigma(1) receptor in the adult rat central nervous system. *Neuroscience* 97, 155–170.
- Bergeron, R., and Debonnel, G. (1997). Effects of low and high doses of selective sigma ligands: further evidence suggesting the existence of different subtypes of sigma receptors. *Psychopharmacology (Berl.)* 129, 215–224.
- Chu, U. B., Ramachandran, S., Hajipour, A. R., and Ruoho, A. E. (2013). Photoaffinity labeling of the sigma-1 receptor with N-[3-(4-Nitrophenyl)propyl]-N-dodecylamine: evidence of receptor dimers. *Biochemistry* 52, 859–868.
- Hayashi, T., and Su, T. P. (2003). Sigma-1 receptors (sigma(1) binding sites) form raft-like microdomains and target lipid droplets on the endoplasmic reticulum: roles in endoplasmic reticulum lipid compartmentalization and export. *J. Pharmacol. Exp. Ther.* 306, 718–725.
- Hayashi, T., and Su, T. P. (2005). The potential role of sigma-1 receptors in lipid transport and lipid raft reconstitution in the brain: implication for drug abuse. *Life Sci.* 77, 1612–1624.
- Hayashi, T., and Su, T. P. (2007). Sigma-1 receptor chaperones at the ER-mitochondrion interface regulate Ca^{2+} signaling and cell survival. *Cell* 131, 596–610.
- Hayashi, T., Tsai, S. Y., Mori, T., Fujimoto, M., and Su, T. P. (2011). Targeting ligand-operated chaperone sigma-1 receptors in the treatment of neuropsychiatric disorders. *Expert Opin. Ther. Targets* 15, 557–577.
- Kourrich, S., Hayashi, T., Chuang, J. Y., Tsai, S. Y., Su, T. P., and Bonci, A. (2013). Dynamic interaction between sigma-1 receptor and Kv1.2 shapes neuronal and behavioral responses to cocaine. *Cell* 152, 236–247.
- Kourrich, S., Su, T. P., Fujimoto, M., and Bonci, A. (2012). The sigma-1 receptor: roles in neuronal plasticity and disease. *Trends Neurosci.* 35, 762–771.
- Martin, W. R., Eades, C. G., Thompson, J. A., Huppler, R. E., and Gilbert, P. E. (1976). The effects of morphine- and nalorphine- like drugs in the nondependent and morphine-dependent chronic spinal dog. *J. Pharmacol. Exp. Ther.* 197, 517–532.
- Martina, M., Turcotte, M. E., Halman, S., and Bergeron, R. (2007). The sigma-1 receptor modulates NMDA receptor synaptic transmission and plasticity via SK channels in rat hippocampus. *J. Physiol.* 578, 143–157.
- Maurice, T., Hiramatsu, M., Itoh, J., Kameyama, T., Hasegawa, T., and Nabeshima, T. (1994). Behavioral evidence for a modulating role of sigma ligands in memory processes. I. Attenuation of dizocilpine (MK-801)-induced amnesia. *Brain Res.* 647, 44–56.
- Monnet, F. P., Debonnel, G., Junien, J. L., and De Montigny, C. (1990). N-methyl-D-aspartate-induced neuronal activation is selectively modulated by sigma receptors. *Eur. J. Pharmacol.* 179, 441–445.
- Navarro, G., Moreno, E., Aymerich, M., Marcellino, D., McCormick, P. J., Mallol, J., et al. (2010). Direct involvement of sigma-1 receptors in the dopamine D1 receptor-mediated effects of cocaine. *Proc. Natl. Acad. Sci. U.S.A.* 107, 18676–18681.
- Shioda, N., Ishikawa, K., Tagashira, H., Ishizuka, T., Yawo, H., and Fukunaga, K. (2012). Expression of a truncated form of the endoplasmic reticulum chaperone protein, sigma1 receptor, promotes mitochondrial energy depletion and apoptosis. *J. Biol. Chem.* 287, 23318–23331.
- Su, T. P., Hayashi, T., Maurice, T., Buch, S., and Ruoho, A. E. (2010). The sigma-1 receptor chaperone as an inter-organellar signaling modulator. *Trends Pharmacol. Sci.* 31, 557–566.
- Trimmer, J. S., and Rhodes, K. J. (2004). Localization of voltage-gated ion channels in mammalian brain. *Annu. Rev. Physiol.* 66, 477–519.

Received: 05 April 2013; accepted: 05 April 2013; published online: 23 April 2013.

Citation: Pabba M (2013) The essential roles of protein-protein interaction in sigma-1 receptor functions. *Front. Cell. Neurosci.* 7:50. doi: 10.3389/fncel.2013.00050
Copyright © 2013 Pabba. This is an open-access article distributed under the terms of the Creative Commons Attribution License, which permits use, distribution and reproduction in other forums, provided the original authors and source are credited and subject to any copyright notices concerning any third-party graphics etc.



STIM1-mediated bidirectional regulation of Ca^{2+} entry through voltage-gated calcium channels (VGCC) and calcium-release activated channels (CRAC)

Osama F. Harraz^{1,2} and Christophe Altier^{3*}

¹ Department of Physiology and Pharmacology, Hotchkiss Brain Institute, Libin Cardiovascular Institute, University of Calgary, Calgary, AB, Canada

² Department of Pharmacology and Toxicology, Faculty of Pharmacy, Alexandria University, Alexandria, Egypt

³ Department of Physiology and Pharmacology, Snyder Institute for Chronic Diseases, Inflammation Research Network, University of Calgary, Calgary, AB, Canada

Edited by:

Leigh Anne Swayne, University of Victoria, Canada

Reviewed by:

Francois Rassendren, Centre National de la Recherche Scientifique, France
J. David Spafford, University of Waterloo, Canada

*Correspondence:

Christophe Altier, Department of Physiology and Pharmacology, Snyder Institute for Chronic Diseases, Inflammation Research Network, University of Calgary, 3330 Hospital Dr. NW, Calgary, AB T2N-4N1, Canada
e-mail: altier@ucalgary.ca

The spatial and temporal regulation of cellular calcium signals is modulated via two main Ca^{2+} entry routes. Voltage-gated Ca^{2+} channels (VGCC) and Ca^{2+} -release activated channels (CRAC) enable Ca^{2+} flow into electrically excitable and non-excitable cells, respectively. VGCC are well characterized transducers of electrical activity that allow Ca^{2+} signaling into the cell in response to action potentials or subthreshold depolarizing stimuli. The identification of Stromal Interaction Molecule (STIM) and Orai proteins has provided significant insights into the understanding of CRAC function and regulation. This review will summarize the current state of knowledge of STIM-Orai interaction and their contribution to cellular Ca^{2+} handling mechanisms. We will then discuss the bidirectional actions of STIM1 on VGCC and CRAC. In contrast to the stimulatory role of STIM1 on Orai channel activity that facilitates Ca^{2+} entry, recent reports indicated the ability of STIM1 to suppress VGCC activity. This new concept changes our traditional understanding of Ca^{2+} handling mechanisms and highlights the existence of dynamically regulated signaling complexes of surface expressed ion channels and intracellular store membrane-embedded Ca^{2+} sensors. Overall, STIM1 is emerging as a new class of regulatory proteins that fine-tunes Ca^{2+} entry in response to endoplasmic/sarcoplasmic reticulum stress.

Keywords: STIM1, Orai, VGCC, CRAC, L-type, T-type, calcium channels, store-operated Ca^{2+} entry

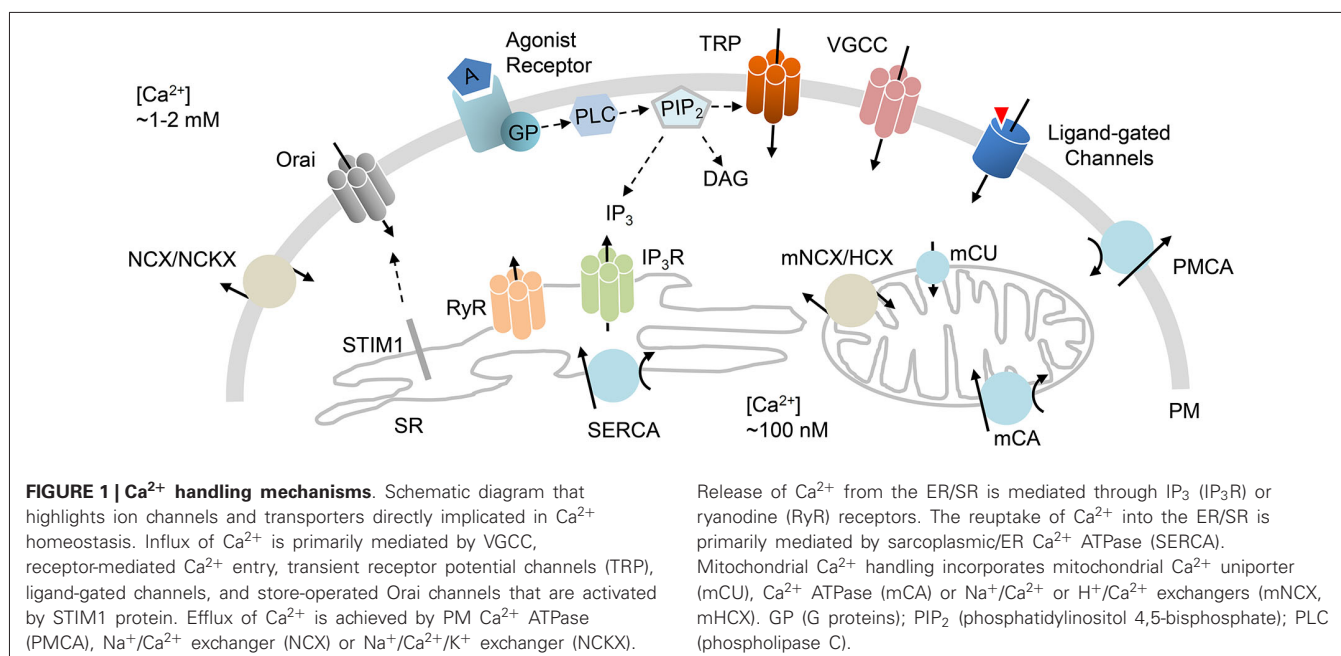
Ca^{2+} HANDLING MECHANISMS

The second messenger calcium (Ca^{2+}) plays a crucial role in a broad range of eukaryotic cellular functions. Regulation of its intracellular concentration ($[\text{Ca}^{2+}]_i$) represents a major determinant that controls signal transduction pathways such as secretion, excitation/contraction coupling, motility, transcription, growth, cell division or apoptosis (Berridge et al., 2003; Catterall, 2011). Precise neural circuit formation and control of neuronal excitability necessitate the tight handling of Ca^{2+} . Further, Ca^{2+} signals are crucial for synaptic transmission and plasticity (Berridge, 1998). In addition, pathophysiological neural insults such as cerebral ischemia can evoke an unwanted rise in Ca^{2+} leading to Ca^{2+} overload toxicity and neuronal cell death (Berridge, 1998; Arundine and Tymianski, 2004).

Strict handling of intracellular Ca^{2+} is necessary to maintain optimized cellular functions. In general, Ca^{2+} signals are modified by the control of Ca^{2+} flux in (entry) and out (efflux) of the cell through plasma membrane (PM) channels and transporters that facilitate Ca^{2+} movement between the extracellular milieu and cytoplasm across a Ca^{2+} concentration gradient (Berridge et al., 2003). In addition, integral proteins localized in the membranes of intracellular stores allow Ca^{2+} release (to

the cytoplasm) and reuptake (into the Ca^{2+} store). The main intracellular Ca^{2+} stores are the endoplasmic reticulum (ER) and sarcoplasmic reticulum (SR). A number of regulatory mechanisms have been proposed to mediate the cellular influx, efflux, release and reuptake of Ca^{2+} , thus achieving Ca^{2+} homeostasis within the cell (Berridge et al., 2003; Stutzmann and Mattson, 2011). Accumulated data suggest that this homeostasis involves the concerted action of Ca^{2+} entry channels at the PM and Ca^{2+} release channels in intracellular ER/SR stores (Figure 1).

Over the past decades, it has been recognized that Ca^{2+} influx into neuronal subcellular compartments (e.g., dendrites, somata, spines, axons) is mediated by two principal means of Ca^{2+} entry. These routes are voltage-gated Ca^{2+} channels (VGCC) and ionotropic neurotransmitter receptors (Berridge, 1998; Catterall, 2011), both routes elicit crucial rises in cytosolic Ca^{2+} in response to different stimuli. VGCC are widely expressed in excitable cells and they trigger Ca^{2+} influx over specific ranges of membrane potentials. Activation of VGCC generates fast neurotransmission at nerve terminals (Bezprozvanny et al., 1995), or excitation-contraction coupling in cardiac, skeletal and smooth muscle cells (Catterall, 2011; Tuluc and Flucher, 2011; Navedo and Santana, 2013). Neurons along with other cell types display an



alternative Ca^{2+} entry mode that is coupled to intracellular Ca^{2+} stores (Gemes et al., 2011). This alternative type of entry, known as capacitative calcium entry, is triggered upon the depletion of Ca^{2+} stores to facilitate store-operated Ca^{2+} entry (SOCE). The latter, SOCE, would in turn replenish the intracellular ER/SR stores (Soboloff et al., 2012). Extensive work on this route of calcium influx has established its functional importance in neurons and its ability to supplement cytosolic Ca^{2+} required for neurotransmission (Berna-Erro et al., 2009; Gemes et al., 2011).

STORE-OPERATED Ca^{2+} ENTRY (SOCE): A STILL-DEVELOPING STORY

About three decades ago, Putney first described the concept of capacitative Ca^{2+} entry (Putney, 1986). According to this concept, the concerted control of both Ca^{2+} influx and Ca^{2+} release from intracellular stores orchestrates Ca^{2+} homeostasis. In other words, Ca^{2+} influx is modulated by the capacity of the cell to hold Ca^{2+} . Several studies showed that stimulus-evoked ER/SR depletion can trigger subsequent influx of extracellular Ca^{2+} into the cytoplasm as a means to replenish Ca^{2+} in intracellular stores (Takemura and Putney, 1989; Muallem et al., 1990). These findings led Putney's model to be revised by indicating that the activation of PM Ca^{2+} channels was a direct consequence of ER/SR depletion (Putney, 1990). Entry of extracellular Ca^{2+} upon store depletion was later suggested to be mediated by Ca^{2+} -release activated channels (CRAC) in a process referred to as SOCE (Hoth and Penner, 1992; Patterson et al., 1999).

The CRAC was first described in 1992 (Hoth and Penner, 1992), but its mechanism of activation was not revealed until 2005 when Cahalan and coworkers identified the STromal Interaction Molecule 1 (STIM1) as the intracellular CRAC component that acts as the Ca^{2+} sensor. Upon store depletion, this sensor STIM1 aggregates and activates the PM Ca^{2+} channel that is necessary for SOCE (Roos et al., 2005; Zhang et al., 2005). First physiological

description of STIM1 as a key component of CRAC was in *Drosophila* S2 cells in which SOCE is the predominant Ca^{2+} entry mechanism. Using RNA interference screens of candidate genes, they reported that *Stim* loss altered SOCE (Roos et al., 2005; Zhang et al., 2005). It was 1 year after the intracellular STIM1 was discovered that the PM component of CRAC was identified. The *Orai* gene, named after the mythological keepers of heaven's gate, was determined as a result of genetic mapping of mutations linked to impaired lymphocyte function (Zhang et al., 2006). The SOCE mechanism was then revised to involve the two key players: (1) STIM, a transmembrane Ca^{2+} sensor protein that is primarily embedded into the SR/ER membrane; and (2) Orai, an integral PM protein being the pore-forming subunit of the CRAC channel (Figures 1, 2A; Soboloff et al., 2012).

Once the key genes governing SOCE were identified, the interplay between STIM1 and Orai was extensively examined. Investigators reported that Orai protein monomers multimerize to form a Ca^{2+} channel whose activity is triggered by interaction with STIM1 (Penna et al., 2008). Further, STIM-Orai Activating Region (SOAR) and CRAC Activation Domain (CAD) were identified as active STIM1 sites necessary to trigger the CRAC current (Park et al., 2009; Yuan et al., 2009). In addition, high-resolution crystal structures of the CAD and the N-terminal region of STIM1 as well as the full-length Orai channel were recently characterized (Stathopulos et al., 2008; Hou et al., 2012; Yang et al., 2012). These latter discoveries represent major landmarks towards the elucidation of the conformational changes of STIM1-Orai complexes as well as the possible interactions with key proteins involved in Ca^{2+} handling mechanisms.

STROMAL INTERACTION MOLECULE (STIM): THE Ca^{2+} SENSOR CONTROLLING Ca^{2+} ENTRY

STIM1 was first reported as a growth modulator (Oritani and Kincade, 1996), and was not implicated in cellular Ca^{2+} dynamics

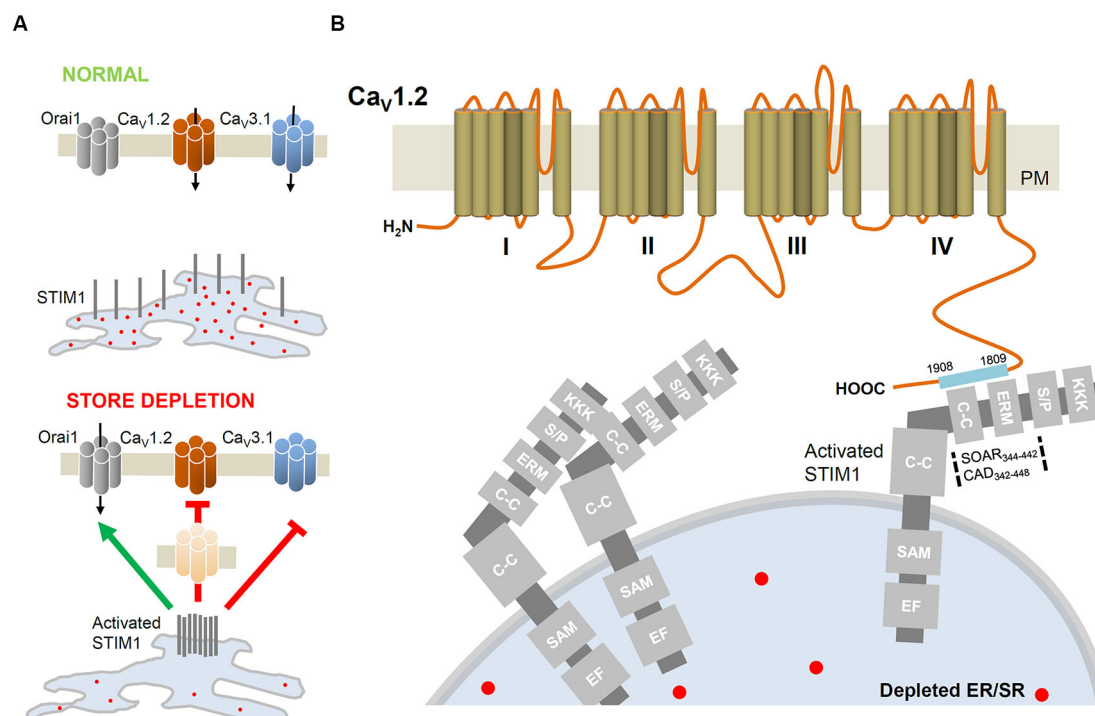


FIGURE 2 | STIM1-mediated regulation of VGCC. (A) In basal conditions, the intraluminal EF-hand of STIM1 is occupied by Ca^{2+} . Upon ER/SR depletion, STIM1 molecules aggregate closer to PM to activate Orai channels but inhibit $\text{Ca}_v1.2$ (L-type; Park et al., 2010; Wang et al., 2010) and $\text{Ca}_v3.1$ (T-type; Nguyen et al., 2013) channels. STIM1-induced internalization of $\text{Ca}_v1.2$ removes functional channels from the cell surface. **(B)** Detailed

interacting sites of STIM1 and the C-terminus of $\text{Ca}_v1.2$. The STIM1 segments CAD (342–448; Park et al., 2010) or SOAR (344–442; Wang et al., 2010) interacts with the C-terminus (1809–1908; Park et al., 2010) of $\text{Ca}_v1.2$. C-C, coiled-coil domain; EF, EF hand motif; ERM, Ezrin-Radixin-Moesin domain; KKK, lysine rich domain; SAM, sterile- α motif; S/P, serine/proline rich domain.

until 2005 (Roos et al., 2005). It became evident that STIM1 proteins function as Ca^{2+} -sensing molecules, resident in the membranes of the intracellular Ca^{2+} stores (ER/SR), that regulate SOCE (Soboloff et al., 2012). STIM1 molecule is ubiquitously expressed and is involved in a wide range of cellular functions. It is an essential component of SOCE in lymphocytes (Liou et al., 2005; Zhang et al., 2005), platelets (Varga-Szabo et al., 2008), neurons (Berna-Erro et al., 2009; Venkiteswaran and Hasan, 2009; Gemes et al., 2011), skeletal muscle cells (Stiber et al., 2008), and cardiomyocytes (Touchberry et al., 2011). When Ca^{2+} stores are depleted, STIM1 molecules aggregate and activate the Orai channels to facilitate Ca^{2+} influx (Soboloff et al., 2012).

The STIM2 was identified as a homologue of STIM1. Both isoforms are ubiquitously expressed in vertebrates and the expression level of STIM1 is generally higher than STIM2 in most tissues (Williams et al., 2001; Oh-Hora et al., 2008). Notably, STIM2 is primarily found in dendritic cells (Bandyopadhyay et al., 2011) and the brain (Williams et al., 2001; Berna-Erro et al., 2009). The two proteins conserve high homology region, but their C- and N-termini display substantial divergence (Soboloff et al., 2012). Interestingly, structural aspects of the two proteins engender subtle differences that are associated with significant functional implications. Although primarily localized to the intracellular ER/SR membranes, approximately 10% of STIM1 proteins are integrated in the PM. This is in stark difference to

STIM2 which, due to an ER-retention sequence in its C-terminus, is exclusively localized in the ER membrane (Soboloff et al., 2006; Saitoh et al., 2011). In addition, STIM1 is a stronger activator of Orai channels when compared to STIM2 (Bird et al., 2009) and STIM2 is more sensitive to small changes in $[\text{Ca}^{2+}]$. These properties of STIM2 and its poor coupling to Orai channels could in theory be essential to limit uncontrolled SOCE (Soboloff et al., 2012). In the following section, our discussion will focus on how STIM1 modulates different Ca^{2+} influx routes.

STROMAL INTERACTION MOLECULE 1 (STIM1) AND Ca^{2+} ENTRY

There are two main stimulus modalities that elicit Ca^{2+} entry: the membrane depolarization in excitable cells versus the ER/SR calcium depletion in non-excitable cells. The VGCC differ from CRAC in being activated by depolarization in response to action potentials or subthreshold stimuli. The STIM1/Orai CRAC complex is activated in response to ER/SR calcium depletion. Noteworthy, both channels are expressed in excitable and non-excitable cells (Kotturi and Jefferies, 2005; Lyfenko and Dirksen, 2008; Stiber et al., 2008). However, VGCC predominate in excitable cells (e.g., neurons, cardiomyocytes, smooth muscle cells) while CRAC currents are prevalent in non-excitable cells (e.g., T-lymphocytes). Both Ca^{2+} channels have received significant attention. In this review we will focus our discussion on the

mechanisms through which STIM1 interaction with CRAC and VGCC modulate Ca^{2+} influx.

STROMAL INTERACTION MOLECULE 1 (STIM1) STIMULATES Ca^{2+} -RELEASE ACTIVATED CHANNELS (CRAC)

In a resting cell, STIM1 exhibits a tubular distribution throughout the ER/SR (Roos et al., 2005). The N-terminus of STIM1 resides inside the ER/SR lumen and possesses an EF-hand that binds Ca^{2+} with low affinity (200–600 nM), and thus acts as a Ca^{2+} sensor. When the lumen of the ER/SR is full of Ca^{2+} , STIM1 EF-hands are saturated with Ca^{2+} ions. In contrast, upon stores depletion, STIM1 molecules aggregate into oligomers (Soboloff et al., 2012) and translocate to sites where the ER/SR membrane is closer to the PM. In these microdomains, STIM1 oligomers form clusters which interact with and activate Orai channels (Figure 2A; Zhang et al., 2006; Penna et al., 2008; Soboloff et al., 2012). STIM1 activates Orai1 by the region identified as STIM1-Orai activating region (SOAR) or CAD to facilitate Ca^{2+} influx. Noteworthy, the small portion of the STIM1 pool integrated into the PM is not required for CRAC channel activation (Park et al., 2009; Yuan et al., 2009).

STROMAL INTERACTION MOLECULE 1 (STIM1) INHIBITS VOLTAGE-GATED Ca^{2+} CHANNELS

SOCE upon ER/SR depletion has been extensively studied since first proposed. Recently, another mechanism of calcium influx was found to be suppressed by store depletion (Park et al., 2010; Wang et al., 2010). This led to the novel term “store-inhibited channels (SIC)” (Moreno and Vaca, 2011); in contrast to store-operated channels that activate upon Ca^{2+} store depletion (Soboloff et al., 2012). The first class of channels identified to be inhibited by store depletion is the voltage-gated Ca^{2+} channel.

Stromal Interaction Molecule 1 (STIM1) inhibits $\text{Ca}_v1.2$ channels

The predominant expression and function of CRAC in non-excitable cells is well reported. The key components of CRAC, STIM and Orai, are also expressed in excitable cells (Stiber et al., 2008; Berna-Erro et al., 2009; Venkiteswaran and Hasan, 2009; Gemes et al., 2011; Touchberry et al., 2011) where VGCC predominate as the main route of Ca^{2+} entry in response to depolarizing stimuli. One subtype of VGCC, the $\text{Ca}_v1.2$ channel, is ubiquitously expressed in neuronal, cardiac and smooth muscle cells. The $\text{Ca}_v1.2$ L-type channel is involved in specific cellular functions and has been long considered as an important target for therapeutic agents such as antiarrhythmic and antihypertensive drugs (Catterall, 2011). In order to understand the coordinated interaction between CRAC and the L-type calcium channel, two studies have examined the role of STIM1 in regulating $\text{Ca}_v1.2$ and Orai1 function. Interestingly, by employing a divergent array of approaches, these studies reported an inhibitory interaction between STIM1 and $\text{Ca}_v1.2$ (Figures 2A, B). This functional crosstalk may explain the predominance of either CRAC or VGCC activity in different tissue types (Park et al., 2010; Wang et al., 2010).

Using excitable cortical neurons and vascular smooth muscle cells, Park et al. (2010) and Wang et al. (2010) assessed VGCC and CRAC functions by monitoring cytoplasmic Ca^{2+} . Unexpectedly,

depletion of ER/SR stores attenuated depolarization-induced $\text{Ca}_v1.2$ activity. Further, depolarization of non-excitable STIM1-rich T-lymphocytes could not evoke a rise in $[\text{Ca}^{2+}]_i$. The modulatory interaction between STIM1 and $\text{Ca}_v1.2$ was emphasized by the observations that: (1) STIM1 overexpression attenuated $\text{Ca}_v1.2$ activity; while (2) $\text{Ca}_v1.2$ -mediated responses were enhanced when STIM1 function or expression was impaired. Direct interaction between STIM1 and $\text{Ca}_v1.2$ proteins was ascertained and a set of experiments, using truncated forms of STIM1, documented that SOAR domain (STIM-Orai activating region, 344–442; Wang et al., 2010) directly interacts with the C-terminus of $\text{Ca}_v1.2$ α_1 subunit (1809–1908; Park et al., 2010). Co-immunoprecipitation analysis confirmed the STIM1- $\text{Ca}_v1.2$ interaction and functional studies revealed that the SOAR domain was necessary and sufficient to suppress $\text{Ca}_v1.2$ current (Figure 2B). A slower inhibitory interaction was further suggested by Park and coworkers, in which the surface expression of $\text{Ca}_v1.2$ decreased as a consequence of long-term internalization of the channel from the PM (Figure 2A; Park et al., 2010). Despite having the same core conclusion, the two reports highlight different perspectives. While Park and coworkers proposed an inhibitory mechanism that attenuates channel expression, Wang et al. found a potential role for Orai1 in the STIM1- $\text{Ca}_v1.2$ inhibitory interaction. Preventing STIM1 expression alone did not abolish $\text{Ca}_v1.2$ channel suppression while the simultaneous inhibition of both STIM1 and Orai1 was necessary to mask $\text{Ca}_v1.2$ inhibition by store depletion. In summary, the two groups reported for the first time that STIM1 effectively attenuates $\text{Ca}_v1.2$ activity.

The description of Ca^{2+} conductances inhibited upon store depletion has major implications for Ca^{2+} signaling in excitable and non-excitable cells. In excitable neuronal cells, VGCC are expressed at higher level than CRAC components and are the predominant Ca^{2+} influx route. In contrast, non-excitable cells display reduced VGCC expression and CRAC represents the main Ca^{2+} entry pathway due to the high expression of STIM1 and Orai (Liou et al., 2005; Zhang et al., 2005; Park et al., 2010). While STIM1 interacts with Orai to facilitate Ca^{2+} influx, a new modulatory role for STIM1 has emerged through which it inhibits Ca^{2+} entry mediated by VGCC. Noteworthy, the ability of STIM1 to reciprocally regulate Orai and $\text{Ca}_v1.2$ would imply that the mode of action of STIM1 is tissue specific. In other words, STIM1 would typically stimulate CRAC in non-excitable cells and inhibit VGCC in excitable cells (Park et al., 2010; Wang et al., 2010; Moreno and Vaca, 2011). This reciprocal modulation of Ca^{2+} entry by STIM1 seems to play a critical role in Ca^{2+} homeostasis by fine-tuning Ca^{2+} entry in cells that simultaneously express both channel types. By providing this missing piece of evidence, these studies resolved the predominant function of one channel over the other despite their co-expression in excitable and non-excitable tissues. That being said, whether other Ca^{2+} channels exhibit analogous or distinct modulation by STIM1 remains unknown.

Stromal Interaction Molecule 1 (STIM1) inhibits T-type Ca^{2+} channels

Recent published experiments revealed that $\text{Ca}_v1.2$ channel is not the only voltage-gated Ca^{2+} channel suppressed by STIM1. Interestingly, a study by Nguyen et al. (2013) showed that

STIM1 attenuates the activity of T-type Ca^{2+} channel. Using cardiomyocyte-derived HL-1 cells, an inhibitory association between STIM1 and $\text{Ca}_v3.1$ was reported and was suggested to limit excessive Ca^{2+} entry. Pathological Ca^{2+} influx in cardiac myocytes can trigger Ca^{2+} overload in the SR and cardiac arrhythmias (Sedej et al., 2010), and STIM1-dependent modulation of $\text{Ca}_v3.1$ could, in theory, restrain such unwanted entry. Indeed, the authors showed that knocking down STIM1 increases T-type Ca^{2+} current density. They further suggested that STIM1 may regulate the expression of T-type α_1 subunits as knocking down STIM1 augmented the surface expression of $\text{Ca}_v3.1$ channel. Whether $\text{Ca}_v3.1$ trafficking or stability at the PM is implicated remains unknown and requires further investigation. Intriguingly, these findings represent a novel regulatory pathway for Ca^{2+} handling in cardiac myocytes. This regulation may be implicated in the modulation of rhythmicity and excitability of native cardiac pacemaker cells where T-type Ca^{2+} channel expression and function is evident (Mangoni et al., 2006; Nguyen et al., 2013).

CONCLUSIONS

The interaction of STIM1 with CRAC or VGCC extends our understanding of the role of STIM1 in cellular Ca^{2+} handling. Recent published work (Park et al., 2010; Wang et al., 2010; Nguyen et al., 2013) described a novel regulatory function for STIM1. Distinct from its role as an ER/SR Ca^{2+} sensor to facilitate Ca^{2+} entry and replenish the stores, STIM1 suppresses the activity of voltage-gated Ca^{2+} channel in excitable cells. This inhibitory association prevents excessive cellular Ca^{2+} influx by mechanisms including direct protein-protein interaction and reduced VGCC surface expression (Park et al., 2010; Wang et al., 2010; Nguyen et al., 2013). This novel concept raises numerous questions that pertain to the dynamic regulation of cellular Ca^{2+} in health and disease. Since STIM1 bi-directionally regulates VGCC and CRAC, SR/ER stress may lead to pathologies related to downstream Ca^{2+} -dependent pathways. In fact, mutations in STIM1 elicit severe immunodeficiency syndromes associated with compromised SOCE (Feske et al., 2010). Impaired STIM-dependent regulation of VGCC and subsequent alterations in Ca^{2+} entry remain to be investigated; as it could be linked to diseases such as epilepsy, cardiac arrhythmia or hypertension. Finally, it will be fundamental to elucidate the cooperated interaction of PM Ca^{2+} channels and their associated subunits and how those signaling complexes respond to ER/SR stress through Ca^{2+} sensors such as STIM1 proteins.

AUTHOR CONTRIBUTIONS

Osama F. Harraz and Christophe Altier wrote the manuscript. Osama F. Harraz produced the figures.

ACKNOWLEDGMENTS

Research in the Altier lab is supported by the Heart and Stroke Foundation of Canada and the Canadian Institutes of Health Research (CIHR). Christophe Altier holds a Canada Research Chair (Tier2). Osama F. Harraz is a Vanier Scholar (CIHR) and is supported by salary studentships from Alberta Innovates (AIHS) and Achievers in Medical Sciences (AIMS).

REFERENCES

- Arundine, M., and Tymianski, M. (2004). Molecular mechanisms of glutamate-dependent neurodegeneration in ischemia and traumatic brain injury. *Cell. Mol. Life Sci.* 61, 657–668. doi: 10.1007/s00018-003-3319-x
- Bandyopadhyay, B. C., Pingle, S. C., and Ahern, G. P. (2011). Store-operated Ca^{2+} signaling in dendritic cells occurs independently of STIM1. *J. Leukoc. Biol.* 89, 57–62. doi: 10.1189/jlb.0610381
- Berna-Erro, A., Braun, A., Kraft, R., Kleinschnitz, C., Schuhmann, M. K., Stegner, D., et al. (2009). STIM2 regulates capacitive Ca^{2+} entry in neurons and plays a key role in hypoxic neuronal cell death. *Sci. Signal.* 2, ra67. doi: 10.1126/scisignal.2000522
- Berridge, M. J., Bootman, M. D., and Roderick, H. L. (2003). Calcium signalling: dynamics, homeostasis and remodelling. *Nat. Rev. Mol. Cell Biol.* 4, 517–529. doi: 10.1038/nrm1155
- Berridge, M. J. (1998). Neuronal calcium signaling. *Neuron* 21, 13–26. doi: 10.1016/S0896-6273(00)80510-3
- Bezprozvanny, I., Scheller, R. H., and Tsien, R. W. (1995). Functional impact of syntaxin on gating of N-type and Q-type calcium channels. *Nature* 378, 623–626. doi: 10.1038/378623a0
- Bird, G. S., Hwang, S. Y., Smyth, J. T., Fukushima, M., Boyles, R. R., and Putney, J. W. Jr. (2009). STIM1 is a calcium sensor specialized for digital signaling. *Curr. Biol.* 19, 1724–1729. doi: 10.1016/j.cub.2009.08.022
- Catterall, W. A. (2011). Voltage-gated calcium channels. *Cold Spring Harb. Perspect. Biol.* 3:a003947. doi: 10.1101/cshperspect.a003947
- Feske, S., Picard, C., and Fischer, A. (2010). Immunodeficiency due to mutations in ORAI1 and STIM1. *Clin. Immunol.* 135, 169–182. doi: 10.1016/j.clim.2010.01.011
- Gemes, G., Bangaru, M. L., Wu, H. E., Tang, Q., Weihrauch, D., Koopmeiners, A. S., et al. (2011). Store-operated Ca^{2+} entry in sensory neurons: functional role and the effect of painful nerve injury. *J. Neurosci.* 31, 3536–3549. doi: 10.1523/jneurosci.5053-10.2011
- Hoth, M., and Penner, R. (1992). Depletion of intracellular calcium stores activates a calcium current in mast cells. *Nature* 355, 353–356. doi: 10.1038/355353a0
- Hou, X., Pedi, L., Diver, M. M., and Long, S. B. (2012). Crystal structure of the calcium release-activated calcium channel Orai. *Science* 338, 1308–1313. doi: 10.1126/science.1228757
- Kotturi, M. F., and Jefferies, W. A. (2005). Molecular characterization of L-type calcium channel splice variants expressed in human T lymphocytes. *Mol. Immunol.* 42, 1461–1474. doi: 10.1016/j.molimm.2005.01.014
- Liou, J., Kim, M. L., Heo, W. D., Jones, J. T., Myers, J. W., Ferrell, J. E., et al. (2005). STIM1 is a Ca^{2+} sensor essential for Ca^{2+} -store-depletion-triggered Ca^{2+} influx. *Curr. Biol.* 15, 1235–1241. doi: 10.1016/j.cub.2005.05.055
- Lyfenko, A. D., and Dirksen, R. T. (2008). Differential dependence of store-operated and excitation-coupled Ca^{2+} entry in skeletal muscle on STIM1 and Orai1. *J. Physiol.* 586(Pt. 20), 4815–4824. doi: 10.1113/jphysiol.2008.160481
- Mangoni, M. E., Trabelsio, A., Leoni, A. L., Couette, B., Marger, L., Le Quang, K., et al. (2006). Bradycardia and slowing of the atrioventricular conduction in mice lacking $\text{Ca}_v3.1/\alpha_1\text{G}$ T-type calcium channels. *Circ. Res.* 98, 1422–1430. doi: 10.1161/01.res.0000225862.14314.49
- Moreno, C., and Vaca, L. (2011). SOC and now also SIC: store-operated and store-inhibited channels. *IUBMB Life* 63, 856–863. doi: 10.1002/iub.547
- Muallem, S., Khademazad, M., and Sachs, G. (1990). The route of Ca^{2+} entry during reloading of the intracellular Ca^{2+} pool in pancreatic acini. *J. Biol. Chem.* 265, 2011–2016.
- Navedo, M. E., and Santana, L. F. (2013). $\text{Ca}_v1.2$ sparklets in heart and vascular smooth muscle. *J. Mol. Cell. Cardiol.* 58, 67–76. doi: 10.1016/j.yjmcc.2012.11.018
- Nguyen, N., Biet, M., Simard, E., Beliveau, E., Francoeur, N., Guillemette, G., et al. (2013). STIM1 participates in the contractile rhythmicity of HL-1 cells by moderating T-type Ca^{2+} channel activity. *Biochim. Biophys. Acta* 1833, 1294–1303. doi: 10.1016/j.bbamcr.2013.02.027
- Oh-Hora, M., Yamashita, M., Hogan, P. G., Sharma, S., Lamperti, E., Chung, W., et al. (2008). Dual functions for the endoplasmic reticulum calcium sensors STIM1 and STIM2 in T cell activation and tolerance. *Nat. Immunol.* 9, 432–443. doi: 10.1038/ni1574
- Oritani, K., and Kincade, P. W. (1996). Identification of stromal cell products that interact with pre-B cells. *J. Cell Biol.* 134, 771–782. doi: 10.1083/jcb.134.3.771

- Park, C. Y., Hoover, P. J., Mullins, F. M., Bachhawat, P., Covington, E. D., Raunser, S., et al. (2009). STIM1 clusters and activates CRAC channels via direct binding of a cytosolic domain to Orai1. *Cell* 136, 876–890. doi: 10.1016/j.cell.2009.02.014
- Park, C. Y., Shcheglovitov, A., and Dolmetsch, R. (2010). The CRAC channel activator STIM1 binds and inhibits L-type voltage-gated calcium channels. *Science* 330, 101–105. doi: 10.1126/science.1191027
- Patterson, R. L., van Rossum, D. B., and Gill, D. L. (1999). Store-operated Ca²⁺ entry: evidence for a secretion-like coupling model. *Cell* 98, 487–499. doi: 10.1016/S0092-8674(00)81977-7
- Penna, A., Demuro, A., Yeromin, A. V., Zhang, S. L., Safrina, O., Parker, I., et al. (2008). The CRAC channel consists of a tetramer formed by Stim-induced dimerization of Orai dimers. *Nature* 456, 116–120. doi: 10.1038/nature07338
- Putney, J. W. Jr. (1986). A model for receptor-regulated calcium entry. *Cell Calcium* 7, 1–12. doi: 10.1016/0143-4160(86)90026-6
- Putney, J. W. Jr. (1990). Capacitative calcium entry revisited. *Cell Calcium* 11, 611–624. doi: 10.1016/0143-4160(90)90016-n
- Roos, J., DiGregorio, P. J., Yeromin, A. V., Ohlsen, K., Lioudyno, M., Zhang, S., et al. (2005). STIM1, an essential and conserved component of store-operated Ca²⁺ channel function. *J. Cell Biol.* 169, 435–445. doi: 10.1083/jcb.200502019
- Saitoh, N., Oritani, K., Saito, K., Yokota, T., Ichii, M., Sudo, T., et al. (2011). Identification of functional domains and novel binding partners of STIM proteins. *J. Cell. Biochem.* 112, 147–156. doi: 10.1002/jcb.22910
- Sedej, S., Heinzel, F. R., Walther, S., Dybkova, N., Wakula, P., Groborz, J., et al. (2010). Na⁺-dependent SR Ca²⁺ overload induces arrhythmogenic events in mouse cardiomyocytes with a human CPVT mutation. *Cardiovasc. Res.* 87, 50–59. doi: 10.1093/cvr/cvq007
- Soboloff, J., Rothberg, B. S., Madesh, M., and Gill, D. L. (2012). STIM proteins: dynamic calcium signal transducers. *Nat. Rev. Mol. Cell Biol.* 13, 549–565. doi: 10.1038/nrm3414
- Soboloff, J., Spassova, M. A., Hewavitharana, T., He, L. P., Xu, W., Johnstone, L. S., et al. (2006). STIM2 is an inhibitor of STIM1-mediated store-operated Ca²⁺ Entry. *Curr. Biol.* 16, 1465–1470. doi: 10.1016/j.cub.2006.05.051
- Stathopoulos, P. B., Zheng, L., Li, G. Y., Plevin, M. J., and Ikura, M. (2008). Structural and mechanistic insights into STIM1-mediated initiation of store-operated calcium entry. *Cell* 135, 110–122. doi: 10.1016/j.cell.2008.08.006
- Stiber, J., Hawkins, A., Zhang, Z. S., Wang, S., Burch, J., Graham, V., et al. (2008). STIM1 signalling controls store-operated calcium entry required for development and contractile function in skeletal muscle. *Nat. Cell Biol.* 10, 688–697. doi: 10.1038/ncb1731
- Stutzmann, G. E., and Mattson, M. P. (2011). Endoplasmic reticulum Ca(2+) handling in excitable cells in health and disease. *Pharmacol. Rev.* 63, 700–727. doi: 10.1124/pr.110.003814
- Takemura, H., and Putney, J. W. Jr. (1989). Capacitative calcium entry in parotid acinar cells. *Biochem. J.* 258, 409–412.
- Touchberry, C. D., Elmore, C. J., Nguyen, T. M., Andresen, J. J., Zhao, X., Orange, M., et al. (2011). Store-operated calcium entry is present in HL-1 cardiomyocytes and contributes to resting calcium. *Biochem. Biophys. Res. Commun.* 416, 45–50. doi: 10.1016/j.bbrc.2011.10.133
- Tuluc, P., and Flucher, B. E. (2011). Divergent biophysical properties, gating mechanisms, and possible functions of the two skeletal muscle Ca(V)1.1 calcium channel splice variants. *J. Muscle Res. Cell Motil.* 32, 249–256. doi: 10.1007/s10974-011-9270-9
- Varga-Szabo, D., Braun, A., Kleinschnitz, C., Bender, M., Pleines, I., Pham, M., et al. (2008). The calcium sensor STIM1 is an essential mediator of arterial thrombosis and ischemic brain infarction. *J. Exp. Med.* 205, 1583–1591. doi: 10.1084/jem.20080302
- Venkiteswaran, G., and Hasan, G. (2009). Intracellular Ca²⁺ signaling and store-operated Ca²⁺ entry are required in Drosophila neurons for flight. *Proc. Natl. Acad. Sci. U S A* 106, 10326–10331. doi: 10.1073/pnas.0902982106
- Wang, Y., Deng, X., Mancarella, S., Hendron, E., Eguchi, S., Soboloff, J., et al. (2010). The calcium store sensor, STIM1, reciprocally controls Orai and CaV1.2 channels. *Science* 330, 105–109. doi: 10.1126/science.1191086
- Williams, R. T., Manji, S. S., Parker, N. J., Hancock, M. S., Van, S. L., Eid, J. P., et al. (2001). Identification and characterization of the STIM (stromal interaction molecule) gene family: coding for a novel class of transmembrane proteins. *Biochem. J.* 357(Pt. 3), 673–685. doi: 10.1042/0264-6021:3570673
- Yang, X., Jin, H., Cai, X., Li, S., and Shen, Y. (2012). Structural and mechanistic insights into the activation of Stromal interaction molecule 1 (STIM1). *Proc. Natl. Acad. Sci. U S A* 109, 5657–5662. doi: 10.1073/pnas.1118947109
- Yuan, J. P., Zeng, W., Dorwart, M. R., Choi, Y. J., Worley, P. F., and Muallem, S. (2009). SOAR and the polybasic STIM1 domains gate and regulate Orai channels. *Nat. Cell Biol.* 11, 337–343. doi: 10.1038/ncb1842
- Zhang, S. L., Yeromin, A. V., Zhang, X. H., Yu, Y., Safrina, O., Penna, A., et al. (2006). Genome-wide RNAi screen of Ca(2+) influx identifies genes that regulate Ca(2+) release-activated Ca(2+) channel activity. *Proc. Natl. Acad. Sci. U S A* 103, 9357–9362. doi: 10.1073/pnas.0603161103
- Zhang, S. L., Yu, Y., Roos, J., Kozak, J. A., Deerinck, T. J., Ellisman, M. H., et al. (2005). STIM1 is a Ca²⁺ sensor that activates CRAC channels and migrates from the Ca²⁺ store to the plasma membrane. *Nature* 437, 902–905. doi: 10.1038/nature04147

Conflict of Interest Statement: The authors declare that the research was conducted in the absence of any commercial or financial relationships that could be construed as a potential conflict of interest.

Received: 23 December 2013; accepted: 29 January 2014; published online: 24 February 2014.

Citation: Harraz OF and Altier C (2014) STIM1-mediated bidirectional regulation of Ca²⁺ entry through voltage-gated calcium channels (VGCC) and calcium-release activated channels (CRAC). *Front. Cell. Neurosci.* 8:43. doi: 10.3389/fncel.2014.00043 This article was submitted to the journal *Frontiers in Cellular Neuroscience*.

Copyright © 2014 Harraz and Altier. This is an open-access article distributed under the terms of the Creative Commons Attribution License (CC BY). The use, distribution or reproduction in other forums is permitted, provided the original author(s) or licensor are credited and that the original publication in this journal is cited, in accordance with accepted academic practice. No use, distribution or reproduction is permitted which does not comply with these terms.



Differential regulation of collapsin response mediator protein 2 (CRMP2) phosphorylation by GSK3 β and CDK5 following traumatic brain injury

Sarah M. Wilson¹, Seul Ki Yeon², Xiao-Fang Yang³, Ki Duk Park² and Rajesh Khanna^{1,3*}

¹ Paul and Carole Stark Neurosciences Research Institute, Indiana University School of Medicine, Indianapolis, IN, USA

² Center for Neuro-Medicine, Brain Science Institute, Korea Institute of Science and Technology, Seoul, Korea

³ Department of Pharmacology, College of Medicine, University of Arizona, Tucson, AZ, USA

Edited by:

Christophe Altier, University of
Calgary, Canada

Reviewed by:

Adam R. Cole, Garvan Institute for
Medical Research, Australia

Hailan Yao, Roskamp Institute, USA

*Correspondence:

Rajesh Khanna, Department of
Pharmacology, College of Medicine,
University of Arizona, Life Sciences
North, Rm 650, PO Box 245050,
1501 North Campbell Drive, Tucson,
AZ 85724, USA
e-mail: rkhanha@email.arizona.edu

Aberrant ion channel function has been heralded as a main underlying mechanism driving epilepsy and its symptoms. However, it has become increasingly clear that treatment strategies targeting voltage-gated sodium or calcium channels merely mask the symptoms of epilepsy without providing disease-modifying benefits. Ion channel function is likely only one important cog in a highly complex machine. Gross morphological changes, such as reactive sprouting and outgrowth, may also play a role in epileptogenesis. Mechanisms responsible for these changes are not well-understood. Here we investigate the potential involvement of the neurite outgrowth-promoting molecule collapsin response mediator protein 2 (CRMP2). CRMP2 activity, in this respect, is regulated by phosphorylation state, where phosphorylation by a variety of kinases, including glycogen synthase kinase 3 β (GSK3 β) renders it inactive. Phosphorylation (inactivation) of CRMP2 was decreased at two distinct phases following traumatic brain injury (TBI). While reduced CRMP2 phosphorylation during the early phase was attributed to the inactivation of GSK3 β , the sustained decrease in CRMP2 phosphorylation in the late phase appeared to be independent of GSK3 β activity. Instead, the reduction in GSK3 β -phosphorylated CRMP2 was attributed to a loss of priming by cyclin-dependent kinase 5 (CDK5), which allows for subsequent phosphorylation by GSK3 β . Based on the observation that the proportion of active CRMP2 is increased for up to 4 weeks following TBI, it was hypothesized that it may drive neurite outgrowth, and therefore, circuit reorganization during this time. Therefore, a novel small-molecule tool was used to target CRMP2 in an attempt to determine its importance in mossy fiber sprouting following TBI. In this report, we demonstrate novel differential regulation of CRMP2 phosphorylation by GSK3 β and CDK5 following TBI.

Keywords: CRMP2, GSK3 β , CDK5, phosphorylation, mossy fiber sprouting, TIMM staining, epileptogenesis, (S)-Lacosamide

INTRODUCTION

Precise regulation of voltage- and ligand-gated ion channels is essential for proper function of both the peripheral and central nervous systems. As perturbations to these tightly-controlled systems can result in diverse neuropathologies, regulators of ion channel function have become prime targets for therapeutic intervention. We have previously demonstrated that the intracellular phosphoprotein collapsin response mediator protein 2 (CRMP2) is a positive regulator of both ligand- and voltage-gated calcium channels (Brittain et al., 2009, 2012a) and can be targeted as such to provide therapeutic relief (Brittain et al., 2011a,b; Wilson et al., 2012a). While phosphorylation of CRMP2 increases its interaction with the N-type voltage-gated calcium channel (Brittain et al., 2012b), we recently discovered a novel posttranslational modification (SUMOylation) that negatively impacts CRMP2's ability to enhance calcium influx (Ju et al., 2013). Intriguingly, through SUMOylation, a previously unidentified link between CRMP2 and trafficking of voltage-gated sodium

channels was unearthed (Dustrude et al., 2013). CRMP2 is therefore in the unique position of potentially possessing the ability to impact voltage-gated calcium and sodium channels, as well as the ligand-gated N-methyl-D-aspartate (NMDA) receptor. A common pathology to which all three of these channel types are thought to contribute is epilepsy (for review see Ghasemi and Schachter, 2011; Oliva et al., 2012; Siwek et al., 2012).

Nearly 2.3 million people in the United States alone are burdened by epilepsy (CDC, 2012), a neurological condition classified by spontaneously recurring seizures (Goddard et al., 1969), with an estimated 150,000 more diagnosed each year (Hirtz et al., 2007; England et al., 2012). It is estimated that nearly half of epilepsy cases are classified as complex partial seizures, the majority of which originate from foci within the temporal lobe (Hauser and Kurland, 1975; Manford et al., 1992a,b; Larner, 1995; Panayiotopoulos, 2005). In many patients, temporal lobe epilepsy (TLE) is initiated by a traumatic event such as traumatic brain injury (TBI), febrile seizures, status epilepticus (SE),

tumors, stroke, or infection (Kharatishvili and Pitkanen, 2010; Yang et al., 2010a; O'Dell et al., 2012). These events are often followed by an asymptomatic latency period lasting upwards of 10 years prior to the development of spontaneous recurring seizures (de Lanerolle et al., 2003; Sharma et al., 2007; Yang et al., 2010a). That these arguably diverse insults can lead to a similar phenotype suggests the possibility of shared epileptogenic mechanisms. The majority of antiepileptic drugs (AEDs) available today target the voltage-gated sodium channel. One of these, Lacosamide (Vimpat®) (R-N-benzyl 2-acetamido-3-methoxypropionamide) ((R)-LCM), does so through a unique mechanism. Instead of affecting current density or steady-state gating kinetics, (R)-LCM selectively enhances sodium channel slow inactivation (Errington et al., 2008). Another characteristic that sets (R)-LCM apart from other AEDs is its ability to target CRMP2 (Beyreuther et al., 2007; Park et al., 2009). Notably, expression levels of CRMP2 have been shown to alter the ability of (R)-LCM to impact sodium channel function (Wang et al., 2010).

Given CRMP2's remarkable ability to regulate ion channel function, it can be at times difficult to consider its many other functions, particularly those for which it was first identified (i.e., neurite outgrowth and guidance) (Goshima et al., 1995). Importantly, of the myriad of CRMP2 functions, it is the ability to promote neurite outgrowth that is impacted by (R)-LCM, not those associated with ion channel function (Wang and Khanna, 2011; Wilson et al., 2012b). CRMP2 promotes neurite outgrowth by two distinct mechanisms: (Brittain et al., 2009) binding and transporting tubulin dimers from the soma to distal projections (Fukata et al., 2002; Kimura et al., 2005) and (Brittain et al., 2012a) stabilizing the growing end of the microtubule by promoting the inherent GTPase activity of tubulin (Chae et al., 2009), the latter of which is impaired by (R)-LCM (Wilson et al., 2012b). Aberrant growth and reorganization of neuronal circuits, specifically that of the dentate mossy fibers within the hippocampus, is commonly observed in post-mortem tissue samples from TLE patients and in animal models of the disease (for review see Koyama and Ikegaya, 2004; Sutula, 2004). Notably, CRMP2 was recently suggested to be involved in mossy fiber sprouting in the SE model of TLE (Lee et al., 2012). Under normal conditions, mossy fibers project from the granule cell layer of the dentate gyrus into the CA3 region of the hippocampus where they form synapses with pyramidal cells (Andersen et al., 1969). During TLE, mossy fibers are observed to innervate the inner molecular layer where they synapse onto the dendrites of other dentate granule cells, leading to the formation of recurrent excitatory circuits (Blaabjerg and Zimmer, 2007). To date, the molecular mechanisms contributing to mossy fiber sprouting are relatively unknown. Recent focus has centered on the involvement of growth-factor cascades, particularly that of the tropomyosin-related kinase receptor B (TrkB). Activation of the TrkB receptor eventually leads to the phosphorylation and inactivation of glycogen-synthase kinase β (GSK3 β) by protein kinase B (Akt) (Cross et al., 1995; Alessi et al., 1996; Bhawe et al., 1999). Inactivation of GSK3 β has been observed following insults commonly associated with TLE, such as TBI (Shapira et al., 2007; Dash et al., 2011; Zhao et al., 2012), hypoxia-ischemia (Sasaki

et al., 2001; Endo et al., 2006; Xiong et al., 2012), and SE (Lee et al., 2012).

The ability of CRMP2 to promote neurite outgrowth is governed by its phosphorylation state. Phosphorylation by a variety of kinases, including GSK3 β , renders CRMP2 inactive (Arimura et al., 2000, 2005; Brown et al., 2004; Cole et al., 2004, 2006; Uchida et al., 2005, 2009; Yoshimura et al., 2005; Hou et al., 2009). Specifically, GSK3 β phosphorylates CRMP2 at threonines 509, 514, and serine 518, thereby reducing its affinity for tubulin (Yoshimura et al., 2005). As inactivation of GSK3 β is observed following TLE-related insults, it is possible that these insults may also lead to a decrease in GSK3 β -phosphorylated (inactive) CRMP2, thereby promoting outgrowth. Indeed we have recently demonstrated that targeting CRMP2 with (R)-LCM can prevent the increased excitatory connectivity of layer V pyramidal neurons in the neocortical isolation (undercut) model of post-traumatic epileptogenesis (Wilson et al., 2012b). Therefore, if loss of CRMP2 phosphorylation is a contributing factor in mossy fiber sprouting, it may be possible to prevent this reorganization through the use of (R)-LCM and its derivatives. In this report we determine if GSK3 β phosphorylation of CRMP2 is altered at various stages following a TLE-related insult, as well as, the impact of GSK3 β inactivation on CRMP2 function. Ultimately, the role of CRMP2 in mossy fiber sprouting is investigated by selectively targeting CRMP2 function *in vivo*.

Lacosamide was originally discovered to be stereoselective, as much higher concentrations of the (S)- configuration are required to halt epileptiform activity both *in vitro* and *in vivo* compared to the (R)- configuration (Andurkar et al., 1999; LeTiran et al., 2001; Lees et al., 2006). In this report we employ the use of (S)-LCM, which retains the ability to target CRMP2-mediated neurite outgrowth without impacting sodium channel function, to determine if GSK3 β phosphorylation of CRMP2 is altered at various stages following a TLE-related insult. Ultimately, the role of CRMP2 in mossy fiber sprouting is investigated by selectively targeting CRMP2 function *in vivo*.

MATERIALS AND METHODS

MATERIALS

All reagents were purchased from Sigma (St. Louis, MO, USA) unless otherwise indicated. (S)-LCM was provided by the laboratory of Dr. Ki Duk Park, Center for Neuro-Medicine, Brain Science Institute, Korea Institute of Science and Technology. A 100 mM solution was made up in dimethylsulfoxide (DMSO) and stored in small aliquots at -20°C . The final concentration of 200 μM was chosen as it phenocopied the effect of CRMP2 siRNA knockdown (data not shown).

CORTICAL NEURON CULTURE

Rat cortical neuron cultures were prepared from cortices dissected from embryonic day 19 (E19) rats as described (Goslin and Banker, 1989), with some modifications. Briefly, cortices were dissected out of E19 rats, and cells were dissociated enzymatically and mechanically (trituration through Pasteur pipette) in a Papain solution (12 U/ml; Worthington) containing Leibovitz's L-15 medium (Invitrogen), 0.42 mg/ml cysteine (Sigma), 250 U/ml DNase 1 (type IV; Sigma), 25 mM NaHCO₃,

penicillin (50 U/ml)/streptomycin (50 µg/ml), 1 mM sodium pyruvate, and 1 mg/ml glucose (Invitrogen). After dissociation, the cells were gently washed by sequential centrifugation in Neurobasal medium containing either 2 mg/ml or 20 mg/ml BSA and Pen/Strep, glucose, pyruvate, and DNase1 (as above) and then plated on poly-D-lysine-coated coverslips or 96-well plates at ~400 cells per mm². Growth media (1 ml/well or 100 µl/well for 12- and 96-well plates, respectively) consisted of Neurobasal medium containing 2% NuSerum, 2% NS21 (Chen et al., 2008), supplemented with penicillin/streptomycin (100 U/ml; 50 µg/ml), 0.1 mM L-Glutamine and 0.4 mM L-glutamax (Invitrogen). 5-fluoro-2'-deoxyuridine (1.5 µg/mL) (Sigma) was added 48 h after plating to reduce the number of non-neuronal cells. After 4 days in culture and 2× each week thereon, half of the growth medium was replaced with medium without 5-fluoro-2'-deoxyuridine.

NEURITE OUTGROWTH

Primary cortical neurons plated on 96-well culture plates were transfected via lipofectamine 2000 (Invitrogen) with EGFP at 4 DIV 48 h before imaging with the ImageXpress Micro (Molecular Devices). Immediately prior to imaging, media was exchanged with sterile phosphate buffered saline (PBS). The overexpression of EGFP allowed for visualization of a small percentage of neurons while maintaining optimal cell densities required for survival. EGFP fluorescence was imaged at 4× magnification. To enable laser-based autofocus, laser offset was determined via z-stack. Optimum exposure time was also determined to prevent saturation.

Analysis of neurite outgrowth was completed using a neurite outgrowth analysis protocol within the MetaXpress software (Molecular Devices). Cell soma and processes are detected by defining separate size and fluorescence intensity threshold parameters. Cells were excluded if they were determined not to be neurons based on morphology, if processes extended beyond the image field, or if no processes were longer than 50 µm. The following parameters are recorded and summarized into a final “total outgrowth” parameter: number of processes, number of branches, mean process length, and maximum process length.

WHOLE-CELL PATCH-CLAMP RECORDINGS

Whole-cell voltage recordings were performed at RT on primary cultured cortical neurons (7 DIV) using an EPC 10 Amplifier (HEKA Electronics). Electrodes were pulled from thin-walled borosilicate glass capillaries (Warner Instruments) with a P-97 electrode puller (Sutter Instrument) such that the final electrode resistances were 2–3 MΩ when filled with internal solutions. The internal solution for recording Na⁺ currents contained (in mM): 110 CsCl, 5 MgSO₄, 10 EGTA, 4 ATP Na₂, and 25 HEPES (pH 7.2, 290–310 mOsm/L). For recording Na⁺ currents, the external solution contained (in mM): 100 NaCl, 10 tetraethylammonium chloride (TEA-Cl), 1 CaCl₂, 1 CdCl₂, 1 MgCl₂, 10 D-glucose, 4 4-AP, 0.1 NiCl₂, 10 HEPES (pH 7.3, 310–315 mOsm/L). Whole-cell capacitance and series resistance (70–80%) were compensated with the amplifier. Cells were considered only when the seal resistance was more than 1 GΩ and the series resistance was less than 10 MΩ. Linear leak currents were digitally subtracted by P/4.

IMMUNOBLOT ASSAY AND QUANTIFICATION

Protein samples were boiled in Laemmli sample buffer for 5 min and fractionated on 4–15% separating SDS polyacrylamide gels. Apparent molecular weights were determined using broad range standards (Fisher). Following electrophoresis, proteins were transferred to PVDF membranes (Invitrogen) for immunoblotting. Membranes were occasionally stained with ponceau (BioRad) to monitor transfer efficiency. Following transfer, membranes were blocked for 1 h in 5% skim milk powder +0.05% BSA in TBST at RT. Primary antibody incubations [goat anti-rabbit GSK3β and GSK3β pSer9 (Millipore), goat anti-rabbit CRMP2 (Sigma), donkey anti-sheep CRMP2 pThr509/514 (Kinasource), goat-anti-rabbit CRMP2 pSer522 (ECM Biosciences), goat anti-rabbit CDK5 (Cell Signaling), or goat anti-mouse βIII-tubulin (Promega)] were either 2 h at RT or overnight at 4°C. Membranes were extensively washed in TBST and incubated in secondary antibody [goat anti-rabbit, goat anti-mouse, or donkey anti-sheep IgG horseradish peroxidase (HRP)] (G Biosciences) or (goat anti-rabbit, goat anti-mouse IgG dylight 650 or 800 conjugated) (Pierce) (1:15,000). Membranes incubated with HRP-conjugated secondary antibodies were washed extensively in TBST prior to probing with Enhanced Chemiluminescence Western blotting substrate (Fisher) before exposure to photographic film. Blots were exposed for a range of durations to ensure the generation of a print in which the film is not saturated. Membranes incubated with dylight-conjugated secondary antibodies were washed extensively in TBST prior to imaging with the LI-COR Odyssey imaging system. Both images obtained from film and LI-COR were digitized and quantified using Un-Scan-It gel V6.1 scanning software (Silk Scientific Inc., Orem), limiting our analysis to the linear range. Immunoblot images were digitized and analyzed using UnscanIt software, limiting analysis to the digital range. Briefly, densitometric values were obtained for each band and normalized to a loading control (tubulin) for each respective sample. In place of a single background measurement, background values for each band were obtained from an directly adjacent area to avoid issues of background discrepancy. To better allow for direct comparisons, measurements for CDK5- and GSK3β-phosphorylated CRMP2 were compared to values for total CRMP2 and Tubulin from the same immunoblot following a stripping and reprobing procedure. The same method was also applied for comparing phosphorylated-GSK3 to total GSK3 and tubulin. While this method provides a direct comparison between levels of each protein within a single, loaded sample, the stripping procedure does decrease the esthetic quality of the immunoblot.

TRAUMATIC BRAIN INJURY

All procedures involving animals were approved by the Institutional Animal Care and Use Committee of Indiana University School of Medicine and were carried out according to NIH guidelines and regulations. Animals were doubly-housed and maintained in a 12 h light/12 h dark cycle environment with access to food and water *ad libitum*. Adult male Sprague–Dawley rats (275–300 g) were subjected to controlled cortical impact (CCI) injury. Rats were anesthetized with a ketamine/xylazine mixture (80 and 5 mg/kg, respectively) and placed in a stereotaxic

frame prior to TBI. Using sterile procedures, the skin was retracted, and a ~4 mm craniotomy was performed ~3 mm lateral to midline and 3 mm posterior to the bregma suture. The skullcap was removed without disruption of the dura. The impacting tip was angled on a medial-lateral plane so that it was perpendicular to the exposed cortical surface. The deformation impact depth was set at 1.5 mm, and the piston velocity was controlled at 3.0 m/s. Following impact, the exposed tissue was covered with bone wax (Henry Schein) and the midline incision was sutured with 5.0 monofilament (Ethicon). Following surgery, animals received a bolus of sterile saline and post-operative analgesic Buprenorphine (0.5 mg/kg). During all surgical procedures and recovery, the core body temperature of the animals was maintained at 36–37°C. Sham animals received the same craniotomy and post-operative care.

IN VIVO ADMINISTRATION OF (S)-LACOSAMIDE ((S)-LCM)

To provide continuous infusion, (S)-LCM was delivered via an implanted osmotic mini-pump (Alzet). To compensate for animal growth over the 4-week treatment period, the animals were weighed prior to surgery and the amount of (S)-LCM was adjusted to account for the expected weight gain and an infusion rate of 2.5 μ l/h to allow for administration of an average of 5 mg/kg per day of (S)-LCM or <0.01% DMSO for vehicle. Immediately following CCI surgery, sterile mini-pumps were subcutaneously implanted. An incision was made on the back, between the shoulder blades. A small pocket was created by carefully separating skin from muscle near the incision site. The mini-pump was placed into the pocket and the incision was closed with 5.0 monofilament.

TISSUE PROCESSING

For immunoblots: at 24 h or 4 weeks post-TBI, animals were sacrificed and transcardially perfused with 0.1 M phosphate buffer. For perfusion, an incision is made in the left ventricle to allow insertion of a needle attached to a peristaltic pump through the ventricle and into the ascending aorta. The needle was clamped into position and a second incision was made in the right atrium for drainage. Following perfusion, brains were extracted and hippocampi ipsilateral and contralateral to the injury site were dissected, frozen in liquid nitrogen, and stored at –80°C. Prior to immunoblot assay, tissue was thawed and homogenized using a sonicator.

For TIMM staining: at 4 weeks following TBI, animals were sacrificed and transcardially perfused (as previously described) with a sodium sulfide perfusate solution (150 mM Na₂S, 8.1 mM Na₂HPO₄, 1.9 mM NaH₂PO₄), followed by 4% paraformaldehyde. Following perfusion, brains were extracted and placed in 4% paraformaldehyde for 24 h at 4°C. Brains were then transferred to 0.1 M phosphate buffer + 30% sucrose for 48 h at 4°C. Tissue was embedded into Optimal Cutting Temperature (OCT) compound (Tissue-Tek) on dry ice. Coronal slices (35 μ m thickness) were made on a cryostat (Leica). Slices were mounted onto gelatin-coated microscope slides and stored at –20°C.

TISSUE STAINING

Tissue sections were allowed to thawed and processed for TIMM staining with the RAPID TIMM Stain Kit (FD

Neurotechnologies). Tissue sections were washed in 0.1 M phosphate buffer 3 times, 3 min each and transferred to the TIMM solution (132 mM Citric Acid, 79.5 mM Sodium Citrate, 153.6 mM Hydroquinone, 5 mM AgNO₃, 30% Gum Arabic), where they were rocked gently in the dark for 45–60 min at 30°C. Sections were then rinsed in ddH₂O for 3 min in the dark, followed by gently washing them in running water for 30 min to remove excess stain. Sections were dehydrated in 50, 75, and 95% ethanol for 3 min each. Sections were incubated in absolute ethanol 3 times, 3 min each and then cleared in xylene (Fisher) 3 times, 3 min each. Coverslips were added using a resinous mounting medium (Aquamount) (Fisher).

Both low and higher magnification images were obtained using a light microscope (Nikon 90i) and scored by three observers blinded to the conditions, based on the scale originally established by Cavazos et al. (1991). Briefly, the scoring system ranks TIMM staining on a scale of 0–5, with 0 being the absence of TIMM granules within the supragranular region and 5 indicating the existence of a dense band of TIMM granules within the supragranular region, extending into the inner molecular layer. To avoid issues of variance among animals, scores were compared from contralateral and ipsilateral hippocampi from the same animal to yield the difference in TIMM scoring (Ipsilateral—Contralateral).

DATA ANALYSIS

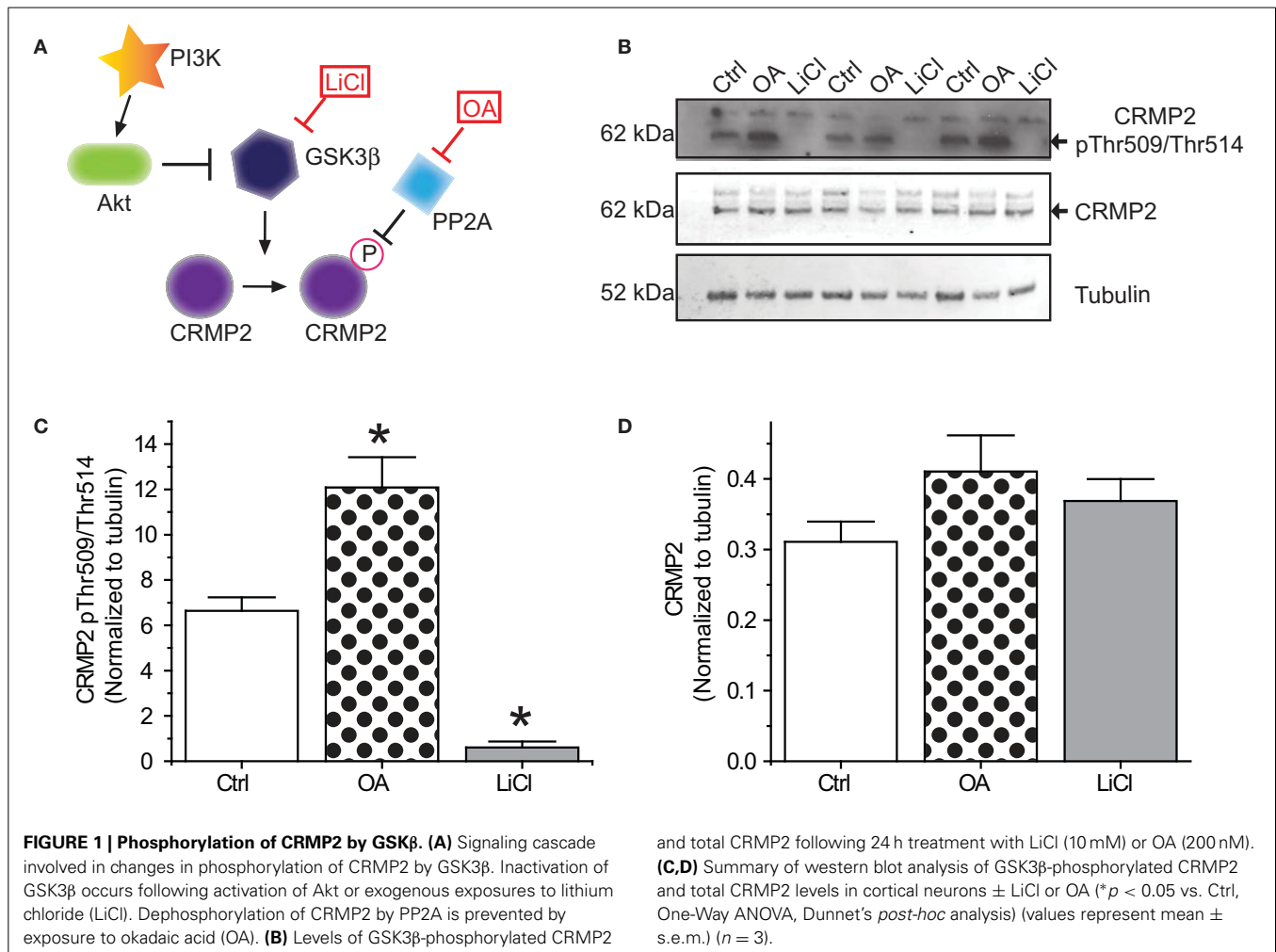
All data points are shown as mean \pm s.e.m. Statistical differences between control and experimental conditions were determined by using ANOVA with a Dunnett's or Tukey's *post-hoc* test or a Student's *t*-test when comparing only two conditions. Values of *p* < 0.05 were judged to be statistically significant.

RESULTS

In regards to its outgrowth-promoting function, the activity of CRMP2 is regulated by its phosphorylation state. In the unphosphorylated form, CRMP2 is considered active and thereby growth-promoting; however, upon phosphorylation by a variety of kinases, most notably GSK3 β , CRMP2 is rendered inactive (Arimura et al., 2000, 2005; Brown et al., 2004; Cole et al., 2004, 2006; Uchida et al., 2005, 2009; Yoshimura et al., 2005; Hou et al., 2009). Tonically active under naïve conditions, GSK3 β is inactivated following insults commonly associated with TLE such as TBI (Shapira et al., 2007; Dash et al., 2011; Zhao et al., 2012), hypoxia-ischemia (Sasaki et al., 2001; Endo et al., 2006; Xiong et al., 2012), and SE (Lee et al., 2012). This inactivation of GSK3 β may lead to an overall decrease in the level of phosphorylated (inactive) CRMP2, thereby promoting neurite outgrowth.

GSK3 β PHOSPHORYLATION OF CRMP2 UNDER NAÏVE CONDITIONS

In order for inactivation of GSK3 β to impact CRMP2 function, a proportion of CRMP2 must be phosphorylated by GSK3 β under normal conditions. Additionally, changes in CRMP2 phosphorylation by GSK3 β should occur on a relatively fast time-scale. To determine the extent of GSK3 β phosphorylation of CRMP2, primary cultured cortical neurons were exposed to the GSK3 β inhibitor Lithium Chloride (LiCl) (10 mM) or the protein phosphatase inhibitor okadaic acid (200 nM) for 18–24 h (Figure 1A). Western blot analysis was performed with



an antibody specific to GSK3β-mediated phosphorylation of CRMP2 at Thr509 and Thr514. Importantly, CRMP2 appears to be phosphorylated by GSK3β under naïve/control conditions (**Figures 1B,C**). Prevention of dephosphorylation by okadaic acid increased CRMP2 phosphorylation by ~2-fold (12.1 ± 1.3) compared to control (6.6 ± 0.6), while LiCl-mediated inhibition of GSK3β resulted in an ~90% loss of CRMP2 phosphorylation (0.6 ± 0.3) ($p < 0.05$) (**Figures 1B,C**). Levels of total CRMP2 protein remained unchanged (control: 0.31 ± 0.03 ; okadaic acid: 0.41 ± 0.05 ; and LiCl: 0.37 ± 0.03) ($p > 0.05$) (**Figure 1D**). This data suggests that a proportion of CRMP2 is phosphorylated by GSK3β under normal conditions and loss of GSK3β activity dramatically results in a near-complete loss of phosphorylated CRMP2 within 18–24 h. GSK3β phosphorylation of CRMP2 appears to be dynamically regulated, as evidenced by active dephosphorylation under control conditions.

GSK3β INHIBITION INCREASES NEURITE OUTGROWTH VIA CRMP2

In regards to its ability to promote neurite outgrowth, phosphorylation by GSK3β effectively inactivates CRMP2 by reducing its affinity for tubulin (Yoshimura et al., 2005). Therefore, inactivation of GSK3β should be growth promoting. To determine if

the LiCl-induced loss of GSK3β-phosphorylated CRMP2 directly alters CRMP2-mediated neurite outgrowth within the same timeframe, EGFP-transfected cortical neurons were exposed to lithium chloride for 18–24 h to determine the effect of GSK3β inhibition on neurite outgrowth (**Figure 2A**). Immediately following exposure, neurons were imaged using the ImageXpress Micro system and neurite outgrowth was determined via the MetaXpress software system. As expected, inhibition of GSK3β increased total outgrowth (154.5 ± 5.9) compared to controls (99.8 ± 4.0) ($p < 0.05$) (**Figures 2B–D**). We had previously demonstrated that (S)-LCM, the inactive enantiomer of (R)-LCM, retains the ability to target CRMP2 function and can therefore be used in place of knockdown strategies to determine the role of CRMP2 in a particular process (Wilson and Khanna, unpublished). To ensure that the LiCl-induced increase in outgrowth was in fact due to changes in CRMP2 activity, the experiment was repeated in the presence of (S)-LCM (200 μM). As (S)-LCM alone decreases outgrowth, it was included in both LiCl-treated and control conditions. Without (S)-LCM, LiCl increased neurite outgrowth by $54.9 \pm 5.9\%$ (**Figure 2D**). In contrast, in the presence of (S)-LCM, LiCl increased neurite outgrowth by $15.3 \pm 5.1\%$ ($p < 0.05$) (**Figures 2D,E**).

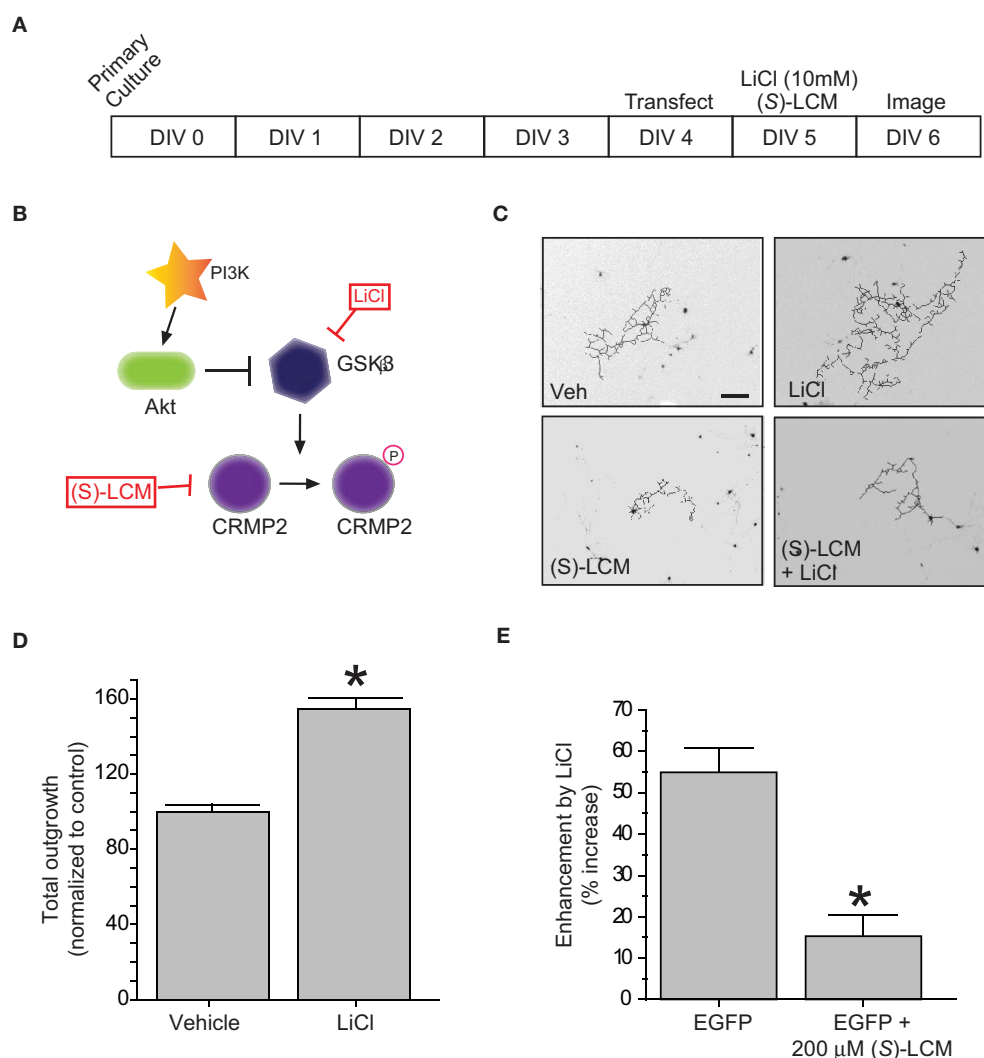


FIGURE 2 | Inactivation of GSK3 β enhances neurite outgrowth in a CRMP2-dependent manner. (A) Experimental timeline. Cortical neurons were transfected with EGFP at 4 DIV and exposed to vehicle (<0.01% DMSO), LiCl (10 mM), (S)-LCM (200 μ M), or LiCl + (S)-LCM for 24 h starting at 5 DIV and imaged at 6 DIV. **(B)** GSK3 β signaling cascade. **(C)** Representative tracings of neurons transfected with EGFP and exposed to

LiCl, (S)-LCM, or both. (Scale bar = 150 μ m). **(D)** Total outgrowth of neurons exposed to LiCl for 24 h (* p < 0.05, student's t -test) (values represent mean \pm s.e.m.). **(E)** Enhancement of outgrowth by LiCl under conditions of (S)-LCM treatment (* p < 0.05 vs. EGFP, One-Way ANOVA, Dunnett's *post-hoc* analysis) (values represent mean \pm s.e.m.) (n = 92–150 cells from 8 separate culture wells).

(S)-LCM DOES NOT TARGET VOLTAGE-GATED SODIUM CHANNELS

It is essential to verify that (S)-LCM is unable to impact voltage-gated sodium channels in this system. Therefore, sodium channel slow inactivation of cultured cortical neurons was determined by holding cells at -70 mV, conditioning to potentials ranging from -100 to $+20$ mV (in $+10$ mV increments) for 5 s, moved to a hyperpolarizing pulse of -120 mV for 150 ms to allow fast-inactivated channels to recover, and a single depolarizing pulse to 0 mV was applied for 15 ms to determine the fraction of channels available (Figure 3A). The addition of 200 μ M (S)-LCM did not alter the onset or extent of slow inactivation (Figures 3B–D). We next determined the effect of (S)-LCM on fast inactivation and steady-state activation. For fast inactivation, cells were held at -80 mV, conditioned to potentials

ranging from -120 to -10 mV (in $+10$ mV increments) for 500 ms and the fraction of available current was determined by a 20 ms test pulse at 0 mV (Figure 3E). For steady-state activation, cells were held at -80 mV and current was measured at potentials ranging from -70 to $+80$ mV (in $+10$ mV increments) for 500 ms (Figure 3E). Neither fast inactivation nor steady-state inactivation was effected by (S)-LCM (Figure 3F).

LOSS OF CRMP2 PHOSPHORYLATION FOLLOWING TBI

The development of TLE following TBI, accounts for 20% of symptomatic epilepsy (Agrawal et al., 2006). Evidence of increased Akt activation within the hippocampus as well as other regions has been observed following TBI (Zhang et al., 2006; Zhao et al., 2012). Corresponding to changes in Akt activity, levels

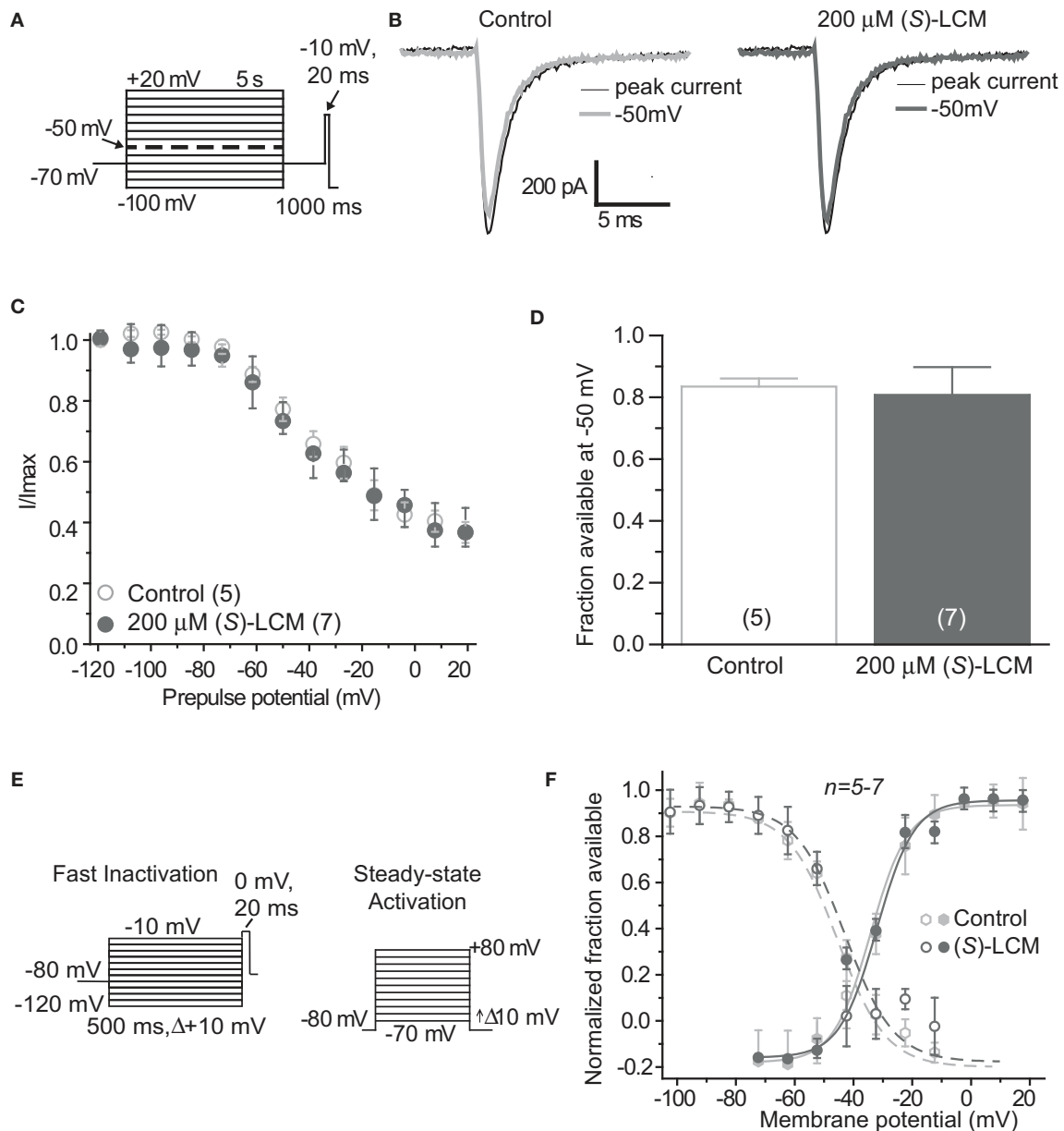


FIGURE 3 | (S)-Lacosamide ((S)-LCM) does not affect biophysical properties of voltage-gated sodium currents in cortical neurons. (A) Voltage protocol for slow inactivation. **(B)** Representative current traces from cortical neurons in the absence (control, 0.1% DMSO) or presence of 200 μ M (S)-LCM. The thin black and thick gray traces represent the currents evoked at -100 and -50 mV, respectively (also highlighted in the voltage protocol as a dashed thick line). **(C)** Summary of steady-state slow activation curves for neurons treated with DMSO (control) or 200 μ M (S)-LCM. No drug-induced slow inactivation was evident at voltages more depolarizing than -80 mV in neurons treated with (S)-LCM. **(D)** Summary of the fraction of current available at -50 mV for neurons treated with

DMSO (control) or 200 μ M (S)-LCM ($p > 0.05$, Student's t -test). **(E)** Voltage protocol for fast inactivation (left) and activation (right). **(F)** Representative Boltzmann fits for steady-state fast inactivation and activation for neurons treated with 0.1% DMSO (control) and 200 μ M (S)-LCM are shown. Values for $V_{1/2}$, the voltage of half-maximal inactivation and activation and the slope factors (k) were derived from Boltzmann distribution fits to the individual recordings and averaged to determine the mean (\pm s.e.m.) voltage dependence of steady-state inactivation and activation, respectively. There were no differences between control and drug for any of the parameters tested ($p > 0.05$, One-Way ANOVA). Data are from 5 to 7 cells per condition.

of phosphorylated (inactive) GSK3 β are also increased following TBI (Shapira et al., 2007; Dash et al., 2011; Zhao et al., 2012). To determine if changes in CRMP2 phosphorylation could be the driving force behind the increased neurite outgrowth in the

hippocampus following TLE-related insults, hippocampal tissue was collected at both early (24 h) and late (4 weeks) phases following TBI in adult male rats. Consistent with previous reports, levels of Ser9-phosphorylated (inactivated) GSK3 β were increased

in the early phase following TBI (1.31 ± 0.08) compared to sham controls (1.00 ± 0.05) ($p < 0.05$) (Figures 4A,B). Importantly, total expression of GSK3 β remained unchanged [(1.00 ± 0.11) vs. (0.81 ± 0.12)] ($p > 0.05$) (Figures 4A,B). The increase in GSK3 β phosphorylation appeared to be transient, as levels did not differ at 4 weeks following TBI (0.97 ± 0.12) compared to sham controls (1.00 ± 0.06) ($p > 0.05$) (Figures 4C,D).

Subsequent to the observed inactivation of GSK3 β , levels of GSK3 β -phosphorylated CRMP2 were reduced in the early phase following TBI (0.52 ± 0.07) compared to sham controls (1.00 ± 0.13) ($p < 0.05$) (Figures 5A,B). No change in total CRMP2 expression was observed [(1.10 ± 0.12) vs. (1.00 ± 0.04)] ($p > 0.05$) (Figures 5A,B). Despite the observed transience of GSK3 β inactivation, levels of GSK3 β -phosphorylated CRMP2 remained reduced in the late phase following TBI (0.62 ± 0.08) compared to sham controls (1.00 ± 0.09) ($p < 0.05$) (Figures 5C,D). These results suggest that there is an increased level of active (unphosphorylated) CRMP2 in both the early and late phases following TBI. Interestingly, while the decrease in CRMP2 phosphorylation at 24 h post-TBI is directly correlated with an inactivation

of GSK3 β , the sustained decrease observed at 4 weeks post-TBI appears to be independent of changes in GSK3 β activity.

"PRIMED" CRMP2 IS DECREASED IN THE LATE, BUT NOT EARLY PHASE FOLLOWING TBI

Phosphorylation of GSK3 β is not the only avenue through which phosphorylation of its substrates is regulated. GSK3 β substrate recognition can be complex, as there is no strict consensus motif, often requiring prior phosphorylation (priming) at a serine slightly c-terminal to the GSK3 β site(s) (DePaoli-Roach, 1984; Fiol et al., 1988). This type of hierarchical phosphorylation allows for complex regulation at multiple levels. In the case of CRMP2, it must first be phosphorylated at serine 522 by the serine/threonine kinase cyclin-dependent protein kinase 5 (CDK5) in order to be phosphorylated by GSK3 β (Yoshimura et al., 2005; Cole et al., 2006) (Figure 6A). Sequential phosphorylation of CRMP2 by CDK5 and GSK3 β has been demonstrated for many facets of CRMP2 function, most importantly, neurite outgrowth and growth cone collapse (Brown et al., 2004; Uchida et al., 2005). As decreased levels of GSK3 β -phosphorylated CRMP2

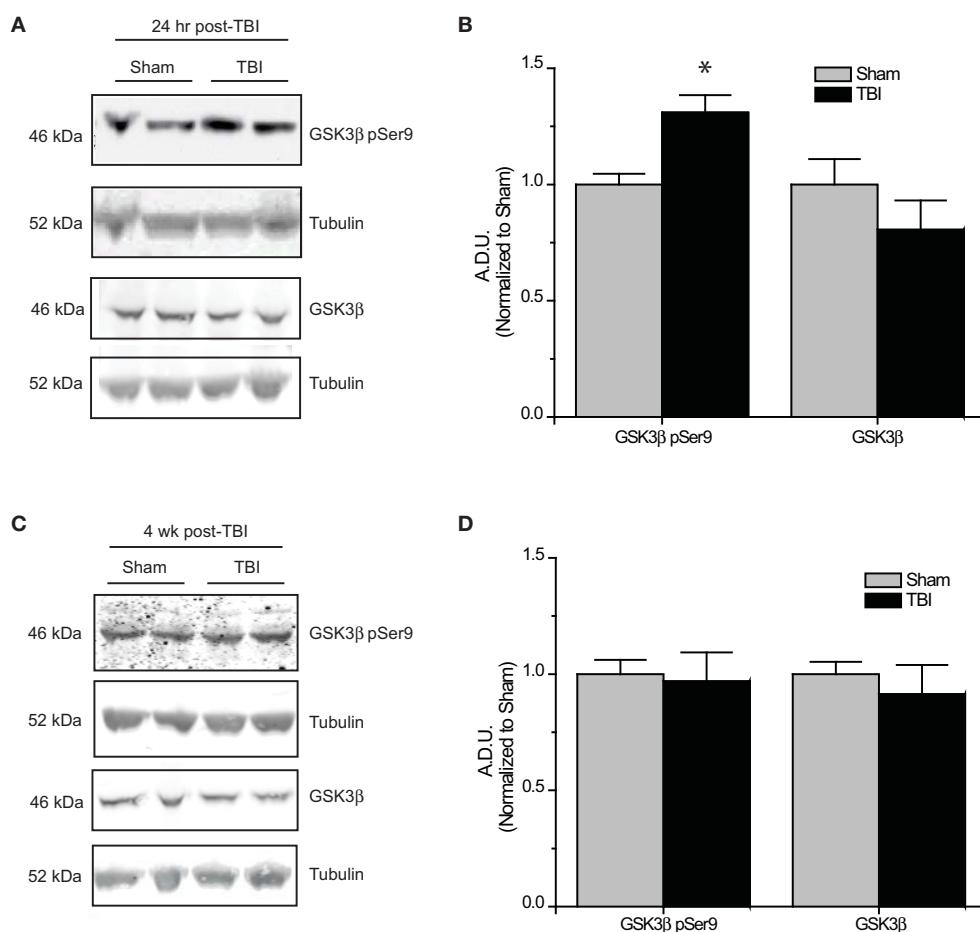


FIGURE 4 | Changes in GSK3 β phosphorylation following TBI. (A) Western blots of phosphorylated and total GSK3 β from hippocampal tissue 24 h following TBI. **(B)** Summary of GSK3 β pSer9 and total GSK3 β levels 24 h following TBI. [Data is depicted as arbitrary densitometric units (A.D.U.)]. **(C)**

Western blots of phosphorylated and total GSK3 β from hippocampal tissue 4 weeks following TBI. **(D)** Summary of GSK3 β pSer9 and total GSK3 β levels 4 weeks following TBI (* $p < 0.05$ vs. sham, Student's t -test) (values represent mean \pm s.e.m.) ($n = 4-5$).

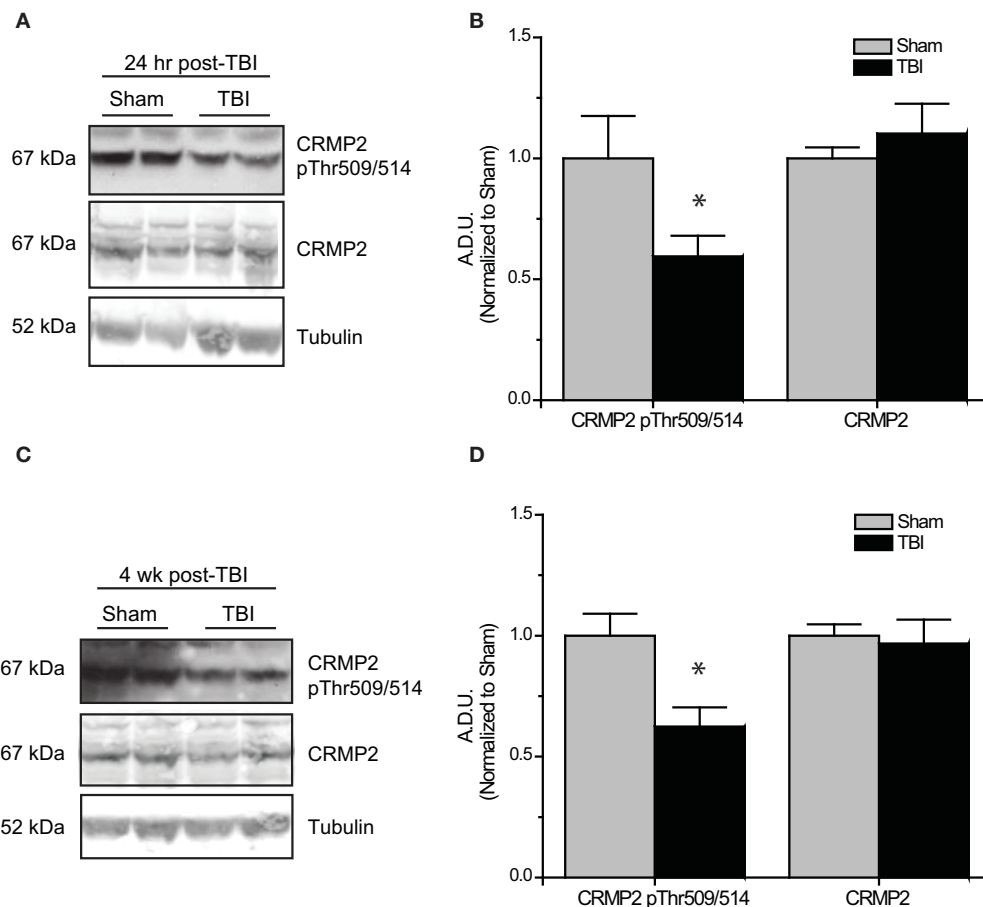


FIGURE 5 | Changes in CRMP2 phosphorylation by GSK3 β following TBI. (A) Western blots of GSK3 β -phosphorylated and total CRMP2 from hippocampal tissue 24 h following TBI. **(B)** Summary of CRMP2 pThr509/514 and total CRMP2 levels 24 h following TBI (raw data represents protein of interest normalized to tubulin and further normalized to sham to allow for easy comparison) [data is represented as arbitrary

densitometric units (A.D.U.)]. **(C)** Western blots of GSK3 β -phosphorylated and total CRMP2 from hippocampal tissue 4 weeks following TBI. **(D)** Summary of CRMP2 pThr509/514 and total CRMP2 levels 4 weeks following TBI. Data was normalized to sham conditions for ease of comparison. (* $p < 0.05$ vs. sham, Student's t -test) (values represent mean \pm s.e.m. from $n = 4-5$).

were observed in the late phase following TBI that were not secondary to changes in GSK3 β expression or activity, it is possible that the changes in levels of GSK3 β -phosphorylated CRMP2 may be attributed to a decrease in phosphorylation by CDK5. Therefore, levels of CDK5-phosphorylated CRMP2 were determined from hippocampal tissue collected at early (24 h) and late (4 weeks) time points following TBI. Notably, CDK5 phosphorylation of CRMP2 at 24 h following TBI did not differ from sham controls [(1.05 ± 0.07) vs. (1.00 ± 0.12)] ($p > 0.05$) (Figures 6B,C). However, at 4 weeks following injury, levels of CDK5-phosphorylated CRMP2 were decreased (0.69 ± 0.07) compared to sham controls (1.00 ± 0.03) ($p < 0.05$) (Figures 6B,C). These results suggest that CRMP2 is differentially regulated during early and late phases following injury. While a loss of GSK3 β activity accounts for decreases in CRMP2 phosphorylation immediately following injury, the same phenotype during later phases is attributed to a loss of priming by CDK5.

EFFECTS OF TARGETING CRMP2 *IN VIVO* ON MOSSY FIBER SPROUTING

As changes in CRMP2 phosphorylation, and presumably activity, are observed within the hippocampus at both early and late time points following TBI, CRMP2 may be involved in both the induction and maintenance of mossy fiber sprouting following injury. To determine the importance of CRMP2 in this phenomenon, osmotic minipumps containing (S)-LCM (140 mg/kg) were implanted (subcutaneously) immediately following TBI surgery in adult male rats. This method allowed for continuous delivery of ~ 5 mg/kg (S)-LCM per day (~ 0.21 mg/kg per hour) over the course of 4 weeks (Figure 7A). The extent of aberrant mossy fiber sprouting is easily identified due to the high amount of chelatable zinc within mossy fibers which can be visualized via a silver-sulfide staining method (TIMM staining) (Timm, 1958; Zimmer, 1973). Therefore, at the cessation of treatment, bilateral hippocampal tissue was obtained and processed for TIMM staining, to reveal the extent of mossy fiber sprouting within the inner molecular layer of the hippocampus.

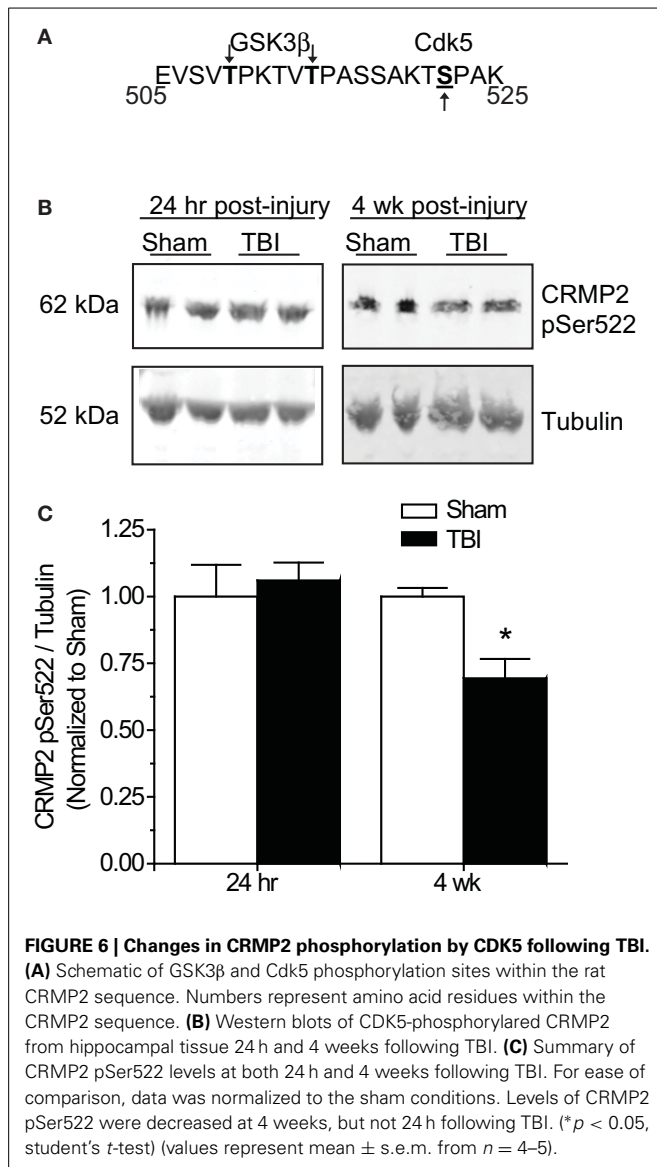


FIGURE 6 | Changes in CRMP2 phosphorylation by CDK5 following TBI. (A) Schematic of GSK3 β and Cdk5 phosphorylation sites within the rat CRMP2 sequence. Numbers represent amino acid residues within the CRMP2 sequence. (B) Western blots of CDK5-phosphorylated CRMP2 from hippocampal tissue 24 h and 4 weeks following TBI. (C) Summary of CRMP2 pSer522 levels at both 24 h and 4 weeks following TBI. For ease of comparison, data was normalized to the sham conditions. Levels of CRMP2 pSer522 were decreased at 4 weeks, but not 24 h following TBI. (* $p < 0.05$, student's t -test) (values represent mean \pm s.e.m. from $n = 4-5$).

As expected, TBI led to increased TIMM differences (1.40 ± 0.25) compared to sham controls (0.25 ± 0.25) ($p < 0.05$) (Figures 7B–D). Importantly, differences in TIMM scores did not differ between sham (0.25 ± 0.25) and naïve animals (0.00 ± 0.32) ($p > 0.05$). Intriguingly, (S)-LCM treatment prevented the TBI-induced increase in TIMM differences (0.40 ± 0.25) compared to animals receiving TBI alone (1.40 ± 0.25) ($p < 0.05$) (Figures 7B–D). However, the changes in TIMM scores following TBI did not differ between animals receiving (S)-LCM (0.40 ± 0.25) and vehicle ($\sim 0.01\%$ DMSO) (1.00 ± 0.00) ($p > 0.05$) (Figures 7C–D). Therefore, it cannot definitively be concluded that CRMP2 is necessary for mossy fiber sprouting following TBI.

DISCUSSION

In order for changes in GSK3 β activity to impact CRMP2 function, a balance of GSK3 β -phosphorylated and unphosphorylated

CRMP2 must be present. Importantly, GSK3 β phosphorylation of CRMP2 appears to be dynamically regulated in naïve neurons, as inhibition of GSK3 β led to an almost complete loss of phosphorylation within 24 h. Additionally, the increase in phosphorylation following okadaic acid exposure provides evidence for active dephosphorylation. Therefore, changes in GSK3 β activity can directly impact CRMP2 function. Indeed, inhibition of GSK3 β led to increases in neurite outgrowth in a CRMP2-dependent manner. Given that inactivation of GSK3 β has previously been demonstrated following TBI, decreased phosphorylation of CRMP2 may account for the changes in neurite elongation and branching observed within the hippocampus. Our findings indicate that TBI leads to decreased GSK3 β phosphorylation of CRMP2 at both 24 h and 4 weeks post-injury. As mossy fiber sprouting is considered a progressive process, the maintained loss of phosphorylation throughout later phases following injury is an important finding. In contrast to early phases following TBI, the loss of GSK3 β phosphorylation at 4 weeks post-injury is likely not attributed to a prolonged inactivation of GSK3 β . In fact, previous reports suggest that levels of Akt-phosphorylated GSK3 β return to baseline within 14 days (Dash et al., 2011). These findings suggest that while CRMP2 may play an integral role in promoting neurite outgrowth both immediately following injury as well as in later phases, the mechanisms underlying the increase in CRMP2 activity during these phases may differ. Indeed, our results revealed that the decrease in GSK3 β -phosphorylated CRMP2 during later phases following injury was in fact attributed to a decrease in priming by CDK5.

Mossy fiber sprouting in TLE can likely be divided into 2 distinct phases: the induction phase, during which sprouting and outgrowth are attributed directly to the precipitating insult such as TBI, hypoxia-ischemia, or SE, and the maintenance phase (Sutula, 2004; Pitkänen and Lukasiuk, 2009). Therefore, early events following injury, such as inactivation of GSK3 β , can be attributed to injury-induced mechanisms (i.e., activation of pro-survival signaling pathways). The latter phase involves processes secondary to the original insult such as hyperexcitability and network synchronization. Interestingly, we have previously demonstrated that CDK5 priming of CRMP2 is decreased in response to prolonged neuronal activity and that the loss of priming is directly translated into a reduction in GSK3 β -phosphorylated CRMP2 (Wilson and Khanna, unpublished). As TBI can lead to progressive hyperexcitability (Yang et al., 2010b), the sustained loss of CRMP2 phosphorylation is potentially due to progressive changes in neuronal function which are secondary to the precipitating injury, such as activity-driven changes in CDK5 function.

Overall, phosphorylation of CRMP2 appears to be differentially regulated through both induction (early) and maintenance (late) phases following TBI. As such, targeting CRMP2-mediated neurite outgrowth throughout these stages may be sufficient to attenuate the progression of mossy fiber sprouting. Indeed, the extent of mossy fiber sprouting in animals that had received continuous administration of (S)-LCM following TBI was markedly decreased compared to untreated animals. However, the trending effect of vehicle administration is a confounding factor that

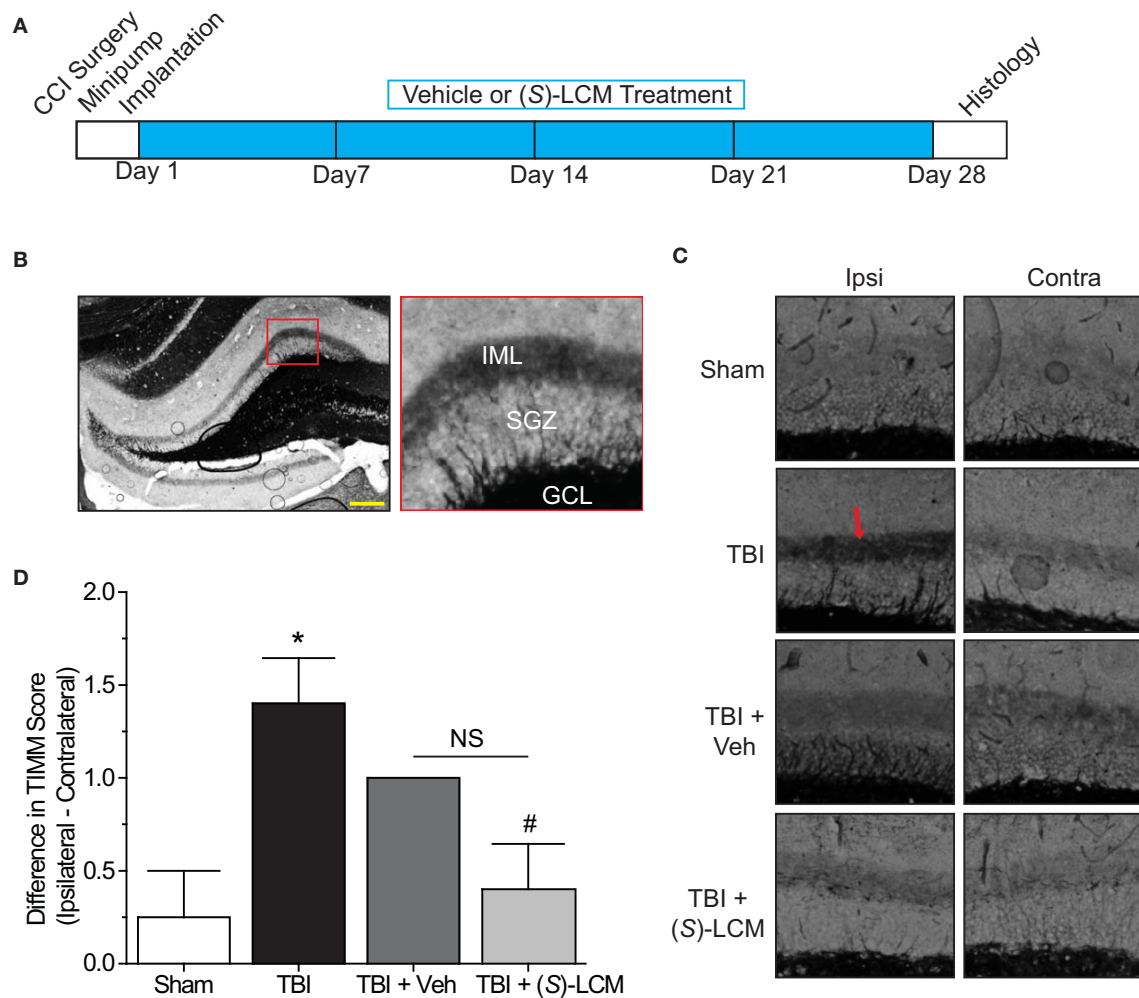


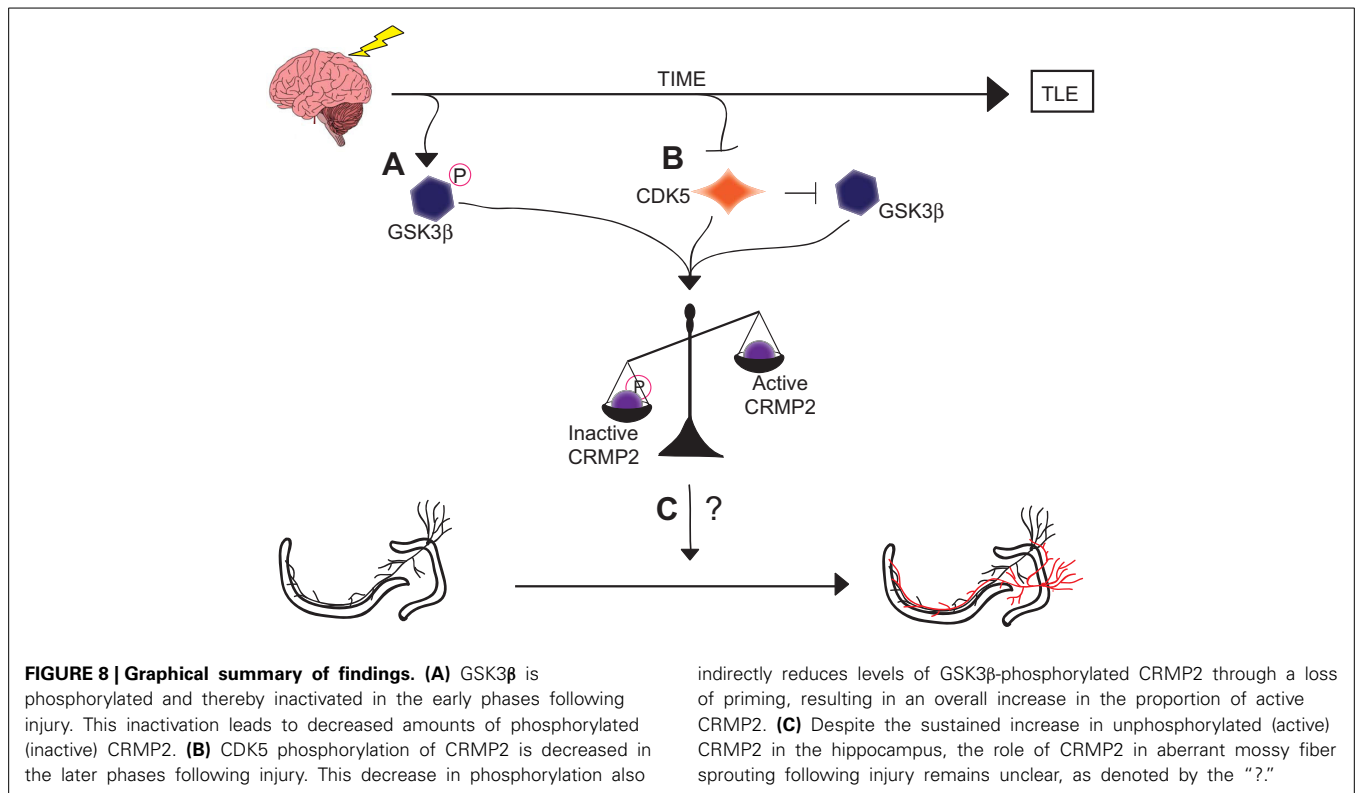
FIGURE 7 | Effects of targeting CRMP2 *in vivo* on mossy fiber sprouting. (A) Timeline of experimental design. Animals received either controlled cortical impact or sham (craniotomy) surgery. Immediately following surgery, animals were implanted with osmotic mini-pumps containing either vehicle or (S)-LCM to be continuously infused at <0.01% DMSO and ~5 mg/kg per day. Following 4 weeks of treatment, tissue samples were prepared for histology. (B) Representative low-magnification image of a TIMM-stained coronal section. Red box depicts region quantified for the extent of mossy fiber sprouting into the inner molecular layer. (C) Representative 10x-magnification images of ipsilateral and

contralateral TIMM-stained hippocampi. TBI led to a dense laminar band of TIMM reactivity within the supragranular zone extending to the inner molecular layer (red arrow). (D) Summary of TIMM scores from animals exposed to sham or TBI surgery \pm vehicle or (S)-LCM. To minimize the impact of variance among animals, data is represented as the difference in TIMM score between ipsilateral and contralateral hippocampi from the same animal. (S)-LCM treatment prevented the TBI-induced increase in mossy fiber sprouting, however did not differ from vehicle. (* $p < 0.05$ vs. sham; # $p < 0.05$ vs. TBI; One-Way ANOVA, Tukey's *post-hoc* analysis) (values represent mean \pm s.e.m. from $n = 4-5$). Scale bar = 250 μ m.

prevents a definitive conclusion from being drawn. Changes in hippocampal cell death likely do not account for the observed changes in TIMM staining, as dentate granule cell survival is typically not impacted by moderate TBI (Lowenstein et al., 1992; Grady et al., 2003). Furthermore, (S)-LCM is unlikely to affect hippocampal cell death as a recent study demonstrated that the parent compound (R)-LCM does not alter neuronal survival following TBI (Pitkanen et al., 2014). The lack of significant separation between (S)-LCM- and vehicle-treated groups may be a result of the nature of administration, despite the previous success observed with infusion of (R)-LCM in a separate study (Licko et al., 2013). While continuous subcutaneous infusion was considered to be preferable over daily intraperitoneal injections, it is

possible that inflammation at the implantation site may have been a factor.

Although the exact role of CRMP2 in mossy fiber sprouting has not yet been determined, it is possible that the loss of GSK3 β phosphorylation immediately following injury contributes to the induction of mossy fiber sprouting while the loss of priming by CDK5 in later phases contributes to the maintenance of mossy fiber sprouting. It is of great interest that these mechanistically distinct events culminate in a similar end-point: an increase in the amount of active CRMP2 (Figure 8). The reduction in mossy fiber sprouting in (S)-LCM-treated animals suggests, at the very least, that CRMP2 may be one factor involved in initiation and progression of mossy fiber sprouting.



AUTHORS AND CONTRIBUTORS

Participated in Research Design—Sarah M. Wilson, Rajesh Khanna. Conducted Experiments—Sarah M. Wilson, Seul Ki Yeon, Xiao-Fang Yang. Performed Data Analysis—Sarah M. Wilson, Seul Ki Yeon, Ki Duk Park, Xiao-Fang Yang. Wrote the Manuscript—Sarah M. Wilson, Rajesh Khanna.

ACKNOWLEDGMENTS

We thank Dr. Weina Ju for help with some of the immunoblots, and members of the Stark Neurosciences Research Institute for helpful comments and discussions. We express many thanks to Dr. Fletcher White and Matthew Ripsch for their generous guidance in experimental design, as well as, the use of their equipment. This work was supported, in part, by a grant a National Scientist Development from the American Heart Association (SDG5280023 to Rajesh Khanna) and a grant from the Showalter foundation (to Rajesh Khanna). Sarah M. Wilson was partially funded by a Stark Fellowship and a Larry Kays Medical Neuroscience award.

REFERENCES

- Agrawal, A., Timothy, J., Pandit, L., and Manju, M. (2006). Post-traumatic epilepsy: an overview. *Clin. Neurol. Neurosurg.* 108, 433–439. doi: 10.1016/j.clineuro.2005.09.001
- Alessi, D. R., Andjelkovic, M., Caudwell, B., Cron, P., Morrice, N., Cohen, P., et al. (1996). Mechanism of activation of protein kinase B by insulin and IGF-1. *EMBO J.* 15, 6541–6551.
- Andersen, P., Bliss, T. V., Lomo, T., Olsen, L. I., and Skrede, K. K. (1969). Lamellar organization of hippocampal excitatory pathways. *Acta Physiol. Scand.* 76, 4a–5a.
- Andurkar, S. V., Stables, J. P., and Kohn, H. (1999). The anticonvulsant activities of N-benzyl 3-methoxypropionamides. *Bioorg. Med. Chem.* 7, 2381–2389. doi: 10.1016/S0968-0896(99)00186-8
- Arimura, N., Inagaki, N., Chihara, K., Menager, C., Nakamura, N., Amano, M., et al. (2000). Phosphorylation of collapsin response mediator protein-2 by Rho-kinase. Evidence for two separate signaling pathways for growth cone collapse. *J. Biol. Chem.* 275, 23973–23980. doi: 10.1074/jbc.M001032200
- Arimura, N., Menager, C., Kawano, Y., Yoshimura, T., Kawabata, S., Hattori, A., et al. (2005). Phosphorylation by Rho kinase regulates CRMP-2 activity in growth cones. *Mol. Cell Biol.* 25, 9973–9984. doi: 10.1128/MCB.25.22.9973-9984.2005
- Beyreuther, B. K., Freitag, J., Heers, C., Krebsfanger, N., Scharfenecker, U., and Stohr, T. (2007). Lacosamide: a review of preclinical properties. *CNS Drug Rev.* 13, 21–42. doi: 10.1111/j.1527-3458.2007.00001.x
- Bhave, S. V., Ghoda, L., and Hoffman, P. L. (1999). Brain-derived neurotrophic factor mediates the anti-apoptotic effect of NMDA in cerebellar granule neurons: signal transduction cascades and site of ethanol action. *J. Neurosci.* 19, 3277–3286.
- Blaabjerg, M., and Zimmer, J. (2007). The dentate mossy fibers: structural organization, development and plasticity. *Prog. Brain Res.* 163, 85–107. doi: 10.1016/S0079-6123(07)63005-2
- Brittain, J. M., Chen, L., Wilson, S. M., Brustovetsky, T., Gao, X., Ashpole, N. M., et al. (2011b). Neuroprotection against traumatic brain injury by a peptide derived from the collapsin response mediator protein 2 (CRMP2). *J. Biol. Chem.* 286, 37778–37792. doi: 10.1074/jbc.M111.255455
- Brittain, J. M., Duarte, D. B., Wilson, S. M., Zhu, W., Ballard, C., Johnson, P. L., et al. (2011a). Suppression of inflammatory and neuropathic pain by uncoupling CRMP-2 from the presynaptic Ca(2+) channel complex. *Nat. Med.* 17, 822–829. doi: 10.1038/nm.2345
- Brittain, J. M., Pan, R., You, H., Brustovetsky, T., Brustovetsky, N., Zamponi, G. W., et al. (2012a). Disruption of NMDAR-CRMP-2 signaling protects against focal cerebral ischemic damage in the rat middle cerebral artery occlusion model. *Channels (Austin)* 6, 52–59. doi: 10.4161/chan.18919
- Brittain, J. M., Piekarz, A. D., Wang, Y., Kondo, T., Cummins, T. R., and Khanna, R. (2009). An atypical role for collapsin response mediator protein 2 (CRMP-2)

- in neurotransmitter release via interaction with presynaptic voltage-gated calcium channels. *J. Biol. Chem.* 284, 31375–31390. doi: 10.1074/jbc.M109.009951
- Brittain, J. M., Wang, Y., Eruvweter, O., and Khanna, R. (2012b). Cdk5-mediated phosphorylation of CRMP-2 enhances its interaction with CaV2.2. *FEBS Lett.* 586, 3813–3818. doi: 10.1016/j.febslet.2012.09.022
- Brown, M., Jacobs, T., Eickholt, B., Ferrari, G., Teo, M., Monfries, C., et al. (2004). Alpha2-chimaerin, cyclin-dependent Kinase 5/p35, and its target collapsin response mediator protein-2 are essential components in semaphorin 3A-induced growth-cone collapse. *J. Neurosci.* 24, 8994–9004. doi: 10.1523/JNEUROSCI.3184-04.2004
- Cavazos, J. E., Golarai, G., and Sutula, T. P. (1991). Mossy fiber synaptic reorganization induced by kindling: time course of development, progression, and permanence. *J. Neurosci.* 11, 2795–2803.
- CDC, CfDCaP. (2012). “Epilepsy in adults and access to care - United States, 2010,” in *MMWR*, Vol. 61 (Washington, DC), 909–913.
- Chae, Y. C., Lee, S., Heo, K., Ha, S. H., Jung, Y., Kim, J. H., et al. (2009). Collapsin response mediator protein-2 regulates neurite formation by modulating tubulin GTPase activity. *Cell. Signal.* 21, 1818–1826. doi: 10.1016/j.cellsig.2009.07.017
- Chen, Y., Stevens, B., Chang, J., Milbrandt, J., Barres, B. A., and Hell, J. W. (2008). NS21: re-defined and modified supplement B27 for neuronal cultures. *J. Neurosci. Methods* 171, 239–247. doi: 10.1016/j.jneumeth.2008.03.013
- Cole, A. R., Causeret, F., Yadirgi, G., Hastie, C. J., McLauchlan, H., McManus, E. J., et al. (2006). Distinct priming kinases contribute to differential regulation of collapsin response mediator proteins by glycogen synthase kinase-3 *in vivo*. *J. Biol. Chem.* 281, 16591–16598. doi: 10.1074/jbc.M513344200
- Cole, A. R., Knebel, A., Morrice, N. A., Robertson, L. A., Irving, A. J., Connolly, C. N., et al. (2004). GSK-3 phosphorylation of the Alzheimer epitope within collapsin response mediator proteins regulates axon elongation in primary neurons. *J. Biol. Chem.* 279, 50176–50180. doi: 10.1074/jbc.C400412200
- Cross, D. A., Alessi, D. R., Cohen, P., Andjelkovich, M., and Hemmings, B. A. (1995). Inhibition of glycogen synthase kinase-3 by insulin mediated by protein kinase B. *Nature* 378, 785–789. doi: 10.1038/378785a0
- Dash, P. K., Johnson, D., Clark, J., Orsi, S. A., Zhang, M., Zhao, J., et al. (2011). Involvement of the glycogen synthase kinase-3 signaling pathway in TBI pathology and neurocognitive outcome. *PLoS ONE* 6:e24648. doi: 10.1371/journal.pone.0024648
- de Lanerolle, N. C., Kim, J. H., Williamson, A., Spencer, S. S., Zaveri, H. P., Eid, T., et al. (2003). A retrospective analysis of hippocampal pathology in human temporal lobe epilepsy: evidence for distinctive patient subcategories. *Epilepsia* 44, 677–687. doi: 10.1046/j.1528-1157.2003.32701.x
- DePaoli-Roach, A. A. (1984). Synergistic phosphorylation and activation of ATP-Mg-dependent phosphoprotein phosphatase by F A/GSK-3 and casein kinase II (PC0.7). *J. Biol. Chem.* 259, 12144–12152.
- Dustrude, E. T., Wilson, S. M., Ju, W., Xiao, Y., and Khanna, R. (2013). CRMP2 protein SUMOylation modulates Nav1.7 channel trafficking. *J. Biol. Chem.* 288, 24316–24331. doi: 10.1074/jbc.M113.474924
- Endo, H., Nito, C., Kamada, H., Nishi, T., and Chan, P. H. (2006). Activation of the Akt/GSK3[beta] signaling pathway mediates survival of vulnerable hippocampal neurons after transient global cerebral ischemia in rats. *J. Cereb. Blood Flow Metab.* 26, 1479–1489. doi: 10.1038/sj.jcbfm.9600303
- Englund, M. J., Liverman, C. T., Schultz, A. M., and Strawbridge, L. M. (2012). Epilepsy across the spectrum: promoting health and understanding. A summary of the institute of medicine report. *Epilepsy Behav.* 25, 266–276. doi: 10.1016/j.yebeh.2012.06.016
- Errington, A. C., Stohr, T., Heers, C., and Lees, G. (2008). The investigational anticonvulsant lacosamide selectively enhances slow inactivation of voltage-gated sodium channels. *Mol. Pharmacol.* 73, 157–169. doi: 10.1124/mol.107.039867
- Fiol, C. J., Haseman, J. H., Wang, Y. H., Roach, P. J., Roeske, R. W., Kowalczyk, M., et al. (1988). Phosphoserine as a recognition determinant for glycogen synthase kinase-3: phosphorylation of a synthetic peptide based on the G-component of protein phosphatase-1. *Arch. Biochem. Biophys.* 267, 797–802. doi: 10.1016/0003-9861(88)90089-6
- Fukata, Y., Itoh, T. J., Kimura, T., Menager, C., Nishimura, T., Shiromizu, T., et al. (2002). CRMP-2 binds to tubulin heterodimers to promote microtubule assembly. *Nat. Cell Biol.* 4, 583–591. doi: 10.1038/ncb825
- Ghasemi, M., and Schachter, S. C. (2011). The NMDA receptor complex as a therapeutic target in epilepsy: a review. *Epilepsy Behav.* 22, 617–640. doi: 10.1016/j.yebeh.2011.07.024
- Goddard, G. V., McIntyre, D. C., and Leech, C. K. (1969). A permanent change in brain function resulting from daily electrical stimulation. *Exp. Neurol.* 25, 295–330. doi: 10.1016/0014-4886(69)90128-9
- Goshima, Y., Nakamura, F., Strittmatter, P., and Strittmatter, S. M. (1995). Collapsin-induced growth cone collapse mediated by an intracellular protein related to UNC-33. *Nature* 376, 509–514. doi: 10.1038/376509a0
- Goslin, K., and Banker, G. (1989). Experimental observations on the development of polarity by hippocampal neurons in culture. *J. Cell Biol.* 108, 1507–1516. doi: 10.1083/jcb.108.4.1507
- Grady, M. S., Charleston, J. S., Maris, D., Witgen, B. M., and Lifshitz, J. (2003). Neuronal and glial cell number in the hippocampus after experimental traumatic brain injury: analysis by stereological estimation. *J. Neurotrauma* 20, 929–941. doi: 10.1089/089771503770195786
- Hauser, W. A., and Kurland, L. T. (1975). The epidemiology of epilepsy in Rochester, Minnesota, 1935 through 1967. *Epilepsia* 16, 1–66. doi: 10.1111/j.1528-1157.1975.tb04721.x
- Hirtz, D., Thurman, D. J., Gwinn-Hardy, K., Mohamed, M., Chaudhuri, A. R., and Zalutsky, R. (2007). How common are the “common” neurologic disorders? *Neurology* 68, 326–337. doi: 10.1212/01.wnl.0000252807.38124.a3
- Hou, S. T., Jiang, S. X., Aylsworth, A., Ferguson, G., Slinn, J., Hu, H., et al. (2009). CaMKII phosphorylates collapsin response mediator protein 2 and modulates axonal damage during glutamate excitotoxicity. *J. Neurochem.* 111, 870–881. doi: 10.1111/j.1471-4159.2009.06375.x
- Ju, W., Li, Q., Wilson, S. M., Brittain, J. M., Meroueh, L., and Khanna, R. (2013). SUMOylation alters CRMP2 regulation of calcium influx in sensory neurons. *Channels* 7, 153–159. doi: 10.4161/chan.24224
- Kharatishvili, I., and Pitkanen, A. (2010). Posttraumatic epilepsy. *Curr. Opin. Neurol.* 23, 183–188. doi: 10.1097/WCO.0b013e32833749e4
- Kimura, T., Watanabe, H., Iwamatsu, A., and Kaibuchi, K. (2005). Tubulin and CRMP-2 complex is transported via Kinesin-1. *J. Neurochem.* 93, 1371–1382. doi: 10.1111/j.1471-4159.2005.03063.x
- Koyama, R., and Ikegaya, Y. (2004). Mossy fiber sprouting as a potential therapeutic target for epilepsy. *Curr. Neurovasc. Res.* 1, 3–10. doi: 10.2174/1567202043480242
- Larner, A. J. (1995). Axonal sprouting and synaptogenesis in temporal lobe epilepsy: possible pathogenetic and therapeutic roles of neurite growth inhibitory factors. *Seizure* 4, 249–258. doi: 10.1016/S1059-1311(95)80001-8
- Lee, C.-Y., Jaw, T., Tseng, H.-C., Chen, I. C., and Liou, H.-H. (2012). Lovastatin modulates glycogen synthase kinase-3 β pathway and inhibits mossy fiber sprouting after pilocarpine-induced status epilepticus. *PLoS ONE* 7:e38789. doi: 10.1371/journal.pone.0038789
- Lees, G., Stohr, T., and Errington, A. C. (2006). Stereoselective effects of the novel anticonvulsant lacosamide against 4-AP induced epileptiform activity in rat visual cortex *in vitro*. *Neuropharmacology* 50, 98–110. doi: 10.1016/j.neuropharm.2005.08.016
- LeTiran, A., Stables, J. P., and Kohn, H. (2001). Functionalized amino acid anticonvulsants: synthesis and pharmacological evaluation of conformationally restricted analogues. *Bioorg. Med. Chem.* 9, 2693–2708. doi: 10.1016/S0968-0896(01)00204-8
- Licko, T., Seeger, N., Zellinger, C., Russmann, V., Matagne, A., and Potschka, H. (2013). Lacosamide treatment following status epilepticus attenuates neuronal cell loss and alterations in hippocampal neurogenesis in a rat electrical status epilepticus model. *Epilepsia* 54, 1176–1185. doi: 10.1111/epi.12196
- Lowenstein, D. H., Thomas, M. J., Smith, D. H., and McIntosh, T. K. (1992). Selective vulnerability of dentate hilar neurons following traumatic brain injury: a potential mechanistic link between head trauma and disorders of the hippocampus. *J. Neurosci.* 12, 4846–4853.
- Manford, M., Hart, Y. M., Sander, J. W., and Shorvon, S. D. (1992a). National General Practice Study of Epilepsy (NGPSE): partial seizure patterns in a general population. *Neurology* 42, 1911–1917. doi: 10.1212/WNL.42.10.1911
- Manford, M., Hart, Y. M., Sander, J. W., and Shorvon, S. D. (1992b). The national general practice study of epilepsy. the syndromic classification of the international league against epilepsy applied to epilepsy in a general population. *Arch. Neurol.* 49, 801–808. doi: 10.1001/archneur.1992.00530320025008
- O'Dell, C. M., Das, A., Wallace, G. T., Ray, S. K., and Banik, N. L. (2012). Understanding the basic mechanisms underlying seizures in mesial temporal lobe epilepsy and possible therapeutic targets: a review. *J. Neurosci. Res.* 90, 913–924. doi: 10.1002/jnr.22829

- Oliva, M., Berkovic, S. F., and Petrou, S. (2012). Sodium channels and the neurobiology of epilepsy. *Epilepsia* 53, 1849–1859. doi: 10.1111/j.1528-1167.2012.03631.x
- Panayiotopoulos, C. P. (2005). *The Epilepsies: Seizures, Syndromes and Management*. Oxfordshire: Bladon Medical Publishing, an imprint of Springer Science+Business Media.
- Park, K. D., Morieux, P., Salome, C., Cotten, S. W., Reamton, O., Eysers, C., et al. (2009). Lacosamide isothiocyanate-based agents: novel agents to target and identify lacosamide receptors. *J. Med. Chem.* 52, 6897–6911. doi: 10.1021/jm9012054
- Pitkanen, A., Immonen, R., Nodde-Ekane, X., Grohn, O., Stohr, T., and Nissinen, J. (2014). Effect of lacosamide on structural damage and functional recovery after traumatic brain injury in rats. *Epilepsy Res.* 108, 653–665. doi: 10.1016/j.eplepsyres.2014.02.001
- Pitkänen, A., and Lukasiuk, K. (2009). Molecular and cellular basis of epileptogenesis in symptomatic epilepsy. *Epilepsy Behav.* 14(1 Suppl. 1), 16–25. doi: 10.1016/j.yebeh.2008.09.023
- Sasaki, C., Hayashi, T., Zhang, W. R., Warita, H., Manabe, Y., Sakai, K., et al. (2011). Different expression of glycogen synthase kinase-3 β between young and old rat brains after transient middle cerebral artery occlusion. *Neurol. Res.* 23, 588–592. doi: 10.1179/016164101101199054
- Shapira, M., Licht, A., Milman, A., Pick, C. G., Shohami, E., and Eldar-Finkelman, H. (2007). Role of glycogen synthase kinase-3 β in early depressive behavior induced by mild traumatic brain injury. *Mol. Cell. Neurosci.* 34, 571–577. doi: 10.1016/j.mcn.2006.12.006
- Sharma, A. K., Reams, R. Y., Jordan, W. H., Miller, M. A., Thacker, H. L., and Snyder, P. W. (2007). Mesial temporal lobe epilepsy: pathogenesis, induced rodent models and lesions. *Toxicol. Pathol.* 35, 984–999. doi: 10.1080/01926230701748305
- Siwek, M., Henseler, C., Broich, K., Papazoglou, A., and Weiergraber, M. (2012). Voltage-gated Ca(2+) channel mediated Ca(2+) influx in epileptogenesis. *Adv. Exp. Med. Biol.* 740, 1219–1247. doi: 10.1007/978-94-007-2888-2_55
- Sutula, T. P. (2004). Mechanisms of epilepsy progression: current theories and perspectives from neuroplasticity in adulthood and development. *Epilepsy Res.* 60, 161–171. doi: 10.1016/j.eplepsyres.2004.07.001
- Timm, F. (1958). Zur Histochemie der Schwermetalle Das Sulfid-Silberverfahren. *Dtsch. Z. Ges. Gerichtl. Med.* 46, 706–711.
- Uchida, Y., Ohshima, T., Sasaki, Y., Suzuki, H., Yanai, S., Yamashita, N., et al. (2005). Semaphorin3A signalling is mediated via sequential Cdk5 and GSK3 β phosphorylation of CRMP2: implication of common phosphorylating mechanism underlying axon guidance and Alzheimer's disease. *Genes Cells* 10, 165–179. doi: 10.1111/j.1365-2443.2005.00827.x
- Uchida, Y., Ohshima, T., Yamashita, N., Ogawara, M., Sasaki, Y., Nakamura, F., et al. (2009). Semaphorin3A signaling mediated by Fyn-dependent tyrosine phosphorylation of collapsin response mediator protein 2 at tyrosine 32. *J. Biol. Chem.* 284, 27393–27401. doi: 10.1074/jbc.M109.000240
- Wang, Y., Brittain, J. M., Jarecki, B. W., Park, K. D., Wilson, S. M., Wang, B., et al. (2010). *In silico* docking and electrophysiological characterization of lacosamide binding sites on collapsin response mediator protein 2 (CRMP-2) identifies a pocket important in modulating sodium channel slow inactivation. *J. Biol. Chem.* 285, 25296–25307. doi: 10.1074/jbc.M110.128801
- Wang, Y., and Khanna, R. (2011). Voltage-gated calcium channels are not affected by the novel anti-epileptic drug lacosamide. *Transl. Neurosci.* 2, 13–22. doi: 10.2478/s13380-011-0002-9
- Wilson, S. M., Schmutzler, B. S., Brittain, J. M., Dustrude, E. T., Ripsch, M. S., Pellman, J. J., et al. (2012a). Inhibition of transmitter release and attenuation of aids therapy-induced and tibial nerve injury-related painful peripheral neuropathy by novel synthetic Ca²⁺ channel peptides. *J. Biol. Chem.* 287, 35065–35077. doi: 10.1074/jbc.M112.378695
- Wilson, S. M., Xiong, W., Wang, Y., Ping, X., Head, J. D., Brittain, J. M., et al. (2012b). Prevention of posttraumatic axon sprouting by blocking collapsin response mediator protein 2-mediated neurite outgrowth and tubulin polymerization. *Neuroscience* 210, 451–466. doi: 10.1016/j.neuroscience.2012.02.038
- Xiong, T., Tang, J., Zhao, J., Chen, H., Zhao, F., Li, J., et al. (2012). Involvement of the Akt/GSK-3 β /CRMP-2 pathway in axonal injury after hypoxic-ischemic brain damage in neonatal rat. *Neuroscience* 216, 123–132. doi: 10.1016/j.neuroscience.2012.04.052
- Yang, L., Afroz, S., Michelson, H. B., Goodman, J. H., Valsamis, H. A., and Ling, D. S. (2010b). Spontaneous epileptiform activity in rat neocortex after controlled cortical impact injury. *J. Neurotrauma* 27, 1541–1548. doi: 10.1089/neu.2009.1244
- Yang, T., Zhou, D., and Stefan, H. (2010a). Why mesial temporal lobe epilepsy with hippocampal sclerosis is progressive: uncontrolled inflammation drives disease progression? *J. Neurol. Sci.* 296, 1–6. doi: 10.1016/j.jns.2010.06.002
- Yoshimura, T., Kawano, Y., Arimura, N., Kawabata, S., Kikuchi, A., and Kaibuchi, K. (2005). GSK-3 β Regulates Phosphorylation of CRMP-2 and Neuronal Polarity. *Cell* 120, 137–149. doi: 10.1016/j.cell.2004.11.012
- Zhang, X., Chen, Y., Ikonomic, M. D., Nathaniel, P. D., Kochanek, P. M., Marion, D. W., et al. (2006). Increased phosphorylation of protein kinase B and related substrates after traumatic brain injury in humans and rats. *J. Cereb. Blood Flow Metab.* 26, 915–926. doi: 10.1038/sj.jcbfm.9600238
- Zhao, S., Fu, J., Liu, X., Wang, T., Zhang, J., and Zhao, Y. (2012). Activation of Akt/GSK-3 β /beta-catenin signaling pathway is involved in survival of neurons after traumatic brain injury in rats. *Neurol. Res.* 34, 400–407. doi: 10.1179/1743132812Y.0000000025
- Zimmer, J. (1973). Changes in the Timm sulfide silver staining pattern of the rat hippocampus and fascia dentata following early postnatal deafferentation. *Brain Res.* 64, 313–326. doi: 10.1016/0006-8993(73)90186-8

Conflict of Interest Statement: The authors declare that the research was conducted in the absence of any commercial or financial relationships that could be construed as a potential conflict of interest.

Received: 05 March 2014; accepted: 29 April 2014; published online: 28 May 2014.

Citation: Wilson SM, Ki Yeon S, Yang X-F, Park KD and Khanna R (2014) Differential regulation of collapsin response mediator protein 2 (CRMP2) phosphorylation by GSK3 β and CDK5 following traumatic brain injury. *Front. Cell. Neurosci.* 8:135. doi: 10.3389/fncel.2014.00135

This article was submitted to the journal *Frontiers in Cellular Neuroscience*.

Copyright © 2014 Wilson, Ki Yeon, Yang, Park and Khanna. This is an open-access article distributed under the terms of the Creative Commons Attribution License (CC BY). The use, distribution or reproduction in other forums is permitted, provided the original author(s) or licensor are credited and that the original publication in this journal is cited, in accordance with accepted academic practice. No use, distribution or reproduction is permitted which does not comply with these terms.



The functionalized amino acid (S)-Lacosamide subverts CRMP2-mediated tubulin polymerization to prevent constitutive and activity-dependent increase in neurite outgrowth

Sarah M. Wilson¹, Aubin Moutal², Ohannes K. Melemedjian², Yuying Wang², Weina Ju^{1,3}, Liberty François-Moutal², May Khanna² and Rajesh Khanna^{1,2,4*}

¹ Paul and Carole Stark Neurosciences Research Institute, Indiana University School of Medicine, Indianapolis, IN, USA

² Department of Pharmacology, College of Medicine, University of Arizona, Tucson, AZ, USA

³ Department of Neurology, The First Hospital of Jilin University, and Jilin University, Jilin, China

⁴ Neuroscience Graduate Interdisciplinary Program, College of Medicine, University of Arizona, Tucson, AZ, USA

Edited by:

Christophe Altier, University of
Calgary, Canada

Reviewed by:

Stephanie Michelle Willerth,
University of Victoria, Canada
Jill Marie Weimer, Sanford
Research, USA

*Correspondence:

Rajesh Khanna, Department of
Pharmacology, College of Medicine,
University of Arizona, 1501 North
Campbell Drive, PO Box 245050,
Tucson, AZ 85724, USA
e-mail: rkhanha@email.arizona.edu

Activity-dependent neurite outgrowth is a highly complex, regulated process with important implications for neuronal circuit remodeling in development as well as in seizure-induced sprouting in epilepsy. Recent work has linked outgrowth to collapsin response mediator protein 2 (CRMP2), an intracellular phosphoprotein originally identified as axon guidance and growth cone collapse protein. The neurite outgrowth promoting function of CRMP2 is regulated by its phosphorylation state. In this study, depolarization (potassium chloride)-driven activity increased the level of active CRMP2 by decreasing its phosphorylation by GSK3 β via a reduction in priming by Cdk5. To determine the contribution of CRMP2 in activity-driven neurite outgrowth, we screened a limited set of compounds for their ability to reduce neurite outgrowth but not modify voltage-gated sodium channel (VGSC) biophysical properties. This led to the identification of (S)-lacosamide ((S)-LCM), a stereoisomer of the clinically used antiepileptic drug (R)-LCM (Vimpat[®]), as a novel tool for preferentially targeting CRMP2-mediated neurite outgrowth. Whereas (S)-LCM was ineffective in targeting VGSCs, the presumptive pharmacological targets of (R)-LCM, (S)-LCM was more efficient than (R)-LCM in subverting neurite outgrowth. Biomolecular interaction analyses revealed that (S)-LCM bound to wildtype CRMP2 with low micromolar affinity, similar to (R)-LCM. Through the use of this novel tool, the activity-dependent increase in neurite outgrowth observed following depolarization was characterized to be reliant on CRMP2 function. Knockdown of CRMP2 by siRNA in cortical neurons resulted in reduced CRMP2-dependent neurite outgrowth; incubation with (S)-LCM phenocopied this effect. Other CRMP2-mediated processes were unaffected. (S)-LCM subverted neurite outgrowth not by affecting the canonical CRMP2-tubulin association but rather by impairing the ability of CRMP2 to promote tubulin polymerization, events that are perfunctory for neurite outgrowth. Taken together, these results suggest that changes in the phosphorylation state of CRMP2 are a major contributing factor in activity-dependent regulation of neurite outgrowth.

Keywords: CRMP2, activity-dependent, neurite outgrowth, (S)-Lacosamide, GSK3 β , Cdk5

INTRODUCTION

Neurite outgrowth is a highly regulated, progressive process, responding to a myriad of intrinsic as well as external cues, such

as network activity. Activity-dependent outgrowth has long been attributed to focal changes in intracellular calcium concentration (Cohan and Kater, 1986; Connor, 1986; Fields et al., 1990; Schilling et al., 1991). The growth promoting aspect of activity is constrained within a small range of calcium concentrations, outside of which retraction and growth cone collapse can occur, suggesting the process is tightly regulated (Cohan and Kater, 1986; Kater et al., 1988; van Pelt et al., 1996). Such regulation allows for a reciprocal relationship between outgrowth and network connectivity (Van Ooyen et al., 1995). A better understanding of

Abbreviations: CRMP2, collapsin response mediator protein 2; DIV, days *in vitro*; E19, embryonic day 19; ELISA, enzyme-linked immunosorbent assay; EGFP, green fluorescent protein; LCM, lacosamide; VGSC, voltage-gated sodium channel; GSK3 β , glycogen synthase kinase 3 β ; Cdk5, cyclin-dependent kinase 5; cAMP, cyclic adenosine monophosphate; RhoK, Rho kinase; CaMKII, calcium/calmodulin dependent protein kinase II; PP1/2A, protein phosphatase 1/2A; MST, microscale thermophoresis.

activity-dependent changes in synaptic organization may provide essential insight into pathological processes involving abnormally high levels of neuronal activity, such as epilepsy.

Mechanistic studies have suggested that the rise in intracellular calcium necessary to promote growth may be attributed to calcium influx through N-methyl-D-aspartate receptors, L-type voltage-gated calcium channels, or both (Kocsis et al., 1994; Wayman et al., 2006). Regardless of the initial route of calcium entry, preventing its secondary mobilization from intracellular stores abolishes the growth promoting effects of depolarization-induced activity (Kocsis et al., 1994). Other than strict calcium dependence, the specific mechanisms underlying activity-dependent outgrowth are relatively unknown. Second messenger systems, especially those responsive to changes in intracellular calcium such as cAMP, have been suggested to play a role (Mattson et al., 1988). Additionally, inhibitors of transcription have also been used to suggest that transcription—most likely of growth promoting genes—may be an important step linking activity to cytoskeletal dynamics (Solem et al., 1995). Further studies also suggest the importance of kinase cascades (Solem et al., 1995; Wayman et al., 2006). Recently, activity-induced outgrowth in cerebellar granule cells was attributed to changes in the kinase GSK3 β and its substrate, collapsin response mediator protein 2 (CRMP2) (Tan et al., 2013). CRMP2 is an intracellular phosphoprotein originally identified for coordinating axon guidance and growth cone collapse (Goshima et al., 1995). More recently, numerous other functions for CRMP2 have been identified, implicating CRMP2 in a variety of neuropathologies (for review see Hensley et al., 2011; Khanna et al., 2012).

Of particular importance to our investigations is the ability of CRMP2 to mediate neurite outgrowth via transport and stabilization of tubulin dimers (Fukata et al., 2002) as well as enhancement of tubulin's intrinsic GTPase activity (Chae et al., 2009). In regards to its outgrowth-promoting function, the activity of CRMP2 is regulated by its phosphorylation state. In the unphosphorylated state CRMP2 is considered active and thereby growth-promoting, however, upon phosphorylation by glycogen synthase kinase 3 β (GSK3 β), cyclin dependent kinase 5 (Cdk5), Rho kinase (RhoK), Ca²⁺/calmodulin-dependent protein kinase II (CaMKII), or Fyn kinases, CRMP2 is rendered inactive (Arimura et al., 2000, 2005; Brown et al., 2004; Cole et al., 2004, 2006; Uchida et al., 2005, 2009; Yoshimura et al., 2005; Hou et al., 2009). Along those same lines, dephosphorylation by the protein phosphatases PP2A and PP1 promotes neurite outgrowth (Zhu et al., 2010; Astle et al., 2011). Elegant studies by the Ohshima and Goshima groups suggest that changes in the phosphorylation state of CRMP2 may allow for dynamic regulation of outgrowth and branching patterns, as phosphorylation by Cdk5 is necessary for proper bifurcation of CA1 apical dendrites as well as organization of dendritic fields (Yamashita et al., 2012; Niisato et al., 2013). In fact, the ability of CRMP2 to coordinate axon guidance/growth cone collapse by Sema3A relies on phosphorylation (Arimura et al., 2005; Uchida et al., 2005, 2009). However, very little is known about the regulation of CRMP2 phosphorylation following neuronal activity. As post-translational modifications serve to regulate numerous processes throughout the

nervous system, including those that are activity-dependent, here we tested the hypothesis that changes in CRMP2 phosphorylation may account for the changes in neurite outgrowth observed following neuronal activity.

In this study we demonstrate that neuronal activity induced by KCl depolarization in cortical neurons led to decreased GSK3 β phosphorylation (residues T509/T514) of CRMP2, which was attributed to reduced priming by Cdk5 (residue S522 of CRMP2). The loss of phosphorylation directly translated into an increase in the amount of CRMP2/tubulin binding, concomitant with an increase in neurite outgrowth. Through the use of a novel small molecule identified herein, we were able to demonstrate an inhibition in CRMP2-facilitated tubulin polymerization without a change in CRMP2-tubulin binding. Consequently, it was determined that activity-driven neurite outgrowth was prevented through inhibition of CRMP2-mediated neurite outgrowth.

MATERIALS AND METHODS

MATERIALS

All reagents were purchased from Sigma (St. Louis, MO, USA) unless otherwise indicated. (S)-LCM, a functionalized amino acid, and some of its derivatives were provided by the laboratory of Dr. Harold Kohn, University of North Carolina, Chapel Hill. A 100 mM solution was made up in dimethylsulfoxide (DMSO) and stored in small aliquots at -20°C . Microscale thermophoresis (MST) labeling solutions and binding buffers were purchased from Nanotemper (München, Germany).

PRIMARY CORTICAL NEURON CULTURE

Primary cortical neurons were prepared from embryonic day 18–19 Sprague–Dawley rats as described (Brittain et al., 2009, 2011a; Wang et al., 2010a) with some modifications. Briefly, cortices were dissected and cell suspensions were plated onto poly-D Lysine-coated glass coverslips. 5-fluor-2'-deoxyuridine (1.5 $\mu\text{g}/\text{mL}$) was added 48 h after plating to reduce the number of non-neuronal cells. The cultures contain $\sim 95\%$ neurons (both excitatory and inhibitory) with the remaining 5% comprised mostly of astrocytes and the occasional microglia. All procedures were in compliance with Institutional Animal Care and Use Committees of the Indiana University School of Medicine and the College of Medicine at the University of Arizona as well as with ARRIVE guidelines.

IMMUNOBLOT ANALYSIS

Lysates were made from cultured cortical neurons at 6 DIV in RIPA buffer containing protease and phosphatase inhibitor cocktails as previously described (Brittain et al., 2009). Samples were boiled in Laemmli sample buffer and separated by electrophoresis on SDS-polyacrylamide gels. Proteins were transferred to polyvinylidene difluoride membranes and blocked at room temperature for 1 h and incubated in primary antibodies CRMP2 (Cat# C2993, Sigma, St. Louis, MO), CRMP2 pThr509/Thr514 (Cat# PB-043, Kinasource, Dundee, Scotland, UK), CRMP2 pSer522 (Cat# CP2191, ECM Biosciences, Versailles, KY), GSK3 β pSer9 (Cat# 5558, Cell Signaling, Danvers, MA), Cdk5 (Cat# 2506, Cell Signaling, Danvers, MA), p35 (Cat# 2680, Cell Signaling, Danvers, MA), GSK3 β (Cat# 9832, Cell Signaling,

Danvers, MA), or Tubulin (Cat# G712A, Promega, Madison, WI) overnight at 4°C. Following incubation in horseradish peroxidase conjugated secondary antibodies, blots were probed with enhanced chemiluminescence Western blotting substrate (Thermo Scientific, Waltham, MA) before exposure to photographic film. Films were scanned, digitized, and quantified using Un-Scan-It gel version 6.1 scanning software (Silk Scientific Inc, Orem, UT).

NEURITE OUTGROWTH IMAGING AND ANALYSIS

Primary cortical neurons were transfected via lipofectamine 2000 (Invitrogen) with enhanced green fluorescent protein (EGFP) at 4 DIV and incubated 24 h in 300 μ M (R)-LCM, LCM derivatives, or vehicle before imaging with ImageXpress Micro (Molecular Devices, Sunnyvale, CA). The overexpression of EGFP allowed for visualization of a small percentage of neurons while maintaining optimal cell densities required for survival. To compare the effects of (S)-LCM and CRMP2siRNA primary cortical neurons were transfected via lipofectamine 2000 with EGFP, control siRNA + EGFP, or CRMP2-siRNA + EGFP at 4 DIV and incubated with 200 μ M (S)-LCM for 24 h before imaging with ImageXpress Micro. Analysis of neurite outgrowth was completed using a neurite outgrowth analysis protocol with the MetaXpress software (Molecular Devices, Sunnyvale, CA). Non-neuronal cells were easily identifiable and excluded based on morphology. Neuronal cell soma and processes are detected by defining separate size and fluorescence intensity threshold parameters. Maximum width and minimum area parameters for determining somas were set to 50 and 300 μ m², respectively. For identifying processes, maximum width and minimum length parameters were set to 8 and 3 μ m, respectively. Cells were excluded if they were determined not to be neurons based on morphology, if processes extended beyond the image field, or if no processes were longer than 50 μ m. The following parameters are recorded and summarized into a final “total outgrowth” parameter: number of processes, number of branches, mean process length, and maximum process length.

PURIFICATION OF RECOMBINANT CRMP2 AND CRMP2_{5ALA} PROTEINS

A CRMP2-GST construct containing 5 amino acids in predicted LCM-binding regions of CRMP2 mutated to alanine (CRMP2_{5ALA}-GST; G360, S363, K418, I420, and P443) was generated by subcloning the mutation containing portion of CRMP2_{5ALA}-EGFP into wild-type CRMP2-GST (using restriction enzymes *RsrII* and *BglII*). Both wild-type and mutant recombinant proteins were purified exactly as described (Brittain et al., 2009; Wang et al., 2010b).

MICROSCALE THERMOPHORESIS (MST) BINDING ANALYSIS

MST, the directed movement of molecules in optically generated microscopic temperature gradients, permits an immobilization-free fluorescence methodology for the analysis of biomolecular interaction (Wienken et al., 2010; van den Bogaart et al., 2012). The thermophoretic movement is determined by the entropy of the hydration shell around the labeled molecule. The solvation entropy and the hydration shell of the macromolecules provide the driving force for the flow, and any change of the

hydration shell of biomolecules due to changes in their primary, secondary, tertiary and/or quaternary structure affects their thermophoretic mobility and can be used to determine binding affinities and enzymatic activities with high accuracy and sensitivity. A microscopic temperature gradient is generated by an infrared laser. In a typical MST-experiment the concentration of the labeled molecule is kept constant while the concentration of the unlabeled interaction partner is varied. NT647-labeled CRMP2 or CRMP2_{5ALA} (500 nM final) was incubated for 10 min at room temperature in the dark with increasing concentrations of (S)-LCM. Thermophoresis analysis was performed on a NanoTemper Monolith NT.115 instrument (25% LED; 25% IR-laser power). The MST curves were fitted with a Hill method using Origin 8.5 software to obtain apparent K_d values for binding interactions.

ELISA-BASED CRMP2-TUBULIN BINDING ASSAY

The 96-well plates (Nunc Maxisorp, Thermo Scientific) were coated with tubulin (200 ng/well, Cytoskeleton Inc.) and incubated at room temperature overnight. The following day the plates were washed and blocked with 3% BSA to minimize non-specific adsorptive binding to the plates. Escalating concentrations of CRMP2 were added to the plates. As a negative control, some wells received escalating concentrations of CRMP2 which was denatured by heating at 95°C for 5 min. The plates were incubated at room temperature with shaking for 2 h. The plates were then washed with PBS containing 0.5% Tween-20 to eliminate unbound CRMP2. The bound CRMP2 was detected by CRMP2 primary antibody (150 ng/ml, Sigma) followed by HRP-conjugated secondary antibody (GE Healthcare). Tetramethylbenzidine (R&D Systems) was used as the colorimetric substrate. The optical density of each well was determined immediately, using a microplate reader (Multiskan Ascent, Thermo) set to 450 nm with a correction wavelength of 570 nm. Data was analyzed by non-linear regression analysis using GraphPad Prism5 (Graph Pad, San Diego, CA).

To determine the effect of (S)-LCM on CRMP2-tubulin binding, 96-well plates were coated with tubulin and incubated overnight. The following day the plates were washed and blocked with 3% BSA to minimize non-specific adsorptive binding to the plate. After the wash all the wells received 1 μ M of CRMP2 and none or escalating concentrations of (S)-LCM. The plates were then incubated at room temperature with shaking for 2 h. This was followed with washes to eliminate the unbound CRMP2. CRMP2 bound to the plates was detected using the method described above.

A cell lysate based ELISA was performed as described above, with some modifications. In tubulin-coated 96-well plates, lysates from cortical cells treated with vehicle, KCl, (S)-LCM, or KCl + (S)-LCM were added. Next, the plates were incubated at room temperature with shaking for 2 h. The plates were then washed to eliminate the unbound proteins. The bound CRMP2 was detected as described above. The optical density of each well was determined immediately, using a microplate reader set to 450 nm with a correction wavelength of 570 nm. The optical densities were normalized to the amount of protein in each sample. Data was analyzed as described earlier.

TURBIDIMETRIC ASSAY FOR TUBULIN POLYMERIZATION

Polymerization of tubulin was performed as previously described (Chae et al., 2009; Wilson et al., 2012a) with modifications. Polymerization was performed in 0.1 M G-PEM buffer (1 mM GTP, 80 mM PIPES, 1 mM EGTA, 1 mM MgCl_2 , pH 7.0), 1 mM Na-GTP (Sigma), and 2 mg/ml tubulin (Cytoskeleton, Inc). CRMP2 proteins (0.2 μM) as well as 3 μM of (*R*)-LCM, (*S*)-LCM or 0.01% DMSO were added to the samples and pipetted onto a 96-well plate at 4°C. Following a 30 min incubation on ice, turbidity changes were assessed at 412 nm using a Synergy™ 2 Multi-Detection Microplate Reader (BioTek Instruments, Inc., San Diego, CA) which had previously been pre-warmed to 37°C. Absorbances were measured over time and compared to background samples which contained only buffer + GTP.

WHOLE-CELL PATCH-CLAMP RECORDINGS

Whole-cell voltage recordings were performed at room temperature on primary cultured cortical neurons using an EPC 10 Amplifier (HEKA Electronics, Germany). Electrodes were pulled from thin-walled borosilicate glass capillaries (Warner Instruments, Hamden, CT) with a P-97 electrode puller (Sutter Instrument, Novato, CA) such that the final electrode resistances were 2–3 M Ω when filled with internal solutions. The internal solution for recording Na^+ currents contained (in mM): 110 CsCl, 5 MgSO_4 , 10 EGTA, 4 ATP Na_2 , and 25 HEPES (pH 7.2, 290–310 mOsm/L). For recording Na^+ currents, the external solution contained (in mM): 100 NaCl, 10 tetraethylammonium chloride (TEA-Cl), 1 CaCl_2 , 1 CdCl_2 , 1 MgCl_2 , 10 D-glucose, 4 4-AP, 0.1 NiCl_2 , 10 HEPES (pH 7.3, 310–315 mOsm/L). Whole-cell capacitance and series resistance were compensated with the amplifier (70–80%). Cells were considered only when the seal resistance was more than 1 G Ω and the series resistance was less than 10 M Ω . Linear leak currents were digitally subtracted by P/4. Neurons were held at -100 mV, conditioned to potentials ranging from -10 to $+20$ mV (in $+10$ mV increments) for 5 s, and then fast-inactivated channels were allowed to recover for 150 ms at a hyperpolarized pulse to -120 mV, and the fraction of channels available was tested by a single depolarizing pulse, to 0 mV, for 15 ms.

KNOCKDOWN OF CRMP2 EXPRESSION BY siRNA

Validated short interfering RNAs (siRNAs) against the rat CRMP2 (5'-ACTCCTTCCTCGTGATACAT-3') sequence (Brittain et al., 2009) and controls (scrambled sequence with approximately the same GC percentage but no sequence homology) were used for CRMP2 knockdown (Invitrogen) in cortical neurons as described (Brittain et al., 2009; Chi et al., 2009; Wilson et al., 2012a). Cells were incubated for 2 days with vector- or scramble siRNA (250 nM) and extent of knockdown was assessed via immunoblot analysis. As previously reported (Chi et al., 2009; Brustovetsky et al., 2014), we observed ~90% knockdown of CRMP2 compared to scramble siRNA (data not shown).

ACTIVITY-DEPENDENT NEURITE OUTGROWTH IMAGING

For analysis of activity-dependent outgrowth, neurons were incubated in vehicle (<0.01% DMSO), 25 mM KCl, 200 μM (*S*)-LCM, or 200 μM (*S*)-LCM + 25 mM KCl for 96 h beginning at

2 DIV. Media was changed at 4 DIV, maintaining KCl levels at 25 mM, at which time neurons were also transfected with EGFP (4 DIV). EGFP-expressing cells were then imaged at 6 DIV. The use of 25 mM KCl is consistent with previous work reporting the involvement of CRMP2 in activity-dependent outgrowth (Tan et al., 2013). Analysis of neurite outgrowth was completed using a neurite outgrowth analysis protocol with the MetaXpress software (Molecular Devices, Sunnyvale, CA).

DATA ANALYSIS

All data points are shown as mean \pm s.e.m. Statistical differences between control and experimental conditions were determined by using ANOVA with a Dunnett's or Tukey's *post-hoc* test or a Student's *t*-test when comparing only two conditions. Values of $p < 0.05$ were judged to be statistically significant.

RESULTS

MODERATE ACTIVITY REDUCES CRMP2 PHOSPHORYLATION BY GSK3 β WITHOUT AFFECTING KINASE ACTIVITY

CRMP2 has recently been suggested as a potential mediator of activity-dependent neurite outgrowth in cerebellar granule neurons (Tan et al., 2013). Unlike other central neurons, cerebellar granule cells require slightly depolarizing conditions for survival *in vitro*. Therefore, it is difficult to generalize this finding to other neuronal populations within the central nervous system. As such, it is not known if CRMP2 is involved in outgrowth induced by depolarization in neurons where it is not necessary for survival. As the ability of CRMP2 to enhance neurite outgrowth is highly dependent upon its phosphorylation state (for review see Khanna et al., 2012), Western blot analysis was used to determine the level of GSK3 β -phosphorylated CRMP2 following acute (30 min) and chronic exposure to KCl (96 h) treatment (Figure 1A). The 96 h KCl treatment was chosen as it reproducibly increased neurite outgrowth. Additionally, as it was unknown how long any biochemical changes, such as phosphorylation, would be sustained, a more acute (30 min) treatment was also used. Treatment with 25 mM KCl reduced the level of GSK3 β -phosphorylated CRMP2 by ~60.8% (acute) and ~54.8% (chronic) compared to control ($p < 0.05$), while total CRMP2 expression did not change (Figures 1B–D). Therefore, exposure to KCl leads to increased levels of active, unphosphorylated CRMP2.

Similar to CRMP2, GSK3 β activity is regulated by changes in phosphorylation state, whereby phosphorylation at GSK3 β Ser9 is sufficient to inhibit its kinase function (Cross et al., 1995). To determine if the decrease in CRMP2 phosphorylation induced by KCl is due to decreased levels of GSK3 β activity, the amount of Ser9-phosphorylated GSK3 β was measured following KCl exposure. Interestingly, neither Ser9 phosphorylation nor total expression of GSK3 β was affected by KCl exposure (Figures 1E–H), suggesting that the decrease in GSK3 β -phosphorylated CRMP2 is not attributed to a change in GSK3 β expression or activity.

MODERATE ACTIVITY REDUCES CDK5 PRIMING OF CRMP2

In the case of CRMP2, substrate recognition by GSK3 β first requires phosphorylation by Cdk5 at a downstream site (Ser522), which “primes” the protein for subsequent GSK3 β

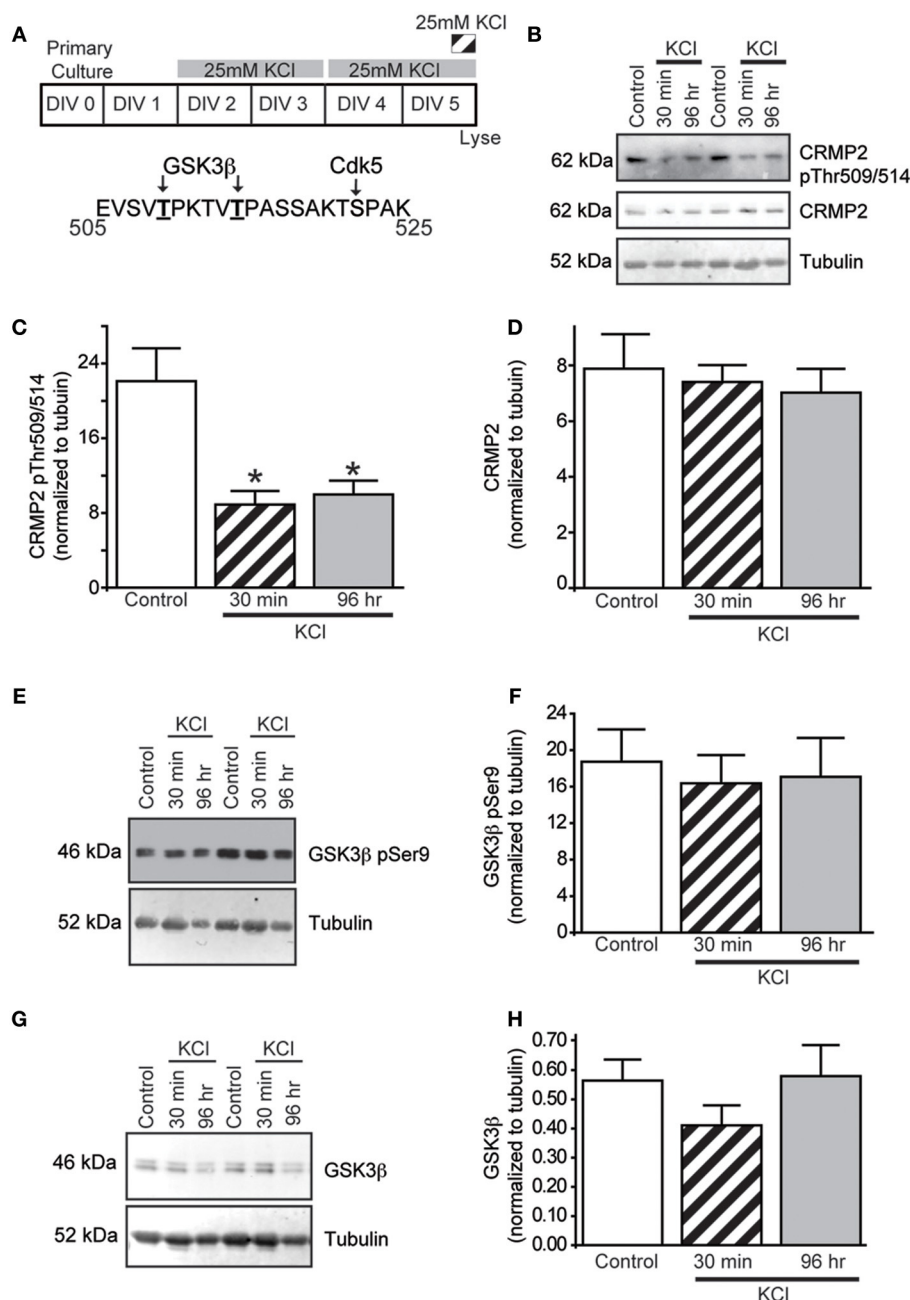
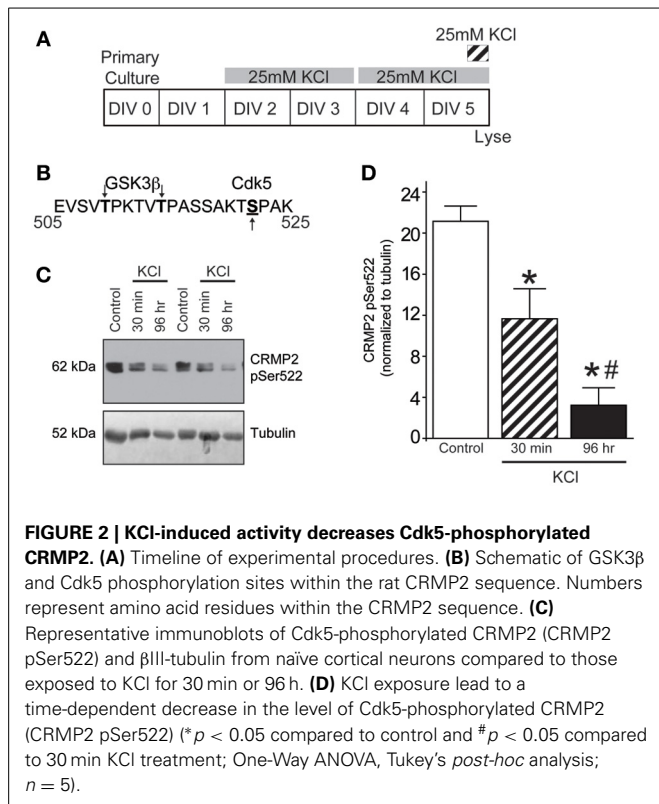


FIGURE 1 | KCl-induced activity decreases GSK3 β phosphorylation of CRMP2 without changing GSK3 β activity or expression. (A) Top: Timeline of experimental procedures. Bottom: Schematic of GSK3 β and Cdk5 phosphorylation sites within the rat CRMP2 sequence. Numbers represent amino acid residues within the CRMP2 sequence. Representative immunoblots of GSK3 β -phosphorylated CRMP2 (CRMP2 pThr509/pThr514), total CRMP2, and β III-tubulin (**B**), inactivated Ser9-phosphorylated GSK3 β and β III-tubulin (**E**), and total GSK3 β and β III-tubulin (**G**) from naïve cortical neurons

compared to those exposed to KCl for 30 min or 96 h. Summary of the relative levels of the indicated proteins (**C,D,F,H**). Expression of GSK3 β -phosphorylated CRMP2 (CRMP2 pThr509/pThr514) is decreased following 30 min or 96 h exposure to KCl (**C**) whereas total CRMP2 expression was not affected by KCl exposures (**D**) (* $p < 0.05$ compared to control; One-Way ANOVA, Tukey's *post-hoc* analysis) ($n = 4$). KCl treatment did not alter phosphorylation of GSK3 β (**F**) nor total GSK3 β expression (**H**) did not change following 30 min or 96 h KCl treatment (One-Way ANOVA, Tukey's *post-hoc* analysis) ($n = 5$).

phosphorylation (Cole et al., 2006) (see **Figure 2B**). Therefore, Western blot analysis of Cdk5-phosphorylated CRMP2 was used to determine if the KCl-induced decrease in GSK3 β phosphorylation is due to a reduction in Cdk5 priming. Both

acute and chronic exposure to KCl (**Figure 2A**) decreased the level of Cdk5-phosphorylated CRMP2 in a time dependent manner by ~44.8% (acute) and ~84.9% (chronic) compared to control ($p < 0.05$) (**Figures 2C,D**), suggesting that the



activity-dependent decrease in GSK3 β -phosphorylated CRMP2 can be attributed to decreased levels of Cdk5-primed CRMP2.

The loss of Cdk5-phosphorylated CRMP2 cannot be attributed to changes in kinase expression as levels of Cdk5 remained consistent following KCl exposure (0.0159 ± 0.0012) compared to control (0.0156 ± 0.0004) ($p > 0.05$) (Supplemental Figure 1). Aside from expression level, Cdk5 activity is primarily determined by the level of its cofactor p35 (Lee et al., 1996; Zhu et al., 2005). However, Western blot analyses reveals that expression of p35 was also not altered following KCl exposure (0.0113 ± 0.0014) compared to control (0.0110 ± 0.0009) ($p > 0.05$), suggesting the loss of Cdk5-phosphorylated CRMP2 is independent of the expression of Cdk5 or its cofactor.

IDENTIFICATION OF AN (R)-LCM DERIVATIVE FOR THE STUDY OF CRMP2-MEDIATED NEURITE OUTGROWTH

The aforementioned data suggest that chronic depolarization via KCl leads to a prolonged loss of both GSK3 β - and Cdk5-phosphorylated CRMP2. As phosphorylation at these sites is canonically known to inactivate the outgrowth-promoting function of CRMP2 (Brown et al., 2004; Cole et al., 2004, 2006; Uchida et al., 2005; Yoshimura et al., 2005), the KCl-induced loss of phosphorylation should translate to an overall increase in CRMP2 activity. However, to determine how the increase in the proportion of active CRMP2 relates to KCl-facilitated neurite outgrowth, it is necessary to preferentially target CRMP2 function. Previously, we demonstrated that the novel anti-epileptic drug (2R)-2-(acetylamino)-N-benzyl-3-methoxypropanamide [(R)-LCM, tradename Vimpat®] could directly impair the ability of CRMP2 to enhance neurite

outgrowth (Wilson et al., 2012a). (R)-LCM purportedly targets steady-state gating kinetics by selectively enhancing sodium channel slow inactivation (Zhu et al., 2005). However, its additional actions on the voltage gated sodium channel (VGSC) render it unsuitable for use as a tool in investigation of CRMP2 functions (Errington et al., 2008; Sheets et al., 2008). Therefore, derivatives of (R)-LCM that were unable to impact VGSC slow-inactivation were screened for their ability to inhibit neurite outgrowth (Table 1). Neurite outgrowth was measured from EGFP-transfected primary cultured cortical neurons using the ImageXpress Micro and MetaXpress software systems (Molecular Devices) following overnight exposure to each derivative. This analysis combines the following measurements: number of primary neurites, number of branches, mean process length, and maximum process length to determine a summary of total outgrowth per cell. The only derivative identified to impact neurite outgrowth was (S)-LCM, which reduced neurite outgrowth by ~35% compared to vehicle (<0.01% DMSO). (R)-LCM was originally determined to be stereoselective, as the (S)-isomer requires much higher concentrations to halt seizure activity *in vivo* (Andurkar et al., 1999; LeTiran et al., 2001). This data suggests that (S)-LCM may retain the ability to target CRMP2.

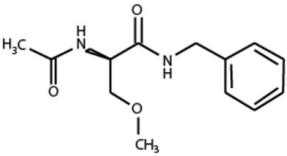
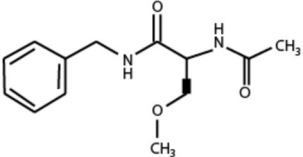
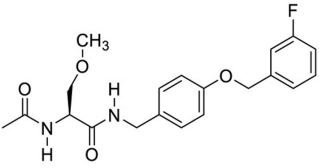
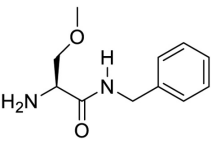
BINDING OF (S)-LCM TO WILDTYPE, BUT NOT MUTANT, CRMP2

MST was used to determine if (S)-LCM could interact with purified CRMP2. Using an infrared laser, precise microscopic temperature gradients are generated within thin glass capillaries filled with a fluorescently labeled protein sample (i.e., CRMP2), and the atomistic movement of molecules along these temperature gradients is monitored in the presence of increasing concentrations of an unlabeled binding partner (S)-LCM (Figures 3A,B). As the concentration of (S)-LCM increased, it bound to CRMP2 thermally diffusing out of the heated infrared spot, resulting in a change in the MST signal and providing a readout of the binding between the CRMP2 and (S)-LCM. NT647-labeled CRMP2 protein was incubated with varying concentrations of (S)-LCM (0.006–100 μ M) and apparent K_d values were obtained by fitting curves using the Hill method. MST experiments revealed that (S)-LCM bound to WT CRMP2 with an apparent K_d of $1.5 \pm 0.01 \mu$ M (Figures 3C,D). Importantly, K_d of (S)-LCM is similar to what is observed for (R)-LCM in this assay ($1.0 \pm 0.04 \mu$ M; Figure 3D) (Wilson and Khanna, 2014). We had previously identified 5 key residues on CRMP2, essential for coordinating (R)-LCM binding and mutated them to alanines to create CRMP2_{5ALA}, whose function mimics that of wildtype CRMP2, yet is not impaired by the presence of (R)-LCM (Wang et al., 2010b; Wilson et al., 2012a) (Figure 3E). MST experiments revealed that (S)-LCM did not interact with NT647-labeled CRMP2_{5ALA} (Figures 3F,G), suggesting that the same binding pocket is necessary for coordinating both (R)- and (S)-LCM binding.

(S)-LCM IMPAIRS THE ABILITY OF CRMP2 TO ENHANCE TUBULIN POLYMERIZATION WITHOUT ALTERING TUBULIN BINDING OR VGSC SLOW-INACTIVATION

It was previously determined that inhibition of CRMP2-mediated neurite outgrowth by (R)-LCM was mediated, not through

Table 1 | Comparison of the ability of lacosamide derivatives to affect VGSC and CRMP2 function.

Compound	Structure	Slow inactivation IC_{50} (μM) ^a	Total outgrowth (% of vehicle) ^b
(R)-LCM		85	81.6 ± 3.7*
(S)-LCM		>1000	66.2 ± 5.9*
Derivative 1		>2400	95.8 ± 4.3
Derivative 2		>1000	98.0 ± 4.5

^aSlow inactivation IC_{50} values were obtained from previous reports (Brittain et al., 2009; Sun et al., 2010).

^bTotal outgrowth represents outgrowth following a 24 h incubation in 300 μM of each compound. For ease of comparison, values were normalized to vehicle. (* $p < 0.05$ vs. vehicle) (Student's *t*-test) (values represent mean ± s.e.m.) ($n = 263$ –394 cells from 8 separate culture wells).

attenuation of tubulin binding, but by impairing the ability of CRMP2 to enhance tubulin polymerization (Wilson et al., 2012a). To ensure that (S)-LCM functions in a similar manner, an ELISA-based competition assay was used to determine the ability of CRMP2 to bind tubulin in the presence of increasing concentrations of (S)-LCM. Similar to what was previously observed for (R)-LCM, binding of CRMP2 and tubulin was not impacted by as much as 1 mM (S)-LCM (Figure 4).

Subsequently, the ability of CRMP2 to enhance tubulin polymerization in the presence of (S)-LCM was examined via turbidimetric assay. Based on the principle that light is scattered by microtubules to an extent that is proportional to the concentration of microtubule polymer, this assay determines the extent of tubulin polymerization by measuring changes in absorbance. Consistent with previous results (Wilson et al., 2012a), the addition of 200 nM recombinant CRMP2 protein dramatically enhanced tubulin polymerization by ~2.8-fold as demonstrated by area under the curve measurements compared to tubulin alone ($p < 0.05$) (Figures 5A,B). Similar to what is observed for (R)-LCM, the ability of CRMP2 to enhance tubulin polymerization was impaired by ~44.0% by as little as 3 μM (S)-LCM ($p < 0.05$) (Figure 5B). Additionally, FM4-64 labeling revealed that (S)-LCM does not impact synaptic bouton size—a phenomenon regulated by CRMP2 (Supplemental Figure 2).

To ensure that (S)-LCM is unable to alter VGSC function at concentrations well above those required for CRMP2 binding,

whole cell recordings were used to measure levels of slow inactivation (Figure 6A). Neither acute nor chronic (24 h) administration of 300 μM (S)-LCM altered the onset or extent of slow inactivation (Figures 6B,D). This concentration was chosen as it greatly surpasses those used for subsequent experiments.

(S)-LCM PHENOCOPIES THE EFFECT OF CRMP2 siRNA ON NEURITE OUTGROWTH

Having demonstrated that (S)-LCM interacts with CRMP2, we next investigated the possible effect of this interaction on CRMP2 function. If (S)-LCM acts to inhibit CRMP2-mediated neurite outgrowth, then its action should mimic the phenotype bestowed by CRMP2 siRNA without the off-target effects on other CRMP2-dependent signaling pathways. Consequently, neurite outgrowth was measured from EGFP-transfected primary cultured cortical neurons using the ImageXpress Micro and MetaXpress software systems (Molecular Devices). Consistent with previous reports (Wilson et al., 2012a), siRNA knockdown of CRMP2 led to a ~37% decrease in total outgrowth (62.6 ± 4.5) compared to control (100 ± 6.6) (see Figures 7A–G). Importantly, neurite outgrowth was not altered by control siRNA (85.1 ± 5.6) ($p > 0.05$). CRMP2 siRNA-mediated reduction in neurite outgrowth was recapitulated by overnight application of 200 μM (S)-LCM, which decreased total outgrowth by ~34% compared to control (66.2 ± 4.5) ($p < 0.05$) (Figures 7A–K). The effects of (S)-LCM and CRMP2 siRNA appeared to mutually occlude one another

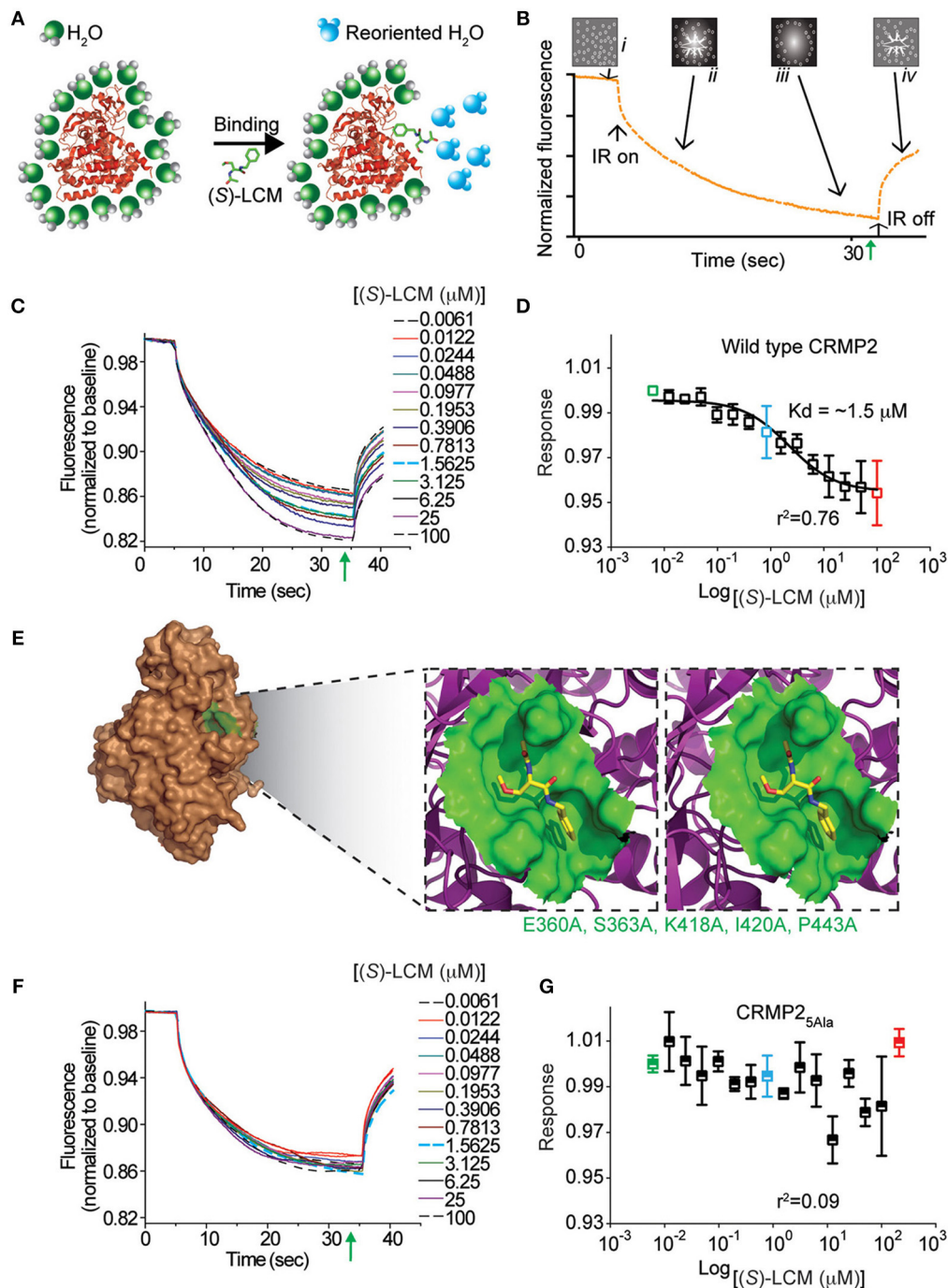


FIGURE 3 | (S)-LCM binds to wildtype CRMP2 in solution measured by microscale thermophoresis (MST). (A) Illustration of hydration shell changes after small molecule [i.e., (S)-LCM] binding to a macromolecule. The changes in the hydration shell properties are detected in the MST instrument. (B) MST assay principle. The four stages in a thermophoresis experiment: (i) initial state (all molecules are randomly distributed); (ii) infrared (IR) laser is turned on, and thermophoresis commences; (iii) steady state flow while IR laser is turned on; and (iv) equilibration to initial state by back-diffusion with IR laser turned off. The green arrow represents the steady-state time point at which the MST measurements were analyzed for the graphs shown in (D,G). (C) MST time traces of concentrations of (S)-LCM ranging from 0.006 to 100 μM . Increasing concentrations altered thermodiffusion of NT-647 labeled

CRMP2. (D) MST values were used to determine dissociation constant for binding of (S)-LCM to wildtype CRMP2, apparent $K_d = 1.5 \pm 0.01 \mu\text{M}$; the curve was fit with an r^2 value of 0.76. (E) Stereo view of the binding site for (S)-LCM within one monomer of the CRMP2 structure (Stenmark et al., 2007; Wang et al., 2010b). (S)-LCM is shown in capped-sticks representation. The amino acids mutated to alanines are indicated in green text. (F) MST time traces of concentrations of (S)-LCM ranging from 0.006 to 100 μM . MST experiments were repeated using NT-647 labeled CRMP2_{5Ala} harboring mutations in residues as indicated in (E). (G) No association could be detected between (S)-LCM and CRMP2_{5Ala}. The data could not be fitted with a curve ($r^2 = 0.09$). A representative range of data points obtained from at least 3 measurements is shown.

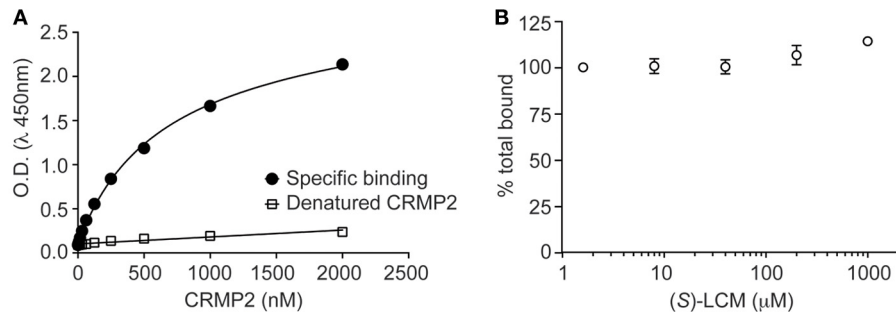


FIGURE 4 | (S)-LCM does not affect tubulin-CRMP2 binding. (A) 96-well plates coated with 200 ng tubulin were incubated with increasing concentrations of recombinant CRMP2 or heat-denatured CRMP2. The Y axis displays the OD₄₅₀ absorbance of the ELISA using CRMP2-specific antibodies. CRMP2 bound to tubulin with half-saturation concentration of ~607 nM.

Binding of heat-denatured CRMP2 demonstrated non-saturable background binding to tubulin. **(B)** Competitive binding assay revealed that (S)-LCM does not abrogate the binding of CRMP2 to tubulin. For **(A,B)**, all measurements were performed in sextuplicate and error bars indicate standard error of the mean. Most of the error bars are smaller than the symbols.

as (S)-LCM was not able to provide a further reduction following CRMP2 knockdown [(71.3 ± 3.3) vs. (62.6 ± 4.5)] ($p > 0.05$) (see **Figures 7A–G**). Total outgrowth is a composite summary of the following parameters: number of branches, number of processes, mean process length, and maximum process length (**Figures 7H–K**), all of which, aside from mean process length, were reduced by both (S)-LCM and CRMP2 siRNA, compared to both control siRNA and no treatment. Combined treatment of CRMP2 siRNA and (S)-LCM did not produce a further reduction in any parameter (data not shown).

TARGETING CRMP2 PREVENTS ACTIVITY DEPENDENT NEURITE OUTGROWTH

Previously, CRMP2 was identified to be involved in activity-dependent neurite outgrowth of cerebellar granule cells (Tan et al., 2013). Unlike other central neurons, cerebellar granule cells require slightly depolarizing conditions for survival *in vitro*. Therefore, it is difficult to generalize this finding to other neuron populations within the central nervous system. As such, it is not known if CRMP2 is involved in outgrowth induced by depolarization in neurons where it is not necessary for survival. To determine the involvement of CRMP2 in activity-driven neurite outgrowth, cortical neurons overexpressing EGFP were exposed to 25 mM KCl and maintained for 96 h to ascertain the extent of activity dependent neurite outgrowth (**Figure 8A**). Consistent with previous findings (Tan et al., 2013), chronic depolarization with 25 mM KCl led to a ~43% increase in total neurite outgrowth (143.1 ± 11.5) compared to control (100 ± 6.6) (**Figure 8B–G**). Notably, blockade of CRMP2-mediated neurite outgrowth by (S)-LCM was sufficient to prevent activity dependent growth induced by KCl (68.4 ± 3.8 vs. 61.7 ± 3.5) ($p > 0.05$). As our earlier data demonstrated that (S)-LCM is not affecting VGSC function in these neurons, these data suggest that KCl-facilitated neurite outgrowth is dependent on CRMP2.

To determine the potential mechanism underlying CRMP2's role in KCl-facilitated neurite outgrowth, we examined the ability of CRMP2 to bind tubulin following chronic exposure to KCl (**Figure 9A**). Lysates from cortical neurons that had been exposed to KCl for 96 h were incubated on tubulin-coated plates. An

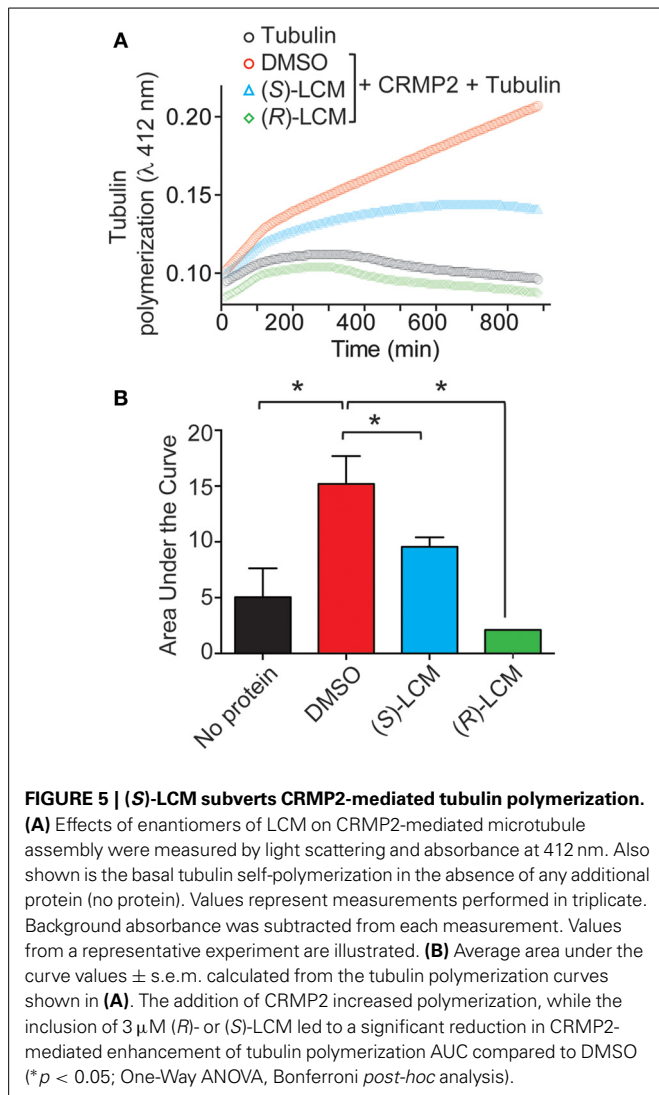
ELISA was then used to determine the amount of bound CRMP2. Consistent with the notion that a loss of phosphorylation should translate into an increase in CRMP2 activity, KCl exposure led to a ~43.5% increase in the binding of CRMP2 to tubulin compared to control ($p < 0.05$) (**Figure 9B**). As (S)-LCM was previously demonstrated to alter CRMP2 function by inhibiting its ability to enhance the intrinsic GTPase activity of tubulin, the addition of (S)-LCM did not alter the effect of KCl on CRMP2/tubulin binding [(143.5 ± 11.9) compared to KCl alone (133.5 ± 4.6)] ($p > 0.05$) (**Figure 9**).

DISCUSSION

Our findings demonstrate that KCl-facilitated neurite outgrowth in cultured cortical neurons is a CRMP2-dependent process. Specifically, neuronal activity led to changes in CRMP2 activity through regulation of its phosphorylation state (**Figure 10**). Interestingly, decreased levels of GSK3β-phosphorylated CRMP2 were observed following activity that were secondary, not to changes in GSK3β expression or activity, but rather decreased CRMP2 priming by Cdk5. CRMP2 has been suggested to be involved in many processes with potential activity-dependent components such as epilepsy, pain, and schizophrenia (Johnston-Wilson et al., 2000; Nakata et al., 2003; Czech et al., 2004; Fallin et al., 2005; Ryu et al., 2008; Brittain et al., 2011a; Wilson et al., 2012a,b). These findings may provide key insight into the importance of CRMP2 within these neuropathologies. Previous work in our lab suggested the potential anti-epileptogenic benefit of targeting CRMP2-mediated neurite outgrowth following CNS insult (Wilson et al., 2012a). The findings presented here further validate CRMP2 as a potential therapeutic target in processes involving maladaptive activity-dependent neurite outgrowth.

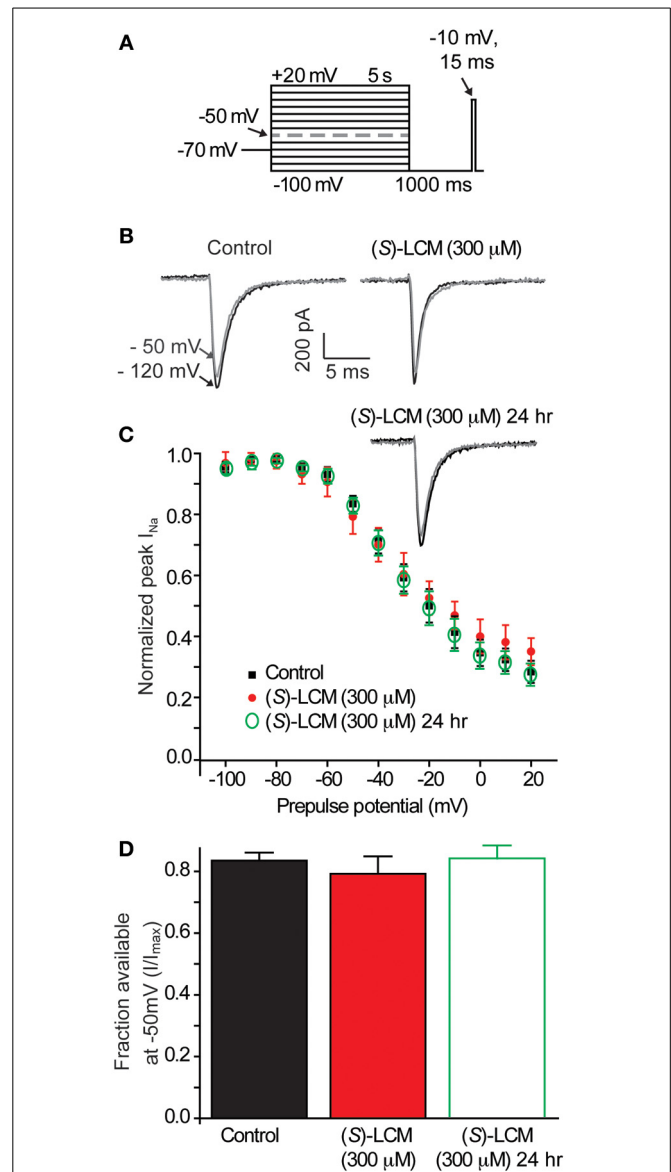
NEURONAL ACTIVITY ALTERS THE PHOSPHORYLATION STATE OF CRMP2

Previous work revealed that phosphorylation of CRMP2 by GSK3β is altered following chronic exposure to KCl in cerebellar granule cells (Tan et al., 2013). Here, we have demonstrated that chronic activity led to decreased levels of GSK3β-phosphorylated CRMP2 in primary cortical neurons as well.



GSK3 β phosphorylation of CRMP2 is potentially regulated by two distinct mechanisms: (1) changes in GSK3 β expression or activity or (2) changes in substrate recognition. Like many substrates, prior phosphorylation of CRMP2 by Cdk5 is required for subsequent phosphorylation by GSK3 β (Cole et al., 2006), providing a level of regulation independent of GSK3 β activity. Our findings suggest that loss of Cdk5 priming is responsible for the activity-driven decrease in GSK3 β -phosphorylated CRMP2. Interestingly, Cdk5 phosphorylation of CRMP2 displayed a time-dependent decrease following KCl exposure while phosphorylation by GSK3 β did not. It is possible that a ceiling effect on GSK3 β phosphorylation of CRMP2 was reached by the amount of Cdk5 phosphorylation that was decreased after only 30 min of KCl exposure. Further reduction in Cdk5 phosphorylation of CRMP2 would therefore not result in additional change in GSK3 β phosphorylation.

At this point, the mechanism underlying the change in Cdk5-phosphorylated CRMP2 is unknown. As the Cdk5 site on CRMP2 (Ser522) has been shown to be resistant to dephosphorylation (Cole et al., 2008), the involvement of protein phosphatases is



unlikely. Unfortunately, mechanisms by which the activity of Cdk5 is regulated following neuronal activity are not well understood. Work by Schuman and Murase suggests that neuronal activity driven by KCl depolarization leads to a decrease in Cdk5 activity that is cofactor independent (Schuman and Murase,

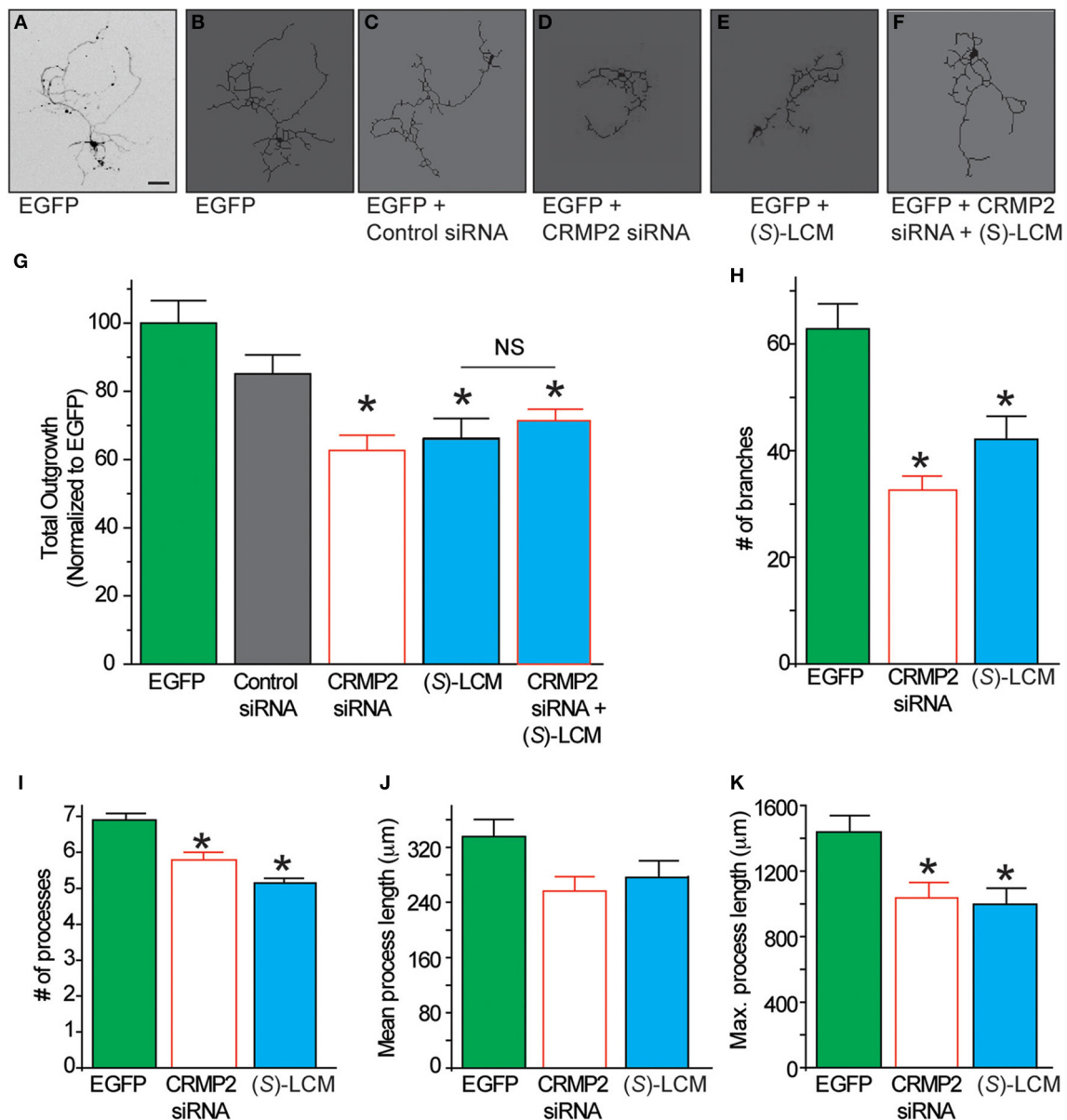


FIGURE 7 | The effect of (S)-LCM on neurite outgrowth phenocopies siRNA knockdown of CRMP2. (A) Representative inverted black and white representative image of a cortical neuron 48 h following EGFP-transfection. (B–F) Representative tracings of neurons transfected with EGFP ± control siRNA, CRMP2 siRNA, 200 μM (S)-LCM, or CRMP2 siRNA + (S)-LCM. (G) Total outgrowth of neurons transfected with EGFP, control siRNA, or CRMP2 siRNA combined with 24 h (S)-LCM treatment (200 μM). CRMP2

siRNA and (S)-LCM reduced outgrowth to a similar level. Combination of CRMP2 and (S)-LCM did not produce a further reduction. (H–K) Comparison of the effects of CRMP2 siRNA and (S)-LCM on # of branches, # of processes, mean process length, and maximum process length. (* $p < 0.05$ vs. EGFP alone, One-Way ANOVA, Tukey's *post-hoc* analysis) (values represent mean ± s.e.m.) ($n = 86$ –320 cells, 8 separate culture wells) (scale bar = 50 μm).

2003). This work has since been corroborated in a report from the Bibb group that demonstrated activity-dependent decreases in Cdk5 activity that were p35 independent (Nguyen et al., 2007). Therefore, future work will seek to identify the events linking neuronal activity to the changes in Cdk5 phosphorylation observed in this study.

The ability of CRMP2 to mediate cytoskeletal dynamics is highly dependent upon its phosphorylation state (for review see

Khanna et al., 2012). In this regard, unphosphorylated CRMP2 is considered active and growth-promoting whereby upon phosphorylation, it is rendered inactive. That CRMP2 is phosphorylated by numerous kinases allows for multiple signaling pathways to converge on a single point, the balance of unphosphorylated (active) and phosphorylated (inactive) CRMP2. Changes in kinase activity that alter this balance should thereby lead to corresponding changes in CRMP2 activity. Therefore, it was not

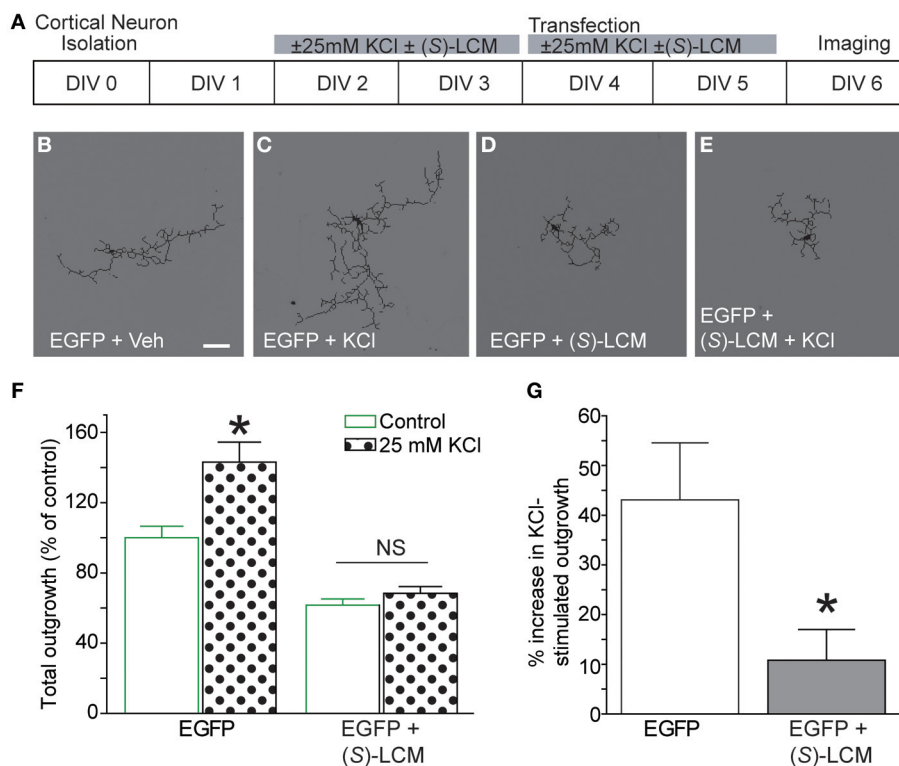


FIGURE 8 | Targeting CRMP2 prevents activity-dependent increase in neurite outgrowth. (A) Timeline of experimental procedures. **(B–E)**

Representative tracings of cortical neurons expressing EGFP and incubated for 96 h in vehicle, 25 mM KCl, 200 μ M (S)-LCM, or 25 mM KCl + 200 μ M (S)-LCM. **(F)** Total outgrowth of cortical neurons exposed to 25 mM KCl in the

presence or absence of 200 μ M (S)-LCM. **(G)** In naïve neurons, KCl exposure increased outgrowth by ~40% compared to vehicle. Co-application of (S)-LCM blunted the KCl-induced increase to ~10% (* p < 0.05 compared to control; Student's t -test) (n = 110–379 cells, across 8 separate culture wells) (scale bar = 50 μ m).

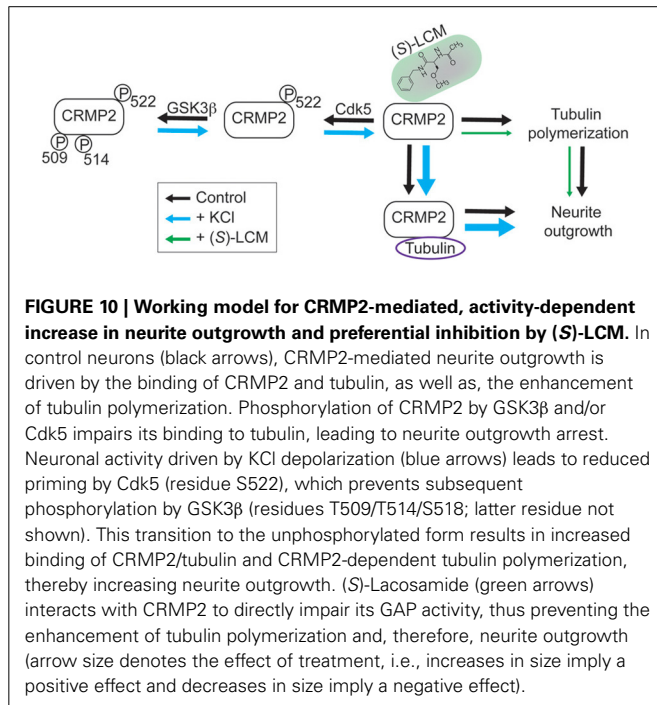
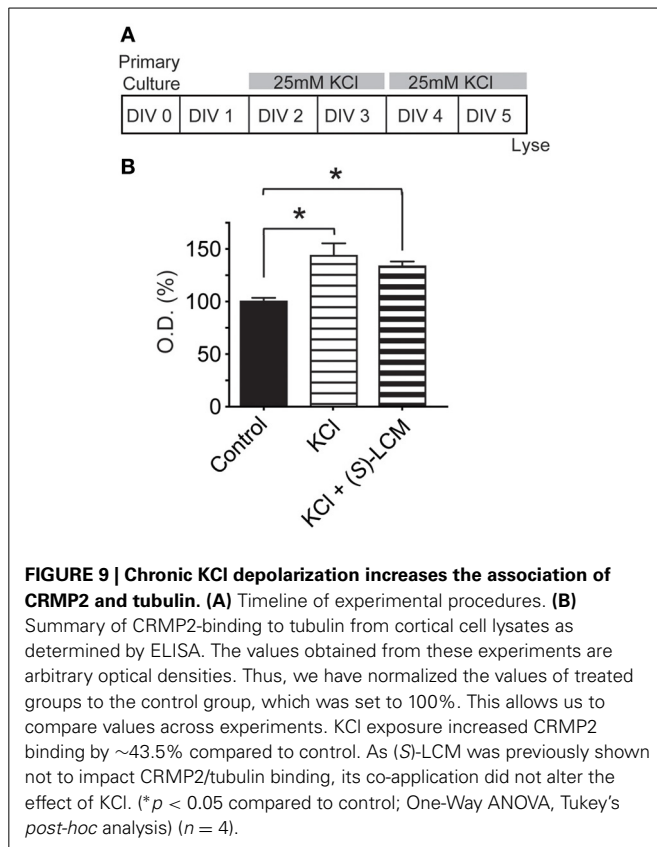
surprising that our findings revealed that the activity-dependent reduction of CRMP2 phosphorylation directly translated into an increase in binding between CRMP2 and tubulin.

(S)-LCM IS A VALUABLE TOOL FOR TARGETING CRMP2-MEDIATED NEURITE OUTGROWTH IN EPILEPTOGENIC PROCESSES

Very few proteins can be considered truly unifunctional. The ability to carry out multiple functions allows for varying levels of dynamic regulation. A drawback of this cellular multitasking is the difficulty in dissecting out specific functions. In the case of CRMP2, the ability to regulate neurite outgrowth is merely one facet of CRMP2 function and its study can be confounded by the role of CRMP2 in other processes such as synaptic transmission (Brittain et al., 2009; Chi et al., 2009), excitotoxicity/neurodegeneration (Castegna et al., 2002; Cole et al., 2006; Sultana et al., 2007; Brittain et al., 2011b, 2012), and migration (Sun et al., 2010), among many others. Therefore, the identification of tools to parse out select functions is invaluable in the dissection of CRMP2's roles within the nervous system. Our findings indicate that (S)-LCM can be used in place of genetic knockdown strategies to preferentially study neurite outgrowth mediated by CRMP2. Aside from a tool for the study of this particular function of CRMP2, (S)-LCM may have therapeutic potential for diseases in which aberrant neurite outgrowth

is known to contribute to the pathology. As more knowledge is gained regarding the role of CRMP2-mediated neurite outgrowth in various pathologies, the ability of (S)-LCM to abrogate this phenomenon may prove extremely valuable.

Activity-dependent neurite outgrowth holds important implications for many pathological conditions, perhaps the most apparent being epilepsy. Therefore, CRMP2 may prove a promising target for therapeutic intervention. Indeed, previous work has demonstrated that targeting CRMP2 via (R)-LCM prevents the aberrant increase in excitatory connectivity in an animal model of posttraumatic epileptogenesis (Wilson et al., 2012a). We also previously showed that following traumatic brain injury (TBI), CRMP2 phosphorylation is decreased concomitantly with increased mossy fiber sprouting in the hippocampus. This biological event is related to tubulin polymerization promoted by non-phosphorylated, active CRMP2. Here, we demonstrate that specific binding of (S)-LCM to CRMP2 results in an inhibition of CRMP2-dependent tubulin polymerization *in vitro* (Figure 5). Since (S)-LCM does not alter slow-inactivation of VGSCs (Figure 6), this compound has fewer off-target effects than its enantiomer parent compound (R)-LCM. This assertion is further supported by the observations that (S)-LCM is more efficient than (R)-LCM in inhibiting neurite outgrowth (Table 1), a CRMP2-dependent event. Thus, we propose that (S)-LCM can be



a molecule of particular interest in targeting aberrant CRMP2-mediated neurite outgrowth in epileptogenesis. As a proof-of-concept, we previously demonstrated that (S)-LCM treatment, in a TBI animal model, resulted in a complete inhibition of mossy

fiber sprouting compared to sham control animals (Wilson et al., 2014).

While the action of (S)-LCM is likely mediated by its ability to impair the enhancement of tubulin polymerization by CRMP2, the effect of (S)-LCM on *every* function of CRMP2 remains untested. At this time, (S)-LCM does not appear to alter tubulin binding nor synaptic bouton size. Additionally, the parent compound (R)-LCM also has no effect on these processes, as well as calcium channel trafficking or glutamate release (Wilson et al., 2012a)—processes altered by changes in CRMP2 function.

ACTIVITY-DRIVEN NEURITE OUTGROWTH IN CULTURED CORTICAL NEURONS IS A CRMP2-DEPENDENT PROCESS, MEDIATED BY CHANGES IN PHOSPHORYLATION STATE

Consistent with the observed changes in CRMP2 phosphorylation and tubulin binding, inhibition of CRMP2 by (S)-LCM prevented the activity-driven increase in neurite outgrowth. As previously mentioned, CRMP2 is capable of mediating neurite outgrowth through two distinct mechanisms: (1) the binding and transport of tubulin dimers (Fukata et al., 2002) and (2) enhancement of the GTPase activity and, therefore, polymerization of tubulin (Chae et al., 2009). While the impact of neuronal activity on the ability of CRMP2 to enhance tubulin polymerization is unknown, our results suggest that an increased association with tubulin accounts for the increase in CRMP2-mediated neurite outgrowth. The ability of (S)-LCM to preclude the effect of KCl on neurite outgrowth lies not within preventing the KCl-facilitated increase in tubulin binding, but rather via simultaneously impairing the ability of CRMP2 to promote tubulin polymerization. This data suggests that the CRMP2's inability to enhance tubulin's GTPase activity, may overrule an increase in affinity for tubulin. Nevertheless, our findings do not rule out the possibility that (S)-LCM's full mechanism of action may include inhibition or enhancement of CRMP2 binding with unknown partner protein(s). Our findings (Figure 10), along with those of Tan et al. (2013), represent two separate reports of the involvement of CRMP2 in activity-driven neurite outgrowth in two distinct cell populations.

AUTHOR CONTRIBUTIONS

Participated in Research Design—Sarah M. Wilson, Aubin Moutal, Yuying Wang, Ohannes Melemedjian, May Khanna, Rajesh Khanna. Conducted Experiments—Sarah M. Wilson, Aubin Moutal, Yuying Wang, Weina Ju, Ohannes Melemedjian, Liberty François-Moutal, May Khanna, Rajesh Khanna. Performed Data Analysis—Sarah M. Wilson, Aubin Moutal, Yuying Wang, Ohannes Melemedjian, Liberty François-Moutal, Rajesh Khanna. Wrote the Manuscript—Sarah M. Wilson, Rajesh Khanna.

ACKNOWLEDGMENTS

We thank members of the Stark Neurosciences Research Institute for helpful comments and discussions. This work was supported, in part, by a National Scientist Development grant SDG5280023 from the American Heart Association and a Neurofibromatosis New Investigator Award NF1000099 from the Department of Defense Congressionally Directed Military Medical Research and

Development Program to Rajesh Khanna. Sarah M. Wilson was partially funded by a Stark Fellowship and a Larry Kays Medical Neuroscience award.

SUPPLEMENTARY MATERIAL

The Supplementary Material for this article can be found online at: <http://www.frontiersin.org/journal/10.3389/fncel.2014.00196/abstract>

REFERENCES

- Andurkar, S. V., Stables, J. P., and Kohn, H. (1999). The anticonvulsant activities of N-benzyl 3-methoxypropionamides. *Bioorg. Med. Chem.* 7, 2381–2389. doi: 10.1016/S0968-0896(99)00186-8
- Arimura, N., Inagaki, N., Chihara, K., Menager, C., Nakamura, N., Amano, M., et al. (2000). Phosphorylation of collapsin response mediator protein-2 by Rho-kinase. Evidence for two separate signaling pathways for growth cone collapse. *J. Biol. Chem.* 275, 23973–23980. doi: 10.1074/jbc.M001032200
- Arimura, N., Menager, C., Kawano, Y., Yoshimura, T., Kawabata, S., Hattori, A., et al. (2005). Phosphorylation by Rho kinase regulates CRMP-2 activity in growth cones. *Mol. Cell. Biol.* 25, 9973–9984. doi: 10.1128/MCB.25.22.9973-9984.2005
- Astle, M. V., Ooms, L. M., Cole, A. R., Binge, L. C., Dyson, J. M., Layton, M. J., et al. (2011). Identification of a proline-rich inositol polyphosphate 5-phosphatase (PIPP)*collapsin response mediator protein 2 (CRMP2) complex that regulates neurite elongation. *J. Biol. Chem.* 286, 23407–23418. doi: 10.1074/jbc.M110.214247
- Brittain, J. M., Chen, L., Wilson, S. M., Brustovetsky, T., Gao, X., Ashpole, N. M., et al. (2011b). Neuroprotection against traumatic brain injury by a peptide derived from the collapsin response mediator protein 2 (CRMP2). *J. Biol. Chem.* 286, 37778–37792. doi: 10.1074/jbc.M111.255455
- Brittain, J. M., Duarte, D. B., Wilson, S. M., Zhu, W., Ballard, C., Johnson, P. L., et al. (2011a). Suppression of inflammatory and neuropathic pain by uncoupling CRMP-2 from the presynaptic Ca(2)(+) channel complex. *Nat. Med.* 17, 822–829. doi: 10.1038/nm.2345
- Brittain, J. M., Pan, R., You, H., Brustovetsky, T., Brustovetsky, N., Zamponi, G. W., et al. (2012). Disruption of NMDAR-CRMP-2 signaling protects against focal cerebral ischemic damage in the rat middle cerebral artery occlusion model. *Channels (Austin)* 6, 52–59. doi: 10.4161/chan.18919
- Brittain, J. M., Piekarczyk, A. D., Wang, Y., Kondo, T., Cummins, T. R., and Khanna, R. (2009). An atypical role for collapsin response mediator protein 2 (CRMP-2) in neurotransmitter release via interaction with presynaptic voltage-gated calcium channels. *J. Biol. Chem.* 284, 31375–31390. doi: 10.1074/jbc.M109.009951
- Brown, M., Jacobs, T., Eickholt, B., Ferrari, G., Teo, M., Monfries, C., et al. (2004). Alpha2-chimaerin, cyclin-dependent kinase 5/p35, and its target collapsin response mediator protein-2 are essential components in semaphorin 3A-induced growth-cone collapse. *J. Neurosci.* 24, 8994–9004. doi: 10.1523/JNEUROSCI.3184-04.2004
- Brustovetsky, T., Pellman, J. J., Yang, X. F., Khanna, R., and Brustovetsky, N. (2014). Collapsin response mediator protein 2 (CRMP2) interacts with N-methyl-D-aspartate (NMDA) receptor and Na⁺/Ca²⁺ exchanger and regulates their functional activity. *J. Biol. Chem.* 289, 7470–7482. doi: 10.1074/jbc.M113.518472
- Castegna, A., Aksenov, M., Thongboonkerd, V., Klein, J. B., Pierce, W. M., Booze, R., et al. (2002). Proteomic identification of oxidatively modified proteins in Alzheimer's disease brain. Part II: dihydropyrimidinase-related protein 2, alpha-enolase and heat shock cognate 71. *J. Neurochem.* 82, 1524–1532. doi: 10.1046/j.1471-4159.2002.01103.x
- Chae, Y. C., Lee, S., Heo, K., Ha, S. H., Jung, Y., Kim, J. H., et al. (2009). Collapsin response mediator protein-2 regulates neurite formation by modulating tubulin GTPase activity. *Cell. Signal.* 21, 1818–1826. doi: 10.1016/j.cellsig.2009.07.017
- Chi, X. X., Schmutzler, B. S., Brittain, J. M., Wang, Y., Hingtgen, C. M., Nicol, G. D., et al. (2009). Regulation of N-type voltage-gated calcium channels (Cav2.2) and transmitter release by collapsin response mediator protein-2 (CRMP-2) in sensory neurons. *J. Cell Sci.* 122(Pt 23), 4351–4362. doi: 10.1242/jcs.053280
- Cohan, C. S., and Kater, S. B. (1986). Suppression of neurite elongation and growth cone motility by electrical activity. *Science* 232, 1638–1640. doi: 10.1126/science.3715470
- Cole, A. R., Causeret, F., Yadirgi, G., Hastie, C. J., McLauchlan, H., McManus, E. J., et al. (2006). Distinct priming kinases contribute to differential regulation of collapsin response mediator proteins by glycogen synthase kinase-3 *in vivo*. *J. Biol. Chem.* 281, 16591–16598. doi: 10.1074/jbc.M513344200
- Cole, A. R., Knebel, A., Morrice, N. A., Robertson, L. A., Irving, A. J., Connolly, C. N., et al. (2004). GSK-3 phosphorylation of the Alzheimer epitope within collapsin response mediator proteins regulates axon elongation in primary neurons. *J. Biol. Chem.* 279, 50176–50180. doi: 10.1074/jbc.C400412200
- Cole, A. R., Noble, W., van Aalten, L., Plattner, F., Meimaridou, R., Hogan, D., et al. (2006). Collapsin response mediator protein-2 hyperphosphorylation is an early event in Alzheimer's disease progression. *J. Neurochem.* 103, 1132–1144. doi: 10.1111/j.1471-4159.2007.04829.x
- Cole, A. R., Soutar, M. P., Rembutsu, M., van Aalten, L., Hastie, C. J., McLauchlan, H., et al. (2008). Relative resistance of Cdk5-phosphorylated CRMP2 to dephosphorylation. *J. Biol. Chem.* 283, 18227–18237. doi: 10.1074/jbc.M801645200
- Connor, J. A. (1986). Digital imaging of free calcium changes and of spatial gradients in growing processes in single, mammalian central nervous system cells. *Proc. Natl. Acad. Sci. U.S.A.* 83, 6179–6183. doi: 10.1073/pnas.83.16.6179
- Cross, D. A., Alessi, D. R., Cohen, P., Andjelkovich, M., and Hemmings, B. A. (1995). Inhibition of glycogen synthase kinase-3 by insulin mediated by protein kinase B. *Nature* 378, 785–789. doi: 10.1038/378785a0
- Czech, T., Yang, J. W., Csaszar, E., Kappler, J., Baumgartner, C., and Lubec, G. (2004). Reduction of hippocampal collapsin response mediated protein-2 in patients with mesial temporal lobe epilepsy. *Neurochem. Res.* 29, 2189–2196. doi: 10.1007/s11064-004-7025-3
- Errington, A. C., Stohr, T., Heers, C., and Lees, G. (2008). The investigational anticonvulsant lacosamide selectively enhances slow inactivation of voltage-gated sodium channels. *Mol. Pharmacol.* 73, 157–169. doi: 10.1124/mol.107.039867
- Fallin, M. D., Lasseter, V. K., Avramopoulos, D., Nicodemus, K. K., Wolyniec, P. S., McGrath, J. A., et al. (2005). Bipolar I disorder and schizophrenia: a 440-single-nucleotide polymorphism screen of 64 candidate genes among Ashkenazi Jewish case-parent trios. *Am. J. Hum. Genet.* 77, 918–936. doi: 10.1086/497703
- Fields, R. D., Neale, E. A., and Nelson, P. G. (1990). Effects of patterned electrical activity on neurite outgrowth from mouse sensory neurons. *J. Neurosci.* 10, 2950–2964.
- Fukata, Y., Itoh, T. J., Kimura, T., Menager, C., Nishimura, T., Shiromizu, T., et al. (2002). CRMP-2 binds to tubulin heterodimers to promote microtubule assembly. *Nat. Cell Biol.* 4, 583–591. doi: 10.1038/ncb825
- Goshima, Y., Nakamura, F., Strittmatter, P., and Strittmatter, S. M. (1995). Collapsin-induced growth cone collapse mediated by an intracellular protein related to UNC-33. *Nature* 376, 509–514. doi: 10.1038/376509a0
- Hensley, K., Venkova, K., Christov, A., Gunning, W., and Park, J. (2011). Collapsin response mediator protein-2: an emerging pathologic feature and therapeutic target for neurodegeneration indications. *Mol. Neurobiol.* 43, 180–191. doi: 10.1007/s12035-011-8166-4
- Hou, S. T., Jiang, S. X., Aylsworth, A., Ferguson, G., Slinn, J., Hu, H., et al. (2009). CaMKII phosphorylates collapsin response mediator protein 2 and modulates axonal damage during glutamate excitotoxicity. *J. Neurochem.* 111, 870–881. doi: 10.1111/j.1471-4159.2009.06375.x
- Johnston-Wilson, N. L., Sims, C. D., Hofmann, J. P., Anderson, L., Shore, A. D., Torrey, E. F., et al. (2000). Disease-specific alterations in frontal cortex brain proteins in schizophrenia, bipolar disorder, and major depressive disorder. The Stanley Neuropathology Consortium. *Mol. Psychiatry* 5, 142–149. doi: 10.1038/sj.mp.4000696
- Kater, S. B., Mattson, M. P., Cohan, C., and Connor, J. (1988). Calcium regulation of the neuronal growth cone. *Trends Neurosci.* 11, 315–321. doi: 10.1016/0166-2236(88)90094-X
- Khanna, R., Wilson, S. M., Brittain, J. M., Weimer, J., Sultana, R., Butterfield, A., et al. (2012). Opening Pandora's jar: a primer on the putative roles of CRMP2 in a panoply of neurodegenerative, sensory and motor neuron, and central disorders. *Future Neurol.* 7, 749–771. doi: 10.2217/fnl.12.68
- Kocsis, J. D., Rand, M. N., Lankford, K. L., and Waxman, S. G. (1994). Intracellular calcium mobilization and neurite outgrowth in mammalian neurons. *J. Neurobiol.* 25, 252–264. doi: 10.1002/neu.480250306
- Lee, K. Y., Rosales, J. L., Tang, D., and Wang, J. H. (1996). Interaction of cyclin-dependent kinase 5 (Cdk5) and neuronal Cdk5 activator in bovine brain. *J. Biol. Chem.* 271, 1538–1543. doi: 10.1074/jbc.271.3.1538

- LeTiran, A., Stables, J. P., and Kohn, H. (2001). Functionalized amino acid anti-convulsants: synthesis and pharmacological evaluation of conformationally restricted analogues. *Bioorg. Med. Chem.* 9, 2693–2708. doi: 10.1016/S0968-0896(01)00204-8
- Matton, M. P., Guthrie, P. B., and Kater, S. B. (1988). Components of neurite outgrowth that determine neuronal cytoarchitecture: Influence of calcium and the growth substrate. *J. Neurosci. Res.* 20, 331–345. doi: 10.1002/jnr.490200307
- Nakata, K., Ujike, H., Sakai, A., Takaki, M., Imamura, T., Tanaka, Y., et al. (2003). The human dihydropyrimidine-related protein 2 gene on chromosome 8p21 is associated with paranoid-type schizophrenia. *Biol. Psychiatry* 53, 571–576. doi: 10.1016/S0006-3223(02)01729-8
- Nguyen, C., Hosokawa, T., Kuroiwa, M., Ip, N. Y., Nishi, A., Hisanaga, S., et al. (2007). Differential regulation of the Cdk5-dependent phosphorylation sites of inhibitor-1 and DARPP-32 by depolarization. *J. Neurochem.* 103, 1582–1593. doi: 10.1111/j.1471-4159.2007.04868.x
- Niisato, E., Nagai, J., Yamashita, N., Nakamura, F., Goshima, Y., and Ohshima, T. (2013). Phosphorylation of CRMP2 is involved in proper bifurcation of the apical dendrite of hippocampal CA1 pyramidal neurons. *Dev. Neurobiol.* 73, 142–151. doi: 10.1002/dneu.22048
- Ryu, M. J., Lee, C., Kim, J., Shin, H. S., and Yu, M. H. (2008). Proteomic analysis of stargazer mutant mouse neuronal proteins involved in absence seizure. *J. Neurochem.* 104, 1260–1270. doi: 10.1111/j.1471-4159.2007.05100.x
- Schilling, K., Dickinson, M. H., Connor, J. A., and Morgan, J. I. (1991). Electrical activity in cerebellar cultures determines Purkinje cell dendritic growth patterns. *Neuron* 7, 891–902. doi: 10.1016/0896-6273(91)90335-W
- Schuman, E. M., and Murase, S. (2003). Cadherins and synaptic plasticity: activity-dependent cyclin-dependent kinase 5 regulation of synaptic beta-catenin-cadherin interactions. *Philos. Trans. R. Soc. Lond. B Biol. Sci.* 358, 749–756. doi: 10.1098/rstb.2002.1256
- Sheets, P. L., Heers, C., Stoehr, T., and Cummins, T. R. (2008). Differential block of sensory neuronal voltage-gated sodium channels by lacosamide [(2R)-2-(acetylaminio)-N-benzyl-3-methoxypropanamide], lidocaine, and carbamazepine. *J. Pharmacol. Exp. Ther.* 326, 89–99. doi: 10.1124/jpet.107.133413
- Solem, M., McMahon, T., and Messing, R. O. (1995). Depolarization-induced neurite outgrowth in PC12 cells requires permissive, low level NGF receptor stimulation and activation of calcium/calmodulin-dependent protein kinase. *J. Neurosci.* 15, 5966–5975.
- Stenmark, P., Ogg, D., Flodin, S., Flores, A., Kottenyova, T., Nyman, T., et al. (2007). The structure of human collapsin response mediator protein 2, a regulator of axonal growth. *J. Neurochem.* 101, 906–917. doi: 10.1111/j.1471-4159.2006.04401.x
- Sultana, R., Boyd-Kimball, D., Poon, H. F., Cai, J., Pierce, W. M., Klein, J. B., et al. (2007). Redox proteomics identification of oxidized proteins in Alzheimer's disease hippocampus and cerebellum: an approach to understand pathological and biochemical alterations in AD. *Neurobiol. Aging* 27, 1564–1576. doi: 10.1016/j.neurobiolaging.2005.09.021
- Sun, Y., Fei, T., Yang, T., Zhang, F., Chen, Y. G., Li, H., et al. (2010). The suppression of CRMP2 expression by bone morphogenetic protein (BMP)-SMAD gradient signaling controls multiple stages of neuronal development. *J. Biol. Chem.* 285, 39039–39050. doi: 10.1074/jbc.M110.168351
- Tan, M., Ma, S., Huang, Q., Hu, K., Song, B., and Li, M. (2013). GSK-3 α /beta-mediated phosphorylation of CRMP-2 regulates activity-dependent dendritic growth. *J. Neurochem.* 125, 685–697. doi: 10.1111/jnc.12230
- Uchida, Y., Ohshima, T., Sasaki, Y., Suzuki, H., Yanai, S., Yamashita, N., et al. (2005). Semaphorin3A signalling is mediated via sequential Cdk5 and GSK3 β phosphorylation of CRMP2: implication of common phosphorylating mechanism underlying axon guidance and Alzheimer's disease. *Genes Cells* 10, 165–179. doi: 10.1111/j.1365-2443.2005.00827.x
- Uchida, Y., Ohshima, T., Yamashita, N., Ogawara, M., Sasaki, Y., Nakamura, F., et al. (2009). Semaphorin3A signaling mediated by Fyn-dependent tyrosine phosphorylation of collapsin response mediator protein 2 at tyrosine 32. *J. Biol. Chem.* 284, 27393–27401. doi: 10.1074/jbc.M109.000240
- van den Bogaart, G., Meyenberg, K., Diederichsen, U., and Jahn, R. (2012). Phosphatidylinositol 4,5-bisphosphate increases Ca²⁺ affinity of synaptotagmin-1 by 40-fold. *J. Biol. Chem.* 287, 16447–16453. doi: 10.1074/jbc.M112.343418
- Van Ooyen, A., Van Pelt, J., and Corner, M. A. (1995). Implications of activity dependent neurite outgrowth for neuronal morphology and network development. *J. Theor. Biol.* 172, 63–82. doi: 10.1006/jtbi.1995.0005
- van Pelt, J., van Ooyen, A., and Corner, M. A. (1996). Growth cone dynamics and activity-dependent processes in neuronal network development. *Prog. Brain Res.* 108, 333–346. doi: 10.1016/S0079-6123(08)62550-9
- Wang, Y., Brittain, J. M., Jarecki, B. W., Park, K. D., Wilson, S. M., Wang, B., et al. (2010b). *In silico* docking and electrophysiological characterization of lacosamide binding sites on collapsin response mediator protein 2 (CRMP-2) identifies a pocket important in modulating sodium channel slow inactivation. *J. Biol. Chem.* 285, 25296–25307. doi: 10.1074/jbc.M110.128801
- Wang, Y., Brittain, J. M., Wilson, S. M., and Khanna, R. (2010a). Emerging roles of collapsin response mediator proteins (CRMPs) as regulators of voltage-gated calcium channels and synaptic transmission. *Commun. Integr. Biol.* 3, 172–175. doi: 10.4161/cib.3.2.10620
- Wayman, G. A., Impey, S., Marks, D., Saneyoshi, T., Grant, W. F., Derkach, V., et al. (2006). Activity-dependent dendritic arborization mediated by CaM-Kinase I activation and enhanced CREB-dependent transcription of Wnt-2. *Neuron* 50, 897–909. doi: 10.1016/j.neuron.2006.05.008
- Wienken, C. J., Baaske, P., Rothbauer, U., Braun, D., and Duhr, S. (2010). Protein-binding assays in biological liquids using microscale thermophoresis. *Nat. Commun.* 1, 100. doi: 10.1038/ncomms1093
- Wilson, S. M., and Khanna, R. (2014). Specific binding of lacosamide to Collapsin Response Mediator Protein 2 (CRMP2) and direct impairment of its canonical function: implications for the therapeutic potential of lacosamide. *Mol. Neurobiol.* doi: 10.1007/s12035-014-8775-9. [Epub ahead of print].
- Wilson, S. M., Ki Yeon, S., Yang, X. F., Park, K. D., and Khanna, R. (2014). Differential regulation of collapsin response mediator protein 2 (CRMP2) phosphorylation by GSK3 β and CDK5 following traumatic brain injury. *Front. Cell. Neurosci.* 8:135. doi: 10.3389/fncel.2014.00135
- Wilson, S. M., Schmutzler, B. S., Brittain, J. M., Dustrude, E. T., Ripsch, M. S., Pellman, J. J., et al. (2012b). Inhibition of transmitter release and attenuation of AIDS therapy-induced and tibial nerve injury-related painful peripheral neuropathy by novel synthetic Ca²⁺ channel peptides. *J. Biol. Chem.* 287, 35065–35077. doi: 10.1074/jbc.M112.378695
- Wilson, S. M., Xiong, W., Wang, Y., Ping, X., Head, J. D., Brittain, J. M., et al. (2012a). Prevention of posttraumatic axon sprouting by blocking collapsin response mediator protein 2-mediated neurite outgrowth and tubulin polymerization. *Neuroscience* 210, 451–466. doi: 10.1016/j.neuroscience.2012.02.038
- Yamashita, N., Ohshima, T., Nakamura, F., Kolattukudy, P., Honnorat, J., Mikoshiba, K., et al. (2012). Phosphorylation of CRMP2 (collapsin response mediator protein 2) is involved in proper dendritic field organization. *J. Neurosci.* 32, 1360–1365. doi: 10.1523/JNEUROSCI.5563-11.2012
- Yoshimura, T., Kawano, Y., Arimura, N., Kawabata, S., Kikuchi, A., and Kaibuchi, K. (2005). GSK-3 β regulates phosphorylation of CRMP-2 and neuronal polarity. *Cell* 120, 137–149. doi: 10.1016/j.cell.2004.11.012
- Zhu, L. Q., Zheng, H. Y., Peng, C. X., Liu, D., Li, H. L., Wang, Q., et al. (2010). Protein phosphatase 2A facilitates axonogenesis by dephosphorylating CRMP2. *J. Neurosci.* 30, 3839–3848. doi: 10.1523/JNEUROSCI.5174-09.2010
- Zhu, Y. S., Saito, T., Asada, A., Maekawa, S., and Hisanaga, S. (2005). Activation of latent cyclin-dependent kinase 5 (Cdk5)-p35 complexes by membrane dissociation. *J. Neurochem.* 94, 1535–1545. doi: 10.1111/j.1471-4159.2005.03301.x

Conflict of Interest Statement: The authors declare that the research was conducted in the absence of any commercial or financial relationships that could be construed as a potential conflict of interest.

Received: 21 May 2014; paper pending published: 17 June 2014; accepted: 26 June 2014; published online: 24 July 2014.

Citation: Wilson SM, Moutal A, Melemedjian OK, Wang Y, Ju W, François-Moutal L, Khanna M and Khanna R (2014) The functionalized amino acid (S)-Lacosamide subverts CRMP2-mediated tubulin polymerization to prevent constitutive and activity-dependent increase in neurite outgrowth. *Front. Cell. Neurosci.* 8:196. doi: 10.3389/fncel.2014.00196

This article was submitted to the journal *Frontiers in Cellular Neuroscience*. Copyright © 2014 Wilson, Moutal, Melemedjian, Wang, Ju, François-Moutal, Khanna and Khanna. This is an open-access article distributed under the terms of the Creative Commons Attribution License (CC BY). The use, distribution or reproduction in other forums is permitted, provided the original author(s) or licensor are credited and that the original publication in this journal is cited, in accordance with accepted academic practice. No use, distribution or reproduction is permitted which does not comply with these terms.



Novel endogenous *N*-acyl amides activate TRPV1-4 receptors, BV-2 microglia, and are regulated in brain in an acute model of inflammation

Siham Raboune¹, Jordyn M. Stuart¹, Emma Leishman¹, Sara M. Takacs¹, Brandon Rhodes¹, Arjun Basnet², Evan Jameyfield¹, Douglas McHugh¹, Theodore Widlanski² and Heather B. Bradshaw^{1*}

¹ Department of Psychological and Brain Sciences, Indiana University, Bloomington, IN, USA

² Department of Chemistry, Indiana University, Bloomington IN, USA

Edited by:

Leigh Anne Swayne, University of Victoria, Canada

Reviewed by:

Christophe Altier, University of Calgary, Canada

Jean Chemin, Centre National de la Recherche Scientifique, France

*Correspondence:

Heather B. Bradshaw, Department of Psychological and Brain Sciences, Indiana University, 1101 East 10th Street, Bloomington, IN 47405, USA
e-mail: hbbradsh@indiana.edu

A family of endogenous lipids, structurally analogous to the endogenous cannabinoid, *N*-arachidonoyl ethanolamine (Anandamide), and called *N*-acyl amides have emerged as a family of biologically active compounds at TRP receptors. *N*-acyl amides are constructed from an acyl group and an amine via an amide bond. This same structure can be modified by changing either the fatty acid or the amide to form potentially hundreds of lipids. More than 70 *N*-acyl amides have been identified in nature. We have ongoing studies aimed at isolating and characterizing additional members of the family of *N*-acyl amides in both central and peripheral tissues in mammalian systems. Here, using a unique in-house library of over 70 *N*-acyl amides we tested the following three hypotheses: (1) Additional *N*-acyl amides will have activity at TRPV1-4, (2) Acute peripheral injury will drive changes in CNS levels of *N*-acyl amides, and (3) *N*-acyl amides will regulate calcium in CNS-derived microglia. Through these studies, we have identified 20 novel *N*-acyl amides that collectively activate (stimulating or inhibiting) TRPV1-4. Using lipid extraction and HPLC coupled to tandem mass spectrometry we showed that levels of at least 10 of these *N*-acyl amides that activate TRPVs are regulated in brain after intraplantar carrageenan injection. We then screened the BV2 microglial cell line for activity with this *N*-acyl amide library and found overlap with TRPV receptor activity as well as additional activators of calcium mobilization from these lipids. Together these data provide new insight into the family of *N*-acyl amides and their roles as signaling molecules at ion channels, in microglia, and in the brain in the context of inflammation.

Keywords: lipid signaling, endocannabinoids, *N*-acyl amides, TRP receptors, microglia

INTRODUCTION

Transient receptor potential channels (TRPs) form a large family of ubiquitous ligand-gated non-selective cation channels that function as cellular sensors and in many cases regulate intracellular calcium. Identification of the endogenous ligands that activate the majority of TRP receptors is still under intense investigation with most of these channels still remaining “orphans” (Vriens et al., 2004; Nilius and Owsianik, 2011; Beech, 2012). Much work has shown that TRPs respond to a variety of external stimuli (e.g., plant-derived lipids), however, most TRP receptors are expressed in areas that would not come in direct contact with external stimuli (e.g., CNS tissue, internal organs, smooth muscle); therefore, the mechanism of direct activation by cellular messengers is still under much debate and research. In the few cases where endogenous ligands have been identified that drive direct activation of TRPs, the majority of these ligands are small lipid molecules, most of which share structural homology (Bradshaw et al., 2013).

Members of the TRPV family that consists of TRPV1-6, of which TRPV1-4 (also known as the thermoTRPs for their

responses to heat) are the most targeted TRP receptors for drug discovery as they are major players in mechanisms of pain and inflammation (Di Marzo et al., 2002; Julius, 2013). TRPV1 (formerly VR1) receptors identification in dorsal root ganglia (DRG) in 1997 was shown to be a molecular integrator of different types of noxious stimuli (Caterina et al., 1997). TRPV1 receptors are mainly expressed in neuronal tissue such as Aδ and C fibers as well as DRG, trigeminal and nodose ganglia, and sensory neurons of the jugular ganglia as well as many brain areas (Tominaga et al., 1998; Caterina and Julius, 2001; Nagy et al., 2004; Starowicz et al., 2008; Cavanaugh et al., 2011a,b). Yet the complete picture of the role of TRPV activity in the CNS is still largely unknown and less still is known about brain TRP activity in the context of pain and inflammation in the brain. Unlocking the mysteries of TRP channel activation will have far-reaching effects on our understanding of cell signaling and pathophysiology in the CNS.

Lipidomics, the field of study focused on identifying and characterizing the full complement of biological lipids, has identified a class of endogenous lipids, *N*-acyl amides, which are providing

a novel avenue from which to studying cellular communication. *N*-arachidonoyl ethanolamine, (Anandamide—the first endogenous cannabinoid identified) is an archetype *N*-acyl amide that is constructed from an acyl group, arachidonic acid, and an amine, ethanolamine via an amide bond. This same structure can be modified by changing either the fatty acid or the amide to form potentially hundreds of lipids (**Figure 1**). More than 70 *N*-acyl amides have been identified in nature and our group has been a driving force behind this work (Bradshaw and Walker, 2005; Tan et al., 2006; Burstein et al., 2007; Hu et al., 2008; Rimmerman et al., 2008; Bradshaw et al., 2009; Hu et al., 2009; Lee et al., 2010; Mchugh et al., 2010; Smoum et al., 2010; Tortoriello et al., 2013).

Multiple members of the *N*-acyl amide class of lipids have been shown to activate a member of the TRPV family (Di Marzo et al., 2002; Julius, 2013). Anandamide was the first *N*-acyl amide shown to activate TRPV1 channels (Zygmunt et al., 1999). *N*-arachidonoyl dopamine (NADA) and *N*-oleoyl dopamine (OLDA), which are structurally similar to the exogenous TRPV1 agonist capsaicin as well as *N*-acyl amide structural analogs to AEA, are more potent endogenous ligand for TRPV1 receptors (Huang et al., 2002; Chu et al., 2003). Additional work showed that *N*-arachidonoyl taurine, which does not activate CB receptors, activates both TRPV1 and TRPV4 receptors (Saghatelian et al., 2006). Likewise, a broader range of *N*-acyl ethanolamides were shown to activate TRPV1 (Movahed et al., 2005), further demonstrating that non-eCB type *N*-acyl amides could also activate TRPs.

Here, we used a unique in-house library of over 70 *N*-acyl amides (for complete listed see Supplemental Table 1) we tested the following three hypotheses: (1) Additional *N*-acyl amides will have activity at TRPV1-4, (2) Acute peripheral injury will drive changes in CNS levels of *N*-acyl amides, and (3) *N*-acyl amides will regulate calcium in CNS-derived microglia. Through these studies we identified 20 novel *N*-acyl amide activators of these TRPVs collectively. We then performed targeted lipidomics using the *N*-acyl amide library on 6 brain regions to determine if acute inflammation by intraplantar paw injection of carrageenan would drive changes in these lipids. Here, we demonstrated that a wide range of lipids are regulated in the brain during acute inflammation and at least 10 of these newly identified TRPV activator lipids are regulated in the brain at 3 h post injection suggesting

that this family of lipids plays important roles in CNS signaling. Finally, we screened BV2 microglial cells with the *N*-acyl amide library to determine if *N*-acyl amides play a role in microglial signaling. In these experiments we show that 6 novel *N*-acyl amide families of lipids active these microglial cells, 5 of which had members that were upregulated 3 h post-carrageenan injection in the brain. Data presented here provide evidence that the TRPV and *N*-acyl amide systems may work together to respond to rapid changes in the neurophysiological environment of acute pain.

MATERIALS AND METHODS

CHEMICALS

Fura-2 AM was purchased from Invitrogen (Carlsbad, CA). 5-Iodoresiniferatoxin (I-RTX) was purchased from Tocris Cookson Inc. (Ellisville, MO). Ruthenium red was purchased from Sigma-Aldrich (St. Louis, MO). 2-Aminoethoxydiphenyl borate (2-APB) and 4- α -Phorbol 12,13-didecanoate (4- α PDD) were purchased from Enzo Life Sciences (Farmingdale, NY). Each of the following *N*-acyl amides were purchased from Cayman Chemical (Ann Arbor, MI): *N*-arachidonoyl ethanolamine (Anandamide; AEA), *N*-oleoyl ethanolamine (OEA), *N*-palmitoyl ethanolamine (PEA), *N*-linoleoyl ethanolamine (LEA), *N*-docosahexaenoyl ethanolamine (DEA), *N*-arachidonoyl glycine (NAGly), and 2-AG. All other reagent-grade *N*-acyl amides were synthesized in house as previously described (Tan et al., 2010). Unless otherwise indicated, all compounds were stored in 100% ethanol, however, assay solutions were made fresh in DMSO prior to every assay. Chemicals used for mass spectrometry were HPLC-grade and include methanol, water, ammonium acetate, and acetic acid. HPLC water and methanol were purchased from VWR International (Plainview, NY). Ammonium acetate and acetic acid were purchased from Sigma Aldrich (St. Louis, MO).

ANIMALS

All protocols were approved by the Indiana University Institutional Animal Care and Use Committee. Adult male Sprague-Dawley rats (Harlan, Indianapolis, IN USA) were used in all experiments. Rats were kept 4 to a cage in standard cages on a 12:12-h light–dark cycle. Food and water were available *ad libitum*. All subjects were adapted to the laboratory environment for a minimum of 2 weeks prior to use in our studies.

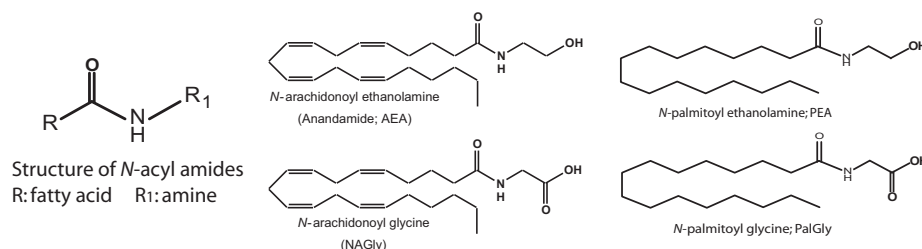


FIGURE 1 | Structure of *N*-acyl amides. *N*-acyl amides studied here have a structure that consists of an acyl group (denoted as R) and an amide bond to an amine (denoted as R₁) and this is depicted as a cartoon structure here (far left). 4 examples of *N*-acyl amide bioactive molecules are also depicted:

N-arachidonoyl ethanolamide (Anandamide; AEA); *N*-arachidonoyl glycine (NAGly); *N*-palmitoyl ethanolamide (PEA); and *N*-palmitoyl glycine (PalGly). These 4 *N*-acyl amide species illustrate that the molecules can differ by changing the acyl group (AEA and PEA) or the amide (AEA and NAGly).

CELL CULTURE

Human embryonic kidney cells (HEK-293) stably expressing human TRPV1-4 and BV-2 cells were cultured as monolayers in T-75 flasks and expanded to passages 15–23. Cells were maintained in Dulbecco's minimum essential medium (DMEM) modified with non-essential amino acids, L-glutamine, and 2.2 g/L sodium bicarbonate and supplemented with 10% fetal bovine serum (FBS) and 1% penicillin-streptomycin (P/S). Cells were subcultured an average of three times a week with Trypsin-EDTA 1× and grown at 37°C in a humidified atmosphere of 5% CO₂ in air; this was done 48 h prior to calcium assays.

CALCIUM (Ca²⁺) IMAGING ASSAY

The effect of the N-acyl amides on calcium mobilization was assessed using a high-throughput 96-wells plate assay adapted from our previous work (Rimmerman et al., 2008). TRPV1 (human), TRPV2 (mouse), TRPV3 (mouse), or TRPV4 (rat)-transfected HEK-293 (TRPV2 cells were a kind gift from Vincenzo DiMarco and the TRPV3 and 4 cells were a kind gift from Michael Caterina) cells were seeded on Cell BIND 96-well flat clear bottom black polystyrene microplates (Corning Life Sciences, Acton, MA) coated with 50 µg/mL poly-D-Lysine (PDL) under the cell culture hood at room temperature, allowing cells to attach to plates. Cells were grown to 75–85% confluence in a monolayer in the culture medium described above for 24–48 h. Prior to all experiments, cells were examined under the microscope to check for optimal confluency and normal morphology.

AGONIST ACTIVITY CALCIUM MOBILIZATION SCREENS

Prior to loading the cells, the selective intracellular fluorescent probe for calcium, Fura-2-acetoxymethyl ester (Fura-2AM), was removed from –20°C and allowed to equilibrate to room temperature while protected from light. Cells were then loaded with 3 µM Fura-2AM at room temperature for 1 h, in HEPES-Tyrode buffer containing 0.05% w/v pluronic F-127 (Invitrogen). HEPES-Tyrode buffer was prepared with HEPES 0.025 mol, NaCl 0.14 mol, KCl 0.0027 mol, CaCl₂ 0.0018 mol, MgCl₂ 0.0005 mol, NaH₂PO₄ 0.0004 mol, and glucose 0.05 mol, and HEPES-Tyrode buffer used in calcium imaging assays was adjusted to pH 7.4 in order to avoid cellular ionic perturbation. After 1 h of Fura-2AM incubation, cells were washed twice and incubated in 175 µL of HEPES-Tyrode buffer for 20 min at room temperature. The plates were scanned for calcium activity using Flex Station II (Molecular Devices, Sunnyvale, CA) at 27°C. After 30 s of baseline recording, cells were challenged with 75 µL of buffer containing N-acyl amide solutions or positive control agonists capsaicin (TRPV1), 2-APB (TRPV2 and 3), 4α PDD (TRPV4), or PAF (BV2) which was first dissolved in DMSO or challenge compounds that were first dissolved in 100% DMSO at different concentrations and then added to buffer for a final DMSO concentration of 0.5% or vehicle (DMSO) alone using the automated fluidic module of Flex Station II.

ANTAGONIST ACTIVITY SCREENS

Similar to the agonist activity assay, cells were incubated at room temperature for 1 h with 3 µM Fura-2AM in HEPES-Tyrode

buffer containing 0.05% w/v pluronic F-127. Cells were then washed twice and resuspended in 175 µL of HEPES-Tyrode buffer containing the 10 µM N-acyl amide mixture or individual compound (depending on the assay) which was first dissolved in 100% DMSO and added to the buffer to make a final concentration of DMSO of 0.5%. or vehicle (DMSO) alone and incubated for 20 min. These plates were then loaded into the FlexStationII and following 30 s of baseline recording, the pre-incubated cells were then challenged with 75 µL of HEPES-Tyrode buffer containing the corresponding positive control agonists capsaicin (TRPV1), 2-APB (TRPV2 and 3), or 4α PDD (TRPV4) which was first dissolved in DMSO. The plates were then scanned for calcium activity using Flex Station II (Molecular Devices, Sunnyvale, CA) at 27°C. The following positive control antagonists were used to compare the level of activity of N-acyl amide mixtures or individual lipids: Iodo-resiniferatoxin (I-RTX; TRPV1), Ruthenium Red (TRV2-4).

IN VIVO INDUCED PAW INFLAMMATION

Male Sprague–Dawley rats remained in their home cage but were placed in the testing room for at least 1 h prior to injection to allow for acclimation to the novel environment. Rats were divided into two groups. Control groups received a 50 µL intraplantar injection of vehicle (saline) into the right hind paw and experimentally-treated animals received a 50 µL intraplantar injection of 3% carrageenan (CG) dissolved in saline into the right hind paw. All solutions of CG or saline were adjusted to pH 7.4.

PAW INFLAMMATION ASSESSMENT AND TISSUE EXTRACTION

Paw inflammation was evaluated in all animals at 3 h following carrageenan injection by using calipers to measure dorsal-to-ventral paw thickness. Rats were euthanized by decapitation and brains removed, placed in Eppendorf tubes and flash-frozen in liquid nitrogen. After brains were frozen, they were quickly dissected and the striatum, thalamus, hippocampus, cerebellum, midbrain and brainstem were placed in individual ependorph tubes, and flash frozen in liquid nitrogen. Tissue samples were kept in a –80°C freezer until used for lipid extraction.

LIQUID CHROMATOGRAPHY/TANDEM MASS SPECTROMETRY (LC/MS-MS)

Levels of each compound were analyzed by multiple reactions monitoring (MRM) mode using an applied Biosystems/MDS Sciex triple quadrupole mass spectrometer API 3000 (Foster City, CA) with electrospray ionization as previously described (Bradshaw et al., 2006; Rimmerman et al., 2008; Lee et al., 2010; Ho et al., 2012; Tortoriello et al., 2013). Samples were loaded using Shimadzu SCL10Avp auto-sampler and chromatographed on a 210 mm Zorbax Eclipse XDB-C18 reversed-phase HPLC column (3.5 µm internal diameter) maintained at 40°C. The flow rate was 200 µL/min achieved by a system comprised of a Shimadzu controller and two Shimadzu LC10ADvp pumps. The Shimadzu LC10ADvp HPLC pumps operated with a starting gradient of 0% mobile phase B which was increased to 100% before returning back to 0%. The mobile phase A consisted of 20/80 MeOH/water containing 1 mM ammonium acetate and mobile

phase B consisted of 100% MeOH containing 1 mM ammonium acetate and 0.5% acetic acid.

DATA ANALYSIS

The analysis of calcium imaging experiments using 96-wells plate was as follows: after 30 s of baseline recording, cells were challenged with the drug, and calcium data per each well was collected every 5 s for a total scan time of 200 s and then calculated as the area under the curve (in relative fluorescence units) using Softmax Pro 5 integration functions (Molecular Devices, Union City, CA). Levels of calcium flux per each treatment group were collected from all repeats and data are presented as mean \pm standard error of the mean (SEM) from at least three different experiments. Graph Pad Prism was used for further statistical analysis. Results were analyzed using One-Way ANOVA with Bonferroni's (calcium imaging data) or Fishers LSD (lipidomics) *post hoc* tests. EC₅₀ are calculated by non-linear regression analysis using the equation for sigmoidal concentration-response curve in Graph Pad Prism 4.0. **p*-value of *p* < 0.05 or #*p*-value of *p* < 0.01 are considered significant.

The 340/380 fluorescence intensity ratio of Fura2AM emission was collected every 5 s for a total scan time of 200 s. Calcium flux per each well was calculated as the area under the curve in relative fluorescence units using Softmax program integration functions. Graph Pad Prism was used for further statistical analysis. The number of repeats per each treatment group varies between 5 and 10 from at least three independent experiments. The majority of mixtures of *N*-acyl amides caused calcium mobilization that was significantly different from vehicle alone when analyzed with an alpha level of *p* < 0.05, however, the effect size was of a low magnitude. In an attempt to narrow down those groups that had the greatest magnitude effect, we set the alpha level to *P* < 0.01.

HPLC/MS-MS data was analyzed as previously described (Bradshaw et al., 2006; Rubio et al., 2007; Rimmerman et al., 2008; Lee et al., 2010; Tan et al., 2010). In brief, the detection of each analyte was based on fragmentation of the precursor ion to yield a daughter ion in the negative ion mode with MRM. The retention times of each of the analyzed compounds were compared to those obtained from their corresponding standards. The area under the curve for the appropriate compound was obtained. The amount of each compound was extrapolated from a calibration curve obtained from analyzing known concentration of synthetic standards and then corrected based up on the extraction efficiency. Final expression of total amounts are in mols/gram tissue (wet wt.). ANOVA analyses were made between 1 h post vehicle and carrageenan injection or 3 h post vehicle or carrageenan injection treatment groups. Individual ANOVAs were performed for each individual lipid family in that there was no a priori assumption that any one lipid specie would have an effect on another, nor would there be interactions between them.

RESULTS

CALCIUM MOBILIZATION OF N-ACYL AMIDE FAMILIES AT TRPV1-4

The first set of experiments were aimed at screening mixtures of each of the *N*-acyl amide families from our unique

library of compounds in each of the TRPV-HEK expression systems. Supplemental Table 1 identifies the complete list of compounds used in the screen and they are grouped as a structural "family" from the categorization of the amine as the grouping mechanism. As an example, all those *N*-acyl glycine molecules that are in the library are considered a unique "family" of compounds and a mixture of each at the same molarity was used as a single screening tool in each of the transfected cell lines. Each of the TRPV1-4 expression systems tested had at least one positive hit with an *N*-acyl amide mixture (Table 2). For agonist activity 4 different families drove calcium in TRPV1-HEK cells, TRPV2 had 2, TRPV3 had 1, and TRPV4 had 2. Whereas, none of the novel *N*-acyl amide mixtures induced calcium mobilization in non-transfected HEK-293 cells (Table 1).

CALCIUM MOBILIZATION OF INDIVIDUAL N-ACYL AMIDES IN TRPV1-4 HEK EXPRESSION SYSTEMS

In a second level of analysis, each individual member of the *N*-acyl amide mixtures that stimulated calcium mobilization in the first screen was tested separately in the same TRPV1-4 HEK/Fura-2AM system. Figure 2 shows an example case of individual *N*-acyl GABA compounds being screened in the TRPV1-HEK system. These experiments with the *N*-acyl GABAs showed a structure-activity relationship for *N*-docosahexaenoyl GABA (D-GABA), *N*-linoleoyl GABA (L-GABA), and *N*-arachidonoyl GABA (A-GABA) all causing significant calcium mobilization; therefore we extended the analysis to include full concentration curves for all *N*-acyl-GABAs. D-GABA, L-GABA, and A-GABA significantly induced concentration-dependent activation of TRPV1 and that each reached an asymptote equivalent to NADA (Figure 2A). Similar to NADA, D-GABA, L-GABA, and A-GABA induced an immediate, sustained increase of calcium (Figure 2B). Supplementary Figures 1–6 show additional data on individual *N*-acyl amide activity in TRPV1-4 HEK systems. These data revealed an additional 5 *N*-acyl amides at TRPV1 (*N*-docosahexaenoyl serine, *N*-docosahexaenoyl glycine, *N*-docosahexaenoyl aspartic acid, *N*-docosahexaenoyl ethanolamide, *N*-linoleoyl ethanolamide), 1 at TRPV2 (*N*-palmitoyl tyrosine), none above the statistical threshold at TRPV3 and 6 at TRPV4 (*N*-arachidonoyl tyrosine, *N*-linoleoyl tyrosine, *N*-palmitoyl tyrosine, *N*-docosahexaenoyl tryptophan, *N*-arachidonoyl tryptophan, *N*-linoleoyl tryptophan). These findings are summarized as a cartoon in Figure 3.

ANTAGONIST ACTIVITY AT TRPV1-4 BY N-ACYL AMIDES

N-acyl amide mixtures listed in Supplemental Table 1 were screened as antagonists at TRPV1-4. As with the agonist screens, we used a known antagonist for each of the TRPV expression systems as our antagonist positive control and challenged the TRPV-HEK expression systems with the same known agonist as in the agonist screens (see Materials and Methods for list of compounds used). Table 2 shows the positive hits for each TRPV expression system. The majority are those that also showed agonist activity also showed antagonist activity (e.g., *N*-acyl GABA mixture is a strong agonist/antagonist at TRPV1), which suggests

Table 1 | Agonist activity of *N*-acyl amides at TRPV1-4.

<i>N</i> -acyl amides (10 μ M mixtures)	Agonist activity				
	Non-transfected HEK-293	TRPV1	TRPV2	TRPV3	TRPV4
<i>N</i> -acyl alanine	7.88 \pm 3.50	16.71 \pm 0.81	45.74 \pm 5.58	14.89 \pm 2.19	30.13 \pm 3.94
<i>N</i> -acyl aspartic acid	11.97 \pm 4.60	95.13 \pm 10.24	6.41 \pm 0.79	26.72 \pm 4.11	25.58 \pm 6.19
<i>N</i> -acyl beta-alanine	5.16 \pm 3.76	22.78 \pm 1.34	23.88 \pm 5.21	21.18 \pm 1.71	9.35 \pm 3.29
<i>N</i> -acyl GABA	−8.15 \pm 4.21	153.08 \pm 10.25	23.58 \pm 5.13	20.24 \pm 2.76	16.00 \pm 2.97
<i>N</i> -acyl glycine	−20.47 \pm 8.29	85.61 \pm 16.80	22.10 \pm 5.43	12.14 \pm 2.98	32.03 \pm 4.23
<i>N</i> -acyl isoleucine	−9.52 \pm 3.25	20.20 \pm 2.71	31.16 \pm 7.62	9.83 \pm 2.23	17.37 \pm 4.39
<i>N</i> -acyl leucine	2.78 \pm 1.79	10.00 \pm 1.92	16.99 \pm 2.19	−2.00 \pm 0.32	4.20 \pm 1.83
<i>N</i> -acyl methionine	−10.34 \pm 4.65	17.02 \pm 2.04	30.67 \pm 5.03	28.65 \pm 4.82	30.46 \pm 4.97
<i>N</i> -acyl phenylalanine	−15.04 \pm 3.00	0.68 \pm 1.75	−5.90 \pm 1.45	−7.55 \pm 1.22	24.13 \pm 3.54
<i>N</i> -acyl proline	−8.21 \pm 2.41	28.34 \pm 5.73	73.35 \pm 2.20	23.92 \pm 3.72	23.84 \pm 4.95
<i>N</i> -acyl serine	−9.98 \pm 6.27	128.76 \pm 29.90	2.87 \pm 2.46	20.56 \pm 1.96	6.28 \pm 1.76
<i>N</i> -acyl threonine	−0.47 \pm 2.52	19.40 \pm 1.01	1.57 \pm 1.37	12.66 \pm 1.05	20.40 \pm 2.27
<i>N</i> -acyl tryptophan	11.39 \pm 2.55	19.33 \pm 2.81	3.94 \pm 1.18	13.46 \pm 1.49	75.59 \pm 7.79
<i>N</i> -acyl tyrosine	−13.72 \pm 5.83	39.05 \pm 2.61	74.78 \pm 15.21	43.61 \pm 2.42	55.59 \pm 7.79
<i>N</i> -acyl valine	−5.14 \pm 4.69	26.63 \pm 3.63	9.01 \pm 1.70	13.42 \pm 3.79	23.86 \pm 4.27
DMSO	−5.46 \pm 2.93	8.10 \pm 0.75	−1.59 \pm 1.68	−0.78 \pm 1.36	2.14 \pm 0.98
Capsaicin (10 μ M)		294.67 \pm 31.31			
NADA (10 μ M)	−11.92 \pm 2.74	220.14 \pm 25.25			
2-APB			238.24 \pm 13.38	121.6 \pm 3.48	
4 α -PDD					76.92 \pm 10.99

Far left column lists the *N*-acyl amide family or control compound that was used as the challenge compounds for each screen. Subsequent columns contain the data from each individual TRPV-HEK expression system as well as the untransfected HEK cells. Values shown are the change in relative fluorescence units of Fura2AM from the 30 s baseline and represent the area of the curve of analysis of 190 s post injection (see example on **Figure 2**). The overwhelming majority of *N*-acyl amide mixtures caused significant increases in baseline calcium at $p = 0.05$ levels over that of the DMSO controls, which were the equivalent to zero. In order to streamline the screening process, we chose to focus on those differences that were only $p \leq 0.01$. Those values in bold black are significantly different from those of the vehicle injection at $p \leq 0.01$.

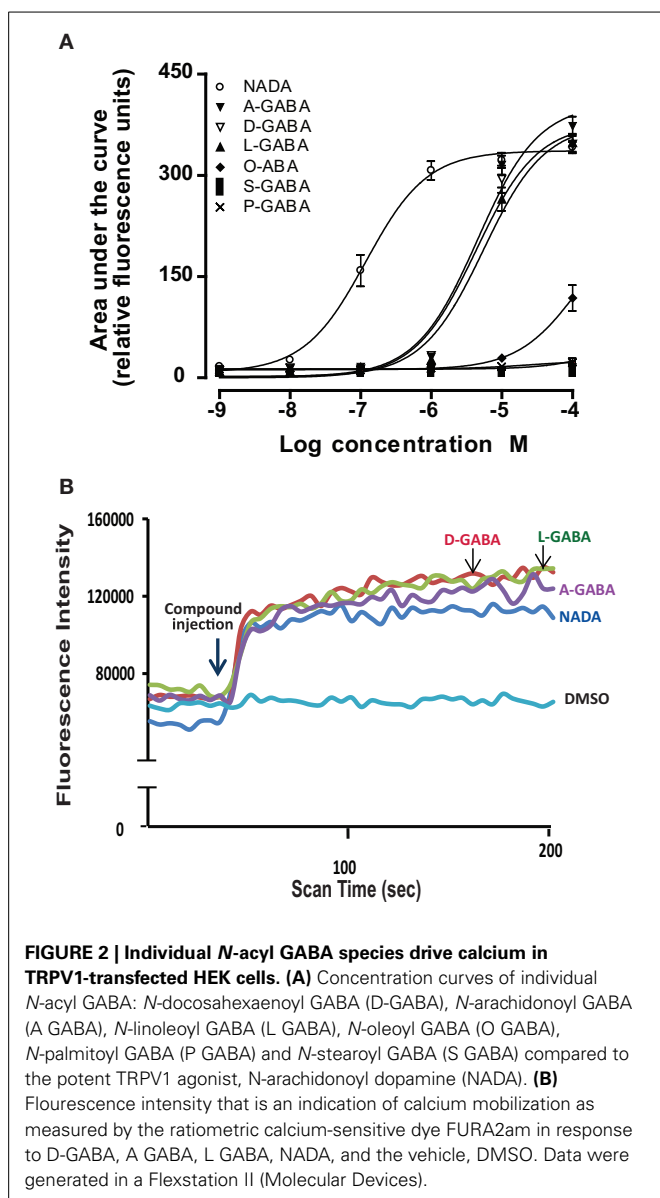
a likely competitive inhibition. Therefore, we focused our efforts for identifying antagonists to those hits that did not have any agonist activity, which singled out the *N*-acyl proline mixture at TRPV1 and the *N*-acyl leucine and *N*-acyl valine mixtures at TRPV3.

ANTAGONIST ACTIVITY ON CALCIUM MOBILIZATION OF INDIVIDUAL *N*-ACYL AMIDES IN TRPV1 AND TRPV3 HEK EXPRESSION SYSTEMS

Of particular interest in the category of the TRPV1 screen was the *N*-acyl proline mixture. This mixture had no agonist activity and a screen of the individual members revealed that *N*-docosahexaenoyl proline is a potent TRPV1 inhibitor (Supplemental Figure 7). Likewise, the *N*-acyl valine mixture had no agonist activity at TRPV3, however, there were 4 individual *N*-acyl valine compounds that act as antagonists (*N*-docosahexaenoyl valine, *N*-linoleoyl valine, *N*-oleoyl valine, *N*-stearoyl valine; Supplemental Figure 8), whereas, the activity of individual *N*-acyl leucine species were not significant. All of the individual *N*-acyl amides that activate or inhibit the TRPV1-4 receptors are summarized in **Figure 3**.

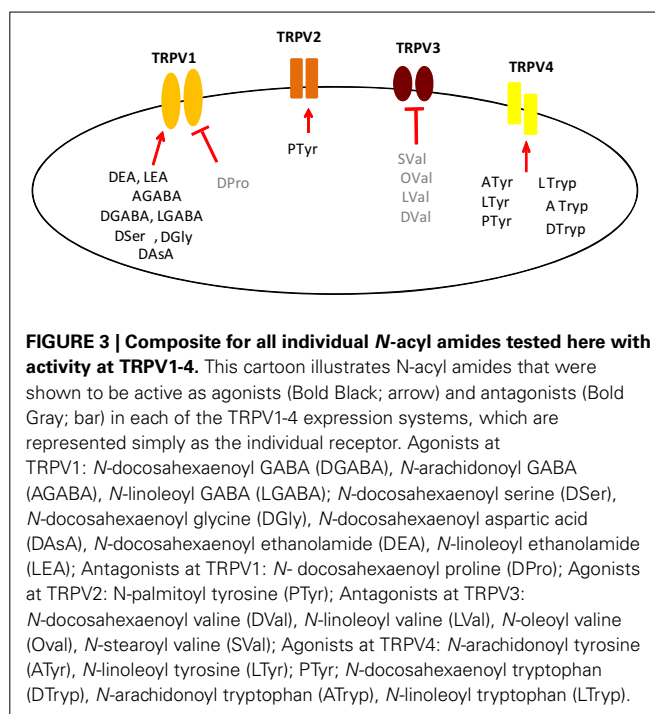
LIPIDOMICS OF 6 DISTINCT BRAIN REGIONS AFTER PERIPHERAL INFLAMMATION REVEAL NOVEL ENDOGENOUS *N*-ACYL AMIDE REGULATION

To address one potential aspect of functional relevance of *N*-acyl amide signaling, we performed a series of targeted lipidomics screens of 75 *N*-acyl amides via HPLC-MS/MS on 6 distinct areas of the brain (striatum, hippocampus, cerebellum, thalamus, mid-brain, and brainstem) in order to survey *N*-acyl amide regulation during an acute inflammatory stimulus. Using the intraplantar carrageenan peripheral inflammation model, we induced an acute inflammatory response and measured changes in brain levels of *N*-acyl amides. Supplemental Figure 9 shows that the levels of edema in the injected paw were significantly greater than vehicle injected at both 1 and 3 h post injection. A majority of all the lipids measured were detected in each of brain areas surveyed and each lipid was found in pmol/gram levels (Supplemental Figure 9 shows matching chromatograms from standards and extracts for 3 *N*-acyl GABA species; Supplemental Table 2 shows all the averaged values for each of the lipids detected in each brain area). Analysis of all lipids in each brain area and comparisons among the four treatment groups was multi-variant. Given that here



were four treatment groups and an *n* of 8 per treatment group, mass spectrometric analysis yielded an enormous quantity of data totaling 14,400 data points for these six brain areas tested (Data shown in Supplemental Table 2). Here, we provide an example of the analysis of those measurements in the hippocampus and striatum.

Out of the 75 spectra analyzed, 48 analytes were detected in hippocampal samples, whereas 57 were detected in striatal samples. Two different levels of analyses were performed. The first level was to compare Veh-1H to CG 1H and then the second level of analysis was to compare Veh-3H and CG-3H. To simplify the analysis into more manageable units, we compared only those lipids within an *N*-acyl amide family in a single ANOVA. For example, only *N*-acyl ethanolamides were compared to the same *N*-acyl ethanolamides. Future studies are aimed at using these data sets in a modeling system to determine if there are predictive



directions of types of *N*-acyl amides or their fatty acid derivatives in a particular direction, but that is beyond the scope of the analysis here.

Table 3 summarizes the results of the 34 *N*-acyl amides that were shown to be modified at either 1 or 3 h post injection as a function of each individual brain area. Of the 12 lipids that were modified (either increasing or decreasing) at the 1 h time point, 6 were found in the hippocampus and 9 of the 12 significantly decreased. This is in stark contrast to the changes in the levels of *N*-acyl amides in the brain 3 h after carrageenan injections wherein all the *N*-acyl amides that were modified by the treatment were significantly higher than those with vehicle injection. Whereas the most differences measured at 1 h post carrageenan were in the hippocampus, the area of the brain with the most dramatic changes in *N*-acyl amides at 3 h post carrageenan were in the striatum and cerebellum. Notably, all brain areas tested had significant increases in *N*-acyl ethanolamides and three of the six (striatum, hippocampus, and cerebellum) all had significant increases in *N*-acyl glycines. Of the 34 *N*-acyl amides that were up or down regulated with peripheral inflammation, 10 showed activity at TRPVs in the assays discussed above and are denoted in gray in **Table 3**.

CALCIUM MOBILIZATION BY N-ACYL AMIDES IN BV-2 MICROGLIAL CELLS

Activation and mobilization by microglia occurs not only during times of mechanical and pathogen-induced tissue damage, but also in times of acute pain (Ji et al., 2013). To test the hypothesis that *N*-acyl amides would drive calcium mobilization in microglia, we screened *N*-acyl amide mixtures in the microglial cell line BV2. Table 5 shows that 5 different *N*-acyl amide family mixtures drive calcium mobilization in BV2 cells, whereas 1

Table 2 | Antagonist activity of *N*-acyl amides at TRPV1-4.

N-acyl amides (10 μ M mixtures)	Antagonist activity			
	TRPV1 (+ CAP)	TRPV2 (+ 2-APB)	TRPV3 (+ 2-APB)	TRPV4 (+ 4 α -PDD)
N-acyl alanine	155.12 \pm 10.33	267.43 \pm 14.53	74.55 \pm 4.34	87.46 \pm 8.03
N-acyl aspartic acid	187.20 \pm 11.78	251.09 \pm 12.01	65.74 \pm 13.38	83.25 \pm 8.34
N-acyl beta-alanine	166.84 \pm 13.52	239.05 \pm 25.01	92.69 \pm 9.95	91.59 \pm 5.26
N-acyl GABA	87.22 \pm 11.12	277.24 \pm 22.89	163.03 \pm 15.23	94.24 \pm 5.71
N-acyl glycine	151.43 \pm 10.3	255.01 \pm 16.16	123.01 \pm 10.80	85.11 \pm 7.15
N-acyl isoleucine	185.08 \pm 5.76	285.96 \pm 30.44	62.73 \pm 3.80	97.22 \pm 5.46
N-acyl leucine	179.18 \pm 13.56	235.66 \pm 22.26	51.37 \pm 3.10	80.25 \pm 6.18
N-acyl methionine	158.93 \pm 14.24	237.28 \pm 18.32	65.15 \pm 5.74	91.50 \pm 9.87
N-acyl phenylalanine	180.70 \pm 10.01	260.15 \pm 28.61	75.64 \pm 22.64	81.56 \pm 4.54
N-acyl proline	95.98 \pm 21.26	-34.61 \pm 26.70	142.49 \pm 6.48	94.16 \pm 11.34
N-acyl serine	196.28 \pm 6.53	234.06 \pm 22.36	69.65 \pm 5.10	94.83 \pm 5.23
N-acyl threonine	197.53 \pm 7.51	210.15 \pm 17.10	81.18 \pm 5.96	83.89 \pm 7.96
N-acyl tryptophan	201.35 \pm 3.26	263.71 \pm 24.69	61.91 \pm 6.13	-99.49 \pm 38.83
N-acyl tyrosine	156.56 \pm 15.15	-116.42 \pm 13.94	58.78 \pm 5.40	-124.36 \pm 22.53
N-acyl valine	174.62 \pm 11.94	240.61 \pm 26.79	39.73 \pm 4.16	37.05 \pm 7.37
DMSO	195.69 \pm 16.42	253.67 \pm 39.42	95.73 \pm 7.01	93.92 \pm 11.55
I-RTX (20 nM)	-22.15 \pm 5.80			
Rethenium red (30 μ M)		64.83 \pm 4.51	41.33 \pm 3.75	-85.52 \pm 34.61

Far left column lists the *N*-acyl amide family or control compound that was used as the pre-incubated compounds for each screen. Challenge compounds are listed under the title of the TRPV-HEK expression system. Values shown are the data from the change in relative fluorescence units of Fura2AM from the 30 s baseline and represent the area of the curve of analysis of 190 s post injection of the positive control challenge compound. Those values in bold black are significantly different from those of the vehicle injection $p \leq 0.01$.

mixture (*N*-acyl phenylalanines) caused a significant depression of the baseline calcium signaling. We chose one mixture, the *N*-acyl GABA lipids to assess activity by individual lipid species. Supplemental Figure 10 shows that there is a structure activity relationship in the *N*-acyl GABA family. Importantly, however, there was no calcium mobilization by capsaicin (Table 4) suggesting that *N*-acyl GABA lipids are likely acting through an alternative receptor.

DISCUSSION

Lipidomics as a field aims to both identify the full complement of biologically active lipids as well as their functional relevance. Here, we have combined a bottom-up approach targeting activity of novel *N*-acyl amide lipids at specific TRPV1-4 receptors and BV2 microglia with a top-down approach of screening the production or metabolism of these lipids in the brain in a model of peripheral inflammation and pain. Together these approaches provide a powerful set of tools that enabled us to discover additional endogenous ligands for TRPV1-4 and microglia as well as determine how these ligands are regulated in the CNS with inflammation, thereby generating a novel hypothesis for the activation and regulation of lipid signaling molecules and their receptors.

BOTTOM-UP LIPIDOMICS OF N-ACYL AMIDES AT TRPV1-4 AND BV-2 MICROGLIA

TRPV receptor activation and regulation as part of the processing of nociceptive information in the periphery and the CNS is not

fully understood. Here, we identified 20 novel *N*-acyl amides as putative ligands for TRPV1-4 channels. These data add to the growing literature that activation of TRP channels follows an opportunistic strategy in which, a wide range of structurally similar endogenous lipids are capable of driving calcium mobilization through these channels (Movahed et al., 2005; Bradshaw et al., 2013). An interesting example of this opportunistic strategy is the evidence here demonstrating that TRPV1 is activated by eight additional novel *N*-acyl amides, including *N*-docosahexaenoyl ethanolamine, which including the previous work by Movahed et al. (2005) brings the number of lipids in the *N*-acyl ethanolamine family alone up to at least 5. One difference between the two studies was the potency of OEA at TRPV1, which was higher than 10 μ M in our hands, therefore, not further investigated here. However, this discrepancy may be due to the very different assay conditions between the two studies. We were able to detect all of these novel TRPV1 agonists except *N*-docosahexaenoyl aspartic acid in the brain. These data support the existing hypothesis that the primary endogenous TRPV1 ligands are long-chain, unsaturated acyl-amides (e.g., AEA; NADA; OLDA) and extends the number of endogenous *N*-acyl amide TRPV1 ligands to at minimum 13. Even though we were unable to test all the individual lipids in our screen at each of the TRPVs tested here, of those that were individually screened the vast majority did not activate TRPV1, suggesting that it is not simply a response to long-chain *N*-acyl amides of any structure. This finding replicates an earlier finding that NAGly and the oxidized AGABA (AGABA-OH) had no activity at

Table 3 | Effects on *N*-acyl amide lipidomics profile in 6 brain areas 1 and 3 h post carrageenan.

	STR		HIPP		CER		THAL		MID		STEM	
	1H	3H	1H	3H	1H	3H	1H	3H	1H	3H	1H	3H
<i>N</i>-acyl alanine												
<i>N</i> -palmitoyl alanine									↓			
<i>N</i> -stearoyl alanine			↑									
<i>N</i> -oleoyl alanine			↓	↑								
<i>N</i> -arachidonoyl alanine #			↓									
<i>N</i> -docosahexaenoyl alanine #		↑										
<i>N</i>-acyl ethanolamine												
<i>N</i> -palmitoyl ethanolamine		↑		↑		↑		↑				↑
<i>N</i> -stearoyl ethanolamine		↑										
<i>N</i> -oleoyl ethanolamine		↑		↑		↑	↓	↑		↑		↑
<i>N</i> -linoleoyl ethanolamine		↑		↑		↑		↑		↑		↑
<i>N</i> -arachidonoyl ethanolamine		↑		↑		↑		↑		↑		↑
<i>N</i> -docosahexaenoyl ethanolamine		↑		↑		↑		↑				
<i>N</i>-acyl GABA												
<i>N</i> -palmitoyl GABA						↑						
<i>N</i> -stearoyl GABA						↑						
<i>N</i> -oleoyl GABA						↑						
<i>N</i> -linoleoyl GABA #		↑				↑						
<i>N</i> -arachidonoyl GABA		↑			↓	↑					↓	
<i>N</i> -docosahexaenoyl GABA						↑						
<i>N</i>-acyl glycine												
<i>N</i> -palmitoyl glycine				↑								
<i>N</i> -stearoyl glycine						↑						
<i>N</i> -oleoyl glycine				↑		↑						
<i>N</i> -linoleoyl glycine			↓			↑						
<i>N</i> -arachidonoyl glycine		↑		↑		↑						
<i>N</i> -docosahexaenoyl glycine #		↑		↑		↑						
Additional <i>N</i>-acyl amides												
<i>N</i> -oleoyl leucine #										↑		
<i>N</i> -stearoyl serine	↓											
<i>N</i> -linoleoyl serine				↑								
<i>N</i> -palmitoyl threonine		↑										
<i>N</i> -palmitoyl tryptophan			↑									
<i>N</i> -stearoyl tryptophan							↑					
<i>N</i> -oleoyl tyrosine						↑						
<i>N</i> -arachidonoyl tyrosine							↑					
<i>N</i> -palmitoyl valine		↑										
<i>N</i> -stearoyl valine			↓									
<i>N</i> -docosahexaenoyl valine #						↑						

These are the summary data of those *N*-acyl amides that were significantly modified (increased or decreased) from the levels measured in the vehicle control and do not represent all lipids tested. All averaged values for all lipids tested are shown in Supplemental Table 2. Six brain areas (STR, striatum; HIPP, hippocampus; CER, cerebellum; THAL, thalamus; MID, midbrain; STEM, brainstem) are depicted in individual columns further separated by the treatment groups 1 hour (1H) and 3 hour (3H) post carrageenan. Those in green with an up arrow showed significant increases from control injections, whereas, those in red with down arrows showed significant decreases from control injections $p = 0.05$. Those in gray are *N*-acyl amides that activated on of the TRPV systems tested here. # Denotes that these compounds had not been previously identified in mammalian brain.

Table 4 | Agonist effects of *N*-acyl amide mixtures on calcium mobilization in BV-2 microglia.

N-acyl amide mixtures 10 μM	BV-2 Microglia
N-acyl alanine	69.48 \pm 3.18
N-acyl aspartic acid	12.73 \pm 0.82
N-acyl beta-alanine	15.33 \pm 1.16
N-acyl GABA	119.56 \pm 2.72
N-acyl glycine	22.91 \pm 1.32
N-acyl isoleucine	8.31 \pm 1.17
N-acyl leucine	56.47 \pm 1.62
N-acyl methionine	33.00 \pm 1.84
N-acyl phenylalanine	(-)-5.07 \pm 2.13
N-acyl proline	102.66 \pm 2.04
N-acyl serine	12.41 \pm 1.35
N-acyl threonine	12.27 \pm 1.00
N-acyl tryptophan	4.83 \pm 1.04
N-acyl tyrosine	19.74 \pm 1.24
N-acyl valine	61.33 \pm 2.17
DMSO	9.09 \pm 0.84
Capsaicin (500 nM)	9.60 \pm 2.54
PAF	49.60 \pm 2.71
Inonomecine	223.92 \pm 5.81

Far left column lists the *N*-acyl amide family or control compound that was used as the challenge compounds for each screen. Values shown are the change in relative fluorescence units of Fura2AM from the 30 s baseline and represent the area of the curve of analysis of 190 s post injection (see example on **Figure 2**). Those values in bold black are significantly higher from those of the vehicle injection, whereas those in bold gray are significantly lower $p \leq 0.01$.

TRPV1 (Barbara et al., 2009). Therefore, the SAR of activity is specific to the oxidation level of the same molecule. In addition, the one antagonist that was identified here, *N*-docosaheptaenoyl proline, is also a long-chain fatty acid amide, providing further evidence of the structural properties of those molecules that successfully interact with the TRPV1 receptor. Therefore, while our and previous data support the hypothesis that TRPV1 is an opportunistic receptor that preferentially is activated by long-chain, unsaturated acyl-amides, it is not activated by all of such molecules in this category.

Similar results were seen with the identification of TRPV4 activators in that of the two *N*-acyl amide mixtures that were hits for agonist activity, three individual members of each were shown to activate the receptor. This was not the case, however, for activity at TRPV2 and TRPV3. Wherein the *N*-acyl proline mixture had the most activity at TRPV2, none of the individual members had a significant effect. While *N*-palmitoyl tyrosine did have a significant effect on calcium mobilization, it was relatively weak compared to the *N*-acyl tyrosine mixture at the same molarity. Likewise, the *N*-acyl tyrosine mixture had the strongest agonist effect at TRPV3, yet none of the individual members showed significant activity. Intriguingly, each of these mixtures also caused antagonist activity in the same expression systems. We hypothesize that there are allosteric effects of individual lipids on members of the same *N*-acyl amide family that would drive one member to have a higher potency than another. This hypothesis will be tested in future studies.

N-acyl amide activity in BV2 microglia also showed similar patterns to those of the TRPVs tested here. 4 of the 5 *N*-acyl amide mixtures that caused calcium mobilization in these BV2 microglia also activated different TRPVs here, with the only exception being *N*-acyl alanine, which did have some activity at TRPV2, though not at the 0.01 p -value; therefore, this was not pursued in these studies. Further studies are aimed at determining if the *N*-acyl alanines are active at additional TRPs. As mentioned previously, however, there was not calcium mobilization with capsaicin in these BV2 cells, suggesting that none of these responses would be through TRPV1. Study of TRP receptor function in microglia is a small but growing field. Although the presence of TRPV1-4 on BV-2 microglial cells has not been fully confirmed, there exists plentiful evidence to suggest a role for TRPVs in microglial signaling. Hassan and colleagues measured the rate of phagocytosis in cultured microglial cells by quantifying the ingestion of fluorescently labeled latex beads. The phytocannabinoid cannabidiol (CBD) boosted the rate of phagocytosis, specifically, 10 μ M CBD increased phagocytosis by 175% over vehicle control. BV-2 microglia do not express the cannabinoid receptors CB₁ or CB₂, thus the effect was not mediated by CB receptor signaling. Pretreating with pertussis toxin, which blocks GPCRs, had no effect on CBD's actions, ruling out GPCR signaling pathways as mediators of this effect. In addition to increasing phagocytosis, CBD caused calcium influx into the microglial cells. The calcium influx was abolished by ruthenium red, a non-selective TRP channel antagonist. Additionally, ruthenium red prevented CBD from increasing phagocytosis. The effects on individual TRPV channels were then investigated: TRPV1 was implicated, as treatment with capsazepine blocked the increase in phagocytosis. Without CBD treatment, the TRPV2 agonist probenecid dose-dependently enhanced phagocytosis *in-vitro*. RT-PCR revealed that TRPV2 mRNA is detectable in untreated BV-2 cells (Hassan et al., 2014).

Immunocytochemistry has shown TRPV1 to be present in rat primary microglial cell lines. However, care must be taken in interpreting these results as knock-out controls are not shown and TRPV1 antibodies can produce artifactual staining. RT-PCR showed that TRPV1 mRNA was present on rat microglia, but not on astrocytes. Interestingly, exposure to TRPV1 agonists like capsaicin-induced apoptosis in these cultured microglial cells. These effects were inhibited by capsazepine, indicating a role for TRPV1 in regulating apoptosis in microglia (Kim et al., 2006). RT-PCR also showed TRPV1 mRNA expression in rat retinal microglial cultures, where it may possibly have a role in regulating intra-ocular pressure (Sappington and Calkins, 2008).

Eight out of 20 of the novel *N*-acyl amides identified here as TRPV1-4 activators are conjugates of docosaheptaenoic acid, which is an omega-3 fatty acid. This is particularly interesting in the context of the recent focus in human nutrition on this class of lipids. Links between omega-3 fatty acids and pain associated with inflammation have been shown and studied for decades, however, the exact molecular mechanism remains elusive (for review see Tokuyama and Nakamoto, 2011). Resolvin molecules are clearly part of the answer (Ji et al., 2011); however, their rapid degradation that perhaps leads to a lack of data on their endogenous production provides a roadblock in our understanding of how these molecules work *in vivo*. In our own hands, we have observed

that *N*-docosahexaenoyl amides are significantly more stable and can be readily measured in tissue. We propose that these *N*-docosahexaenoyl amides may even act as more stable precursor molecules for the more reactive and fast-lived resolvins.

Unlike the resolvins species of lipids, *N*-acyl amides in brain are relatively straightforward to measure using methanolic extractions, partial purification on C18 solid phase extraction columns and HPLC-MS/MS analysis (Bradshaw et al., 2006; Rimmerman et al., 2008; Bradshaw et al., 2009; Smoum et al., 2010). We recently identified 47 of those measured here in *Drosophila*, demonstrating that these simple bioactive lipids are not unique to mammals or the brain (Tortoriello et al., 2013). That nearly a third of those measured here were modified by peripheral inflammation suggests that they are of the type of lipids that are rapidly made on demand and are likely part of the myriad of signaling systems that are engaged during both a stress-inducing and painful event.

TOP-DOWN LIPIDOMICS OF N-ACYL AMIDES IN THE CNS

Carrageenan injections into the paw are a reliable model of acute inflammation that is associated with thermal and mechanical allodynia and hyperalgesia as well as the suite of learning a motivated behaviors associated with the response to noxious stimuli (Fecho et al., 2005). Here, we demonstrate a wide-range of regulation of *N*-acyl amides in six different regions of the brain; however, we will focus our discussion on the hippocampus and the striatum in that they showed the most dynamic changes in *N*-acyl amides with peripheral inflammation. It is important to note that they both play important and evolving roles in pain and inflammation.

Both the striatum and hippocampus have been heavily implicated as CNS regions involved in pain processing and perception (Malow and Olson, 1981; McEwen, 2001; Ploghaus et al., 2001; Ferre et al., 2009; Barcelo et al., 2012), and our study confirms that there are changes in the production of these putative *N*-acyl amide signaling molecules in the striatum and hippocampus due to inflammatory pain. However, one of the major limitations of this study is the heterogeneity of these brain areas. While both regions are discrete and easy to dissect from the brain, both the striatum and hippocampus are also responsible for a host of functions. The hippocampus is particularly noted for its role in consolidation of long-term memories and spatial memory in rodents. Constant dendritic remodeling and neurogenesis make the hippocampus capable of learning new associations such as avoidance behaviors to painful stimuli (Ploghaus et al., 2001). The hippocampus is also very susceptible to glucocorticoids for instance those released in response to a painful, stressful situation. McEwen hypothesizes that the neurochemical and morphological changes in the hippocampus may cause changes in chronic pain perception (McEwen, 2001). Indeed, patients with effectively managed chronic pain versus those whose pain persists despite treatment have an increased pain threshold and are able to more sensitively discriminate between different levels of pain (Malow and Olson, 1981).

Similarly, the striatum is involved in regulating a variety of processes. The striatum is best known for its role in planning and modulating motor movement by integrating sensory and motor

information. However, parts of the striatum respond exclusively to noxious stimuli (Barcelo et al., 2012). While dopaminergic neurons are densely expressed in the striatum and implicated in pain processing, CB₁ receptors form heteromers with D₂, A_{2A}, and μ opioid receptors indicating potential novel mechanisms of endocannabinoid function in the striatum beyond retrograde signaling and inhibition of neurotransmitter release (Ferre et al., 2009). Therefore, increases in AEA shown here may play a role in the CB₁ response as well as in the TRPV1 response.

CONCLUSIONS

These studies represent a novel direction in ion channel research in the CNS. Blending our knowledge of lipidomics of *N*-acyl amides and TRPV channel activity has allowed us to discover a connection between the two of which the depth of has yet to be tested. We propose that this is merely the beginning of our understanding of how these systems work in concert and hypothesize that the co-evolution of *N*-acyl amides and ion channels plays a major role in a wide range of cellular signaling beyond the mammalian brain.

SUPPLEMENTARY MATERIAL

The Supplementary Material for this article can be found online at: <http://www.frontiersin.org/journal/10.3389/fncel.2014.00195/abstract>

REFERENCES

- Barbara, G., Alloui, A., Nargeot, J., Lory, P., Eschaliere, A., Bourinet, E., et al. (2009). T-type calcium channel inhibition underlies the analgesic effects of the endogenous lipoamino acids. *J. Neurosci.* 29, 13106–13114. doi: 10.1523/JNEUROSCI.2919-09.2009
- Barcelo, A. C., Filippini, B., and Pazo, J. H. (2012). The striatum and pain modulation. *Cell. Mol. Neurobiol.* 32, 1–12. doi: 10.1007/s10571-011-9737-7
- Beech, D. J. (2012). Integration of transient receptor potential canonical channels with lipids. *Acta Physiol. (Oxf.)* 204, 227–237. doi: 10.1111/j.1748-1716.2011.02311.x
- Bradshaw, H. B., Raboune, S., and Hollis, J. L. (2013). Opportunistic activation of TRP receptors by endogenous lipids: exploiting lipidomics to understand TRP receptor cellular communication. *Life Sci.* 92, 404–409. doi: 10.1016/j.lfs.2012.11.008
- Bradshaw, H. B., Rimmerman, N., Hu, S. S., Burstein, S., and Walker, J. M. (2009). Novel endogenous N-acyl glycines identification and characterization. *Vitam. Horm.* 81, 191–205. doi: 10.1016/S0083-6729(09)81008-X
- Bradshaw, H. B., Rimmerman, N., Krey, J. F., and Walker, J. M. (2006). Sex and hormonal cycle differences in rat brain levels of pain-related cannabinimetic lipid mediators. *Am. J. Physiol. Regul. Integr. Comp. Physiol.* 291, R349–R358. doi: 10.1152/ajpregu.00933.2005
- Bradshaw, H. B., and Walker, J. M. (2005). The expanding field of cannabinimetic and related lipid mediators. *Br. J. Pharmacol.* 144, 459–465. doi: 10.1038/sj.bjp.0706093
- Burstein, S. H., Adams, J. K., Bradshaw, H. B., Fraioli, C., Rossetti, R. G., Salmons, R. A., et al. (2007). Potential anti-inflammatory actions of the elmiric (lipoamino) acids. *Bioorg. Med. Chem.* 15, 3345–3355. doi: 10.1016/j.bmc.2007.03.026
- Caterina, M. J., and Julius, D. (2001). The vanilloid receptor: a molecular gateway to the pain pathway. *Annu. Rev. Neurosci.* 24, 487–517. doi: 10.1146/annurev.neuro.24.1.487
- Caterina, M. J., Schumacher, M. A., Tominaga, M., Rosen, T. A., Levine, J. D., and Julius, D. (1997). The capsaicin receptor: a heat-activated ion channel in the pain pathway. *Nature* 389, 816–824.
- Cavanaugh, D. J., Chesler, A. T., Braz, J. M., Shah, N. M., Julius, D., and Basbaum, A. I. (2011a). Restriction of transient receptor potential vanilloid-1

- to the peptidergic subset of primary afferent neurons follows its developmental downregulation in nonpeptidergic neurons. *J. Neurosci.* 31, 10119–10127. doi: 10.1523/JNEUROSCI.1299-11
- Cavanaugh, D. J., Chesler, A. T., Jackson, A. C., Sigal, Y. M., Yamanaka, H., Grant, R., et al. (2011b). Trpv1 reporter mice reveal highly restricted brain distribution and functional expression in arteriolar smooth muscle cells. *J. Neurosci.* 31, 5067–5077. doi: 10.1523/JNEUROSCI.6451-10
- Chu, C. J., Huang, S. M., De Petrocellis, L., Bisogno, T., Ewing, S. A., Miller, J. D., et al. (2003). N-oleoyldopamine, a novel endogenous capsaicin-like lipid that produces hyperalgesia. *J. Biol. Chem.* 278, 13633–13639. doi: 10.1074/jbc.M211231200
- Di Marzo, V., Blumberg, P. M., and Szallasi, A. (2002). Endovanilloid signaling in pain. *Curr. Opin. Neurobiol.* 12, 372–379. doi: 10.1016/S0959-4388(02)00340-9
- Fecho, K., Nackley, A. G., Wu, Y., and Maixner, W. (2005). Basal and carrageenan-induced pain behavior in Sprague-Dawley, Lewis and Fischer rats. *Physiol. Behav.* 85, 177–186. doi: 10.1016/j.physbeh.2005.03.018
- Ferre, S., Goldberg, S. R., Lluís, C., and Franco, R. (2009). Looking for the role of cannabinoid receptor heteromers in striatal function. *Neuropharmacology* 56(Suppl. 1), 226–234. doi: 10.1016/j.neuropharm.2008.06.076
- Hassan, S., Eldeeb, K., Mills, P. J., Bennett, A. J., Alexander, S. P., and Kendall, D. A. (2014). Cannabidiol enhances microglial phagocytosis via transient receptor potential (TRP) channel activation. *Br. J. Pharmacol.* 171, 2426–2439. doi: 10.1111/bph.12615
- Ho, K. W., Ward, N. J., and Calkins, D. J. (2012). TRPV1: a stress response protein in the central nervous system. *Am. J. Neurodegener. Dis.* 1, 1–14.
- Hu, S. S., Bradshaw, H. B., Benton, V. M., Chen, J. S., Huang, S. M., Minassi, A., et al. (2009). The biosynthesis of N-arachidonoyl dopamine (NADA), a putative endocannabinoid and endovanilloid, via conjugation of arachidonic acid with dopamine. *Prostaglandins Leukot. Essent. Fatty Acids* 81, 291–301. doi: 10.1016/j.plefa.2009.05.026
- Hu, S. S., Bradshaw, H. B., Chen, J. S., Tan, B., and Walker, J. M. (2008). Prostaglandin E2 glycerol ester, an endogenous COX-2 metabolite of 2-arachidonoylglycerol, induces hyperalgesia and modulates NFκB activity. *Br. J. Pharmacol.* 153, 1538–1549. doi: 10.1038/bjp.2008.33
- Huang, S. M., Bisogno, T., Trevisani, M., Al-Hayani, A., De Petrocellis, L., Fezza, F., et al. (2002). An endogenous capsaicin-like substance with high potency at recombinant and native vanilloid VR1 receptors. *Proc. Natl. Acad. Sci. U.S.A.* 99, 8400–8405. doi: 10.1073/pnas.122196999
- Ji, R. R., Berta, T., and Nedergaard, M. (2013). Glia and pain: is chronic pain a gliopathy? *Pain* 154, S10–S28. doi: 10.1016/j.pain.2013.06.022
- Ji, R. R., Xu, Z. Z., Strichartz, G., and Serhan, C. N. (2011). Emerging roles of resolvins in the resolution of inflammation and pain. *Trends Neurosci.* 34, 599–609. doi: 10.1016/j.tins.2011.08.005
- Julius, D. (2013). TRP channels and pain. *Annu. Rev. Cell Dev. Biol.* 29, 355–384. doi: 10.1146/annurev-cellbio-101011-155833
- Kim, S. R., Kim, S. U., Oh, U., and Jin, B. K. (2006). Transient receptor potential vanilloid subtype 1 mediates microglial cell death *in vivo* and *in vitro* via Ca²⁺-mediated mitochondrial damage and cytochrome c release. *J. Immunol.* 177, 4322–4329. doi: 10.4049/jimmunol.177.7.4322
- Lee, S. H., Raboune, S., Walker, J. M., and Bradshaw, H. B. (2010). Distribution of endogenous farnesyl pyrophosphate and four species of lysophosphatidic acid in rodent brain. *Int. J. Mol. Sci.* 11, 3965–3976. doi: 10.3390/ijms11103965
- Malow, R. M., and Olson, R. E. (1981). Changes in pain perception after treatment for chronic pain. *Pain* 11, 65–72. doi: 10.1016/0304-3959(81)90139-1
- Mcewen, B. S. (2001). Plasticity of the hippocampus: adaptation to chronic stress and allostatic load. *Ann. N.Y. Acad. Sci.* 933, 265–277. doi: 10.1111/j.1749-6632.2001.tb05830.x
- Mchugh, D., Hu, S. S., Rimmerman, N., Juknat, A., Vogel, Z., Walker, J. M., et al. (2010). N-arachidonoyl glycine, an abundant endogenous lipid, potently drives directed cellular migration through GPR18, the putative abnormal cannabidiol receptor. *BMC Neurosci.* 11:44. doi: 10.1186/1471-2202-11-44
- Movahed, P., Jonsson, B. A., Birnir, B., Wingstrand, J. A., Jorgensen, T. D., Ermund, A., et al. (2005). Endogenous unsaturated C18 N-acyl ethanolamines are vanilloid receptor (TRPV1) agonists. *J. Biol. Chem.* 280, 38496–38504. doi: 10.1074/jbc.M507429200
- Nagy, I., Santha, P., Jancso, G., and Urban, L. (2004). The role of the vanilloid (capsaicin) receptor (TRPV1) in physiology and pathology. *Eur. J. Pharmacol.* 500, 351–369. doi: 10.1016/j.ejphar.2004.07.037
- Nilius, B., and Owsianik, G. (2011). The transient receptor potential family of ion channels. *Genome Biol.* 12:218. doi: 10.1186/gb-2011-12-3-218
- Ploghaus, A., Narain, C., Beckmann, C. F., Clare, S., Bantick, S., Wise, R., et al. (2001). Exacerbation of pain by anxiety is associated with activity in a hippocampal network. *J. Neurosci.* 21, 9896–9903.
- Rimmerman, N., Bradshaw, H. B., Hughes, H. V., Chen, J. S., Hu, S. S., Mchugh, D., et al. (2008). N-palmitoyl glycine, a novel endogenous lipid that acts as a modulator of calcium influx and nitric oxide production in sensory neurons. *Mol. Pharmacol.* 74, 213–224. doi: 10.1124/mol.108.045997
- Rubio, M., Mchugh, D., Fernandez-Ruiz, J., Bradshaw, H., and Walker, J. M. (2007). Short-term exposure to alcohol in rats affects brain levels of anandamide, other N-acyl ethanolamines and 2-arachidonoyl-glycerol. *Neurosci. Lett.* 421, 270–274. doi: 10.1016/j.neulet.2007.05.052
- Saghatelian, A., McKinney, M. K., Bandell, M., Patapoutian, A., and Cravatt, B. F. (2006). A FAAH-regulated class of N-acyl taurines that activates TRP ion channels. *Biochemistry* 45, 9007–9015. doi: 10.1021/bi0608008
- Sappington, R. M., and Calkins, D. J. (2008). Contribution of TRPV1 to microglia-derived IL-6 and NFκB translocation with elevated hydrostatic pressure. *Invest. Ophthalmol. Vis. Sci.* 49, 3004–3017. doi: 10.1167/iovs.07-1355
- Smoum, R., Bar, A., Tan, B., Milman, G., Attar-Namdar, M., Ofek, O., et al. (2010). Oleoyl serine, an endogenous N-acyl amide, modulates bone remodeling and mass. *Proc. Natl. Acad. Sci. U.S.A.* 107, 17710–17715. doi: 10.1073/pnas.0912479107
- Starowicz, K., Cristino, L., and Di Marzo, V. (2008). TRPV1 receptors in the central nervous system: potential for previously unforeseen therapeutic applications. *Curr. Pharm. Des.* 14, 42–54. doi: 10.2174/138161208783330790
- Tan, B., Bradshaw, H. B., Rimmerman, N., Srinivasan, H., Yu, Y. W., Krey, J. F., et al. (2006). Targeted lipidomics: discovery of new fatty acyl amides. *AAPS J.* 8, E461–E465. doi: 10.1208/aapsj080354
- Tan, B., O'dell, D. K., Yu, Y. W., Monn, M. F., Hughes, H. V., Burstein, S., et al. (2010). Identification of endogenous acyl amino acids based on a targeted lipidomics approach. *J. Lipid Res* 51, 112–119. doi: 10.1194/jlr.M900198-JLR200
- Tokuyama, S., and Nakamoto, K. (2011). Unsaturated fatty acids and pain. *Biol. Pharm. Bull.* 34, 1174–1178. doi: 10.1248/bpb.34.1174
- Tominaga, M., Caterina, M. J., Malmberg, A. B., Rosen, T. A., Gilbert, H., Skinner, K., et al. (1998). The cloned capsaicin receptor integrates multiple pain-producing stimuli. *Neuron* 21, 531–543. doi: 10.1016/S0896-6273(00)80564-4
- Tortoriello, G., Rhodes, B. P., Takacs, S. M., Stuart, J. M., Basnet, A., Raboune, S., et al. (2013). Targeted lipidomics in *Drosophila melanogaster* identifies novel 2-monoacylglycerols and N-acyl amides. *PLoS ONE* 8:e67865. doi: 10.1371/journal.pone.0067865
- Vriens, J., Owsianik, G., Voets, T., Droogmans, G., and Nilius, B. (2004). Invertebrate TRP proteins as functional models for mammalian channels. *Pflugers Arch.* 449, 213–226.
- Zygmunt, P. M., Petersson, J., Andersson, D. A., Chuang, H., Sorgard, M., Di Marzo, V., et al. (1999). Vanilloid receptors on sensory nerves mediate the vasodilator action of anandamide. *Nature* 400, 452–457.

Conflict of Interest Statement: The authors declare that the research was conducted in the absence of any commercial or financial relationships that could be construed as a potential conflict of interest.

Received: 28 March 2014; accepted: 24 June 2014; published online: 01 August 2014.
 Citation: Raboune S, Stuart JM, Leishman E, Takacs SM, Rhodes B, Basnet A, Jameyfield E, McHugh D, Widlanski T and Bradshaw HB (2014) Novel endogenous N-acyl amides activate TRPV1-4 receptors, BV-2 microglia, and are regulated in brain in an acute model of inflammation. *Front. Cell. Neurosci.* 8:195. doi: 10.3389/fncel.2014.00195
 This article was submitted to the journal *Frontiers in Cellular Neuroscience*.
 Copyright © 2014 Raboune, Stuart, Leishman, Takacs, Rhodes, Basnet, Jameyfield, McHugh, Widlanski and Bradshaw. This is an open-access article distributed under the terms of the Creative Commons Attribution License (CC BY). The use, distribution or reproduction in other forums is permitted, provided the original author(s) or licensor are credited and that the original publication in this journal is cited, in accordance with accepted academic practice. No use, distribution or reproduction is permitted which does not comply with these terms.